

Investigation into non-aqueous remedial conservation treatments for iron-tannate dyed organic materials

A thesis submitted to the University of Manchester for the degree of
Doctor of Philosophy
in the Faculty of Engineering and Physical Sciences

2012

Helen Wilson

School of Materials

Table of contents
TABLE OF CONTENTS

List of Tables	8
List of Figures	10
List of Equations	15
List of Schemes	17
Abstract	18
Declaration and copyright statement	19
Peer-reviewed publications and posters and websites	20
Acknowledgements, dedication, and preface	21
List of abbreviations	22
1. INTRODUCTION	24
1.1 The importance of cultural heritage	24
1.2 The Science and Heritage Programme	25
1.3 The British Museum	25
1.4 Project background	25
1.5 Research aims	26
1.6 Methodology and thesis structure	26
2. ANALYTICAL TECHNIQUES	28
2.1 μ -X-ray Fluorescence (μ -XRF)	28
2.1.1 Theory	28
2.1.2 Equipment	29
2.1.3 Usage in cultural heritage	30
2.2 Scanning Electron Microscopy with Energy Dispersive X-ray (SEM-EDX) analysis	30
2.2.1 Theory and equipment	30
2.2.2 Uses in cultural heritage	32
2.3 Colour measurement	32
2.3.1 Theory	33
2.3.2 Equipment	35
2.3.3 Uses in cultural heritage	35
2.4 Electron Paramagnetic Resonance (EPR) Spectroscopy	36
2.4.1 Theory	36
2.4.2 Equipment	38
2.4.3 Usage in cultural heritage	39
2.5 Gel Permeation Chromatography with Multi Angle Laser Light Scattering detector (GPC-MALLS)	40
2.5.1 Theory	40
2.5.2 Equipment and method	42
2.5.3 Uses in cultural heritage	42
2.6 pH testing	42
2.6.1 Theory	42
2.6.2 Equipment	44
2.6.3 Usage in cultural heritage	47
2.7 Bathophenanthroline testing	47
2.7.1 Theory	47
2.7.2 Equipment	48
2.7.3 Usage in cultural heritage	49
2.8 Viscometry	49
2.8.1 Theory	50
2.8.2 Equipment	50
2.8.3 Usage in cultural heritage	51
2.9 Tensile testing	51
2.9.1 Theory	52
2.9.2 Equipment	53
2.9.3 Uses in cultural heritage	54
3. UNDYED MODEL TEXTILES	55
3.1 Historic iron-tannate dyed materials	55
3.2 Aims for model textiles	55
3.3 Choice of model textiles	56
3.3.1 Cellulosic textiles	57
3.3.2 Proteinaceous textiles	58
3.4 Cellulosic model textile properties and reactivity	59
3.4.1 Cotton	59
3.4.1.1 Formation	60
3.4.1.2 Chemical composition and fibre structure	60
3.4.1.3 Cellulose	63
3.4.1.4 Microfibrils	64
3.4.1.5 Properties	65

3.4.1.6 Reactivity	68
3.4.1.7 Cotton dyeing	75
3.4.2 Abaca	77
3.4.2.1 Abaca plant	77
3.4.2.2 Fibre production	78
3.4.2.3 Fibre structure	78
3.4.2.4 Composition	79
3.4.2.5 Mechanical properties	82
3.4.2.6 Reactivity	83
3.5 Proteinaceous model textile properties and reactivity	85
3.5.1 Wool	85
3.5.1.1 Composition of keratin	85
3.5.1.2 Crosslinks	90
3.5.1.3 Structure of wool fibres	91
3.5.1.4 Reactivity	96
3.5.1.5 Wool dyeing	103
3.5.1.6 Properties	105
3.5.2 Silk	107
3.5.2.1 Fibroin composition	108
3.5.2.2 Fibroin structure	108
3.5.2.3 Mechanical properties	111
3.5.2.4 Reactivity	112
3.6 Conclusions	116
4. MODEL IRON-TANNATE DYES	118
4.1 Iron-tannate dye composition and properties	118
4.1.1 Reagents	118
4.1.2 Iron-polyphenol dye complex	119
4.1.3 Other metal-polyphenol complexes	126
4.1.4 Iron oxidation state in iron-tannate dyes	127
4.1.5 Colour	129
4.1.5.1 Factors affecting the colour of the dyed material	129
4.1.6 Acidity	132
4.1.6.1 Dye formulation	132
4.1.6.2 Substrate	133
4.1.6.3 Age	133
4.1.7 Interaction of dye and fibres	133
4.1.7.1 Application of the first reagent	133
4.1.7.2 Application of the second reagent	135
4.1.7.3 The effect of dyebath pH on dye-fibre interactions	136
4.1.8 Metal ion reactivity	136
4.2 Iron-tannate dye usage	138
4.3 Historic dye formulations	141
4.4 Iron-tannate dye detection	143
4.4.1 Chemical techniques	144
4.4.1.1 Bathophenanthroline indicator paper	144
4.4.1.2 Other tests	146
4.4.2 Analytical techniques	146
4.4.2.1 X-ray fluorescence (XRF)	146
4.4.2.2 High-performance liquid chromatography (HPLC)	147
4.4.2.3 Spectroscopic techniques	148
4.5 Iron-tannate dyes as catalysts	149
4.5.1 Oxidation	149
4.5.1.1 Autoxidation	149
4.5.1.2 Metal ion catalysed oxidation	151
4.5.2 Hydrolysis	154
4.5.3 Volatile organic compounds	158
4.5.4 Cycle of degradation	158
4.5.5 Variable condition of iron-tannate dyed objects	159
4.5.6 Storage recommendations for organic materials	161
4.6 Model dye development	161
4.6.1 Aims of the model dyes	162
4.6.2 Experimental method	163
4.6.3 Results of the textile dyeing experiments	164
4.6.4 Discussion	167
4.6.4.1 Two-stage versus one-stage dyeing	167
4.6.4.2 Effect of the order of two-stage dyeing, T-I or I-T, on dyeing	169
4.6.4.3 Effect of repeat dyeing on fabric colour	170

Table of contents

4.6.4.4 Dyeing of cellulosic materials relative to proteinaceous materials	170
4.6.4.5 Effect of temperature on dyeing – General trends	170
4.6.4.6 Gall powder extract	173
4.6.4.7 Reproducibility	174
4.6.4.8 Effect of varying reagent concentrations on dyeing	174
4.6.4.9 Effect of different immersion times on dyeing	175
4.6.4.10 Effect of varying the liquor: fabric ratio on dyeing	176
4.6.4.11 Effect of addition of copper on dyeing	176
4.6.5 Influence of results on the dye formulations	176
4.7 Conclusions	179
5. MODEL IRON-TANNATE DYED TEXTILES	180
5.1 Production	180
5.1.1 Dyeing of the model textiles	180
5.1.2 Summary of the 14 model textiles	182
5.2 Experimental techniques	183
5.2.1 X-ray fluorescence (XRF)	183
5.2.2 Surface pH	184
5.2.3 Bathophenanthroline tests	184
5.2.4 Colour measurements	184
5.2.4.1 Unaged model textiles	185
5.2.4.2 Aged model textiles	185
5.2.5 Tensile testing	187
5.2.5.1 Unaged model textiles	187
5.2.5.2 Aged model textiles	187
5.2.6 Electron paramagnetic resonance (EPR) analysis	188
5.2.7 Scanning electron microscopy-energy dispersive X-ray (SEM-EDX) analysis	189
5.2.7.1 Cross-sections	189
5.2.7.2 Model textiles	190
5.2.8 Gel permeation chromatography-multi-angle light scattering (GPC-MALLS)	191
5.2.9 Accelerated ageing	192
5.2.9.1 Assessing the effect of dye formulation 1 (c1/p1) on the cotton, abaca, wool, and silk model textiles	192
5.2.9.2 Assessing the effect of dye type on the cotton and silk model textiles	192
5.3 Characterisation of unaged model textiles - Results and discussion	193
5.3.1 Effect of dye application on the structure of the textiles	193
5.3.2 Extent of dyeing into the textile fibres	200
5.3.3 Homogeneity testing	203
5.3.3.1 XRF	203
5.3.3.2 Bathophenanthroline testing	205
5.3.3.3 Surface pH	208
5.3.3.4 Tensile testing	210
5.3.3.5 Colour measurement	211
5.3.3.6 GPC-MALLS	213
5.3.3.7 EPR	215
5.4 Characterisation of c1 and p1 dyed model textiles during accelerated ageing – Results and discussion	219
5.4.1 Surface pH	219
5.4.2 Colour measurement	220
5.4.3 Tensile testing	222
5.4.4 EPR	223
5.4.5 GPC-MALLS	227
5.4.6 SEM	231
5.5 Effect of dye type on textile stability – Results and discussion	234
5.5.1 Colour measurement	234
5.5.2 Tensile testing	238
5.6 Overall discussion	241
5.6.1 Homogeneity of the dyeing	241
5.6.2 Stability to thermal ageing	241
5.6.3 Comparison of iron-gall ink and iron-tannate dye data	242
5.7 Conclusions	243
6. IRON-TANNATE DYED CULTURAL HERITAGE	245
6.1 Experimental	245
6.1.1 Historic samples	245
6.1.2 Analytical techniques	260
6.1.2.1 XRF	260
6.1.2.2 Colour measurement	261
6.1.2.3 Bathophenanthroline testing	261

6.1.2.4 EPR	261
6.1.2.5 GPC-MALLS	261
6.1.2.6 Surface pH testing	261
6.1.2.7 SEM-EDX	261
6.2 Results and Discussion	262
6.2.1 XRF	262
6.2.2 Spectrophotometry	266
6.2.3 Bathophenanthroline testing	267
6.2.4 EPR	268
6.2.5 GPC-MALLS	270
6.2.6 Surface pH testing	271
6.2.7 SEM-EDX	273
6.3 Conclusions	286
7. ACCELERATED AGEING	288
7.1 Aims	289
7.2 Accelerated ageing theory	289
7.2.1 Rates of reaction	290
7.2.1.1 The Arrhenius equation	291
7.2.2 Methods of accelerated ageing	294
7.2.3 Natural ageing versus accelerated ageing	295
7.3 Accelerated ageing methods in use	298
7.3.1 Conditions used	298
7.3.2 Discussion of suitability of conditions for this research	299
7.4 Experimental method	300
7.4.1 Model textiles used	300
7.4.2 Equipment used	300
7.4.3 Conditions investigated	300
7.4.4 Analytical methods	302
7.4.4.1 Subjective handling tests	302
7.4.4.2 Tensile testing	302
7.4.4.3 Colorimetry	303
7.4.4.4 Surface pH	303
7.4.4.5 GPC-MALLS	303
7.5 Results and discussion	303
7.5.1 Subjective handling tests	303
7.5.2 Tensile testing	306
7.5.3 Colorimetry	309
7.5.3.1 Undyed textiles	309
7.5.3.2 Dyed textiles	312
7.5.4 Surface pH	315
7.5.5 GPC-MALLS	317
7.6 Choice of accelerated ageing conditions for use in Treatment Test 1 (Chapter 9)	319
7.7 Natural ageing studies	321
7.8 Conclusions	321
8. STABILISATION TREATMENTS FOR IRON-TANNATE DYED TEXTILES	322
8.1 Conservation strategies	322
8.2 Theory of stabilisation	322
8.2.1 Antioxidants	323
8.2.1.1 Metal ion chelators	324
8.2.1.2 Peroxide decomposers	327
8.2.1.3 Radical scavengers	328
8.2.1.4 Efficacy of antioxidants	329
8.2.2 Deadifiers	329
8.2.3 Calcium phytate treatment	333
8.2.4 Consolidants	335
8.2.5 Solvents – Aqueous vs non-aqueous	335
8.2.6 Conclusions	337
8.3 Chemicals for experimentation	338
8.3.1 Antioxidants	339
8.3.1.1 Tinuvin 292	340
8.3.1.2 Tinuvin 144	340
8.3.1.3 Irganox 1135	340
8.3.1.4 Irganox 1425	341
8.3.1.5 1-ethyl-3-methylimidazolium bromide (EBr)	341
8.3.1.6 (+)- α -tocopherol	342
8.3.1.7 Magnesium phytate	342
8.3.1.8 Etidronic acid	343

Table of contents

8.3.1.9 Melaneze (synthetic melanin)	343
8.3.2 Deacidifiers	343
8.3.2.1 Calcium bicarbonate (calcium hydrogencarbonate)	343
8.3.2.2 Magnesium ethoxide	344
8.4 Solvents for experimentation	344
8.4.1 Ethanol (100% ethyl alcohol) and IMS (ethyl alcohol denatured)	344
8.4.2 Tetrachloroethylene (1,1,2,2-tetrachloroethene)	345
8.4.3 n-Hexane	345
8.4.4 Cyclosiloxane D5	345
8.5 Solvent-model textile compatibility	346
8.5.1 Experimental Method	346
8.5.2 Analytical techniques	347
8.5.2.1 Colorimetry	347
8.5.2.2 Microscopy	347
8.5.2.3 SEM	348
8.5.3 Results and discussion	348
8.5.3.1 General observation	348
8.5.3.2 Colorimetry	350
8.5.3.3 Microscopy	351
8.5.3.4 SEM	351
8.5.4 Conclusions	352
8.6 Solvent-chemical combinations	352
8.6.1 Experimental method	352
8.6.2 Results and discussion	352
8.7 Treatment concentrations	353
8.8 Conclusions	355
9. STABILISATION TREATMENT TEST 1 - UNAGED COTTON AND SILK	356
9.1 Experimental method	356
9.1.1 Treatment solutions	356
9.1.2 Treatment application	358
9.1.3 Accelerated ageing	358
9.1.4 Analysis	359
9.1.4.1 Micro-pH testing	359
9.1.4.2 Colorimetry	360
9.1.4.3 Subjective handling tests (Cc1)	361
9.1.4.4 Tensile testing	362
9.1.4.5 Viscometry	362
9.1.4.6 SEM-EDX	363
9.1.4.7 EPR spectroscopy	363
9.1.4.8 GPC-MALLS	363
9.2 The effect of treatment application on the model textiles – Results and discussion	364
9.2.1 Micro-pH testing	364
9.2.2 Colorimetry	367
9.2.3 SEM-EDX	373
9.2.4 GPC-MALLS	378
9.2.5 EPR spectroscopy	380
9.3 The effect of the treatments on the stability of the model textiles during accelerated ageing – Results and discussion	381
9.3.1 Micro-pH testing	381
9.3.2 Subjective handling tests	383
9.3.3 Viscometry	385
9.3.4 Tensile testing	386
9.3.5 EPR spectroscopy	389
9.3.6 Colorimetry	390
9.3.7 GPC-MALLS	400
9.4 The technical merits of the most successful treatments	405
9.5 Fulfilment of the aims of the treatment	406
9.6 Conclusions	407
10. STABILISATION TREATMENT TEST 2 – PRE-AGED MODEL TEXTILES	409
10.1 Determination of the highest concentration of T292 to be used in Stabilisation Treatment Test 2	409
10.1.1 Experimental method	409
10.1.2 Results and discussion	410
10.1.3 Summary	410
10.2 Effect of solvent immersion on the conditions of fragile pre-aged model textiles	410
10.2.1 Experimental	410
10.2.1.1 Microscopy and SEM-EDX analysis	411

Table of contents

10.2.1.2 GPC-MALLS	411
10.2.1.3 XRF of GE-immersed samples	411
10.2.2 Results and discussion	412
10.2.2.1 General observations and SEM-EDX	412
10.2.2.2. GPC-MALLS	417
10.2.3 Summary	418
10.3 Treatment Test 2	419
10.3.1 Experimental method	419
10.3.1.1 Accelerated Ageing	419
10.3.1.2 Treatment application	420
10.3.1.3 Analytical methods for treated samples before accelerated ageing	423
10.3.1.4 Analytical methods for treated samples after 1 week of accelerated ageing (70°C and 65% RH)	424
10.3.2 Results and discussion - Treated pre-aged samples before accelerated ageing	424
10.3.2.1 Subjective handling tests	424
10.3.2.2 Colorimetry	425
10.3.2.3 Surface pH	429
10.3.3 Treated pre-aged samples after accelerated ageing – Results and discussion	431
10.3.3.1 Colorimetry	431
10.3.3.2 Tensile testing	437
10.3.4 Identification of most successful treatments	440
10.3.5 Summary	442
10.4 Conclusions	442
11. CONCLUSIONS AND FURTHER WORK	444
11.1 Conclusions	444
11.1.1 Model iron-tannate dyed textiles	444
11.1.2 Accelerated ageing	444
11.1.3 Treatments	445
11.2 Original contributions to knowledge	447
11.2.1 Model iron-tannate dyed textiles	447
11.2.2 Analytical techniques	447
11.2.3 Antioxidants and deacidifiers for iron-tannate dyed organic materials	448
11.2.4 The study of a range of historic objects at the British Museum	448
11.3 Retrospective changes to this project	449
11.4 Further work	449
11.4.1 Optimisation of treatments	449
11.4.2 Application method investigation	450
11.4.3 Light ageing of the dyed model textiles	450
11.4.4 Lifetime ageing studies of iron-tannate dyed cultural heritage	450
11.4.5 Use longer accelerated ageing times	450
11.4.6 Application to a modern iron-tannate dyed textile	451
11.4.7 Determination of acceptable levels of change to an object during treatment	451
11.4.8 Methods of iron-tannate dye identification	451
11.4.9 Further investigation into iron-tannate dyed objects in the British Museum's collection	451
REFERENCES	453
APPENDICES	476
Appendix 1 Chemistry Central Journal publication, 2012	476
Appendix 2 ICOM-CC 16th Triennial Conference publication, 2011	490
Appendix 3 IIC 2010 Congress poster, 2010	499
Appendix 4 ICON CF10 conference poster, 2010	500
Appendix 5 Experimental methods for the 16 iterative experiments (Section 4.6.2) used to produce the dye formulations detailed in Table 4.3	501
Appendix 6 XRF Fe ratios of historic samples	505
Appendix 7 Samples of the model textiles (see Table 5.1 for dye formulations)	512

Word count: 139829 (excluding preliminary pages and appendices)

List of tables
LIST OF TABLES

Table 3.1	Source and description of undyed model textiles	57
Table 3.2	Composition of abaca fibre	79
Table 3.3	Properties of abaca	82
Table 3.4	Amino acid composition of wool keratin	86
Table 3.5	Amino acid residue content in silk fibroin and sericin	108
Table 4.1	Iron-gallate and iron-tannate complexes most likely to occur in acidic iron-tannate dyes	120
Table 4.2	A summary of the results of 16 iterative experiments in which dyebath conditions were varied to assess the effects of these on textile colouration	165
Table 4.3	Outline of dye formulations based on results from small-scale laboratory experiments	177
Table 4.4	The final model dye formulations following adaptation at the University of Manchester's dyehouse	178
Table 4.5	The method of washing the model textiles prior to dyeing	178
Table 5.1	Model dye formulations	182
Table 5.2	Summary of the model textiles used in this project and their abbreviations	182
Table 5.3	Variation in colour coordinates between SCI/100 and SCE/100 data as a % of SCI/100 and SCE/100 data	186
Table 5.4	The effect of dye application on the iron and copper content of the model textiles as determined using XRF and bathophenanthroline test papers	204
Table 5.5	The effect of dye application on the breaking load, extension, and surface pH of the model textiles	209
Table 5.6	The effect of dye application on the colour of the model textiles	212
Table 5.7	The effect of dye application on the average molecular weight and carbonyl content of cotton	213
Table 5.8	The changes in iron(III), copper(II), and radical content in the model textiles following dye application	216
Table 5.9	Effect of accelerated ageing (80°C and 58% RH) on the surface pH of the p1 and c1 dyed model textiles	219
Table 5.10	Changes in overall colour (E_{00}^*), colour coordinates, breaking load (N), and extension (%) of substitute textiles during accelerated ageing (80°C and 58% RH)	220
Table 5.11	The changing iron(III) content and environment and radical content in the c1/p1 dye formulation dyed model textiles during accelerated ageing (80°C and 58% RH)	223
Table 5.12	The change in average molecular weight and molecular weight distribution of CU and Cc1 with accelerated ageing (80°C and 58% RH)	227
Table 5.13	Changes in overall colour and colour coordinates of the cotton and silk model textiles due to accelerated ageing (70°C and 65% RH) for up to 39 days	234
Table 5.14	The effect of dye type on the tensile properties of cotton and silk after accelerated ageing (70°C and 65% RH)	238
Table 6.1	Images, British Museum (or other) registration numbers, and descriptions of the objects analysed in this chapter	246
Table 6.2	Semi-quantitative XRF analysis of iron in black or brown areas of British Museum and other objects	265
Table 6.3	Results of bathophenanthroline testing and XRF on a selection of historic iron-tannate dyed cellulosic materials and cellulosic model textiles	267
Table 6.4	Molecular weight and carbonyl content of samples from two British Museum objects compared to a severely degraded dyed cotton model textile sample	270
Table 7.1	Accelerated ageing conditions tested	301
Table 7.2	The effect of different accelerated ageing conditions on the strength and colour of the model textiles as determined using subjective testing	304
Table 7.3	The effect of using cycling and stable RH during accelerated ageing on the breaking load and extension of the dyed and undyed model textiles	308
Table 7.4	The change in colour of the undyed model textiles after accelerated ageing with stable and cycling RH methods	309
Table 7.5	The change in colour of the dyed (p1 and c1) model textiles after accelerated ageing with stable and cycling RH methods	312
Table 7.6	The surface pH of the dyed and undyed model textiles after accelerated ageing with stable and cycling RH methods	315
Table 7.7	The effect of different accelerated ageing methods on the molecular weight and PDI of CU and Cc1 model textiles	318
Table 7.8	The effect of different accelerated ageing methods on the carbonyl content of CU and Cc1 model textiles	318
Table 8.1	Antioxidants, deacidifiers and solvents under investigation in this project	338
Table 8.2	Error values in changes in colour parameters for the model textiles	347
Table 8.3	General observations during immersion and drying of dyed model textiles in a variety of	348

List of tables

	solvents	
Table 8.4	Hazards of the solvents determined by MSDS	349
Table 8.5	The change in colour parameters of unaged cotton and silk model textiles due to 30 minute immersion in different solvents	350
Table 8.6	The compatibility of the chemicals with the solvents	353
Table 8.7	Chemical concentrations used in Treatment Test 1 (Chapter 9)	354
Table 9.1	The concentrations of the treatment solutions used in Treatment Test 1	357
Table 9.2	Approximate error in the colorimetric data due to variation in model textile colour prior to treatment or accelerated ageing	361
Table 9.3	The effect of treatment application on the colour and pH of Cc3 and the colour of CU	364
Table 9.4	The effect of treatment application on the pH and colour of Sp3 and the colour of SU	366
Table 9.5	The effect of the application of a selection of treatments to Cc3 on the GPC-MALLS molecular weight, carbonyl content, polydispersity index, and molecular weight distribution	378
Table 9.6	The effect of dye application to Cc3 on the iron(III) ion content, ratio of bound and unbound iron(III) ions and radical content	380
Table 9.7	The change in pH upon accelerated ageing of unaged and aged Cc3 fabrics	382
Table 9.8	The effect of the treatments on the handle, colour, and DP of the treated Cc3 textiles after accelerated ageing (2 weeks at 80°C and 65% RH)	384
Table 9.9	Breaking load and extension of treated and untreated of Sp3 after accelerated ageing (4 weeks at 80°C and 65% RH)	388
Table 9.10	The effect of accelerated ageing on the iron(III) ion and radical content of the model textiles	389
Table 9.11	Change in colour of Cc3 samples after accelerated ageing (80°C and 65% RH) for 2 and 4 weeks as determined using colorimetry	391
Table 9.12	Change in colour of CU samples after accelerated ageing (80°C and 65% RH) for 2 and 4 weeks as determined using colorimetry	392
Table 9.13	The effect of accelerated ageing (4 weeks at 80°C and 65% RH) on the colour of treated and untreated dyed (Sp3) and undyed (SU) silk samples	397
Table 9.14	Effect of treatments on the molecular weight, molecular weight distribution, polydispersity index and carbonyl content of a selection of Cc3 textiles during accelerated ageing (2 weeks at 80°C and 65% RH) on carbonyl content of Cc3 after accelerated ageing	400
Table 10.1	The concentrations of T292 solutions tested on Sp3 samples	410
Table 10.2	Effects of solvent immersion on colour and weight of pre-aged cotton and abaca samples, observation of wetting out and drying times, and indication of which samples were analysed with SEM-EDX	412
Table 10.3	Si content in GE immersed samples determined using XRF	416
Table 10.4	Changes in molecular weight, polydispersity index, and carbonyl content in aged (4 weeks aged at 80°C and 35-80% RH cycling every 3 hours) and fragile Cc1 due to immersion in solvents	417
Table 10.5	Treatment application conditions for pre-aged model textiles	421
Table 10.6	Colour change in pre-aged model textiles due to treatment application	427
Table 10.7	Surface pH of a selection of treated and untreated pre-aged samples prior to accelerated ageing	430
Table 10.8	The effect of treatments on the discolouration of the pre-aged model textiles during accelerated ageing (1 week at 70°C and 65% RH)	432
Table 10.9	The effect of treatments on the breaking load and extension properties of the model textiles after accelerated ageing	439

List of figures
LIST OF FIGURES

Figure 2.1	Electron and radiation processes in the XRF technique	28
Figure 2.2	Schematic of SEM instrument	31
Figure 2.3	Interaction of electrons with sample surface and volume of sample generating the signals	32
Figure 2.4	Diagram to illustrate the CIE $L^*a^*b^*$ colour space and the $L^*C^*h^\circ$ colour coordinates	34
Figure 2.5	A representation of Zeeman splitting of the energy levels of an unpaired electron with increasing strength of an external magnetic field	36
Figure 2.6	Typical absorbance and first derivative EPR spectra	39
Figure 2.7	Surface pH testing electrode and pH meter with micro-pH electrode analysing sample (inset)	46
Figure 2.8	The bathophenanthroline test strips used to identify soluble iron(II) and iron(III) ions (using 1% aqueous ascorbic acid solution) on a variety of model and historic textiles as well as the semi-quantitative colour chart and the structure of bathophenanthroline	48
Figure 2.9	Photograph of the viscometry equipment (excepting the water bath) used at the Centre for Sustainable Heritage, UCL	51
Figure 2.10	Photograph of the Instron 4411 tensile tester at the University of Manchester testing an aged dyed silk sample	53
Figure 3.1	From left to right: Samples of the undyed cotton, abaca, silk, and wool model textiles used in this project	57
Figure 3.2	An example of a bogolanfini in good condition (British Museum registration number: Af1987,07.9) and a Japanese hina doll with inset image of losses to its silk hair (British Museum registration number: 1981,0808.227) © The Trustees of the British Museum	59
Figure 3.3	The structure of cellulose with intramolecular hydrogen bonds	64
Figure 3.4	Typical stress-strain curves for cotton and other fibres at 20°C and 65% RH	67
Figure 3.5	The absorption and desorption of moisture by cellulose with changing RH at 25°C	72
Figure 3.6	Possible oxidation products of hydroxyl groups on anhydroglucose in cellulose	75
Figure 3.7	Some of the monosaccharides present in the hemicellulose of abaca	80
Figure 3.8	The structure of pectic acid	81
Figure 3.9	The structure, isoelectric point, and concentration [mol%] of acidic, basic, sulphur-containing, and heterocyclic amino acid residues in wool	87
Figure 3.10	The structure, isoelectric point (when given), and concentration [mol%] of polar and non-polar amino acid residues in wool	88
Figure 3.11	The amphoteric character of amino acids	89
Figure 3.12	The types of crosslinks present in wool	91
Figure 3.13	Explanation of the primary and secondary structure of the 8c-1 protein of the wool intermediate filament p.75	94
Figure 3.14	Morphology of a wool fibre	94
Figure 3.15	Principle steps in the formation of lanthionine from cystine	98
Figure 3.16	Four models for the sheet structure formed by hydrogen bonds	110
Figure 3.17	The formation of a lysinoalanine crosslink in silk in alkaline conditions	114
Figure 4.1	The classification of tannins into four major types based on their structural characteristics	119
Figure 4.2	Pourbaix diagram for iron in water at equilibrium and at 25°C	128
Figure 4.3	Coordination structures of copper in silk prepared at pH 4.18 (a and b), pH 4.53 (c), and pH 10.60 (d)	134
Figure 4.4	The structure of decagalloyl glucose, one of a range of polyphenols that can be present in tannic acid	135
Figure 4.5	Degradation of black weft of a textile previously owned by the Queen of Madagascar, 1753 (British Museum registration number: Af,SLMisc2105)	139
Figure 4.6	Bathophenanthroline testing of dyed and undyed areas of a strip of Kuba cloth from this PhD project	145

List of figures

Figure 4.7	Factors affecting the stability of iron-tannate dyed organic materials. Scheme adapted from schemes of factors affecting the stability of paper	160
Figure 4.8	Photographs of one-stage samples dyed using a 24 h old dyebath (left) and a fresh dyebath (right)	167
Figure 4.9	Photographs of two-stage samples dyed using the I-T order (left) and the T-I order (right)	168
Figure 4.10	Photographs of samples dyed using an I-T two-stage process at different temperatures	171
Figure 4.11	Photographs of samples dyed using a T-I two-stage process at different temperatures	172
Figure 5.1	Image of samples of each model textile (dyed and undyed) produced for this project	183
Figure 5.2	Undyed and dyed (unaged and aged) cotton samples prepared for qualitative analysis (left) and a sample of dyed wool (pictured on the right with the components required for the preparation) prepared using the newly developed method for quantitative analysis	188
Figure 5.3	BSE SEM micrograph comparing Ac1 (left) and AU (right) at $\times 14$ magnification	194
Figure 5.4	BSE SEM micrographs of undyed (left) and c1 dyed (right) abaca at $\times 50$, $\times 100$, and $\times 650$ magnifications	195
Figure 5.5	BSE SEM micrographs of undyed (left) and c1 dyed (right) cotton at $\times 50$, $\times 100$, and $\times 650$ magnifications	196
Figure 5.6	SEM micrograph and EDX spectrum of unaged Cc3 at $\times 250$ magnification and close up of the iron signal	197
Figure 5.7	BSE SEM micrographs of undyed (left) and p1 dyed (right) silk at $\times 50$, $\times 100$, and $\times 950$ or $\times 650$ magnifications	198
Figure 5.8	SEM micrograph and EDX spectrum of unaged Sp3 at $\times 250$ magnification	199
Figure 5.9	BSE SEM micrograph comparing Wp1 (left) and WU (right) at $\times 10$ magnification	199
Figure 5.10	BSE SEM micrographs of undyed (left) and p1 dyed (right) wool at $\times 50$, $\times 100$, and $\times 650$ magnifications	200
Figure 5.11	SEM micrographs and EDX spectra of a dyed abaca (A), cotton (B), and silk (C and D) fibres in cross-section. The dyed silk fibres in C are from the interior of the yarn while those in D are on the crown of the weave	201
Figure 5.12	SEM micrograph and EDX spectrum of a dyed wool fibre near the crown of the weave	202
Figure 5.13	The iron and copper content of dyed model textiles as determined using XRF	204
Figure 5.14	The effect of dyeings on the surface pH of the model textiles	208
Figure 5.15	The effect of dyeing methodology on the strength and extensibility of the model textiles	210
Figure 5.16	The effect of dye application on the reflectance spectra of the cellulosic (upper) and proteinaceous (lower) model textiles	211
Figure 5.17	The effect of the application of different dye formulations on the molar mass distribution of the cotton substrate	214
Figure 5.18	First derivative EPR spectra of c2 dyed and undyed cotton and abaca	215
Figure 5.19	Comparison between the total iron content (ratio determined using XRF) and the relative Fe(III) ion content (determined using EPR) in the dyed unaged model textiles	217
Figure 5.20	The colour change (E_{00}^*) of the undyed and p1/c1 dyed model textiles during 4 weeks of accelerated ageing (80°C and 58% RH)	221
Figure 5.21	The changing breaking load (N) of the model textiles for 0, 1, 2, 3 and 4 weeks accelerated aged (80°C and 58% RH)	222
Figure 5.22	The changes in iron(III) and radical content in Cc1 (upper) and Sp1 (down) during accelerated ageing (80°C and 58% RH) for 0, 1, 2, and 4 weeks. NB: the unaged Cc1 and Sp1 sample was analysed separately from the aged samples but under the same experimental conditions	225
Figure 5.23	The changing radical content in Ac1 with accelerated ageing (80°C and 58% RH) for 1, 2, and 4 weeks	226

List of figures

Figure 5.24	The changing carbonyl content and theoretical carbonyl content due to oxidation in CU and Cc1 during accelerated ageing (80°C and 58% RH)	228
Figure 5.25	The change in molar mass distribution of cellulose in Cc1 with accelerated ageing (80°C and 58% RH)	229
Figure 5.26	The negative correlation between breaking load and carbonyl content of samples during ageing	229
Figure 5.27	SEM micrographs of 4 week aged (80°C and 58% RH) and unaged Cc1 and Ac1 samples at $\times 100$ or $\times 150$ and $\times 650$ magnifications	232
Figure 5.28	SEM micrographs of 4 week aged (80°C and 58% RH) and unaged Sp1 and Wp1 samples at $\times 100$ or $\times 150$ and $\times 650$ magnifications	233
Figure 5.29	The effect of dye formulation type on the extent of colour change (E_{00}^*) in cotton and silk model textiles during accelerated ageing (70°C and 65% RH)	235
Figure 5.30	The effect of dye type on the breaking load of cotton warp and weft as a % breaking load retained during accelerated ageing (70°C and 65% RH)	239
Figure 5.31	The effect of dye type on the breaking load of silk as a % breaking load retained during accelerated ageing (70°C and 65% RH)	239
Figure 6.1	XRF spectrum of silk hair from a Hina doll in the British Museum's collection	261
Figure 6.2	XRF spectrum of a cellulosic sample from an Apatani rain cape in the British Museum's collection	262
Figure 6.3	Reflectance spectra of iron-tannate dyed cultural heritage compared to aged (80°C and 58% RH) and unaged model textiles	266
Figure 6.4	The correlation between XRF and bathophenanthroline test data of historic iron-tannate dyed and undyed textiles and model iron-tannate dyed and undyed cellulosic textiles	268
Figure 6.5	EPR spectra (upper image) of historic iron-tannate dyed materials and accelerated aged (80°C, 58% RH) Ac1 and Cc1 model textiles with close-up of the radical section of the spectra (lower image)	269
Figure 6.6	The molar mass distribution of two historic cotton samples from the British Museum	270
Figure 6.7	Comparison between the surface pH of some historic iron-tannate dyed materials and aged and unaged cellulosic model textiles. The piu piu/Moari cloak samples were provided by Louise Bacon from the Horniman Museum.	271
Figure 6.8	SEM micrographs at $\times 25$ and $\times 150$ magnifications of undyed and dyed sections of a broken piece of historic New Zealand flax piu piu or Maori cloak from the Horniman Museum (provided by Louise Bacon)	273
Figure 6.9	SEM micrograph at $\times 500$ magnification and EDX spectrum of the surface of a dyed section of piu piu or Maori cloak. Samples provided by Louise Bacon from the Horniman Museum.	275
Figure 6.10	SEM micrograph and XRF spectra of point analyses of the surface of an incised undyed section of piu piu or Maori cloak at $\times 150$ magnification. Samples provided by Louise Bacon from the Horniman Museum.	276
Figure 6.11	SEM micrographs of black coloured samples from a fragile banana fibre belt from the Caroline Islands (19 th Century) and a fragile Apatani rain cape from the British Museum's collection	277
Figure 6.12	SEM micrograph and EDX spectrum of a dyed fibre from a black dyed 19 th Century belt from the Caroline Islands (no registration number)	278
Figure 6.13	SEM micrograph at $\times 500$ magnification and EDX spectrum of a cellulosic fibres from an Apatani rain cape (1957, As11,9)	279
Figure 6.14	SEM micrographs at $\times 25$, $\times 150$, and $\times 500$ magnifications of a piece of fragile iron-tannate dyed cotton from an Akali Sikh turban (As2005,0727.1.o)	280
Figure 6.15	SEM micrograph $\times 500$ magnification and EDX spectra of a section of dyed Akali Sikh turban (As2005,0727.1.o)	281
Figure 6.16	SEM micrographs at $\times 25$, $\times 150$, and $\times 500$ magnifications of unaged undyed raffia (left) and accelerated aged iron-tannate dyed raffia that was produced and supplied by Mark Sandy (Camberwell College of Arts)	283

List of figures

Figure 6.17	SEM micrograph at $\times 500$ magnification and EDX spectrum of an iron-tannate dyed aged raffia sample produced by Mark Sandy (Camberwell College of Arts)	284
Figure 6.18	SEM micrograph $\times 500$ magnification and EDX spectra of an unaged undyed raffia sample provided by Mark Sandy (Camberwell College of Arts)	285
Figure 7.1	The effect of stable and cycling RH ageing on the breaking load of dyed model textiles	306
Figure 7.2	The effect of using cycling and stable RH during accelerated ageing on the extension of the dyed and undyed model textiles	307
Figure 7.3	The change in colour of the undyed model textiles due to accelerated ageing using cycling and stable RH	310
Figure 7.4	The change in colour of the dyed (p1/c1) model textiles due to accelerated ageing using cycling and stable RH	313
Figure 7.5	The variation in surface pH of c1 and p1 dyed model textiles with different accelerated ageing methods	316
Figure 7.6	The changing molar mass distribution of Cc1 during accelerated ageing with stable RH (80°C, 58% RH)	317
Figure 7.7	The changing molar mass distribution of Cc1 during accelerated ageing with cycling RH (80°C, 35-80% RH)	317
Figure 8.1	The treatment of iron gall inked documents during a visit to the Zeeuws Archief, Middelburg, The Netherlands in 2007	333
Figure 8.2	The chemical structures of antioxidants used in this project. A: Tinuvin 292 (Top: Bis(1,2,2,6,6-pentamethyl-4-piperidiny)-sebacate, Bottom: 1-(methyl)-8-(1,2,2,6,6-pentamethyl-4-piperidyl sebacate), B: Irganox 1135, C: Tinuvin 144, D: Irganox 1425, E: phytic acid, F: 1-ethyl-3-methylimidazolium bromide, G: (+)- α -tocopherol, H: Synthetic melanin, I: etidronic acid.	339
Figure 8.3	The chemical structure of calcium carbonate	343
Figure 8.4	The chemical structure of magnesium ethoxide	344
Figure 8.5	Chemical structures of the solvents used in this project. A: ethanol, B: IMS includes a small percentage of methanol (depicted) as well as ethanol, C: tetrachloroethylene, D: cyclosiloxane D5, E: hexane.	346
Figure 8.6	The change in colour of unaged cotton and silk model textiles due to 30 minute immersion in different solvents	350
Figure 9.1	Cotton and silk dyed (c3 and p3) and undyed treated samples prepared for accelerated ageing	359
Figure 9.2	Change in colour (E_{00}^*) of dyed and undyed cotton due to treatment application (for colour changes in Cc3 textiles >1)	368
Figure 9.3	The effect of treatment application on the colour of Sp3 (for $E_{00}^* > 1$)	371
Figure 9.4	The effect of treatment application on the colour of SU (for $E_{00}^* > 0.5$)	371
Figure 9.5	SEM micrographs at $\times 250$ magnification (left) and enlarged sections (right) of untreated and treated Cc3 before accelerated ageing	373
Figure 9.6	SEM micrographs at $\times 250$ magnification (left) and enlarged sections (right) of untreated and treated Sp3 before accelerated ageing	374
Figure 9.7	SEM micrograph and EDX spectrum of the Cc3 sample following immersion in the ME30 treatment solution for 30 minutes	376
Figure 9.8	SEM micrograph and EDX spectrum of surface deposits on Sp3 yarns treated with T292-6/ME30	377
Figure 9.9	The effect of treatment application on the molar mass distribution of the cellulose in Cc3	378
Figure 9.10	The effect of treatment application on the EPR spectrum of Cc3	380
Figure 9.11	Correlation between the pH of treated Cc3 textiles before accelerated ageing (2 weeks at 80°C and 65% RH) and the resulting DP after ageing	386
Figure 9.12	The breaking load (N) and extension (%) of treated and untreated Sp3 model textiles after accelerated ageing	387
Figure 9.13	The first-derivative EPR spectra of treated aged Cc3 samples	389
Figure 9.14	The change in colour of a selection of treated Cc3 (upper) and CU (lower) samples following 2 and 4 weeks of accelerated ageing (80°C and 65% RH)	393

List of figures

Figure 9.15	The correlation between initial pH and the change in overall colour of treated Cc3 during accelerated ageing (80°C and 65% RH)	394
Figure 9.16	The change in colour of a selection of treated Sp3 (upper) and SU (lower) samples following 4 weeks of accelerated ageing (80°C and 65% RH)	398
Figure 9.17	The carbonyl content of unaged (0) and two week aged (2) treated and untreated Cc3 textiles determined using GPC-MALLS in two batches one of which is denoted by 'a'	401
Figure 9.18	The effect of treatments on the molar mass distribution of cellulose in Cc3 after two weeks of ageing (80°C and 65% RH)	403
Figure 9.19	Correlation between overall change in colour (E_{00}^*) with overall change in carbonyl content in treated samples with ageing	405
Figure 10.1	SEM micrographs of untreated pre-aged dyed (c1) cotton and pre-aged dyed (c1) cotton that has been immersed for 30 minutes in deionised water, cyclosiloxane D5, or IMS	413
Figure 10.2	SEM micrographs of untreated pre-aged dyed (c1) abaca and pre-aged dyed (c1) abaca that has been immersed for 30 minutes in deionised water, cyclosiloxane D5, or IMS	413
Figure 10.3	Figure 10.3. SEM micrograph and EDX spectrum of the surface deposits on un-immersed pre-aged dyed cotton. In spectra 1 and 3 a point and an area, respectively, with surface deposits are analysed. In spectrum 2 an area without surface deposits is analysed	414
Figure 10.4	Figure 10.4. SEM micrograph and EDX spectrum of the surface deposits on un-immersed pre-aged dyed abaca. Spectra 1 and 4 are of phytoliths (silicon plant bodies) that are naturally present in abaca	415
Figure 10.5	The effect of solvent immersion on the molar mass distribution of fragile Cc1 (4 weeks aged at 80°C and 35-80% RH)	418
Figure 10.6	Colour change in pre-aged model textiles due to treatment application	425
Figure 10.7	The change in lightness of samples due to treatment application	426
Figure 10.8	The change in redness (+ a^*) and greenness (- a^*) of samples due to treatment application	428
Figure 10.9	The change in blueness (- b^*) and yellowness (+ b^*) of samples due to treatment application	428
Figure 10.10	The effect of the treatments on the discolouration of pre-aged model textile samples during accelerated ageing (1 week at 70°C and 65% RH)	431
Figure 10.11	Correlation between surface pH of pre-aged samples and overall colour change (E_{00}^*) after further accelerated ageing (1 week at 70°C and 65% RH) for dyed textiles	433
Figure 10.12	The change in lightness of the pre-aged treated samples due to the treatment on accelerated ageing	435
Figure 10.13	The change in redness (+ a^*) and greenness (- a^*) of treated and untreated pre-aged samples following accelerated ageing	435
Figure 10.14	Correlation between surface pH of pre-aged samples and change in redness (+ a) after further accelerated ageing (1 week at 70°C and 65% RH) for dyed textiles	436
Figure 10.15	The change in blueness (- b^*) and yellowness (+ b^*) of treated and untreated pre-aged samples following accelerated ageing	437
Figure 10.16	The effect of treatments on the breaking load of the model textiles after accelerated ageing	438

LIST OF EQUATIONS

Equation 2.1	$\Delta E_{00} = \sqrt{\left(\left(\frac{\Delta L'}{k_L S_L}\right)^2 + \left(\frac{\Delta C'}{k_C S_C}\right)^2 + \left(\frac{\Delta H'}{k_H S_H}\right)^2 + R_T \left(\frac{\Delta C'}{k_C S_C}\right) \left(\frac{\Delta H'}{k_H S_H}\right)\right)}$	34
Equation 2.2	$E = g_e \mu_B B_0$	37
Equation 2.3	$E = h = g_e \mu_B B_0$	37
Equation 2.4	$\frac{N_u}{N_l} = e^{\frac{-\Delta E}{kT}} = e^{\frac{-g_e \mu_B B_0}{kT}}$	38
Equation 2.5	$M_n = \frac{\sum_i M_i N_i}{\sum_i N_i}$	41
Equation 2.6	$M_w = \frac{\sum_i M_i^2 N_i}{\sum_i M_i N_i}$	41
Equation 2.7	$PDI = \frac{M_w}{M_n}$	41
Equation 2.8	$pH = -\log_{10}(a_{H^+})$	43
Equation 2.9	$K_w = \frac{a_{H^+} \times a_{OH^-}}{a_{H_2O}}$	43
Equation 2.10	$pK_w = pH + pOH$	44
Equation 2.11	$E_{measure} = E_{ref} - 2.303 \frac{RT}{nF} \times pH$	45
Equation 2.12	$\frac{t}{t_0} = \frac{y}{y_0}$	50
Equation 2.13	$DP^{0.85} = 1.1 \cdot [y]$	50
Equation 2.14	$\text{Stress (Nm}^{-2}\text{)} = \frac{\text{Force (N)}}{\text{Cross-sectional area (m}^2\text{)}}$	52
Equation 2.15	$\text{Strain} = \frac{\text{Elongation (mm)}}{\text{Initial length (mm)}}$	52
Equation 2.16	$\text{Extension (\%)} = \text{Strain} \times 100\%$	52
Equation 2.17	$\text{Strain} = \frac{\text{Stress}}{\text{Young's modulus}}$	52
Equation 2.18	$\text{Tenacity (Ntex}^{-1}\text{)} = \frac{\text{Force applied at break (N)}}{\text{Linear density (tex)}}$	53
Equation 5.1	$\text{Ratio} = \left(\frac{A_e}{A_c}\right) \times 1000$	183
Equation 5.2	$\text{Relative integral of y} = \frac{\text{Peak area of y}}{\text{Peak area of x}} \times \frac{\text{Mass of x}}{\text{Mass of y}}$	189
Equation 5.3	$REG = 1000 (1/Mn)$	191
Equation 5.4	$\text{Oxidised groups} = \text{Overall carbonyl content} - REG$	191
Equation 7.1	$S = \left(\frac{DP^o}{DP}\right) - 1$	290

List of figures

Equation 7.2	$k = Ae^{-\frac{E_a}{RT}}$	291
Equation 7.3	$\ln k = \ln A - \frac{E_a}{RT}$	292
Equation 8.1	$\text{I}^\cdot + \text{HO}^\cdot \rightarrow \text{I}^\cdot + \text{HO}^\cdot$	327
Equation 8.2	$\text{I}^\cdot + \text{I}^\cdot \rightarrow \text{I}_2^\cdot$	327
Equation 8.3	$2\text{I}^\cdot + 2\text{H}^+ + \text{H}_2\text{O}_2 \rightarrow \text{I}_2 + 2\text{H}_2\text{O}$	327
Equation 8.4	$\text{I}_2 + 2\text{H}_2\text{O}_2 \rightarrow 2\text{I}^\cdot + 2\text{H}^+ + \text{O}_2$	327
Equation 8.5	$2\text{HO}^\cdot + \text{I}_2 + \text{H}_2\text{O}_2 \rightarrow 2\text{I}^\cdot + 2\text{H}_2\text{O} + \text{O}_2$	327
Equation 9.1	$\frac{t}{t_0} = \frac{y}{y_0}$	362
Equation 9.2	$\text{DP}^{0.85} = 1.1 \cdot [\text{y}]$	362

List of schemes
LIST OF SCHEMES

Scheme 2.1 The self-ionisation of water into hydroxide and hydronium ions.	43
Scheme 3.1 Oxidation of cystine residues to cysteic acid	99
Scheme 3.2 Disulphide cross-link formation	100
Scheme 3.3 A mechanism of photoyellowing of wool by the formation of aldehyde groups from cystine	101
Scheme 4.1 Formation of iron(III)-gallate and iron(III)-pyrogallol complexes from iron(II) ions and gallic acid as proposed by Krekel	121
Scheme 4.2 The formation of semi-quinones and quinones from phenols and an excess of ferric ions	122
Scheme 4.3 Oxidation of iron(II) to iron(III) by oxygen	127
Scheme 4.4 Charge-transfer in an iron(III) pyrogallol complex	130
Scheme 4.5 Acid-catalysed degradation of iron(III) pyrogallol	132
Scheme 4.6 Proposed autoxidation mechanism	150
Scheme 4.7 Possible initiation mechanism for autoxidation in hydrocarbons	151
Scheme 4.8 Production of superoxide by ferrous ion and oxygen and subsequent oxidation of an organic substrate	152
Scheme 4.9 Iron-catalysed decomposition of hydrogen peroxide	152
Scheme 4.10 Proposed mechanism for ferric iron catalysed degradation of hemicellulose	153
Scheme 4.11 Degradation of cellulose by metal ions via a Lewis acid mechanism	153
Scheme 4.12 Acid hydrolysis of oxidised cellulose	156
Scheme 4.13 Acid hydrolysis of peptide bond in protein based on the mechanism of acid hydrolysis of esters	156
Scheme 4.14 The mechanism for β -alkoxy-elimination of cellulose in an alkaline environment	157
Scheme 4.15 Alkaline hydrolysis of peptide bonds	158

Abstract
ABSTRACT

Helen Louise Wilson
The University of Manchester
Doctor of Philosophy
Investigation into non-aqueous remedial conservation treatments for iron-tannate dyed organic materials
August 2012

Iron-tannate dyes have been used for thousands of years and on many continents to colour materials that are now part of our cultural heritage shades of black, grey, or brown. Cellulosic and proteinaceous yarns and woven textiles have been dyed with iron-tannate dyes to form objects or components of objects for domestic and ceremonial use. Unfortunately, the longevity and useful lifetime of iron-tannate dyed objects is threatened by the dye itself which accelerates the degradation of organic materials through metal-catalysed oxidation and acid-catalysed hydrolysis. The accelerated degradation causes weakening, discolouration, and embrittlement of the organic materials at a faster rate than undyed equivalents and if left unimpeded, weakens the objects to the point that they are no longer able to be exhibited without damage. In some cases the degradation is so great that the dyed areas of the objects have crumbled to dust. At present there is no suitable chemical stabilisation method available with which to inhibit this degradation. An aqueous treatment is available for successfully stabilising paper containing iron gall ink; iron gall ink is chemically similar to iron-tannate dye. However, the aqueous nature of this treatment makes it unsuitable for weakened fibres, water soluble components, and water sensitive materials which may be part of a composite material containing iron-tannate dye. Non-aqueous treatments are therefore urgently needed in order to preserve our iron-tannate dyed cultural heritage for future generations.

In this project a range of non-aqueous antioxidants and a non-aqueous deacidifier (described in Chapter 8) were tested alongside existing aqueous treatment in order to establish their ability to slow down the degradation of a range of model iron-tannate dyed textiles (Chapters 9 and 10). Model textiles were developed as part of the project (Chapters 3-5) to be substitutes for historic materials in these stabilisation studies. Validation of the model textiles for this purpose (Chapter 6) involved the comparison of the model textiles with selected historic iron-tannate dyed objects within the British Museum's collection (Chapter 6). The historic objects and the properties of the model textiles before and after accelerated ageing (Chapters 5 and 6) and before and after treatment application (Chapters 9 and 10) have been characterised using a variety of analytical techniques (Chapter 2). In order to determine which accelerated ageing conditions were the most suitable for this project various combinations of elevated temperature and either cycling or stable relative humidity were tested for their ability to produce noticeable changes in the properties of the dyed model textiles within four weeks of ageing (Chapter 7).

This project is an AHRC/EPSRC funded Science and Heritage Programme PhD in which the British Museum has been a collaborative institution. Among other wider dissemination methods, research from this project has been presented to the public on numerous occasions at gallery tours and Science Day events at the British Museum.

Declaration
DECLARATION

No portion of the work referred to in this thesis has been submitted in support of an application for another degree or qualification of this or any other university or other institute of learning.

COPYRIGHT STATEMENT

- i. The author of this thesis (including any appendices and/or schedules to this thesis) owns certain copyright or related rights in it (the “Copyright”) and she has given The University of Manchester certain rights to use such Copyright, including for administrative purposes.
- ii. Copies of this thesis, either in full or in extracts and whether in hard or electronic copy, may be made **only** in accordance with the Copyright, Designs and Patents Act 1988 (as amended) and regulations issued under it or, where appropriate, in accordance with licensing agreements which the University has from time to time. This page must form part of any such copies made.
- iii. The ownership of certain Copyright, patents, designs, trademarks and other intellectual property (the “Intellectual Property”) and any reproductions of copyright works in the thesis, for example graphs and tables (“Reproductions”), which may be described in this thesis, may not be owned by the author and may be owned by third parties. Such Intellectual Property and Reproductions cannot and must not be made available for use without the prior written permission of the owner(s) of the relevant Intellectual Property and/or Reproductions.
- iv. Further information on the conditions under which disclosure, publication and commercialisation of this thesis, the Copyright and any Intellectual Property and/or Reproductions described in it may take place is available in the University IP Policy (see <http://www.campus.manchester.ac.uk/medialibrary/policies/intellectualproperty.pdf>), in any relevant Thesis restriction declarations deposited in the University Library, The University Library’s regulations (see <http://www.manchester.ac.uk/library/aboutus/regulations>) and in The University’s policy on presentation of Theses.

Chemistry Central Journal

Helen Wilson, Chris Carr, Marei Hacke. (2012). Production and validation of model iron-tannate dyed textiles for use as historic textile substitutes in stabilisation treatment studies. *Chemistry Central Journal*, 6(44).

ICOM-CC (International Council of Museums – Committee for Conservation)

Wilson H, Carr C, Hacke M, Cruickshank P, Daniels V, Stacey R, Rigout M: Investigation of non-aqueous remedial treatments for iron-tannate dyed textiles. In *ICOM-CC 16th Triennial Conference, 19-23 September 2011, Lisbon*. pp. 1-9. Lisbon, Portugal: ICOM-CC; 2011:1-9.

ICON (Institute of Conservation)

Gill L, Wilson H, Mackenzie B: Group news and graduate voice: CF10's winning student posters [Poster entitled 'Developing chemically unstable model textiles for treatment evaluation' by Helen Wilson]. *ICON News* 2010, 28:22-25. This poster was awarded the prize for best poster by the judges at the Icon CF10 – Conservation in Focus conference, Cardiff, 24th -26th March 2010.

IIC (International Institute for Conservation of Historic and Artistic Works)

Wilson H: Investigation into iron diffusion into wool, silk, cotton and abaca textiles using SEM-EDX [Poster]. In *IIC 2010 Congress - Conservation and the Eastern Mediterranean, 20th - 23rd September 2010; Istanbul, Turkey*. IIC; 2010. Accessible online at: <http://www.iiconservation.org/node/2769> (accessed 03/07/12)

Textile Research Journal

Wilson H, Carr C, Hacke M, Rigout M, Rigby S, Fisher K, Potthast A, Henniges U: Evidence of oxidation and acid hydrolysis in the degradation of iron-tannate dyed organic materials. *Textile Research Journal*. (In Preparation, 2012)

Studies in Conservation

Wilson H, Cruickshank P, Carr C, Hacke M, Daniels V, Rigout M: Investigation of non-aqueous remedial treatments for iron-tannate dyed silk textiles. *Studies in Conservation*. (In Preparation, 2012)

WEBPAGES

http://www.ucl.ac.uk/silva/heritagescience/Research_Projects/projects/CRS/HWilson

http://www.britishmuseum.org/research/research_projects/black-dyed_organic_materials.aspx

ACKNOWLEDGEMENTS

I would like to thank my supervisors, Prof. Chris Carr and Dr. Muriel Rigout from the University of Manchester and Dr Marei Hacke, Dr Vincent Daniels, Pippa Cruickshank, and Dr Rebecca Stacey who supervised during Dr Hacke's maternity leave, for their great support and encouragement and continued interest throughout this project.

Thanks go to AHRC, EPSRC, the British Museum, the University of Manchester, and the Brommelle Memorial Fund for their financial and other support throughout the project. Thanks also to the Science and Heritage Programme and more specifically, to Prof. May Cassar and Debbie Williams for the organisation and coordination of this initiative.

This project has involved significant collaboration and consequently I'd like to thank the following people for their assistance at various points in the project: Phil Cohen for his dyeing expertise, Adrian Handley for his tensile testing assistance, Dr Huw Owens for his colour knowledge, Dr Stephen Rigby and Dr Karl Fisher for the EPR analysis from the University of Manchester; Dr David Pegg for the use of and assistance with the environmental chamber at the National Gallery, London; Mark Sandy and Mike Yianni for the use of and assistance with the environmental chambers at Camberwell College of Arts, London; Matija Strli for the training and use of the viscometry equipment at UCL's Centre for Sustainable Heritage, London; and Dr. Ute Henniges and Prof. Antje Potthast for the training and use of the GPC-MALLS equipment at BOKU, Vienna and subsequent editorial support. Additionally I'd like to thank: the staff at the Department of Conservation and Scientific Research at the British Museum for making me feel welcome and answering my queries; Dr Duncan Hook for training me in the use of the XRF equipment and Nigel Meeks for training me in the use of the SEM-EDX equipment; the conservators and curators who have helped in the project including Helen Wolfe for facilitating access to the collections; and Dr Catherine Higgitt and Dr JD Hill for their assistance in the running of the PhD at the British Museum.

Finally I'd like to extend huge thanks to my family and friends, particularly my fiancé, Simon Curtis, and parents, Richard and Liz Wilson, and brother, Chris Wilson. Their constant support and encouragement and frequent chats have enabled me to maintain a good balance between my work life and home life and have thus enabled me to work to the best of my ability and with constant enthusiasm for this research area.

DEDICATION

I dedicate this thesis to my parents and grandparents. Particularly to my parents for their endless support and to my grandfather, Peter Utley, who recognised the value of education and kindly gave me the financial means to extend the term of this PhD, enabling me to produce a thesis of which I am proud.

PREFACE

Prior to starting this PhD project in 2008 Helen Wilson graduated from the University of Oxford with a Master's degree in Chemistry (MChem) (2007) and completed a one year ICON HLF Conservation Science Internship with Dr Nicholas Eastaugh at the Pigmentum Project, London (2007-2008). The fourth year of the MChem degree involved a self-organised conservation science project in collaboration with paper conservator Ally Greathead at the Ashmolean Museum, Oxford. The resulting dissertation was entitled 'Analysis of the current research into the chemistry of Iron Gall Ink and its implications for Paper Conservation'.

List of abbreviations
LIST OF ABBREVIATIONS

Institutions

BOKU	University of Natural Resources and Life Sciences, Vienna
ICOM-CC	International Council of Museums – Committee for Conservation
ICON	Institute of Conservation
IIC	International Institute for Conservation of Historic and Artistic Works

Analytical techniques

EPR	Electron Paramagnetic Resonance
GPC-MALLS	Gel Permeation Chromatography with Multi Angle Laser Light Scattering detector
SEM-EDX	Scanning Electron Microscopy with Energy Dispersive X-ray analysis
XRF	X-ray Fluorescence analysis

Model textiles

Dye formulation ^a		Model textile			
		Cotton	Abaca	Wool	Silk
Undyed	U	CU	AU	WU	SU
Dyes for cellulosic model textiles	c1	Cc1	Ac1		
	c2	Cc2	Ac2		
	c3	Cc3			
Dyes for proteinaceous model textiles	p1			Wp1	Sp1
	p2			Wp2	Sp2
	p3				Sp3

a. See Table 5.1 for detailed information on the dye formulations

Accelerated aged model textiles

0s, 1s, 2s, 3s, and 4s, e.g. CU-1s	Model textiles accelerated aged using 80°C and 58% RH (stable RH) for 0 (i.e. unaged), 1, 2, 3, and 4 weeks, respectively, e.g. 1 week aged undyed cotton.
0c, 1c, 2c, 3c, and 4c, e.g. Sp1-3c	Model textiles accelerated aged using 80°C and 35-80% RH every 3 hours (cycling RH) for 0, 1, 2, 3, and 4 weeks, respectively, e.g. 3 week aged dye formulation 1 dyed silk.

Treatment chemicals and solvents

AT	(+)-alpha-Tocopherol
EBR	1-ethyl-3-methylimidazolium bromide
I1135	Irganox 1135
I1425	Irganox 1425
T144	Tinuvin 144
T292	Tinuvin 292
PA	Phytic acid
EA	Etidronic acid
M	Melaneze
PA (MP)	Phytic acid used to produce magnesium phytate
MC (MP)	Magnesium carbonate used to produce magnesium phytate
CB	Calcium bicarbonate
ME	Magnesium ethoxide
EtOH	Ethanol (100%)
IMS	Industrial methylated spirits
T	Tetrachloroethylene
H	n-Hexane
GE	Cyclosiloxane D5 (GreenEarth®)

List of abbreviations

Treatment codes used in Chapter 9

Treatment code	Chemical mass ^b	Concentration, M		Treatment code	Chemical mass ^b	Concentration, M	
		Dyed ^c	Undyed ^c			Dyed ^c	Undyed ^c
AT2	2	0.00052	0.00047	T144-2	2	0.00033	0.00029
AT3	3	0.00078	0.0007	T144-3	3	0.00049	0.00044
AT6	6	0.00155	0.00141	T144-6	6	0.00098	0.00088
AT6/ME30 ^a	6	0.00157	0.00141	T144-6/ME30	6	0.00099	0.00088
AT200	200	0.05146	0.05146	T144-450	450	0.07282	0.07282
EA0.4	0.4	0.00019	0.00017	T292-2	2	0.00025	0.00023
EA0.4/ME30	0.4	0.00019	0.00017	T292-3	3	0.00038	0.00034
EA2	2	0.00097	0.00087	T292-6	6	0.00077	0.00069
EA4	4	0.00195	0.00174	T292-6/ME30	6	0.00077	0.00069
EA4/ME30	4	0.00195	0.00174	T292-260	260	0.03277	0.03277
EBR6	6	0.00335	0.003	PA (MP5/2CB5)	5	0.00098	0.00044
EBR30	30	0.01675	0.015	PA (MP15/2CB15)	15	0.00244	0.00218
EBR60	60	0.0335	0.03001	PA (MP30/2CB30)	30	0.00487	0.00436
I1135-2	2	0.00057	0.00051	MC (MP5/2CB5)	0.82	0.00108	0.00107
I1135-3	3	0.00086	0.00077	MC (MP15/2CB15)	4.66	0.00617	0.00562
I1135-6	6	0.00172	0.00154	MC (MP30/2CB30)	9.37	0.01241	0.01125
I1135-43	43	0.01229	0.01229	PA3	3	0.00047	0.00044
I1135-43/ME30	43	0.01229	0.01229	PA15	15	0.00243	0.00219
ME6	6	0.00558	0.00502	PA30	30	0.00486	0.00438
ME30	30	0.02793	0.02496	PA30IMS/ME300	30	0.00487	0.00436
ME60	60	0.05603	0.05				

a. A separate application of ME30 was made to a treated sample;

b. Mass of chemical in 300 ml of solvent as approximate % textile weight;

c. In some cases, concentrations for undyed and dyed textiles vary because of differing textile masses; the mass of chemical per mass of textile is equal. In other cases the concentration is independent of textile mass.

Treatment codes used in Chapter 10

Set (Treatment code)	Chemical	Chemical concentration (M)	Mass of chemical as % of textile mass					Mean	SD
			CU and SU	Cc2 and Sp2	Cc3 and Sp3	AU and WU	Ac2 and Wp2		
A (untreated)	None								
B (MP/2CB)	MC (MP)	0.012	10	10	10	6	5	8	2
	PA (MP)	0.002	13	13	13	8	6	10	3
	CB ^a	0.037	63	59	59	36	30	49	13
C (EBR/T292-3)	EBR	0.033	66	62	62	38	31	52	14
	T292	0.033	298	279	279	173	142	234	64
D (EBRT292-3)	EBR	0.033	66	62	62	38	31	52	14
	T292	0.033	298	279	279	173	142	234	64
E (T292-3)	T292	0.033	298	279	279	173	142	234	64
F (T292-15)	T292	0.163	1483	1387	1387	860	705	1164	318

a. Estimated value. See Note 'b' for Table 10.5 for more details.

1 INTRODUCTION

1.1 The importance of cultural heritage

Changing perceptions about the importance of the various aspects of our ancestral past has resulted in a gradual development and broadening of the definition of ‘cultural heritage’. Essentially, cultural heritage is the legacy from our past, and it increases and adapts as time progresses. Cultural heritage can be organised into three groups: tangible, intangible and natural cultural heritage. Tangible cultural heritage includes moveable heritage such as the objects present in museums, immovable heritage such as monuments, and underwater heritage such as shipwrecks. Intangible cultural heritage includes traditions such as the knowledge and skills needed to produce traditional crafts, and natural cultural heritage includes natural sites that have cultural aspects such as cultural landscapes (Jokilehto 2005; UNESCO 2007).

Cultural heritage, and consequently its preservation, is important for many reasons:

1. Economics - The arts and heritage sector accounts for 10% of the UK’s GDP and over £20 billion is added to the UK GDP by heritage tourism (more than the car industry or advertising). In 2007/2008, every £1 spent in the heritage sector attracted £2 from other sources (Arts Council England 2010);

2. Community and quality of life - Cultural heritage improves quality of life, regenerates local economies and encourages local enterprises, making regenerated areas more attractive to work and live in (Arts Council England 2010). It can enable the development of the intellectual, spiritual, emotional and moral aspects of people and consequently increases the range of options open to all (UNESCO 2001);

3. Identity - Cultural heritage improves understanding of our own individual and cultural past, forging a sense of belonging and identity in relation to our own culture. This understanding is an essential part of our liberty and one which is viewed by UNESCO as a human right. It also enables better understanding of other cultures and consequently aids inter-cultural respect and dialogue (Caple 2000; UNESCO 2001; UNESCO 2007);

4. Creativity - Inspiration can be drawn from our own and other cultural traditions resulting in improved ideas for creative industries (Arts Council England 2010);

5. Understanding of the world to improve the future - Understanding of the world, both past and present can be improved through the remembrance and study of cultural

1.2 The Science and Heritage Programme

heritage. This understanding can help control the present and influence the future (Caple 2000).

1.2 The Science and Heritage Programme

This 5 year programme was established in 2006 following recommendations from the House of Lords. Its aim was to improve collaboration between the science and heritage sectors, developing capacity for research and supporting new researchers. The funding provided by the Arts & Humanities Research Council (AHRC) and the Engineering & Physical Sciences Research Council (EPSRC) was used to establish 7 Interdisciplinary Grants, 8 Post Doctoral Fellowships, 13 Research Clusters, and 10 Collaborative Research Studentships (of which this PhD project is one) that involved collaboration between science and heritage sectors (UCL 2012).

1.3 The British Museum

This PhD project is in collaboration with the Conservation and Scientific Research Department of the British Museum. The British Museum is world-renowned for its extensive collection of objects from around the world and its high-quality research. The Museum was the first national public museum that was established in 1753 by an Act of Parliament following Sir Hans Sloane's bequest of his collection (over 71,000 objects) to King George II for the nation on his death (Trustees of the British Museum 2012a). Subsequent acquisitions have resulted in a growing collection, an increasing proportion of which (currently 2 million objects) is searchable via the British Museum's online collection database. The Museum has ten curatorial and research departments of which the Conservation and Scientific Research Department with which this project is affiliated is one. This department plays a valuable role in the preservation of the collection by providing scientific results that affect the way the objects are stored, conserved, and displayed. It also contributes to the fulfilment of the British Museum's legal responsibility (according to the 1996 Treasure Act) to process treasure finds from England and Wales of which around 50 cases occur per year (Trustees of the British Museum 2012b).

1.4 Project background

For hundreds of years it has been known that iron-tannate dyes have an adverse effect on the stability of the organic materials they colour; its usage has been highly regulated and in some cases forbidden on high quality goods at various points in history for this reason (Hofenk de Graaff 2002). Through catalytically-active iron ions and the high acidity of the dyes, metal-catalysed oxidation and acid hydrolysis can occur in iron-tannate dyed

1.5 Research aims

substrates at an accelerated rate compared to undyed equivalents. For iron-tannate dye containing objects that are now part of our cultural heritage such as those at the British Museum, their longevity is threatened by the dye and the fact that at present there is no suitable treatment with which to inhibit this accelerated degradation. Significant research into the degradation behind iron gall inks (Kolar and Strlic 2006) which are chemically similar to iron-tannate dyes (Barker 2002; Hofenk de Graaff 2002) has resulted in the development of a now widely accepted aqueous stabilisation treatment for use on iron gall inked paper (Neevel 2002). The relatively few studies into the efficacy of this treatment at stabilising iron-tannate dyed textile materials suggest that it could be a useful stabilisation treatment (Daniels 1999a; Sato, Okubayashi and Sato 2011). However, the aqueous nature of the treatment prevents its usage on iron-tannate dyed materials containing water-sensitive components such as degraded organic material, water sensitive dyes, or metals (Daniels 1999b). Research into non-aqueous treatments is therefore urgently needed to bring the conservation community closer to a suitable method of preservation of iron-tannate dyed cultural heritage.

1.5 Research aims

The aims of this research are three-fold:

1. To develop a range of model iron-tannate dyed textiles that are valid substitutes for iron-tannate dyed historic material in stabilisation treatment studies and that are relevant to the iron-tannate dyed materials in the British Museum's collection;
2. To determine an accelerated ageing method that causes detectable changes in the tensile properties of the model iron-tannate dyed textiles within four weeks of exposure;
3. To identify a variety of non-aqueous antioxidants and deacidifiers for use on the model textiles and to determine the efficacy of the developed treatments involving these chemicals, at stabilising the model textiles. By comparing with the already established aqueous treatment the efficacy of this treatment on the model textiles can also be determined.

1.6 Methodology and thesis structure

To achieve these aims model iron-tannate dyed textiles have been developed (Chapters 3-5) and comparison of the properties of these materials has been made to a range of historic iron-tannate dyed materials including some from the British Museum's collection (Chapter 6). The analytical techniques used throughout this project have been reviewed in Chapter 2 and an accelerated ageing method has been chosen for use in the treatment tests following the testing of a variety of accelerated ageing conditions on the model textiles (Chapter 7).

1.6 Methodology and thesis structure

The treatments that are investigated in this research are detailed in Chapter 8 and the efficacy of the treatments on unaged and aged model iron-tannate dyed textiles is assessed in Chapters 9 and 10, respectively. Conclusions of this research are summarised in Chapter 11 along with recommendations for future work. Peer-reviewed papers and posters from this project are presented in Appendices 1-4.

2 ANALYTICAL TECHNIQUES

2.1 μ -X-ray Fluorescence (μ -XRF)

XRF is a qualitative and to a certain extent, a quantitative surface technique. It enables identification of the elements present in a small sample area and if the sample surface is homogeneous, with commercially available quantitation standards, elemental concentration can be calculated to within 2-10% error (Strlic, Kolar, Selih, Budnar, Simcic, Kump, Necemer, Marinsek and Pihlar 2006). Since the samples used in this research were organic materials with inhomogeneous, rough surfaces which lack commercially available quantitation standards, the accuracy of the quantification provided by the spectrometer is uncertain for this research. A study into the error involved in the determination of iron content in iron gall ink on manuscripts has been published and it was found that 78% of the total uncertainty was due to the inhomogeneous surface structure of the paper (Virro, Mellikov, Volobujeva, Sammelselg, Asari, Paama, Jürgens and Leito 2008). Nevertheless, calculation of the ratio between the areas of the Compton peak¹ and the elemental peak in question can be used for semi-quantitative comparison. This method was used in this thesis for comparison of iron content in dyed and undyed samples.

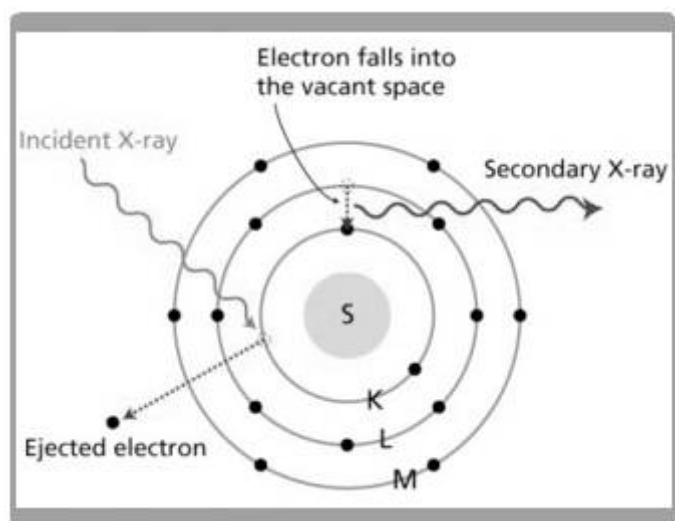
2.1.1 Theory

Figure 2.1 Electron and radiation processes in the XRF technique (Oxford Instruments plc 2008)

¹ The Compton peak arises from primary X-ray photons which are inelastically scattered due to interaction with an electron.

2.1 μ -XRF

When an atom is irradiated with primary X-ray photons, an electron from an inner (low energy) orbital such as a K shell may be ejected (Figure 2.1). The energy needed to eject the electron must be less than that of the incident X-ray photon. The energy that is not absorbed is scattered and is recorded in the XRF spectrum as the Compton peak. Photons that are elastically scattered through the sample (i.e. are not absorbed) are recorded in the XRF spectrum as a continuous spectrum (background spectrum) with a peak corresponding to the X-ray source (e.g. Mo or Rh). The vacancy created in the sample by the ejected electron is filled by an electron from a higher energy level such as the L shell. On moving to this lower energy level, the electron emits an X-ray photon (secondary X-ray) with energy equal to the difference between the higher and lower energy levels. Differences between specific orbitals are characteristic of the atom involved and therefore enable the identification of the elements present in a sample (Atkins and de Paula 2002a). By quantifying the number of photons released by a particular element for a set time, a count rate (intensity) can be determined. The intensity gives an approximate indication of concentration of the elements present in the sample area (Oxford Instruments plc 2008).

2.1.2 *Equipment*

An XRF spectrometer contains an X-ray tube, a detector (e.g. Si(Li) detector) to convert received X-ray photons into a charge, an analogue to digital convertor to convert the charge from the detector into pulses, and a multi-channel analyser to count the pulses and enable a spectrum of counts against energy to be displayed on a computer screen. In the X-ray tube electrons are produced by heating a tungsten filament and are accelerated through a large voltage towards the target (e.g. Mo or Rh). Incident X-ray photons are emitted when the high speed electrons collide with the target and are directed towards the sample through a window of light material such as aluminium. Depending on the detector type (energy-dispersive (EDX) or wavelength-dispersive (WDX)), the X-ray photons are sorted by either their energy or wavelength, respectively. The signal-to-noise ratio of the EDX (Si(Li) detector) detectors is increased through cooling e.g. by liquid nitrogen or Peltier cooling. Unlike WDX, EDX does not require a crystal and detects all wavelengths of radiation simultaneously, resulting in smaller equipment and rapid analysis. However EDX has poorer resolution of low energy radiation (wavelengths $> 0.8 \text{ \AA}$) than WDX, can detect only elements equal to or greater than $Z=11$ (Na) rather than $Z=4$ (Be), and has lower sensitivity to elements producing a weak signal if elements producing a strong signal are present (Whiston 1987).

2.2 SEM-EDX analysis

Portable handheld XRF devices are now available which enable an in situ elemental analysis of objects (Bruker AXS 2012). For historic textiles the handheld XRF devices are suitable for qualitative elemental analysis only but are useful when sampling or the movement of either the object or XRF spectrometer to the other is not possible (Luxford, Thickett and Wyeth 2011).

2.1.3 Usage in cultural heritage

XRF is particularly useful for analysis of delicate, valuable objects such as those within the British Museum as it is a non-contact, non-destructive technique (when using a low energy primary X-ray source). Varying types of XRF have been used to research the metal content of iron gall inks in historic documents (Strlic, Kolar, Selih, Budnar, Simcic, Kump, Necemer, Marinsek and Pihlar 2006; BrukerAXS 2009; Hahn 2010; Bicchieri, Monti, Piantanida, Pinzari, Iannuccelli, Sotgiu and Tireni 2012; Bruker Nano GmbH 2012). The composition of textiles (Findlay 1989; Green and Daniels 1990; Katayama, Ide-Ektessabi, Funahashi and Nishimura 2008; Luxford, Thickett and Wyeth 2011), metal threads (Muros, Warmlander, Scott and Theile 2006), iron-tannate dyed materials (Wills and Hacke 2007) and pigments (Skelton and Lee-Whitman 1986) have also been analysed using XRF. XRF is frequently used in combination with SEM (Section 2.2).

2.2 Scanning Electron Microscopy with Energy Dispersive X-ray (SEM-EDX) analysis

Scanning Electron Microscopy (SEM) is a powerful analytical technique with great versatility. High and variable magnification enables specimen surfaces to be carefully examined and imaged. In combination with EDX, knowledge of the type and location of elements in a specific area or spot of the specimen can be determined.

2.2.1 Theory and equipment

A beam of electrons is produced using an electron gun (Figure 2.2). There are several kinds of electron gun including a thermionic electron gun in which a cathode of tungsten is heated to temperatures of approximately 2800K. The electron beam is accelerated by application of a 1-30kV positive voltage on the perforated anode which allows the electron beam through. The current of the electron beam can be altered and the beam focussed through the use of a negatively charged Wehnelt electrode placed between the anode and cathode. The beam then passes through a condenser lens, objective lens aperture, scanning coil, and objective lens before reaching the sample. The lenses and aperture focus the beam

2.2 SEM-EDX analysis

while the scanning coil moves the beam across the sample surface. Typically the entire system is operated under vacuum conditions.

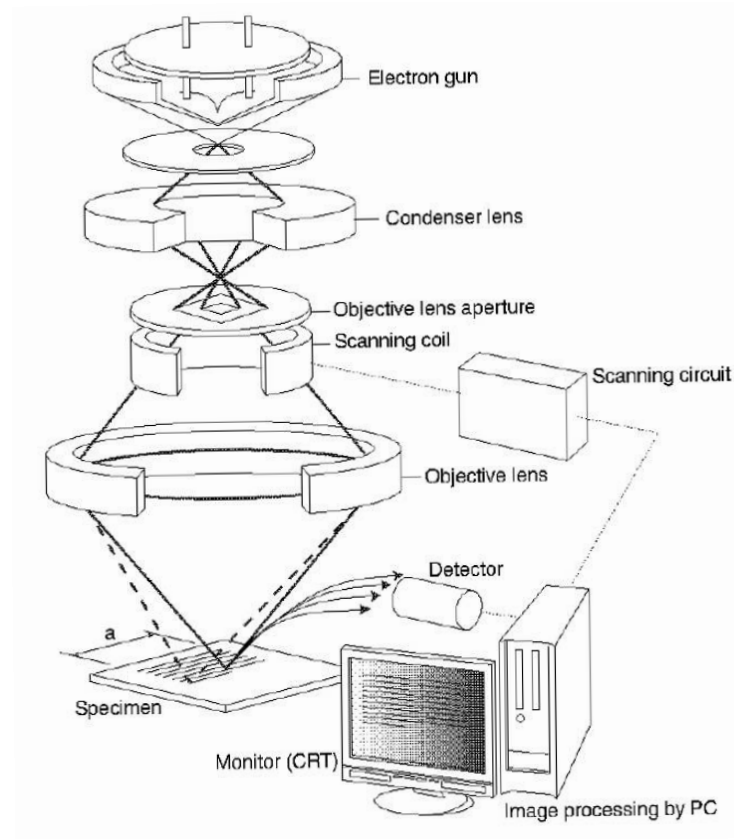


Figure 2.2 Schematic of SEM instrument (Jeol Ltd. and Jeol Datum Ltd. 2009)

Interaction of the electron beam with the sample surface results in the release of secondary electrons, backscattered primary electrons, Auger electrons, X-rays, and cathodoluminescence from the surface. Some electrons are also elastically or inelastically scattered through the sample. A secondary electron detector (Everhart-Thornley, E-T, or through the lens, TTL, detector depending on its location) detects the secondary and backscattered electrons and transmits an amplified signal to the display unit. Backscattered electrons have higher energy than secondary electrons and provide information from the outer 10 – 100 nm within the sample (Figure 2.3). Backscattered electrons are sensitive to changes in elemental mass with lighter atomic number atoms resulting in fewer electrons scattered and a darker area on the SEM image. The X-rays are detected using EDX (EDS) which converts the X-rays into an electric current enabling measurement of elements from B to U simultaneously.

2.3 Colour measurement

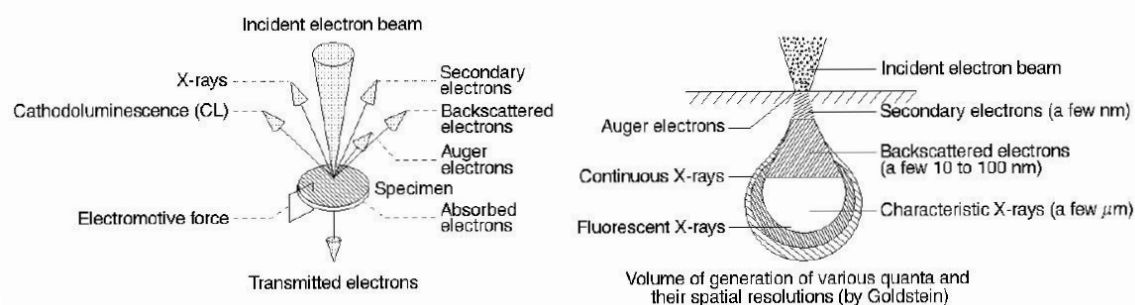


Figure 2.3 Interaction of electrons with sample surface and volume of sample generating the signals (Jeol Ltd. and Jeol Datum Ltd. 2009)

Unlike a high vacuum SEM, in variable pressure SEM instruments such as the Hitachi S-3700N at the British Museum, non-conducting samples do not need to be coated with metal or graphite coatings before analysis. This enables water-containing organic materials such as the textiles used in this research to be analysed quickly and with minimal damage if a low accelerating voltage, small probe current, and short times at high magnification are used. In addition, for objects which are smaller than the chamber, sampling is not necessary which makes this an essentially non-destructive technique (Jeol Ltd. 2009; Jeol Ltd. and Jeol Datum Ltd. 2009).

2.2.2 Uses in cultural heritage

The information gained from SEM-EDX complements that gained from techniques such as XRF. The SEM technique has been used in mechanistic decay studies involving metal corrosion, identification of fakes, determination of historical manufacture methods, and identification of biological materials such as different types of wood used in an object. SEM in combination with EDX or WDX is frequently used in heritage science to study the surface and composition of materials such as paper and iron gall ink (Sistach 1990; Wagner, Bulska, Hulanicki, Heck and Ortner 2001; Rouchon, Pellizzi, Duranton, Vanmeert and Janssens 2011), metal threads (Hacke, Carr, Brown and Howell 2003), weighted silks (Garside, Wyeth and Zhang 2010a), textiles (Hofmann-de Keijzer and Hartl 2005), and pigments (Vargas, Arias, Rodriguez and Erbez 2006).

2.3 Colour measurement

Visible reflectance spectroscopy enables accurate description of the colour of a material by colorimetry and/or spectrophotometry. It is a non-destructive analytical technique which involves irradiation of a surface with a known illuminant (often D65 radiation which simulates daylight) and measurement of the reflected light. Since organic materials

2.3 Colour measurement

including iron-tannate dyed textiles often change colour with ageing, colour measurement is an effective and rapid technique to monitor the degradation of a material and the effects of treatment application.

2.3.1 Theory

Pure white light is a combination of all of the different wavelengths of radiation in the visible region (360-780 nm), though not all of the same intensity (Christie 2001). The extent to which these different wavelengths of energy are absorbed (by chromophores) or scattered on contact with a surface determines the colour of the surface. The scattered (reflected) light that interacts with the retina causes a colour to be perceived that is complementary to the wavelengths of radiation absorbed. For example, the absorption of blue light ($\lambda = 435\text{-}480\text{ nm}$) by a surface from incident white light causes the surface to appear yellow since the red and green wavelengths are reflected. These combine additively to give an overall yellow colouration (Christie 2001).

There are two main methods of colour measurement. Spectrophotometry is the measurement of the intensity of discrete wavelengths of radiation (typically analysed at 10 nm intervals) throughout the visible spectrum presented as a reflectance spectrum of the surface analysed. Colorimetry however involves the measurement of the intensity of light reflected from a surface that is collected through three (or four) optical filters. Measured using a colourimeter, colorimetry produces numerical values to describe the colour of the surface using colour spaces (Billmeyer and Saltzman 1966).

Colour spaces have been developed to express the colour of an object or light source easily and accurately, often numerically. Many colour spaces have been developed including XYZ tristimuli values, Yxy colour space, $L^*C^*h^\circ$ colour space, and Hunter Lab colour space, but the CIE $L^*a^*b^*$ colour space is the most popular.

Introduced by the Commission Internationale de L'Éclairage in 1976, CIE $L^*a^*b^*$ colour space is a uniform colour space (Figure 2.4) in which equal distances on the chromaticity diagram represent perceived colour differences (ΔE^*_{ab}) of equal value. The L^* -axis indicates lightness with values of 0-100 representing black to white respectively. The a^* chromaticity axis indicates redness ($+a^*$) and greenness ($-a^*$) while the b^* -axis indicates yellowness ($+b^*$) and blueness ($-b^*$). Colour differences (ΔE^*_{ab}) between samples described by CIE $L^*a^*b^*$ (1976) are calculated as Euclidean distances using a colour

2.3 Colour measurement

difference formula such as that in Equation 2.1 (Billmeyer and Saltzman 1966; Minolta Co. Ltd. 1998; Sistach, Gibert and Areal 1999; Kolar, Sala, Strlic and Selih 2005):

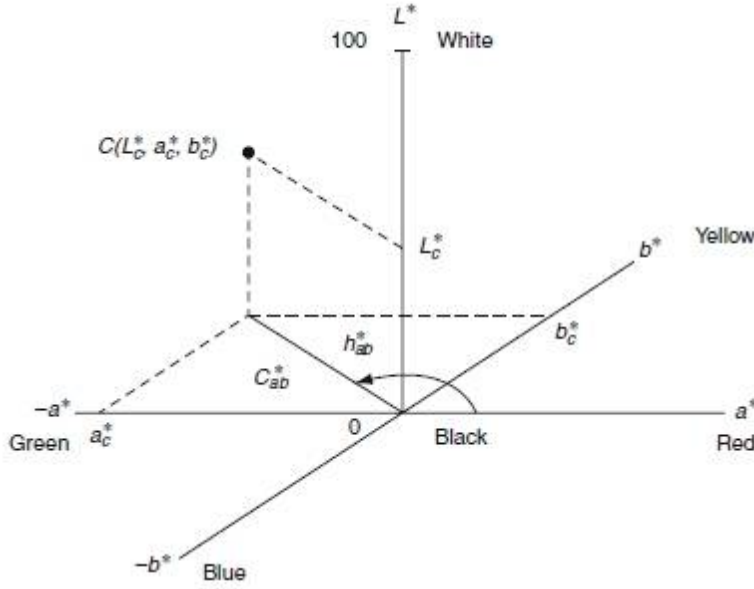


Figure 2.4 Diagram to illustrate the CIE $L^*a^*b^*$ colour space and the $L^*C^*h^\circ$ colour coordinates (Klein 2010)

In 2000, the CIE2000 colour difference equation (Equation 2.1) was released which improved upon the 1976 and 1994 versions. This new equation includes weighting functions for lightness (L^*), chroma (C^*), and hue (h°). To improve performance for blue colours, an interactive term between chroma and hue differences is included. Finally, a scaling factor has been introduced for the CIE $L^*a^*b^*$ a^* scale to improve the performance of grey colours. The CIE2000 colour difference equation has provided significantly better results than those from other colour spaces (Luo, Cui and Rigg 2001). However, three discontinuities and their magnitudes due to the formula have been reported (Sharma, Wu and Dalal 2005).

$$\Delta E_{00} = \sqrt{\left(\left(\frac{\Delta L'}{k_L S_L} \right)^2 + \left(\frac{\Delta C'}{k_C S_C} \right)^2 + \left(\frac{\Delta H'}{k_H S_H} \right)^2 + R_T \left(\frac{\Delta C'}{k_C S_C} \right) \left(\frac{\Delta H'}{k_H S_H} \right) \right)} \quad \text{Equation 2.1}$$

A fuller description of Equation 2.1 can be found elsewhere (Luo, Cui and Rigg 2001).

The point at which a ΔE^*_{ab} becomes perceptible is important when considering the effect of treatments on samples in heritage science since minimal colour change is required. Approximately 50% of observers can perceive a ΔE^*_{ab} of 1. However, differences in factors such as colour, surface texture, background, viewing angle, and illumination level

2.3 Colour measurement

result in the majority of people noticing a $\Delta E_{ab}^* < 1$ only 19% of the time. Typically the majority of people notice a colour difference of $\Delta E_{ab}^* \geq 3$ (Gilchrist and Nobbs 1999; Kolar, Strlic and Pihlar 2006). In one study into iron gall ink on paper (Reissland and Cowan 2002) a $\Delta E_{00}^* = 1.7$ value was deemed as a 'just perceptible' colour change based on the fastness grades in the BS EN 20105-A02:1995/ISO 105-A02:1993 1995, 1993 standards.

2.3.2 Equipment

Spectrophotometers such as the Konica/Minolta CM-2600d used at the British Museum include: a source of light (e.g. Xenon source with UV-filter to approximate D65); a light trap (Ulbricht sphere with coarse, white internal surface) into which the light is released; an objective optical waveguide for the light reflected from the sample at a set angle, e.g. 10° ; a concave diffraction grating to diffract the light; a reflection grating (concave) to collimate the diffracted light; and a silicon photodiode array to convert the light into electrical signals for the computer to process. In some spectrophotometers a reference beam is also incorporated using a separate identical optical system to that used for the reflected light from the sample. The software of the system calculates both spectrophotometric and colorimetric data. Tristimulus colorimeters are connected to a computer and contain a light source, grating, and R , G , B filters which transmit red, green, and blue light, respectively, and photocells which convert the light into electrical signals for software to produce colorimetric data (Klein 2010). Scanning devices that have been calibrated to colour standards are also being used in place of spectrophotometers and colorimeters (Kolar, Strlic and Pihlar 2006).

2.3.3 Uses in cultural heritage

Colour measurement is a common analytical technique in the analysis of cultural heritage since changes in colour of objects due to either degradation or the application of treatments need to be minimised (Kolar, Strlic and Pihlar 2006). Spectrophotometry and colorimetry have therefore been used to characterise the colour of iron-tannate complexes on paper and textiles and monitor their changes with age (Sistach, Gibert and Areal 1999; Te Kanawa, Thomsen, Smith, Miller, Andary and Cardon 1999; Csefalvayova, Havlinova, Ceppan and Jakubikova 2007) and/or treatment application (Kolar, Sala, Strlic and Selih 2005; Havlinova, Minarikova, Hanus, Jancovicova and Szaboova 2007). Colour measurements of textiles (Hallett and Howell 2005; Manhita, Ferreira, Vargas, Ribeiro, Candeias, Teixeira, Ferreira and Dias 2011) and paper (Zervos and Moropoulou 2005) without iron-tannate complexes, photographs (Fenech, Strlic, Degano and Cassar 2010), paintings

2.4 Electron Paramagnetic Resonance (EPR) Spectroscopy

(Bacci, Casini, Cucci, Picollo, Radicati and Vervat 2003), pigments (Frausto-Reyes, Ortiz-Morales, Bujdud-Perez, Magana-Cota and Mejia-Falcon 2009) and stone (Pouli, Fotakis, Hermosin, Saiz-Jimenez, Domingo, Oujja and Castillejo 2008) have also been undertaken.

2.4 Electron Paramagnetic Resonance (EPR) Spectroscopy

(Meybeck and Meybeck 1978; Banwell and McCash 1994; Atkins and de Paula 2002c)

EPR was used in this research to determine the presence of radicals and metal ions in iron-tannate dyed organic materials. Additionally information about the chemical environment of the metal ions and the type of radicals was gained.

2.4.1 Theory

Also known as electron spin resonance (ESR), EPR is a magnetic resonance spectroscopic technique that detects paramagnetic species with a lifetime typically greater than 10^{-6} s (Meybeck and Meybeck 1978; Banwell and McCash 1994; Atkins and de Paula 2002c). Paramagnetic species such as free radicals (organic or inorganic) and some transition metal ions (complexed or uncomplexed) contain one or more unpaired electrons. When there is an unpaired electron in a molecule there is a net spin of $\frac{1}{2}$ (spin quantum number, s) and two spin levels defined by the spin magnetic quantum numbers (m_s) = $+\frac{1}{2}$ and $-\frac{1}{2}$, because the direction of electron spin can be up or down, respectively. These levels are degenerate until an external magnetic field is applied at which point the $m_s = +\frac{1}{2}$ level for which the magnetic moment of the electron is anti-parallel to the applied magnetic field, is raised in energy and the $m_s = -\frac{1}{2}$ level for which the magnetic moment of the electron is parallel to the applied magnetic field is lowered in energy in a phenomenon known as Zeeman splitting (Figure 2.5).

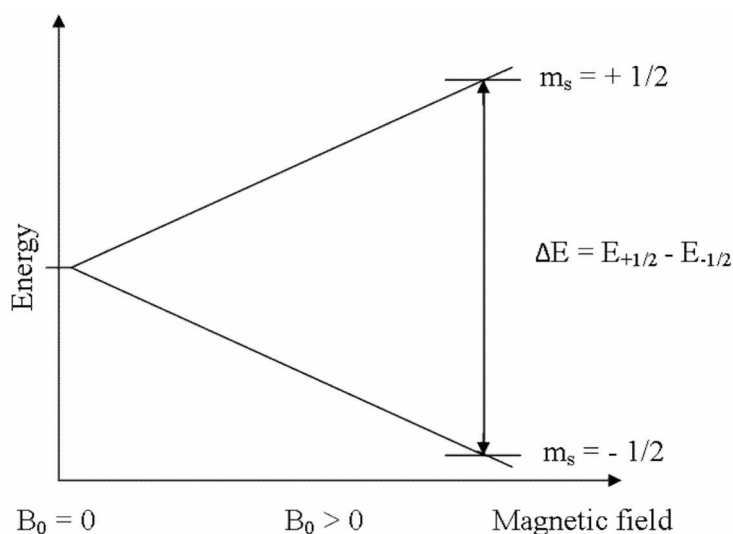


Figure 2.5 A representation of Zeeman splitting of the energy levels of an unpaired electron with increasing strength of an external magnetic field

2.4 Electron Paramagnetic Resonance (EPR) Spectroscopy

The difference in energy between the two spin levels (ΔE) increases with increasing strength of the external magnetic field (B_0) according to the Equation 2.2.

$$\Delta E = g_e \mu_B B_0 \quad \text{Equation 2.2}$$

where g_e is the electron's g-factor (≈ 2.0023 for a 'free' electron), μ_B is the Bohr magneton ($9.724 \times 10^{-24} \text{ JT}^{-1}$), and B_0 is the magnetic field strength (T). The g-factor is affected by local magnetic fields resulting from the structure of the complex or radical in which it exists. A typical g-factor for a *d*-metal complex where the unpaired electron is often localized to a specific orbital between two atoms is 0-6 because the electron experiences spin-orbit coupling if the orbital angular momentum is greater than 0 (i.e. is not an s-orbital). In radicals, the unpaired electron is relatively 'free' as it is in an orbital that covers the entire molecule and so typical g-factors for radicals are close to that for the 'free' electron i.e. 1.9-2.1 for inorganic radicals and 2.0027 for organic radicals (Banwell and McCash 1994; Atkins and de Paula 2002c). The size of ΔE is therefore characteristic of a specific type of environment for an unpaired electron at a specific B_0 . This enables determination of the type of paramagnetic species, i.e. radical or transition metal complex, and in many cases, the nature of the environment of that species, e.g. octahedral or tetrahedral complex of a transition metal and the type of ligands involved. The high sensitivity of EPR to the concentration of a paramagnetic compound enables EPR to be used to estimate the quantity of paramagnetic compound present (Banwell and McCash 1994).

Resonance between an applied electromagnetic radiation and the energy difference between the two m_s levels of an electron in an external magnetic field occurs when the frequency (ν) of each and therefore the energy, $h\nu$ (where h is Planck's constant, $\sim 6.63 \times 10^{-34} \text{ Js}$), is the same (Equation 2.3).

$$\Delta E = h\nu = g_e \mu_B B_0 \quad \text{Equation 2.3}$$

At this point an electron in the lower energy level can be raised to the upper energy level through the absorption of radiation of energy ($h\nu$) that is equal to ΔE . When there are more electrons in the lower energy level than in the upper, overall resonance absorption of the applied radiation equal to ΔE occurs. The smaller the ratio of the number of electrons in the upper level (N_u) to the number of electrons in the lower level (N_l), the stronger the signal possible before the point of saturation is reached, where $N_u = N_l$ and when no

2.4 Electron Paramagnetic Resonance (EPR) Spectroscopy

resonance absorption occurs. The Boltzmann law determines this ratio (Equation 2.4) and shows that to increase the EPR signal either the temperature can be lowered or B_0 increased (thus increasing ΔE) (Meybeck and Meybeck 1978).

$$\frac{N_u}{N_l} = e^{\frac{-\Delta E}{kT}} = e^{\frac{-g\mu_B B_0}{kT}}$$

Equation 2.4

Where k is the Boltzmann constant ($1.38065 \times 10^{-23} \text{ JK}^{-1}$) and T is the temperature in Kelvin.

Typically in EPR experiments, a fixed electromagnetic radiation frequency in the microwave region is used with a changing external magnetic field strength. The absorption of the microwave radiation with changing field strength is recorded. Consequently, to improve signal the temperature of the experiment is lowered, for example to 10K through the use of liquid helium, rather than B_0 being raised.

2.4.2 Equipment

Samples can be analysed in any physical state using EPR, however complications can arise in gas phase samples due to the free rotation of molecules. Quartz or Suprasil (synthetic quartz) tubes are used to contain the sample during analysis since glass contains iron and other contaminants (Atkins and de Paula 2002c). An EPR spectrometer includes a cavity for the sample, a source (klystron) of monochromatic microwave radiation (typically operating at 9.5 GHz), an electromagnet (typically operating at $\sim 0.34 \text{ T}$) with additional coils to enable the magnetic field to be varied, and a crystal detector (Meybeck and Meybeck 1978; Banwell and McCash 1994). A plot of the microwave absorption against the field strength is obtained from the spectrometer but usually it is the first-derivative of this spectrum that is used for evaluation (Figure 2.6). This is because identifying the point of maximum absorption and calculating the intensity of the signal is most accurate from the first-derivative spectrum (Banwell and McCash 1994).

The presence of hyperfine structure in the EPR spectrum can occur due to the interaction of the magnetic moment of the unpaired electron with that of neighbouring nuclei. Additionally, if there is more than one unpaired electron, coupling can occur between the magnetic moments of the multiple unpaired electrons, causing the appearance of fine structure in the EPR spectrum (Banwell and McCash 1994). These structures provide information about the chemical environment of the paramagnetic species.

2.4 Electron Paramagnetic Resonance (EPR) Spectroscopy

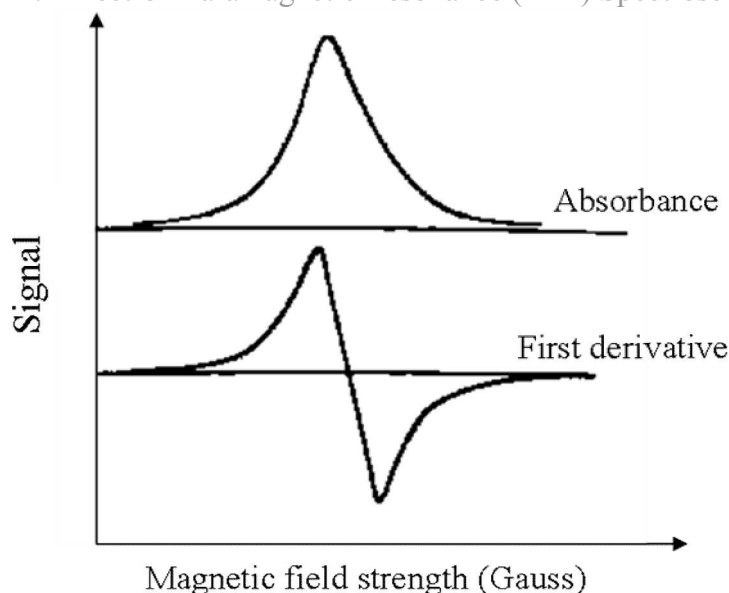


Figure 2.6 Typical absorbance and first derivative EPR spectra (Meybeck and Meybeck 1978)

2.4.3 Usage in cultural heritage

EPR is useful for the study of degradation reactions such as oxidation, that involve the formation of radicals (Mills and White 1994), for the understanding of metal ion binding in fibres (Kokot and Feughelman 1973; Chen, Lu, Yao, Pan and Shen 2005), and for the dating of materials (Boutaine, David and Dudley 2006; Kabacinska, Krzyminiowski, Dobosz and Nawrocka 2012). Extensive research into polymers has also been carried out using EPR (Meybeck and Meybeck 1978).

Samples as small as 1 cm long threads can be analysed using EPR which are recoverable after analysis. These factors are important when studying cultural heritage for which sampling must be kept to a minimum and be as non-destructive as possible. Despite this, EPR has been used relatively little in the analysis of cultural heritage to date. Nuclear magnetic resonance (NMR) which is very similar to EPR but which does not require an unpaired electron has been used to a much greater extent because it is applicable to a wider range of materials (Atkins and de Paula 2002c), a review of such analysis in cultural heritage has been published (Capitani, Di Tullio and Proietti 2012). Published examples of the use of EPR for cultural heritage materials includes the study of stone (Brilli, Conti, Giustini, Occhiuzzi, Pensabene and De Nuccio 2011), marble (Polikreti and Maniatis 2004), pigments (Orsega, Agnoli and Mazzocchin 2006; Negut, Bercu and Dului 2012), clay (Presciutti, Capitani, Sgamellotti, Brunetti, Costantino, Viel and Segre 2005), waterlogged leather (Bardet, Gerbaud, Le Pape, Hediger, Tr  n and Boumlil 2009), and

2.5 Gel Permeation Chromatography with Multi-Angle Laser Light Scattering detector (GPC-MALLS)

paper (Attanasio, Capitani, Federici, Paci and Segre 1995a; Attanasio, Capitani, Federici and Segre 1995b; Capitani, Emanuele, Segre, Fanelli, Fabbri, Attanasio, Focher and Capretti 1998).

2.5 Gel Permeation Chromatography with Multi Angle Laser Light Scattering detector (GPC-MALLS)

GPC is a form of size exclusion chromatography (SEC) that with a MALLS and refractive index (RI) detector can be used to determine the average molecular weight, the molecular weight distribution, and the polydispersity index of a polymeric sample (Malawer 1995). Depending on the availability of a specific fluorescence labeller, functional groups such as carbonyl or carboxyl groups of a polymeric sample can be detected when a fluorescence detector is attached to the GPC-MALLS system (Henniges, Prohaska, Banik and Potthast 2006). Profiles of carbonyl content in polymers relative to their molecular weight can be achieved. Samples as small as 5 mg can be analysed which is advantageous for the analysis of cultural heritage (Henniges, Prohaska, Banik and Potthast 2006). The validity of fluorescence labelling of functional groups for use on cellulosic materials has been established (Rohrling, Potthast, Rosenau, Lange, Borgards, Sixta and Kosma 2002) and it has subsequently been used to investigate iron gall ink on paper (Henniges, Reibke, Banik, Huhsman, Hahner, Prohaska and Potthast 2008) and the stabilising effect of the calcium phytate/calcium bicarbonate treatment on such samples (Henniges and Potthast 2008). In this project, collaboration with Antje Potthast and Ute Henniges at the University of Natural Resources and Life Sciences (BOKU), Vienna enabled me to undertake a one month placement at BOKU in July 2011, during which a range of samples were analysed using GPC-MALLS to aid understanding of the iron-tannate dye catalysed degradation mechanism and efficacy of treatments tested.

2.5.1 Theory

As a polydisperse material (one with polymer chains of different molecular weights) passes through a column it is separated according to the hydrodynamic volume of the polymers in the solvent used. The largest polymers are eluted first because they are unable to access the pores in the column. The smallest polymers are eluted last because they can access the pores in the column and therefore follow a different and longer path through the column compared to the larger molecules. The polymers therefore pass through the detectors at different times based on their size. The MALLS detector determines the molecular weight of the polymer and the RI detector the concentration. Using a fluorescence detector the

2.5 Gel Permeation Chromatography with Multi-Angle Laser Light Scattering detector (GPC-MALLS)

quantity of labelled groups (e.g. carbonyl) can be determined. It is assumed that there is no interaction between the polymers and the column, or the polymers with each other and that the correlation between hydrodynamic volume and molecular mass is constant. It is also assumed that the solvent has enabled all of the polymers to align themselves in a characteristic manner, such as in random coils that can be described by their hydrodynamic volumes rather than them being in their fully extended form (Malawer 1995; Trathnigg 1995).

The overall carbonyl group content in cellulose arises from reducing end groups (REGs) at the end of the cellulose chains (one per chain), and from carbonyl groups introduced through oxidation along the cellulose molecule. This overall carbonyl content is calculated by the fluorescence labelling method. Differentiation between the two types of groups cannot be made at present but indirect calculation of the REGs (i.e. theoretical REG content) can be made using the reciprocal of M_n (kg/mol) multiplied by 1000. This assumes that all of the REGs are in their chain form rather than their ring form and that no carbonyl groups have been oxidised to carboxylic acids. By subtracting the REG content from the overall carbonyl content a theoretical value of carbonyl groups that were formed by oxidation can be calculated. The standard deviation of the carbonyl content determined using GPC-MALLS is <5%, while that of M_w is ~5%, and that of M_n is ~10%. These are based on long-term analyses of standard pulps (Potthast, Henniges and Banik 2008).

Since both the weight averaged molecular weight (M_w) (Equation 2.6) and number averaged molecular weight (M_n) (Equation 2.5) of the sample is calculated the polydispersity index (PDI) (Equation 2.7) can also be calculated. This indicates the narrowness of the molecular weight distribution i.e. the monodispersity of the sample. For synthetic polymer a PDI < 1.1 indicates the sample is monodisperse (Atkins and de Paula 2002b).

$$M_n = \frac{\sum_i M_i N_i}{\sum_i N_i}$$

Equation 2.5

$$M_w = \frac{\sum_i M_i^2 N_i}{\sum_i M_i N_i}$$

Equation 2.6

$$PDI = \frac{M_w}{M_n}$$

Equation 2.7

Where M_i is the mass of a particular polymer chain in the sample and N_i is the number of polymer chains with mass M_i .

2.5.2 *Equipment and method*

The technique of fluorescence labelling of cellulose is described in detail elsewhere (Rohrling, Potthast, Rosenau, Lange, Borgards, Sixta and Kosma 2002) but requires that the sample be disintegrated and suspended in water, labelled with a fluorescence labeller, dissolved, diluted, and filtered before being injected into the GPC column. Carbazole-9-carboxylic acid [2-(2-amiooxyethoxy)ethoxy]amide (CCOA) is used in a zinc acetate buffer (pH 4) to label the carbonyl groups in cellulosic polymers by forming covalent bonds with the aldehyde and keto groups. Carboxyl groups are not labelled by CCOA. *N,N*-dimethylacetamide/lithium chloride 9% (v/w) (DMAc/LiCl) is used to dissolve the sample and DMAc to dilute to the appropriate GPC conditions. Once injected a pump ensures that it is forced through the column along with the mobile phase (DMAc/ LiCl 0.9% (v/w)) which has been degassed and filtered to ensure no air bubbles or impurities enter the system (Malawer 1995).

2.5.3 *Uses in cultural heritage*

GPC-MALLS specifically has been used on cellulosic pulps (Rohrling, Potthast, Rosenau, Lange, Borgards, Sixta and Kosma 2002; Potthast, Rohrling, Rosenau, Borgards, Sixta and Kosma 2003) including those from iron gall ink manuscripts (Henniges and Potthast 2008; Henniges, Reibke, Banik, Huhsmann, Hahner, Prohaska and Potthast 2008) and textiles (Henniges, Bjerregaard, Ludwig and Potthast 2011). GPC (or SEC) has also been used on cellulose nitrate (Quye, Littlejohn, Pethrick and Stewart 2011), cotton linters (Emsley, Ali and Heywood 2000), and silk (Hallett and Howell 2005; Nilsson, Vilaplana, Karlsson, Bjurman and Iversen 2010).

2.6 pH testing

Acids and bases can greatly affect the stability and lifetime of organic materials (e.g. acid hydrolysis or alkaline degradation). Therefore it is important to establish the acidity of a material when considering conservation strategies for its stabilisation or storage (Tse 2007).

2.6.1 *Theory*

Brønstedt-Lowry acids and bases are substances that donate and accept hydronium ions (protons, H^+), respectively, in aqueous solution. The extent to which this donation or acceptance occurs determines if the acid or base is strong (fully dissociates in water) or weak (only dissociates partially as determined by the equilibrium constant). The acidity or alkalinity of the extractable components of a material can be indicated by the pH of its aqueous solution. It is important to understand that only the extractable hydronium ions

2.6 pH testing

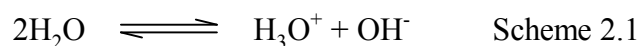
that are able to move to the method of detection are being measured and that consequently, pH does not indicate total acidity. Non-extractable acids such as cellulosic carboxyl groups or compounds such as the practically insoluble alkaline earth carbonates used to deacidify paper are not detected (Smith 2011). By increasing the extraction time more of the alkaline earth carbonates can be detected giving more reliable pH results (Strlic, Kolar, Kocar, Drnovsek, Selih, Susic and Pihlar 2004). Consequently, pH is not a useful indicator of the quantity of deacidifier required to neutralise all the acid present in a sample (including the non-dissociated weak acids), nor the amount of alkaline reserve present in a sample (Smith 2011). Additionally, the pH of a material is only valid and meaningful when the material contains water under ambient conditions for example, hygroscopic organic materials, because it is the acidity of an aqueous solution. For completely dry objects the concept of pH is irrelevant (Chamberlain and Coupe 1961; Tse 2007).

The pH of a solution is equal to the negative logarithm of the hydrogen ion activity (a_{H^+}) (Equation 2.8).

$$\text{pH} = -\log_{10}(a_{H^+}) \quad \text{Equation 2.8}$$

The activity is equal to the concentration of hydronium ions multiplied by the activity coefficient. In dilute solution the activity coefficient equals 1 and so the activity and concentration of hydronium ions are equal (Alliance Technical Sales Inc 2012). Therefore, in dilute solutions, pH is a measure of the concentration of hydronium ions and is measured on a scale of 0-14 when relative to pure water. This scale arises because of the self-ionisation of pure water and the classification of pure water as being neutral. Other self-ionising solvents (e.g. alcohol) can be used in the determination of the pH of a solution but they require a different scale (Galster 1991; Tse 2007).

Pure water self-ionises into hydroxide and hydronium ions (Scheme 2.1) to an extent defined by K_w (Equation 2.9).



Scheme 2.1 The self-ionisation of water into hydroxide and hydronium ions.

$$K_w = \frac{a_{H^+} \times a_{OH^-}}{a_{H_2O}} \quad \text{Equation 2.9}$$

2.6 pH testing

Since the dissociation is very small, the activity of water is assumed to be constant.

Consequently, the dissociation constant of water, K_W , is the product of the activities, or concentrations in dilute solution, of the hydronium and hydroxide ions. At 25°C, K_W is close to 10^{-14} M^2 since the concentration of both the hydrogen and hydroxide ions in pure water at 25°C is 10^{-7} M . pK_W is therefore 14 at 25°C, while pH and pOH are 7 (Equation 2.10).

$$pK_W = \text{pH} + \text{pOH} \quad \text{Equation 2.10}$$

where pK_W and pOH are the negative logarithms of K_W and the concentration of hydroxide ions, respectively (Atkins and de Paula 2002b).

Since pure water is considered neutral, pH 7 is considered the neutral pH. The addition of hydronium ions to a solution increases the concentration, and therefore the activity, of the hydronium ions and thus decreases the pH. Conversely, the addition of hydroxide ions to the solution increases the activity of the hydroxide ions and increases the pH. Rarely are pH values outside of the 0 (acidic) to 14 (alkaline) scale needed (Tse 2007).

2.6.2 Equipment

Several reviews of the methods and equipment available for the pH testing of cultural heritage, including their technical merits, have been published (Saverwyns, Sizaire and Wouters 2002; Strlic, Kolar, Kocar, Drnovsek, Selih, Susic and Pihlar 2004; Tse 2007). Consequently only a brief discussion is presented here.

The pH of a solution can be measured colorimetrically or potentiometrically. Colorimetric pH determination involves the use of indicator papers, pens, or solutions that contain organic dyes that change colour at certain hydronium ion concentrations. This is a subjective method of assessment which provides semi-quantitative results only.

Potentiometric pH determination gives quantitative results since it uses a pH meter to measure the potential difference between the indicator electrode and a reference electrode. These electrodes can be separate or combined into one. The reference electrode produces a constant voltage while the indicator electrode produces a voltage that is proportional to the

2.6 pH testing

concentration of hydronium ions in the solution (detected by a sensing membrane glass)²

The pH meter calculates the difference between the voltages (E_{measure}) of the reference (E_{ref}) and indicator electrodes and displays it as a pH value after conversion using the Nernst equation (Equation 2.11). There is a 59.2 mV change per unit pH and the voltage at pH 7 is 0. Positive mV corresponds to pH < 7 (acidic) while negative mV corresponds to pH > 7 (alkaline).

$$E_{\text{measure}} = E_{\text{ref}} - 2.303 \frac{RT}{nF} \times pH \quad \text{Equation 2.11}$$

where R is the gas constant (8.314 JK⁻¹mol⁻¹), T is the absolute temperature (K), F is the Faraday electrochemical constant (96487 Cmol⁻¹), and n is the ionic charge, i.e. n = 1 for hydronium ions (Tse 2007; Alliance Technical Sales Inc 2012).

pH measurements are highly temperature dependent. Changes in temperature from 25°C at pH 7 are compensated for through the use of temperature sensors at the time of pH measurement. Other factors that affect pH results include the sample:water ratio, extraction time, water quality, ionic strength and composition of the solution, contaminants on the sample or containers used in the analysis, and interfering substances that can block or coat the sensing membrane or reference junction (Tse 2007).

Depending on the type of electrode available, pH measurements of hot or cold aqueous extracts, of a drop of distilled water on the surface of a material (Figure 2.7), or of extracts of particularly small samples (micro-pH testing) can be taken. In this project micro-pH testing and surface pH testing have been used on model and historic textiles.

² Detailed information on the construction and working of pH electrodes is presented in the following sources: Emerson Process Management (2010). Application data sheet 43-002/rev.C: The theory of pH measurement, Rosemount Analytical Inc, Alliance Technical Sales Inc (2012). A guide to pH measurement - the theory and practice of laboratory pH applications, Alliance Technical Sales Inc.

2.6 pH testing

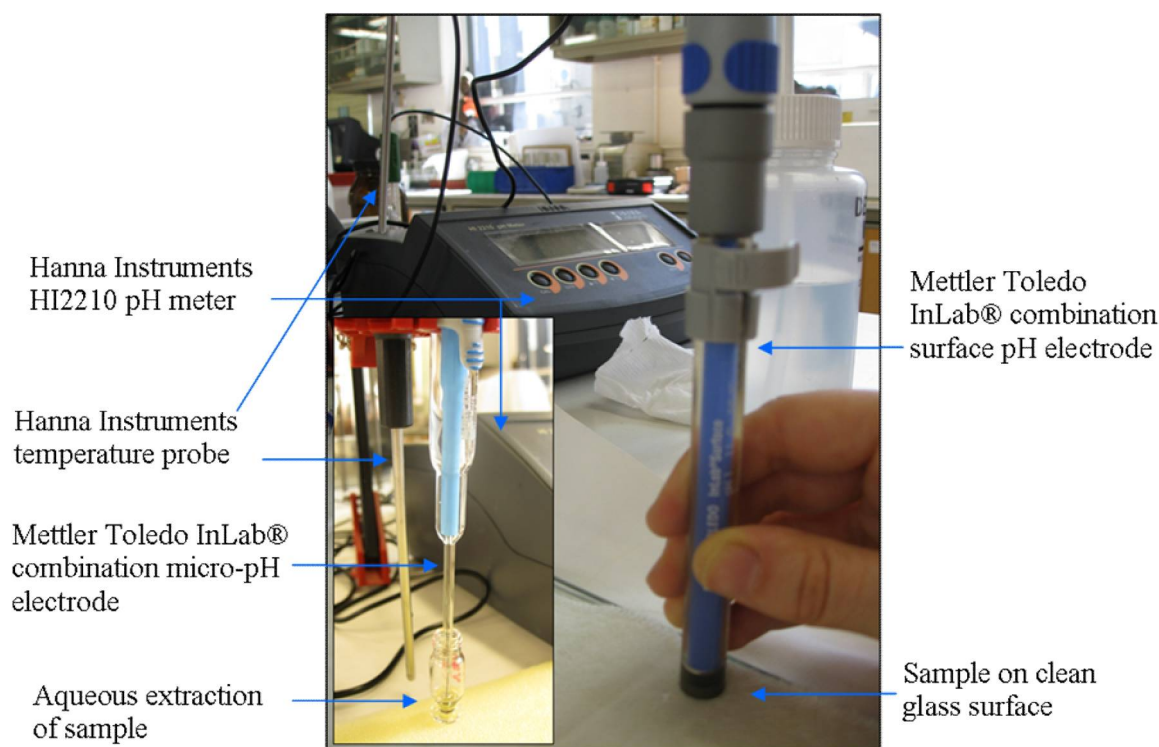


Figure 2.7 Surface pH testing electrode and pH meter with micro-pH electrode analysing sample (inset)

International standards exist for the pH testing of paper (ASTM D778-97; TAPPI T 435; TAPPI T 509; ISO 6588-1:2005 2005; ISO 6588-2:2005 2005) and fibres (ASTM D2165-94 2000) or textiles (BS EN ISO 3071:2006 2006) by aqueous extract and of paper by surface pH testing (TAPPI T 529 om-09). Note that the pH obtained through surface pH testing is likely to differ from that obtained through extraction methods particularly if the water used in the surface pH test has remained on the surface of the material rather than dissipating into the material during the test. The variation in results for the same sample measured in different laboratories using the above standards can be as much as 0.5 pH units. The recommended extraction methodologies are often not followed directly as the size of sample required (often 1-2 g for extraction methods) is unacceptable to remove from cultural heritage objects. This has resulted in the development of micro-pH analytical techniques (Saverwyns, Sizaire and Wouters 2002; Strlic, Kolar, Kocar, Drnovsek, Selih, Susic and Pihlar 2004; Vuori and Tse 2005b) and the use of surface pH and colorimetric methods which require significantly smaller quantities of sample (as little as 50 μg for micro-pH testing) and water (Banik 2011) but can have their own undesirable side effects e.g. tidelines from surface pH testing. Ways to ensure that non-standard methods of pH testing are still reliable have been recommended (Tse 2007; Banik 2011) but despite this

2.7 Bathophenanthroline testing

Banik (Banik 2011) still questions the reliability and significance of the pH results of paper obtained with the methods currently available.

2.6.3 Usage in cultural heritage

pH testing is widely used in conservation to aid the development of strategies for the treatment and storage of objects by improving understanding of the condition and degradation rate of an object and the efficacy of treatments (Tse 2007). pH testing has been used in ageing studies of organic materials such as paper (Slavin and Hanlan 1992; Zou, Uesaka and Gurnagul 1996b) and cotton (Zervos and Moropoulou 2005). Both colorimetric methods of pH testing (Hanus, Makova, Ceppan, Minarikova, Hanusova and Havlinova 2009) and potentiometric methods have been used to identify the acidity of iron gall ink manuscripts (Kolar, Stolf, Strlic, Pompe, Pihlar, Budnar, Simcic and Reissland 2006; Csefalvayova, Havlinova, Ceppan and Jakubikova 2007). The efficacy of treatments on paper with iron gall ink (Havlinova, Minarikova, Hanus, Jancovicova and Szaboova 2007) and the pH of iron-tannate dyed *Phormium tenax* (Daniels 1999b) and iron weighted silk has also been investigated (Garside, Wyeth and Zhang 2010b).

2.7 Bathophenanthroline testing

The bathophenanthroline test papers developed by Neevel and Reissland (Neevel and Reissland 2005) to detect soluble iron(II) ions in paper are now commercially available (Preservation Equipment Ltd. 2012). They are a useful low technology method of identifying the presence of soluble iron(II) ions in many materials thus aiding the identification of those materials most at risk from iron-catalysed degradation.

2.7.1 Theory

Bathophenanthroline (4, 7-diphenyl-1, 10-phenanthroline) forms a magenta-coloured complex (1:1, 2:1, and 3:1) of low water solubility with iron(II) ions. Soluble iron(II) concentrations as low as 1 ppm (i.e. 1 mgL⁻¹) produce visible colour change in the test strip and when either 1% (w/v) aqueous ascorbic acid solution (pH ~ 2.5) or 1% aqueous sodium dithionite solution (pH ~ 6.5) is added to a used test strip, the presence of any transferred iron(III) ions can also be ascertained through their reduction to detectable iron(II). Unlike with other iron(II) indicator papers which use water soluble indicators such as 2,2'-dipyridyl, the low solubility of the iron(II)-bathophenanthroline complexes prevents the transfer of the coloured indicator to the object. The prevention of the indicator paper staining the sample during testing is vital when testing cultural heritage objects.

2.7 Bathophenanthroline testing



Figure 2.8 The bathophenanthroline test strips used to identify soluble iron(II) and iron(III) ions (using 1% aqueous ascorbic acid solution) on a variety of model and historic textiles as well as the semi-quantitative colour chart (Vuori and Tse 2005a) and the structure of bathophenanthroline

2.7.2 Equipment

When testing for iron(II) ions a piece of indicator paper which can be as small as 0.5 cm × 1 cm, is wetted with a drop of deionised water and blotted to remove excess water before being placed on the sample area. The indicator is pressed onto the sample by hand for 30 s with a piece of melinex between the paper and hand to prevent contamination of the paper. During air-drying (2 min) the indicator paper will turn magenta in the presence of iron(II) ions; the intensity of colour being proportional to iron(II) content (up to 50 ppm (Vuori and Tse 2005a)) (Figure 2.8). If the aim of the test is to determine the efficacy of a treatment at removing iron(II) and iron(III) ions or making them catalytically inactive, Neevel (Neevel 2009) advises that 1% aqueous solution of sodium dithionite should be used to reduce transferred iron(III) ions to detectable iron(II) ions due to its neutral pH which prevents the breakdown of iron(III)-gallate complexes. However, when identifying the presence of iron gall ink, a 1% aqueous solution of ascorbic acid is recommended to reduce iron(III) to iron(II) since here the breakdown of transferred iron(III)-gallate complexes and subsequent release of iron(III) for reduction is beneficial to the aim of the test. There are many variables within this testing method such as contact time, water content of the paper, surface texture of the sample, porosity of the sample, competing complexation reactions, pH conditions of the test, and the presence of other metals (Neevel 2009) that make the results of bathophenanthroline tests unsuitable for quantitative determination of iron content. However, a colour code has been developed which indicates the level of soluble iron ions detected as being 1, 10, 25, and 50+ ppm based on the results from test strips

2.8 Viscometry

immersed into aqueous iron(II) sulphate solutions of different concentration (Vuori and Tse 2005a). This colour code was not intended for quantitative analysis but to provide a method of recording of colour intensity to aid comparison with the results from other researchers, and of identification and prioritisation of the objects most at risk from iron-catalysed degradation. The application of bathophenanthroline test paper to detect iron ions in textiles has been suggested (Barker 2002) and investigated (Vuori and Tse 2005a). The test strips were concluded to be successful at identifying the presence of iron ions in most cellulosic materials as well as proteinaceous materials such as silk and collagen. However, they were not reliable for the identification of iron ions in wool. The unavailability of the iron(II) ions for complexation with bathophenanthroline was suggested to be due to the tight binding between the many sulphhydryl (-SH) groups in keratin and the iron(II) ions (Vuori and Tse 2005a).

2.7.3 Usage in cultural heritage

The ability of the bathophenanthroline test to identify the presence of soluble iron(II) ions (and iron(III) ions once they have been reduced to iron(II) ions) rapidly in many cellulosic and proteinaceous (except wool) materials makes it a valuable tool for paper and textile conservators. The test is used as a standard test in some conservation studios (Vuori and Tse 2005a) and has been used in published research into the identification of iron(II) ions in manuscripts (Hanus, Makova, Ceppan, Minarikova, Hanusova and Havlinova 2009; Titus, Schneller, Huhsmann, Hahner and Banik 2009), textiles (Vuori and Tse 2005a), and baskets (Wills and Hacke 2007), as well as the monitoring of the results of treatment application to iron gall ink documents (Eusman 2002; Rouchon, Pellizzi, Duranton, Vanmeert and Janssens 2011).

2.8 Viscometry

Viscometry (or viscosimetry), is used to calculate the intrinsic viscosity of fluids such as solutions of dissolved polymers. The molecular weight of polymeric solutions (average molecular weight if the solution is polydisperse) and therefore the DP (or average DP) of dissolved polymers can be determined viscometrically. This is useful in conservation science because DP affects the strength of fibres and consequently the strength and flexibility of the woven textiles or paper sheets from which the polymer originates (Zou, Gurnagul, Uesaka and Bouchard 1994). The use of viscometry to monitor the degradation of paper caused by iron gall ink has been validated and the resulting DP values found to correlate linearly to a limited extent with bursting strength (due to the large random error involved in the bursting strength data) (Kolar and Strlic 2004).

2.8.1 Theory

The viscosity of a fluid is its internal resistance to flow which increases (i.e. the solution flows at a slower rate) with decreasing temperature (Nelkon and Parker 1971). Viscometry of a polymer such as cellulose requires dissolution of the sample e.g. cotton fibres, in a solvent such as cupriethylenediamine (CED). The time for the solution to pass between two marks on the capillary-tube viscometer is compared with the efflux time of the pure solvent. The intrinsic viscosity number ($[\eta]$) is calculated using Equation 2.12 and the Wetzel-Elliot-Martin's equation (Wetzel, Elliot and Martin 1953). Average molecular weight of the polymer is calculated from the intrinsic viscosity using the Mark-Houwink-Sakurada equation and the average DP is calculated using the Evans and Wallis equation (Equation 2.13) (Kolar, Strlic and Pihlar 2006).

$$\frac{t}{t_0} = \frac{\eta}{\eta_0} \quad \text{Equation 2.12}$$

Where t and t_0 are the efflux times of the polymer solution and solvent, respectively, and η/η_0 is the viscosity ratio.

$$\text{DP}^{0.85} = 1.1 \cdot [\eta] \quad \text{Equation 2.13}$$

The high alkalinity of CED can cause the depolymerisation of degraded, oxidised cellulose and therefore there is a systematic error involved in this method of DP determination. Additionally, it is assumed that the textile contains 5% water from the atmosphere (Strlic, Kolar, Zigon and Pihlar 1998).

2.8.2 Equipment

There are many types of viscometer including manual (e.g. glass capillary) and automatic types (Poulten Selfe & Lee Ltd 2004). The manual viscometer equipment used in this project was at the Centre for Sustainable Heritage, UCL and is depicted in Figure 2.9. This equipment included a water bath to warm the dissolved sample to $25.0 \pm 0.1^\circ\text{C}$ before being put into the viscometer (BS ISO 5351:2010 2010), a glass capillary-tube viscometer with water jacket maintained at $25.0 \pm 0.1^\circ\text{C}$, a stopwatch to measure the time it takes the solution to pass between two marks on the viscometer, and a suction pump to bring the solution into the viscometer to start the test.

2.9 Tensile testing

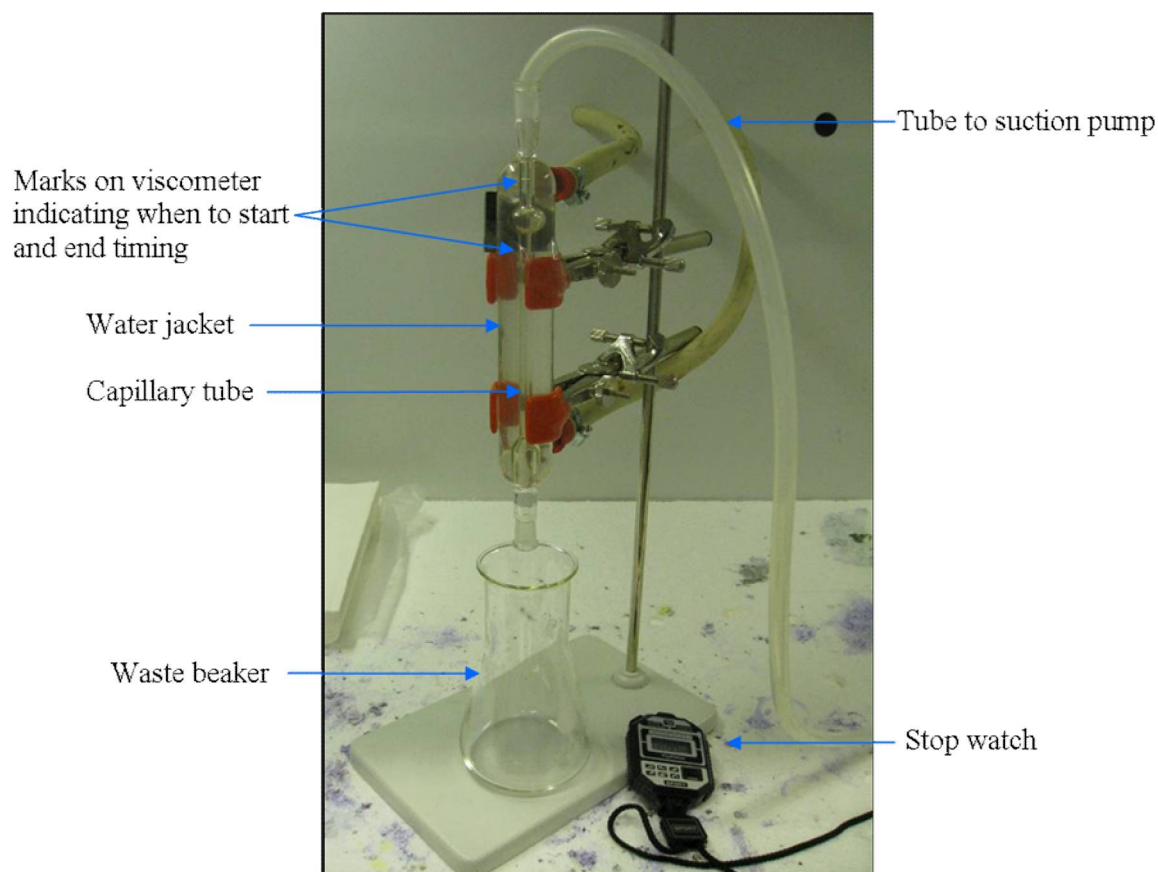


Figure 2.9 Photograph of the viscometry equipment (excepting the water bath) used at the Centre for Sustainable Heritage, UCL

2.8.3 Usage in cultural heritage

Standards exist for the viscometric determination of the DP of cellulosic pulps (ASTM D1795-96 2001; D1795-96(2007)e1 2007; ASTM D6188-97 2008; BS ISO 5351:2010 2010). In cultural heritage viscometry has been used in the study of the degradation of cellulose (Feller, Lee and Bogaard 1986) in paper (Whitmore and Bogaard 1994) and cotton (Sharples 1954), of the effects of iron gall ink on paper (Kolar and Strlic 2004; Kolar, Strlic and Pihlar 2006), of the effects of stabilising treatments on paper (Stefanis and Panayiotou 2007), and to assist in the lifetime estimation of iron gall ink manuscripts (Strlic, Csefalvayova, Kolar, Menart, Kosek, Barry, Higgitt and Cassar 2010). Viscometry has also been used on silk (von Lerber, Pentzien, Strlic and Kautek 2005).

2.9 Tensile testing

There are many types of mechanical testing, e.g. folding endurance (BS ISO 5626:1993 1994), bursting strength (BS EN ISO 2758:2003 2002), tearing resistance (BS EN ISO 1974:2012 2012), zero-span tensile strength (BS ISO 15361:2000 2001; ASTM D5804-97 2002), and tensile testing (ASTM D5034-95 2001; ASTM D5804-97 2002; ASTM D5035-

2.9 Tensile testing

95 2003). Tensile testing involves the application of tension to a sample (for example, a length of yarn or strip of textile or paper) to determine its breaking load and elongation at break. Organic polymeric materials such as cellulose weaken with age as the polymer chains are broken and the DP decreases (Zou, Gurnagul, Uesaka and Bouchard 1994). Tensile testing enables this weakening to be quantified which is useful for investigating the rate of degradation of a material and monitoring the efficacy of stabilisation treatments.

2.9.1 Theory

When a load is applied to a material the material experiences a force of tension and stretches (elongates). The load and elongation of a sample can be normalised to give the stress and strain (or extension), respectively, according to Equations 2.14-2.16, making them suitable for comparison with different types of fibre of the same fineness.

$$\text{Stress (Nm}^{-2}\text{)} = \frac{\text{Force (N)}}{\text{Cross-sectional area (m}^2\text{)}} \quad \text{Equation 2.14}$$

$$\text{Strain} = \frac{\text{Elongation (mm)}}{\text{Initial length (mm)}} \quad \text{Equation 2.15}$$

$$\text{Extension (\%)} = \text{Strain} \times 100\% \quad \text{Equation 2.16}$$

When the strain of a material is proportional to the applied stress, the material obeys Hooke's Law (Equation 2.17) and will regain all or the majority of its original dimensions once the load is removed. Reversible deformation such as this is called elastic deformation and gives a straight line on a load-elongation or stress-strain curve.

$$\text{Strain} = \frac{\text{Stress}}{\text{Young's modulus}} \quad \text{Equation 2.17}$$

The gradient of this straight line is the initial or Young's modulus which indicates the resistance of the material to small forces of tension. In fibres, elastic deformation occurs when primary and secondary bonds in the amorphous regions of the fibre are being stretched and broken (Booth 1968). However, as the polymer chains move past each other plastic deformation occurs where the original form of the sample is not regained after the removal of the load. This causes the gradient of the stress-strain curve to bend. The continuing rearrangement of the polymer chains with the increase in stress can cause the polymer to become more resistant to deformation and consequently the gradient changes again. Eventually the polymer chains are broken and the sample is torn apart. This is the breaking point of the sample from which, the breaking load (N) and extension at break (%) and therefore the material's strength and extensibility, can be established. Additionally the

2.9 Tensile testing

specific strength (tenacity) of the sample can be calculated (Equation 2.18) which is measured in mNtex^{-1} or gftex^{-1} where a tex is gkm^{-1} and gf is grams force. Since the tenacity is normalised with respect to fibre density, samples of different fineness can be directly and reliably compared (Booth 1968).

$$\text{Tenacity (Ntex}^{-1}\text{)} = \frac{\text{Force applied at break (N)}}{\text{Linear density (tex)}} \quad \text{Equation 2.18}$$

2.9.2 Equipment



Figure 2.10 Photograph of the Instron 4411 tensile tester at the University of Manchester testing an aged dyed silk sample

An electromechanical tensile tester such as the Instron 4411 tensile tester at the University of Manchester (Figure 2.10) typically includes a frame in which two crossheads (stiff beams) are mounted. One of these is moved prior to testing to set the gauge length required while the other is moved electromechanically during the testing to apply tension to (i.e. to load) the sample. Loading of the sample can occur at a constant rate of extension, constant rate of loading, or constant rate of stress (Booth 1968). The sample is held in grips or jaws that are attached to the crossheads. The grips in Figure 2.10 are pneumatic flat-faced grips that were made at the University of Manchester. In-between the grip and the crosshead that is moved during testing is the load cell which contains a strain gauge that converts the force of tension into an electrical signal with which a computer produces a stress-strain or load-extension curve.

2.9 Tensile testing

The Instron tester is a versatile piece of equipment with a wide range of accessories available (e.g. load cell, grips, and jaw faces) to optimise the equipment for the role required (INSTRON 2012). Additionally, the extension speed and gauge length can also be altered. Many factors affect tensile test results including the sample alignment in the grips/jaws which should be parallel to the direction of force to be applied (ASTM D5035-95 2003), and the temperature and relative humidity of the environment during testing; for example, increasing humidity increases the strength of cotton but decreases the stiffness while increasing temperature decreases both (Hearle 2007). For hygroscopic samples it is important to tensile test all samples under the same environmental conditions to ensure the comparability of the results. Ideally, samples should be pre-conditioned for a minimum of 8 hours for animal fibres and 6 hours for cellulosic fibres (ASTM D5035-95 2003) to ensure the moisture content within the sample is the same as that needed for testing. Sample length also affects the results, particularly the extension results. For the extension results to be valid the same level of pre-tensioning of the sample prior to clamping as well as the same gauge length must be used on all samples to ensure the same length of sample is being tested (ASTM D5035-95 2003). The history of the sample (e.g. chemical treatment or previous tension application), the form of the sample (e.g. yarn or woven textile), and the capacity of the machine (e.g. maximum load detectable) can also affect tensile testing results (Booth 1968).

2.9.3 *Uses in cultural heritage*

Tensile testing has been used as a form of mechanical testing in studies into silk (Hallett and Howell 2005; Garside and Brooks 2006; Garside, Wyeth and Zhang 2011), raffia (Sandy and Bacon 2008), cotton (Zervos and Moropoulou 2005), iron-tannate dyed silk (Sato, Okubayashi, Sukigara and Sato 2011) and *Phormium tenax* (Daniels 1999b), accelerated ageing methods (Nilsson, Vilaplana, Karlsson, Bjurman and Iversen 2010), and paper stabilisation treatments (Stefanis and Panayiotou 2007).

3 UNDYED MODEL TEXTILES

The model dyed textiles have two components; the model textile material and the model dyestuff. The development of both are dealt with separately in this chapter and Chapter 4, respectively, while the final combined model dyed textiles are characterised and summarised in Chapter 5.

3.1 Historic iron-tannate dyed materials

Iron-tannate dyes have been used to colour a wide variety of proteinaceous and cellulosic materials. Based primarily on catalogue information for objects at the British Museum and occasionally on scientific analysis (microscopy by Dr. Caroline Cartwright at the British Museum has identified iron-tannate dyed abaca), materials dyed with iron-tannate dye at the British Museum were found to include leather, skin, silk, cotton, abaca (*Musa textilis*), New Zealand flax (*Phormium tenax*), bark cloth, raffia, and palm fibres (see Chapter 6). In addition there are unidentified cellulosic materials such as those used in basketry (Egyptian and North American), African masks, and objects such as belts and loin cloths from Oceania.

3.2 Aims for model textiles

The model textiles were produced for this project to be valid substitutes for historic iron-tannate dyed materials during the testing of a variety of conservation treatments. Consequently, some of the undyed model textiles acquired for this project were subjected to iron-tannate dyeing, accelerated ageing, immersion in a range of antioxidants and deacidifiers, and multiple analyses, sometimes destructive.

In order for the results of the conservation treatment tests to be of most use to the conservation community, the undyed model textiles must:

- a. be representative of the materials dyed with iron-tannate dye throughout history and within the British Museum's collections;
- b. be relatively homogenous in dimensions and colouration to minimise error in analytical results;
- c. be of suitable quantity for all analyses to be completed and comprehensive natural ageing experiments to be undertaken.

3.3 Choice of model textiles

When choosing the material types to be used in this project the following factors were considered: relevance to iron-tannate dyed objects in the British Museum, examples reported in the literature, chemical composition, availability, and cost. The former was the first factor that was investigated and was found to be more complicated than expected. While the British Museum has a database for its collection (Merlin), relevant terms such as 'iron-tannate dye' and 'black dye' were rarely stated in the entries and so searches for these were generally unsuccessful. The wide range of shades of colour of iron-tannate dyed objects (browns, greys, and blacks) made the search for 'black dye' to be of limited value. However, even if all the colours were searched for some objects would still be missed, e.g. the Akali Sikh turban (As2005,0727.1.o) which was known prior to the start of this project to contain iron-tannate dye (Pullan and Baldwin 2008) and the catalogue entry for which listed its colour as blue due to the presence of indigo. Searches based on objects that were known from literature to contain iron-tannate dye such as black or brown dyed objects from New Zealand (Daniels 1995) or bogolanfini from Africa (Donne 1973) were more successful but would not identify lesser known iron-tannate dyed object types. A survey of the collection was not considered possible in the time-frame of this project and so instead, with the assistance of conservator Pippa Cruickshank, curators were asked to identify any black dyed materials within their departments, particularly those that were in poor condition. This led to numerous suggestions which were subsequently located in the stores and where possible sampled. When the objects were black/brown/grey in colour and were in poor condition (e.g. brittle, weak, fragmented, losses) the material types that were reported in the catalogue were used to give an indication of the types of iron-tannate dyed materials likely to be present at the British Museum (Section 3.1). XRF analysis of the samples acquired was later undertaken to indicate the likelihood of these objects containing iron-tannate dye (Chapter 6).

Due to the need for large quantities of material with homogenous structure throughout, woven textiles rather than non-woven materials such as leather, skin, or bark cloth became the chosen form of the model textiles. Woven textiles rather than individual fibres were chosen because of the increased sample size this would allow. Larger sample sizes increase the overall sample homogeneity, improve handle-ability, and enable aesthetic changes due to treatments to become noticeable. Importantly, woven textiles were closer to the form of many of the British Museum objects that were thought to contain iron-tannate dye and that need stabilising.

3.3 Choice of model textiles

Consequently, the resulting four woven textile materials were chosen as the model textiles for this research: abaca, cotton, wool, and silk (Table 3.1). Further detail behind the choice of each is reported in Sections 3.3.1 and 3.3.2.

Table 3.1 Source and description of undyed model textiles

Model textile and reference code	Description	Supplier
Cotton (CU)	Plain woven, scoured, bleached, 100% cotton fabric (135 g/m ²)	Phoenix Calico Limited
Abaca (AU)	Undyed, unstiffened, natural double strand pinokpok	Parkin Fabrics Limited
Wool (WU)	100% wool botany serge (190 g/m ²)	Whaleys (Bradford) Limited
Silk (SU)	Scoured, degummed, plain weave silk (220 g/m ²)	Professor J. Shao, Zhejiang Sci-Tech University, Hangzhou, PRC.



Figure 3.1 From left to right: Samples of the undyed cotton, abaca, silk, and wool model textiles used in this project

3.3.1 Cellulosic textiles

Iron gall ink is chemically similar to iron-tannate dye (Barker 2002; Hofenk de Graaff 2002). The extensive research into the degradation caused by and stabilisation treatments for iron gall ink on paper forms much of the background research for this project. Paper made from cotton linters or historical rag paper has been used in the majority of research into iron gall ink (Neevel 2002; Kolar, Mozir, Balazic, Strlic, Ceres, Conte, Mirruzzo, Steemers and De Bruin 2008). The use of woven cotton in this project will enable comparison with iron gall ink research and also reflects the presence of iron-tannate dyed cotton in the British Museum's collections in objects such as bogolanfini (British Museum

3.3 Choice of model textiles

registration number: Af1987,07.9, Figure 3.1) and an Akali Sikh turban (British Museum registration number: 2005,0727.1). A scoured and bleached cotton textile was sourced to ensure that contaminants such as metal ions which may be a source of error in the experiments in this project were minimised. While scouring and bleaching may not have been used on all historic cotton iron-tannate dyed textiles it is likely that it will have been used on some.

Abaca (*Musa textilis*) is a leaf fibre which was chosen to represent the many cellulosic iron-tannate dyed materials present in the British Museum's collections that are less crystalline and that contain less cellulose than the seed fibre cotton. These include: *Phormium tenax* (New Zealand flax) which is used in New Zealand to create baskets, cloaks, and piu piu (ceremonial skirts); basketry materials such as those used in Egypt and North America; and raffia which is used in Africa to make Kuba cloths. Fibre identification by Dr. Caroline Cartwright at the British Museum has confirmed that abaca has been used in two British Museum objects (British Museum registration numbers: 1906,5.24.8 and 1904-282). It is highly likely that many more iron-tannate dyed British Museum objects, particularly those originating from Polynesia, also contain abaca. The least processed abaca (i.e. no stiffening) was chosen to better mimic the historic manufacturing techniques used to produce the iron-tannate dyed abaca objects in the British Museum's collection.

3.3.2 Proteinaceous textiles

A few studies into the understanding or stabilisation of iron-tannate dyed proteinaceous materials have been reported. These have been on silk and have investigated the degradation of iron-tannate dyed silk or consolidation options (Yanagi, Yasuda and Hirabayashi 1994; Sato and Okubayashi 2010; Garside, Wyeth and Zhang 2010b; Sato, Okubayashi and Sato 2011). Non-aqueous antioxidant/deacidification stabilisation methods have not been investigated. Silk is an important textile to assess within this research study because of the popular method of weighting silks using iron ions and tannins (Hacke 2008). In the British Museum collections, iron-tannate dyed silk is present as the black hair (sugaito) of Japanese hina-dolls (British Museum registration numbers: 2001,1129.1 and 1981,0808.227, Figure 3.1). A scoured degummed silk was chosen to give an efficiently dyed model textile with minimal impurities.



Figure 3.2 An example of a bogolanfini in good condition (British Museum registration number: Af1987,07.9) and a Japanese hina doll with inset image of losses to its silk hair (British Museum registration number: 1981,0808.227) © The Trustees of the British Museum

Wool was chosen as a model textile material because it differs from silk in that it is composed of keratin rather than fibroin. Historic dye manuals confirm that wool (Rosetti 1548; Haigh 1800) was iron-tannate dyed in the past, however, there is little currently identified within the British Museum's collections. Non-collection iron-tannate dyed wool samples from Islamic¹ and British² carpets have been identified in this project (Chapter 6). The botany serge wool is a woven textile that had been dyed at the University of Manchester prior to the project and was in stock as a result.

3.4 Cellulosic model textile properties and reactivity

3.4.1 Cotton

Approximately 50% of the worldwide consumption of fibres is of cotton (Wakelyn, Bertoniere, French, Zeronian, Nevell, Thibodeaux, Blanchard, Calamari, Triplett, Bragg, Welch, Timpa, Goynes Jr., Franklin, Reinhardt and Vigo 1998). Cotton fibres are the seed hairs of the fruit (cotton boll) of trees of the genus *Gossypium*. Grown in warm

¹ Supplied by Anna Beselin, carpet conservator at the Museum of Islamic Art, Berlin.

² Supplied by Heather Tetley, carpet conservator at Tetley Studios, UK.

3.4 Cellulosic model textile properties and reactivity

environments, the major production sites are North and South America, Africa, India, and Asia. *Hirsutum*, *barbadense*, *arboretum*, and *herbaceum* are the four domesticated species of cotton of most commercial importance. Continual development through breeding programmes constantly improves the cotton available to consumers.

Once harvested the cotton bolls are ginned (cleaned) to remove trash and seeds from the fibres. Approximately 750 lbs of cottonseed is produced by ginning for every 500 lbs of fibre produced. Fibre quality and physical attributes of the cotton are assessed during classification and finally sent to textile mills. Fibres of 1 inch or longer are spun into yarn. These are called lint and are located at the base of the cotton seed. Other types of fibres (fuzz and linters) have different properties to lint and are located in different locations to the lint. Fuzz is primarily located towards the top of the seed (Wakelyn, Bertoniere, French, Zeronian, Nevell, Thibodeaux, Blanchard, Calamari, Triplett, Bragg, Welch, Timpa, Goynes Jr., Franklin, Reinhardt and Vigo 1998).

3.4.1.1 Formation

Cotton fibres are long single cells grown from separate epidermal cells on the outer integument of cotton fruit ovules. Mature cotton fibres are hollow, dead, dried cell walls with bean-shaped cross-section and convolutions along their length. These convolutions enable cotton fibres to be spun into yarn (Wakelyn, Bertoniere, French, Zeronian, Nevell, Thibodeaux, Blanchard, Calamari, Triplett, Bragg, Welch, Timpa, Goynes Jr., Franklin, Reinhardt and Vigo 1998). The development of cotton fibres is well documented and is divided into four overlapping stages: initiation, elongation, secondary-wall thickening, and maturation. Fibre lengths are genetically controlled and, depending on genotype, can be 1-6 cm in length. Length-to-width (aspect) ratios of cotton fibres range from 1,000-3,000 with 4,000 occasionally reached by some mature fibres (Hsieh 2007).

3.4.1.2 Chemical composition and fibre structure

Cotton is a highly crystalline, fibrillar and ordered fibre comprising of approximately 90% cellulose I. The molecular weight of the cellulose in cotton is greater than that in any other plant fibres (Hsieh 2007). The cotton fibre is formed from an outer cuticle, primary cell wall, secondary cell wall, lumen cell wall, and lumen.

Cuticle and non-cellulosic materials

The cuticle is essentially a layer of non-cellulosic materials. In cotton, non-cellulosic materials including pectins (0.4-1.2%), proteins (0.7-1.6%), waxes (0.4-1.2%), inorganics

3.4 Cellulosic model textile properties and reactivity

(0.7-1.6%), and other materials (0.5-8.0%) which are present on the cuticle and primary cell wall or in the lumens of cotton fibres. Non-cellulosic content varies with plant variety, maturity, and growing conditions. Increasing fibre maturity coincides with decreasing content of non-cellulosic materials. As a result, the small quantities of these materials are difficult to detect in mature fibres (Hsieh 2007).

The proteins in cotton fibres are primarily located in the lumen as protoplasmic residue but are also found in the primary cell wall. Free amino acids including glutamic acid, aspartic acid, serine, and threonine have been detected in the primary cell wall (Wakelyn, Bertoniere, French, Zeronian, Nevell, Thibodeaux, Blanchard, Calamari, Triplett, Bragg, Welch, Timpa, Goynes Jr., Franklin, Reinhardt and Vigo 1998).

Pectic substances including free pectic acid and insoluble iron, magnesium, and calcium pectates, are located in the primary cell wall.

Cotton wax is a combination of high molecular weight, long chain, predominantly saturated fatty acids and alcohols, resins, sterols, sterol glucosides, and saturated and unsaturated hydrocarbons. The wax is located primarily in the primary cell wall and by acting as a lubricant, aids cotton spinning. However, in addition to pectins, cotton waxes contribute to raw cotton's hydrophobicity (low wettability) which can have negative consequences when dyeing (Wakelyn, Bertoniere, French, Zeronian, Nevell, Thibodeaux, Blanchard, Calamari, Triplett, Bragg, Welch, Timpa, Goynes Jr., Franklin, Reinhardt and Vigo 1998).

Organic acids and inorganic salts are also present in cotton fibres in very low and highly variable quantities. Metal ions originally in the soil are present in cotton fibres. Potassium, magnesium, and calcium are the most prevalent metals with concentrations of 1000-6500 ppm, 400-1200 ppm, and 400-1200 ppm respectively. In addition, iron ions and copper ions are present at levels of 30-90 ppm and 1-10 ppm, respectively (Wakelyn, Bertoniere, French, Zeronian, Nevell, Thibodeaux, Blanchard, Calamari, Triplett, Bragg, Welch, Timpa, Goynes Jr., Franklin, Reinhardt and Vigo 1998).

Hot water soluble phosphorus compounds are present in cotton but these can precipitate out in the presence of alkali earth metals. Use of hard water during scouring is therefore not recommended as it can result in precipitates forming rather than being removed (Hsieh 2007).

Mild alkali scouring and bleaching in preparation for dyeing removes most of these non-cellulosic materials. Once the non-cellulosic materials have been removed from a raw cotton fibre, only cellulose remains (Wakelyn, Bertoniere, French, Zeronian, Nevell, Thibodeaux, Blanchard, Calamari, Triplett, Bragg, Welch, Timpa, Goynes Jr., Franklin, Reinhardt and Vigo 1998).

Primary cell wall

Cellulose constitutes less than 50% of the primary cell walls of cotton fibres (Nevell and Zeronian 1985). Non-cellulosic polymers, uronic acid, various proteins, and neutral sugars are also present in the primary cell wall. The degree of polymerisation (DP) of this cellulose is between 2,000 and 6,000 with a broad distribution of molecular weights (Hsieh 2007). The cellulose is randomly arranged into a criss-crossed network of fibrils. A winding layer is present next to the secondary cell wall as a “lacy” network of helical microfibrils. The primary cell wall and winding layer inhibit outward expansion of the secondary cell wall on swelling making the latter less accessible to damage (Wakelyn, Bertoniere, French, Zeronian, Nevell, Thibodeaux, Blanchard, Calamari, Triplett, Bragg, Welch, Timpa, Goynes Jr., Franklin, Reinhardt and Vigo 1998). Research on the development of cotton fibres suggest that the primary cell wall is 30% crystalline compared to the 70% crystallinity of mature fibres (Hearle 2007).

Secondary cell wall

The secondary cell wall contains 94% of the total fibre material and is essentially pure cellulose (DP approximately 14,000). The molecular weight distribution is more uniform and the cellulose is more crystalline than that in the primary cell wall (Hearle 2007; Hsieh 2007).

During secondary cell wall development, layers of cellulose microfibrils are laid down on the inside of the previously formed primary cell wall at the rate of one layer per day. The fibrils are laid down in spirals with angles (compared to the fibre axis) ranging from 35° to 20° depending on whether the layer is an outer or inner layer, respectively. The angles are constant within each layer until the spiral direction reverses at reversals along the fibre length (Hearle 2007). These reversals can be seen under the primary cell wall as ridges. By maturity, the secondary cell wall is 12-20 µm thick. The thickness of this layer affects the fineness of the fibre (mass per unit length) as well as its strength, reactivity, and dyeability. The degree of thickening of the secondary cell wall is a measure of fibre maturity

(Wakelyn, Bertoniere, French, Zeronian, Nevell, Thibodeaux, Blanchard, Calamari, Triplett, Bragg, Welch, Timpa, Goynes Jr., Franklin, Reinhardt and Vigo 1998).

Lumen

The lumen contains dried protoplasmic residue, is almost as long as the fibre, and takes up approximately 5% of the cross-sectional area of mature cotton fibres. A thin cell wall provides a barrier for the lumen and is in some cases undetectable (Nevell and Zeronian 1985; Wakelyn, Bertoniere et al. 1998).

Pores

Pores and channels are formed during fibre development, and collapse on drying, the extent dependent on the extent of drying. When dry, small pores exist next to areas where the chains are strained, and where the residues and hydroxyl groups are highly disrupted from alignment and orientation. Water molecules are very small and can penetrate these tiny pores, interfering with the intermolecular hydrogen bonding within (Rowland 1977). Scouring, bleaching, and dewaxing all increase the pore size. In cotton, the pores have void volumes of 0.7-3.4%.

3.4.1.3 Cellulose

There are many levels of organisation within the cotton fibre that makes it a complex structure which is still not fully elucidated. There are different types of cellulose (I-IV) but raw cotton contains cellulose I in predominantly the I β form with 10% type I α . Cellulose I β is monoclinic and has two cellulose chains in its unit cell compared to one in the triclinic cellulose I α due to a longitudinal displacement of adjacent sheets of cellulose chains. The mercerisation of raw cotton converts some or all of the cellulose I into cellulose II depending on conditions and concentrations used (O'Sullivan 1997; Wakelyn, Bertoniere, French, Zeronian, Nevell, Thibodeaux, Blanchard, Calamari, Triplett, Bragg, Welch, Timpa, Goynes Jr., Franklin, Reinhardt and Vigo 1998; Jarvis 2003).

Cellulose is a rigid, long, unbranched polymer constructed from β -1,4-D(+)-glucopyranose units linked by 1,4-glucosidic ether bonds (Figure 3.3). Neighbouring glucose residues are rotated 180° to each other around the ether bond to make a repeating cellobiose unit of 1.03 nm in length. Rotation around the C-O-C bonds is restricted by steric interactions.

3.4 Cellulosic model textile properties and reactivity

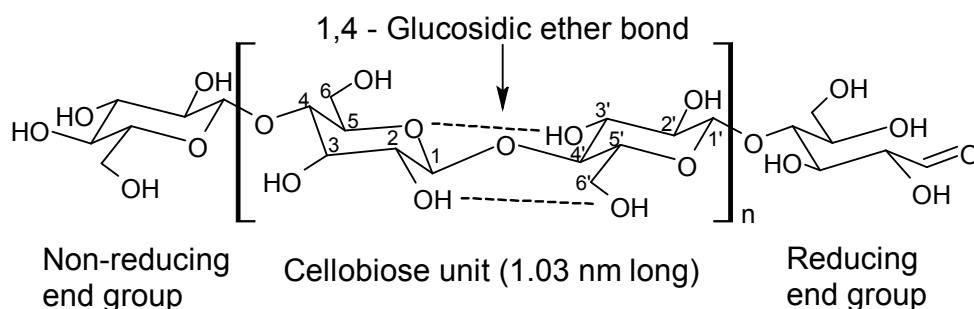


Figure 3.3 The structure of cellulose with intramolecular hydrogen bonds (Hearle 2007; Bruckle 2011)

There are two secondary hydroxyl groups (C-2 and C-3) and one primary hydroxyl group (C-6) per anhydroglucose unit which facilitate widespread inter- and intra-molecular hydrogen bonding (Hearle 2007; Hsieh 2007). In cellulose I β intramolecular hydrogen bonding occurs as shown in Figure 3.3. Hydrogen bonding between the O6-H and O3 of a residue in an adjacent chain also occurs (O'Sullivan 1997; Wakelyn, Bertoniere et al. 1998). The hydrogen bonds in cellulose I are 0.275 nm long (O'Sullivan 1997) however the nature of the hydrogen bonding in cellulose I α is still uncertain (Jarvis 2003).

There is a reducing (O1-H) and non-reducing end (O4-H) within every cellulosic chain (Figure 3.3); a hemi-acetal and hydroxyl group, respectively. While the reducing end is highly reactive the low quantity within fibres makes their contribution to overall reactivity in general minimal (Nevell and Zeronian 1985; Wakelyn, Bertoniere et al. 1998).

Cellulose chains have high strength and modulus when put under tension. There is also high rigidity for in-plane bending but cellulose can be twisted and bent out of the plane. There are a wide range of chain lengths of cotton cellulose but a peak in the distribution of molecular weights at 2×10^5 corresponds to a chain length of 0.5 μ m and molecular aspect ratio of 1000:1 (Hearle 2007). DPs of cotton can exceed 20,000 and most molecular weight values of cotton range between 10^4 and 5×10^6 . Cotton fibres are approximately 3000 times longer than cellulose chains (Wakelyn, Bertoniere, French, Zeronian, Nevell, Thibodeaux, Blanchard, Calamari, Triplett, Bragg, Welch, Timpa, Goynes Jr., Franklin, Reinhardt and Vigo 1998).

3.4.1.4 Microfibrils

Individual cellulose chains hydrogen bond together (0.835 nm apart) to form sheets. Van der Waals forces exist between adjacent sheets (0.79 nm apart) with the chains aligned in the same direction (parallel arrangement). Molecular modelling suggests that Van der

3.4 Cellulosic model textile properties and reactivity

Waals forces are very important in the lattice energy of cotton. Out of a lattice energy of approximately 20 kcal/mol, 17 or 18 kcal/mol are due to the Van der Waals forces, the rest being attributed to hydrogen bonding. Note that CH-O bonds were not included in the calculations (Wakelyn, Bertoniere, French, Zeronian, Nevell, Thibodeaux, Blanchard, Calamari, Triplett, Bragg, Welch, Timpa, Goynes Jr., Franklin, Reinhardt and Vigo 1998). The cellulose chains are packed together into microfibrils, which are further organised into macrofibrils (fibrils). The fibrils are used by the plant to form the cell walls and in a mature fibre the fibril diameter can be 4.22 nm (Hearle 2007).

In some fibres, electron microscopy has identified the presence of elementary fibrils (protofibrils) of cellulose with a periodicity of approximately 3.5-4.2 nm. During formation, the elementary fibrils associate together to form microfibrils with a periodicity of 10 nm. However, the elementary fibril is not confirmed in cotton. Indeed, Jarvis reports that the microfibrils of cotton (*Gossypium* spp.) are made from single crystals 4-5 nm wide with approximately 30% of the chains at the surface (Jarvis 2003). Within these crystalline structures, non-crystalline areas arise from the discontinuities caused by chains ending within the crystalline structure as well as crystallite bending and twisting. In addition, the hydroxyl groups on fibril surfaces can have various orientations which cause disorder and non-uniform hydrogen bonding. Imperfect microfibril packing makes cotton 92.6-94.7% crystalline. However others have calculated the crystallinity as approximately 66% and others as low as 40-45% (O'Sullivan 1997; Wakelyn, Bertoniere, French, Zeronian, Nevell, Thibodeaux, Blanchard, Calamari, Triplett, Bragg, Welch, Timpa, Goynes Jr., Franklin, Reinhardt and Vigo 1998; Hearle 2007).

3.4.1.5 Properties

The properties of cotton vary greatly with type of cotton, location of cotton on the seed, and stage of cotton development (Hsieh 2007). Fibre lengths can vary from 5 cm to 1.5 cm while linear density varies from 1 dtex to 3 dtex for superfine Sea Island cotton to coarse Asiatic cotton, respectively. The cell wall density (i.e. lumen not included) is 1.55 g/cm³ when dry, 1.52 g/cm³ at 65% RH, and 1.38 g/cm³ when wet (Hearle 2007).

Cotton's strength (ability to resist force) originates from the rigid structure of cellulose, the extensive inter-and intra-molecular hydrogen bonding, and its crystalline, ordered structure. Bond strengths, maturity, and crystalline orientation also affect cotton's strength. The collapse of the cell wall and increase in convolution angles on dehydration make dry fibres break at greater strain and lower force than hydrated fibres (Hsieh 2007). Longer, finer

3.4 Cellulosic model textile properties and reactivity

fibres, and those of higher molecular weight with narrow molecular weight distribution are generally stronger than other cotton fibres.

The strength of single fibres is measured as tenacity (stress) which is the force per mass per length of fibre measured in mN/tex or gf/tex where a tex is g/km and gf is grams force. The United States Department of Agriculture's Agricultural Marketing Service (USDA AMS) have described cottons with HVI (high volume instrument) tenacity below 20 g/tex as being very weak and those above 30 as being very strong (Gordon 2007). Tenacities of cotton fibres ranging from 13 to ~32 gf/tex have been reported (Wakelyn, Bertoniére, French, Zeronian, Nevell, Thibodeaux, Blanchard, Calamari, Triplett, Bragg, Welch, Timpa, Goynes Jr., Franklin, Reinhardt and Vigo 1998).

The tenacities of cotton bundles are also measured as they include fibre-fibre interactions. These strengths increase with decreasing spiral angle. The 25° spiral angle of Egyptian cotton relates to 44 gf/tex bundle strength. Coarser cottons with 45° spiral angles are much weaker than Egyptian cottons. Asian cottons which have much shorter fibres than Egyptian cottons have a typical bundle strength of 18 gf/tex (Wakelyn, Bertoniére, French, Zeronian, Nevell, Thibodeaux, Blanchard, Calamari, Triplett, Bragg, Welch, Timpa, Goynes Jr., Franklin, Reinhardt and Vigo 1998).

Individual fibres are on average stronger than bundles of fibres due to the high fibre variability within the bundle. Immature fibres with only a primary cell wall have been found to have one sixth of the strength and half the tenacity of a mature fibre with a secondary cell wall (Hearle 2007).

Increasing humidity increases the strength of cotton but decreases the stiffness while increasing temperature decreases both (Hearle 2007). At 55% RH the tenacity of cotton was 25.8 g/tex while at 75% RH it was 29.1 g/tex (Gordon 2007). The knot strength of cotton is 91% of the tensile strength.

Elastic recovery is the ratio of recovered to total extension of a material after a specified cycle application and removal of force. In cotton, cyclic strain tests show a hysteresis loop. Increasing stress and strain increases the unrecovered extension while increasing the strain lowers the recovery curve to below the elongation curve (Hearle 2007). At 1% extension elastic recovery is 0.9 while it is 0.4 at the elongation at break (approximately 6%).

3.4 Cellulosic model textile properties and reactivity

Applying tension to dry cotton fibres causes the fibre convolutions to be removed. 3.8% extension untwists part of the fibre, 6.8 % fully untwists the whole fibre, and 7.4% breaks the fibre. The helical structure of the fibrils also adds to the extension properties of cotton. In addition, the reversal points of the fibrils untwist, increasing the helix angle and further extending the fibre. The shear stress caused by this moves round the fibre until it reaches the weak point at the boundary between the curved ends and the concave section of the bean-shaped fibre cross-section. At this point the fracture tears across the concave section. Unlike in dry fibres, the fibrils in wet fibres break individually as the inter-fibrillar hydrogen bonds are broken by water (Hearle 2007). The release of internal stresses by water enables the fibre to extend further so that at almost saturation point the elongation at break can be 10% while at low RH it can be only 5% (Wakelyn, Bertoniere, French, Zeronian, Nevell, Thibodeaux, Blanchard, Calamari, Triplett, Bragg, Welch, Timpa, Goynes Jr., Franklin, Reinhardt and Vigo 1998).

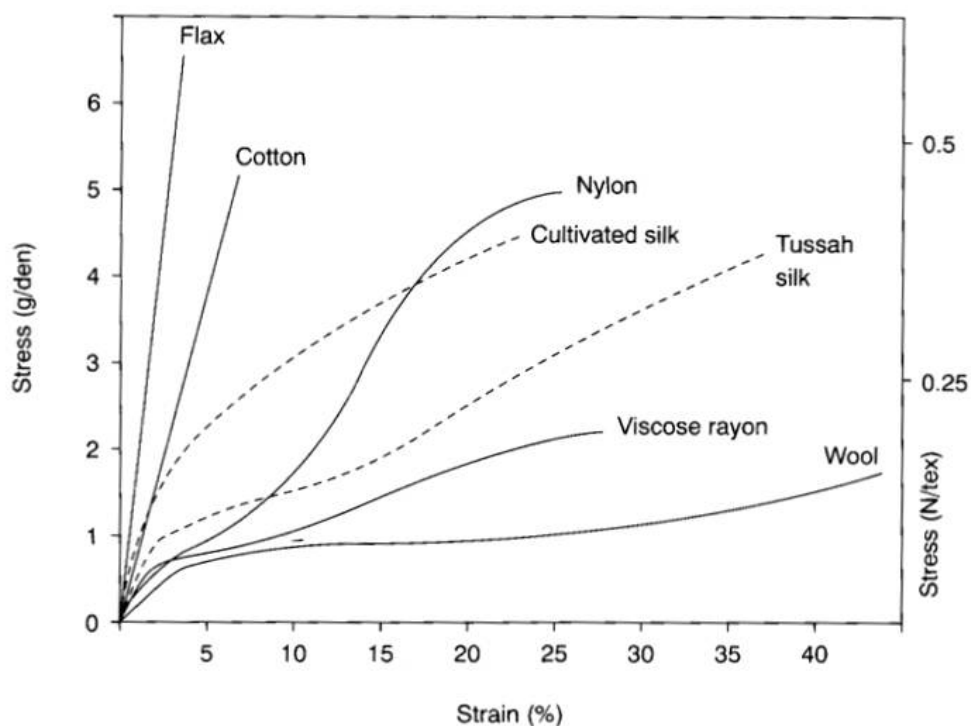


Figure 3.4 Typical stress-strain curves for cotton and other fibres at 20°C and 65% RH (Robson 1985)

The Young's modulus is the ratio of stretching stress per unit cross-sectional area to elongation per unit length. It is affected by the covalent bonding along the cellulose crystals. The initial Young's modulus for cotton ranges from approximately 80 g/den for Sea Island cotton to 40 g/den for Asian cotton. Upon release of a stretching force, the

3.4 Cellulosic model textile properties and reactivity

cotton is plastically deformed and it does not return to its original dimensions (Wakelyn, Bertoniere et al. 1998; Hearle 2007).

Swelling recovery eliminates or reduces the 'permanent' extension remaining after elongation of a dry fibre (Hearle 2007). Cotton has a toughness ranging from 5-15 mN/tex which is increased if it is swollen and dried without tension, but decreased if dried under tension (Wakelyn, Bertoniere, French, Zeronian, Nevell, Thibodeaux, Blanchard, Calamari, Triplett, Bragg, Welch, Timpa, Goynes Jr., Franklin, Reinhardt and Vigo 1998).

Fine fibres of cotton have lower torsional rigidity than coarser fibres. Torsional rigidity is the torque needed to give a unit twist or angular deflection between the ends of a specimen of unit length. Fine Egyptian cottons have a rigidity of 1-3 mN/m² compared to coarser Indian fibres, 7-11 mN/m² (Wakelyn, Bertoniere, French, Zeronian, Nevell, Thibodeaux, Blanchard, Calamari, Triplett, Bragg, Welch, Timpa, Goynes Jr., Franklin, Reinhardt and Vigo 1998). Shear modulus is the modulus of rigidity which is lower in wet than dry cotton fibres due to the bonding of water. As a result, resistance to convolution untwisting is decreased and the shear modulus for both reversal rotation and helical structure extension are decreased (Hearle 2007).

3.4.1.6 Reactivity

As most of the non-cellulosic materials are removed prior to treatments such as dyeing, the reactivity of cotton is essentially that of cellulose and cotton's supramolecular structure (Wakelyn, Bertoniere, French, Zeronian, Nevell, Thibodeaux, Blanchard, Calamari, Triplett, Bragg, Welch, Timpa, Goynes Jr., Franklin, Reinhardt and Vigo 1998). Reactions with oxidising agents and acids are directly of relevance to this research and so are focussed on in this section. Other reactions by cellulose include esterification and etherification which are only very briefly mentioned.

Accessible areas

When dehydrated, cotton fibre reactivity differs around the bean-shaped cross-section due to the forces imparted by this shape. For example, fibrils are packed tighter in regions of spiral reversal and on the highly curved ends of the bean-shaped cross-section. These areas are therefore less accessible to reagents than adjacent areas. The concave and convex areas of the cross-section are less densely packed which makes them more accessible but the concave section is the most accessible and therefore most reactive due to the structure

opening up through the tangential compressive forces it experiences (Nevell and Zeronian 1985; Hsieh 2007).

On a more molecular level, the chemical reactivity of cellulose is dominated by that of the hydroxyl groups. Swelling pre-treatments, reagents, and reaction conditions affect the order of hydroxyl accessibility and total accessibility. The C-6 hydroxyl group in virgin cotton is more reactive than either the C-2 or C-3 while under alkaline conditions the C-2 hydroxyl group is most reactive. Greater reactivity is also found in the hydroxyl groups on the surfaces of fibrils compared to those within fibrils. This is because unlike the cellulose chains on the surfaces of the fibrils, the cellulose chains inside the fibrils are densely packed with hydroxyl groups bound by intra- or inter-molecular hydrogen bonds to neighbouring hydroxyl groups. Consequently the hydroxyl groups inside the fibrils are less accessible and less reactive than those on the surface. Reactions start in the more accessible regions of the fibre, notably the non-crystalline regions such as the surfaces of crystalline areas and intercrystalline areas (Nevell and Zeronian 1985; Wakelyn, Bertoniere et al. 1998; Jarvis 2003; Hearle 2007; Hsieh 2007).

Esterification and Etherification

Esterification reactions include nitration, sulphation, and acetylation and most often occur in acidic conditions. In comparison, etherification often occurs in alkaline conditions (Hsieh 2007).

Oxidation

Oxidising agents such as hypochlorites, peroxides, permanganates, and dichromates attack cellulose readily. The conversion of hydroxyl groups into carbonyl and aldehyde groups (reducing oxycellulose) or carboxyl groups (acidic oxycellulose) is often non-specific. Reduced oxycellulose is more sensitive to chain length-reducing alkali than cellulose and it can be further oxidised to acidic oxycellulose (Hsieh 2007). Aldehydes have much stronger reducing powers than ketones (Wakelyn, Bertoniere, French, Zeronian, Nevell, Thibodeaux, Blanchard, Calamari, Triplett, Bragg, Welch, Timpa, Goynes Jr., Franklin, Reinhardt and Vigo 1998).

Among other routes, heat, light, and oxygen can initiate autoxidation of cellulose. Free radicals are produced which can form peroxy and later, hydroperoxy radicals. The latter are particularly reactive, initiating a chain reaction in which hydrogen abstraction, peroxide formation on the cellulose chains, and peroxide decomposition become just some of the

3.4 Cellulosic model textile properties and reactivity

propagation routes. Recombination of radicals and the presence of inhibitors such as radical scavengers lead to free radical termination pathways. Recombination of two radicals in separate cellulosic chains results in crosslinks between the chains which can increase the brittleness of the fibres (Strlic and Kolar 2005).

Oxidised cellulose is sensitised towards β -elimination chain cleavage which decreases the DP and therefore strength of cellulose. Chain cleavage can also occur directly through the formation of a C-1 radical (Fellers, Iversen, Lindstrom, Nilsson and Rigdahl 1989).

Acid treatment

Mineral acids such as H_2SO_4 , HCl and HNO_3 swell or dissolve cellulose at different concentrations. Swelling begins above 50% concentration in H_2SO_4 solutions while at 60% concentration cellulose is randomly hydrolysed into small molecular-weight (MW) fractions. Temperature, acid concentration, and treatment time affect the extent of hydrolysis which causes severe loss in mechanical strength (Batra 1998a).

During hydrolysis, glycosidic bonds are broken which results in a decrease in DP and tensile strength and an increase in aldehyde content due to the formation of a further terminal reducing functionality with each scission. The mechanism involves initial protonation of the glycosidic O (step 1) followed by breaking of the bond to form a carbonium ion (step 2). Nucleophilic attack of the carbonium ion by a hydroxide ion stabilises the residue (step 3). Step two in this three step mechanism is the rate determining step (Wilson and Parks 1979; Feller, Lee and Bogaard 1986; Wakelyn, Bertoniere, French, Zeronian, Nevell, Thibodeaux, Blanchard, Calamari, Triplett, Bragg, Welch, Timpa, Goynes Jr., Franklin, Reinhardt and Vigo 1998).

The rate of acid hydrolysis goes through three stages. Initially the rate of hydrolysis is very fast (10,000 times faster than the rate of stage two) due to 'weak links' in the structure. These weak glycosidic bonds are under unusually large stress which has developed during polymer formation. In addition it is possible that weak links arise from oxidation products within the cellulose chain. Glycosidic bonds with neighbouring carbonyl or carboxyl groups are weaker than those with adjacent hydroxyl groups. Once all of these bonds have been broken, random hydrolysis in the accessible non-crystalline regions occurs. Finally, the crystallites are attacked (Fellers, Iversen et al. 1989; Wakelyn, Bertoniere et al. 1998; Strlic and Kolar 2005).

Alkali treatment

Glycosidic bonds are fairly stable in neutral and alkaline conditions, requiring high temperatures or strong alkali before β -alkoxy elimination occurs. However, if oxidised groups (alkoxy-carbonyl groups) are present in the cellulose, β -alkoxy elimination can occur at low temperatures and in mild alkali. Consequently, alkaline hydrolysis can become a major degradation mechanism in cellulosic materials that have been strongly deacidified (Wilson and Parks 1979; Bicchieri and Pepa 1996; Daniels 1996).

β -alkoxy elimination occurs when there is an electron-withdrawing group in the β position to an ether group and when the α -carbon atom has an acidic hydrogen atom. This acidic hydrogen atom is removed by the base which initiates the elimination of the alkoxy group and cleavage of the ether bond resulting in the formation of an unsaturated product. The transformation of the C-1 aldehyde group on the unsaturated product by the Lobry de Bruyn-Van Eckenstam transformation into a C-2 ketone enables the elimination process to start again. The resulting 'peeling reaction' stops when a crystalline region is reached or the chain is fully depolymerised. The peeling reaction occurs when there is a carbonyl group at the C-6 or C-2 position but not at the C-3 position which forms saccharinic acid (Daniels 1996; Wakelyn, Bertoniere et al. 1998).

Mercerisation using sodium hydroxide causes cotton to swell. Swelling results in a more circular fibre cross-section, decreased lumen size, and fewer convolutions. Crystallite lengths are reduced by this treatment, increasing moisture regain but decreasing crystallinity. Higher concentrations of sodium hydroxide enable the crystalline regions to be attacked as well as the amorphous regions because the sodium ions are less hydrated. Varying degrees of conversion of cellulose I to cellulose II can occur as previously mentioned (Wakelyn, Bertoniere, French, Zeronian, Nevell, Thibodeaux, Blanchard, Calamari, Triplett, Bragg, Welch, Timpa, Goynes Jr., Franklin, Reinhardt and Vigo 1998).

Moisture adsorption

Moisture regain is the mass of adsorbed water:oven-dry mass of fibre (%). Moisture content is the mass of adsorbed water:total fibre mass (%).

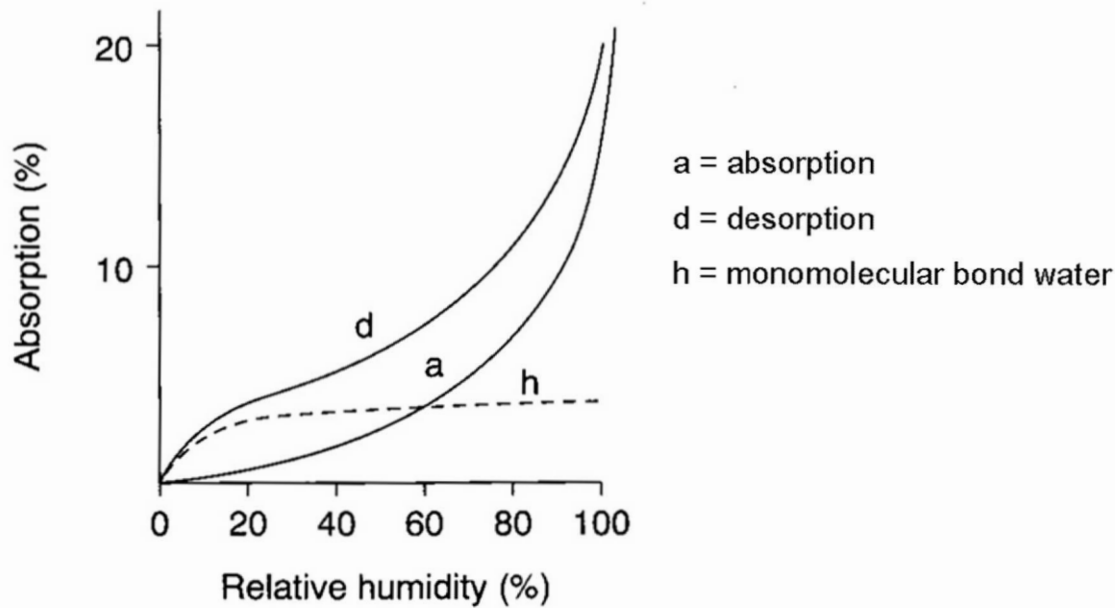


Figure 3.5 The absorption and desorption of moisture by cellulose with changing RH at 25°C (Timar-Balazsy and Eastop 1998) p.15

The regain-RH curve for cotton is a hysteresis curve in which the equilibrium regain during desorption is higher than during adsorption (Figure 3.5). The adsorption regain of cotton at 20°C and 65% RH is 7-8% while the desorption regain is 0.9% more. A regain of 8.5% is recommended when calculating the mass of cotton for commercial purposes (Hearle 2007). Morton and Hearle provide a concise molecular explanation for the hysteresis (Morton and Hearle 1997). Dry fibres have crosslinks in non-crystalline areas where chains are close to one another. In a completely wet fibre, the cross-links are broken having been replaced by water and the chains are relatively far apart. Active sites become free with either the breaking of cross-links or evaporation of water and these new active sites will quickly form a new bond; either a hydrogen bond with water or a cross-link. Clearly, the closer the chains are together, the more likely the new bond will be a cross-link. The cross-links found in drier fibres keep the chains closer together than in hydrated fibres and as such cross-links are more likely to form in the drier fibre than water adsorption. Therefore, in the same atmosphere, an initially dry cotton sample will retain more cross-links than an initially wet sample, resulting in a hysteresis.

3.4 Cellulosic model textile properties and reactivity

Moisture regain is affected by temperature so that up to 85% RH, increasing the temperature from 50°C to 110°C at a specific relative humidity results in a decrease in the moisture regain of cotton. At 20% RH, this reduction is 0.9% which doubles to 1.8% at 70% RH.

The principal direction of swelling in cotton fibres on adsorption of moisture is in the transverse direction. Values between 7% and 23% diameter swelling of cotton from dry to wet fibres have been quoted by researchers (Hsieh 2007). The first water molecules adsorbed by dry fibres hydrogen bond to available hydroxyl groups in the inter-crystalline areas and on the surface of the crystalline regions. While hydroxyl groups are on the surface of the crystallites, the O of the glycosidic bond is half a molecule lower in the surface of the crystallite making it inaccessible (Wakelyn, Bertoniere et al. 1998; Hearle 2007). These directly bound water molecules are held close to the cellulose structure so that the fibre volume increase due to this water is less than that of the same quantity of liquid water. Consequently, fibre density increases during this phase of water adsorption. Later water molecules bind either directly, to the remaining available hydroxyl groups on the crystallite surfaces, or indirectly, to directly bound water molecules. Indirect hydrogen bonds are weaker than direct hydrogen bonds. The water molecules now pack similar to liquid water and the volume increase becomes the same as liquid water. Density decreases during this phase. In total, three layers of water molecules form in the amorphous regions before water is held by capillary forces in pores of 110 nm at 99% RH (Morton and Hearle 1997; Wakelyn, Bertoniere et al. 1998; Hearle 2007).

Heating

Heat can cause dehydration and depolymerisation. The extent of each and which one predominates depends on the temperature, heating rate, and presence of acid or alkali catalyst. Dehydration is favoured in the presence of acid catalysts while depolymerisation is favoured with alkali catalysts. Low temperatures favour dehydration and increases charring while higher temperatures release volatile compounds from the fibre. Heating cotton to 120°C doesn't affect the strength of the fibre though there is a slight increase in carboxyl and carbonyl groups and a slight lowering of DP (Wakelyn, Bertoniere, French, Zeronian, Nevell, Thibodeaux, Blanchard, Calamari, Triplett, Bragg, Welch, Timpa, Goynes Jr., Franklin, Reinhardt and Vigo 1998). At 150°C the fibre tensile strength and molecular weight decrease (Hsieh 2007).

3.4 Cellulosic model textile properties and reactivity

During dehydration, inter-molecular water from the cellulose, and water from the lumen is removed. The former causes the formation of inter-molecular hydrogen bonds while the latter causes the collapse of the fibre. Dehydrated mature cotton fibres have a bean-shaped cross-section and are twisted along their length. There can be 3.9 to 6.5 twists per mm of fibre and the twist direction reverses one to three times per mm. Spiral reversals are linked to the spiralling microfibrils in the secondary cell wall which are visible as ridges underneath the primary wall. The angle of these microfibrils with respect to fibre axis differs during development of the fibre until angles of 20-30° are achieved in maturity. Dehydration of cotton fibres can result in crimp, 11 to 13 per cm in some cases, due to variations in forces on drying (Hearle 2007; Hsieh 2007).

The extent of dehydration affects the way in which the fibres fracture. Breaks occur in the areas adjacent to reversals but they start in the line of weakness along the boundary between the concave area and the highly curved ends of the bean-shaped cross-section (Hearle 2007).

Heat can also initiate oxidation through the scission of bonds to form radicals and cause cross-linking between cellulose chains via a condensation reaction between two hydroxyl groups from different chains. Cellulose that has been exposed to light is more sensitive to thermal degradation due to the presence of activated chemical bonds and reactive compounds such as hydroperoxides. Small molecules such as carbon dioxide, carbon monoxide, and water can be released during thermal degradation due to the scission of covalent bonds (Timar-Balazsy and Eastop 1998).

Photodegradation

The strong covalent bonds in cellulose cause cellulose to strongly absorb UV light below 200 nm. Slight absorption is seen between 200 and 300 nm and very weak absorption (due to reducing end groups) occurs up to 400 nm. The absorption of light causes homolytic scission of bonds of energy equal to that absorbed and forms radicals. Direct photolysis of cotton can occur by the absorption of 254 nm radiation by an unknown species. This degradation is independent of the presence of oxygen. Substances such as dyes and metal oxides can cause photosensitised degradation of cotton by absorption of light above 310 nm. The excited states of these substances cause the degradation of cellulose which is dependent on oxygen (Wakelyn, Bertoniere, French, Zeronian, Nevell, Thibodeaux, Blanchard, Calamari, Triplett, Bragg, Welch, Timpa, Goynes Jr., Franklin, Reinhardt and Vigo 1998).

3.4 Cellulosic model textile properties and reactivity

The radicals formed from homolytic scission of covalent bonds can cause oxidation of the cellulose (photo-oxidation). This can oxidise the hydroxyl groups on the cellulose to form carbonyl and carboxyl groups and can also cause scission of the glycosidic ether bonds (some of the possible oxidation products are shown in Figure 3.6). Photo-oxidation therefore increases the acidity of the cotton, increases its susceptibility to alkaline degradation (through introduction of carbonyl groups), and decreases the DP of the cellulose and therefore decreases the tensile strength of the cotton. The reducing power and solubility of the cellulose are also increased on photo-oxidation (Timar-Balazsy and Eastop 1998; Wakelyn, Bertoniere, French, Zeronian, Nevell, Thibodeaux, Blanchard, Calamari, Triplett, Bragg, Welch, Timpa, Goynes Jr., Franklin, Reinhardt and Vigo 1998).

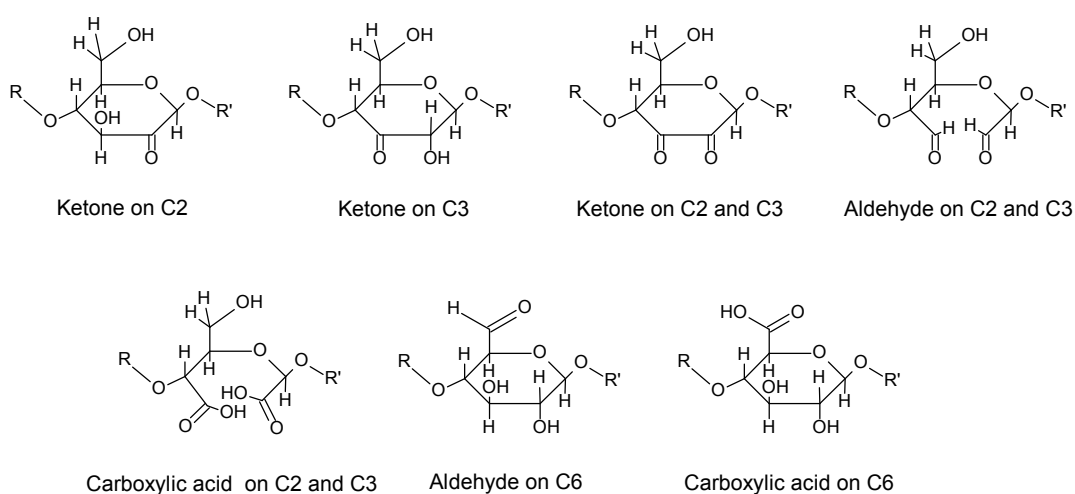


Figure 3.6 Possible oxidation products of hydroxyl groups on anhydroglucose in cellulose (Timar-Balazsy and Eastop 1998)

3.4.1.7 Cotton dyeing

Cotton can be dyed as fibre, yarn, or fabric. Best dyeing results are obtained by removing impurities and non-cellulosics using techniques such as mercerisation, desizing, and scouring prior to dyeing. Mature fibres are favoured because immature fibres tend to dye unevenly and have high numbers of breaks and faults in spinning and weaving (Wakelyn, Bertoniere, French, Zeronian, Nevell, Thibodeaux, Blanchard, Calamari, Triplett, Bragg, Welch, Timpa, Goynes Jr., Franklin, Reinhardt and Vigo 1998).

There are many types of dyes which can be used on cotton including azoic, direct, reactive, vat, and sulphur dyes. With the exception of reactive dyes, all of the above dyes bind to cotton by interchain hydrogen bonding and Van der Waals forces. Reactive dyes form covalent bonds with the C6 hydroxyl groups. Sulphur and vat dyes have a more

3.4 Cellulosic model textile properties and reactivity

complicated dyeing procedure than most dyes because the initial dye is usually insoluble in water and conversion to the soluble leuco form of the dye is required prior to dyeing. At this stage, the dye can penetrate into the fibres at which point the dye can be re-oxidised back to its insoluble keto form inside the fibre. These dyes are therefore trapped in the fibres by the end of the procedure. Basic dyes are not usually used on cottons.

Pigments are insoluble in water whereas dyes are, at least at some stage in the dyeing process, soluble in water. Pigments can be used to colour cotton but a polymeric binder is required to adhere the pigment to the fibre. Colouration can be achieved by batch exhaustion, printing, and padding application methods.

Hemicelluloses are virtually absent from cotton but play an important role in dyeing in cellulosic materials such as jute and possibly also abaca which have higher hemicellulose contents (Deo and Desai 1999).

When dyeing with black tea and metal mordant including iron and copper, Deo and Desai noted that a dyebath at pH 4 produced the deepest shade of dye. The shade decreased with increasing pH. It was postulated that this could be due to tea compounds acting as a cationic dye in acidic conditions (Deo and Desai 1999).

3.4.2 *Abaca*

The abaca plant (*Musa textilis*) is a member of the Musaceae family of plants which also includes the banana tree (*Musa sapientum*). Indigenous to the Philippine Islands where there are 200 varieties (Jarman 1998), abaca has been used by the native population to make textiles for centuries. Exportation to the West began in the early 19th century as abaca's superiority over hemp in the areas of marine cordage and hawsers became known (Cook 1993a). The English and Americans gave abaca its alternative name 'manila hemp' in the 1880s. However, this is a misnomer as abaca is a hard fibre while hemp is soft (Batra 1998a).

Today abaca is produced predominantly in the Philippines and Ecuador as well as being grown in other South-east Asian countries. In 2007, 60,000 tonnes of abaca was produced in the Philippines and 10,000 tonnes in Ecuador. In addition to being used for ropes, twine, netting, and sack cloth, abaca is pulped to make high quality writing paper, tea bags, and Japanese yen bank notes (30% abaca). Abaca's high tensile strength has enabled it to be used as a strengthening composite material for under floor panelling in some Mercedes-Benz A-class cars (FAO UN 2009). In addition, abaca has replaced the carcinogenic and often banned asbestos (Armecin and Gabon 2008).

3.4.2.1 *Abaca plant*

Abaca is a fast growing plant between 5 and 10 m tall which can be harvested in 18 months. In a mature plant, 12-30 stalks exist in a cluster. The stalks can be at different stages of development to each other and 2.5 to 6 m tall. Each stalk is formed from 12-25 overlapping leaf sheaths around a core that originates from the fleshy central core of the plant. Only the central sheaths extend to the top of the stalk so that the stalk is wider at the base (15-30 cm diameter) than at the top (typically less than 5 cm). The stalk transports water and nutrients from the roots to the leaves (Batra 1998a; Armecin and Gabon 2008). 90% of the stalk is water and sap, 2-5% is fibre, and 8-5% is soft, cellular tissue. The sheaths narrow along their length until they form a point. The top of this narrowed part forms the central stem of leaf-like foliage (fronds) when it unfurls from the stem. The fronds can be 1-2 m long and almost 0.3 m wide. At maturity, the sheath formation ends and the core of the stalk continues to grow to form the flower spike prior to flowering. After flowering the abaca plants produce approximately 80 mm long inedible banana-like fruits (Saleeby 1915; Batra 1998a).

3.4 Cellulosic model textile properties and reactivity

Each sheath contains three layers; the outer, middle, and inner layers. The outer layer includes the epidermis and consists of bundles of fibres distributed in a matrix of soft tissue. The middle layer contains fibrovascular tissue which transports water, and the inner layer is made from soft, cellular tissue (Batra 1998a).

3.4.2.2 Fibre production

Abaca fibre is a leaf fibre that can be removed manually (stripping) or mechanically (decortication) from the sheath. The first stage of stripping involves desheathing the stem/stalk of the abaca plant and flattening the sheaths. The sheaths are cut from the bottom of the plant and the leaves (fronds) are removed. A knife is used to cut between the outer and middle layer of a sheath enabling a strip (tuxy) 50-80 mm wide to be pulled from its length. Tuxying continues until all fibre has been removed from the sheath. Scraping of the tuxies by pulling between a wooden block and serrated knife (400-2000 serrations/m or no serration) under large pressure removes residual pulp. Larger serration density or no serration produces the finest fibres. The Hagotan machine can scrape 6-8 times as many tuxies as people (Cook 1993a; Jarman 1998; Batra 1998a). Spindle stripping machines are available instead of manual stripping of the tuxies (Jarman 1998).

Decortication machines such as the Krupp or Robey convert fresh stalks into bundles of sorted abaca fibres via a conveyor belt, crushing press, crushing rollers, rope belt and decorticator. While decortication results in less waste than stripping, the fibres produced suffer processing damage and are not as lustrous or strong as stripped fibres (Batra 1998a).

The quality and quantity of the abaca fibre obtained from the sheaths depends on their location within the stem and their width. Fibres up to 3 m long can be obtained. Four grades of fibre are obtained from sheaths within four sheath groups; the outside, adjacent-to-outside, middle, and inner sheaths. Fibre colour, colour uniformity, handling, cleanliness, and drying method also factor into the grading of abaca fibres with the best grades being for light beige fibres that are fine, very strong, and lustrous (Batra 1998a; FAO UN 2009).

3.4.2.3 Fibre structure

In comparison to wool, silk, and cotton, research into the structure and composition of abaca is relatively sparse. The data in this section comes primarily from Batra who compiled data about abaca and other long vegetable fibres from many sources (Batra 1998a). The results of other more recent articles are also reported including a particularly

thorough investigation into the chemical composition of abaca (Del Rio and Gutierrez 2006).

Unlike cotton fibres which are single-cell systems, abaca fibres are composed of aggregates of polygonal-shaped ultimates (multiple cells). In multiple-cell systems such as this, natural polymers such as resins, gums, middle lamella, and cementing and encrusting materials bind the ultimates together to form the aggregate. The aggregates in abaca are typically surrounded by a layer of silica filled stegma cells which remain as residue on burning. The ultimates in these aggregates have large oval to circular lumen and occasionally, thin cell walls. The ultimates are smooth and lustrous in length with tapering ends similar to individual abaca fibres (Cook 1993a; Batra 1998a). Abaca fibres produced using a range of manual and mechanical extraction methods were found to have fibres between 4.14 and 5.05 mm long and 18.56 – 21.69 μm diameter. A lumen between 9.46 and 13.21 μm wide, and a cell wall between 3.28 and 5.11 μm thick were also detected (FAO/CFC/UNIDO/FIDA c2004). X-ray diffraction has highlighted a prevalence of helical fibrils in the Musa fibres and estimates the spiral angle of abaca to be 22.5° (Batra 1998a).

Abaca fibre crystallinity has been reported as being 52%. This increased with alkali treatment to 62% due to the removal of amorphous lignin and hemicellulose during the treatment.

3.4.2.4 Composition

Table 3.2 Composition of abaca fibre

Reference	Abaca fibre composition (%)						
	Cellulose	Hemicellulose	Lignin	Pectin	Water solubles	Fat and waxes	Moisture
(Batra and Turner 1998b)	63.2	19.6	5.1	0.5	1.04	0.2	10.0
(Kelley, Rowell, Davis, Jurich and Ibach 2004)	62.5	12 (xylose only)	8.0				
(Sun, Fang, Goodwin, Lawther and Bolton 1998; Sun, Fang, Goodwin, Lawther and Bolton 1998)	60.4-63.6	20.8	7.6-8.5	0.8	4.9 (hot water soluble)		
(Cook 1993a)	~77.0		~9.0				0.0
(FAO/CFC/UNIDO/FIDA c2004) ^a	61.95-64.69	14.49-17.64	8.44-9.86		1.14-2.05 (hot water soluble)		

Note for Table 3.2:

a. Range of values dependent on method of production.

3.4 Cellulosic model textile properties and reactivity

The composition of abaca from a variety of sources is presented in Table 3.2. Unlike for cotton, abaca contains a significant amount of hemicellulose and lignin which can affect the reactivity of the fibre compared to cotton.

Hemicelluloses are low molecular weight (100-200 DP), branched polysaccharides (often heteropolysaccharides) that are present in the cell wall and middle lamella of some plant fibres. Hemicelluloses are hygroscopic and amorphous and increase the flexibility of fibres due to the quantity of water they can bind (Timar-Balazsy and Eastop 1998).

Approximately 21% of abaca is hemicellulose, and the major monosaccharide is xylose. Smaller quantities of glucose, arabinose, uronic acids, galactose, mannose, and trace amounts of rhamnose (Figure 3.7) were detected in hemicellulose extracts in varying amounts depending on the extraction method.

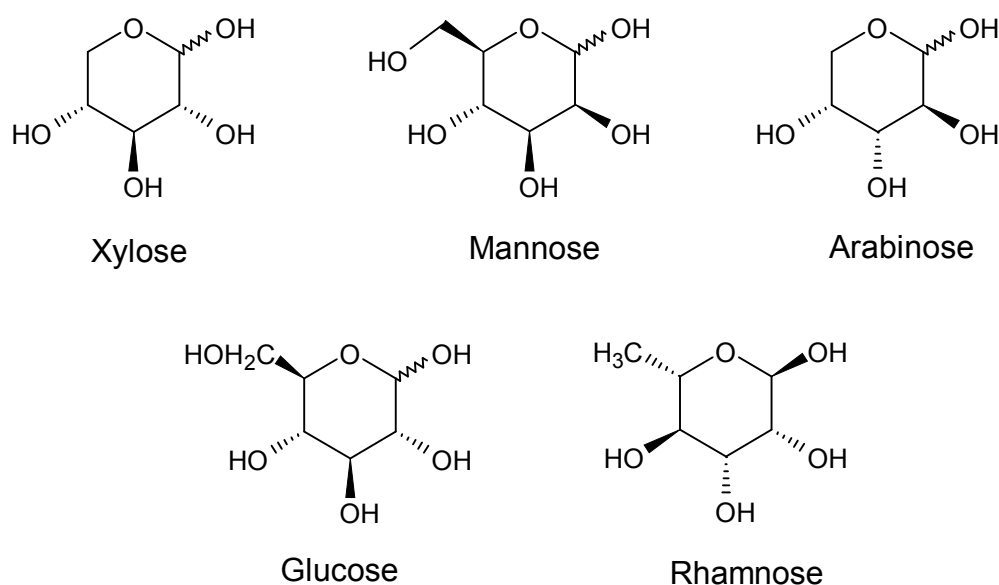


Figure 3.7 Some of the monosaccharides present in the hemicellulose of abaca

FTIR results corroborate the implications from compositional data that the major components of the hemicelluloses in abaca are arabinoxylan, glucoxylan, and/or xylan. The molecular average weights varied from 75,000 to 227,000 depending on extraction method. 5.6% of the 20.8% of the hemicellulose in abaca is soluble in 1% NaOH while 15.3% is isolated using 17.5% NaOH. Some of the hemicellulose has been shown to be closely associated with the surface of the cellulose since despite extraction with 17.5% NaOH and subsequent acid hydrolysis of the extract, xylose (1.75 – 2.40%), mannose (0.1 -1.18%), arabinose (0.1-0.37%), and trace amounts of rhamnose and galactose remained, along with 96.04 – 98.00% glucose (Sun, Fang, Goodwin, Lawther and Bolton 1998; Sun, Fang, Goodwin, Lawther and Bolton 1998).

Lignin is a complex structure that is still not fully understood. It is thought to be a hydrophobic, rigid, acidic, and amorphous network of polymers of phenolic alcohols and is present in the middle lamella and cell wall of 'woody fibres' (Timar-Balazsy and Eastop 1998). Between 5 and 9% of abaca has been identified as lignin (Table 3.2) and 67.7-73.9% of this has been shown to be syringyl lignin units. Syringyl units link the majority of hemicellulose to lignin in hemicellulose-lignin complexes in the cell wall. Small amounts of the hydroxycinnamic acids *p*-coumaric acid and ferulic acid are also present which form linkages between polysaccharide chains and lignin via ester and ether bonds, respectively. The content of *p*-coumaric acid is exceptionally high in abaca compared to in other monocotyledons such sisal, and is significantly greater than that of ferulic acid in abaca (Sun, Fang, Goodwin, Lawther and Bolton 1998; Del Rio and Gutierrez 2006; Del Rio, Gutierrez, Rodriguez, Ibarra and Martinez 2007). A study into the structure of lignin in abaca has been undertaken using 2D NMR (Martinez, Rencoret, Marques, Gutierrez, Ibarra, Jimenez-Barbero and del Rio 2008).

Pectin is usually located in the cell wall and middle lamella of cellulosic fibres and accounts for less than 1% of abaca fibres. The main component of pectin is pectic acid (Figure 3.8), a polymer of D-galacturonic acid monomers linked by 1,4-bonds. Some of the C5 carboxylic acid groups in pectin exist as water insoluble salts with magnesium or calcium while others exist as methyl esters. Water-soluble pectin is often removed from fibres during processing (Timar-Balazsy and Eastop 1998).

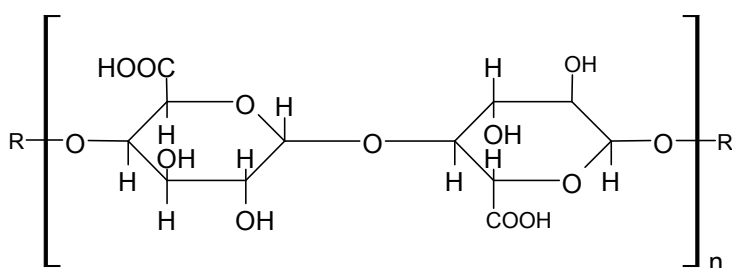


Figure 3.8 The structure of pectic acid

A detailed study into the 0.51% of lipophilic extracts (non-polar extracts) from abaca fibre (Marques, del Rio and Gutierrez 2010) identified the presence of fatty acids (9 mg per 100 mg of extract), steroid hydrocarbons (3 mg/100 mg), steroid ketones (4 mg/100 mg), free sterols/triterpenols (25 mg/100 mg – mainly sitosterol and 7-oxositosterol), sterol glycosides (2 mg/100 mg), and sterol/triterpenol esters (1 mg/100 mg).

3.4.2.5 Mechanical properties

The multicellular nature of abaca means that the mechanical properties are influenced by the interaction between the middle lamella substances and the ultimate fibres. Data for various mechanical properties from a variety of sources are presented in Table 3.3.

Table 3.3 Properties of abaca

Property	Value from references		
	(Batra 1998a)	(Jarman 1998)	(FAO/CFC/UNIDO/FIDA c2004)
Crystallinity of untreated abaca (%)	52		
Degree of Polymerisation	1990		
Porosity (%)	17-21		
Apparent density (g/cc)	1.2, 1.1		
True density (g/cc)	1.45, 1.40		
Linear density (Tex)		4.2-44.4	
Specific heat (cal/g/°C)	0.322		
Volume swelling in water (%)	42.2		
Absorption regain (%) at 65% RH and 20°C	9.5		
Difference between desorption and absorption regains at 65% RH and 20°C	-		
Tensile strength (kg/sq.mm)		140, 85	
Tensile strength (kgf/g.m.)			32.58-51.95
Extension at break (%)	2.5-2.7	8.0, 7.8	
Elongation (%)	2-4.5		2.39-5.39
Fineness (d-tex)	42, 319, 414		
Tenacity (g/d-tex)	3.6, 6.8, 5.5		
Work of rupture	-, 0.77, 0.09		
Fineness (km/kg)	32		
Breaking length (km)	32-69		
Modulus of Rupture (nM/tex)	6		

Stress-strain curves of abaca are steep and linear. Small initial extensions of long vegetable fibres such as abaca lead to high fibre recovery. After repeated loading and unloading, abaca retained significant levels of tenacity (breaking stress) and showed only small levels of permanent set and hysteresis loss (Batra 1998a).

Knotting and unknotting abaca results in a minimal decrease in breaking strength and is greater for wet than dry abaca fibres. Tenacity is lost when twisted rather than untwisted abaca is stretched. The knot efficiency (ratio of knot tenacity:straight tenacity) of abaca drops to 22.4% i.e. tenacity when knotted is approximately one fifth of that when straight. In these experiments abaca broke at 2.65% extension when straight and 2.70% after knotting and unknotting.

2.5 years of dry storage of abaca at 20°C led to the % elongation to rupture decreasing by a quarter and tenacity (g/den) decreasing by an average of 4.2%.

3.4.2.6 Reactivity

Moisture absorption, desorption and swelling

As in cotton, water molecules hydrogen bond to the hydroxyl groups on the carbohydrate fractions of abaca. In dry fibres, the first molecules bind directly to the hydroxyl groups while subsequent water molecules bind to other hydroxyl groups or bound water molecules. The tight packing of carbohydrate chains in the crystalline regions of cellulose prevents absorption of water molecules. Moisture absorption occurs primarily in the amorphous regions of cellulose. The interaction of moisture with abaca is more complicated than that with cotton because abaca also contains hemicelluloses, polyuronides, and lignin. The amorphous nature of the first two of these compounds increase abaca's moisture absorption ability; hemicellulose is more hygroscopic, and therefore swells more than cellulose. However, lignin's hydrophobicity decreases the moisture absorption ability of abaca. Layers of lignin close to the fibre surface and inside the inner middle lamella of bast, seed, and leaf fibres, impedes moisture diffusion into the cell walls. (Timar-Balazsy and Eastop 1998; Batra 1998a). However, the hydrophobicity of lignin decreases with age and degradation and so moisture absorption ability of abaca may increase with age.

Abaca's 9.5% absorption regain at 65% RH and 20°C is comparable to that of cotton (7-8%) and mercerised cotton (8-12%). It is more than scoured cotton, 6%, but less than scoured wool, 14%.

Alkali

The complicated structure of leaf and bast fibres makes their reactivity more complex than that of pure cellulose. The extent of degradation/modification depends on the different reactivity's of the different components of the middle lamella and the changes in structure as treatments continue.

Hemicelluloses which form the majority of the middle lamella are dissolved in alkali. Depending on the concentration, temperature, and extraction time, approximately 44 – 94% of the total hemicelluloses, and approximately 17 – 31% of total lignin in abaca can be dissolved in sodium hydroxide. Treatment of abaca with dilute alkali has been shown to cause preferential removal of small molecular chains from hemicellulose to leave hemicelluloses with molecular average weights of 75,000 – 130,000 while treatment with

3.4 Cellulosic model textile properties and reactivity

strong alkali caused dissolution of larger hemicelluloses resulting in molecular average weights of 123,000 – 227,000 (Sun, Fang, Goodwin, Lawther and Bolton 1998). The breakage of structure stabilising chemical linkages enables the fibre to swell. Swelling opens the structure further which then enables the alkali to act deeper. In dilute alkali the interfibrillar and intercrystalline regions are accessible and so swell. Swelling in the interfibrillar regions causes changes in the crystal structure of the fibres (Batra 1998a). Fibres of abaca can be separated from strands by boiling in alkali (Cook 1993a).

Between 15.78 and 22.40% of abaca fibres stripped using a variety of methods dissolved in 1% NaOH while only 1.14-2.05% dissolved in hot water, and 0.72-3.05% dissolved in alcohol-benzene (FAO/CFC/UNIDO/FIDA c2004).

Acids

Hemicellulose reacts similarly to cellulose but faster than cellulose due to the greater accessibility of the polymer chains arising from its amorphous nature. Consequently, hemicellulose can undergo acid hydrolysis and be broken down into its monosaccharides. These can then form coloured compounds that discolour the fibres or acidic compounds that increase the rate of acid hydrolysis, or even compounds with functional groups that can form free-radicals easily, thus contributing to the oxidation of the fibre (Timar-Balazsy and Eastop 1998). Gradual hydrolysis of cellulose and xylose occurs in organic acids such as formic, oxalic, tartaric, and acetic acids when the temperature is increased (Batra 1998a).

Lignin is naturally acidic due to the phenols in its structure and is therefore resistant to acid. Consequently, unless mechanical action is involved, it can maintain the fibrous structure of the fibres when all cellulose and hemicellulose has been degraded, e.g. in strong aqueous sulphuric acid (Batra 1998a).

Bleaching

A typical two stage bleaching process involves sodium chlorite followed by hydrogen peroxide. Hemicelluloses are dissolved and lignin is removed. Consequently, bleached fibres can be up to 25% lighter in weight and weaker than unbleached fibres (Batra 1998a).

Photosensitivity

Oxidation of the cellulose, hemicellulose, and lignin in abaca fibres can be initiated by light, particularly UV. This causes the breakdown of the polymers into their respective monomers which can form coloured or acidic products (Timar-Balazsy and Eastop 1998).

3.5 Proteinaceous model textile properties and reactivity

Lignin is particularly sensitive to light as it contains chromophores that give lignin its yellow colour and that enable photo-oxidation to be rapid in ambient conditions. Photo-oxidation of lignin causes yellow/brown discolouration and an increase in acidity and increase free-radical content (Timar-Balazsy and Eastop 1998; Batra 1998a).

3.5 Proteinaceous model textile properties and reactivity

3.5.1 Wool (Maclaren and Milligan 1981; Cook 1993; Jones, Rivett et al. 1998; Hocker 2002)

Wool refers not only to all animal hair but more specifically to that produced by domesticated sheep (Hocker 2002). Raw wool can contain up to 50% contaminants such as suint, dirt, wool wax, vegetable matter and sand. Suint is dried sweat secreted by the subiferous glands of the sheep and contains water soluble carboxylic acids and their salts. Wool wax is secreted by the sebaceous glands of the sheep and contains hydrophobic fatty alcohols and fatty acids (Maclaren and Milligan 1981; Broadbent 2001). These are removed on scouring which involves agitation of the wool in hot, soapy solutions. The genetic variety of breeds of sheep as well as their diet, health and climate affects factors such as the crimp, diameter and length of wool fibres.

3.5.1.1 Composition of keratin

The polymerisation of amino acid monomers produces a proteinaceous polymer. The type, proportion, and sequence of amino acids in the polymer constitute the primary structure of the polymer. The proportion of amino acids present in wool (Jones, Rivett and Tucker 1998) is illustrated in Figures 3.8 and 3.9 and Table 3.4.

All types of wool are made from α -keratin, a fibrous proteinaceous polymer formed through polymerisation of amino acid monomers to form protein molecules arranged in a right-handed coil (α -helix) conformation. This protein form is distinguishable from the β -pleated sheet conformation present in silk and feathers by its α X-ray diffraction pattern. The α -helix structure is stabilised by many weak hydrogen bonds between amide groups (N-H) and carbonyl (C=O) groups four residues along the chain. There are 3.6 residues in one coil and each coil is 540 nm apart from the next coil (repeat distance). Combinations of 21 different amino acids (residues) make up the wool polypeptide chains but the relative ratio of each may change even within the same type of wool (Maclaren and Milligan 1981; McMurphy 1996; Hocker 2002).

3.5 Proteinaceous model textile properties and reactivity

The 21 amino acids present in wool differ in their side chains which may be acidic, basic, hydrophobic (non-polar), hydrophilic (polar), sulphur-containing, or heterocyclic (Figures 3.7 and 3.8).

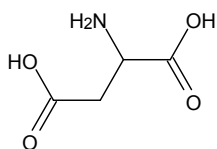
Table 3.4 Amino acid composition of wool keratin

Amino acid residue	Amino acid residue content in wool (%)		
Reference	(Needles 1986)	(Leeder and Marshall 1982)	(Gillespie, Broad and Reis 1969)
Wool type	Average content for major varieties of wool	Merino sheep wool	English Leicester × Merino sheep 1390
Alanine	3-5	5.4	4.13
Arginine	8-11	6.9	21.7
Aspartic acid ^a	6-8	6.6	4.87
Glutamic acid ^b	12-17	11.9	8.57
Glycine	5-7	8.2	4.94
Cysteine ^c	10-15	10.0	10.61
Histidine	2-4	0.8	1.50
Isoleucine	3-5	3.1	2.36
Leucine	7-9	7.7	5.60
Lysine	0-2	2.8	4.49
Methionine	0-1	0.4	0.40
Phenylalanine	3-5	2.8	1.82
Proline	5-9	7.2	4.57
Serine	7-10	10.5	7.10
Threonine	6-7	6.3	4.27
Tryptophan	1-3	- ^d	- ^d
Tyrosine	4-7	3.7	2.26
Valine	5-6	5.7	4.08
NH ₃	- ^d	- ^d	- ^d

Notes for Table 3.4:

- Includes asparagine;
- Includes glutamine;
- Contributes to cystine;
- The value cannot be obtained by acid hydrolysis method;
- Not included.

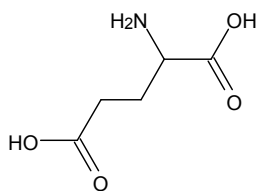
Acidic residues



Aspartic acid (Asp)

pH 2.8

Wool: 5.9

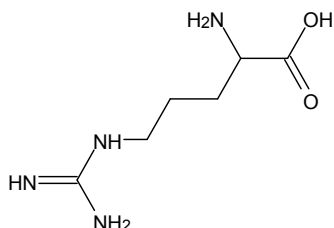


Glutamic acid (Glu)

pH 3.2

Wool: 11.1

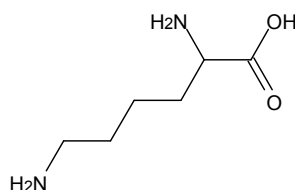
Basic residues



Arginine (Arg)

pH 10.8

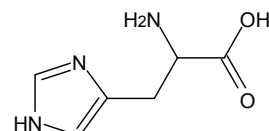
Wool: 6.2



Lysine (Lys)

pH 10.0

Wool: 2.7

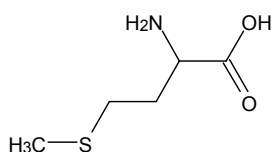


Histidine (His)

pH 7.6

Wool: 0.8

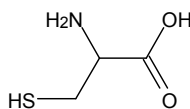
Sulphur-containing residues



Methionine (Met)

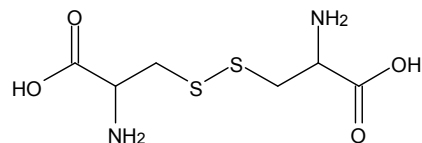
pH 5.7

Wool: 0.5



Cysteine (CysH)

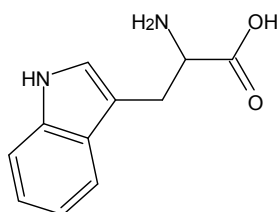
pH 5.1

Wool: 13.1^a


Cystine (Cys)

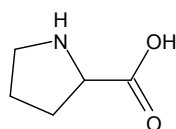
pH -

Heterocyclic residues



Tryptophan (Try)

pH 5.9

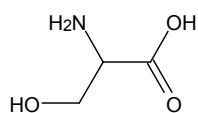
Wool: -^b


Proline (Pro)

pH 6.3

Wool: 6.6

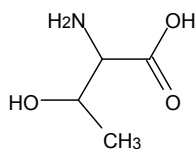
Figure 3.9 The structure, isoelectric point (Timar-Balazsy and Eastop 1998), and concentration [mol%] (Jones, Rivett and Tucker 1998) of acidic, basic, sulphur-containing, and heterocyclic amino acid residues in wool. Notes for Figure 3.9: a. contributes to cystine, and b. the value is unobtainable on acid hydrolysis.

Polar residues

Serine (Ser)

pH 5.7

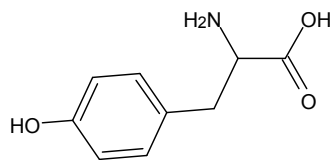
Wool: 10.8



Threonine (Thr)

pH 5.6

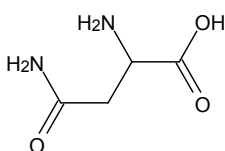
Wool: 6.5



Tyrosine (Tyr)

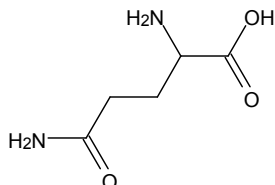
pH 5.7

Wool: 3.8



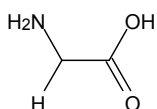
Asparagine (Asn)

pH -



Glutamine (Gln)

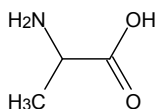
pH -

Non-polar residues

Glycine (Gly)

pH 6.0

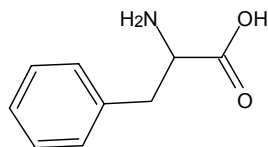
Wool: 8.6



Alanine (Ala)

pH 6.0

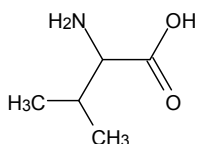
Wool: 5.2



Phenylalanine (Phe)

pH 5.5

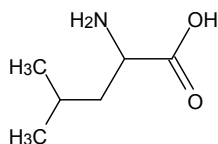
Wool: 2.5



Valine (Val)

pH 6.0

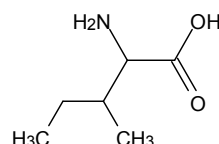
Wool: 5.7



Leucine (Leu)

pH 6.0

Wool: 7.2



Isoleucine (Ileu)

pH 6.0

Wool: 3.0

Figure 3.10 The structure, isoelectric point (when given) (Timar-Balazsy and Eastop 1998), and concentration [mol%] (Jones, Rivett and Tucker 1998) of polar and non-polar amino acid residues in wool (Asn and Gln hydrolyse to Asp and Glu)

Of particular importance are the cystine residues which are the main source of sulphur within wool and which stabilise the wool fibre through the formation of disulphide crosslinks. There are approximately 800-850 $\mu\text{mol/g}$ of both acidic (aspartic and glutamic acids) and basic (arginine, lysine, and histidine) residues in wool which imparts amphoteric character (Maclaren and Milligan 1981; Hocker 2002). The isoelectric point of wool is the pH at which the protein residues show amphoteric properties, existing as electrically

3.5 Proteinaceous model textile properties and reactivity

neutral zwitterions, (Figure 3.11), and it varies depending on the source, condition, composition, and purity of the protein. Consequently, while the isoelectric point of wool is around pH 5.5 (Broadbent 2001), in textile conservation it is considered to be in the pH 5-7 region (Timar-Balazsy and Eastop 1998) as within this range there is little acid or base bound to wool (Broadbent 2001).

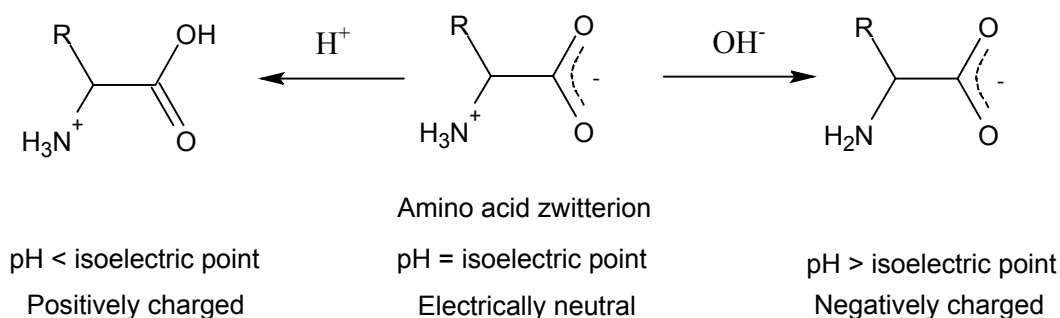


Figure 3.11 The amphoteric character of amino acids

It is also important to note that while deprotonated carboxylic acid groups and protonated amino groups are basic and acidic, respectively (Hocker 2002), those at the N- and C-terminals contribute little to the acidic and basic capability of wool. All of the basic groups attract acid dyes but the side chains of lysine and histidine can also bond covalently with reactive dyes.

Keratin protein fractions

The sequence of amino acid residues in the polypeptide chains of wool vary with breed of sheep (Maclaren and Milligan 1981). There are four fractions of proteins of wool each of which are made up of a number of protein families which consist of closely related members. These fractions are extracted from wool after reduction and carboxymethylation and are: the low sulphur fraction (LSF) which has less sulphur than whole wool, the high sulphur fraction (HSF) which contains more sulphur than whole wool, the ultrahigh sulphur fraction (USF) and finally, the high Gly/Tyr fraction (HGT) (Hocker 2002). 50-60% of the original fibre weight is due to low-sulphur proteins which are partly helical in conformation and contained in the microfibrils (Jones, Rivett and Tucker 1998). None of the other fractions contain protein arranged in helices. Most of the high-sulphur proteins are located in the non-crystalline matrix of cortical cells and their possible tightly folded configurations are stabilised by disulphide bonds. These intra-chain disulphide bonds are the most probable cause of fibre matrix swelling after immersion of fibres in water or formic acid. Little is known about ultrahigh-sulphur proteins apart from that nearly a third

3.5 Proteinaceous model textile properties and reactivity

of the residues are half-cystine residues. High Gly/Tyr proteins have been located in orthocortical cells, possibly originating from the cuticle and cell membranes (Maclaren and Milligan 1981; Morton and Hearle 1997; Jones, Rivett et al. 1998).

3.5.1.2 Crosslinks

Five types of structure stabilising crosslinks are present in wool fibres (Figure 3.12):

1. Hydrophobic bonds can be formed between non-polar side groups on opposite polymer chains, e.g. valine and phenylalanine);
2. Disulphide bonds which are the major type of crosslink in wool are produced from cystine residues. Disulphide bonds between different polypeptide chains make a single network molecule with low lateral swelling and high wet strength. A combination of stress, heat, and water can rearrange disulphide bonds;
3. Salt bridges are formed between the ionised side chains of acidic and basic residues. These crosslinks are pH-sensitive, occurring around the isoelectric point of the fibre when there is a high content of ionised side groups. Salt-bridges are formed via ionic bonding between a glutamate or aspartate residue and a protonated lysine or arginine residue (Morton and Hearle 1997);
4. Covalent iso-dipeptide linkages are formed between an aspartate or glutamate residue and a lysine residue;
5. H-bonding between hydrogen-donating and accepting groups, amides in particular, also stabilise the wool structure. Hydrogen bonds occur between the –NH- and –CO- of groups in neighbouring main chains as well as between hydroxyl groups in side chains (Morton and Hearle 1997). Due to these bonds, wool properties are greatly affected by water, acid, and alkali which can break H-bonds (Maclaren and Milligan 1981; Timar-Balazsy and Eastop 1998; Hocker 2002).

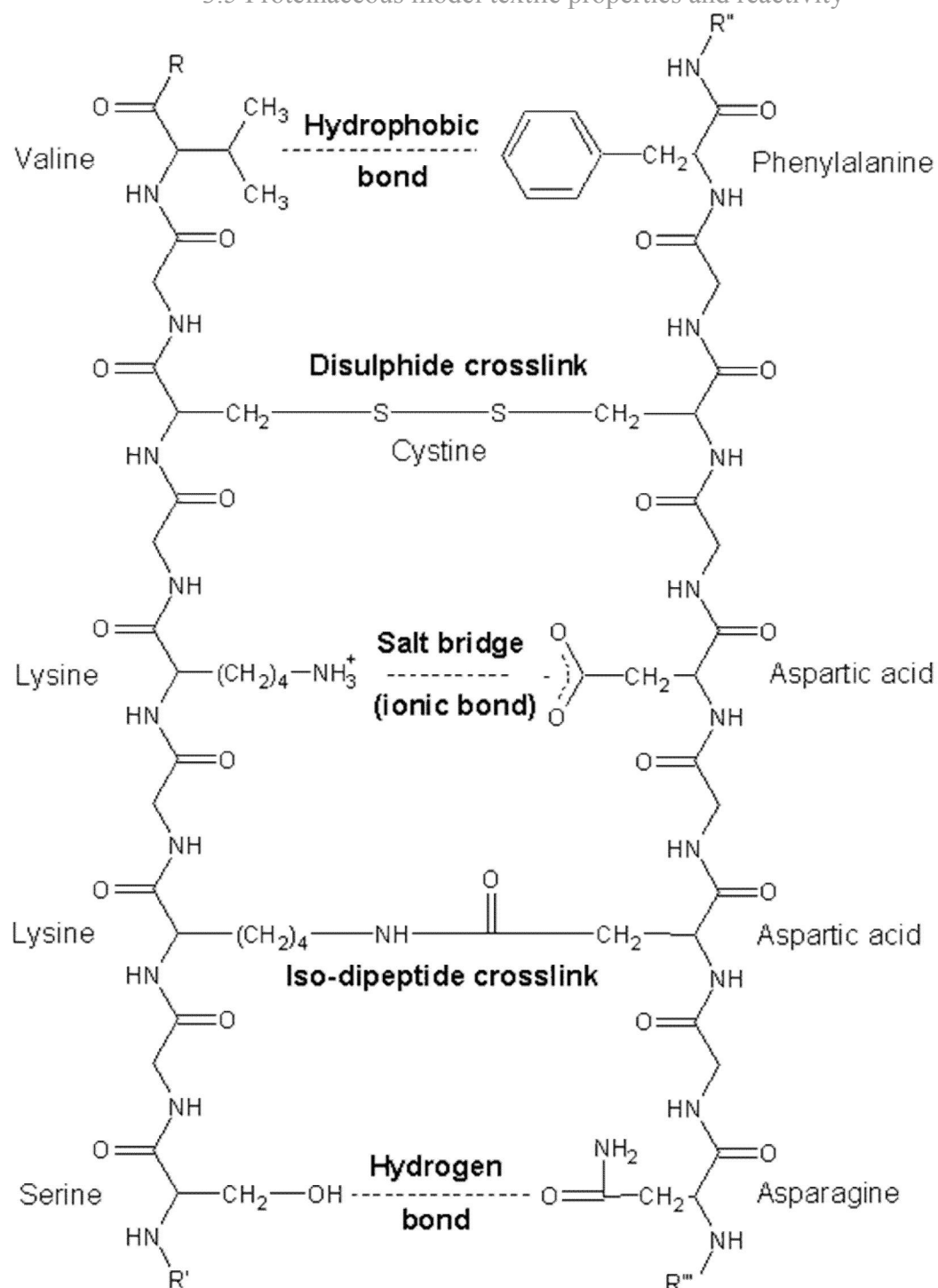


Figure 3.12 The types of crosslinks present in wool (Timar-Balazsy and Eastop 1998; Broadbent 2001)

3.5.1.3 Structure of wool fibres

Wool fibres are composed of the cuticle, cortex, and cell membrane complex (CMC). Coarse fibres may also have a medulla. A wool fibre is approximately circular in cross-section and often wavy, tapering from the root to the tip. The elasticity of the crimp

(waviness) often present in wool fibres causes long retention times of the resultant bulk and softness of woollen fabrics (Morton and Hearle 1997).

Cuticle

There are different types of cuticle cells including those that completely encompass the fibre with one cell in a spiral structure, or two semi-cylindrical cells or finally, three or four crooked cells. The cells involved will be of different dimensions meaning that the often quoted cuticle cells dimension of 20µm wide, 30 µm long and 0.5-0.8 µm thick are correct for only some (Phan, Thomas and Heine 1995). These cells, which are slightly bent and almost rectangular in shape, cover the fibre by overlapping like the tiles on a roof. The degree of overlap, number of scales per cm, degree of scale exposure and resulting thickness of the cuticle partly depends on the coarseness of the fibre. Cuticle cells closer to the fibre core are thinner than those near the surface. Very fine fibres with a diameter of 15 µm or less have a single layer of cuticle cells which overlap spirally towards the fibre tip (Phan, Thomas and Heine 1995; Hocker 2002). Transmission electron microscopy of longitudinal sections of wool has shown that a single layer of scales covers the orthocortex compared to two or three layers covering the paracortex. Cuticle cells covering the paracortex expose 30% of the total cell length and are 40% longer than those covering the orthocortex which have approximately 20% of the cell length exposed. The exposed ends of the cuticular scales point towards the fibre tip which results in directional frictional properties depending on whether an applied surface is moved with or against the scale direction. While noticeably separate at the exposed ends, neighbouring cuticle cells merge together towards the root of the cell, sharing the same endocuticle (Phan, Thomas and Heine 1995; Hocker 2002).

Cuticle cells consist of four parts; the approximately 2.5nm thick epicuticle, the A- and B-layer of the enzyme-resistant exocuticle, and the enzyme-digestible endocuticle. The epicuticle is not the sulphur-rich Allwörden membrane it was once thought to be (Phan, Thomas and Heine 1995). Instead it is an inert protein layer containing iso-dipeptide bonds. Resistant to alkalis, oxidising agents, and proteolytic enzymes, the epicuticle is bound via thioester linkages to a hydrophobic fatty acid layer of chiral 18-methyl eicosanoic acid (18-MEA). This fatty acid layer is the surface of the wool fibre and may in fact be integrated into the epicuticle rather than a separate layer. The sulphur-rich (35% S) A-layer of the exocuticle is highly crosslinked with disulphide and iso-dipeptide bonds. The B-layer has less crosslinking than the A-layer due to a lower quantity of S (20% S). The high sulphur content and cross-linked nature of the exocuticle makes it amorphous and highly resistant

to degradation. The very low sulphur content of the endocuticle makes this more reactive than the exocuticle and the preferential diffusion pathway for water and other reagents into the fibre core due to its permeability (Cook 1993b; Jones, Rivett and Tucker 1998; Timar-Balazsy and Eastop 1998; Hocker 2002).

Cell membrane complex (CMC)

The CMC essentially ‘cements’ the cortical cells together and separates the cortical cells from the cuticle cells. There is much yet to learn about CMC but it is thought that its two main components are the intercellular material (δ - layer) and modified plasma membranes (β -layers). It is possible that an intracellular membrane band (i-layer) also exists. CMC is often viewed as non-keratinous because it contains low levels of cystine, 1% in intercellular cement (Leeder 1986). The resulting low levels of disulphide bonds explain the swelling and accessibility properties of the δ - layers, the likely constituents of which are proteins and lipids (Jones, Rivett and Tucker 1998). The CMC contains lipids and proteins (desmosomes) and coats the cortical cells in a 25nm thick layer (Maclaren and Milligan 1981; Hocker 2002). The CMC contributes about 4-6% of wool fibres; 1.5% of this material is resistant membranes, 1.5% lipids, and 1-3% are intercellular cement (Leeder 1986; Wortmann, Wortmann and Zahn 1997). Only the lipids and intercellular cement form a continuous phase throughout the fibre which can act as a diffusion pathway according to Brady’s CMC-Diffusion model. The fact that this continuous phase would be approximately 3% weight of the wool made Wortmann, Wortmann and Zahn question this model (Wortmann, Wortmann and Zahn 1997).

Cortex (Wortmann and Zahn 1994; Hocker 2002)

The polypeptide chains of wool are arranged as α -helices with bulky side groups on the exteriors of the helices. This unstretched structure is stabilised by intra-molecular hydrogen bonds between amide groups and carboxylic acid groups, four residues apart. Both protein and DNA sequencing have enabled the elucidation of the primary structure of wool keratins, KIP (Figure 3.13). The polypeptide chain has an N- and a C- terminal domain (non-helical). In between these are four segments of residues in helical conformation and approximately 47 nm in total length: 1A, 1B, 2A, and 2B. The linkers L1, L12, and L2 separate the segments. Both combinations of 1A, L1, and 1B as well as 2A, L2, and 2B are equal in their 20-21 nm length. In the helical segments the amino acids are arranged in heptads which is why the columns in the figure are labelled a to g, of which a and d have predominantly hydrophobic side chains. Molecular dynamic simulations suggest that

3.5 Proteinaceous model textile properties and reactivity

unlike segment 1A, linker segment L12 is not inherently stable in the α -helix conformation (Hocker 2002).

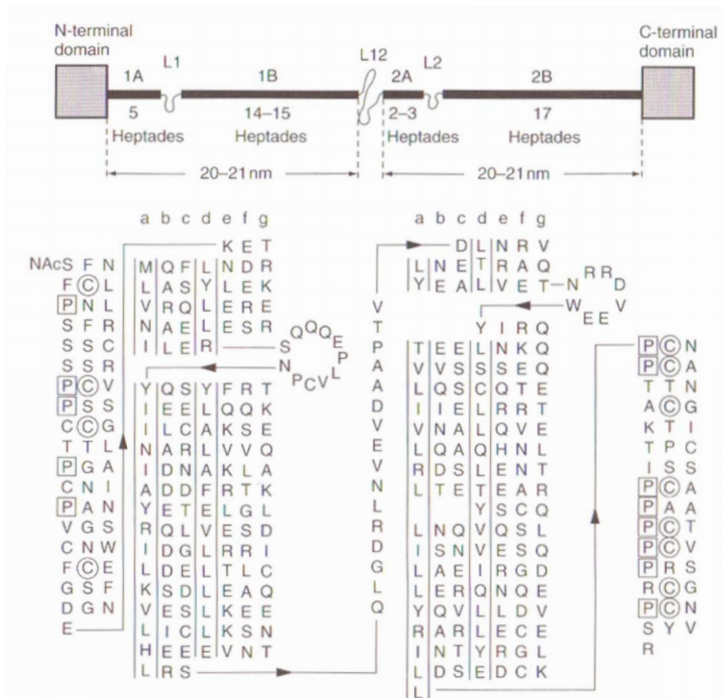


Figure 3.13 Explanation of the primary and secondary structure of the 8c-1 protein of the wool intermediate filament (Hocker 2002) p.75

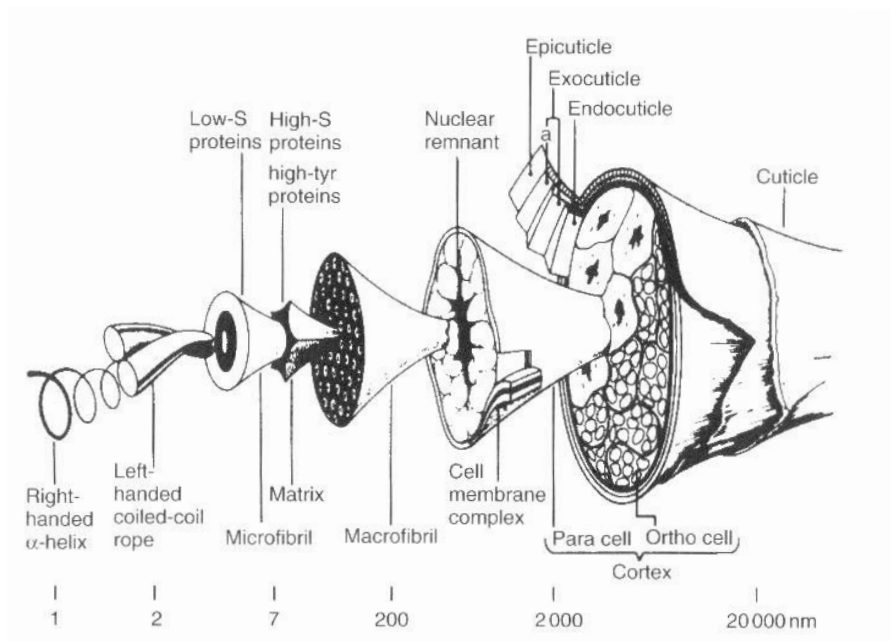


Figure 3.14 Morphology of a wool fibre (Rippon 1992)

One acidic KIP coils together with a basic KIP to form a hetero-dimer. This coiled coil is primarily formed due to their hydrophobic behaviour which brings hydrophobic residues in

3.5 Proteinaceous model textile properties and reactivity

a and d closer to each other. Salt-bridges (ionic bonds) between residues c and g further stabilise the dimer (Hocker 2002).

Two rows of end-on packed dimers form the protofilament. Stabilisation occurs by the anti-parallel combination of the rows so that the 2B sections overlap. This overlap enables the lateral formation of disulphide bonds. Four KIP chains are present in the protofilament cross-section, which has a diameter of 2.8 nm (Hocker 2002).

Two protofilaments combine to form a protofibril which contains 8 KIPs in its cross-section. Combination of two protofibrils forms a half filament which on doubling with another half filament forms the 8-10 nm diameter intermediate filament (microfibril, KIF) (Hocker 2002).

Bundles of 500-800 microfibrils surrounded by a 10 nm thick matrix of interfilament material (KAP) constitute macrofibrils. There are more than a hundred types of KAPs, some are heavily crosslinked, as well as five acidic Type I KIFs and five basic Type 2 KIFs. At their widest point, macrofibrils have a diameter of 100-300 nm and are surrounded by intermacrofibrillar matrix material consisting of cytoplasmatic and nuclear remnants of the keratinocytes (Morton and Hearle 1997; Hocker 2002).

Combination of 5-20 macrofibrils forms a spindle-shaped cortex cell which is 2-6 μm wide and 45-100 μm long. Cortex cells account for roughly 90% of the wool fibre mass and are present in the core as two types: orthocortex cells (60-90%) and paracortex cells (40-10%) (Figure 3.14). In the orthocortex, the macrofibrils are noticeably separated and microfibrils are present in hexagonal arrangements. In the paracortex, the macrofibrils are less well separated and the densely packed microfibrils are arranged randomly as well as hexagonally (Hocker 2002). In coarse fibres paracortex cells encircle a core of orthocortex cells while in fine fibres (less than 25 μm or so) the ortho and para cortices form two half-cylinders of bilateral symmetry which twist spirally along the fibre length. This causes the paracortex to be on the inside edge of crimp in the fibre and the orthocortex to be on the outside edge. Unlike the orthocortex cells, every paracortex cell contains nuclear remnants and cytoplasmic residue. The orthocortex has a lower S-content than the paracortex and stains more readily with acid or basic dyes and salts of lead, mercury, silver and gold, enabling differentiation between the two (Maclaren and Milligan 1981; Cook 1993; Jones, Rivett et al. 1998; Hocker 2002).

Medulla

The medulla has been described as ‘a central stream of cells interspersed with vacuoles’ (Jones, Rivett and Tucker 1998, p.373). It can be a hollow canal or even a hollow tubular network which can run through wool fibres. A greater proportion of medullated cells is a characteristic of medium and coarse wools as they can be completely absent or invisible in fine fibres (Cook 1993; Morton and Hearle 1997; Jones, Rivett et al. 1998). Often the coarse wools with medullated cells dye to a lighter shade than those without due to internal light diffusion of the medulla and a thinner cortex to dye (Cook 1993b).

3.5.1.4 Reactivity (Maclaren and Milligan 1981)

Chemical reactions can affect both the side chains and main peptide chain of proteins. Some reactions of side chains which are not elaborated upon here include esterification, alkylation, acylation and arylation.

Acids (Maclaren and Milligan 1981; Cook 1993b; Jones, Rivett and Tucker 1998; Timar-Balazsy and Eastop 1998; Simpson 2002)

While acid has no effect on the disulphide bonds (excepting disulphide interchange to which the disulphide bonds are susceptible in concentrated acid), acid can break the structure-stabilising H-bonds and salt linkages (if below the iso-electric point).

Peptide chains can be partially or completely hydrolysed into smaller chains or individual residues in a random manner by acid-catalysed hydrolysis. This decreases the average DP of the polymer chains. The peptide bonds adjacent to aspartic acid followed by glycine and serine are the most labile. If sulphonic acid groups (RSO_3H) have been formed in the polymers by scission of disulphide bonds, for example during photo-oxidation, acid hydrolysis of nearby peptide links will occur. 6 M HCl is used in an evacuated sealed tube at 105°C for 24 hours to fully hydrolyse proteins in preparation for amino acid analysis (Simpson 2002). This procedure destroys tryptophan and partially destroys cystine, serine, and threonine. When exposed to strong acid for a long time, asparagine and glutamine residues are converted to aspartic and glutamic acid by conversion of the amide groups to carboxylic acids and releasing ammonia in the process. This occurs faster than hydrolysis of peptide bonds. During partial hydrolysis, an acyl shift at serine and threonine residues ($\text{N} \rightarrow \text{O}$ migration) as well as disulphide interchange occurs.

3.5 Proteinaceous model textile properties and reactivity

The amine side chains ($-\text{CRR}'\text{CH}_2\text{NH}_2$) can also be converted to dehydroalanine ($\text{RR}'\text{C}=\text{CH}_2$) by acid. The alkene is a chromophore which can lead to yellowing of wool (Timar-Balazsy and Eastop 1998).

Overall, acid environments cause wool to exhibit weight loss, a decrease in tensile fibre wet strength, a decrease in urea/bisulphite solubility, and yellow discolouration.

Nevertheless, formic, acetic, or sulphuric acids are still used in the dyeing of wool. Sulphuric acid is also used in the carbonising of cellulosic contaminants within wool. By using the recommended conditions of pH 4.0-5.5 and a temperature less than 100°C, damage to wool during dyeing with acid can be minimised (Lewis 1992).

When immersed in an acidic or alkaline solution in the range of pH 3-10, equilibration can take up to one hour. This slow equilibration is due to initial absorption at the fibre surface causing an electrostatic barrier which hinders further absorption. This equilibration time can be significantly reduced through incorporation of a neutral salt such as KCl (Simpson 2002).

Alkalis (Maclaren and Milligan 1981; Jones, Rivett and Tucker 1998; Timar-Balazsy and Eastop 1998; Simpson 2002)

Undegraded wool is particularly sensitive to alkali and oxidised wool even more so, with damage occurring at a significant rate at low alkali concentrations and room temperature. When exposed to alkali solutions of pH 11 or higher for even short periods of time at room temperature, hydrolysis of peptide bonds and alkaline degradation of cystine can occur. Just 5% NaOH solution can dissolve wool while 2% NaCl can decrease the rate of alkaline degradation. Alcoholic solutions increase the extent of alkaline degradation of wool because it swells the fibre more than water does.

The cystine residues can be broken by hydroxide ions to form thiol and sulphenic acid (RSOH) side groups. The latter is unstable and so forms sulphur, water, and dehydroalanine (Figure 3.15). An autocatalytic cycle is started when sodium sulphite is formed since this can break disulphide bonds. Alternatively the sulphenic acid can form an aldehyde side group and release hydrogen sulphide. The aldehyde can contribute to the discolouration (yellow/grey/ brown) of wool, particularly if it is conjugated with other unsaturated bonds and can also direct hydrolysis to the peptide bonds nearby. A lanthionine residue can be formed through combination of dehydroalanine and thiol side

3.5 Proteinaceous model textile properties and reactivity

groups (Timar-Balazsy and Eastop 1998) or through direct attack at the β -carbon on the cystine residue by a hydroxide ion (Simpson 2002). Lanthionine cross-links are sensitive to alkali and photolysis but are resistant to acid.

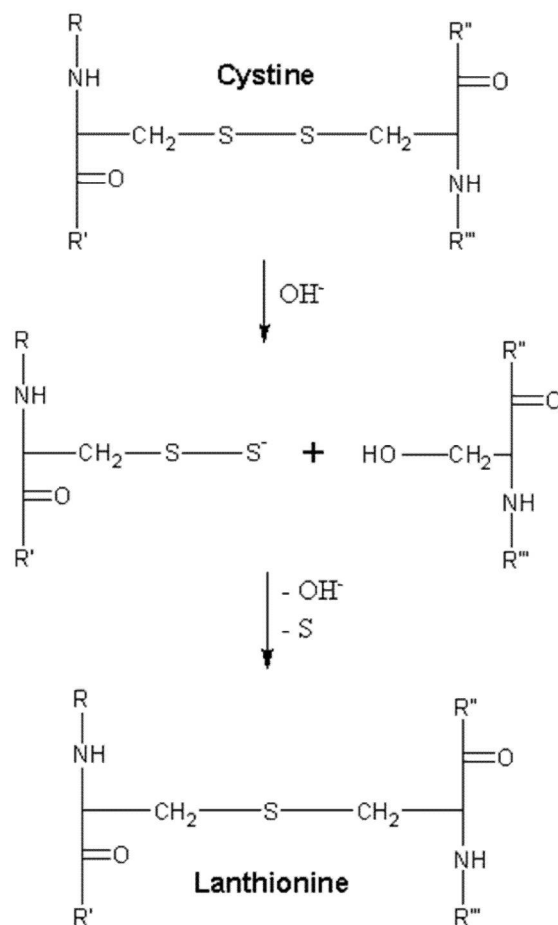


Figure 3.15 Principle steps in the formation of lanthionine from cystine (Simpson 2002)
p.138

Lysinoalanine crosslinks can be formed by interaction of dehydroalanine originally from cystine or cysteine, and an amine side group such as that on lysine, or by reaction of serine and lysine. Other products are also produced in small amounts. Whether the crosslinks are inter- or intra-molecular affects the resulting fibre properties. The lowered urea/bisulphite solubility of wool treated with alkali compared to untreated is due to the slow replacement of reducible disulphide crosslinks with non-reducible inter-molecular crosslinks.

In strong alkali, cystine, lysine, arginine, threonine, and serine are partially destroyed while ornithine, lanthionine, lysinoalanine, pyruvic acid, β -aminoalanine, and ornithinoalanine are produced. The amide groups of asparagine and glutamine residues are hydrolysed to the carboxylic acid groups of aspartic and glutamic acids and produce ammonia as a byproduct. The sulphur content of wool decreases by up to 50% with the release of sulphide and sulphate. Hot alkaline solutions cause the complete dissolution of wool fibres.

3.5 Proteinaceous model textile properties and reactivity

Immersion of a protein sample in a 0.1M NaOH solution at 65°C for 1 hour constitutes the BS 3568:1988 alkali solubility test. This test indicates the extent of protein degradation by the percentage of protein dissolved (10% solubility is usual for undamaged wool). Loss of cystine crosslinkages and salt linkages, increasing carbonyl content e.g. from alkali degradation or photo-oxidation, and acid damage all increase the alkali solubility of wool while new, stable crosslinkages decrease the solubility (Timar-Balazsy and Eastop 1998; Simpson 2002).

Strong alkaline solutions can be used to impart a shrink-resist effect while dilute solutions of sodium hydroxide and tri-sodium phosphate have been used to increase wool's dye affinity. Mild alkali in organic solvents partially breaks down the covalent bonds linking fatty acids to the fibre surface, resulting in a more hydrophilic fibre.

Treatment of wool with alkali therefore causes increased rapidity of fibre dye uptake, increased swelling in water, decreasing alkali solubility, a decrease in the handle (feel) of the wool and increased yellowing. Nonionic, neutral detergents are therefore preferred to alkaline soaps when washing or scouring.

Oxidising agents (Maclaren and Milligan 1981; Jones, Rivett and Tucker 1998; Simpson 2002)

There are many residues in wool which are vulnerable to oxidation including cystine, cysteine, methionine, and tryptophan. The abundance of cystine and its sensitivity to oxidants gives rise to strength loss. Some disulphide bonds are oxidised to sulphonic acid groups.

Complete oxidation converts cystine residues into cysteic acid (Scheme 3.1).



Scheme 3.1 Oxidation of cystine residues to cysteic acid

Intermediate products are formed when the oxidant is not in excess. In industry, hydrogen peroxide is used to bleach wool, while chlorine and permanganate are used separately to shrink-proof wool.

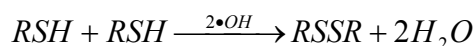
Reducing agents (Maclaren and Milligan 1981; Jones, Rivett and Tucker 1998)

On reduction for example by thioglycollate, sulphites, bisulphites, or phosphines, the disulphide bonds in wool are converted to thiols i.e. cystine residues produce two cysteine residues. Reduction of 20% of the disulphide bonds in wool can be used in industry to impart shrink resistance and increase the ease of setting. However if too many disulphide bonds are broken the fibre strength is decreased to unacceptable levels. However, for protein analysis, complete cleavage of the disulphide bonds is required. Especially in alkaline solutions, cysteine residues can be oxidised to disulphide bonds by dissolved oxygen. To prevent this reformation alkylation with iodoacetate for example is performed.

Photodegradation (Maclaren and Milligan 1981; Cook 1993; Jones, Rivett et al. 1998; Simpson 2002)

The absorption of UV near 254 nm by disulphide bonds causes the formation of a radical species, proposed to be a cystinyl radical cation ($RSSR^{\cdot+}$) which can absorb at 600 nm (Millington and Church 1997; Millington 2000). This species can be oxidised by atmospheric oxygen and is thought to be the only species which forms partially oxidised cystine species (Millington and Church 1997; Millington 2000). This and other radicals can initiate photo-oxidation of the polymer which causes the introduction of carbonyl and carboxyl groups (e.g. cysteic acid) into the polymer chain and can cause cleavage of the peptide bonds, decreasing the average DP of the wool. Secondary bonds as well as salt linkages are also broken. The breaking of these bonds causes an increase in the solubility and elongation of the wool, decreases its strength, and increases its susceptibility to attack by acids and bases by increasing the accessibility of the polymer chains.

At the same time new cross-links including disulphide (Scheme 3.2), peptide, lanthionine, and lysinoalanine, are formed. These increase the brittleness and rigidity of the wool by bringing the polymer chains closer together (Timar-Balazsy and Eastop 1998).

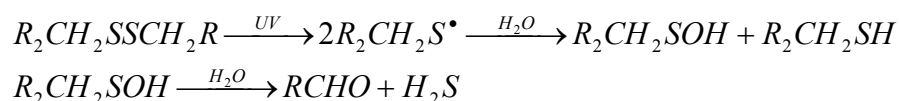


Scheme 3.2 Disulphide cross-link formation

Both yellowing (UV light <331 nm) and bleaching (visible light >398 nm) of wool can occur depending on the wavelength of radiation absorbed. The rate of yellowing is greatly affected by moisture and metal ion content of the wool (Smith 1975; Jones, Rivett et al. 1998; Shimizu 2000). The rate of yellowing is ten times faster in humid conditions than in

3.5 Proteinaceous model textile properties and reactivity

dry with aldehyde groups being introduced via sulphenic acid side groups as shown in Scheme 3.3 (Timar-Balazsy and Eastop 1998).



Scheme 3.3 A mechanism of photoyellowing of wool by the formation of aldehyde groups from cystine

Cupric and ferric ions have been found to photosensitise the formation of glycyI free-radicals (Smith 1974; Smith 1975). When exposed to UV for 50 hours, the yellowness index of untreated wool changed more than those of wool treated individually with copper and iron salts. However, the iron treated wool produced the least change in yellowness index after 50 hours of UV exposure (Bendak, Raslan and Salama 2008). Iron had a better yellowing resistance effect on wool than copper. The tensile properties of untreated wool compared to those of wool pre-treated with copper and iron salts at 40°C and 60°C were almost the same (Bendak, Raslan and Salama 2008).

Photo-oxidation can lead to problems when processing wool as fibre weakening can cause breakage during processing and cysteic acid formed from oxidation of cystine can damage the epicuticle and cause uneven dyeing. The cleavage of disulphide bonds and the introduction of charged sulphonate groups enables ‘weathered’ wool to swell more with water.

In addition to cystine and cysteine, other amino acids that are particularly susceptible to photolysis include proline, histidine, isoleucine, leucine, tryptophan, threonine, phenylalanine, methionine and tyrosine.

Effect of heat (Cook 1993b; Jones, Rivett and Tucker 1998; Timar-Balazsy and Eastop 1998).

Heat can initiate oxidation by causing homolytic scission of chemical bonds to form radicals. Homolytic scission of O-O bonds in peroxides can occur in ambient conditions.

Increasing temperature causes increasing water loss from the wool until it is dessicated. Above 100°C inter-chain peptide bonds can form between carboxylic acid and amino side groups such as glutamic acid and lysine, respectively. This changes the water absorption properties of the wool. Wool contracts when heated to 128°C and 140°C in sealed tubes.

3.5 Proteinaceous model textile properties and reactivity

Contraction depends on the rate of heating. Above 180°C yellow or brown discolouration of the wool can occur as small groups are eliminated from the wool along with ammonia and hydrogen sulphide.

Heating wool in water to temperatures above 50°C decreases its urea/bisulphite solubility due to the formation of lanthionine and lysinoalanine crosslinks. When boiled for a long time, wool loses its flexibility/softness and becomes weak.

Moisture

Wool is a particularly hygroscopic fibre which under normal atmospheric conditions can hold 16-18 % of its weight in moisture. 33% water is bound at 100% RH and it holds up to 200% of its dry weight when immersed in water. This can lead to significant mechanical damage to the fibre if it is already weakened by chemical degradation (Timar-Balazsy and Eastop 1998).

Water absorption by wool liberates heat (exothermic) and causes swelling of the fibre (Cook 1993b). The CMC in particular swells considerably due to a lack of covalent disulphide bonds. In the isoelectric region of wool (pH 5-7), wool fibres can swell up to 35-40% in width and 1-2% in length. Outside of this region, even more swelling can be expected due to the breakage of salt linkages (Timar-Balazsy and Eastop 1998).

As with other polymeric fibres, the sigmoid shaped absorption and desorption isotherms of wool form a hysteresis. The water quantity absorbed by wool when equilibrated at constant temperature and differing relative humidities differs depending on whether the wool was initially wet or dry. The equilibrium water content (ewc) at a specific relative humidity is greater for the wool which was initially wet than for the wool that was initially dry. This means that the desorption isotherm is above the absorption isotherm on a water absorbed (%) vs relative humidity graph.

The generally accepted explanation for the formation of sigmoid-shaped isotherms is that the initial steep gradient up to about 5% RH (approximately 3% ewc) originates from water molecules hydrogen-bonding with the hydrophilic groups on side and main chain groups in the fibre. Secondly, between 5 and 70% RH (3 and 15% ewc) the water molecules bind to sites on the main or side chains which bind water molecules with less energy or to water molecules already bound to groups on the chains. As a result, these water molecules are bound less strongly than those in the first stage and the isotherm gradient lowers. Finally,

between 70 and 100% RH, the isotherm gradient increases again as new binding sites are introduced. These new sites arise from the swelling in the fibres which breaks structure-stabilising hydrogen bonds in and between the protein chains.

The breakage of hydrogen bonds and formation of new sites in wool fibres at high RH or after immersion in water also explains why equilibration of initially wet wool to a high RH at set temperature results in a greater ewc than for the initially dry wool equilibrated to the same conditions (Jones, Rivett and Tucker 1998).

3.5.1.5 Wool dyeing (Sideris, Holt et al. 1990; Thomas and Phan 1990; Parton 2002)

Wool can be dyed in many stages of its production from loose stock to woven fabric. The types of dyes used at each stage can differ due to the processing demands on the dyed material that will follow. Loose stock for example will be heavily processed after dyeing to produce woven fabric and so a dye of high fastness is required. To ensure level dyeing of a woven fabric, a dye with suitable migration properties is needed. Larger dye molecules migrate more slowly than smaller dye molecules generally resulting in higher fastness properties. An exception to this is afterchrome dyeing, the first stage of which is the application of low molecular weight acid levelling dyes which have relatively poor fastness properties but migrate quickly through the material. The second stage involves the application of chromium which enables the dye to co-ordinately bond with the fibre, thus increasing its fastness properties (Parton 2002).

The use of water as the solvent in dyeing has been found to cause preferential dyeing of the orthocortex (Sideris, Holt and Leaver 1990). This is thought to be due to the smaller distance the dye has to diffuse to reach the orthocortex, typically through a single cortical cell, compared to the paracortex which has multiple cortical cells through which the dye must diffuse (Brady 1990). Non-aqueous solvents were found to restrict dye diffusion to the CMC (Sideris, Holt and Leaver 1990). Level dyeing throughout the fibre was only achieved with water alone.

Dye Diffusion (Leeder 1986; Brady 1990; Leeder, Holt, Rippon and Stapleton 1990; Wortmann, Wortmann and Zahn 1997; Simpson 2002)

Simpson (Simpson 2002) describes three stages in the dye transfer from an aqueous bath. Firstly, the dye must diffuse to the fibre surface. This process can be made more even by the use of efficient equipment and thorough mixing of the dye solution. Secondly, the dye has to transfer across the surface. The diffusion barrier resulting from the cuticle's surface

3.5 Proteinaceous model textile properties and reactivity

lipid (F) layer and underlying highly crosslinked protein (A) layer causes dyes to penetrate through damaged areas or the cuticle cell junctions rather than directly through undamaged cuticular scales. Then the dyes transfer into adjacent A-layers and exocuticle and through the lightly cross-linked non-keratinous material, endocuticle, and intermacrofibrillar materials of the CMC. Intermacrofibrillar cement provides channels for dye molecules to diffuse through and the greater content in the ortho compared to the paracortex leads to differences in dyeing properties. Typically, acid dyes preferentially dye the paracortex while the majority of dyes with basic groups preferentially dye the orthocortex (Leeder, Holt, Rippon and Stapleton 1990). In stage three, the dyestuffs transfer to the heavily cross-linked high-sulphur matrix proteins which surround the cortical cell microfibrils (Simpson 2002). At equilibrium, the areas of initial diffusion are usually devoid of dye molecules. At this stage, anionic dye molecules are present only in the high-sulphur regions ensuring maximum wet fastness. If the dyestuff remains in the non-keratinous material, it is possible for the rapid diffusion out of the fibre to occur i.e. poor wet fastness.

Acidic dyebaths

Interestingly, Cook and Fleischfresser noted that large water-soluble anion polymers such as Synthapret BAP (MW approx 3000) diffuse readily into wool fibres when wool has a net positive charge $\text{pH} \leq 4$. Decreasing the pH increased the sorption rate. These polymers are based on poly-(propylene oxide) with no bulky aromatic rings, resulting in small cross-sectional areas. Staining revealed that the orthocortex contained more of the Synthapret BAP than the paracortex (Cook and Fleischfresser 1984).

However, dyeing in strong acid conditions such as pH 2.0, leads to the modification of wool keratins in the microfibrils as well as attack of non-keratinous parts. Wet bundle tenacity decreases, alkaline solubility increases and proteinaceous compounds are also released. Increasing the dyeing time in these strongly acidic solutions causes more damage. The least damage to wool during dyeing was thought to occur with solutions at pH 2.6-4.0 (Thomas and Phan 1990), however pH 4-5.5 is now the most accepted pH range (Lewis 1992).

On immersion of the wool into an acid bath, the wool first adsorbs the small protons which can diffuse faster than the larger anions. The higher affinity of wool for the anions compared to the protons leads to substitution of the protons once the anions have diffused to the sites of proton adsorption (Fonteneau Tamime and Viallier 2000).

Metal ion mordants

Metal ions are required as a mordant in some dyeings. Modern dyes use copper, cobalt, nickel, and in particular, chromium as mordants but toxicological and ecological drawbacks has led to the tightening of government regulations on their usage. Recently investigations have begun to find more environmentally-friendly mordants such as iron for use with modern dyes (El-Shishtawy and Kamel 2002). The specific interactions of metal ions with wool are discussed in more detail in Chapter 4.

3.5.1.6 Properties

Dimensions

Typical fibre lengths of fine wools are about 38-125 mm, medium wools 65-150 mm and long wools 125-375 mm (Cook 1993b). The crimp of wool means that when fully extended, wool fibres can be twice their original length.

The average diameter widths of fine wool fibres can be 17µm, compared to that of medium wool, 24-34 µm, and long wool, approximately 40 µm. Wool fibres are generally thicker than cotton fibres and have an oval cross-section.

Crimp

The wavy structure of wool (crimp) is present in three planes, and is related to the spiralling of the orthocortex and paracortex along the fibres. Crimp imparts elasticity to the fibres and enables fibres twisted together to form a yarn that stays together. Higher quality wools such as merino wools can have 12 waves per cm while lower quality wools can have 2 waves per cm (Cook 1993b).

Mechanical properties

The CMC acts as the chemical and physical weak link in wool fibres. As well as being preferentially attacked by many chemicals including acids and reducing agents, its lack of disulphide bonds enables it to break easily under stress. Longitudinal extension often results in intermacrofibrillar boundaries or cell boundaries being broken. Increasing humidity leads to swelling of the CMC which would usually suggest it would become weaker. Instead, it has been found that increasing humidity leads to increased abrasion resistance, possibly due to the improved ability of the CMC to dissipate energy (Leeder 1986).

Elastic properties

At 2% and 20% extension, wool has an elastic recovery of 99% and 63%, respectively. A small contribution to this recovery is made by the natural crimp of wool but primarily it is due to the α -helical sections of the intermediate filaments (Cook 1993b).

On stretching wool, the H-bonds stabilising the α -helical structure in α -keratin are broken and the polymer chains are extended to form the β -pleated sheets of β -keratin in which new H-bonds are formed to stabilise the structure. An increase in β -pleated sheet structure occurs in both cortical and cuticle cells, particularly in the early stages of stretching. The most change is seen in the cortical cells. Stretching can also cause a small decrease in order along the polymer chains (Church, Corino and Woodhead 1998). The transformations from α -helices to β -pleated sheets can be reversible for the A-filaments in the cortical cells which are suitably short to result in unhindered extension and lack covalent, intermolecular bonds which would also hinder the transformation. The yield point of wool is reached when all the A-filaments are extended. In the post-yield region the long, uncrosslinked 1B segments can be extended irreversibly. Also during this region, the 2B section opens up to varying degrees depending on the sulphur bonds present in it. The cross-linking disulphide bonds hinder the extension of the α -keratins. However, if conditions are such that the disulphide bonds are relaxed through disulphide interchanges, faster than strain is applied, the 2B section can transform under constant stress like the A-sections and the post-yield region disappears. Under normal conditions such as in water at 20°C however, the 1B section is more perfectly aggregated and thus barely accessible to the transformation. Hence only the 1A, 2A and 2B sections will be in the β -form when the wool fibre breaks at 60-70% strain. Increasing the temperature increases the accessibility of the 1B section, thus increasing the breaking strain. This increase can continue until most if not all of the α -helical material in the intermediate filaments is converted to the β -structure (Wortmann and Zahn 1994).

Under normal conditions wool has an elongation at break is 25-35%, a tenacity of 8.8-15.0 cN/tex (1.0-1.7 g/den) and tensile strength of 1190-2030 kg/cm². Under wet conditions the elongation of break is 25-50% and its tenacity is 7-14 cN/tex (0.8-1.6 g/den) (Cook 1993b).

3.5.2 *Silk* (Hearle and Peters 1963; Cook 1993; McMurry 1996; Robson 1998)

There are many varieties of insects and spiders that can produce silk, but it is the silk of the *Bombyx mori* caterpillar (commonly referred to as a silkworm) which is of most commercial importance. Feeding on mulberry leaves alone, the caterpillar forms a silk cocoon to protect itself during metamorphosis. To do this, liquid silk is extruded through two channels in the spinneret located in the caterpillar's head. The two silk filaments (brins) harden on exposure to the air and are 'glued' together by sericin to form one thread (bave) with an average diameter of 15-25 μm . Sericin is an amorphous material and is the main contributor to the colour of the silk, which can be white, yellow or green in hue. This continuous fibre is laid down in figure-of-eight movements and can be up to 1.6km long (Cook 1993b; Robson 1998).

To prevent destruction of the long filaments when the moth emerges, the cocoons are heated to kill the caterpillars inside. When needed, the silk is unwound from the cocoon by a process called 'reeling' which uses hot water to soften the sericin prior to winding. 500-800 m of silk can be obtained for use as a continuous-filament yarn, while shorter fibres can be combined as 'spun silk' (Hearle and Peters 1963; Robson 1998). Degumming removes the sericin from yarns or woven fabrics using hot soapy water and gives the silk lustre. Up to 25% of the weight of raw silk will be lost during the degumming process (Robson 1998). A degummed, semi-transparent silk fibre twists longitudinally and has a very smooth surface. The cross-section from the silk of the *Bombyx mori* is roughly triangular with rounded corners. Other moths produce different cross-sections.

Microvoids exist in silk filaments parallel to the fibre axis and rod-like in shape. Variations in size and distribution of these microvoids between individual filaments may be due to differences in fibre source or spinning conditions (Robson 1998).

Liquid sericin has greater water content (86%) than liquid silk which prevents its conversion to the β -form enabling it to remain separate from the silk which does convert. On exposure to air the sericin solidifies to an amorphous adhesive coating which contains many hydrogen bonds. Sericin accounts for 25% of the weight of a silk cocoon. Aspartic acid, serine and glycine are the main components of *B. mori* sericin. Residues with polar side chains are three times more prevalent than those with non-polar groups and of these, 60% have hydroxyl groups, 30% acidic and 10% basic. The relatively high quantity of acidic groups in the filament contributes to sericin's isoelectric point being 4.0 (Robson 1998).

3.5.2.1 Fibroin composition

Silk is made from fibroin, rather than keratin by condensation of α -amino acids. One fibroin molecule can be approximately 140 nm long (Morton and Hearle 1997). The amino acid content of silk fibroin and sericin is presented in Table 3.5. Overall, silk contains high proportions of glycine, alanine, serine, and tyrosine with low proportions of acidic and basic side groups (Hearle and Peters 1963; Cook 1993b). There is on average a total of two to three times more acidic groups than basic groups in fibroin with usually more aspartic than glutamic acid and more arginine than histidine and lysine (Robson 1998). The isoelectric region of silk fibroin is between pH 3 and 7 and the isoelectric point can be around pH 2.8 (Timar-Balazsy and Eastop 1998).

Table 3.5 Amino acid residue content in silk fibroin and sericin

Amino acid residue	Amino acid residue content in silk (%)				
	Silk protein type	Fibroin ^a	Fibroin	Fibroin	H-chain L-chain
Alanine	29-35	30.3	29.4	29.8	14.2
Arginine	0-2	0.9	0.5	0.2	4.5
Aspartic acid	1-3	1.5	1.3	0.7	14.8
Glutamic acid	1-2	1.2	1.0	0.7	9.2
Glycine	36-43	43.7	44.6	49.4	9.2
Cysteine	0	0.0	0.2	_{-b}	_{-b}
Histidine	0-1	0.4	0.1	0.1	2.3
Isoleucine	_{-b}	0.9	0.7	0.1	7.8
Leucine	0-1	0.7	0.5	0.1	7.5
Lysine	0-1	0.2	0.3	0.1	1.2
Methionine	0	0.9	0.1	_{-b}	0.4
Phenylalanine	1-2	1.2	0.6	0.4	2.7
Proline	0-1	0.5	0.4	0.3	3.2
Serine	13-17	9.9	12.1	11.3	9.0
Threonine	1-2	0.7	0.9	0.5	3.0
Tryptophan	0-1	_{-b}	0.1	_{-b}	_{-b}
Tyrosine	10-13	5.2	5.2	4.6	2.8
Valine	2-4	1.8	2.2	2.0	6.4
Reference	(Needles 1986)	(Yanagi, Kondo and Hirabayashi 2000)	(Robson 1998)	(Robson 1998)	(Robson 1998)

Notes for Table 3.5:

a. Average value of amino acid residue content in fibroin;

b. Not stated.

3.5.2.2 Fibroin structure

There are two major polypeptide components in *B. mori* fibroin which are linked by a disulphide bond: a heavy component with MW of approximately 350,000 daltons (H-chain) and a light component with a MW of approximately 25,000 daltons (L-chain). In addition P25 (c. 30,000 daltons) is a small glycoprotein which binds by hydrophobic non-covalent interactions to the H-L disulphide-linked fibroin dimer. The molar ratio of H-chain:L-

chain:P25 is 6:6:1 (Schoeser, MacDonald and Marcondalli 2007; Hardy, Romer and Scheibel 2008).

The H-chain is hydrophobic and consists of 5263 residues of predominantly Gly (45.9%), Ala (30.3%), and Ser (12.1%). The H-chain contributes to silk's 62-66% crystallinity through the 12 crystalline domains involving the following residue sequence: Gly-Ala-Gly-Ala-Gly[Ser-Gly(Ala-Gly) n] 8 Ser-Gly-Ala-Ala-Gly-Tyr where 'n' is usually two and the mean is always 2 (Hearle and Peters 1963). This sequence is also known as (GAGAGS) n (Takahashi, Gehoh and Yuzuriha 1999). These residues have small side groups enabling close, highly ordered packing. The crystalline regions are further divided into sub-domains involving approximately 70 residues and are separated by 11 amorphous domains of 31 residues in irregular GT~GT sequence (Takahashi, Gehoh et al. 1999; Ha, Gracz et al. 2005; Schoeser, MacDonald et al. 2007). The L-chain doesn't contribute to the crystalline parts of the fibroin as it contains many residues with bulky side groups which prevent the occurrence of high order and close packing that is seen in the H-chain (Morton and Hearle 1997; Robson 1998; Takahashi, Gehoh et al. 1999). In addition, the L-chain is relatively elastic and more hydrophilic than the H-chain. The L-chain contains 244 residues including small percentages of most residues with the largest percentages in Asp/Asn, Ala, Gly, Glu/Gln, and Ser. Importantly, the L-chain contains three cystine residues, two of which can form an intramolecular disulphide bridge while the third forms a disulphide bridge between the L- and H- chains. The very small quantities of cystine and its partial degradation during degumming explain why cystine is often reported to be absent in silk (Robson 1998; Schoeser, MacDonald et al. 2007; Hardy, Romer et al. 2008).

In crystalline regions, the polypeptide chains align themselves in an extended form anti-parallel to one-another in β -pleated sheets. Hydrogen bonding between the amide N-H groups and C=O groups from adjacent chains leads to an approximate 0.92 nm interchain separation. Hydrophobic interactions enable β -pleated sheets to pack on top of each other with chains aligned along the fibre axis.

Recent new evidence suggests that the previously accepted silk fibroin model is no longer applicable. A fully accepted model of silk fibroin has yet to be found. It was previously thought that β -pleated sheets packed together in an anti-parallel arrangement (Figure 3.16) with the H side-groups of the glycine residues facing one-another and the methyl and hydroxymethyl side chains of alanine and serine facing one-another. This polar-anti-parallel arrangement would give intersheet separation distances of 0.35 nm and 0.57 nm,

3.5 Proteinaceous model textile properties and reactivity

respectively (Marsh, Corey et al. 1955; Hearle and Peters 1963; Robson 1998). However, research by Takahashi, Gehoh and Yuzuriha suggests that an anti-polar-anti-parallel arrangement is more likely, where the methyl groups of the alanine residues point alternately to either side of the sheet (Takahashi, Gehoh and Yuzuriha 1999). This leads to a single intersheet separation distance of 0.93 nm. Zhou et al have since suggested that the β -pleated sheets are arranged parallel rather than anti-parallel to one-another (Schoeser, MacDonald and Marcondalli 2007). It should be noted that while residues such as tyrosine with larger side groups do not fit into these crystallite models, their absence cannot be assumed (Robson 1998).

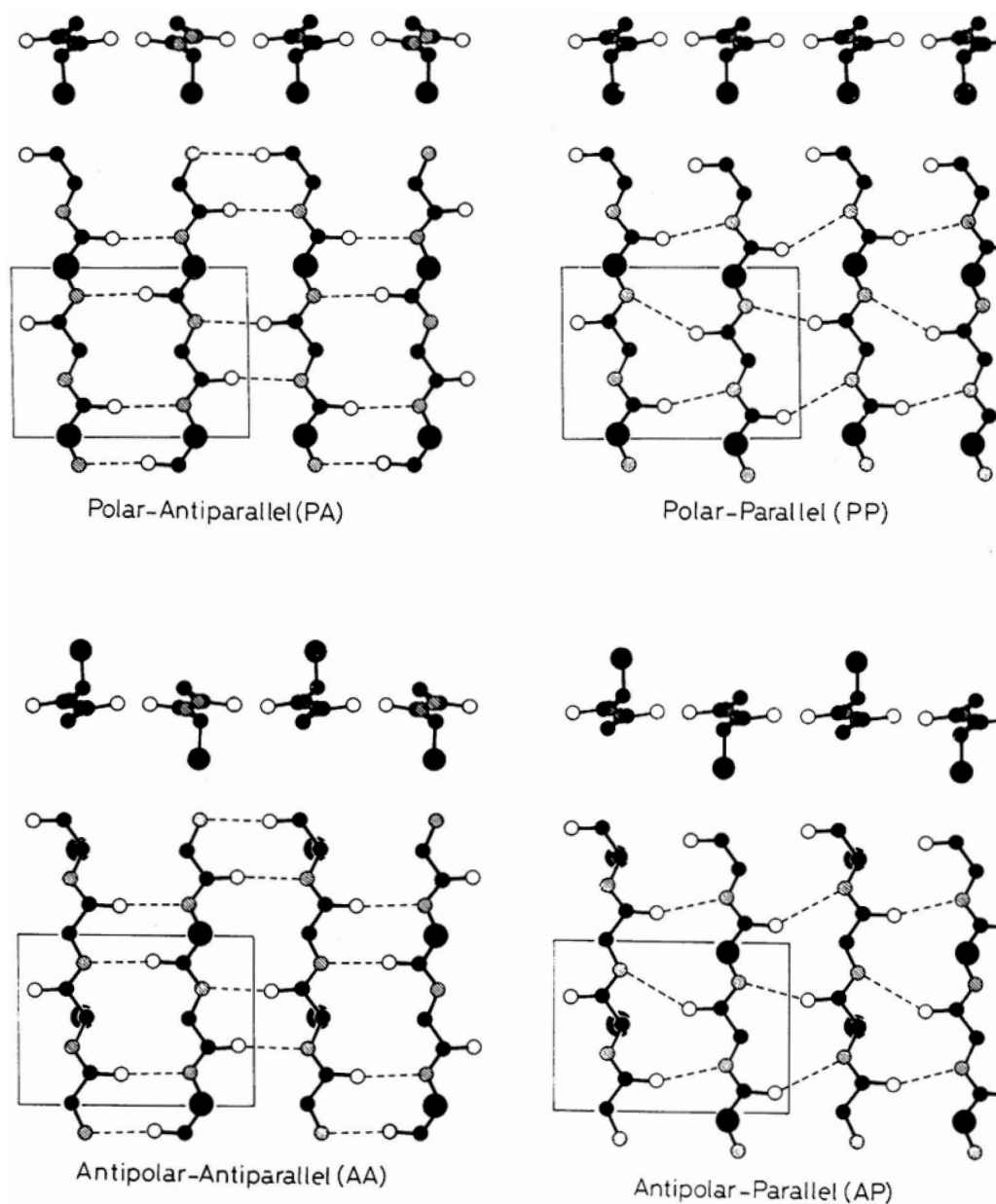


Figure 3.16 Four models for the sheet structure formed by hydrogen bonds (Takahashi, Gehoh and Yuzuriha 1999, p.130)

3.5.2.3 Mechanical properties

The high (approximately 60%) crystallinity of silk and close packing of its molecules enables the intermolecular forces of attraction to have maximum effect (Timar-Balazsy and Eastop 1998). This imparts great strength to the silk (30.9-44.1 cN/tex) with wet strength 75-85% that of the dry strength (Cook 1993b). The crystalline and extended nature of the polypeptide chains prevents great extension of silk filaments when they are pulled leading to slippage of the chains within the filaments after only a small amount of distortion. Cook reports silk to have a 20-25% elongation at break under normal conditions and 33% at 100% RH. Silk's low elasticity is demonstrated by its plastic deformation beyond 2% extension of original length. Even with very slow elastic recovery it never regains its original length (Cook 1993b).

Cultivated silk recovers from low stresses of less than 1 g/den and has a low yield strain. At 20% strain i.e. close to breaking point for both silk, silk recovers by 33%. Finer fibres recover more successfully than thicker fibres. In addition, moisture content greatly affects the elastic recovery of silk. At strains of 1%, increasing humidity decreases the recovery while at 5% and 10% the opposite is found. Up to strains of 5% both silk and wool are nearly perfect elastic fibres (Robson 1998).

Typical values for silk include strain $26 \pm 5\%$, stress 710 ± 130 MPa and a modulus of 9.5 ± 1.6 GPa for single degummed silk fibroin filaments $12.9 \pm 1.4\mu\text{m}$ in size (Schoeser, MacDonald and Marcondalli 2007).

Silk is tougher than any other natural fibre and is comparable to that of nylon. In addition, silk's breaking stress and breaking extension also compare favourably to nylon's. Silk's initial modulus which indicates stiffness is greater than that of nylon and wool but less than flax and polyester. Silk has a lower yield point than nylon which is partly due to its low yield strain. This means that it reaches the point where plastic deformation occurs at lower strains than for nylon. Increased fibre fineness leads to increased breaking stress, initial modulus, Young's modulus and crystallinity and decreased breaking extension in silk (Robson 1998).

Elongation

Application of tension causes an initial deformation predominantly in the amorphous regions. The initial modulus, resistance to deformation, is affected by the proportion of amorphous regions, interaction of amorphous with crystalline regions and the degree of

3.5 Proteinaceous model textile properties and reactivity

binding of the randomly arranged chains to one another. The high initial modulus of silk indicates relatively high interchain bonding in both the amorphous and crystalline regions. When the interchain bonds remain intact on extension there will be complete elastic recovery when the force is released. If interchain bonds break the recovery will be inelastic as randomly arranged chains within the amorphous regions extend and slip past one another and the crystalline regions (Robson 1998). This behaviour leads to a low modulus yield plateau in the stress-strain curve. If new bonds are formed in this deformed state, the silk will be permanently deformed. As the chains become more extended the crystalline region takes the load until it is too large, at which point the fibroin breaks and intrachain hydrogen and possibly peptide bonds are broken.

3.5.2.4 Reactivity

Moisture absorption

Due to the low content of sulphur and high content of serine in fibroin, the main intermolecular bonds will be predominantly hydrogen bonds within the main chain. In addition there are small quantities of hydrogen bonds and salt linkages in the side chains (Morton and Hearle 1997). This makes silk hygroscopic. At 20°C and 65% RH silk absorbs approximately 10 w% in water (Schoeser, MacDonald and Marcondalli 2007). Water is absorbed first by the amorphous regions in the silk. Competition ensues between water molecules and free reactive side-groups to form crosslinks between fibroin chains. These crosslinks ‘loosen’ the structure resulting in an increase in extensibility and a decrease in force required to rupture the fibre. These trends are further exaggerated if the water becomes absorbed into the crystalline regions (Robson 1998). At 100% RH silk absorbs 35% of its weight in water while at 65% RH silk absorbs up to 30% of its dry weight in water. In liquid water silk fibres swell mainly in the transverse direction (16.5-18.7%) with only ~1.3% swelling in the axial direction (Timar-Balazsy and Eastop 1998). Any salts or impurities within the water are also absorbed by the silk (Cook 1993b) and some inorganic salts such as calcium salts, can cause a decrease in axial length with simultaneous transverse swelling (Timar-Balazsy and Eastop 1998). This has a great effect when considering aqueous treatments for aged silks.

Soaking silk in water at 20°C and 95°C increases its extensibility, a trend that further increases with increasing temperature (Robson 1998).

3.5 Proteinaceous model textile properties and reactivity

Silk fibroin can become desiccated with exposure to RH < 40% or with heat. Since water acts as a plasticiser in the amorphous areas of fibres, desiccated silk is rigid and brittle, and loses some of its softness (Timar-Balazsy and Eastop 1998).

Acid (Cook 1993b; Robson 1998; Timar-Balazsy and Eastop 1998; Schoeser, MacDonald and Marcondalli 2007)

Silk is more sensitive to acid than wool due to its low cystine content since the disulphide bonds of cystine are resistant to acid. Dilute acids can rapidly hydrolyse the peptide bonds in the accessible, amorphous regions of silk. This is followed by a much slower attack of the less accessible regions, the rate of which can be increased with increasing temperature or textile agitation. Acid also breaks H-bonds and salt linkages in the silk. Salt linkages occur around the isoelectric point of the silk and are broken by suppression of the dissociation of the carboxyl group and formation of salts with strong mineral acids. The isoelectric point for silk is when the silk proteins are electrically neutral (i.e. an equal number of cationic and anionic groups exist). This occurs around pH 2.8, depending on factors such as fibre source, composition, and condition, and enables salt linkages to occur which help to stabilise the tertiary structure of silk. Silk is most stable and resistant to chemical degradation at this point. The gradual protonation or deprotonation of side groups below and above the isoelectric point, respectively, results in the gradual increase in bound acid and base and decrease in salt linkages. The isoelectric region (between pH 3 and 7 for silk) is the region over which silk is most stable to physical and chemical attack, having little bound acid or alkali and consequently retaining many or all of its salt linkages (Timar-Balazsy and Eastop 1998; Broadbent 2001). The random nature of acid hydrolysis weakens and embrittles silk through the cleavage of peptide bonds anywhere along the polymer chain.

The use of acid can be controlled to produce desirable effects upon silk. For example, crepe effects can be produced using concentrated sulphuric acid which can contract silk fibres by shrinking up to 40% in length with simultaneous swelling of the width. The sheen and softness of silk can also be improved with sulphuric acid. However, sulphuric acid also introduces sulphamine side groups into the polymer through reaction with amino groups and these can direct hydrolysis to nearby peptide bonds. Alternatively, dilute solutions of acids such as tartaric or citric acid can harden silk under mild conditions to produce scroop (rustling effect).

Alkali

The lack of alkaline-sensitive cystine in silk makes silk less susceptible to alkaline degradation than wool. Weak alkali solutions cause minimal damage to the silk because unlike the random nature of acid hydrolysis, in alkaline degradation only peptide bonds at the end of polymer chains are broken (depolymerisation). However, concentrated alkaline solutions e.g. caustic soda, cause alkaline hydrolysis which decreases silk's strength and lustre and can completely dissolve silk fibroin (Cook 1993b). Hot alkali decreases the quantity of serine and threonine residues by one third and releases ammonia.

Alkali also breaks H-bonds and salt linkages that help stabilise the secondary and tertiary structures of silk. This can cause structural changes that can leave the silk more susceptible to degradation.

Additionally, alkali can enable the formation of lysinoalanine crosslinks (Figure 3.17). β -elimination of serine or cystine residues to form dehydroalanine residues is thought to be involved. The addition of ϵ -amino group of a lysine residue to dehydroalanine's double bond forms lysinoalanine. Less than 10% of the lysinoalanine formed in silk originates from cystine unlike 75% in wool. Serine forms the remaining lysinoalanine (Robson 1998). These crosslinks decrease the fibre's flexibility and its ability to absorb water.

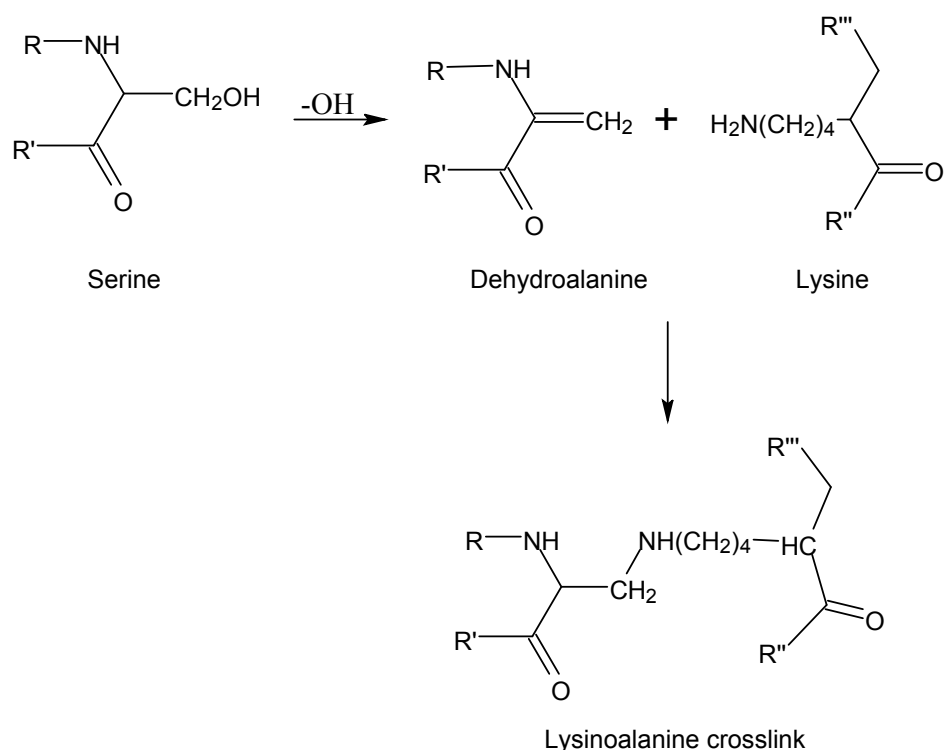


Figure 3.17 The formation of a lysinoalanine crosslink in silk in alkaline conditions (Robson 1998)

Oxidation

The complex oxidation reactions of silk occur at the peptide bonds, tyrosine side chains, and at the amino terminal residues of main chains. Complexes similar to those formed between urea and amino groups and peptide bonds are thought to form with peroxide. The tyrosine side chains are oxidised to acids and the peptide chains are broken at the tyrosine residues. Oxidation leads to reduced solubility of silk fibroin. This is thought to be due to the formation of crosslinks involving tyrosine residues or the reaction of p-quinone with a free amino group (Robson 1998).

Oxidising agents such as hydrogen peroxide and peracids are carefully used in industry to bleach silk which can be yellow even after degumming.

Artificial ageing by light, heat, and a combination of heat and high humidity has indicated that the resulting decrease in tensile strength was solely due to the breaking of the fibroin chain and that this correlated with an increase in acidity at least until a 50% drop in performance. This acidity increase is suggested to arise from the breaking of peptide bonds, salt linkages, and H-bonds which may stabilise the secondary structure. Acid and basic groups are located primarily in the amorphous regions of silk fibroin which are more susceptible to degradation than the crystalline regions. The breaking of bonds in these amorphous regions would free up some of the acid groups, increasing the acidity (Kim, Zhang and Wyeth 2008).

Photodegradation

Of all the natural fibres, silk is the most sensitive to light. The reactions involved in photodegradation are complex and not fully understood but it is known that UV is the most damaging component of light (Robson 1998). UV light (220-370 nm) causes photoyellowing while visible light bleaches silk (Lewis 1989; Timar-Balazsy and Eastop 1998). In particular, the yellowing of silk occurs due to the degradation of tryptophan and this is accelerated by the presence of tyrosine (Robson 1998).

Photoactive residues in proteins include tryptophan (λ_{max} - 280 nm), tyrosine (λ_{max} - 275 nm), phenylalanine (λ_{max} - 257 nm), leucine, threonine, and disulphide bonds. While silk contains very little cystine and phenylalanine it contains double the quantity of tyrosine

3.6 Conclusions

and a third less tryptophan than wool. UV affects the residues in the amorphous regions of the fibroin and causes the fibre to discolour, weaken, and become rigid and brittle. The degree of crystallinity in irradiated silk fibroin remains constant; however the degree of orientation within the crystalline regions decreases. Fibroin molecules within these disordered β -pleated sheets could also be degraded by UV (Robson 1998).

Photodegradation is thought to start with the breaking of hydrogen bonds. Subsequent oxidation of tryptophan and tyrosine, possibly to quinones, results in chromophoric groups that cause yellow/grey/brown/light-pink discolouration of silk and the production of radicals. The radicals can cause cleavage of the peptide bonds close to the tryptophan or tyrosine groups by a variety of mechanisms; each produce more chromophoric groups and some produce small, coloured, often water-soluble degradation products and ammonia. Hydrogen peroxide is thought to play an intermediary role. Crosslinks can form between an oxidised tyrosine and a lysine residue and between two activated tyrosine residues. These can occur before cleavage of peptide and disulphide bonds (Lewis 1989; Robson 1998; Timar-Balazsy and Eastop 1998).

The rate of photodegradation is increased by the presence of oxygen, moisture, and some metal ions (Robson 1998). Cations of copper and nickel inhibit degradation but those of zinc, iron(III), and chromium increase it (Robson 1998; Shimizu 2000).

Dye diffusion

Unlike wool, silk fibres have no surface barrier with which to inhibit dye diffusion. Consequently, fast dye uptake can occur at lower temperatures than with wool (Brady 1990).

3.6 Conclusions

A range of iron-tannate dyed organic materials including cotton, abaca, wool, silk, leather, skin, New Zealand Flax (*Phormium tenax*), and raffia, were identified in historic objects at the British Museum through discussion with curators, searches of the British Museum's catalogue, and XRF analysis (Chapter 6). Consideration of the aims of the model textiles to be produced in this project, the form of the historic iron-tannate dyed materials at the British Museum, the availability of materials, the high quantity of material required, and the high homogeneity required led to the choice of woven cotton, abaca, wool, and silk textiles for the organic materials to be used in this project. The composition, formation, properties, and reactivity of each material have been discussed as there are slight

3.6 Conclusions

differences for each material type that can affect the extent of dyeing and iron-tannate dye catalysed degradation. Abaca for example has a higher non-cellulosic component (approximately 35%) than cotton (approximately 10%) and some of these components e.g. hemicellulose (approximately 21% of abaca) are more susceptible to acid hydrolysis than cellulose. Wool has a hydrophobic outer cuticle which silk, and the other fibres, do not have and this could affect the extent of dye penetration into the fibres and subsequent iron-tannate dye catalysed degradation.

4 MODEL IRON-TANNATE DYES**4.1 Iron-tannate dye composition and properties****4.1.1 Reagents**

The essential reagents in iron-tannate dyes are iron ions and tannins which are dissolved in water and either combined together before application to a textile or applied separately to a textile in two stages. Textile dyeing manuals and other literature describing iron-tannate dyeing from the 16th century onwards often identify sources of iron ions as being: iron sulphate also known as copperas, green vitriol or Roman vitriol; iron acetate (produced from pieces of iron in acetic acid); or iron-rich mud from stagnant water areas such as swamps or river beds where the iron present is maintained as Fe(II) due to anaerobic bacterial reduction. Tannins (condensed, hydrolysable, or a mixture) (Figure 4.1) were sourced from plant material such as gallnuts (e.g. Aleppo or oak), bark (e.g. alder or oak), leaves (e.g. sumach), seeds (e.g. Tamarind) or fruit (e.g. divi divi) (Rosetti 1548; Mascall 1589; Haigh 1800; Bancroft 1813; Martin 1813; Packer 1830; Baird 1850; Bird 1876; Hurst 1892a; Forbes 1956; Donne 1973; Daniels 1995; Cardon 2007; Leed 2008; Ziegler 2008; Karolia, Nagrani and Raval 2009).

Hydrolysable tannins are glucose esters of phenolic acids such as gallic acid and ellagic acid and were the preferred tannin type because they form blue-black coloured iron(III)-tannate dye complexes on combination with iron ions (Khanbabaee and van Ree 2001). Condensed tannins (proanthocyanidins) are oligomers or polymers of flavan-3-ol (catechin) monomers (Khanbabaee and van Ree 2001) which form green-black coloured dye complexes on combination with iron ions (Daniels 1997, 1998; Daniels 2000; More, Smith, Te Kanawa and Miller 2000). Daniels (Daniels 1997, 1998) noted that while useful for tanning leather, condensed tannins are less useful for iron-tannate dyes and references Mitchell who reports that ‘iron-greening’ tannins cause iron-gall inks to leave rust-like stains after six months and that consequently, only ‘iron-blueing’ tannins are suitable for ink (Daniels 2000). The reagent sources listed above are just a small selection of the wide range used by dyers all over the world based on the tannic acid and iron ion sources available to them.

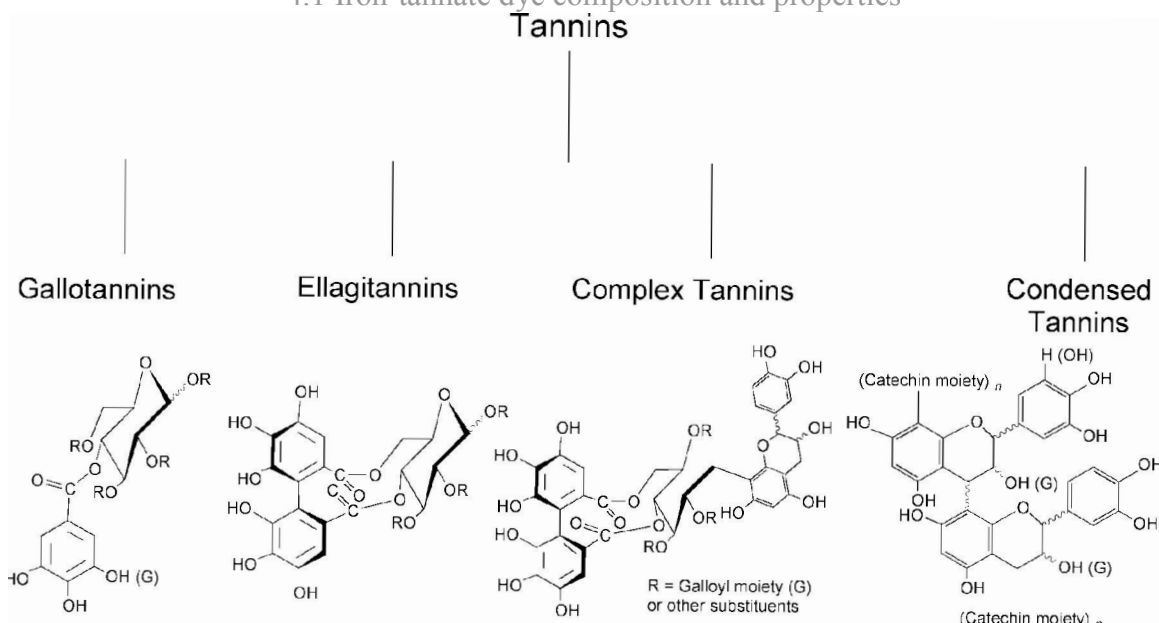


Figure 4.1 The classification of tannins into four major types¹ based on their structural characteristics (Khanbabaee and van Ree 2001) p.643

Additional reagents were often intentionally added to iron-tannate dyes including logwood, Prussian blue, copper sulphate, soured wine, vinegar, egg shells, and urine (Rosetti 1548). Metals such as titanium, vanadium, chromium, manganese, cobalt, nickel, copper, zinc, mercury, and lead were often unintentionally added as impurities in a reagent, in this case, iron sulphate. These ions have been identified within iron gall ink documents using an in-air PIXE method (Budnar, Simcic, Ursic, Rupnik and Pelicon 2006; Kolar, Stolf, Strlic, Pompe, Pihlar, Budnar, Simcic and Reissland 2006). In a study of 97 documents, six contained ink with a molar ratio of copper to iron higher than 60% and 32 had a copper to iron ratio higher than 10%. The molar ratios of other transition metals to iron were less than for copper. Calcium and potassium were also detected and suggested to arise from gum Arabic (Kolar, Stolf, Strlic, Pompe, Pihlar, Budnar, Simcic and Reissland 2006).

4.1.2 Iron-polyphenol dye complex

The structures of iron-tannate dye complexes are still not fully understood. Several studies have been undertaken in which iron(II) ions, iron(III) ions, or metallic iron have been combined with hydrolysable tannic acids or its phenolic hydrolysis products such as gallic

¹ The four major tannin types are: “(1) Gallotannins are all those tannins in which galloyl units or their *meta*-depsidic derivatives are bound to diverse polyol-, catechin-, or triterpenoid units. (2) Ellagitannins are those tannins in which at least two galloyl units are C-C coupled to each other, and do not contain a glycosidically linked catechin unit. (3) Complex tannins are tannins in which a catechin unit is bound glycosidically to a gallotannin or an ellagitannin unit. (4) Condensed tannins are all oligomeric and polymeric proanthocyanidins formed by linkage of C-4 of one catechin with C-8 or C-6 of the next monomeric catechin.” Khanbabaee, K. and T. van Ree (2001). "Tannins: Classification and Definition." *Natural Product Reports* **18**: 641-649, p. 643

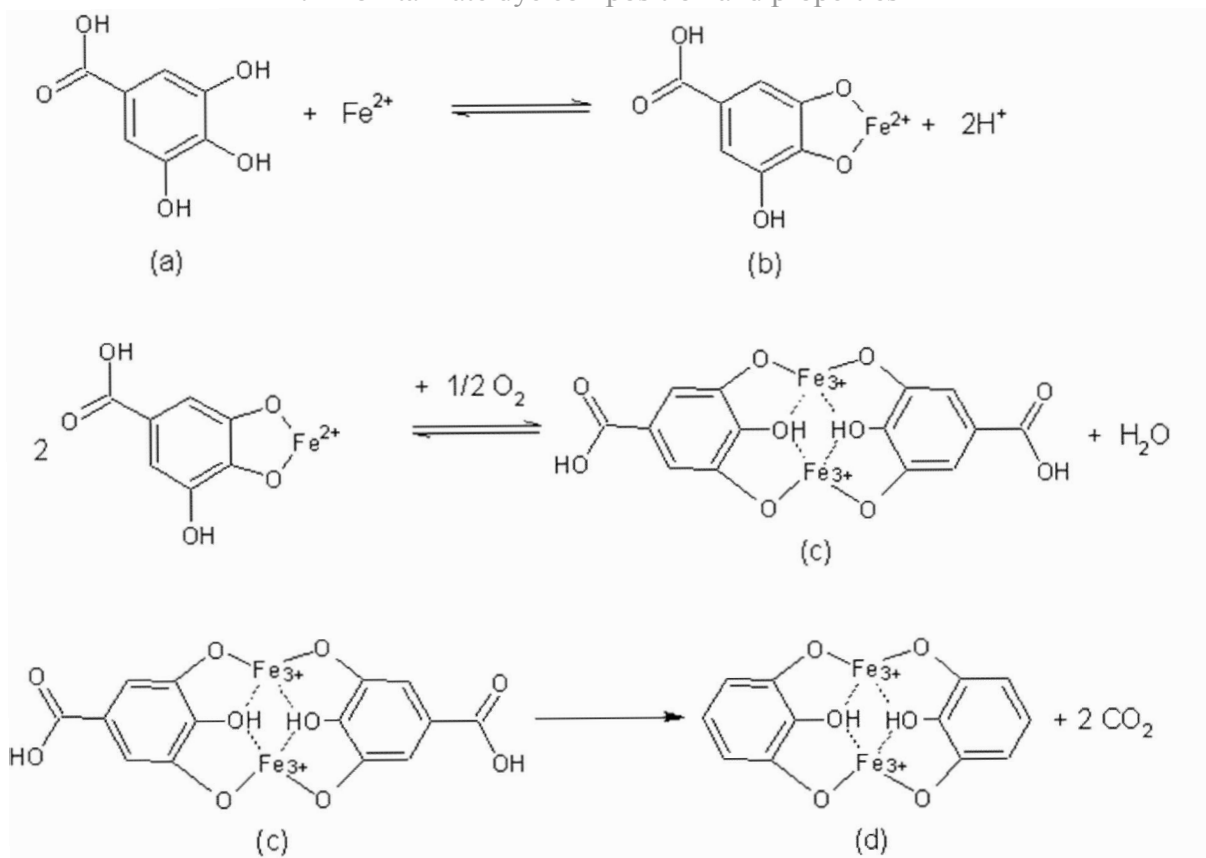
4.1 Iron-tannate dye composition and properties

acid, ellagic acid, and pyrogallol (Tasneem, Kazmi and Sultana 1991; Wunderlich 1991; Qureshi and Kazmi 1994; Wunderlich 1994; Marmolle, Leize, Mila, Van Dorsselaer, Scalbert and Albrecht-Gary 1997; Krekel 1999; Hynes and O'Coinceanainn 2001; Jaen, Gonzalez, Vargas and Olave 2003; Wilson 2007; Sungur and Uzar 2008).

In aqueous polyphenol solutions with a concentration <1% it has been found that hydrolysis of iron into oxides and oxyhydroxides predominates (Jaen, Gonzalez, Vargas and Olave 2003). However, above a 1% polyphenol concentration, complexation with the polyphenol predominates. Research suggests that the rate of reaction of iron with polyphenols is concentration dependent (Jaen, Gonzalez, Vargas and Olave 2003) with the rate increasing with increasing polyphenol concentration. Pyrogallol and tannic acid (5%) showed similar kinetic behaviour on combination with iron, and the conversion of metallic iron to iron-tannate complexes was found to be first order (Iglesias, Garcia de Saldana and Jaen 2001). Rate constants for complex formation have been calculated for gallic acid and iron (Tasneem, Kazmi and Sultana 1991; Marmolle, Leize, Mila, Van Dorsselaer, Scalbert and Albrecht-Gary 1997; Hynes and O'Coinceanainn 2001) and tannic acid and iron (Sungur and Uzar 2008) but are considered beyond the scope of this thesis and the details are omitted.

Under acidic conditions 1:1, 1:2, and 2:2 iron(III):gallic acid complexes are formed (Darbour 1980; Krekel 1999; Delamare and Repoux 2001; Hynes and O'Coinceanainn 2001; Jaen, Gonzalez, Vargas and Olave 2003). According to Krekel (Krekel 1999) both 1:1 iron(II):gallic acid and iron(III):pyrogallol complexes are also formed; the former during his proposed two step production of the 2:2 iron(III):gallic acid complex (Scheme 4.1), and the latter only if unbound iron(III) ions are present to enable decarboxylation of the gallic acid moieties (Scheme 4.1). The 1:1 iron(II):gallic acid complex has been identified using ToF-SIMS but it is uncertain if its presence was due to primary ion bombardment and fragmentation of the 2:2 complex, or if it was present in the sample prior to analysis (Delamare and Repoux 2001). However, iron(II) compounds were identified after combination of metallic iron and pyrogallol (5%) (Jaen, Gonzalez, Vargas and Olave 2003).

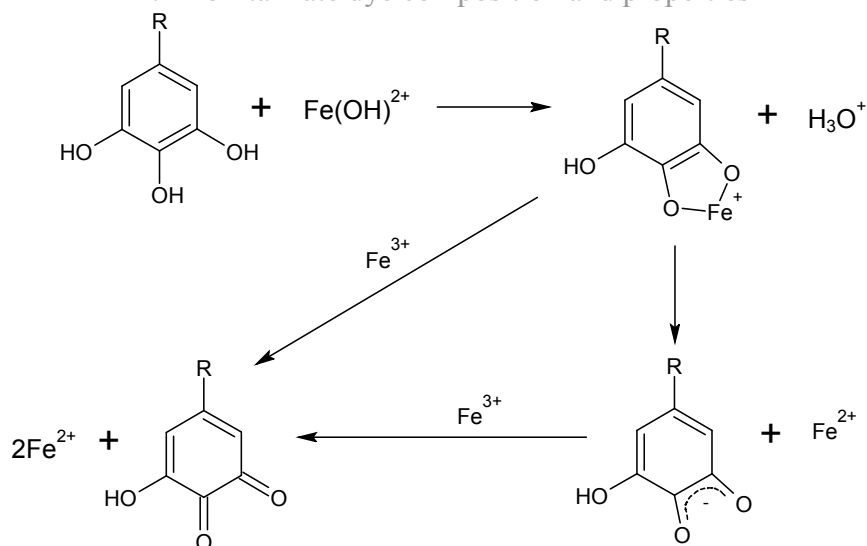
4.1 Iron-tannate dye composition and properties



Scheme 4.1 Formation of iron(III)-gallate and iron(III)-pyrogallol complexes from iron(II) ions and gallic acid as proposed by Krekel (Krekel 1999). On combination of gallic acid (a) and iron(II) sulphate in water a water-soluble, colourless 1:1 iron(II)-gallic acid complex (b) is formed via a metal catalysed deprotonation reaction when the gallic acid is protonated (Hynes and O'Coinceanainn 2001). Upon oxidation with dissolved oxygen in the water, (b) becomes an insoluble, blue-black 2:2 iron(III)-gallic acid complex (c). After iron(III)-catalysed decarboxylation of (c) the resulting 2:2 iron(III):pyrogallol complex (d) is planar with the four oxygen atoms from four water molecules (two above and two below the plane) completing the octahedral environments of the iron(III) ions. This octahedral environment is highly probable in (c) also, however using molecular modelling computations it has been suggested that the iron(III) ions are in tetrahedral arrangement with the gallic acid molecules, making (c) non-planar (Delamare and Repoux 2001).

The 1:1 complex is increasingly unstable with increasing acidity, being decomposed to a quinone and iron(II) ion by an internal electron transfer, Scheme 4.2. Depending on the conditions the electron transfer can occur via a protonated complex (Hynes and O'Coinceanainn 2001). Under neutral and alkaline conditions 1:2 and 1:3 iron(III):gallic acid complexes have been identified (Kipton, Powell and Taylor 1982). The formation of a 1:3 complex at pH 8 from both 1:1 and 1:2 complexes has been studied and found to be faster from the former (Qureshi and Kazmi 1994).

4.1 Iron-tannate dye composition and properties



Scheme 4.2 The formation of semi-quinones and quinones from phenols and an excess of ferric ions (Hynes and O'Coinceanainn 2001)

Additionally, Wunderlich (Wunderlich 1991) proposed a 1:1 hexaganol iron(III):gallic acid framework in which each iron(III) ion was bound to four gallic acids in an octahedral arrangement. Two gallic acids were bound via vicinal dihydroxyl groups while the other two were bound via the hydroxyl of the carboxylic acid group. Each of these gallic acids could bind to more iron ions to complete the framework proposed. However, the method of production was not comparable to the production of iron gall inks or iron-tannate dyes, unlike the previously mentioned studies, since it involved the combination of iron(III) chloride with gallic acid on a gel matrix. Consequently, it is uncertain if this structural framework is present in either iron-gall inks or iron-tannate dyes.

A study involving iron(III) chloride hexahydrate and tannic acid rather than gallic acid found that 1:1 ($\text{pH} < 3$), 2:1 ($\text{pH} 3\text{--}7$), and 4:1 ($\text{pH} > 7$) iron(III):tannic acid complexes can be formed at varying pHs (Sungur and Uzar 2008). In a separate study in which metallic iron was mixed with tannic acid, 1:1 iron(III):tannic acid complexes were identified throughout the experiment with 1:2 complexes developed at a later stage (Iglesias, Garcia de Saldana and Jaen 2001). A 1:1 iron(II):tannic acid complex was proposed if the iron(II) had not first been oxidised to iron(III). While structures of these complexes were not presented, research suggests that hydroxyl groups, particularly the ortho-dihydroxyl groups in the galloyl (3, 4, 5-trihydroxybenzene) moieties of tannic acids are important in iron binding. Additionally, other unstated sites are thought to be involved (Khokhar and Owusu Apenten 2003). For tannic acid in which five digallic acids can be bound to one glucose molecule via ester linkages, these sites could be the carbonyl groups of the ester linkages and neighbouring hydroxyl groups in the digallic acid, or the carbonyl of an ester link with

4.1 Iron-tannate dye composition and properties

oxygen from an adjacent ester link, or possibly with the oxygen of the glucose ring. The latter two suggestions may be less energetically favourable than the first due to the closer proximity of neighbouring groups.

Apart from Wunderlich's proposal of a crystalline complex, the iron complexes proposed for iron-tannate dyes tend to be small compounds. In research into the complexation of copper(II) and zinc(II) ions to polyphenols including tannic acid, gallic acid, and pyrogallol, the insoluble nature of the complexes was considered (McDonald, Mila and Scalbert 1996). It was proposed that in order for the complex of soluble copper ions and soluble polyphenol compounds to be less soluble than the reagents, or even insoluble in water:

- a. the polarity of the polyphenol could be reduced;
- b. a neutral complex could be formed such as $M(LH_3)M(LH_3)M$ which has been suggested to form from gallic acid and copper ions (McDonald, Mila and Scalbert 1996) and involves complexation via the carboxyl groups as well as the ortho-dihydroxy groups of the gallic acids. Catechol hydroxyl groups (ortho dihydroxyl) of tannins bind more strongly to iron(III) than carboxyl groups (Smith, Te Kanawa, Miller and Fenton 2001);
- c. the complex could be of high molecular weight. This could occur by two methods. Firstly, semi-quinones or quinones that can be produced through copper-catalysed autoxidation of tannic acid (Balla, Kiss and Jameson 1992) can polymerise and complex with copper ions to form high molecular weight, insoluble complexes. Secondly, due to the many ortho-dihydroxy groups in tannic acid, polymerisation can occur by the complexation of multiple copper ions which can each complex with separate tannic acids to make a large structure (McDonald, Mila and Scalbert 1996).

Potentially similar polymerisation could occur to iron-tannate and iron-gallate complexes to produce high molecular weight compounds. For small charged molecules, polymerisation to form high molecular weight molecules could explain the insoluble nature of iron-tannate and iron-gallate complexes. In addition to insolubility, the larger the molecule's size the lower its diffusional properties and consequently, the more permanent and wash fast the dye will be.

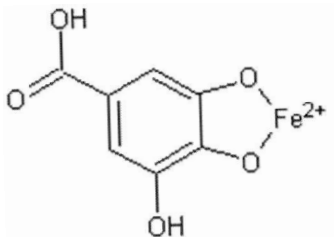
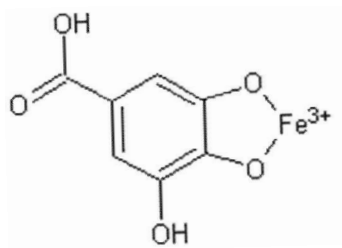
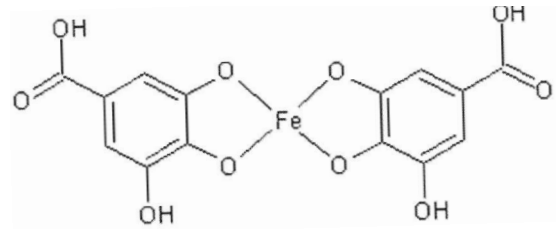
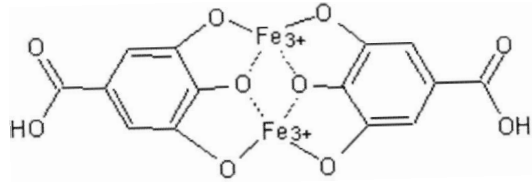
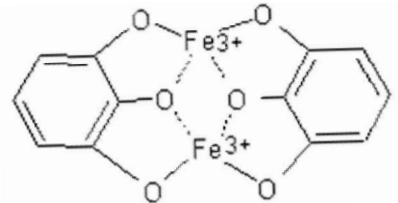
4.1 Iron-tannate dye composition and properties

Aggregation of iron-tannate or iron-gallate dye molecules by weak intermolecular bonds such as van der Waals' and/or hydrogen bonds, rather than polymerisation could occur to produce high molecular weight iron-tannate or iron-gallate aggregates (Wilson 2007). As seen with vat dyes such as indigo (Aspland 1997), the extent of aggregation of a molecule can increase with the planarity and linearity of the molecule and many of the iron-gallate molecules discussed in this section are indeed planar (see Table 4.1 for molecular structures). A well known example in vat dyeing is the indigo molecule which aggregates through intermolecular hydrogen bonding to varying levels depending on the environment to achieve distinct colours (Christie 2001).

In summary, since iron-tannate dyes are acidic (Section 4.16), the most likely complexes present in iron-tannate dyes include the 1:1 iron(II):gallic acid complex, 1:1, 1:2, 2:2 iron(III):gallic acid complexes, and the 1:1 and 2:1 iron(III):tannic acid complexes (Table 4.1). Since tannins can reduce iron(III) ions to iron(II) ions (see Section 4.14), both 1:1 and 2:1 iron(II):tannic acid complexes may also be present. The majority of these complexes are unstable in neutral or alkaline conditions. Though rarely mentioned in the literature, polymerisation may occur to produce large high molecular weight iron-tannate compounds. When formed inside the fibre, these large polymers can become trapped due to their size and so the dyed textile exhibits good wash fastness and permanence. High molecular weight aggregates may also be formed particularly from planar molecules via van der Waals' and/or intermolecular hydrogen bonds, which would also impart good wash fastness if formed within the fibres. Similar aggregation via intermolecular hydrogen bonding is known to occur with indigo molecules.

4.1 Iron-tannate dye composition and properties

Table 4.1 Iron-gallate and iron-tannate complexes most likely to occur in acidic iron-tannate dyes

Iron(II):gallic acid	
<p>1:1 iron(II):gallic acid</p>  <p>Soluble and colourless (Krekel 1999)</p>	
Iron(III):gallic acid/pyrogallol	
<p>1:1 Iron(III):gallic acid</p> 	<p>1:2 iron(III):gallic acid</p> 
<p>2:2 iron(III):gallic acid</p> 	<p>2:2 Iron(III):pyrogallol</p> 
Iron(III) and iron(II):tannic acid	
<p>1:1 Iron₇ — tannic acid</p>	<p>2:1 Iron₂ — tannic acid</p>

4.1.3 Other metal-polyphenol complexes

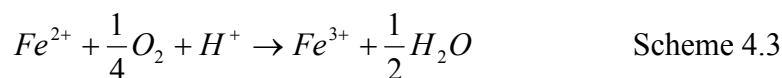
As previously mentioned, metals other than iron such as titanium, vanadium, chromium, manganese, cobalt, nickel, copper, zinc, mercury, and lead can be present in iron-gall inks and iron-tannate dyes (Budnar, Simcic, Ursic, Rupnik and Pelicon 2006; Kolar, Stolf, Strlic, Pompe, Pihlar, Budnar, Simcic and Reissland 2006). These metal ions can be present due to intentional (i.e. addition of copper sulphate) and unintentional (i.e. as impurities in reagents) additions to the ink or dye formulation. For example, vitriol, a source of iron sulphate, contained many impurities dependent on the location of the mine from which it was sourced. A study of two types of vitriol identified sulphates of copper, aluminium, zinc, and manganese in addition to iron sulphate (Krekel 1999). Of these, Neevel (Neevel 2002) states that only the iron(II) ions and iron(III) ions bind to gallic acid and gallotannic acid, and Krekel (Krekel 1999) states that combination of pure copper(II) sulphate with gallic acid results in only soluble brown products. However, while zinc ions have been shown to form insignificant quantities of precipitates with gallic acid and pyrogallol and low quantities with tannic acid (McDonald, Mila and Scalbert 1996), evidence suggests that copper ions do bind to gallic acid, pyrogallol, and tannic acid (McDonald, Mila and Scalbert 1996; Cruz, Diaz-Cruz, Arino, Tauler and Esteban 2000; Andrade Jr., Dalvi, Silva Jr., Lopes, Alonso and Hermes-Lima 2005), and aluminium(III) ions have formed complexes with condensed polymers at neutral pH (Kennedy and Powell 1985). In a pH 5 buffered solution (buffered to counteract the increasing acidity on complex formation), the ratio of copper:tannic acid was dependent on reagent concentration with the maximum being limited by the quantity of ortho-dihydroxyphenyl and/or carbonyl coordination groups in the ligand (McDonald, Mila and Scalbert 1996; Cruz, Diaz-Cruz, Arino, Tauler and Esteban 2000). Research (McDonald, Mila and Scalbert 1996) suggested that two gallic acid molecules bound to three copper ions through use of both ortho-dihydroxyphenyl groups and the carboxyl group to give the uncharged $M(LH_3)_3M$ complex. As with iron-tannate and iron-gallate complexes, the stability of the copper-tannate and copper-gallate complexes was pH dependent (McDonald, Mila and Scalbert 1996). In a separate study, 6:1 to 8:1 copper(II):tannic acid complexes were produced (Andrade Jr., Dalvi, Silva Jr., Lopes, Alonso and Hermes-Lima 2005). The binding involved may be $Cu(O)_4$ in which four phenolic hydroxyl groups are bound to one copper(II) ion. This structure has been identified using EPR to analyse silk fibroin that had been pre-treated with tannic acid prior to treatment with cuprammonia solution (pH 10.6) (Chen, Lu, Yao, Pan and Shen 2005).

4.1.4 Iron oxidation state in iron-tannate dyes

Both the formation of iron(II) and iron(III) gallic and tannic acid complexes have been discussed with oxidation of iron(II) ions occurring in aerated solutions both when complexed and uncomplexed. It could be expected that the iron in iron-tannate dyes only exists as iron(III), however significant quantities of both iron(II) and iron(III) ions have been identified in oxygenated solutions of iron ions and pyrogallol in the pH range of 2.5-5.5 (Kipton, Powell and Taylor 1982). Iron(II) ions have also been identified in iron gall inks of 15th (Darbour, Bonnassies and Flieder 1981), 16th (Wagner, Bulska, Stahl, Heck and Ortner 2004), and 18th (Neevel 1995) century documents and modern model samples (Wagner, Bulska, Stahl, Heck and Ortner 2004) in proportions ranging from approximately 15% to 52% of the total iron content. Since iron(II) ions participate in the Fenton reaction, knowledge of their presence in iron gall inks and presumably in iron-tannate dyes also is important.

The ratio of iron(II):iron(III) ions in a dye is affected by several competing processes.

1. Oxidation of iron(II) to iron(III) by oxygen (Scheme 4.3).



The rate of oxidation increases with decreasing acidity, i.e. increasing pH. Qualitative evidence suggests that above pH 4 only minute traces of oxygen are needed to oxidise iron(II) but that below pH 4 the rate of oxidation could be low enough to enable iron(II) ions to be present (Kipton, Powell and Taylor 1982).

Figure 4.2 is a Pourbaix diagram for iron which identifies the most thermodynamically stable form of iron at equilibrium, at a varying pH and standard potentials (E). Figure 4.2 also shows the regions of passive, corrosive and immune behaviour of iron at different pH and standard potentials. A more negative potential indicates a greater probability that the compound will be reduced while a more positive potential indicates a greater probability that the compound will be oxidised. A limitation of the Pourbaix diagram is that the kinetics of the reaction, i.e. how fast it goes, is not indicated (Scott and Eggert 2009; McCafferty 2010).

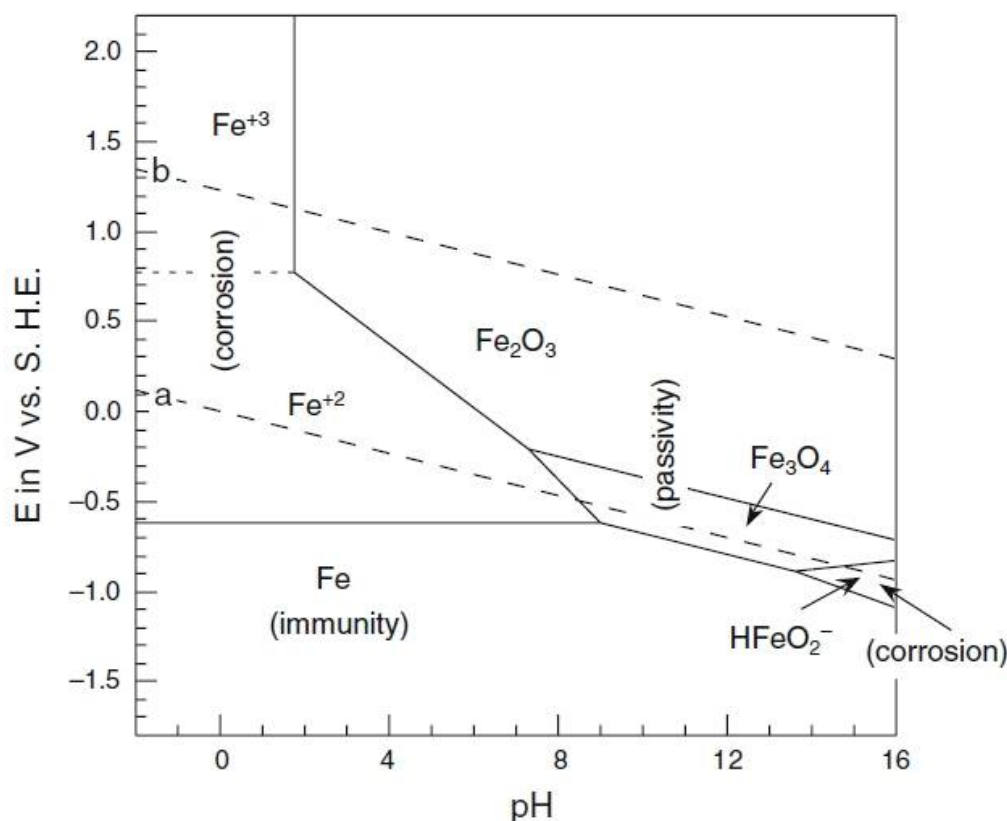


Figure 4.2 Pourbaix diagram for iron in water at equilibrium and at 25°C (McCafferty 2010) p.104

2. Formation of stable iron(III)-tannate complexes.

At equilibrium and low pH, iron(III) is the most favourable oxidation state of iron. Therefore, following Le Chateliers Principle, the formation of stable iron(III)-tannate complexes increases the rate of oxidation of iron(II) by decreasing the concentration of unbound iron(III) in the system (Kipton, Powell and Taylor 1982).

3. Reduction of iron(III) to iron(II) by polyphenols of the ink or dye.

Gallic acid and pyrogallol are phenolic molecules that can rapidly reduce iron(III) at pH 2-3 to iron(II) (Kipton, Powell and Taylor 1982). This is due to the similar reduction potential for ortho-quinone \rightarrow polyphenol [0.713 V (SHE) for pyrogallol and 0.799 V (SHE) for gallic acid] and for iron(III) \rightarrow iron(II) [0.771 V (SHE)] (Kipton, Powell and Taylor 1982; Martinez and Stern 1999; Jaen, Gonzalez, Vargas and Olave 2003). This reduction can also occur to copper(II) ions [copper(II) \rightarrow copper(I) = 0.16 V (SHE)] (Balla, Kiss and Jameson 1992; Atkins and de Paula 2002b). In each case, reduction of metal ions can occur when complexed to a polyphenol or uncomplexed, and can occur by the complexed polyphenol or by a separate polyphenol. Under low pH conditions electron transfer from an iron(III)-gallate complex has been found to go

4.1 Iron-tannate dye composition and properties

via a protonated iron(III)-gallate complex (Hynes and O'Coinceanainn 2001). The polyphenols that are separate from the iron they reduce are oxidised to semi-quinones (phenoxyl radicals) prior to quinones and it is possible that those that are complexed to the iron they reduce are also oxidised to semi-quinones (Hynes and O'Coinceanainn 2001; Andrade Jr., Dalvi, Silva Jr., Lopes, Alonso and Hermes-Lima 2005; Andrade Jr., Ginani, Lopes, Dutra, Alonso and Hermes-Lima 2006). Semi-quinones of hydrolysable tannins, condensed tannins, and pyrogallol have been detected in EPR studies using horseradish peroxidase and hydrogen peroxide (Bors, Michel and Stettmaier 2000). This reduction has been proposed to occur at the natural pH of mixtures of gallic acid with metallic iron (Jaen, Gonzalez, Vargas and Olave 2003) which are likely to be comparable to the pH of iron-tannate dye formulations. Cu(II) ions are also reduced by ortho-dihydroxybenzene at pH 4.5-5.5 and form semi-quinones and quinones as a byproduct (Balla, Kiss and Jameson 1992).

4. Reduction of iron(III) ions by organic radicals and aldehydes of the substrate. Some organic radicals (other than polyphenols) such as glucose, as well as aldehydes, can also reduce iron(III), and these compounds increase in concentration with increasing oxidation of the iron-tannate dyed substrate (Strlic, Selih and Kolar 2006).

If metallic iron is included in the dye formulation, iron(II) ions can also arise from its anodic dissociation, Figure 4.2. (Kipton, Powell and Taylor 1982; Iglesias, Garcia de Saldana and Jaen 2001; Jaen, Gonzalez, Vargas and Olave 2003).

4.1.5 Colour

Iron-tannate dyed organic materials are typically black immediately after dyeing but can also be grey or brown and often turn browner with age. Reflectance spectra of model iron gall ink documents (Sistach, Gibert and Areal 1999) and traditionally dyed New Zealand flax (*Phormium tenax*) (Te Kanawa, Thomsen, Smith, Miller, Andary and Cardon 1999) have been used to characterise the changing colour of iron-gall inks and iron-tannate dyes during ageing.

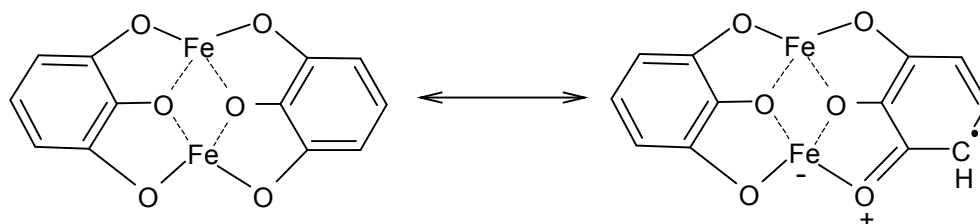
4.1.5.1 Factors affecting the colour of the dyed material

a. The iron-tannate dye complex.

The colour of the iron-tannate dye complex is due to a reversible light-induced charge-transfer across an Fe-O bond of the complex (Scheme 4.4) (Krekel 1999). The conjugated double bond system formed from the charge-transfer absorbs a broad range of visible

4.1 Iron-tannate dye composition and properties

energy with a maximum around 620 nm at pH 4 that gives iron(III)-pyrogallol its blue-black colour (Sistach, Gibert and Areal 1999).



Scheme 4.4 Charge-transfer in an iron(III) pyrogallol complex

Different iron-polyphenol complexes have different colours. Solutions of iron(III) gallate complexes were blue-purple (λ_{max} 548 \pm 3 nm) with a 1:2 stoichiometry at pH 7.5, and red-purple (λ_{max} 499 \pm 2 nm) with a 1:3 stoichiometry (pH 10.5). In contrast iron(III) pyrogallol solutions of pH < 3 were amber, between pH 4.5-7.2 were purple-grey, and with a pH > 7.2 were red-purple (Kipton, Powell and Taylor 1982). The increasing redness of the complexes above pH 7 is important when considering neutralisation of the acid in iron-tannate dyed textiles as part of a conservation treatment. Significant change of colour of a sample due to treatment application is undesirable.

b. Iron-tannate dye formulation.

The reagents used including their purity, source, quantity, and freshness affect the colour of the dyed material. In model iron gall inks the inclusion of equal quantities of copper and iron ions caused the ink to have a greenish tint due to the formation of green copper hydroxycarbonates (Sistach 1990). For tannic acid sources the time of year when the source is harvested and length of time between harvesting and use is important as the quantity of tannic acid in a source varies throughout the year and decreases over time once harvested. Decreasing tannic acid content will lead to a paler ink or dye for the same mass of reagent as one with a higher tannic acid content. The production method including length of exposure to the reagents, pH of dyeing solutions, and temperature of solutions as well as water supply can also affect the colour achieved by the dye (O'Connor and Richards 1999).

The many variables and the frequent ambiguity in historic dye formulations caused low reproducibility of black dyeing. Even with the detailed dye formulations of the 19th century, black dyes were thought by both merchants and dyers to be the most difficult dyes to match (Anonymous 1898). By the end of the 19th century, black dyeing had become the

4.1 Iron-tannate dye composition and properties

most important branch of silk dyeing requiring highly skilled dyers who often specialised in black dyeing (Hurst 1892).

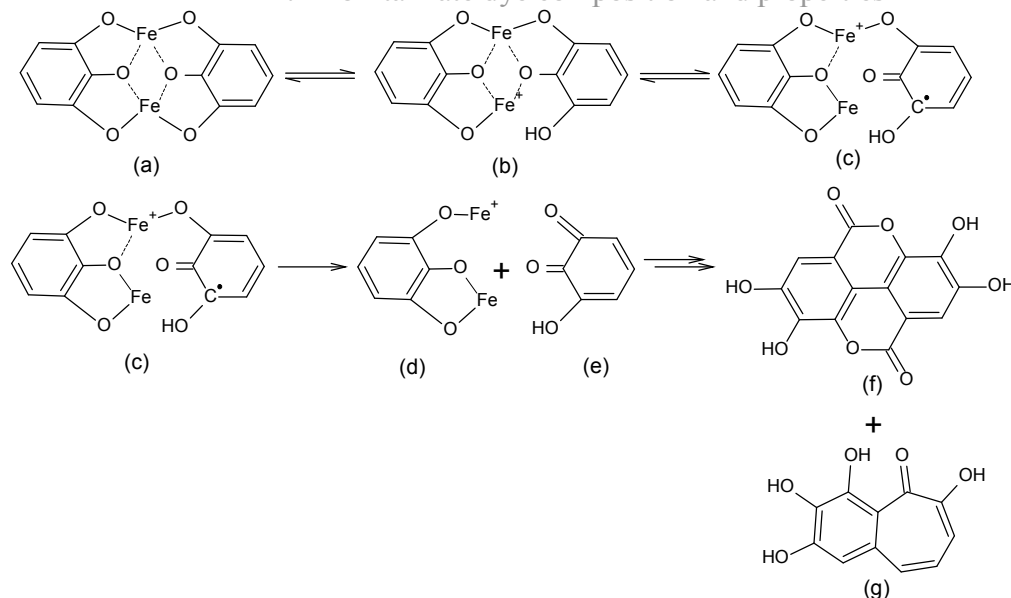
c. Coloured degradation products.

Oxidation and acid hydrolysis of the substrate, breakdown of the iron-tannate dye complex, and oxidation of polyphenols can all lead to coloured degradation products (Kipton, Powell and Taylor 1982; Sistach, Gibert and Areal 1999; Daniels 2000).

Oxidation introduces carbonyl groups into the polymer chain which along with acid hydrolysis, breaks the polymer chain into small molecules such as sugars. Carbonyl groups such as aldehydes are chromophores that can absorb light in the near visible region and can cause discolouration to the fibre if they form part of a larger conjugated system. Increasing conjugation lowers the energy of the light absorbed as the energy gap between the ground and excited states decreases, thus increasing the quantity of light absorbed in the visible region by the oxidised fibre. This gives oxidised fibres a yellow, yellow/brown colouration (Sykes 1970; Timar-Balazsy and Eastop 1998). Large coloured compounds can be formed via condensation reactions with the small molecules that result from depolymerisation of the polymer chains (Sistach, Gibert and Areal 1999; Whitmore 2011). Glucose, originating from the depolymerisation of cellulose, can form furans that can react to produce coloured compounds. The rate of discolouration therefore increases with: light which accelerates oxidation; acid which can catalyse the condensation of small molecules into larger, coloured compounds; and increasing RH as the water molecules bring the reagents together for reaction to occur. Through reaction with oxidised or unoxidised polymer chains, coloured compounds can become bound to the polymer chains in the fibres and therefore insoluble in water. Unbound coloured compounds are water soluble and so can be removed by washing the substrate (Whitmore 2011).

Acid catalysed breakdown of the black complex through interaction with light forms 1,2-benzoquinone (Scheme 4.5) which then forms brown degradation compounds such as ellagic acid (yellow-brown) (**f**) and purpurogallin (reddish brown) (**g**). Gallic acid and ellagic acid can be further degraded to produce polymeric compounds of polyphenols similar to humic acid (Slawinska, Slawinski, Polewski and Pukacki 1979; Neevel 2006).

4.1 Iron-tannate dye composition and properties



Scheme 4.5 Acid-catalysed degradation of iron(III) pyrogallol (Sistach, Gibert and Areal 1999)

Oxidation of phenols such as gallic acid can occur in acid and alkaline environments by oxygen or by iron(III) ions and results in quinones via semi-quinone intermediates. Ortho-quinones can undergo secondary reactions including phenolic coupling in environments above pH 7 (Kipton, Powell and Taylor 1982). Above pH 8 the black complex in iron gall ink is dissolved as phenols are irreversibly oxidised and a reddish brown solution including purpurogallin is formed (Krekel 1999).

The presence of high quantities of iron(III) in the dye will also increase the brown tone of the dye through the formation of brown coloured iron(III) oxides and oxide-hydroxides (Sistach 1990; Emsley 1998; Krekel 1999; Neevel 2006).

4.1.6 Acidity

4.1.6.1 Dye formulation

The high acidity of iron-tannate dyes and iron gall inks is due to the iron source, tannin source, and any other reagents added to the dye or ink formulation. Unbound iron contributes to the acidity by forming acidic hydration products (Shahani and Hengemihle 1986; Neevel 2002). The counterion of the iron can form acidic compounds during iron-tannate or iron-gallate complex formation, e.g. sulphuric acid (Krekel 1999). The tannic or gallic acids contain labile hydroxyl and carboxyl groups which can contribute to the acidity when not complexed to iron; the pH of dissolved tannins varies for tannin type but is 2.8 for tannic acid (10 g/L) (McDonald, Mila and Scalbert 1996). Additionally, the inclusion

4.1 Iron-tannate dye composition and properties

of other reagents will affect the acidity, for example vinegar will lower the pH or urine will raise it. Consequently, the pH of fresh iron gall inks has been found to range from 1.5 to 3.7 (Sistach and Espedaler 1993; Krekel 1999). Analysis of a variety of model inks suggest that the more acidic inks are darker in colour due to the presence of more tannic acid with which iron ions can complex (thus forming darker inks) and as a result can produce more sulphuric acid, making the ink more acidic (Sistach 1990).

4.1.6.2 Substrate

When applied to a substrate the pH of the ink or dye can be altered by components of the substrate such as calcium carbonate in parchment, and alum in paper. Analysis of historic iron gall ink documents has identified ink lines of pH 3.7 - 7.1 (Kolar, Stolfa, Strlic, Pompe, Pihlar, Budnar, Simcic and Reissland 2006), and an Akali Sikh turban (2005, 7-27.1) has been identified with an aqueous pH of 4.1. Modern iron-tannate dyed New Zealand flax from a piupiu (ceremonial skirt produced by the Maori) was found to have an aqueous pH of 4.5 – 6.5 while an historic equivalent had a pH of 3.5 - 4.3 (Daniels 1999b).

4.1.6.3 Age

An increase in acidity of an iron-tannate dyed substrate can also occur with ageing due to oxidation.

4.1.7 *Interaction of dye and fibres*

Iron-tannate dyes are metal-complex or mordant dyes which can be applied to textiles either in one step using a pre-mixed solution of tannic acid and iron ions in water, or in two-steps by sequential application of pure reagent solutions. The order of dyebath application in the two-step process can vary so that either iron ions or tannic acid are applied first and are therefore the mordant. Consequently fibre/iron/tannic acid, or fibre/tannic acid/iron interactions will predominate depending on the sequence of application (Bhattacharya and Shah 2000).

4.1.7.1 Application of the first reagent

Metal ions may be applied first to the textile. The binding of ferrous ions to the fibre may in part be due to Van der Waals forces (Hofenk de Graaff 2002). Aluminium ions have been found to bind non-specifically to wool via Van der Waals forces due to the high charge of the aluminium ions which can either interact with induced dipoles or those inherently present in the wool (Hartley 1968c). Additionally, metal ions can bind by co-ordinate or ionic bonds to hydroxyl, carbonyl, carboxyl, imine, amine, and thiol

4.1 Iron-tannate dye composition and properties

functionalities on the polymer chains of the fibres (Guthrie and Laurie 1968; Hartley 1968b; Hartley 1968c; Bird 1972; Fukatsu and Isa 1986; Kokot 1993; Shimizu 2000; Smith, Te Kanawa, Miller and Fenton 2001); copper ions bind more strongly than iron ions, particularly to thiols (Maclaren and Milligan 1981; Letelier, Lepe, Faundez, Salazar, Marin, Aracena and Speisky 2005; Letelier, Sanchez-Jofre, Peredo-Silva, Cortes-Troncoso and Aracena-Parks 2010). While most or all of these functionalities are present in wool and silk, it is the carboxyl groups that are the major binding site for metal ions (Maclaren and Milligan 1981; Chen, Lu, Yao, Pan and Shen 2005). Since wool contains more aspartic acid, glutamic acid (Guthrie and Laurie 1968), and thiols (Hearle and Peters 1963) than silk it is possible that wool could bind more metal ions than silk, if the groups are accessible to the metal ions and if the groups are ionised. Whether the groups are ionised depends on the pH of the environment and the iso-electric point of the fibres (see the next section for more information). Under acidic conditions (pH 4.18), two types of coordination between copper and the carboxylate groups in silk have been identified using ESR (structures a and b in Figure 4.3) (Chen, Lu, Yao, Pan and Shen 2005). When using the quantity of closed chain of terminal base and of Cu(II) a complex involving both oxygen and nitrogen donor groups on polymer side chains at pH 4.53 was proposed, structure c in Figure 4.3 (Shimizu 2000). Under alkaline conditions (pH 10.60) a complex involving the amide groups of the peptide chain has been identified (structure d in Figure 4.3) (Chen, Lu, Yao, Pan and Shen 2005).

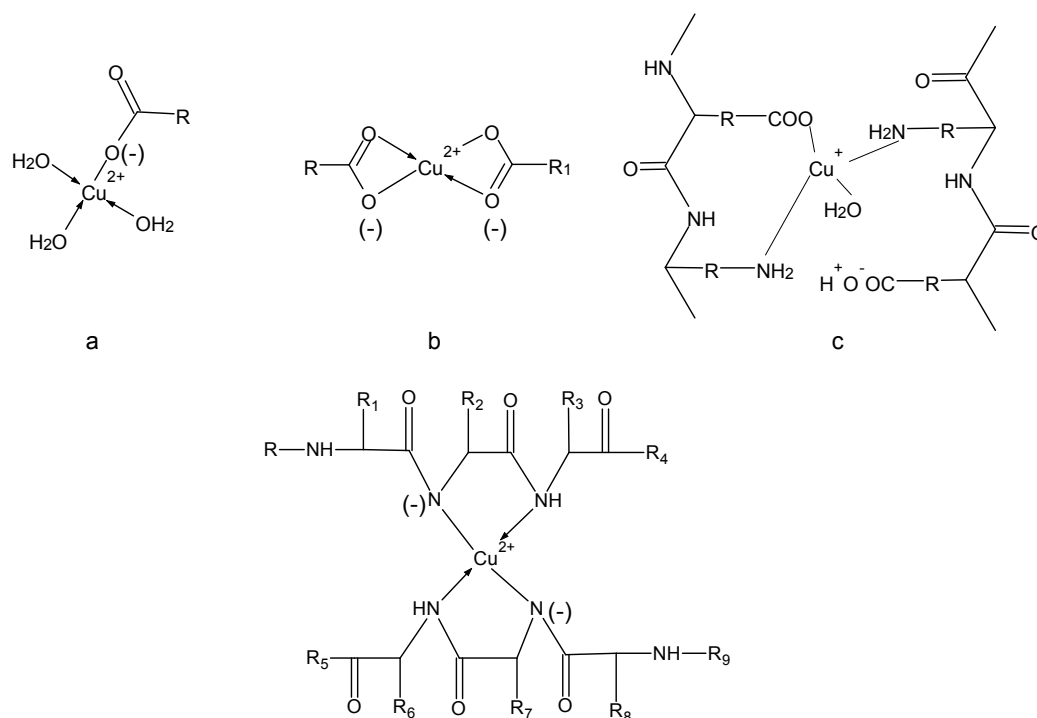


Figure 4.3 Coordination structures of copper in silk prepared at pH 4.18 (a and b), pH 4.53 (c), and pH 10.60 (d) (Shimizu 2000; Chen, Lu, Yao, Pan and Shen 2005)

4.1 Iron-tannate dye composition and properties

Only carbonyl, carboxyl, and hydroxyl groups are present in cotton and abaca, and in unoxidised cellulose, the hydroxyl groups are the major binding sites for metal ions since they are the most abundant groups present. Abaca contains more hydroxyl and carboxyl groups than cotton due to its higher hemicellulose and lignin content (Sun, Fang, Goodwin, Lawther and Bolton 1998; Hsieh 2007).

Tannin rather than metal ions may be applied first to the textile. Tannins contain a significant quantity of phenolic hydroxyl groups (Figure 4.4) which can hydrogen bond to carbonyl and carboxyl groups in textile fibres. Any carbonyl or carboxyl groups present may hydrogen bond to the hydroxyl or amine groups in fibres. Additionally, tannin molecules are large and can interact with the fibres by Van der Waals forces (Hearle and Peters 1963; Christie 2001; Frazier, Deaville, Green, Stringano, Willoughby, Plant and Mueller-Harvey 2010).

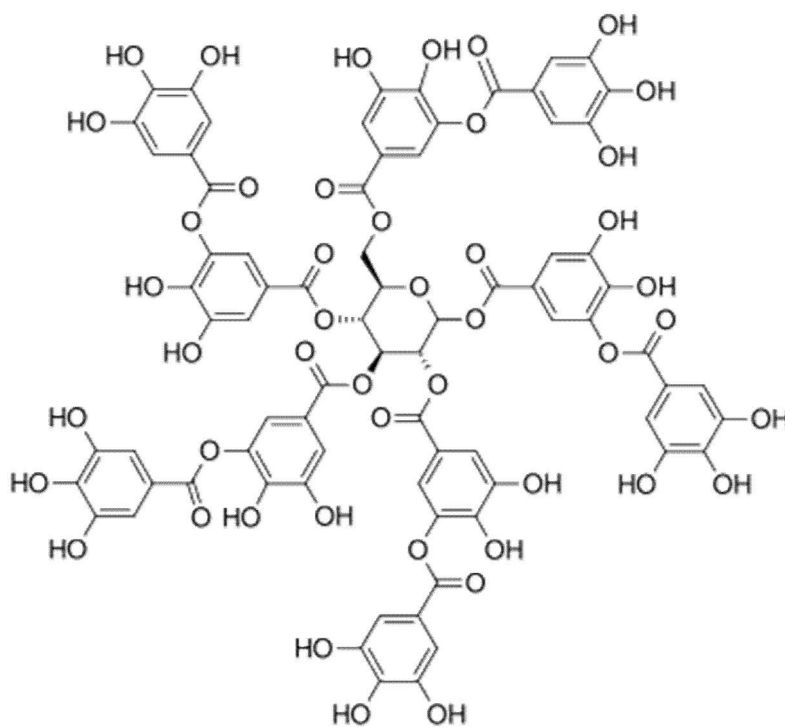


Figure 4.4 The structure of decagalloyl glucose, one of a range of polyphenols that can be present in tannic acid

4.1.7.2 Application of the second reagent

When the second reagent is applied to textile treated with the first reagent, iron-tannate dye complexes are formed bound to the fibre. This binding, in addition to the slow diffusion behaviour of the unbound iron-tannate complexes, due to their low solubility and large size, result in iron-tannate dyes being wash resistant (Burkinshaw and Kumar 2008).

4.1.7.3 The effect of dyebath pH on dye-fibre interactions

The pH of the dyebath can affect the uptake of metal cations and tannic acid by affecting the form and availability of the functional groups that bind to the metal ions and tannic acids (Hartley 1968a; Hartley 1968b; Hartley 1968c; Hartley 1970a; Bird 1972). In acidic conditions such as those during iron-tannate dyeing, the ionisation of carboxyl and hydroxyl groups in cellulosic fibres will be suppressed. Consequently, while the tannic acid has plenty of hydroxyl sites to hydrogen bond to, the metal ions have fewer negatively charged sites in the fibres with which to bind. The effect of dyebath pH on the binding within proteinaceous textiles is determined by the isoelectric point of the fibre. The isoelectric points of wool and silk (approximately 5.6 and 2.8, respectively (Timar-Balazsy and Eastop 1998)) are the pH values at which the proteins are electrically neutral, having an equal quantity of positive (e.g. $-\text{NH}_3^+$) and negative (e.g. $-\text{COO}^-$) groups. The isoelectric point can vary with many factors including fibre type, composition, and so in textile conservation, pH 3-7 is considered to be the isoelectric region of silk and pH 5-7, the isoelectric region of wool (Timar-Balazsy and Eastop 1998). In these regions the proteinaceous fibres have few acidic or basic groups and are at their most stable due to the presence of salt linkages between the anionic and cationic groups. While the fibre is electrically neutral at the isoelectric point ionic binding can still occur. Above the isoelectric point, the ammonium groups will gradually become deprotonated while the carboxylate groups will remain ionised. In wool, deprotonation of ammonium groups occurs between pH 8 and 13 (Broadbent 2001). Consequently the fibre will be slightly negatively charged. In this case it is likely that both carboxylate and amine functionalities will be able to bond with the metal cations while anions will be electrostatically repelled (Figure 4.3). Below the isoelectric point the carboxylate anions will be protonated and the ammonium groups will remain charged. The protonation of carboxylate groups in wool occurs between pH 1.5 and 4.5. Consequently, the fibre will be slightly positively charged. In this case anions can bind to the protonated amine groups while metal cations will be repelled from the fibre and/or bind to remaining carboxylate or amine groups (Timar-Balazsy and Eastop 1998; Shimizu 2000; Broadbent 2001).

4.1.8 Metal ion reactivity

Unbound metal ions are able to participate in the Fenton reaction, thus accelerating the oxidation and acid hydrolysis of the substrate. Unbound ions can be present due to an excess of iron sulphate being used in the ink or dye formulation, for example, in 104 historic iron gall ink recipes there was predominantly 50% more iron than was needed for complex formation (Neevel 1995), and due to the breakdown of the dye complex. Unlike

4.1 Iron-tannate dye composition and properties

for iron-gall ink documents, iron-tannate dyed textiles are often washed after dyeing and this can remove the majority or all of the soluble unbound metal ions (Hofenk de Graaff 2002). Therefore, unlike for iron-gall ink documents where the excess of iron in the dye formulations can be a significant contributor to the quantity of unbound ions in the ink, the gradual breakdown of iron-tannate dye complexes throughout the textile's lifetime may be the major source of unbound iron ions in iron-tannate dyed textiles.

The iron bound in iron-tannate complexes is thought to not participate in the Fenton reaction and some studies support this view (Lopes, Schulman and Hermes-Lima 1999). However, subsequent studies have suggested that this may be incorrect and that reaction with hydrogen peroxide does occur but that the hydroperoxyl radical is immediately trapped by the tannic acid. It is possible that a phenoxyl radical is formed as a result (Andrade Jr., Ginani, Lopes, Dutra, Alonso and Hermes-Lima 2006). Radical trapping of hydroxyl radicals by copper-tannic acid complexes has also been demonstrated (Andrade Jr., Dalvi, Silva Jr., Lopes, Alonso and Hermes-Lima 2005). This phenoxyl radical will be significantly more stable than the initial hydroperoxyl radical though it may still contribute to the oxidation of the inked or dyed substrate through radical propagation. The trapping of hydroperoxyl radicals by complexed tannic acid is also proposed for copper(I)-tannic acid complexes (Andrade Jr., Dalvi, Silva Jr., Lopes, Alonso and Hermes-Lima 2005).

The presence of other metal ions in iron-tannate dyes and iron gall inks can also accelerate substrate degradation. The efficiency of transition metals at catalysing the Fenton reaction in solutions of pH 5.5-9.5 has been shown to vary with pH (Strlic, Kolar, Selih, Kocar and Pihlar 2003; Selih, Strlic, Kolar and Pihlar 2007). Ions such as cobalt, chromium, manganese, and nickel behave similarly to iron in that as the pH increases, the rate of reaction of hydroxyl radical production, i.e. the Fenton reaction, increases. This increase is particularly rapid from around pH 7.7, up to around pH 8.5, after which the rate decreases. For copper, the reaction rate increase is slower than for iron but by pH 8.5 it increases rapidly rather than decreases. Consequently, in alkaline environment such as that for deacidified paper or textiles, copper rather than iron ions may be the most reactive and degradative. Zn(II) however has been shown to have anti-oxidant properties in the Fenton-like reaction mixtures in the pH range 5.5-9.5 (Strlic, Kolar, Selih, Kocar and Pihlar 2003).

4.2 Iron-tannate dye usage

Iron-tannate dyeing has been reported in Africa (Ayed and Alatrache 1997/1998; Ottenberg 2007), Australia and Oceania (Petrosian-Husa 1995), Europe (Daniels 1995; O'Connor and Richards 1999), Asia, South America (O'Connor and Richards 1999) and North America. The British Museum has iron-tannate dyed objects from most of these continents made from a range of natural fibres and textiles including abaca, wool, cotton, silk, bark cloth, raffia, and New Zealand flax (*Phormium tenax*). Assessment of the likelihood that a range of British Museum objects contain iron-tannate dyes is presented in Chapter 6. Examples include the use of New Zealand flax by the Maori to make clothing such as *piu piu* (Registration number: Oc1994, 04.112), belts and cloaks (e.g. Registration number: Oc1995, Q.17) as well as baskets for food collection or personal possessions (e.g. Registration number: Oc1994, 4.98) (Pendergrast and Starzecka 1996). Bogolanfini (Registration number: Af1956, 27.10) are, among other locations and people, produced in Western Sudan by the Bamana of Mali by mud-dyeing cotton material for everyday wear (e.g. for men's shirts and women's wrap-around skirts), for ceremonial purposes (e.g. for girl's initiation rites or hunter's attire) and now, tourism (Donne 1973; Toerien 2003). An important and popular use of iron-tannate dyes was the weighting of silks which suffer from severe accelerated degradation due to the high quantities of metal ions and tannins that the silk can absorb. These black weighted silks were produced throughout Europe and beyond in the 19th century (Hofenk de Graaff 2004) and were used, among other things, for clothing such as dresses, or items such as black ribbons or threads. Iron-tannate dyed raw silk was used for the hair on Japanese hina-dolls (Registration number: 2001, 1129.1).

The simplicity of iron-tannate dye production has led to the suggestion that it was used in Prehistoric times and was possibly the first occurrence of the dyeing of textiles and skin (Forbes 1956; Robinson 1969; Cardon 2007). Literature reports the usage of iron-tannate dyes such as those from iron acetate and oak galls since Antiquity (Forbes 1956; Brunello 1973) and around the 7th century in Japan, ancient methods were used to develop a mud-dyeing method unique to the production of Oshima Pongee silk (The Association for the Promotion of Traditional Craft Industries 2009-2011). During the Middle Ages in the Mediterranean, iron-tannate dyeing of wool and silk was highly regulated by authorities and guilds. The degradative effect of iron-tannate dyes on the textiles it coloured led to the prohibition of its usage on the finest quality wools. Rather than combinations of powdered galls and iron acetate as used in negre black, combinations of woad, alum and madder as in bruneta black were favoured.

4.2 Iron-tannate dye usage

With the invention of the printing machine in the mid-15th century, information was made available to a much wider audience. Previously, dye recipes were often secret, passed on only when necessary by word of mouth through generations of dyers, but with books such as *The Plictho* of Gioanventura Rosetti of 1548 (Rosetti 1548), some of these recipes were recorded for the benefit of interested parties for centuries to come.

By the mid-17th century, Dutch dyers were predominantly dyeing wool black using iron-tannate dyes which were previously forbidden by guilds in favour of a much less damaging method of woad or indigo with madder (Hofenk de Graaff 2002). As was the case in the Mediterranean in the Middle Ages, the use of iron-tannate dyes on wool and silk was often highly regulated by authorities and guilds due in part to the known degradative nature of the dye.

During the 18th century, exploration of New Zealand by Western travellers resulted in the iron-tannin dyeing methods of the Maori being more widely known and recorded. In the 20th century the African mud-dyeing methods used in the production of bogolanfini (Donne 1973) and Hu Ronko shirts (Ottenberg 2007) had been recorded.



Figure 4.5 Degradation of black weft of a textile previously owned by the Queen of Madagascar, 1753 (British Museum registration number: Af,SLMisc2105)

Physical evidence for the early use of iron-tannate dyes is harder to gain than for undyed equivalent materials since the dye can significantly decrease the lifetime of the dyed material. Consequently, sometimes a lack of material has become the evidence for the use of iron-tannate dyes. A possible example of the use of iron-tannate dyes in the Middle Ages exists in the complete destruction of woollen weft in a piece of medieval woollen cloth discovered in the old city of Montpellier (Cardon 1990). A similar situation can be seen on a textile (Af, SLMisc2105) in the British Museum's collection dated to 1753,

4.2 Iron-tannate dye usage

which belonged to the Queen of Madagascar and is possibly made of banana fibre (Figure 4.5). In this example, unidentified black dyed weft is still visible but has deteriorated in many places leaving the coloured warp intact.

Physical evidence dates the use of iron-tannate dyes to approximately 3600 years ago with the ancient Egyptians during the 18th Dynasty (1550-1292 BC). Examples of iron-tannate dyed basketry from this period are present in the British Museum's collections (Wills and Hacke 2007). An early example of iron-tannate dye usage in Europe exists in woollen textile fragments from the Hallstatt Period (800-400 BC) of the Iron Age. These were preserved in the Hallstatt salt caves (Hofmann-de Keijzer and Hartl 2005) due to salt impregnation, constant climate, and lack of light. The presence of the degradation phenomena on the wool fibres correlated well with presence of copper or iron-tannate dye (Joosten, van Bommel, Keijzer and Reschreiter 2006).

Today, silk mud-dyeing to make Amami Oshima Pongee in Japan is still practiced (The Association for the Promotion of Traditional Craft Industries 2009-2011). The production of bogolanfini or bogolanfini inspired mud cloths has increased significantly since 1990 for economic and political reasons (Toerien 2003). However prior to this, mud dyeing production was diminishing as modern dyed textiles became cheaper and more favourable and skills were being passed on to fewer of the next generation (Imperato and Shamir 1970). As of 2007 the production of Hu Ronko shirts in Northern Sierra Leone was in serious decline due to the loss of skills resulting from the 1992-2002 Civil war (Ottenberg 2007). In New Zealand, iron-tannate dyes are still being used at Te Puia, Rotorua where there are weaving and carving schools designed to keep traditional Maori skills alive (New Zealand Maori Arts and Crafts Institute (Te Puia) 2010). Karolia, Nagrani and Raval (Karolia, Nagrani and Raval 2009) have continued the use of natural dyes, including iron-tannate dyes, in their venture to add value to Khadi textiles which are a symbol of patriotism in India.

4.3 Historic dye formulations

Analysis of historic iron-tannate dye recipes from the 16th to 20th centuries demonstrated that there are a great many variations in methods and ingredients (Rosetti 1548; Mascall 1589; Haigh 1800; Bancroft 1813; Martin 1813; Packer 1830; Bird 1876; Donne 1973; Cardon 1990; Petrosian-Husa 1995; Ayed and Alatrache 1997/1998; O'Connor and Richards 1999; Te Kanawa, Thomsen, Smith, Miller, Andary and Cardon 1999; Hofenk de Graaff 2004). Early recipes such as those by Rosetti (Rosetti 1548) are usually simple and often ambiguous in the quantities and timings involved while later recipes such as those noted by Hurst (Hurst 1892a) are particularly complicated and specific. Variations exist in immersion times, the number and type of repeat dyeings, and method of application of reagents i.e. application of iron ions and tannic acids simultaneously via one solution (one-stage method), or the separate application of each reagent (two-stage method) and the order of application in the latter case. Temperatures, reagent concentrations, reagent types, and reagent combinations also vary.

Recipes 1-5 demonstrate different methods, reagents, and the complexities of iron-tannate dyeing from the 16th to the 20th centuries.

Recipe 1 – Example of a 16th century one-stage dyeing process.

‘To dye skeins black.

37. Measure a little crushed gallnut and allow it to boil in a small pot with water. When you have boiled it a little, take away all the gallnuts and put into it as much Roman vitriol as was the gallnut, and a little gum arabic. Give it one boil and put in your skeins and allow to boil a little, and you will have good luster and black.’ (Rosetti 1548) p.104

The ‘dye’ in this recipe is in actual fact an ink and is an example of a recipe involving only the basic reagents needed (tannins and iron).

Recipe 2 - Example of a 19th century two-stage dyeing process and silk weighting.

The following is an outline of the detailed recipe for ‘Another black’ given on pp.46-47 of Hurst’s *Silk dyeing, Printing and Finishing* (Hurst 1892a).

Firstly, a tannin bath using chestnut extract is made to souple (soften) the silk. This is followed by immersion of the silk into a bath of pyrolignite of iron (iron liquor) formed from combination of iron and pyroligneous acid, for half an hour. The silk is then removed from the bath, wrung to remove excess liquid and hung to oxidise for several hours before the first two stages are repeated. ‘Two repetitions will give a fair black, weighted to about 50 per cent.; four will give about 100 per cent.; eight up to 200 per cent.; fourteen or

4.3 Historic dye formulations

fifteen up to 400 per cent.’(Hurst 1892a) p.46. The baths would be refreshed with new liquor or scrap iron. Once complete, brightening of the silk could be achieved using oil.

Recipe 3 – Example of the use of Prussian blue, addition of tin salts, combined tannin sources and a two-stage dyeing process i.e. iron and tannin dyeing is applied separately, in a 19th century tannin dye recipe.

The following is a summary of the detailed recipe for a ‘Fine Souple Black’ described on pages 44-46 of Hurst’s *Silk Dyeing, Printing and Finishing* (Hurst 1892a).

Firstly, mordanting of the silk using a bath of ‘basic sulphate of iron’ was required followed by a bath of soda crystals which causes the deposition of iron soap onto the fibres which increases the weight of the silk (Hurst 1892a) p.37. The third step involved dyeing the silk blue using ‘a bath of yellow prussiate and potash acidified with hydrochloric acid’ i.e. Prussian blue. A bath of extracts of galls and divi divi² was then produced to soften the silk over 2-3 hours, after which it would be left until the bath was cold. Upon removal from this bath, tin crystals were added, and the silk re-immersed and worked for between half an hour and an hour. The fifth step required the silk to be immersed in bath of soap before being wrung and washed. If the silk wasn’t the desired depth of black steps 4 and 5 could be repeated with an ‘immersion in a weak iron bath, if necessary’. Step six was to brighten the silk through the use of oil.

Recipe 4 – example of an early 19th century one-stage dyeing recipe with unspecified quantities of reagents or lengths of times of immersion.

‘To dye Linen of a Black colour.- Take filings of iron, wash them, and add to them the bark of elder-tree: boil them up together, and dip your linen therein.’(Martin 1813) p.287.

Recipe 5 – example of 20th century mud dyeing of bogolanfini by the Bamana or Bambara of western Sudan summarized by J.B. Donne (Donne 1973) p.1.

‘1. The small leafy branches of *Anogeissus leiocarpus* and *Combretum glutinosum* are gently pounded in a mortar and then soaked in water for twenty-four hours. White cloth woven from local cotton is dipped in the resulting solution and then placed in the sun for several hours. This process dyes (or perhaps it would be better to say ‘stains’) the cloth a bright yellow, the side exposed to the sun being a deeper yellow than the underside.

² The Divi divi is a leguminous tree grown in South America and the West Indies the fruit of which is often required for dyeing recipes due to their 40-50 per cent tannin content.
<http://www.faculty.ucr.edu/~legneref/botany/tandye.htm>

4.4 Iron-tannate dye detection

2. Mud collected from a still pond, and allowed to stand for a year in a pot, is now used to paint in the background, outlining the intended designs, which stand out in yellow against the mud. When the cloth has dried, the mud is washed out leaving yellow designs on a black background. (This process may be repeated, sometimes several times).’

These yellow designs are then bleached white to leave a white on black design.

4.4 Iron-tannate dye detection

Black dyes other than iron-tannate dyes, which are not known to accelerate degradation of the substrate have been used throughout history. The use of woad followed by madder or weld was very common but it was expensive compared to iron-tannate dyes due to the need for a deep dark blue colour from the woad (Cardon 1990). In place of woad, indigo was also used (Hofenk de Graaff 2002) and during the 19th century, silk was sometimes dyed with potassium ferrocyanide (Prussian blue) prior to being dyed black with iron and tannin sources (Hurst 1892; van Oosten 1994). Other black dyes mentioned in literature include the use of manganese dioxide, soot, charcoal (Wilson 1979) and logwood. In Samoa, a black dye also known as ‘lama’ is used on Siapo (Samoa tapa cloth made from the bark of trees from the mulberry family) and is made by combining the burnt residue of the candlenut tree with ‘O’a’ which is a brown dye extracted from the bark of the blood tree (Hein 2008). In the 19th century a new range of black dyes, developed from coal tar became available to dyers; the best of these, which were also difficult to dye on silk, were Aniline black and Alizarine black (Hurst 1892). Black dyes available now included acid, sulphur, reactive, and direct black dyes.

The identification of iron-tannate dye in an object is important since the presence of the dye can significantly decrease the lifetime of the object. An indication of the likelihood of a black, brown, or grey dyed organic material being iron-tannate dyed can be gained by knowledge of the time, method, and location of production. The use of iron-tannate dyes on Maori artefacts is well reported for example. If such knowledge is unknown or uncertain then assessment of the condition of the dyed object could help since an unusual level of brittleness and weakness when compared to undyed equivalent material of the same age and history would suggest the presence of iron-tannate dye. Iron-tannate dyes can also be identified using a variety of analytical or chemical techniques that identify the presence of iron or tannins or both.

4.4.1 Chemical techniques

Iron-tannate dyes are chemically detectable through the boiling of a sample in 10% sulphuric acid which breaks down the iron-tannate complex, releasing iron which is detectable in the sulphuric acid. This causes a significant lightening of the original brown colour which is reversed if an excess of ammonia is added to the sulphuric acid decoction. A separate sample can be boiled with tin(II) chloride. This will turn yellow or orange if the samples was dyed with a plant extract containing tannins and hydroxyflavones (Schweppe 1986).

4.4.1.1 Bathophenanthroline indicator paper

A simple, low technology method of detecting the presence of soluble iron salts on the surface of an object is with bathophenanthroline indicator paper. Developed for the detection of iron(II) ions in paper objects (Neevel and Reissland 2005), this indicator paper is also effective at detecting the presence of soluble iron on many cellulosic materials such as cotton, New Zealand flax, and linen as well as non-keratinous proteinaceous materials such as silk and skin. The test involves contact between the object and a damp piece of bathophenanthroline paper for 30 seconds on paper (Neevel 2009). However, 2-3 minutes has been used on cellulosic and proteinaceous woven and non-woven materials and these longer contact times are especially needed for non-keratinous proteinaceous samples. Keratinous materials such as wool have generally proven unresponsive to the indicator paper, possibly due to the strong bonding between iron and thiols in the fibre (Vuori and Tse 2005a). An insoluble magenta coloured complex is formed on the bathophenanthroline paper when soluble iron(II) is present (Figure 4.6). The presence of unbound iron(III) ions can be determined by applying a drop of 1% (w/v) aqueous solution of ascorbic acid (pH 2.5) or 1% aqueous solution of sodium dithionite (pH 6.5) to the bathophenanthroline paper after testing for iron(II) ions; the latter is preferable due to its more neutral pH (6.5) which, unlike with ascorbic acid solutions, prevents the bathophenanthroline from breaking down iron(III)-gallic acid complexes and releasing iron (Neevel 2009). Any iron(III) ions present are reduced to iron(II) and so intensify the magenta colour of the strip. Issues in the efficacy of this test at determining unbound iron ion content and the formation of the magenta coloured complex is discussed elsewhere (Neevel 2009).

4.4 Iron-tannate dye detection

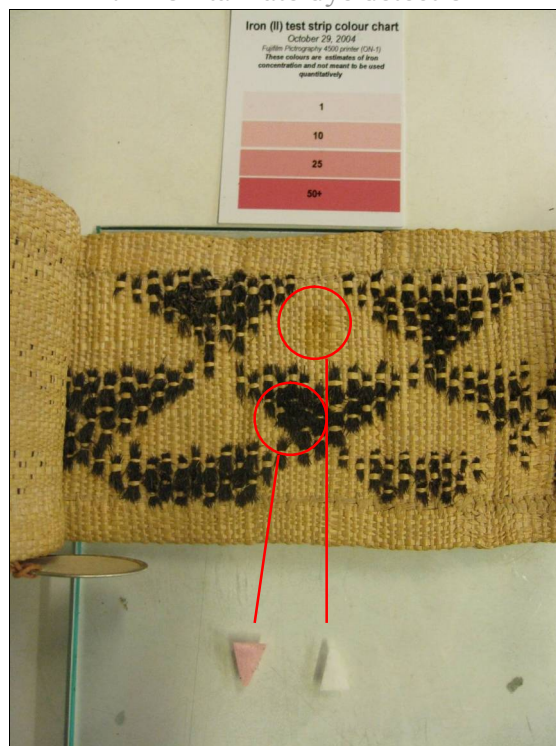


Figure 4.6 Bathophenanthroline testing of dyed and undyed areas of a strip of Kuba cloth from this PhD project

An iron(II) test strip colour chart has been developed to aid conservators in prioritising the stabilisation treatments of the textiles most at risk of iron-catalysed degradation (Vuori and Tse 2005a). Indeed, for textiles, the use of this indicator paper lies in this prioritisation, and not, as is the case for iron gall ink on paper objects, in the identification of the presence of iron-tannate complexes. This is because washing of iron-tannate dyed textiles removes the soluble iron that the indicator paper is used to detect, thus some washed iron-tannate dyed textiles could give a negative response when tested with bathophenanthroline indicator paper. Unless treated with an aqueous solution, iron gall ink documents are unlikely to have been washed and therefore retain soluble iron ions. The efficacy of the aqueous phytate treatment on iron gall ink documents can be assessed through the use of bathophenanthroline paper tests (Neevel 2009).

Even with the colour chart, the indicator paper cannot be used to accurately quantify the iron present in a sample as only soluble or weakly complexed iron will be detected.

A non-bleeding test for copper(II) ions has also been developed that can detect levels of copper(II) as low as 10-25 ppm (Neevel 2006).

4.4.1.2 Other tests

There are several chemical spot tests for tannins in leathers that are based on the assessment of colour changes to the sample including ones using ferric chloride or vanillin (Falcao and Araujo 2011). These may not be of use to dark coloured samples. The presence of hydrolysable tannins in a sample can also be established by using nitrite to react with ellagic acid and recording the maximum absorbance at 538 nm of the red dinitrosyl adduct spectrophotometrically. A test procedure for use on ink has been published but the process was recommended for studying the degradation of iron gall ink only since there were occasions when ellagic acid was identified in non-iron gall ink samples or was not identified in some iron gall ink samples (Neevel 2006).

4.4.2 Analytical techniques

The most accurate assessment of whether iron-tannate dye is present can be gained through detection of high levels of iron and tannins in the dyed organic material. This can be achieved in several ways:

4.4.2.1 X-ray fluorescence (XRF)

XRF can detect elements including iron (soluble, insoluble, bound, unbound, iron(II), and iron(III)) in a sample. Handheld XRF devices are on the market which can be used in-situ with the object in question. These can analyse areas as small as 5 by 6 mm and identify elements with atomic mass equal to or greater than that of magnesium when the vacuum pump attachment is used (Luxford, Thickett and Wyeth 2011). Alternatively, the object could be moved to a larger portable or fixed XRF machine or a sample can be taken. As little as a 1 cm long fibre can be analysed by the ArtTax μ -XRF spectrometer at the British Museum and elements down to and including sodium can be identified when helium purging is used. However, greater sample size will provide a larger signal which will allow for more accurate assessment of the quantity of iron present. When a 0.65 mm collimator is used the oval region of the sample being analysed is approximately 1.1 by 0.9 mm. The technique is non-destructive when low energy and short time spans are used, and when a sample is not removed it is also non-invasive, a desirable combination for conservators.

The higher the iron content the greater the likelihood that iron-tannate dye is present. However, the use of Prussian blue in the production of black dyes (Hurst 1892; van Oosten 1994) can complicate evaluation since the iron is present in a stable hexacyanoferrate complex and is therefore not a catalyst for substrate degradation. Iron as well as aluminium and silica is also a common contaminant of museum objects that can be acquired during

4.4 Iron-tannate dye detection

object production, storage, and handling (Dussubieux, Naedel, Cunningham and Alden 2005). It is therefore important to analyse an equivalent undyed area of an object to identify the background levels of iron before concluding on the likelihood of a material being dyed with iron-tannate dye.

XRF has been used to identify and study iron gall inks on paper (Wagner, Bulska, Hulanicki, Heck and Ortner 2001; Hahn, Kanngiesser and Malzer 2005; Bicchieri, Monti, Piantanida and Sodo 2008; Hahn 2010), and iron-tannate dyes on a range of substrates (Findlay 1989; Ayed and Alatrache 1997/1998; Wakui, Yatagai, Kohara, Sano, Ikuno, Magoshi and Saito 2001; Wakui, Yamazaki and Saito 2002; Wills and Hacke 2007). Energy dispersive X-ray fluorescence has also been used in combination with scanning electron microscopy in the technique SEM-EDX to analyse the distribution of metal ions in iron gall ink samples on paper and parchment (Sistach 1990; Vuori and Tse 2005a; Virro, Mellikov, Volobujeva, Sammelselg, Asari, Paama, Jürgens and Leito 2008) and metal ions in wool (Green and Daniels 1990).

Other techniques that have been used to detect iron in dyed textiles but which are less readily available to conservators include: Atomic Absorption Spectrometry (AAS) (Ayed and Alatrache 1997/1998), Inductively Coupled Plasma – Atomic Emission Spectroscopy (ICP-AES) (Wakui, Yatagai, Kohara, Sano, Ikuno, Magoshi and Saito 2001; Wakui, Yamazaki and Saito 2002), Inductively Coupled Plasma-Mass Spectrometry (ICP-MS) (Dussubieux, Naedel, Cunningham and Alden 2005), and Particle-induced X-ray Spectroscopy (PIXE) (Budnar, Simcic, Ursic, Rupnik and Pelicon 2006). Neutron activation analysis (NAA) has also been used to identify metal ions including iron in silk, however the stability of lead isotopes mean that they are not identified using this technique (Miller and Reagan 1989). An overview of some of these and other techniques that are most frequently used to determine the type and quantity of metals present in paper has been published (Strlic, Kolar, Selih, Budnar, Simcic, Kump, Necemer, Marinsek and Pihlar 2006).

4.4.2.2 High-performance liquid chromatography (HPLC)

HPLC has been used to detect dye compounds including tannic acids in wool (Masschelein-Kleiner, Lefebvre and Geulette 1981; Hofmann-de Keijzer and Hartl 2005; Joosten, van Bommel, Keijzer and Reschreiter 2006) and silk (van Oosten 1994). HPLC chromatograms of some tannins have been published however identification of the

different types of tannin is difficult since often only ellagic acid is detected (Hofenk de Graaff 2004).

4.4.2.3 Spectroscopic techniques

A variety of spectroscopic techniques have been used to distinguish iron gall inks from other black or brown inks on paper. These analyses are based on the differing absorption and reflectance properties of iron gall inks compared to other brown or black inks such as bistre, carbon, and sepia. Iron gall ink absorbs strongly in the 550 – 700 nm range of the visible region and reflects strongly in the 950 – 2500 nm near infrared (NIR) region. Carbon inks and sepia absorb strongly in the NIR region however iron gall inks with low iron-tannin ratios or that were thinly applied can be difficult to identify from bistre inks. A summary of such research until c.2005 has been produced (Neevel 2006).

Using fibre-optics reflectance spectroscopy, iron gall inks were found to be distinguishable from sepia and bistre inks by the strong absorption of 550 – 700 nm light (Neevel 2006). Limitations of this technique include the comparable reflectance spectra of the iron gall ink to bistre ink when the iron gall ink is thinly applied, low in iron, or contains degraded dye complexes.

Near Infrared spectroscopy (NIR) can be a useful method of identifying iron gall inks because they reflect light in the NIR region (Havermans, Aziz and Penders 2005). False Colour Infrared Imaging (Havermans 2003; Havermans, Aziz and Scholten 2003) can be used to distinguish iron gall inks from other inks. It can also indicate regions of the sample where carbonising has started before it is detectable with the naked eye areas as the carbon-rich areas absorb NIR strongly.

A method of NIR spectroscopy in combination with chemometric data evaluation has been reported which enables a reliable indication of the DP and pH of paper with and without iron gall ink (Strlic, Csefalvayova, Kolar, Menart, Kosek, Barry, Higgitt and Cassar 2010). Using the calculated DP values, an estimation of the time it will take for the sample to become too fragile to handle without damage occurring (DP = 400) can be calculated.

NIR spectroscopy has been applied to historic silk to aid determination of the condition of the textiles (Garside, Wyeth and Zhang 2011; Luxford, Thickett and Wyeth 2011).

However, poor NIR spectra are acquired from black materials and so it may not be suitable for use on black iron-tannate dyed textiles (Garside, Wyeth and Zhang 2011). Since NIR

4.5 Iron-tannate dyes as catalysts

spectroscopy has been successfully used for brown iron gall inks on paper, the techniques may be more successful on brown iron-tannated dyed textiles. A detailed reference data set and reliable condition model is needed to accurately determine the condition of the materials being analysed (Luxford, Thickett and Wyeth 2011). This has been attempted for iron gall ink on paper (Strlic, Csefalvayova, Kolar, Menart, Kosek, Barry, Higgitt and Cassar 2010) and silk (not black) (Garside, Wyeth and Zhang 2011) but more work is needed to extend these data sets and produce ones for other materials.

4.5 Iron-tannate dyes as catalysts

Textiles dyed with iron-tannate dye often experience catalysed degradation. Without intervention, this leads to embrittlement, discolouration, and fibre loss in a much shorter time than experienced by non-iron-tannate dyed textiles. Van Oosten (van Oosten 1994) reports that black dyed silk fibre that had been weighted eight fold could crumble within a few weeks when exposed to sunlight.

The problem of iron-tannate dyes causing the accelerated deterioration of textiles has been known for several centuries (Haigh 1800; Bancroft 1813). Throughout Europe trade guild regulations frequently forbade the use of iron-tannate dyes on the highest quality textiles. Instead, black dyes formed without iron were favoured, using multiple dyeings with less degradative dyes such as indigo and madder (Cardon 1990; Hofenk de Graaff 2002).

The theory for the degradation experienced by iron-tannate dyed objects predominantly originates from extensive research into the comparable damage caused by the chemically similar iron gall inks to paper (Havermans and de Feber 1999; Sistach, Gibert and Areal 1999; de Feber, Havermans and Defize 2000; Kolar and Strlic 2006; Csefalvayova, Havlinova, Ceppan and Jakubikova 2007). The inks catalyse the natural degradation processes of oxidation and acid hydrolysis, initiating a continuous cycle of degradation. Significantly less research has been undertaken on the mechanism of substrate degradation by iron-tannate dyes (Daniels 1999b; More, Smith, Te Kanawa and Miller 2000).

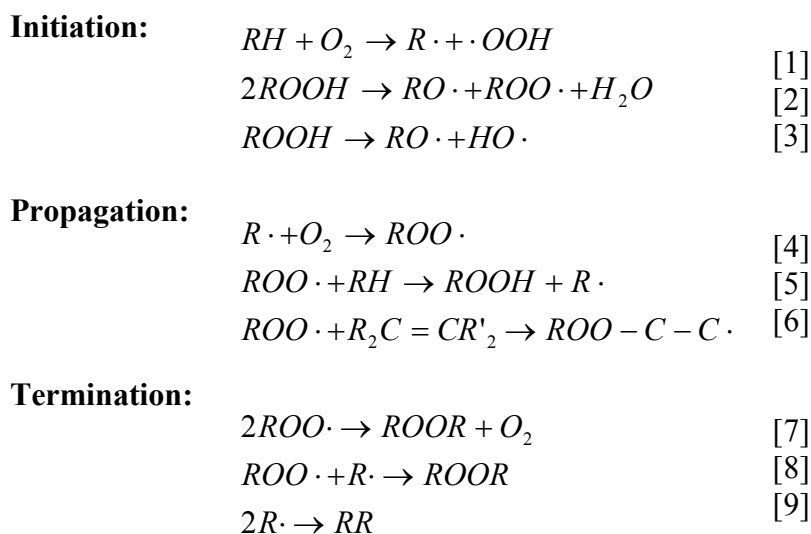
4.5.1 Oxidation

4.5.1.1 Autoxidation

Autoxidation is an autocatalytic mechanism of oxidation of organic substrates that occurs via free radicals. There are three mechanistic stages to autoxidation (Scheme 4.6): initiation, propagation, and termination. Initiation is the stage when radicals are initially formed. When there is no or very little peroxide present, the major process of initiation is

4.5 Iron-tannate dyes as catalysts

by hydrogen abstraction from an organic material by oxygen, (1) in Scheme 4.6. As well as organic radicals, hydrogen peroxide or peroxide radicals are formed during this process. This is a slow process and so once there is enough peroxide present, decomposition of the peroxide becomes the major initiation step (2 and 3). This produces highly reactive and unselective hydroxyl radicals. Once a radical has been formed it can either propagate to form a new radical (4-6) or react with another radical in a termination reaction that produces a non-radical product (7-9). Propagation can occur by direct coupling of an organic radical with oxygen (4), hydrogen abstraction from an organic substrate by a radical (5), or addition of a radical to an unsaturated bond (6). The coupling reaction is a very fast reaction unless the initial radical is highly resonance stabilised. Consequently, hydrogen abstraction is the rate determining step of autoxidation and it typically occurs intermolecularly. Due to the fast coupling reaction in normal O₂ pressure and moderate temperature, recombination of two alkylperoxyl radicals is the major termination step (7). Under low O₂ pressure or when the radical is so highly resonance stabilised that it has not coupled with oxygen, recombination of two alkyl radicals (9) or an alkyl and an alkylperoxyl radical (8) can occur (Al-Malaika 1993).

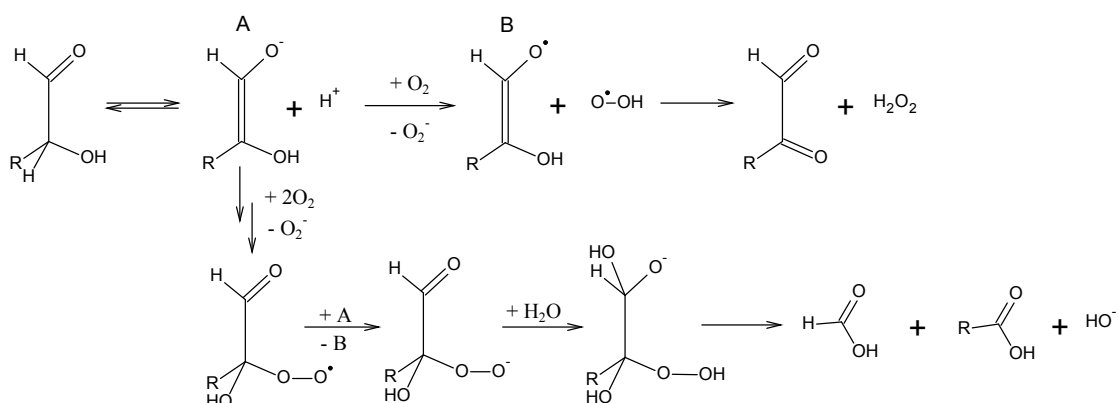


Scheme 4.6 Proposed autoxidation mechanism (Al-Malaika 1993)

Autoxidation begins slowly at first as there is little or no peroxide present with which to form radicals rapidly. The initial method of production of hydrogen peroxide is not fully known but for cellulosic materials it has been postulated to be due to the interaction of oxygen with the terminal aldehyde groups of cellulose chains (Thornalley and Stern 1984; Kolar and Strlic 2006) (Scheme 4.7). This reaction is accelerated in alkaline conditions. While superoxide may not be able to abstract a hydrogen atom from glucose, it is

4.5 Iron-tannate dyes as catalysts

eliminated from polymer chains through decomposition or recombination, which forms hydrogen peroxide and singlet oxygen (Kolar and Strlic 2006). Hydrogen peroxides can also form through the interaction of semi-quinone radicals, oxygen, and alcohol groups. Semi-quinones are formed through interaction of quinones (derived from oxidation) and light (Sistach, Gibert and Areal 1999). The emission of reactive oxygen species, proposed to be hydrogen peroxide, during iron-gall ink catalysed degradation of paper has been identified (Strlic, Menart, Cigic, Kolar, De Bruin and Cassar 2010).



Scheme 4.7 Possible initiation mechanism for autoxidation in hydrocarbons (Thornalley and Stern 1984; Strlic, Kolar, Kocar and Rychly 2005)

As the peroxide content increases, the rate of oxidation increases and the reaction becomes autocatalytic as the peroxides form peroxy radicals that cause the production of more peroxides on the polymer chain that in turn form more peroxides and so on. The time it takes to reach this stage, i.e. the induction period can be decreased through the presence of initiators such as metal ions, light, heat, or hydrogen peroxide or extended through the use of antioxidants. The rate of autoxidation finally decreases (Al-Malaika 1993) due to the decreasing quantity of sites available for oxidation.

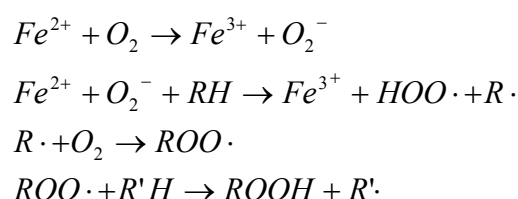
H-abstraction by peroxy/hydroxyl radicals (5) introduces a radical into the polymer chain which can cause the formation of crosslinks (6) and carboxylic acid groups (Scheme 4.6). The brittleness and acidity of the textile is therefore increased.

4.5.1.2 Metal ion catalysed oxidation

Unbound ferric and ferrous ion can be present in iron-tannate dyed substrates from the dyeing process and/or breakdown of the iron-tannate complex. Research has shown that there is typically an excess of iron ions with respect to tannins in iron gall ink recipes resulting in unbound reactive iron ions (Neevel 1995); it is likely that this is also true for iron-tannate dye recipes however washing may remove these soluble iron ions from the

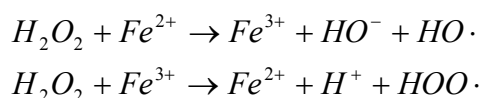
textile (Hofenk de Graaff 2002). Remaining unbound iron ions can catalyse the oxidation of polymers in iron-tannate dyed textiles by a number of mechanisms:

1. *Direct production of organic radicals via initial formation of superoxide (Scheme 4.8).* (Scott 1993b; Neevel 1995). Ferrous ions can reduce ground state oxygen to superoxide. Reduction of the superoxide and H-abstraction from a polymer can form a peroxy radical and an organic, alkyl radical that can couple with oxygen to give another peroxy radical. The peroxy radicals can abstract more hydrogen to form peroxides (Botti, Mantovani and Ruggiero 2005).



Scheme 4.8 Production of superoxide by ferrous ion and oxygen and subsequent oxidation of an organic substrate (Scott 1993b; Neevel 1995);

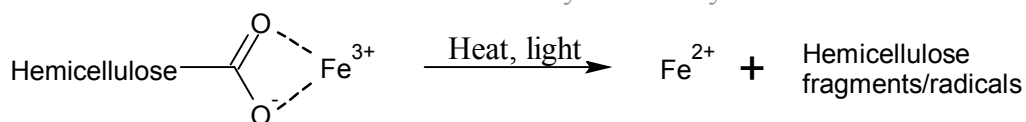
2. *Ferrous ion catalysed decomposition of hydroperoxides via the Fenton reaction (Scheme 4.9).* The comparable stability of the ferric and ferrous ions enables hydroperoxides to be decomposed by redox reactions of the iron. Regeneration of the ferrous ion by reaction of the ferric ion with hydroperoxide makes this a catalytic cycle.



Scheme 4.9 Iron-catalysed decomposition of hydrogen peroxide (Scott 1993b)

3. *Ferric ions can also catalyse the degradation and oxidation of cellulosic polymers by binding to unesterified carboxylic acid groups in hemicellulose (Scheme 4.10.).* The resulting decarboxylation reaction, initiated by light or heat, breaks the polymer chain to which the carboxylic acid group was attached and releases radicals. The free radicals can then oxidise the polymer (More, Smith, Te Kanawa and Miller 2000).

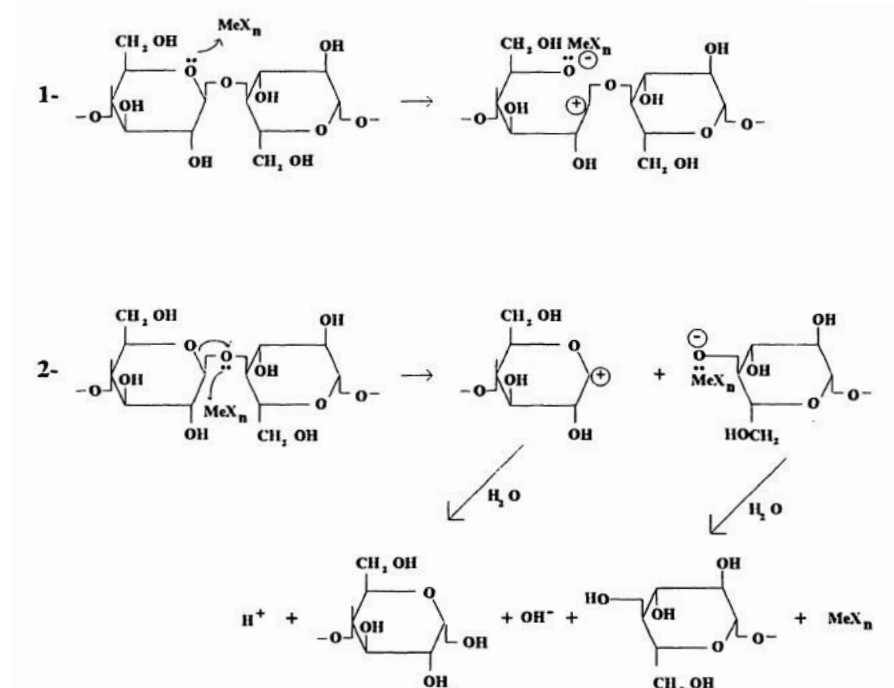
4.5 Iron-tannate dyes as catalysts



Scheme 4.10 Proposed mechanism for ferric iron catalysed degradation of hemicellulose (More, Smith, Te Kanawa and Miller 2000);

4. Metal catalysed cellulose degradation via a Lewis mechanism (Scheme 4.11).

The degradation of cellulose via a Lewis acid mechanism rather than a radical mechanism has been verified in iron and copper doped papers, Scheme 4.11 (Bicchieri and Pepa 1996). It was concluded that copper ions oxidise the hydroxyl groups on cellulose faster than iron. The copper ions caused preferential oxidation of the C2 and C3 hydroxyl groups which caused the opening of the pyranose ring (the rate determining step) prior to the formation of aldehyde groups. The iron ions behaved differently to the copper ions by preferentially oxidising the C6 hydroxyl groups. These results were confirmed in a separate study (Calvini and Gorassini 2002). The greater extent of oxidation made the copper doped papers more susceptible to alkaline degradation than the iron doped paper. It was therefore concluded (Bicchieri and Pepa 1996) that iron ions catalyse cellulose degradation predominantly by cleavage of the glucosidic bond (mechanism 2 in Scheme 4.11) whereas copper ions predominantly cause ring opening of the glucopyranose ring (mechanism 1 in Scheme 4.11).



Scheme 4.11 Degradation of cellulose by metal ions via a Lewis acid mechanism (Bicchieri and Pepa 1996)

Particularly through the Fenton reaction, unbound iron ions can accelerate the oxidation of organic materials.

4.5.2 Hydrolysis (Wilson and Parks 1979; Bicchieri and Pepa 1996; Baranski, Lagan and Lojewski 2005)

Hydrolysis of polymers can occur in acid and alkaline environments and are illustrated in Schemes 4.12, 4.13, 4.14 and 4.15, respectively. In contrast to undegraded cotton, abaca, and silk, which are particularly sensitive to acid, undegraded wool is particularly sensitive to alkali (Maclaren and Milligan 1981; Jones, Rivett and Tucker 1998; Simpson 2002). However, with increasing degradation the susceptibility for all of these fibres to both acid and alkali increases.

During hydrolysis cleavage of a polymer chain occurs, forming two polymer chains in the process. Acid hydrolysis occurs predominantly in the accessible (amorphous) regions of the fibres since these regions enable the broken chain fragments to move apart from one-another and are also accessible to water, which is a reactant and catalyst in the reaction (Whitmore 2011). Crystalline regions of fibres can undergo acid hydrolysis depending on factors such as the temperature, type of acid, concentration of acid, length of exposure to the acid, and condition of the polymer (Timar-Balazsy and Eastop 1998). By cleaving the polymer chains between crystallites, the DP decreases significantly which causes a significant decrease in tensile strength and wet strength of the fibre. However when a polymer chain, that is attached to a crystallite by one end only or is not attached to a crystallite at all, is broken significant strength loss is not seen, and smaller degradation products are formed. The increasingly short polymer chains that are attached to crystallites can align better than they did when they were longer and attached to two crystallites. Additionally, increasing cleavage of bonds can cause the aggregation of smaller chains into new crystalline regions. Consequently, an increase in crystallinity of the fibre can occur with acid hydrolysis (Fan, Gharpuray and Lee 1987; Whitmore 2011) and has been measured in cellulosic samples using X-ray diffraction (Sandy, Manning and Bollet 2010). In cellulosic materials hydrolysis also causes an increase in aldehyde content as each chain break forms a new reducing end group (Scheme 4.12). These groups can be oxidised to carboxylic acids, further increasing the acidity of the system. In proteinaceous materials the amide bonds are broken to form a carboxylic acid end group and an amine end group (Scheme 4.13) (Whitmore 2011).

4.5 Iron-tannate dyes as catalysts

The rate of acid hydrolysis goes through three stages. Initially the rate of hydrolysis is very fast (10,000 times faster than the rate of stage two) due to ‘weak links’ in the structure. In cellulose, weak glycosidic bonds are under unusually large stress which has developed during polymer formation. In addition it is possible that weak links arise from oxidation products within the cellulose chain. Glycosidic bonds with neighbouring carbonyl or carboxyl groups are weaker than those with adjacent hydroxyl groups. Once all of these bonds have been broken, random hydrolysis in the accessible non-crystalline regions occurs. In pure cellulosic papers acid hydrolysis has been shown to occur at a steady rate and follow first order reaction kinetics (Zou, Gurnagul, Uesaka and Bouchard 1994). Finally, the crystallites are attacked, particularly when oxidation or swelling increases accessibility of the chains in the crystallites (Fellers, Iversen, Lindstrom, Nilsson and Rigdahl 1989; Timar-Balazsy and Eastop 1998; Wakelyn, Bertoniere, French, Zeronian, Nevell, Thibodeaux, Blanchard, Calamari, Triplett, Bragg, Welch, Timpa, Goynes Jr., Franklin, Reinhardt and Vigo 1998; Strlic and Kolar 2005).

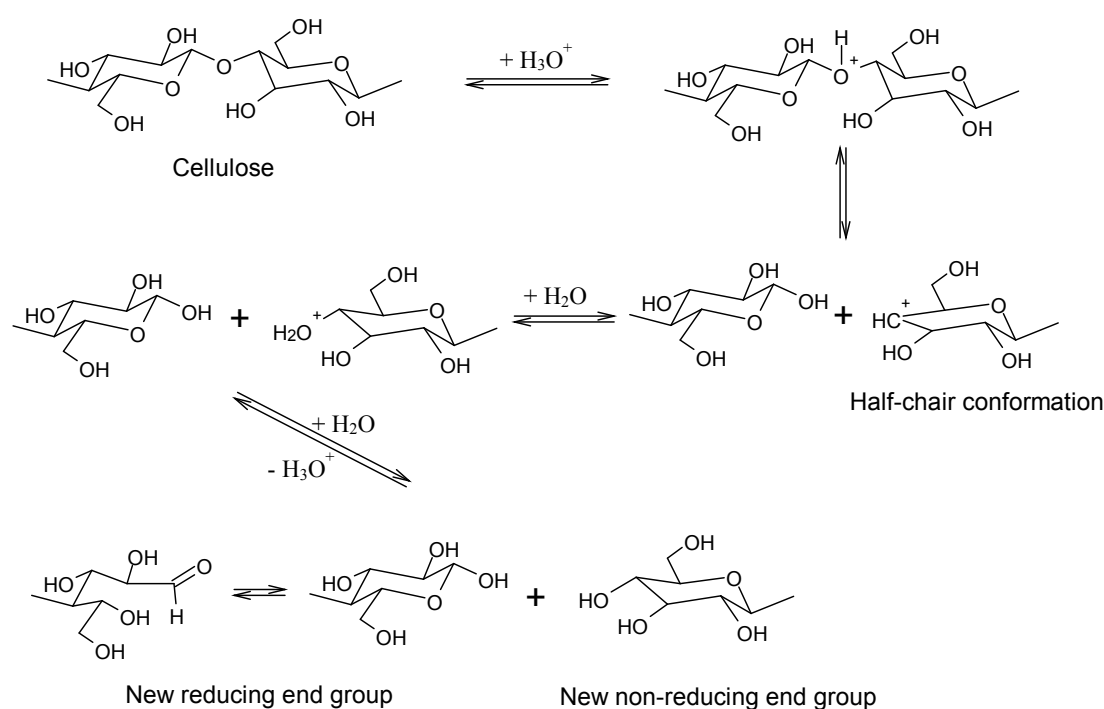
The rate of acid hydrolysis is catalysed by acidity, temperature, and water content in the fibres. The rate of hydrolysis of cellulose in paper increases 10-fold for every unit decrease in pH since it is a catalyst in the reaction (Whitmore 2011). Increasing temperature increases the rate of hydrolysis by many mechanisms including: increasing the rate of diffusion of reactants to reaction sites; increasing the quantity of molecules with the activation energy required to for a successful reaction; and, through increased molecular motion, increasing the ability for distortion of molecules (e.g. in the half-chair formation needed in the acid hydrolysis of cellulose, Scheme 4.12) and separation of chain fragments after scission (Whitmore 2011). An increase in temperature of 5°C causes an approximate doubling of the rate of acid hydrolysis in paper (Erhardt and Mecklenburg 1995). Increasing water content in the fibres increases the rate of acid hydrolysis as water acts as a reactant, and as a transport medium and plasticiser (Whitmore 2011).

When all the bonds in the amorphous regions are broken a levelling off of the polymer is observed since subsequent attack on crystallites is very slow and so little subsequent change in DP occurs. The value of the LODP is dependent on the polymer type as it is the average length of the crystallites in the polymer, and it is independent of the temperature or acidity of the environment. In cellulose, the LODP is reached when 2-5% of the sample has been hydrolysed (Fan, Gharpuray and Lee 1987) and has been reported as ranging between 150 and 250 (Shroff and Stannett 1985; Zou, Uesaka and Gurnagul 1996a; Emsley, Ali and Heywood 2000). In a study of historic iron gall inked papers the average

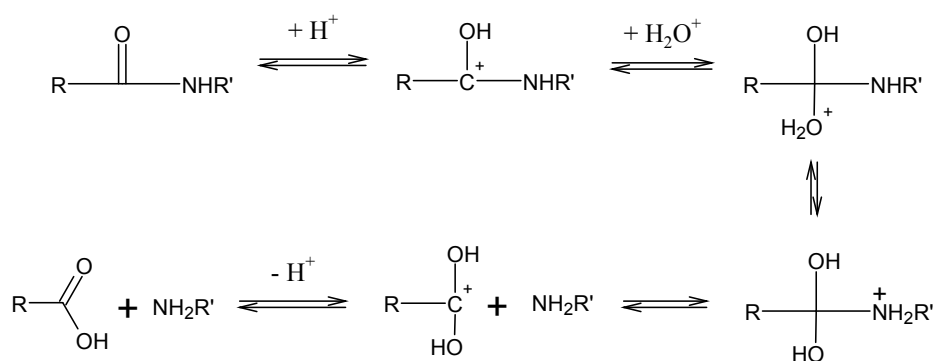
4.5 Iron-tannate dyes as catalysts

DP of 3 extremely degraded papers was 400 and this was subsequently used to identify papers at high risk of mechanical damage during handling (Strlic, Csefalvayova, Kolar, Menart, Kosek, Barry, Higgitt and Cassar 2010).

Acid-catalysed hydrolysis (Schemes 4.12 and 4.13) is a major degradation pathway for iron-tannate dyed textiles due to the high acidity of iron tannate dyes that originates from the reagents and byproducts of dye complex formation and the acids formed through oxidation of the substrate. A high concentration of weak acids such as acetic acid formed during the degradation of cellulose can be equally or more damaging than a low concentration of strong acid such as sulphuric acid which can be a byproduct of iron-tannate dye complex formation (Shahani and Harrison 2002).



Scheme 4.12 Acid hydrolysis of oxidised cellulose (Sykes 1970; Whitmore 2011)

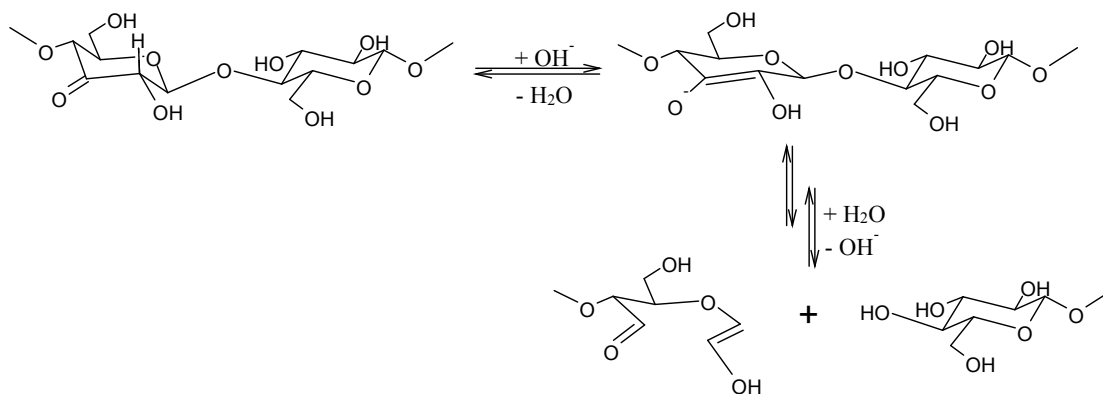


Scheme 4.13 Acid hydrolysis of peptide bond in protein based on the mechanism of acid hydrolysis of esters (Sykes 1970)

4.5 Iron-tannate dyes as catalysts

Attempts to stabilise acidic materials using deacidification methods can leave objects with mildly alkaline pH values such as pH 8. Unoxidised cellulose is relatively stable in mildly alkaline solutions but oxidised cellulose is particularly sensitive due to the presence of carbonyl groups throughout the polymer chain rather than only at the end of chain (reducing end group). These groups enable β -alkoxy-elimination to occur in oxidised cellulose as in Scheme 4.14 (Whitmore 2011). In β -alkoxy-elimination the bond to the carbon atom that is two atoms away is broken. Therefore, depending on where the oxidised group is in the cellulose (e.g. C2, C3, or C6) determines whether the glucosidic bond in cellulose is broken. Carbonyl groups at C2 or C3 will break the glucosidic bond in chains in the amorphous regions and cause a decrease in DP and tensile strength. In unoxidised cellulose the aldehydes of the reducing end groups are the only carbonyl groups present. These cause the separation of the terminal glucose unit only so that a 'peeling' reaction occurs. Significant changes in tensile strength are not seen by this method, hence the relative stability of unoxidised cellulose in mildly alkaline environments (Timar-Balazsy and Eastop 1998).

Since the rate of alkaline hydrolysis increases 10-fold for every unit increase in pH (Whitmore 2011), alkaline hydrolysis can be the major degradation pathway in deacidified objects.

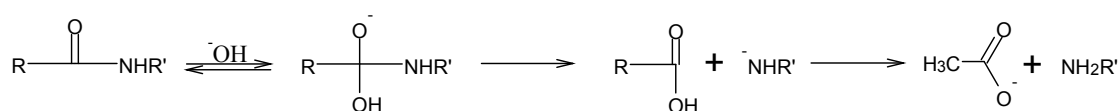


Scheme 4.14 The mechanism for β -alkoxy-elimination of cellulose in an alkaline environment (Sykes 1970; Whitmore 2011)

For protein polymers the amide bonds can be broken in alkaline conditions, Scheme 4.15. Again attack is primarily at chain ends in unoxidised chains but can be throughout the chains if carbonyl groups are present since these groups cause the scission of the peptide bonds close to them. Alkali cleaves disulphide bond crosslinks and salt bridges in

4.5 Iron-tannate dyes as catalysts

proteinaceous fibres and forms new crosslinks. Sulphenic acid side groups (RSOH) formed from the breakage of the disulphide bonds can form aldehyde groups and hydrogen sulphide (H₂S) in alkali. Consequently, wool is particularly sensitive to alkali as it contains many disulphide crosslinks. Silk however does not contain disulphide bonds and so it is more resistant to mild alkali than it is to acid, particularly when unoxidised, since acid hydrolysis is random (Timar-Balazsy and Eastop 1998).



Scheme 4.15 Alkaline hydrolysis of peptide bonds (Sykes 1970)

4.5.3 Volatile organic compounds

Volatile organic compounds are low molecular weight molecules that can be formed and released from organic materials during oxidation and acid hydrolysis. Acetic acid, vanillin, acetaldehyde and furfural were some of the most abundant volatile organic compounds emitted from a pure cotton linter paper and a groundwood pulp paper (pre-conditioned to 23°C and 50% RH) during up to 30 days of ageing at 100°C (Ramalho, Dupont, Egasse and Lattuat-Derieux 2009). The effect of iron gall ink on VOC emission from paper has been investigated and found to have a significant effect on the VOCs emitted (Havermans and de Feber 1999). 11 VOCs including furfural, formic acid, furan, and acetic acid were emitted from the iron gall inked paper compared to the two (methanol and furfural) emitted from the reference paper. The evolution of acetic acid from the acetyl groups in the hemicellulose of iron-tannate dyed *Phormium tenax* (New Zealand flax) has been demonstrated (Daniels 1999b). The formation of acidic VOCs such as acetic acid can cause acid hydrolysis to objects exposed to them.

4.5.4 Cycle of degradation

Oxidation and acid hydrolysis reinforce each other, particularly in cellulosic fibres where the reducing end groups formed by cleavage of the cellulose chain via acid hydrolysis can be oxidised to carboxylic acid groups by oxidation, which then accelerate acid hydrolysis. The presence of iron-tannate dyes can accelerate these processes as detailed above so that a destructive and ongoing cycle of substrate degradation is initiated. Consequently iron gall inked and iron-tannate dyed organic materials can show the following properties much sooner than undyed equivalents (James 2000; Shahani and Harrison 2002):

4.5 Iron-tannate dyes as catalysts

- a. Weaker due to the decrease in the DP of the polymer chains;
- b. Embrittled due to crosslinking between polymer chains which decreases flexibility, and due to the decrease in the DP of the polymer chains;
- c. Hydrophobic due to crosslinking between polymer chains ;
- d. Discoloured due to the breakdown of the iron-tannate dye complex and coloured degradation products;
- e. Increasing acidity due to oxidation of carbonyl groups to carboxylic acids.

4.5.5 Variable condition of iron-tannate dyed objects

Many iron-tannate dyed objects at the British Museum are in very poor condition.

Examples include a cotton Akali Sikh turban (Registration number: 2005, 0727.1) (Pullan and Baldwin 2008) and a vegetable fibre Apatani rain cape (Registration number: As1957, 11.9) which require minimal handling due to their fragility; the turban is even too fragile to be displayed. Complete or partial losses have occurred to the black dyed weft of a textile previously owned by the Queen of Madagascar (Registration number: Af, SLMisc2105), to the dark brown regions of Micronesian loin cloth of banana or hibiscus fibre (Registration number: Oc1904C3.282), and to the iron-tannate dyed silk hair of numerous Japanese Hina dolls (e.g. Registration number: AS1981, 0808.227). Both the flap of a brittle Ojibwa iron-tannate dyed skin bag (Registration number: 1937.6-17.1) (Daniels 1997, 1998; Cruickshank, Daniels and King 2009) and an exceedingly fragile and fragmented banana fibre belt (Cruickshank and Morgan 2011) have needed lining to physically stabilise them.

However there are also iron-tannate dyed objects in the British Museum that are surprisingly in relatively good condition. For example all of the British Museum bogolanfini are in good condition (Wolfe 2012), (e.g. Registration numbers: Af1956, 27.10 and Af1987, 07.4), as is a dark blue Adinkra cloth (Registration number: Af1935, 1005.2). Apart from age of the object, the condition of an iron-tannate dyed object will be affected by many factors which can be roughly divided into endogenous (internal) and exogenous (external) factors as shown in Figure 4.7 (Reissland 2002; Strlic, Kolar and Scholten 2005).

4.5 Iron-tannate dyes as catalysts

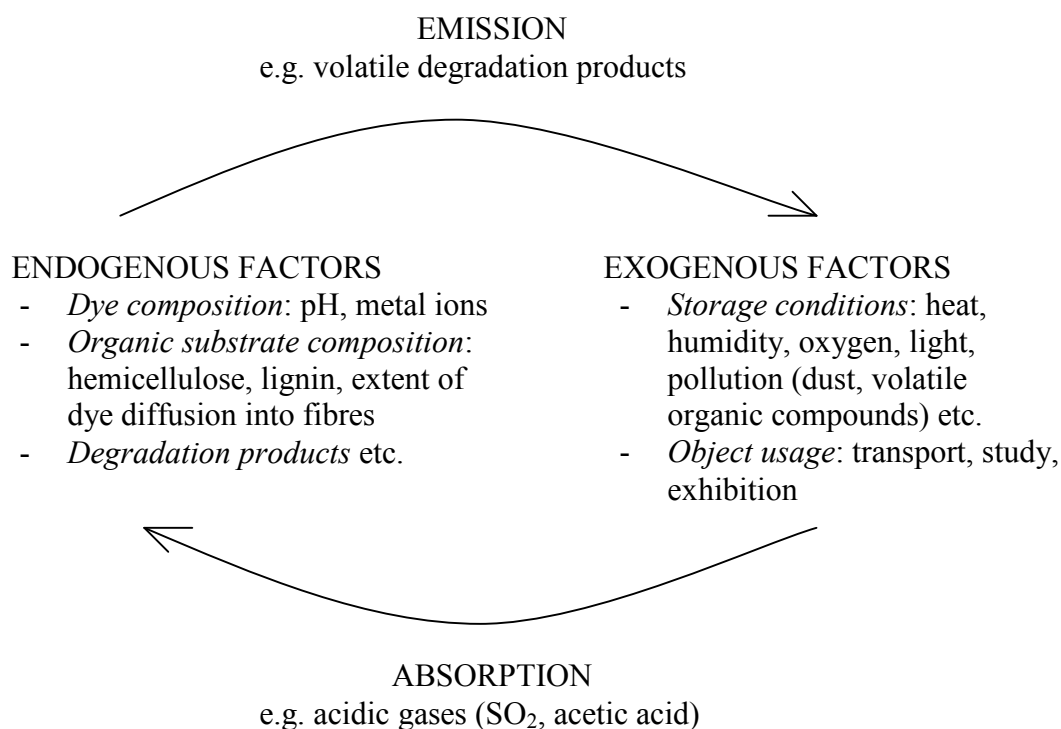


Figure 4.7 Factors affecting the stability of iron-tannate dyed organic materials. Scheme adapted from schemes of factors affecting the stability of paper (Reissland 2002; Strlic, Kolar and Scholten 2005)

Overall, all materials incorporating iron-tannate complexes within their structure are likely to experience accelerated degradation at some time in their lifetime, but the point of initiation of this acceleration will differ depending on the factors in Figure 4.7. Most notably, the onset of accelerated degradation may be later for objects that have been washed such as iron-tannate dyed bogolanfini, than for those that have not such as iron-gall ink documents, since washing removes water-soluble catalysts such as acids and metal ions. Consequently, initial degradation of washed iron-tannate dyed objects may be primarily due to autoxidation rather than both metal ion-catalysed oxidation and acid hydrolysis as in iron gall inked materials (Hofenk de Graaff 2004). The increasing acidity of polymers during oxidation will cause the eventual increase in the rate of acid hydrolysis and also the breakdown of the iron-tannate dye complex. The latter will release iron ions which can then participate in the Fenton reaction, causing metal ion-catalysed oxidation and therefore, accelerated degradation.

4.5.6 Storage recommendations for organic materials

Since oxidation and acid hydrolysis reinforce one-another, particularly in cellulosic materials, and are catalysed by iron gall inks and iron-tannate dyes, retardation of the degradation is needed as soon as possible in order to extend the lifetime of the object as much as possible. In order to preserve these objects the rate of degradation must be decreased. This can be achieved by controlling the environment (preventive conservation) or treating the object (interventive conservation) as listed below (Reissland and Cowan 2002; Shahani and Harrison 2002; Saunders 2006):

- a. Lowering temperature and keeping it stable slows down chemical reactions;
- b. Lowering RH and keeping it stable slows down chemical reactions;
- c. Lowering light levels and filtering UV to minimise photodegradation;
- d. Anoxic (oxygen-free) environment will retard oxidation;
- e. Introducing an alkaline reserve to neutralise acidity;
- f. Using a reducing agent to reduce carboxylic acids and carbonyl groups back to alcohols;
- g. Introducing an antioxidant to slow down oxidation such as a peroxide decomposer, metal ion chelator, chain breaking electron donor or acceptor and/or a UV absorber (Scott 1993a).

Further information on the preservation options for iron-tannate dyed objects is discussed in Chapter 7.

4.6 Model dye development

For this project, large quantities of unaged iron-tannate dyed textile of known composition and production history were required in order to gain the most accurate results from stabilisation treatment studies. Historic iron-tannate dyed material could not fulfil these requirements and would not be used if it could fulfil them, due to ethical considerations. Consequently model dyes needed to be developed that could be applied to the model textiles selected in Chapter 3. A few model inks or dyes have been produced in other research projects. For example, a model iron gall ink that has been used in many studies into iron gall ink on paper was proposed by Neevel (Neevel 1995). In this formulation, a ratio of iron ions:tannin (5.5:1) was used along with gum Arabic that was representative of the ratio that occurred in a range of historic iron gall ink recipes. Iron-tannate dye formulations have also been developed for use on small quantities of yarns/fibre bundles and/or textiles of silk (Sato and Okubayashi 2010), New Zealand flax (More, Smith, Te

4.6 Model dye development

Kanawa and Miller 2000), and raffia (Sandy and Bacon 2008). In this project, much larger quantities of material were needed that were representative of the materials in the British Museums collections. Consequently, three model dyes were developed through a combination of critical analysis of historical iron-tannate dye recipes, and laboratory and dyehouse-based experimentation.

4.6.1 Aims of the model dyes

The models dyes must:

- a. be applied evenly to cause even acceleration of degradation of the substrate;
- b. leave an excess of iron ions in the textile in order to accelerate degradation;
- c. significantly accelerate the rate of degradation of the model dyed textiles compared to the rate of degradation of the undyed equivalent. Preferably significant strength loss should occur within 4 weeks of accelerated ageing in order for the project to be completed on time;
- d. cause accelerated degradation results that are comparable to those found in iron-tannate dyed objects in the British Museum's collections;
- e. be economically and logistically viable.

Critical analysis of historic iron-tannate dye formulations led to the identification of a wide range of variables that could affect the textile colouration achievable by the dye (see Section 4.3 for more details). The vast array of historical dye formulations and reagents suggested that no single recipe could be viewed as representative of all. However, iron ions and tannic acids were present in all of the recipes. Consequently, three dye formulations were developed based around combinations of iron sulphate and tannic acids. Dye formulation 1 is the purest as it uses only iron ions and tannic acids. Dye formulations 2 and 3 include "impurities" (copper ions and extract of gall powder, respectively) that were common in the iron sources and the tannic acid sources, respectively, of historical dye formulations. Multiple sources of tannic acid were often used in historical dye formulations. To reflect this, a 50:50 mixture of non-purified tannic acid from Chinese galls and purified tannic acid from sumach was used in model dye formulations one and two. The quantity of copper sulphate pentahydrate used in dye formulation 2 was based on one of two highly researched model iron gall inks that were developed for the InkCor project at the ICN (Stijnman 2006). In these model recipes, the copper sulphate pentahydrate was introduced as a vitriol impurity at levels of 10% and 1% of the weight of iron sulphate heptahydrate. The larger of two quantities was chosen for dye formulation 2 to enable the effects of the metal ions to be more noticeable. Extract of gall powder rather

than whole oak galls was chosen to replace tannic acid in dye formulation 3 as the greater surface area should mean more tannic acid and gallic acid is released on soaking.

4.6.2 Experimental method

16 laboratory experiments using iron(II) sulphate heptahydrate, copper(II) sulphate pentahydrate, purified and non-purified tannic acids, and gall powder were designed to produce dye formulations that were optimised for their ability to colour the textiles in an economic and logistically viable manner. The experimental methods are summarised in Appendix 5 and were designed to assess the effect of the variables identified in historic iron-tannate dye recipes (Section 4.3) on the colour of the samples. Specifically, the effect of immersion times, repeat dyeing, reagent ratio, reagent concentrations, the solution temperatures, two-stage versus one-stage dyeing processes and the tannin-iron or iron-tannin order in the two-stage process, on dyeing “quality” were investigated.

For all lab-scale experiments, 5 cm x 5 cm squares of wool, abaca, cotton, and silk were used in solutions made up to 250 ml (unless otherwise stated). The majority of experiments involved different conditions for the proteinaceous and cellulosic materials. In these cases samples of wool, silk, and cotton were included in the ‘wool’ dyebath while samples of cotton, abaca, and silk were included in the ‘abaca’ dyebath. The cotton and silk in the wool and abaca dyebaths, respectively, ensured a comparison could be made between them and the other fabrics in the dyebaths.

Tap water rather than distilled water was the chosen solvent for the majority of the experiments because only tap water would be used at the University of Manchester’s dyehouse. However, the tap water in London where the experiments were undertaken is hard compared to the soft water in Manchester. This hardness caused the undesirable precipitation of metal ion salts during these experiments. Later experiments therefore used deionised water as the solvent in London.

Samples were put into the dyebaths wet and rinsed after completion of every dyebath in tap water of similar temperature to the dyebath. Wetting of the samples involved immersion in tap water until the samples were saturated. The dyebaths were stirred manually several times during immersion and temperatures were monitored with a thermometer. Dyebaths were either at room temperature or a temperature maintained by a hot plate. Fresh solutions were used in each dyebath which were made near to the time of immersion unless otherwise stated.

4.6 Model dye development

All experiments except for Experiment 2 which investigated the effect of temperature on textile colouration (see Appendix 5) involved the removal of a sample after one dyeing cycle while the other samples continue on to a second dyeing cycle. Experiment 1 included a further dyeing cycle. At the end of each cycle a sample of each material was removed from the dyebath and a new one added to keep the liquor: fabric ratio constant. Samples were blotted dry with paper towel and air-dried on completion of the dyeing process. If a complete dyeing process took several days the samples were re-wetted prior to immersion in the dyebaths. Samples were then stored in labelled paper envelopes rather than plastic sample bags to prevent surface contamination with plasticisers.

The colour of the dried dyed samples from each test was compared side-by-side in a well-lit area by the same assessor. Objective analysis using spectrophotometry was not necessary since characterisation of the colour change would have added little to the process of dye optimisation and the data evaluation would have been time-consuming. The most successful conditions in each test i.e. those that produced suitably dark dyed samples with the least reagent usage, were continued on to further tests until dye recipes were formulated which were balanced between sample colour, and economic and logistical viability of the method. The optimised dye recipes were then scaled up for use on industrial dyeing equipment at the University of Manchester where further adjustment occurred.

4.6.3 Results of the textile dyeing experiments

Overall the greatest depth of colour of the fabrics was achieved using a:

1. Two-stage dyeing method rather than a one-stage dyeing method;
2. Dyebath order of tannin-iron (T-I) for the cellulosic fabrics and iron-tannin (I-T) for the proteinaceous fabrics;
3. Dyebaths of low temperature for the cellulosic fabrics and of moderate temperatures of 55°C for the proteinaceous fabrics. The variation of colouration of the proteinaceous fabrics with temperature was more complicated than that for the cellulosic fabrics;
4. Immersion times in heated solutions of iron sulphate of approximately one hour. Minimal improvement in fabric colouration occurred with immersion times greater than one hour and caused undesirable precipitation of iron oxide in the dyebath;
5. Repeat of the dyeing steps which greatly increased the colour yield.

More detailed results are presented in Table 4.2.

4.6 Model dye development

Table 4.2 A summary of the results of 16 iterative experiments in which dyebath conditions were varied to assess the effects of these on textile colouration

Overall factor under study	Specific factor under study	Cotton	Abaca	Wool	Silk
One-stage dyeing method	Effect on depth of shade of freshness of dyebath solution	Fresh solution produced darker dyed materials than less fresh solutions			
Two-stage dyeing method	Dyebath order that achieved best depth of black/grey shade	Tannin application first followed by separate iron sulphate application (T-I)			Trend unclear as often very similar results obtained
	Two-stage vs one-stage dyeing methods	Two-stage process is more effective than one-stage with equal reagent concentrations and gives better wash-fastness			
Repeat dyeing		Improved depth and levelness of colour			
Temperature	Effect of temperature increase on depth of black/grey shade when using Iron-Tannin application order (on application of each only)	Similar beige colour throughout	Decreasing pale grey colouration	Increase up to 55°C and brown colouration at 90°C	Increasing brown colouration
	Effect of temperature increase on depth of black/grey shade when using Tannin-Iron application order (on application of each only)	Decrease	Slight increase	Increase	Slight increase
	Conditions to achieve best depth of black shade (one application of each reagent only)	Tannin-Iron 20°C	Tannin-Iron 90°C but very similar to Tannin-Iron 55°C	Iron-Tannin 55°C	Tannin-Iron 55°C though Tannin-Iron 20°C gave a similarly dark and less brown colouration. NB: in a subsequent test repeat dyed Iron-Tannin 55°C gave a darker coloured silk than repeat dyed Tannin-Iron 20°C

4.6 Model dye development

Overall factor under study	Specific factor under study	Cotton	Abaca	Wool	Silk
Reagent concentration	Effect on depth of colour of increasing both tannic acid and iron sulphate together by the same proportion	Increase			
	Lowest concentration that achieved sufficient depth of shade	One tenth of that used initially			One fifth of that used initially
	Effect on depth of colour of increasing tannic acid concentration only	No significant change in colour			
	Effect on depth of colour of increasing iron sulphate concentration only	No significant change in colour in one experiment but in another where the concentration of iron was increased greatly there was an increase in depth of shade, most notably on the cotton and abaca			
Liquor: fabric ratio	Effect on depth of shade of decreasing the liquor: fabric ratio	Increasing	Similar levels of dark colouration	Increasing	Increasing
Immersion times (per reagent)	Effect on depth of shade of increasing immersion time up to 24 h	Increase (2, 3, and 4 h immersion times gave similar results after single application of dye reagents)			
	Single dye application with 24 h immersion time vs repeat application using 2 h immersion time	Similar result but repeat dyeing with 2 h immersion times produced slightly darker samples		Repeat dyeing with 2 h immersion times gave significantly darker and less brown results	
	Effect on depth of shade of using 1 h immersion time for iron sulphate dyebaths and 3 h immersion time for tannin acid dyebaths rather than 2 h each	Minimal and there was no orange precipitation (thought to be iron oxide) that occurred with 2 h and greater length immersion times			
Gall powder as tannic acid source	Ratio of gall powder: tannic acid needed to create similar depths of shade	2:1 produces most similar results NB: since tannic acid quantity in a source can vary this result may not be the case with other natural tannin sources			
Gallic acid as a substitute for tannic acid	Effect on depth of shade compared to equivalent mass of tannic acid	Gallic acid didn't dissolve in the 20°C dyebath and so the samples were not dyed black		Increased	Increased
Copper(II) sulphate	Effect on depth of shade of the addition of copper sulphate pentahydrate to the iron sulphate dyebaths at 10% concentration of the iron sulphate	Increased	Increased	Decreased and resulted in a visually observable greenish tint	Decreased

4.6.4 Discussion

4.6.4.1 Two-stage versus one-stage dyeing

Visual examination of the dyed fabrics (Figures 4.8 and 4.9) clearly showed that the two-stage dyeing method, where the samples were sequentially immersed in separate dyebaths of iron(II) sulphate and tannic acid, led to greater fabric colouration than those obtained from the one-stage dyeing method where the reagents were combined in one dyebath. Similar results were noted with the dyeing of cotton and jute with tea tannins (Deo and Desai 1999). Also, the application of an after-treatment of tannic acid and iron(II) sulphate to nylon-6,6 using the single-stage process resulted in samples with typically lower rub-resistance than those treated with the two-stage process (Burkinshaw and Kumar 2008). The freshly made one-stage dyebath solutions dyed the samples more (greater depth of colour) than the 24 hour old dyebath.

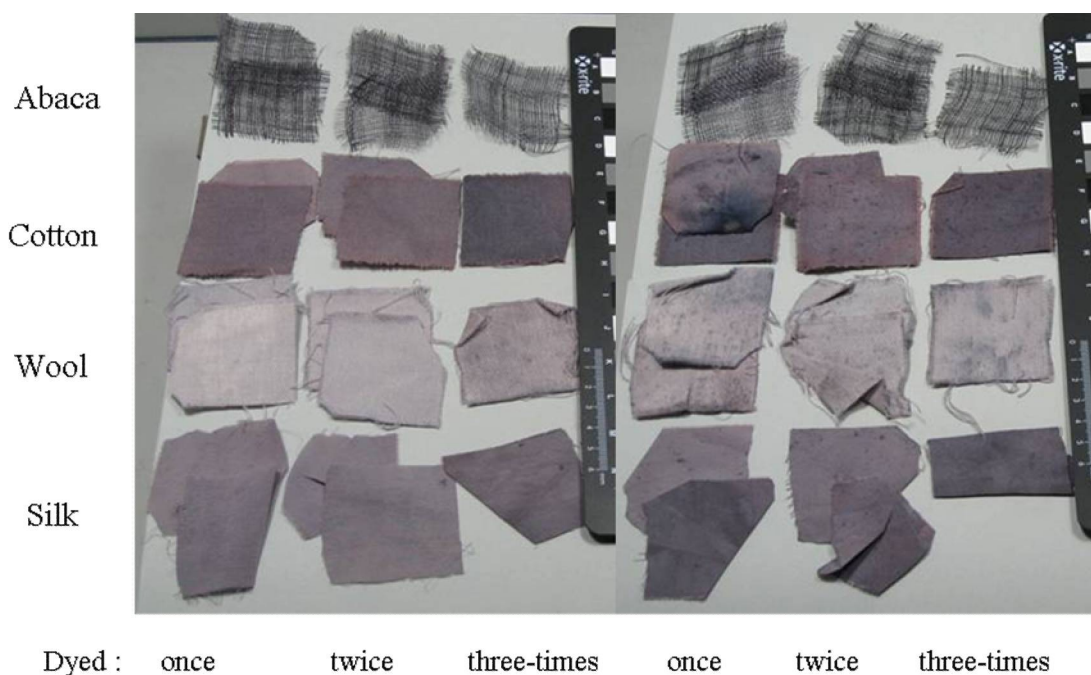


Figure 4.8 Photographs of one-stage samples dyed using a 24 h old dyebath (left) and a fresh dyebath (right)

4.6 Model dye development

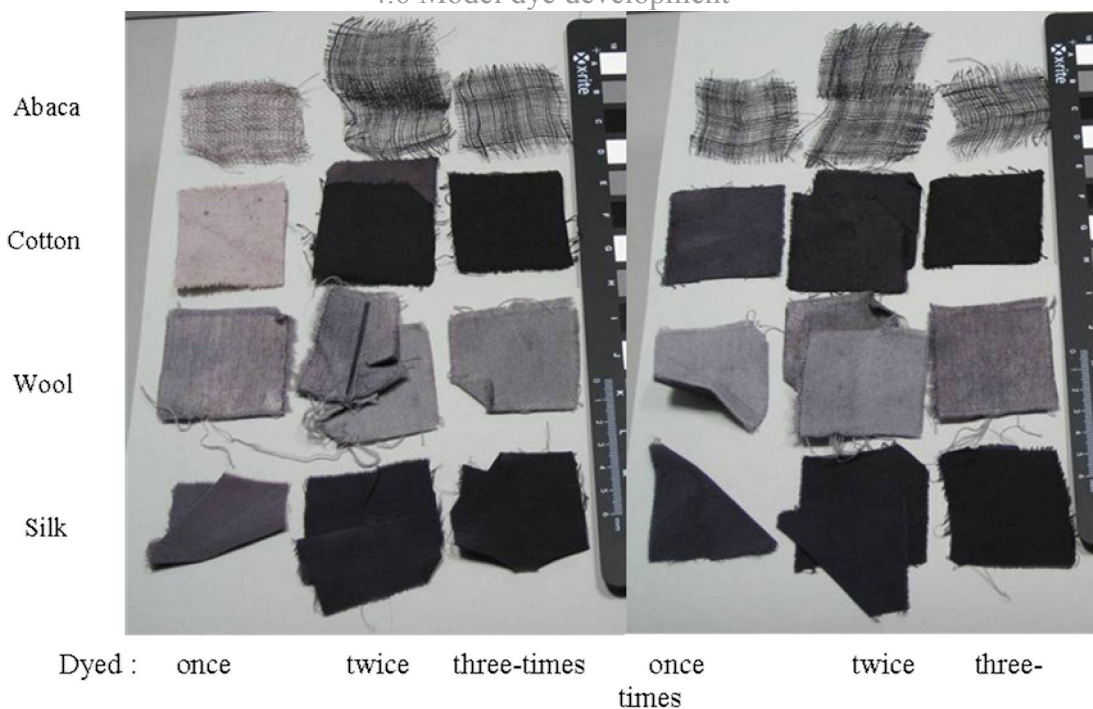


Figure 4.9 Photographs of two-stage samples dyed using the I-T order (left) and the T-I order (right)

The order of increasing depth of black colouration of dyed samples was found to be: 24 hour old one-stage solution < freshly prepared one-stage solution < two-stage application (Figures 4.8 and 4.9). This is inversely proportional to the extent of expected complex formation in the dyebaths prior to sample immersion. The simultaneous presence of the tannic acid and iron(II) sulphate in the one-stage dyebath enables complex formation to occur in the dyebath solution prior to fabric sample immersion. The longer the solution has been exposed to the air, the more oxidation and complex formation can occur (i.e. the 24 hour old solution compared to the freshly prepared solution). Complex formation outside the fibres has two effects. Firstly, the quantity of reagents available for complexation within the fibres is continuously decreased. Even if all the available reagents reacted in the sample fibres the dyed result would be less than that seen in the equivalent two-stage samples. Secondly, the iron-tannate complex is larger than the individual reagents and may aggregate to form even larger aggregates. The ability of these larger molecules or aggregates to diffuse into and out of the fibres will be less than that of the individual reagents. This would cause complexes formed outside the fibres to penetrate the fibre periphery only or stay on the fibre surface. Such complexes or aggregates may be more easily washed off than those that are within the interior of the fibre (Burkinshaw and Kumar 2008). Indeed, when washing the samples from these experiments, it was observed

that the effluent was more discoloured (purple) from the one-stage dyed samples compared to the two-stage dyed samples.

In contrast, the use of individual dyebaths in the two-stage process enables one reagent, smaller than the complex and with greater diffusional properties, to penetrate the fibres. When washed and immersed in the second dyebath, the second reagent will complex with the first reagent primarily inside the fibre. Complexation of any of the first reagent remaining on the surface of the fibres will also occur. Consequently, the majority of the dye is formed within the fibres from where it is less able to be removed due to the large size of the complex. Two-stage dyed materials are therefore dyed darker than one-stage and have superior wash-fastness properties.

4.6.4.2 Effect of the order of two-stage dyeing, T-I or I-T, on dyeing

Figure 4.9 demonstrates that the cellulosic materials are dyed significantly darker using the tannin-iron (T-I) method than the iron-tannin (I-T) method when once dyed. The darkness of I-T dyed cellulosic samples improves greatly when repeat dyed because essentially the materials have been dyed in a T-I manner once (I-T, I-T). These results were confirmed through the use of a cotton sample in the wool dyebaths (I-T, 55°C) throughout these experiments. Wool dyed significantly darker when the I-T rather than T-I method was used. Silk dyed well using both methods with T-I once dyed superior to I-T once dyed, but I-T repeat dyed being darker than T-I repeat dyed.

The differences between results from the I-T and T-I two-stage methods depend on the success of binding of the first reagent to the fibres. The success of the T-I method in the cellulosic fabrics is due to the large quantity of hydroxyl groups in cellulose and hemicellulose that can hydrogen bond with tannic acid, in addition to Van der Waals forces and substantivity imparted through physical size of the acid. Conversely, the lack of ion binding sites such as carboxylic acid or amine groups in cellulose explains the failure of the I-T method. The pale colouration that did occur with these samples could be due to the binding of iron ions to the fibre via Van der Waals. Both proteinaceous materials contain carboxylic acid and amine groups for metal ion binding and hence the I-T method is a success. In addition, side groups containing hydroxyl, amine, and thiol groups are present in wool and silk which will enable hydrogen bonding with tannic acid. Hence, the T-I method is also a success with wool and silk. The pH of the dyebath solutions will have an effect on the success of the dyeing methods on the proteinaceous textiles due to the

isoelectric points of the fibres and the resulting states of the acidic and basic groups.

Further information on this can be found in Section 4.1.7.3.

4.6.4.3 Effect of repeat dyeing on fabric colour

Repeating the dyeing process improves the darkness of the dyed samples and improves the levelness of the colouration (decreases the visible variation in colour across the sample's surface). This indicates that sites on the fibres to which the dye binds were still available following one and two dyeing cycles.

4.6.4.4 Dyeing of cellulosic materials relative to proteinaceous materials

It was noted that the cellulosic materials dyed faster than the proteinaceous materials. Certainly wetting out of materials was quickest with silk and cotton, and slowest with wool.

The hydrophobic cross-linked nature of the wool fibre cuticle decreases diffusion rates of water and small dye molecules into the fibres. These diffusion barriers are not present in the other model materials and so they dye and wet out faster than wool (Maclaren and Milligan 1981; Jones, Rivett and Tucker 1998; Wakelyn, Bertoniere, French, Zeronian, Nevell, Thibodeaux, Blanchard, Calamari, Triplett, Bragg, Welch, Timpa, Goynes Jr., Franklin, Reinhardt and Vigo 1998).

4.6.4.5 Effect of temperature on dyeing – General trends

Generally, increasing the temperature of the dyebaths between 20 and 90°C resulted in an increase in the depth of the brown tone of the resulting dyed fabrics (Figures 4.10 and 4.11). This was particularly noticeable for the I-T dyed fabrics, with I-T dyed 90°C samples exhibiting the deepest brown shade.

Increasing the temperature in the I-T dyebaths caused a slight decrease in colouration of the cotton and abaca, an increase in darkness of wool up to 55°C with a very brown colour at 90°C, and an increase in brown tone of silk.

The depth of black/grey colouration of the T-I samples decreased for cotton when the temperature was increased. It is possible that a slight increase in depth of colour occurred for abaca and silk with increasing temperature while there was a significant increase for wool.

4.6 Model dye development

Wool was dyed significantly darker at 55°C using the I-T order, more so than any other combination. Generally the I-T dyebath order resulted in darker results than T-I equivalents with the exception of the 90°C I-T sample which was more brown than black. T-I 90°C was the second darkest wool sample but was much lighter than the I-T 55°C.

When dyed once the T-I silk samples were darker than the I-T samples. T-I 55°C was the darkest (90°C was too brown to be black) and T-I 20°C was second darkest when dyed just once. However, in a separate part of the experiment repeat dyeing of the silk at 55°C using the I-T order significantly improved the colour of the silk, making it darker than the once dyed samples and the T-I repeat dyed samples at 20°C.

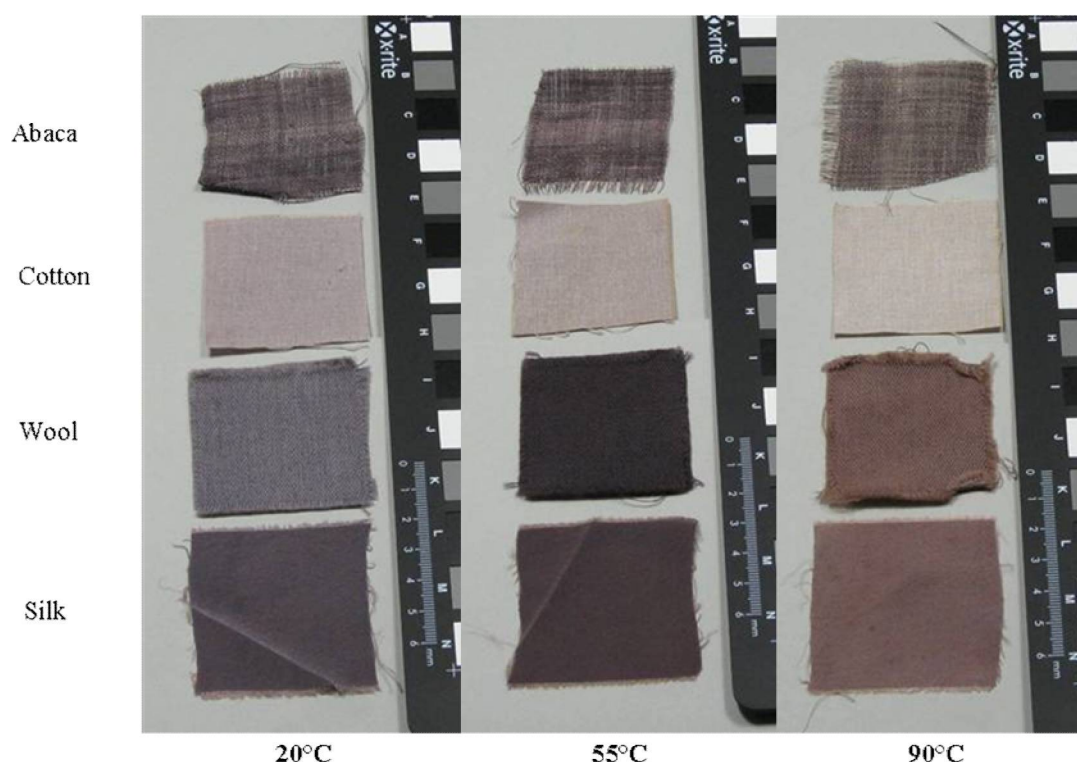


Figure 4.10 Photographs of samples dyed using an I-T two-stage process at different temperatures

4.6 Model dye development

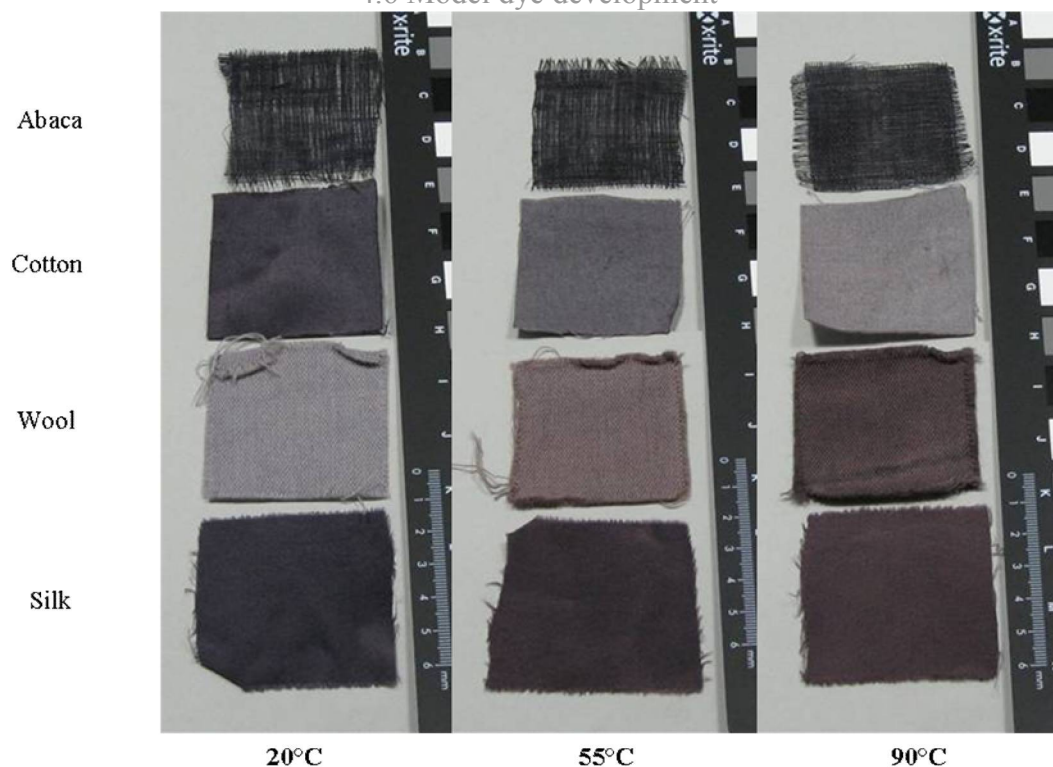


Figure 4.11 Photographs of samples dyed using a T-I two-stage process at different temperatures

Cotton was barely dyed when once dyed using the I-T method but did dye to a brown-grey when repeat dyed at 55°C in subsequent tests. All T-I samples were successful on the first dyeing, with best results at lower temperature. T-I 20°C was the darkest with T-I 55°C the second darkest. The repeat dyed I-T sample (from subsequent tests) was not darker than the T-I 20°C fabric.

Abaca dyed very well in the T-I dyebath order. It was difficult to tell which temperature provided the darkest black however the order of T-I 90°C followed by T-I 55°C was confirmed as best. The I-T dyebath dyed the abaca but only to a pale grey. The greater uptake of iron, and therefore dye, by abaca compared to cotton is likely to be due to the higher hemicellulose content in abaca than in cotton which contains carboxylic acid groups to which iron ions can bind (Sun, Fang, Goodwin, Lawther and Bolton 1998; Hsieh 2007).

Increasing the temperature will cause an increase in the rate of dyeing but, the point of equilibrium and therefore the final colouration that is achievable by the dye system will change depending on the dyeing system involved. Increasing temperature increases the rate of a reaction through the increase in molecular motion imparted to the molecules of the system. The rate of diffusion of molecules into the fibres and the number of successful

4.6 Model dye development

collisions between reactants increases with temperature. However, depending on the thermodynamics of the reaction involved, increasing the temperature can alter the point of equilibrium between the opposing reactions according to the Le Chatelier's principle. Since the adsorption of a dye to a fibre is typically exothermic, an increase in the temperature of the system will cause the equilibrium to shift towards the endothermic reaction, i.e. desorption of the dye from the fibre. In this case, higher dyeing temperatures will cause decreasing colouration of the fabrics as is seen most notably with the cotton samples. Increasing temperature also decreases the extent of aggregation of the dye since aggregation is slightly exothermic. The concentration of single molecules that can diffuse into the fibre therefore increases, causing an increase in colouration of the fabrics. Once aggregation of dye molecules has become insignificant, increasing the temperature will cause colouration results based on the thermodynamics of the reaction as mentioned above (Sumner 1989; Broadbent 2001).

The increase in temperature in the iron sulphate dyebath caused damage/discoloration to immersed fibres, particularly after immersion times of 1 hour in heated solutions. This effect was not present with either the tannin dyebath nor the iron dyebath after the tannin had been completed and was particularly noticeable when the iron dyebath was heated. This is likely to be due to the oxidation of the ferrous ions in the dyebath solution to coloured iron oxides which may associate with, and therefore discolour, the fibres. The rate of oxidation will increase with temperature. Once tannic acid has been applied to the fabric the oxidation of the iron(II) ions will be competing with the complexation of the iron(II) ions with the bound tannic acid. The above results suggest that complexation with tannic acid is more energetically and thermodynamically favourable than the oxidation of the iron(II) ions.

4.6.4.6 Gall powder extract

Similar dyeing results were obtained by use of gall powder extract compared to gall powder in place of tannic acid. However, equal quantities of gall powder and tannic acid led to different results with gall powder being less successful than tannic acid. This is because a greater range of compounds are present in gall powder than pure tannic acid. Consequently, a greater quantity of gall powder will need to be extracted for use in dye formulation 3 than the quantity of tannic acid that will be used in dye formulations 1 and 2. Extract was therefore used in the dyehouse to prevent gall powder blocking the drains when the dyebath was emptied.

4.6.4.7 Reproducibility

Throughout all of these experiments, colour reproducibility was variable. Often, samples dyed in different dyebaths under supposedly the same conditions were visibly different. Insufficient stirring and variability in reagent concentrations/measurements are likely to have contributed to these differences.

4.6.4.8 Effect of varying reagent concentrations on dyeing

Increasing the reagent concentration led to improved depth of colouration for all samples. This was due to the increased reagent concentration gradient between the dye bath solution and the textile which causes the equilibrium to be attained quicker than in dyebaths with lower reagent concentrations. If the equilibrium is not reached in the immersion times used, differences in rate of equilibrium attainment will lead to colour differences in the dyed samples. If the equilibrium is reached in the immersion times used, darker dyeing will occur because the concentration of dye in the fibre will be greater.

It was found that under the conditions used, cotton and abaca were dyed dark enough for use in this research project, but higher reagent concentrations were necessary for wool and silk. This could be due to the greater combined mass per metre of the wool and silk fabrics compared to the cotton and abaca and/or structural differences between the fibres.

Changes to reagent ratio were evaluated to determine whether improved colouration was possible but the results from varying the reagent ratios was inconclusive. Initial increases in the concentration of each reagent individually led to minimal changes in colouration of the fabrics. However, a larger change in the concentration of the iron ions was later used and this caused an increase in the colouration of the cellulosic samples and silk using T-I and 20°C. Silk dyed using I-T and 55°C decreased in colour with the increase in iron, while the colouration of wool may have increased. This suggested that the previous changes in concentrations of reagents may have been too small to cause visually observable changes in colouration. The increase in colouration of the cellulosic textiles suggested that iron was a limiting factor in the colour yield of the dyeing method. The reason for the decrease in the colouration of the silk using the I-T and 55°C method was uncertain.

4.6.4.9 Effect of different immersion times on dyeing

Increasing the immersion times of the fabric samples in the dye baths increased the colour strength of the fabrics with repeat applications. This is likely to be due to an increased exhaustion and interactions between reagents and fibres that would increase the colouration of the fabrics until a dynamic equilibrium was established. Keeping the samples immersed in the dye baths after equilibrium has been established causes no change in colouration since the rates of adsorption and desorption of dye onto and from the fibre are equal.

The equilibrium in the cellulosic dye baths was not reached in this experiment since the use of the 24 hour immersion time in the repeat dyeing of the cellulosic materials led to noticeably darker results than in the samples produced using 2, 3, and 4 hour immersion times. The proteinaceous dye baths appeared to reach equilibrium after 3 hours since the samples produced using 4 hour and 24 hour immersion times were very similarly coloured but still darker than the fabrics produced using 2 or 3 hour immersion times. However, a false equilibrium can occur where the equilibrium is between the dye bath solution and the surface of the fibre rather than the inside of the fibre. This can lead to the fibre being ring-dyed rather than dyed throughout (Sumner 1989). Ring dyeing of fibres with iron-tannate dye could cause catalysed degradation predominantly in the outer parts of the fibre and not the inner parts which are responsible for the strength of the fibre. Consequently, ring dyeing of fibres is undesirable for this project.

Decreasing the iron dyebath immersion time to 1 hour for the proteinaceous materials made little difference to the resulting colour. Precipitation of orange iron oxides occurred for immersion times in heated solution greater than 1 hour. A similar situation for Cu(II) ion uptake by wool has been reported in which the Cu(II) ion uptake levelled off after 30 minutes (Bendak, Raslan and Salama 2008). By increasing the tannic acid dyebath immersion to 3 hours to maintain an overall 4 hour dye completion time, the dyed material was marginally darker than fabrics with 2 hour immersion times per dyebath. This could occur if most of the iron ion adsorption occurred within the first hour and complete complexation of the adsorbed ions occurred in more than 2 or even 3 hour immersion times. In these cases the samples immersed for 3 hours will likely result in more complexes being formed and hence a darker colour.

4.6.4.10 Effect of varying the liquor:fabric ratio on dyeing

Decreasing the liquor:fabric ratio from ~118:1 to ~71:1 to ~24:1 visibly increased colour strength of the dyed wool, cotton, and silk. Abaca dyed darkly in all repeat dyed samples. Unlevel dyeing of wool and silk from the wool dyebath occurred using the lowest liquor:fabric ratio of 22:1 (50 ml solution) probably due to inefficient stirring. However, some areas were darker than other wool or silk samples in this experiment and so they are viewed as a continuation of the trend of decreasing ratio, increasing darkness. This is because decreasing the liquor:fabric ratio increases the concentration of dye in the fibres at equilibrium (exhaustion, %) (Broadbent 2001).

4.6.4.11 Effect of addition of copper on dyeing

The addition of copper to the iron sulphate dyebaths increased the darkness of the T-I dyed abaca, cotton and silk (20°C) but decreased the darkness of the I-T dyed wool, silk and cotton (55°C). The wool was particularly pale with the addition of copper and had a visually observable greenish tint. This observation is likely due to the application of heat to the wool dyebaths and possibly also to the use of the iron dyebath first. Krekel (Krekel 1999) noted that combination of pure copper sulphate and gallic acid results in soluble brown products being formed. Any of these coloured compounds remaining in the dyed textiles would affect the shade of grey expected.

4.6.5 Influence of results on the dye formulations

These preliminary colouration studies led to an outline for the dye formulations (Table 4.3). The reagent concentrations of these dye formulations were scaled up for use at the University of Manchester's dyehouse and optimised for the model dyes. Slight adaptations to the dye formulations at the dyehouse were made e.g. the inclusion of an extra iron sulphate dyebath in the proteinaceous dyeings (p1, p2, and p3), to further optimise the model dyes. The final dye formulations are presented in Table 4.4. Dye formulations with greater colour yields could have been chosen but the darker colouration they could achieve was thought to be out weighed by the greater cost of reagents or more complicated production methods.

4.6 Model dye development

Table 4.3 Outline of dye formulations based on results from small-scale laboratory experiments

	Wool and silk	Cotton and abaca
Conditions in all dye formulations		
Dyebath temperature (°C)	55	Room temperature
Two-stage dye bath order	1. Iron sulphate 2. Tannic acid	1. Tannic acid 2. Iron sulphate
Immersion times (hours)	1. 1 2. 3	1. 2 2. 2
Dyeing machine	Winch	Jigger
Dye formulations 1 (p1 and c1) ^a and 2 (p2 and c2)		
Dye bath quantity (l)	200	60
Approximate total fabric mass for 10 m lengths of each fabric (kg)	2.70	3.20
Approximate liquor: fabric ratio	74:1	19:1
Iron sulphate heptahydrate per dye bath (kg)	1.10	0.74
Tannic acid per dye bath (kg)	1.30	0.90
Copper sulphate pentahydrate per dye bath in dye formulation 2 only (kg)	0.10	0.08
Minimum number of repeats	1	1
Dye formulations 3 (p3 and c3) (for silk and cotton fabrics only) ^b		
Dye bath quantity (l)	200	60
Approximate mass of a 10 m length of fabric (kg)	0.70	1.70
Approximate liquor: fabric ratio	286:1	35:1
Iron sulphate heptahydrate per dye bath (kg) ^c	0.28	0.39
Gall powder per dye bath (kg) ^d	1.05	1.40
Copper sulphate pentahydrate per dye bath (kg)	-	-
Minimum number of repeats	1	1

Notes for Table 4.3:

a. Dye formulations 1, 2, and 3 are labelled as p1, p2, and p3 for the proteinaceous fabrics, respectively, and c1, c2, and c3 for the cellulosic fabrics, respectively;

b. Dye formulation 3 was planned to be applied to cotton and silk only to lower economic costs and model textile numbers. The quantity of solution in the dye bath could not be reduced to maintain the same liquor: fabric ratio in c3/p3 as was planned for c1/p1 and c2/p2 because the machines were at their minimum capacity already. An extra material was not added into the dye to maintain the liquor: fabric ratio because the extra material could have taken up some of the dye which may have made the materials from c3/p3 less comparable with those from c1/p1 and c2/p2;

c. The quantity of iron sulphate heptahydrate per dye bath was calculated as follows (demonstrated for silk):
Iron sulphate heptahydrate mass (in p1) \times (mass of silk in p1/total mass of wool and silk in p1);

d. The quantity of gall powder to be extracted in water was calculated as follows (demonstrated for silk):
2(Tannic acid mass (in p1) \times [mass of silk in p1/total mass of wool and silk in p1]).

4.6 Model dye development

Table 4.4 The final model dye formulations following adaptation at the University of Manchester's dyehouse

Dye code		Substrate	Liquor: Fabric ^a	Dyebath A ^b	Dyebath B	Dyebath A+	Dyeing sequence
Proteinaceous	p1	Wool + silk	200 : 3.23	0.02 M FeSO ₄ .7H ₂ O 55°C, 1 hour	6.5 g.L ⁻¹ TA 55°C, 3 hours	0.009 M FeSO ₄ .7H ₂ O 55°C, 1 hour	A B A B A+
	p2	Wool + silk	200 : 3.23	0.02 M FeSO ₄ .7H ₂ O + 0.002 M CuSO ₄ .5H ₂ O 55°C, 1 hour	6.5 g.L ⁻¹ TA 55°C, 3 hours	0.009 M FeSO ₄ .7H ₂ O + 0.0009 M CuSO ₄ .5H ₂ O 55°C, 1 hour	A B A B A+
	p3	Silk	200 : 0.62	0.005 M FeSO ₄ .7H ₂ O 55°C, 1 hour	3.5 g.L ⁻¹ Gx 55°C, 3 hours	0.002 M FeSO ₄ .7H ₂ O 55°C, 1 hour	A B A B A+
Cellulosic	c1	Cotton + abaca	60 : 2.01	15g.L ⁻¹ TA 20°C, 2 hours	0.04 M FeSO ₄ .7H ₂ O 20°C, 2 hours	-	A B A B A B
	c2	Cotton + abaca	60 : 2.01	15 g.L ⁻¹ TA 20°C, 2 hours	0.04 M FeSO ₄ .7H ₂ O + 0.005 M CuSO ₄ .5H ₂ O 20°C, 2 hours	-	A B A B A B
	c3	Cotton	60 : 1.22	16.6 g.L ⁻¹ Gx 20°C, 2 hours	0.024 M FeSO ₄ .7H ₂ O 20°C, 2 hours	-	A B A B A B

Notes for Table 4.4:

a. Ratio in litres of dyebath:total mass of fabric in kilograms;

b. TA: 50:50 mixture of non-purified and purified tannic acid extracts from Chinese galls and sumac; Gx: non-purified gall powder;

c. In p1, the final quantity of iron (A+) was added directly to final dyebath B but in p2 and p3, it was applied in a separate dyebath due to substantial and problematic foam formation in p1. Since an unknown quantity of tannic acid remained in the final dyebath B in p1 when the iron (A+) was added, the effective concentration of iron ions available for binding with tannic acid on or within the textile fibres is lower than that in p2 and p3.

Prior to dyeing the model textiles were washed to remove impurities as detailed in Table 4.5.

Table 4.5 The method of washing the model textiles prior to dyeing

	Winch machine	Dye Jigger machine
Fabric	10 m of wool 10 m of silk	10 m of abaca 10 m cotton
Water (l)	200	60
Sodium Carbonate (kg)	0.2	0.06
Non-ionic detergent (kg)	0.4	0.06
Temperature (°C)	50	50
Quantity of material (m ²)	1. 34.5 2. 20 (20 m of silk only)	43
Drying method	Hydroextractor and tumble drier (low heat) or air dry	Mangle and hot rollers

4.7 Conclusions

Model dyes have been developed for the model textiles detailed in Chapter 3 following critical analysis of historical iron-tannate dye formulations, small-scale laboratory experimentation, and adaptation at the University of Manchester's dyehouse facilities. These dyes will colour the model textiles shades of grey to black. Accelerated ageing of the dyed fabrics will establish if they fulfil the other aims of the model textiles, i.e. that they degrade at an accelerated rate compared to undyed equivalents and produce similar results to those seen in historic British Museum objects.

5 MODEL IRON-TANNATE DYED TEXTILES

The nature of the undyed model textiles and the dye formulations are discussed separately in Chapters 3 and 4, respectively. Chapter 5 discusses the dyeing of the model textiles and assesses the ability of the dye formulations to fulfil the aims stated in Chapter 3.

To fulfil the stated aims the model dye formulations must:

- a. be applied evenly to cause even acceleration of degradation of the substrate;
- b. leave an excess of iron ions in the textile in order to accelerate degradation;
- c. significantly accelerate the rate of degradation of the model dyed textiles compared to the rate of degradation of the undyed equivalent. Preferably showing significant strength loss within 4 weeks of accelerated ageing in order for the project to be completed on time;
- d. cause accelerated degradation results that are comparable to those found in iron-tannate dyed objects in the British Museum's collections;
- e. be economically and logistically viable.

Aim 'e' has already been achieved as it was a key consideration during the development of the dye formulations during Chapter 4. Through the characterisation of colour, pH, and metal ion distribution of the model textiles prior to accelerated ageing the success of the model dyes at achieving aims 'a' and 'b' are determined in this chapter. Analysis of accelerated aged samples also enable assessment of the success of the model dyes at fulfilling aim 'c' in this chapter. Aim 'd' is considered in Chapter 6.

Much of the work presented in this chapter has been published in the peer-reviewed, online, and open access Chemistry Central Journal (Wilson, Carr and Hacke 2012). Posters featuring some of the work in this chapter have also been presented at the national conference, ICON CF10 in Cardiff, 24th-26th March 2010 (Gill, Wilson and Mackenzie 2010) and at the international IIC 2010 Istanbul Congress – Conservation and the Eastern Mediterranean (Wilson 2010) and are presented in Appendices 4 and 3, respectively.

5.1 Production

5.1.1 *Dyeing of the model textiles*

The final dye formulations differed for proteinaceous and cellulosic materials (p1-3 and c1-3, respectively) and are summarised in Table 5.1. Due to practicalities of handling, wool and silk were dyed together in a Winch machine and cotton and abaca were dyed together in a jigger machine. Neither machine has model numbers but both were produced

5.1 Production

by Sir James Farmer Norton, a now defunct Manchester-based textiles machine manufacturer. The colouration of the wool and silk textiles dyed on the Winch machine were observed to more closely resemble the results from the lab-based dye experimentation (Chapter 4) than the cotton and abaca textiles that were dyed in the jigger. The textiles in the Winch machine were in direct contact with the dyebath more frequently than the textiles in the jigger. Consequently, when considering historical dyeing methods where organic materials were immersed in the dye solution for certain lengths of time (as was also the case during the dye experimentation in this project), the Winch machine may replicate the historic dyeing conditions more accurately than the jigger machine.

The fabrics were pre-washed using sodium carbonate and non-ionic detergent to remove any impurities prior to dyeing as detailed in Chapter 2. The dyebaths were made up fresh for each application and the fabrics were re-wetted before immersion. The reagents were dissolved in a small amount of tap water before adding them to the dyebaths and diluting to the correct volume. The non-purified tannic acid extracts from Chinese galls and the purified tannic acid extracts from sumac were fully soluble in water and were used in dye formulations 1 and 2 as received. However, the non-purified gall powder was only partially soluble and would have blocked the drains of the dyeing machines if used as received. Therefore, the tannic acid in the gall powder was extracted by soaking in a bucket of tap water for several days prior to dyeing (16.6 gL^{-1} and 3.5 gL^{-1} for c3 and p3 dye formulations, respectively). The concentrated extract was then diluted to the correct volume in the treatment dyebaths. Once the last tannic acid bath had been completed for wool and silk (B), additional metal ions (iron sulphate or iron sulphate and copper sulphate) were added to the bath (A+) which was then left for 1 hour before washing as usual.

The pH of clear and colourless dyebath solutions was tested using pH-Fix 0-14 Fisherbrand pH indicator strips and found to be typically pH 4 to 6 for both tannic acid solutions and metal ion solutions. The fabrics were rinsed twice in tap water for five minutes between dyebaths and after the final dyebath. All fabrics except abaca which was air dried due to its stiffness, were dried using a hydroextractor and tumble drier with low thermal and mechanical action.

Table 5.1 Model dye formulations

Dye code		Substrate	Liquor: Fabric ^a	Dyebath A ^b	Dyebath B	Dyebath A+	Dyeing sequence
Proteinaceous	p1	Wool + silk	200 : 3.23	0.02 M FeSO ₄ .7H ₂ O 55°C, 1 hour	6.5 g.L ⁻¹ TA 55°C, 3 hours	0.009 M FeSO ₄ .7H ₂ O 55°C, 1 hour	A B A B A+
	p2	Wool + silk	200 : 3.23	0.02 M FeSO ₄ .7H ₂ O + 0.002 M CuSO ₄ .5H ₂ O 55°C, 1 hour	6.5 g.L ⁻¹ TA 55°C, 3 hours	0.009 M FeSO ₄ .7H ₂ O + 0.0009 M CuSO ₄ .5H ₂ O 55°C, 1 hour	A B A B A+
	p3	Silk	200 : 0.62	0.005 M FeSO ₄ .7H ₂ O 55°C, 1 hour	3.5 g.L ⁻¹ Gx 55°C, 3 hours	0.002 M FeSO ₄ .7H ₂ O 55°C, 1 hour	A B A B A+
Cellulosic	c1	Cotton + abaca	60 : 2.01	15g.L ⁻¹ TA 20°C, 2 hours	0.04 M FeSO ₄ .7H ₂ O 20°C, 2 hours	-	A B A B A B
	c2	Cotton + abaca	60 : 2.01	15 g.L ⁻¹ TA 20°C, 2 hours	0.04 M FeSO ₄ .7H ₂ O + 0.005 M CuSO ₄ .5H ₂ O 20°C, 2 hours	-	A B A B A B
	c3	Cotton	60 : 1.22	16.6 g.L ⁻¹ Gx 20°C, 2 hours	0.024 M FeSO ₄ .7H ₂ O 20°C, 2 hours	-	A B A B A B

Notes for Table 5.1:

a. Ratio of dyebath volume (l):total mass of fabric (kg);

b. TA: 50:50 mixture of non-purified and purified tannic acid extracts from Chinese galls and sumac; Gx: non-purified gall powder;

c. In p1, the final quantity of iron (A+) was added directly to final dyebath B but in p2 and p3, it was applied in a separate dyebath due to substantial and problematic foam formation in p1. Since an unknown quantity of tannic acid remained in the final dyebath B in p1 when the iron (A+) was added, the effective concentration of iron ions available for binding with tannic acid on or within the textile fibres is lower than that in p2 and p3.

5.1.2 Summary of the 14 model textiles

In total, approximately 8 – 10 metres of 14 model textiles were produced for use in this project. 10 of these model textiles were iron-tannate dyed and consist of approximately 80 m² of material. The abbreviations used to refer to the model textiles from now on are detailed in Table 5.2 and used in Figure 5.1 to identify the model textiles depicted.

Samples of the model textiles are included in Appendix 7.

Table 5.2 Summary of the model textiles used in this project and their abbreviations

Dye formulation ^a	Model textile			
	Cotton	Abaca	Wool	Silk
Undyed	CU	AU	WU	SU
c1	Cc1	Ac1		
c2	Cc2	Ac2		
c3	Cc3			
p1			Wp1	Sp1
p2			Wp2	Sp2
p3				Sp3

Note for Table 5.2:

a. See Table 5.1 for detailed information on the dye formulations.

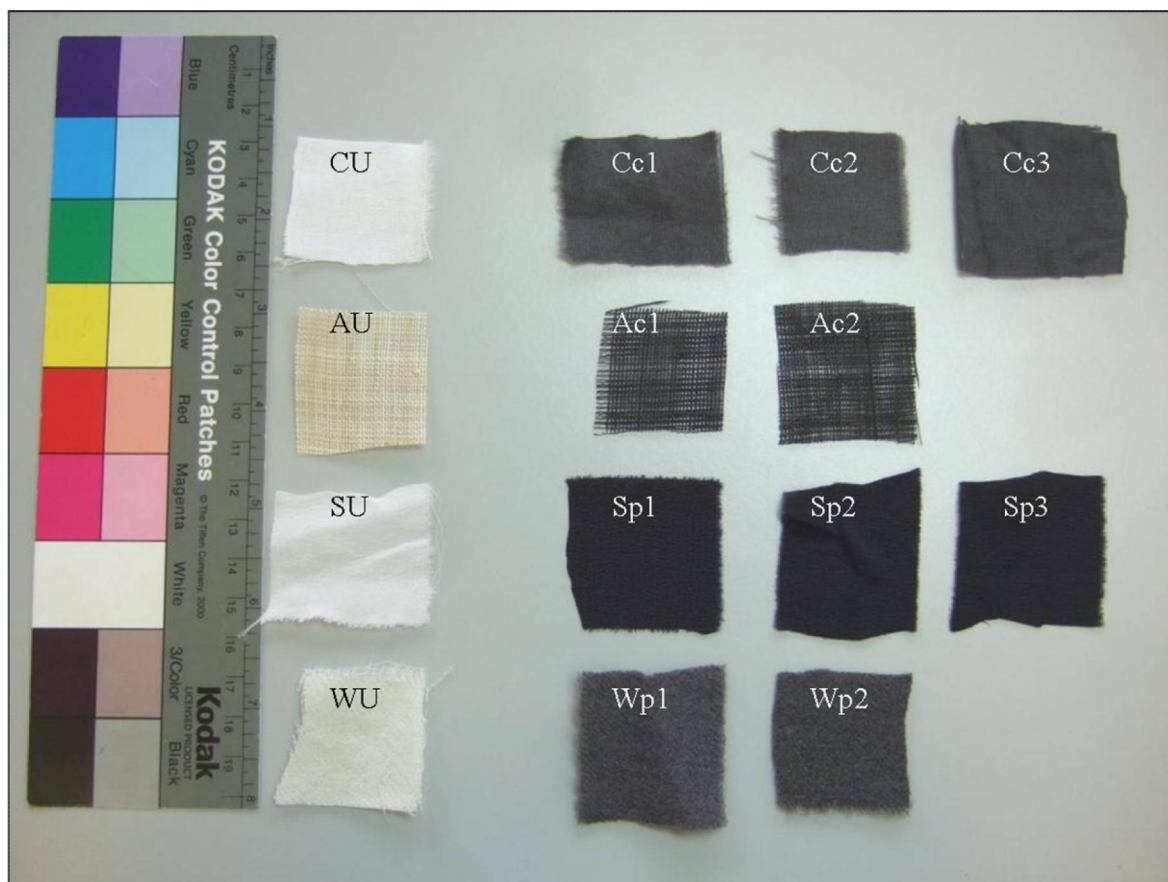


Figure 5.1 Image of samples of each model textile (dyed and undyed) produced for this project

5.2 Experimental Techniques

Some or all of the following analytical techniques (XRF, colour measurement, surface pH, GPC-MALLS, EPR, and tensile testing) were used to characterise the properties of unaged and aged (Section 5.2.9) model textiles.

5.2.1 X-ray fluorescence analysis (XRF)

An ArtTax μ -XRF spectrometer with molybdenum X-ray tube was used for semi-quantitative analysis of the elemental content of the model textiles. Single thicknesses of model textiles were analysed on filter paper for 100 s, using a 1.5 mm collimator, 50 kV, and 500 μ A in air. 8 analyses per model textile were obtained with the same textile alignment. The net peak areas of elements (A_e) and the Compton peak (A_c) were calculated by ArtTax4.9 software using the Bayes deconvolution method. The net elemental peak areas were normalised to the Compton peak using Equation 5.1.

$$Ratio = \left(\frac{A_e}{A_c} \right) \times 1000 \quad \text{Equation 5.1}$$

5.2 Experimental techniques

The mean ratios and standard deviations iron and copper were calculated from the 8 ratios calculated per model textile.

5.2.2 *Surface pH*

Individual sheets of textile were laid on a clean glass sheet and a drop of deionised water added. Before analysis it was ensured that the water dispersed into the fabric rather than remaining as a drop on the surface. In some cases more than one drop of water was needed to wet the textile sufficiently for successful measurement. A Mettler Toledo InLab®Surface pH electrode attached to a Hanna Instruments HI2210 pH meter with temperature probe was then applied to the wet area and held in place until the pH value stabilised. Ten analyses per model textile were made on randomly selected locations of randomly selected textile sheets. pH 4.01 and pH 7.01 buffer solutions were used to calibrate the equipment prior to analysis.

5.2.3 *Bathophenanthroline tests*

The method of testing for iron(III) ions in textiles using bathophenanthroline paper was described by Vuori and Tse (Vuori and Tse 2005a). A drop of deionised water was added to a small triangle of bathophenanthroline test paper. The excess water was blotted from the surface of the test paper using filter paper. The wet test paper was put onto the sample area for analysis and a piece of melinex placed on top. These were pressed onto the sample for 3 minutes to ensure good contact between the test paper and sample surface. Care was taken not to press too firmly as this could damage the sample. Upon removal from the sample, the test paper was air dried for 2 minutes before it was cut in half. To one of these halves, a drop of 1% ascorbic acid was applied to convert any iron(III) to iron(II). When dry, the test papers were compared to a colour chart prepared by Vuori and Tse (Vuori and Tse 2005a) and the category of iron content that compared best with the test papers was noted. Plastic tweezers were used to handle the test papers to minimise contamination of the test papers with iron from the tweezers. Metal scissors were used to cut the test paper.

5.2.4 *Colour measurements*

Spectrophotometric and colorimetric data was collected using a Konica/Minolta CM-2600d spectrophotometer, Spectramagic 3.60 software, and the following settings: SCI+SCE, medium aperture, UV included, 10° observer, and D65 illuminant. The spectrophotometer was calibrated using a white standard before analysis and the textiles were analysed on black velvet.

5.2.4.1 Unaged model textiles

10 randomly selected sheets of each model textile were analysed in 3 randomly selected locations to provide mean, standard deviation, and coefficient of variation L^* , a^* , b^* values of SCE/100 data. The standard deviation and coefficient of variation values for SCE/100 data were not collected. The unaged abaca samples were folded so that two layers were measured simultaneously due to the looseness of the weave compared to the other textiles. One layer of the cotton, silk, and wool was analysed.

5.2.4.2 Aged model textiles

Assessing the effect of dye formulation 1 (c1/p1) on the cotton, abaca, wool, and silk model textiles

The same method of colorimetry was employed for the unaged model textiles except that average CIE L^* , a^* , b^* values were calculated by the software from 5 randomly selected locations on each aged model textile. Again, CIE2000 was used to calculate the ΔE_{00}^* , ΔL^* , Δa^* , Δb^* from SCE/100 data from the aged textile compared to the unaged equivalent textile

Assessing the effect of dye type on the cotton and silk model textiles

Spectrophotometry of each sample was performed prior to and after accelerated ageing using the method detailed in Section 5.2.4.1 except the average CIE L^* , a^* , b^* values were calculated by the software from 5 randomly selected locations on each aged model textile and that one layer of all textiles were analysed. The CIE2000 colour difference formula was used to calculate the difference in colour (ΔE_{00}^*) between the samples prior to and after ageing. By analysing each sample prior to ageing and using that data as the unaged comparison rather than the data from the unaged sample set, error due to natural variation in colouration of the model textiles was eliminated. The ΔL^* , Δa^* , and Δb^* values were calculated by subtraction of the unaged values of a sample from the aged values of the same sample.

The CIE2000 colour difference formula was used to calculate the ΔE_{00}^* , ΔL^* , Δa^* , Δb^* from SCE/100 data from the aged textile compared to the unaged equivalent textile. SCE/100 data was chosen for evaluation of colour changes in aged model textiles because it excluded the specular component which could be a source of error in the textiles with more reflective surfaces such as abaca and silk. However, SCI and SCE data for the unaged model textiles differed little from each other (Table 5.3); typically less than 1.2%

5.2 Experimental techniques

variation in L^* , and less than 10% variation in a^* and b^* . The b^* SCI/100 data was consistently slightly greater than the SCE/100 data and the a^* data was consistently lower than the SCE/100 data, but the L^* data varied between being higher and lower.

Table 5.3 Variation in colour coordinates between SCI/100 and SCE/100 data as a % of SCI/100 and SCE/100 data

Model textile ^a	Divisor ^b	L^*	a^*	b^*	% difference		
					L^*	a^*	b^*
CU	SCE/100	84.4	-0.2	0.5	-0.1	35.1	39.6
	SCI/100	84.3	-0.3	0.7	-0.1	26.0	28.4
Cc1	SCE/100	35.8	0.7	-4.5	-0.3	-3.8	-3.1
	SCI/100	35.7	0.7	-4.3	-0.3	-4.0	-3.2
Cc2	SCE/100	33.7	0.8	-5.0	-0.3	-2.3	-2.5
	SCI/100	33.6	0.8	-4.9	-0.3	-2.3	-2.6
Cc3	SCE/100	29.7	0.6	-4.7	-0.3	-1.1	-2.7
	SCI/100	29.6	0.6	-4.6	-0.3	-1.1	-2.8
AU	SCE/100	74.2	1.9	13.4	0.0	-1.7	1.0
	SCI/100	74.2	1.9	13.6	0.0	-1.7	1.0
Ac1	SCE/100	21.4	0.6	-2.5	1.2	-8.5	-10.9
	SCI/100	21.7	0.6	-2.2	1.1	-9.3	-12.2
Ac2	SCE/100	23.1	0.5	-2.9	1.0	-4.0	-8.3
	SCI/100	23.3	0.5	-2.6	0.9	-4.2	-9.1
SU	SCE/100	75.5	-0.1	0.8	-0.2	36.8	23.3
	SCI/100	75.4	-0.2	1.0	-0.2	26.9	18.9
Sp1	SCE/100	20.6	1.5	-4.2	0.6	-1.4	-6.7
	SCI/100	20.7	1.5	-3.9	0.6	-1.4	-7.2
Sp2	SCE/100	18.8	1.6	-4.5	-0.5	-0.6	-3.3
	SCI/100	18.8	1.6	-4.4	-0.5	-0.6	-3.5
Sp3	SCE/100	17.6	1.4	-4.4	1.1	-0.8	-7.4
	SCI/100	17.8	1.4	-4.1	1.1	-0.8	-8.0
WU	SCE/100	78.5	-1.0	6.5	-0.1	5.7	2.9
	SCI/100	78.4	-1.1	6.7	-0.1	5.4	2.8
Wp1	SCE/100	33.6	1.3	-1.2	-0.3	-1.2	-9.3
	SCI/100	33.5	1.3	-1.1	-0.3	-1.3	-10.3
Wp2	SCE/100	30.9	1.0	-1.1	-0.4	-4.2	-7.0
	SCI/100	30.8	0.9	-1.0	-0.4	-4.4	-7.6

Notes for Table 5.3:

- See Table 5.2 for explanation of model textile codes;
- Calculated using the difference between SCI/100 and SCE/100 values of a colour coordinate divided by the divisor (either SCI/100 or SCE/100). The resulting value was multiplied by 100 to give the % values in the table.

5.2.5 Tensile testing

5.2.5.1 Unaged model textiles

10 mm wide strips of cotton and silk textiles and 11 fibres wide strips of abaca (all 70 – 100 mm long) were tested using an Instron 4411 tensile tester with 500 N static load cell and Series IX software. The warp direction of the cotton and abaca, and the weft direction of the silk were tested. The strips had been conditioned to approximately 21°C and 50% RH overnight before testing. Between eight and ten strips were analysed per sample (as sample size allowed) using a 50 mm gauge length and 10 mm min⁻¹ extension speed as used by Garside, Wyeth and Zhang (Garside, Wyeth and Zhang 2010a). The samples were placed centrally, vertically, and slightly slack in the clamps. Wool was not tested because the strength of the material caused the strips to slip from the jaws when extended under these conditions. Yarn testing would be more suitable but was not possible in the timeframe of the project.

5.2.5.2 Aged model textiles

Assessing the effect of dye formulation 1 (c1/p1) on the cotton, abaca, wool, and silk model textiles

The same method was employed as in Section 5.2.5.1 for the unaged model textiles however Ac1 was too brittle and weak to be prepared without damage after 2 weeks of ageing at 80°C and 58% RH, and so has not been analysed beyond 2 weeks of ageing. Exponential trend lines were fitted to tensile testing data using MS Excel.

Assessing the effect of dye type on the cotton and silk model textiles

The dyed (c1, c2, c3, p1, p2, and p3) and undyed cotton (warp and weft) and silk (weft only) samples were assessed for breaking load and extension after 0, 14, 21, 28, and 35 (cotton) or 39 (silk) days of accelerated ageing (70°C and 65% RH). Since the samples of the same type originated from the same pre-cut pieces of model textile, it can be confidently assumed that the tensile properties of the unaged samples are comparable to those for the aged samples prior to ageing. The same equipment and method was employed as described in Section 5.2.5.1 except that six strips of each sample were tested following conditioning overnight to 54+/- 14% RH and 21+/-1°C and a 10 mm gauge length was used. The gauge length was chosen to support the tensile testing results in Chapter 10 (Treatment test 2). Exponential trend lines were fitted to tensile testing data using MS Excel.

5.2.6 Electron paramagnetic resonance analysis (EPR)

Electron paramagnetic resonance (EPR) was used to investigate the types and quantities of radicals and iron(III) present in a selection of aged and unaged model iron-tannate dyed samples. Undyed equivalents were analysed for comparison. Three yarns (5 cm long for silk, 2 cm long for cotton, and 1.5 cm long for wool and abaca) taken from randomly selected areas of each sample were wrapped around a quartz capillary tube and attached using PTFE tape. The samples occupied no more than 2.5 cm of the end of the capillary tube. The capillary tube and sample were placed inside a quartz EPR tube for analysis. This method enabled the rapid removal of the samples from the EPR tube and capillary tube without visible contamination of either tube as well as retention of the sample. It also provided information that was more representative of the whole sample in a time-efficient manner through the single analysis of three yarns rather than single or multiple analyses of single yarns.



Figure 5.2 Undyed and dyed (unaged and aged) cotton samples prepared for qualitative analysis (left) and a sample of dyed wool (pictured on the right with the components required for the preparation) prepared using the newly developed method for quantitative analysis

Continuous wave X-band (approximate microwave frequency 9.4 GHz) EPR spectra were obtained using a Bruker ELEXSYS E500 EPR spectrometer equipped with a Super High Q (SHQE) cylindrical EPR resonator. The experimental temperature of 10 K was maintained using liquid helium boil-off gas flow via an Oxford Instruments ESR900 helium flow cryostat and LT600 helium transfer line. The temperature was determined using a Cernox

5.2 Experimental techniques

sensor within the cryostat linked to an Oxford Instruments ITC503 temperature controller. For the detection of high spin iron signals, the microwave power was 0.5 M_w (milliwatts), the modulation amplitude was 5 G (gauss) and the sweep width was 4000 G. For the detection of radical signals the microwave power was 20 μW, the modulation amplitude was 1.5 G and the sweep width was 150 G.

Following analysis the model textile samples were weighed. Relative integrals of radicals and iron(III) ions were calculated using the following equation to enable inter-sample comparison:

$$\text{Relative integral of } y = \frac{\text{Peak area of } y}{\text{Peak area of } x} \times \frac{\text{Mass of } x}{\text{Mass of } y} \quad \text{Equation 5.2}$$

where ‘x’ is the sample with the highest peak out of the range of samples being compared and ‘y’ is the sample of interest. The peak areas refer to either the sum of the areas of all the iron(III) peaks (e.g. O_h and T_d/unbound peaks) or the radical peak areas in the spectrum and were calculated by the software. Calculation of the percentage of bound and unbound iron was calculated by assigning the sample in the data set with the greatest intensity of O_h bound iron(III) as having 100% bound iron to which all other samples were normalised. The iron(III) in this sample will not be 100% bound but nevertheless this assumption allows the comparison of the iron(III) coordination in different samples to be simplified. O_h bound iron(III) ions gave signals in the EPR spectrum at around g~8 and g~4.25. The latter being under the T_d bound iron(III) peak. Calculation of the total iron in these peaks, assuming that all iron at g = 4.26 is O_h iron, gave the quantity of O_h bound iron for comparison with the equivalent value in different samples. For a particular sample, the value calculated for the O_h was subtracted from the experimentally recorded signal for iron to give the proportion of unbound iron(III) ions. The quantity of O_h bound iron(III) was assumed to be consistent.

5.2.7 Scanning electron microscopy-energy dispersive X-ray (SEM-EDX) analysis

5.2.7.1 Cross-sections

Cross-sections of 1 cm × 0.5 cm pieces of model textile were embedded in resin (bisphenol A-epichlorohydrin) in sample pots that were evacuated to remove air bubbles from the resin and sample. Once dry the cross-sections were ground down to reveal the cross-section of the embedded textiles and cut down at the opposite end of the cross-section to a depth of 1 cm using a laith. The surfaces of the cross-sections containing the textile samples were initially polished using a 3 μm MD-MOL circular magnetic disc (attached to

5.2 Experimental techniques

a metal plate rotating at 250 rpm) with 3 μm diamond paste. The surfaces were finished by polishing with 1 μm MD-NAP disc and 1 μm diamond paste. Diamond paste was removed from the surfaces of the cross-sections by placing them in a beaker of warm soapy water in an ultrasonic machine for 2-3 minutes before further rinsing and drying.

Analysis of the cross-sections was undertaken using an Hitachi Ultra High Resolution S-4800 FE-SEM and an Hitachi VP-SEM S-3700N (30 Pa). The SEMs were operated at 20 kV and a 12 mm working distance for all analyses. Elemental analysis was conducted using an Oxford Instruments energy dispersive X-ray analyser with INCA software. EDX spectra were collected for varying lifetimes after optimisation of the iron peak versus total time taken for analysis: 200 s for abaca and silk; 200-300 s for cotton and 500-1000 s for wool. Dyed and undyed samples of the same material were analysed using the same conditions for comparison.

5.2.7.2 Model textiles

Unaged

Backscattered secondary electron (BSE) imaging of the surfaces of the p1/c1 dyed model textiles was undertaken using an Hitachi VP-SEM S-3700N (30 Pa) operated at 20 kV and an approximate 23 mm working distance. Images were taken of representative areas of each sample at $\times 50$, $\times 100$, $\times 150$, and $\times 650$ magnifications. Due to charging effects particularly on the abaca and wool samples, there are slight variations in the analysis conditions in order to produce the optimal image. EDX analysis of these samples was not undertaken.

Cc3 and Sp3 samples were analysed for surface deposits and, using EDX, for the elemental content of surface deposits. For this the Hitachi VP-SEM S-3700N (30 Pa) was used with an Oxford Instruments energy dispersive X-ray analyser and INCA software. The SEMs were operated at 20 kV and a 10.6-14.1 mm working distance (generally ~ 11 mm). EDX spectra were collected over 50 s. The data from these analyses are qualitative only due to the variation in working distance and lack of calibration method for these materials.

Aged

Similar conditions to those used to analyse the unaged model textiles were used to analyse the 4 week aged (80°C, 58% RH) Cc1, Ac1, Sp1, and Wp1 model textiles. Comparison between these analyses and those of the unaged equivalent model textiles was made to

5.2 Experimental techniques

determine if accelerated ageing had caused any consistently significant alterations to the surfaces of the textiles.

5.2.8 Gel permeation chromatography-multi-angle light scattering (GPC-MALLS)

GPC-MALLS was used to analyse both the aged and unaged cotton textiles. Carbonyl groups in 20-25 mg of disintegrated sample were fluorescence labelled using carbazole-9-carboxylic acid [2-(2-amiooxyethoxy)ethoxy]amide (CCOA) in a zinc acetate buffer solution (pH 4). The washed and dried labelled samples were then dissolved using *N,N*-dimethylacetamide/lithium chloride 0.9% (v/w) (DMAc/LiCl) and the resulting solution was diluted and filtered before being passed through the GPC column. In the column the cellulose molecules are separated by their hydrodynamic volume (the largest molecules are eluted first). A multi-angle laser light scattering detector (MALLS) in combination with a refractive index (RI) detector enable the calculation of the molecular weight of the molecules using the light scattering equation that is detailed in a review by Philip Wyatt (Wyatt 1993). The fluorescence detector also allows the calculation of oxidised groups in the molecules. Using this analytical set up which has been used in the analysis of paper and iron gall ink on paper (Rohrling, Potthast, Rosenau, Lange, Borgards, Sixta and Kosma 2002; Potthast, Rohrling, Rosenau, Borgards, Sixta and Kosma 2003; Henniges, Reibke, Banik, Huhsmann, Hahner, Prohaska and Potthast 2008), the average molecular weight (M_w and M_n), polydispersity index (PDI), and overall carbonyl content can be calculated. An approximation as to the number of carbonyl groups in a sample that have arisen from hydrolysis, i.e. reducing end groups (REGs) and oxidation can be calculated using Equations 4.3 and 4.4.

$$\text{REG} = 1000 (1/M_n) \quad \text{Equation 5.3}$$

where M_n is the number averaged molecular mass in kg/mol.

And,

$$\text{Oxidised groups} = \text{Overall carbonyl content} - \text{REG} \quad \text{Equation 5.4}$$

The number average degree of polymerisation (DP_n) can be calculated by dividing the number average molecular weight (M_n) by the molecular mass of one anhydroglucose unit (0.162 kgmol^{-1}).

The total carbonyl content in the samples arises from reducing end groups of the cellulose and the oxidised groups along the polymer chain (Potthast, Henniges and Banik 2008).

5.2 Experimental techniques

Acid hydrolysis causes the REGs to increase at a rate of one per scission of the cellulose chain (Whitmore and Bogaard 1994). M_n is the number average molecular weight of cellulose which is calculated by dividing the total weight of the sample by the number of molecules. The number of molecules equals the number of reducing end groups (one per cellulose chain) and this number increases by one with each chain scission. The theoretical quantity of carbonyl groups that are reducing end groups ($\mu\text{mol/g}$) was calculated by the reciprocal of M_n (kg/mol) multiplied by 10^3 . This assumes that the M_n was correct (note that there is an expected standard deviation of 10% for M_n values), that none of the REGs have been oxidised to carboxylic acids, and that oxidation causes negligible chain scission (Potthast, Henniges and Banik 2008).

5.2.9 Accelerated ageing

5.2.9.1 Assessing the effect of dye formulation 1 (c1/p1) on the cotton, abaca, wool, and silk model textiles

Fabric samples (at least 10 cm by 15 cm) of undyed and c1 and p1 dyed model textiles were accelerated aged at 80°C and 58% RH for 1, 2, 3, and 4 weeks using a Sanyo Gallenkamp Environmental Chamber (reference 8291) at The National Gallery, London. The samples were arranged into two stacks, one for dyed samples and one for undyed samples. Within the stacks the samples were organised in the following order on the perforated metal shelf: abaca (on the metal shelf), cotton, silk, and wool (top of the pile). The stacks were moved around the shelf during the ageing to minimise any location-dependent variations in environmental conditions but the order of the stacks was not rotated.

5.2.9.2 Assessing the effect of dye type on the cotton and silk model textiles

Samples of CU, Cc1, Cc2, Cc3, SU, Sp1, Sp2, and Sp3 were prepared for accelerated ageing as below and exposed to 70°C and 65% RH for up to 39 days. Six samples of silk (approximately 15 cm x 13-16 cm) were prepared per model textile from one 30 cm x 47 cm piece, each sample being incorporated into a separate stack. Twelve samples of cotton (approximately 15 cm x 13-16 cm) were prepared per model textile from two 30 cm x 43 cm pieces. Two pieces were prepared so that tensile testing of the warp and weft could occur on individual samples. The silk and cotton model textiles were stacked separately and undyed textiles were included in the stacks with dyed materials but were separated from the dyed materials by two pieces of paper (Munktell CXD pHoton Aqua Forte High Wet Strength absorbent paper, 90gsm). Two pieces of paper were placed at the bottom and

5.2 Experimental techniques

top of the stacks and the differently dyed textiles were separated by single pieces of paper. Cotton tying tape was used to loosely keep the stack together. Pencil notations of dye type were put on the bottom right corner of the papers on which the samples lay. The top paper of the stack was noted in pencil as C0, C1, C2 and so on until C5 for cotton and S0 to S5 for silk. From the bottom to the top the sample order was: c3 or p3, c2 or p2, c1 or p1, U and for the cotton samples piece A was placed on top of piece B. The warp direction on each sample was marked with an arrow using a biro and all samples were aligned in the stack so that the warp ran from front to back of the stack.

The dimensions of the stacks required their placement over two shelves in a WK3-180/40 environmental chamber at Camberwell College of Arts. Only five of the six stacks per textile type were aged. One stack of each textile type was retained unaged for tensile testing. The shelves were positioned within the central third of the chamber and stacks 1 and 2 were placed on the higher shelf, while stacks 3-5 were placed on the lower shelf. The chamber had recently been calibrated and was reported to have shown even temperature distribution throughout the chamber. Silk stacks were placed directly on the shelves with the equivalent cotton stacks on top of them. 70°C and 65% RH conditions were chosen to cause a slightly slower rate of degradation than that produced by the usual conditions used in this project (80°C and 65% RH). A slower rate of degradation might enable greater information to be obtained from the cotton samples than is usually obtained, since the majority of strength loss is seen within the first week of ageing. Additionally these conditions were used in Treatment Test 2 (Chapter 10). Due to a malfunction in the environmental chamber samples aged longer than 39 days were not obtained but had been planned. The malfunction required that the chamber be turned off. The remaining cotton stack and remaining two silk stacks remained in the chamber for 3 weeks and 2 days before removal and were damp on removal, having been exposed to humidity but not elevated temperature. The 39 day aged silk was the only sample analysed that had been in the chamber following the malfunction. The two other stacks (one of cotton and one of silk) were not analysed as they were not aged longer than the other samples.

5.3 Characterisation of unaged model textiles - Results and discussion

5.3.1 *Effect of dye application on the structure of the textiles*

SEM was used to observe the surface of the undyed model materials and those dyed with p1/c1 with a view to establishing any surface damage or deposits.

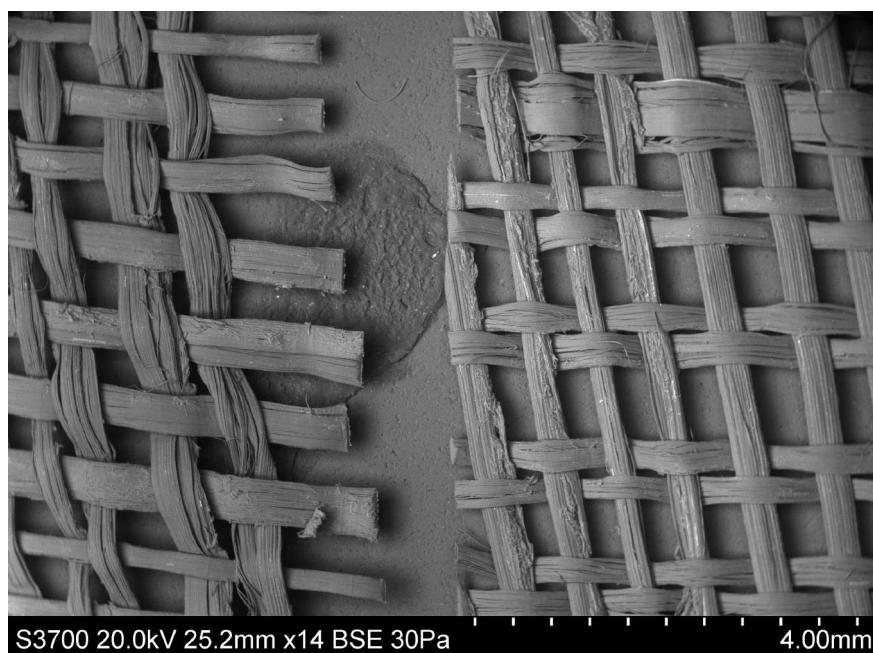


Figure 5.3 BSE SEM micrograph comparing Ac1 (left) and AU (right) at $\times 14$ magnification

The BSE images clearly showed the use of knotting of abaca fibre bundles to make long yarns for the weaving of the textile. Dyeing caused the abaca fibre bundles to separate and widen, decreasing the gaps between them, and caused longitudinal splitting of some of the fibre bundles (Figures 5.2 and 5.3). Surface contaminants such as that seen in Figure 5.4 (B – dyed) remained throughout the dyeing process.

Dyeing caused the cotton fibres to move within the yarn, making the gaps in the weave smaller (Figure 5.5). Fibres on the surface of the Cc1 sample appeared flatter than those on the surface of the CU samples. Defibrillation has also occurred in some dyed fibres. Using EDX on Cc3 (Figure 5.6) iron was detected in areas of the fibres without particles as well as in some of the surface particles. A calcium-rich surface deposit was also identified.

The tight weave of the silk was slightly loosened after dyeing with p1 (Figure 5.7). The yarn surfaces were severely abraded during the dyeing process and have resulted in the splitting of yarns. Using EDX on Sp3 (Figure 5.8) iron was detected in both surface deposits and fibres. High levels of Al and S were identified in the surface deposits analysed and in one case high levels of Ca and K were also present.

5.3 Characterisation of unaged model textiles – Results and discussion

Dyeing the wool caused the fibres to become entangled (felting) to such an extent that the weave was barely discernable (Figures 5.7 and 5.8). The surface scales of the individual fibres appear in similar condition after dyeing.

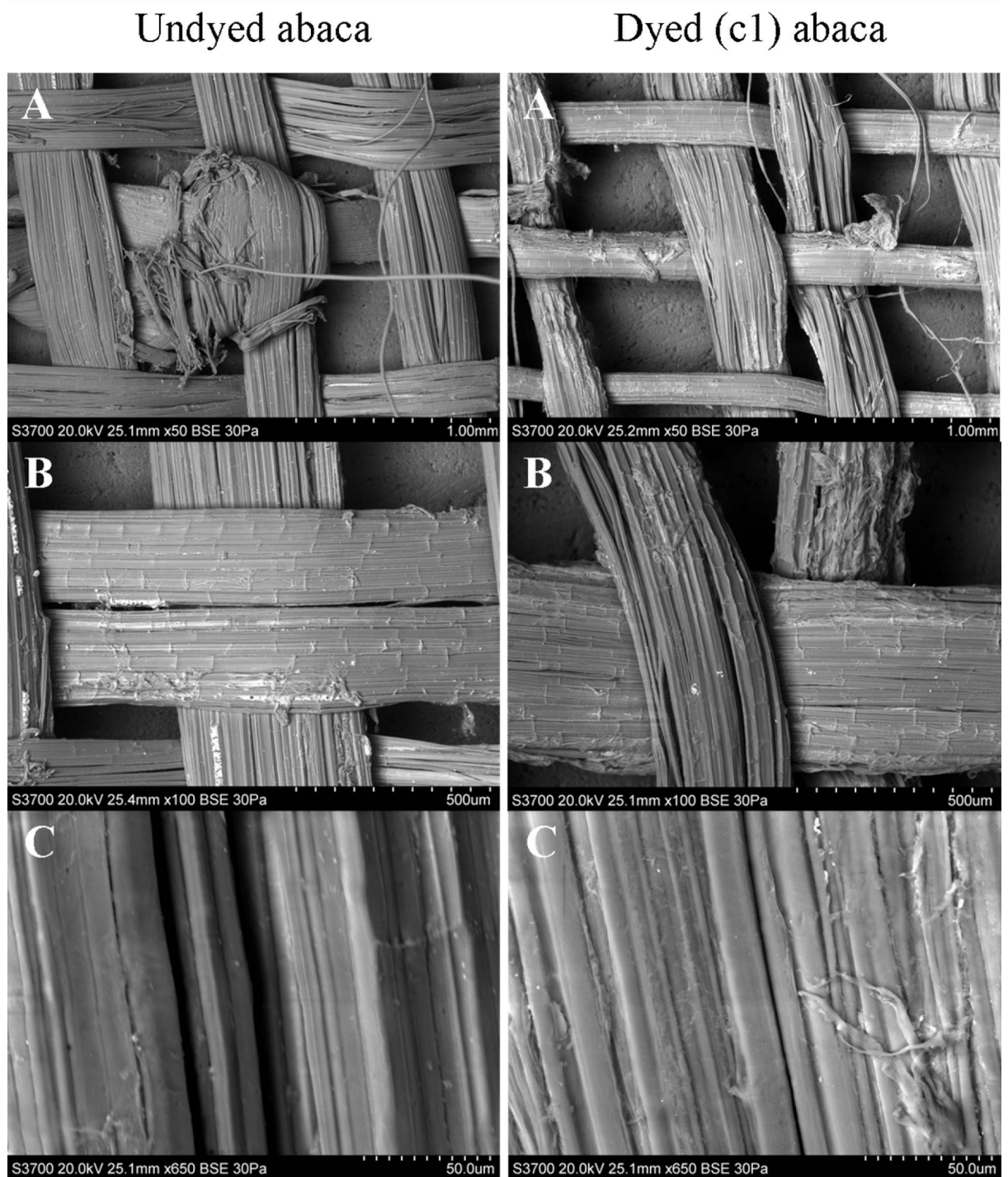


Figure 5.4 BSE SEM micrographs of undyed (left) and c1 dyed (right) abaca at $\times 50$, $\times 100$, and $\times 650$ magnifications

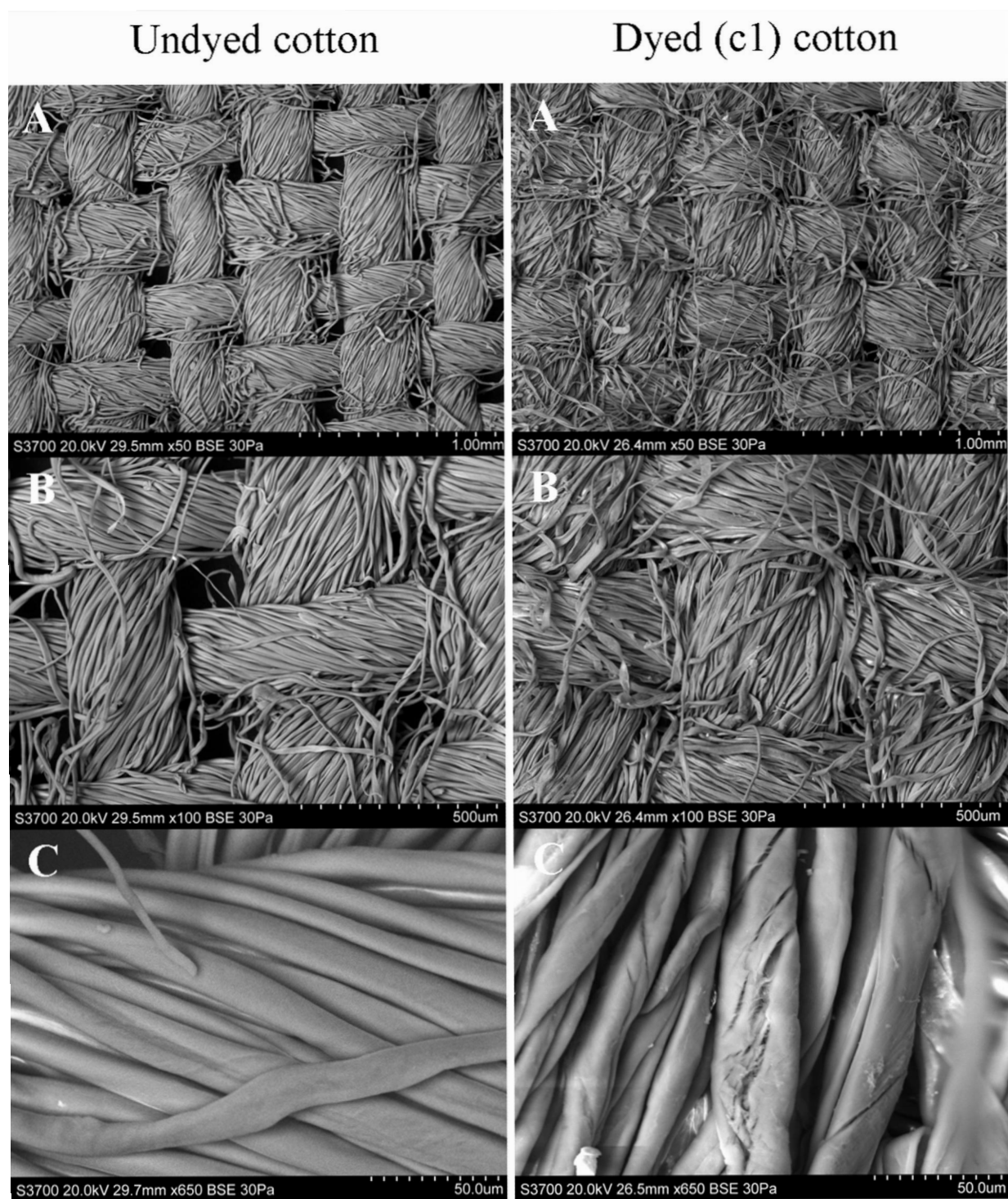


Figure 5.5 BSE SEM micrographs of undyed (left) and c1 dyed (right) cotton at $\times 50$, $\times 100$, and $\times 650$ magnifications

5.3 Characterisation of unaged model textiles – Results and discussion

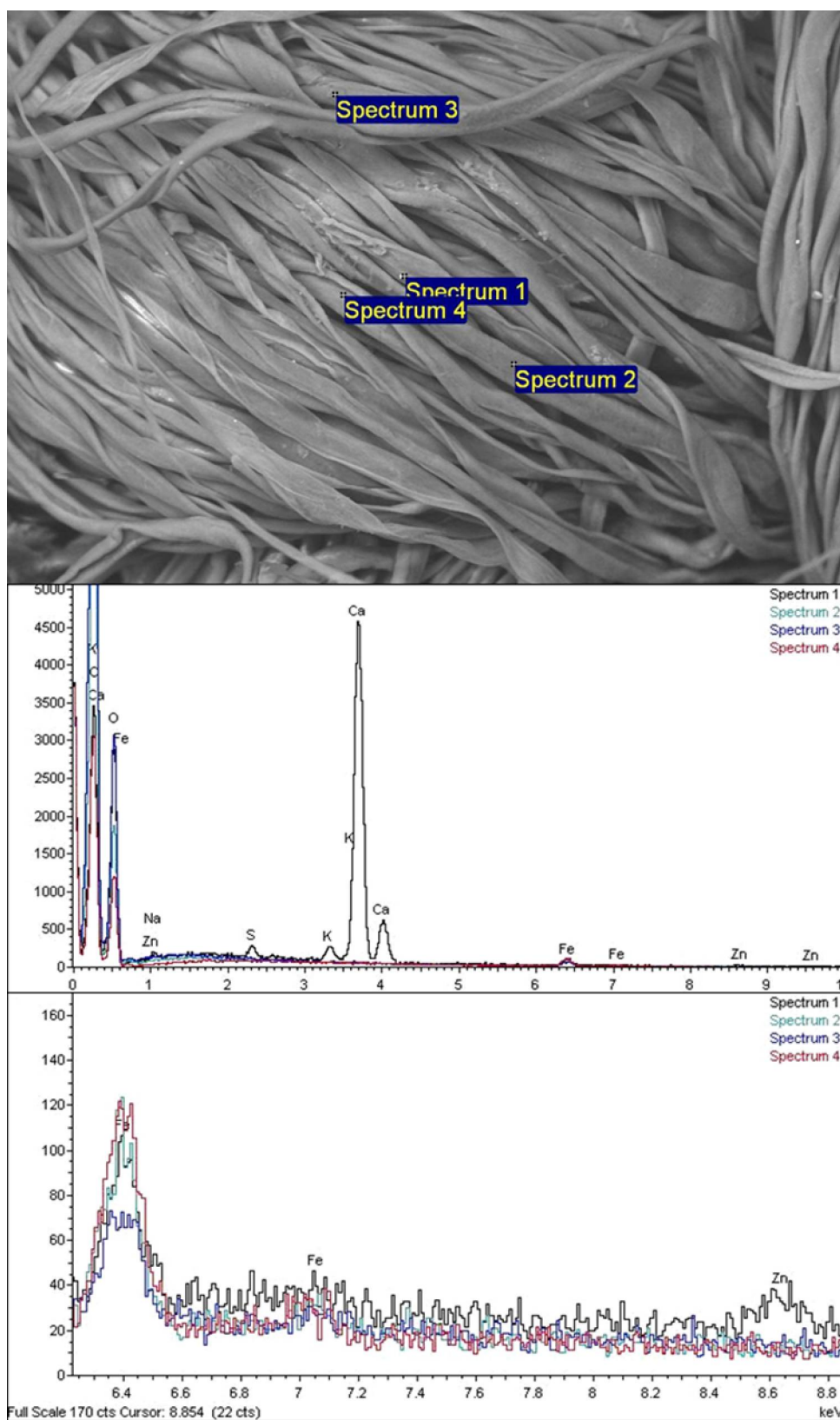


Figure 5.6 SEM micrograph and EDX spectrum of unaged Cc3 at $\times 250$ magnification and close up of the iron signal

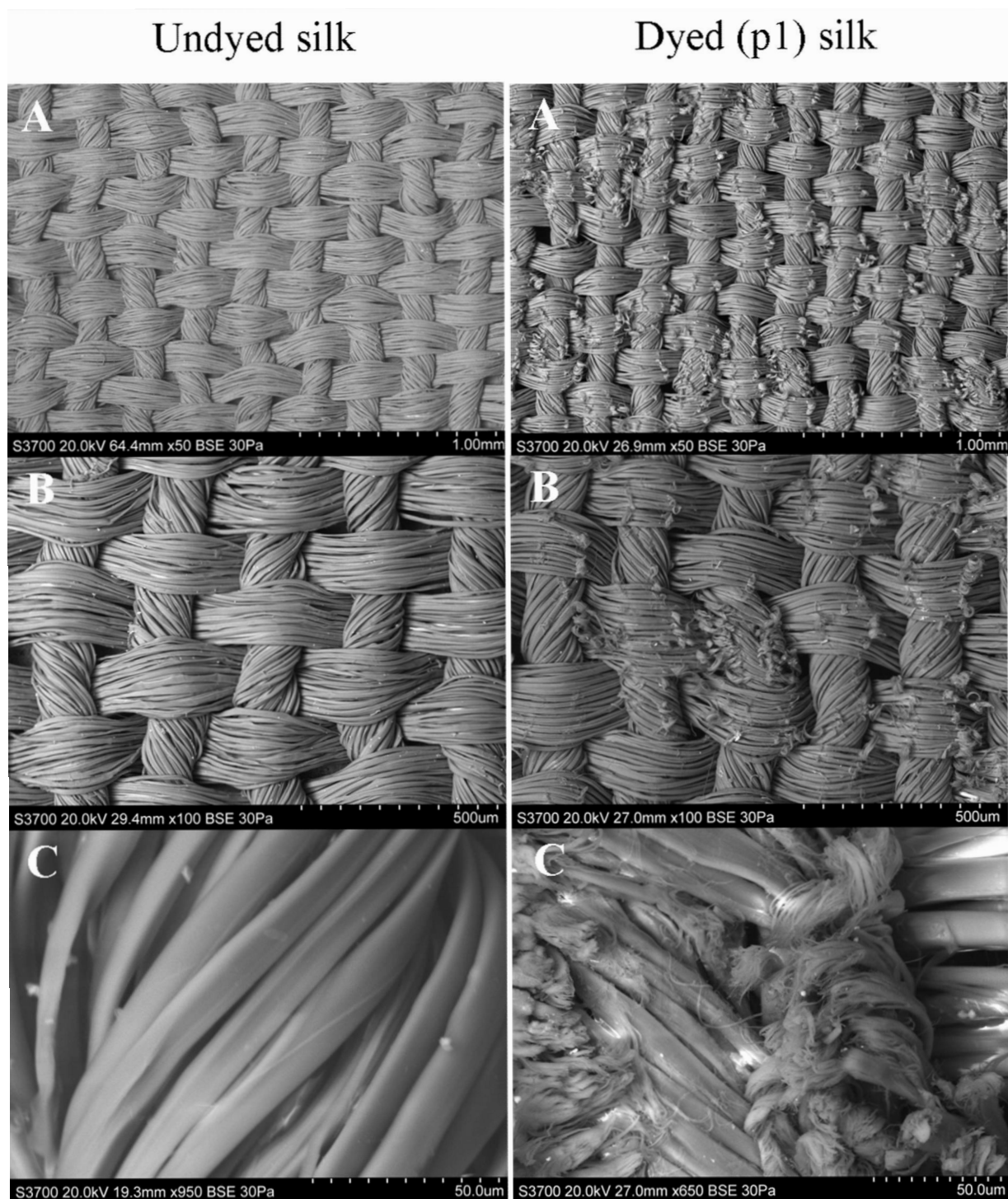


Figure 5.7 BSE SEM micrographs of undyed (left) and p1 dyed (right) silk at $\times 50$, $\times 100$, and $\times 950$ or $\times 650$ magnifications

5.3 Characterisation of unaged model textiles – Results and discussion

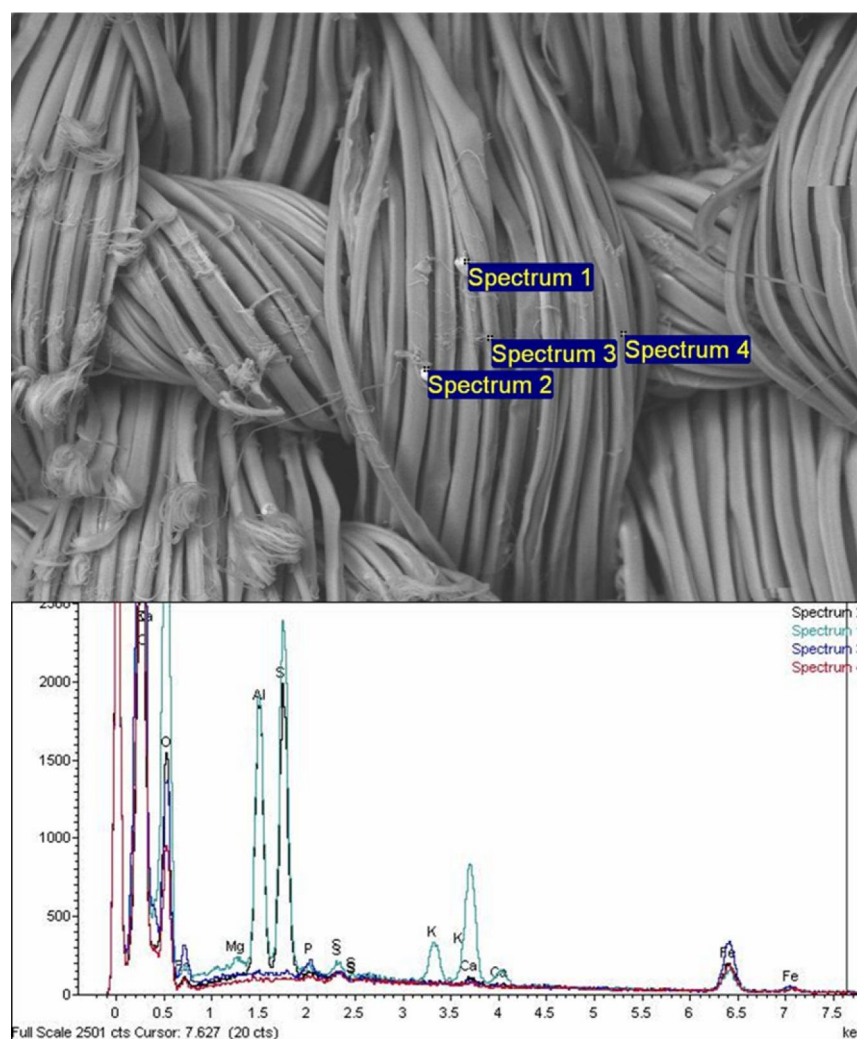


Figure 5.8 SEM micrograph and EDX spectrum of unaged Sp3 at ×250 magnification

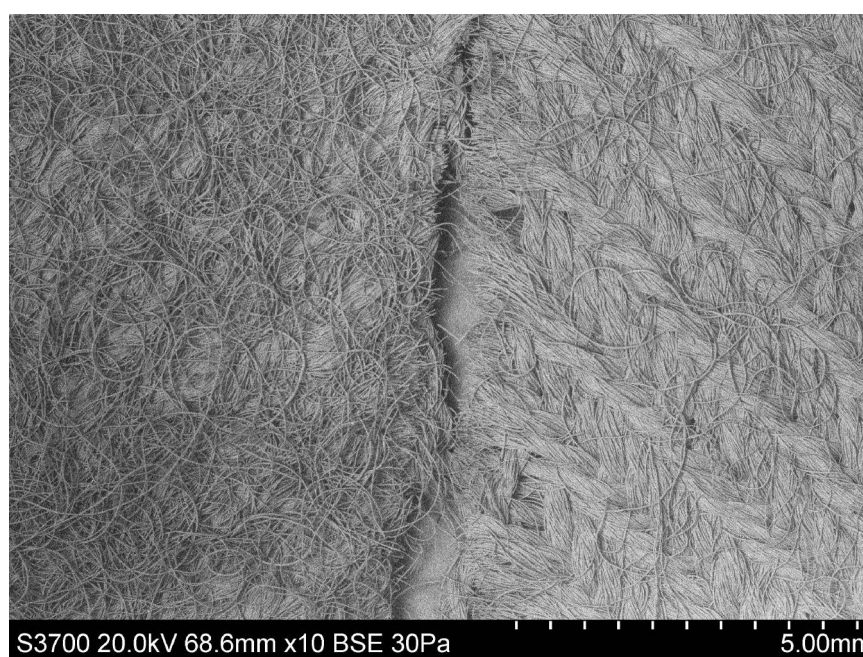


Figure 5.9 BSE SEM micrograph comparing Wp1 (left) and WU (right) at ×10 magnification

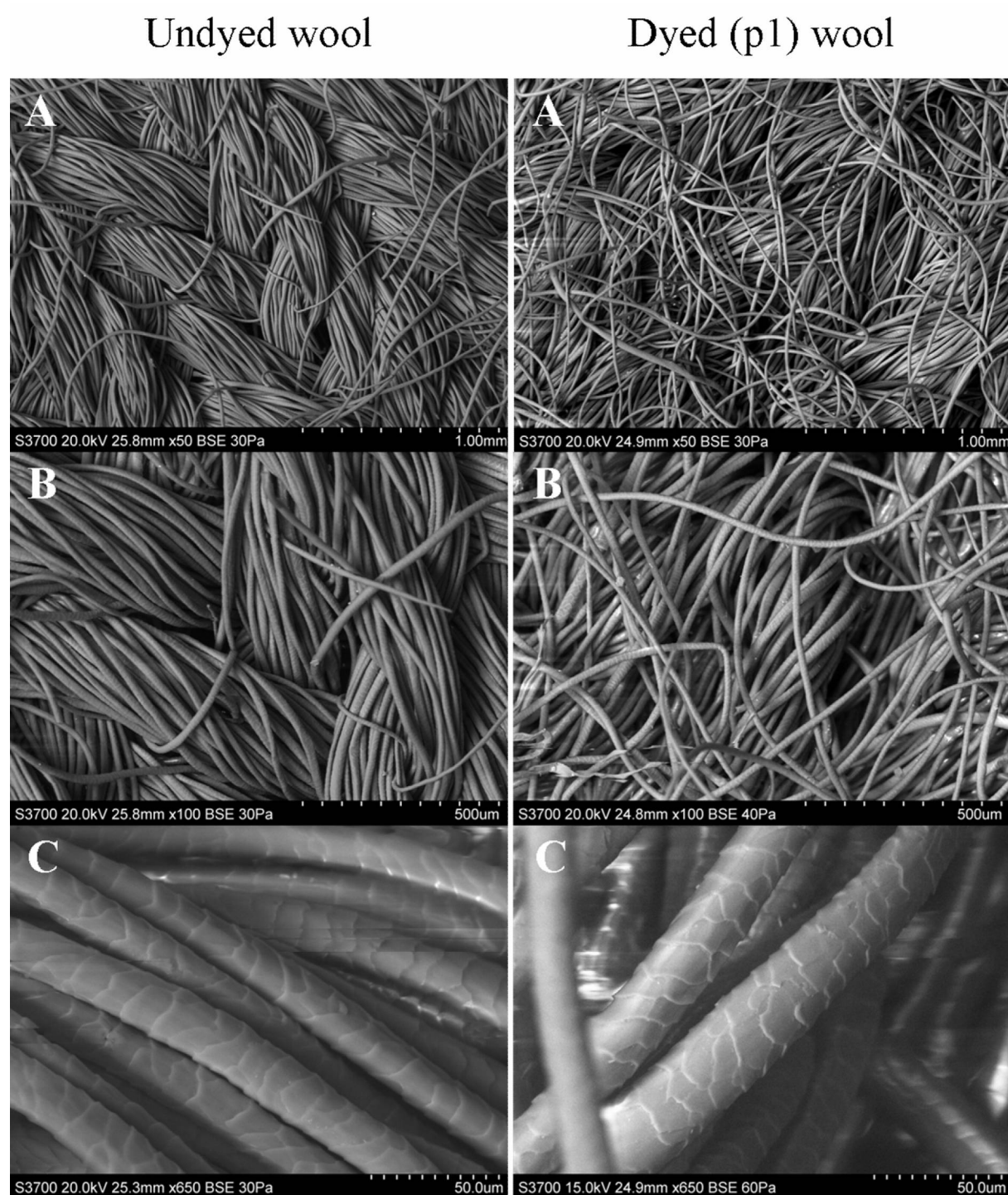


Figure 5.10 BSE SEM micrographs of undyed (left) and p1 dyed (right) wool at $\times 50$, $\times 100$, and $\times 650$ magnifications

5.3.2 *Extent of dyeing into the textile fibres*

The high reactivity of the hydroxyl radicals formed during metal-catalysed oxidation means that the most oxidative damage to a fibre will occur close to the location of hydroxyl radical formation, i.e. the metal ions. Consequently, SEM-EDX was used to

5.3 Characterisation of unaged model textiles – Results and discussion

analyse cross-sections of a range of dyed (c1 and p1) and undyed model textiles to determine the location of metal ions throughout the cross-section.

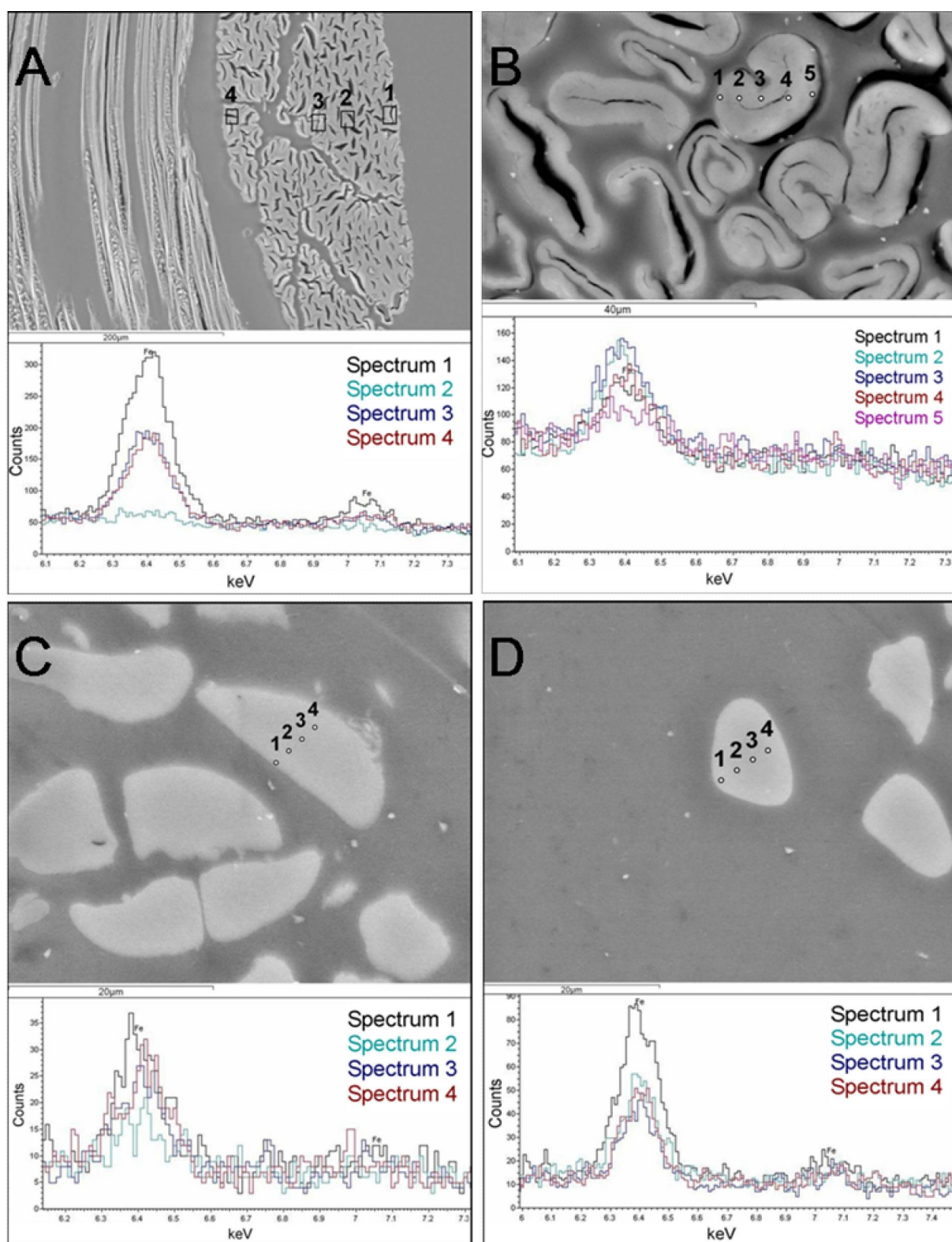


Figure 5.11 SEM micrographs and EDX spectra of a dyed abaca (A), cotton (B), and silk (C and D) fibres in cross-section. The dyed silk fibres in C are from the interior of the yarn while those in D are on the crown of the weave

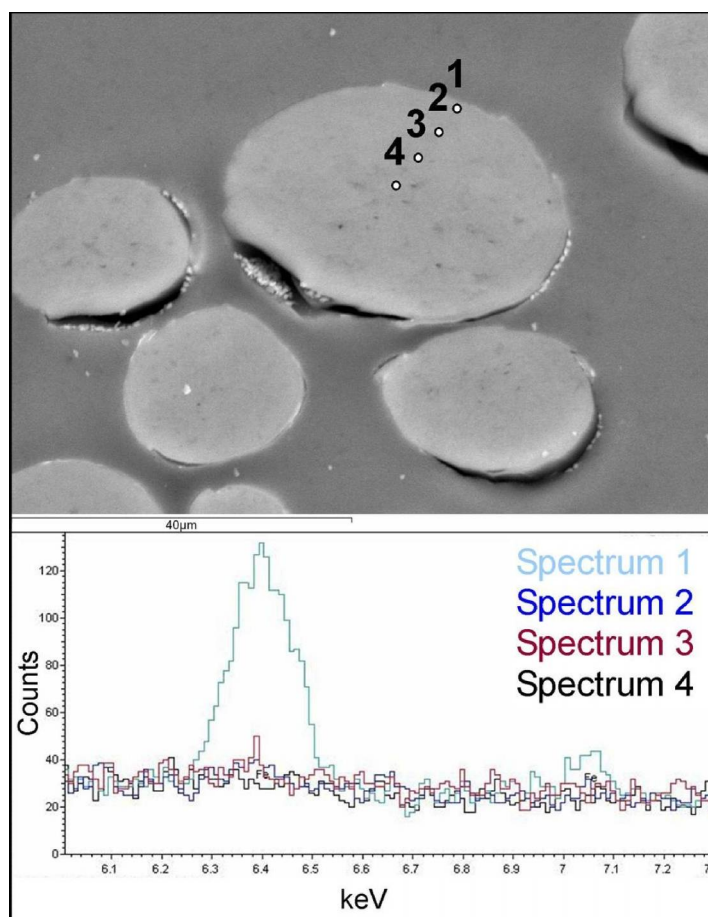


Figure 5.12 SEM micrograph and EDX spectrum of a dyed wool fibre near the crown of the weave

It was determined that detectable levels of iron were present in all the dyed model textiles tested but in none of the undyed.

As can be seen in Figure 5.11 the fibre bundles/yarns of the cotton, abaca, and silk are made up of individual fibres. SEM-EDX analysis was undertaken across the fibre bundles/yarns and individual fibres of those fibre bundles/yarns. For the individual fibres of dyed abaca, cotton, and silk, iron was easily detected on the edge and in the interior of each fibre. An iron concentration gradient decreasing from the edge to the interior of a fibre was often seen and its intensity could depend on the fibre's location within the fibre bundle/yarn. This variation of iron content with location within the fibre bundle/yarn correlates well with variation in accessibility of different parts of a fibre bundle/yarn to the dye. The more accessible an area is e.g. due to being on the surface of the fibre bundle/yarn or due to the presence of a crack into the fibre bundle/yarn (Figure 5.11A), the greater the iron content detected. In contrast, the iron in the wool fibres was primarily located on the outer surface of the fibres (cuticle) with minimal or no iron detected inside the fibres

5.3 Characterisation of unaged model textiles – Results and discussion

(cortex), Figure 5.12. This can be attributed to the highly cross-linked hydrophobic cuticle layer in the wool fibres that restricts the diffusion of water-based dye into the fibre cortex (Simpson 2002). This cuticle layer is not present in silk or the cellulosic textiles, thus explaining why these textiles contain iron throughout the fibres. The use of a higher temperature during dyeing, such as the 90-100°C usually used for wool dyeing rather than the 55°C used in these dye formulations, may improve dye diffusion into the wool fibres. However, 55°C was selected for use for the proteinaceous dyeings in this project in order to minimise thermal damage to the simultaneously dyed silk.

Some of the iron ions detected by SEM-EDX will be unbound/uncomplexed and catalytic. The small size of the ions suggest that, if not located close to bound iron (dye complexes), the unbound ions will be located further into the fibres. Consequently, unbound ions will be present throughout the cotton, abaca, and silk fibres but only in the cuticle of wool fibres. This correlates well with the strength loss seen in the accelerated ageing studies. Accelerated degradation throughout the cotton, abaca and silk fibres caused severe strength loss while wool suffered accelerated degradation in the cuticle only, thus retaining much of its strength.

5.3.3 Homogeneity testing

5.3.3.1 XRF

Variations in overall metal ion content in the model textiles could cause variations in rates of metal-catalysed degradation, particularly if some of the metal ions are unbound. Consequently XRF was used to identify the homogeneity of metal ion distribution throughout the model textiles through the calculation of standard deviation and coefficient of variation of iron and copper content (Table 5.4).

5.3 Characterisation of unaged model textiles – Results and discussion

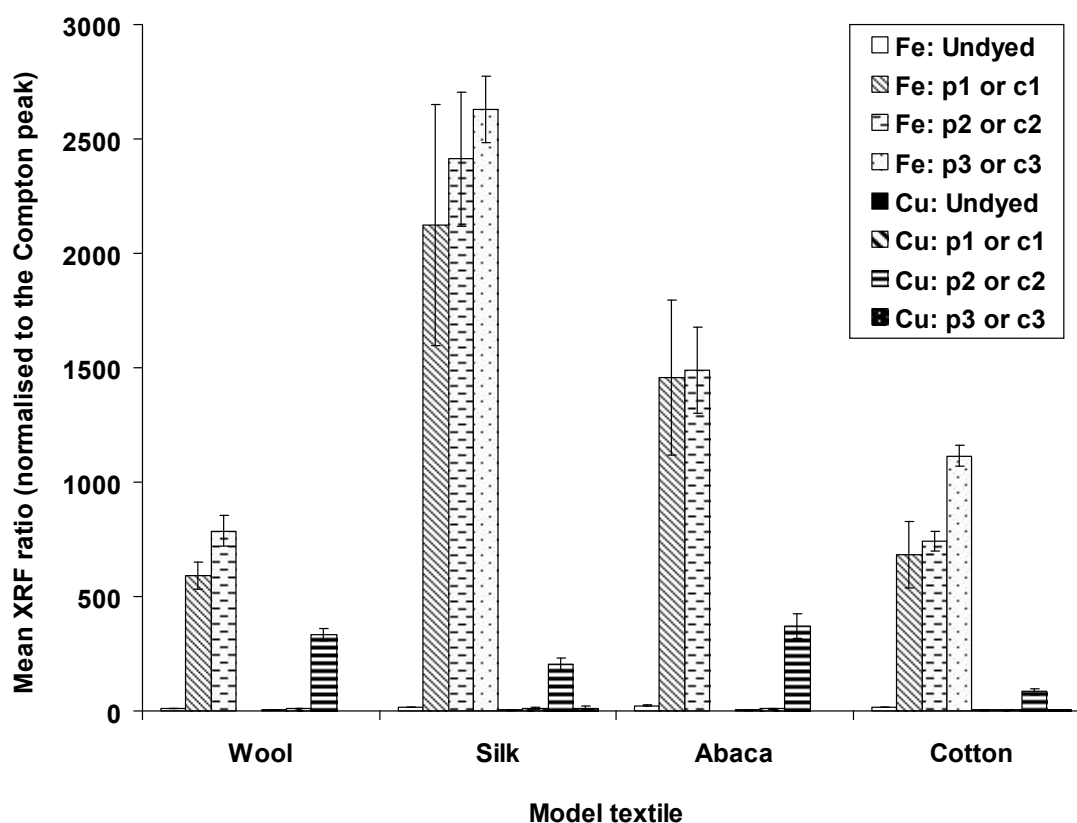


Figure 5.13 The iron and copper content of dyed model textiles as determined using XRF

Table 5.4 The effect of dye application on the iron and copper content of the model textiles as determined using XRF and bathophenanthroline test papers

Model textile ^a	XRF ^b (elemental ratios)		Correlation to colour chart ^d	
	Fe	Cu	Unbound Fe ²⁺	Total unbound iron ^d
WU	12 (1) ^c	5 (1) ^c	0	0
Wp1	590 (60)	11 (1)	0	0
Wp2	786 (68)	333 (27)	0	0
SU	17 (2)	4 (1)	ND ^e	ND ^e
Sp1	2124 (526)	9 (5)	0	0
Sp2	2413 (292)	204 (26)	0	0
Sp3	2628 (145)	11 (10)	0	0
AU	24 (5)	4 (3)	0	0
Ac1	1459 (338)	9 (2)	10	25
Ac2	1490 (190)	371 (53)	1	10
CU	15 (1)	3 (1)	0	0
Cc1	683 (145)	5 (3)	10	10
Cc2	742 (41)	83 (11)	0	10
Cc3	1115 (44)	3 (3)	10	10

Notes for Table 5.4:

- See Table 5.2;
- Iron and copper content ratios (net elemental peak area: net Compton peak area) multiplied by 1000;
- Standard deviations of mean data are in parentheses;
- Colour chart for the response of bathophenanthroline test paper to unbound ferrous ions devised by Vuori and Tse (Vuori and Tse 2005a);

5.3 Characterisation of unaged model textiles – Results and discussion

- e. Determined by using 1% ascorbic acid to reduce unbound ferric ions to detectable ferrous ions;
- f. Not done.

All dye formulations introduced significant quantities of iron and copper (p2 and c2 only) ions into the textiles (Table 5.4 and Figure 5.13). The differences in iron content between c1/p1, c2/p2, and p3 dyed textiles are statistically insignificant. However, c3-dyed cotton resulted in a statistically significant higher level of iron in the textile than occurred with the other dye formulations. It is possible that this was due to a greater quantity of tannic acid and gallic acid being present in the gall powder extract than in the Chinese gall and sumach tannic acids used in c1, c2, p1, and p2. The exact quantity of tannic acid in the gall powder was unknown but it was assumed to be lower than that in an equal mass of purified tannic acid, and so a quantity of gall powder that was approximately double the mass of the tannic acid used in the other dyes, and proportional to the mass of the textiles in c3 and p3 was used. Dye formulation 3 also achieved the most uniform metal ion distribution (a maximum of 6% variation from the mean). This was below the 10% variation in iron content that was achieved in model iron gall ink on paper samples that were viewed as being reasonably uniform (Kolar, Strlic and Pihlar 2006). To make these samples, paper had been immersed in iron gall ink and dried between felts. The least uniform metal ion distribution in the model textiles was achieved using dye formulation 1 (a maximum of 25% variation from the mean). These variations in iron content may have been caused by the production method, particularly the efficacy of post-dyeing rinsing.

5.3.3.2 Bathophenanthroline testing

While XRF detects total iron content, bathophenanthroline test paper detects only unbound ferrous ions. Through the reduction of unbound ferric ions to unbound ferrous ions the total unbound iron content can be indicated. However, due to the many areas for variation in method (Neevel 2009) and the limited colour categories to compare samples with in the colour chart produced by Vuori and Tse (Vuori and Tse 2005a), the use of bathophenanthroline paper is qualitative only and inter-sample comparison is unreliable. As expected, no unbound iron ions were detected on the undyed materials. However, no unbound iron ions were detected on the dyed proteinaceous materials either. The inability of the bathophenanthroline test at identifying the presence of iron ions in proteinaceous materials has already been recognised (Vuori and Tse 2005a). Unbound ferrous ions and in some cases ferric ions (after reduction to ferrous ions) were detected in the cellulosic dyed textiles. The colour chart devised by Vuori and Tse enabled the categorisation of unbound

5.3 Characterisation of unaged model textiles – Results and discussion

ferrous and total iron content (ferrous and ferric) in ppm as noted in Table 5.4 but the large range of each category makes this test unsuitable for rigorous inter-sample comparison. Many of the cellulosic dyed samples were at the 10 ppm level and while there were differences between samples categorised at the 10 level, these differences were not able to be noted with accuracy due to the lack of a comparative scale. Consequently, they were noted simply as 10 in the results table. The use of colorimetry to analyse the results may be of use but this will require the development of a calibrated scale such as that in the colour chart and the method may require the use of larger test pieces in order to provide complete coverage of the aperture of the spectrophotometer.

In this study, ascorbic acid was used to reduce ferric iron into the detectable ferrous iron. However, the acidity of the 1% ascorbic acid solution is such that it can destroy iron-tannate dye complexes, releasing the iron that was previously complexed. This can give an unclear reading as to the quantity of unbound ferric iron and so it has been recommended that a neutral reducing agent such as sodium dithionite be used instead of 1% ascorbic acid solution (Neevel 2009).

The bathophenanthroline test papers are detecting the unbound iron ions that remain after the post-dyeing rinsing. Since the majority of the soluble unbound metal ions will have been removed in the post-dyeing rinsing, it follows that the majority of iron present in the dyed model textiles is bound either in iron-tannate complexes or directly to the fibre. The iron-tannate complex can be either physically bonded to the fibres via van der Waals' forces (Hearle and Peters 1963; Christie 2001; Frazier, Deaville, Green, Stringano, Willoughby, Plant and Mueller-Harvey 2010) or bonded via the mordant of the dye. In the cellulosic dye formulations tannic acid was applied first and therefore acts as the mordant. This will cause fibre/tannic acid/iron interactions to predominate (Bhattacharya and Shah 2000). In the proteinaceous dye formulations the iron ions (and copper ions in p2) were applied first and therefore act as the mordant. Thus, in the proteinaceous textiles fibre/iron/tannic acid interactions will predominate. Direct binding of iron and copper ions can occur with hydroxyl, carbonyl, and carboxyl groups in the cellulosic and proteinaceous fibres in addition to amine, amide, and thiol groups in the proteinaceous textiles (Hearle and Peters 1963; Fukatsu and Isa 1986; Christie 2001). The greater proportion of carboxyl-containing non-crystalline components, such as hemicellulose, in the abaca compared to cotton (Sun, Fang, Goodwin, Lawther and Bolton 1998; Hsieh 2007) explains why the dyed abaca textiles contain more metal ions than the simultaneously dyed cotton textiles.

5.3 Characterisation of unaged model textiles – Results and discussion

Copper ions bind more strongly than iron ions, particularly to thiols (Maclaren and Milligan 1981; Letelier, Lepe, Faundez, Salazar, Marin, Aracena and Speisky 2005; Letelier, Sanchez-Jofre, Peredo-Silva, Cortes-Troncoso and Aracena-Parks 2010) and as wool contains more thiols (Hearle and Peters 1963) in addition to aspartic acid and glutamic acid (Guthrie and Laurie 1968) than silk, wool p2 contains more copper than silk p2. Thiol content in the wool cuticle, where it is likely most of the dye exists, could be increased during the dyeing process through the hydrothermal breakdown of disulphide bonds (Maclaren and Milligan 1981). However, the silk dyed textiles contain more iron than the simultaneously dyed wool samples. This is likely to be due to the highly cross-linked and hydrophobic cuticle of the wool fibres which is not present on the silk fibres (Simpson 2002); this will inhibit diffusion of the iron-tannate dye into the core of the wool fibres, thus minimising uptake of the dye. In addition, silk has between 2 and 3 times more carboxylic acid groups than amino groups (Robson 1998) while wool has approximately equal quantities of each (Broadbent 2001), consequently silk has potentially more mordant binding sites.

Out of all of these, carboxylate anion groups ($-\text{COO}^-$) are the major binding sites in wool (Maclaren and Milligan 1981) and silk (Chen, Lu, Yao, Pan and Shen 2005). This is due to the isoelectric points of wool and silk which are approximately at pH 5.6 and 2.8, respectively (Timar-Balazsy and Eastop 1998) and the pH of the dyebaths for the model textiles ranged between pH 4 and 6. The isoelectric points of wool and silk are the pH values at which the proteins are electrically neutral, having equal quantities of positive (e.g. $-\text{NH}_3^+$) and negative (e.g. $-\text{COO}^-$) functional groups. In the pH range present in the dyebaths it is likely that the silk fibroin will be slightly negatively charged which will attract the metal cations. By co-ordinate bonds the metal ions can bind to un-ionised groups such as amines and hydroxyl groups while by ionic bonds the metal ions can bind to negatively charged groups such as carboxylate and sulphonate groups (Hartley 1968b; Hartley 1968c; Bird 1972). In the pH range present in the dyebaths it is likely that the wool will be either slightly positively charged due to groups such as protonated amines, which will repel the metal cations, or will be electrically neutral. In this case, the metal ions can bind to by co-ordinate bonds to un-ionised groups such as amine groups, and by ionic bonds to the ionised carboxyl groups. The majority or all of the carboxyl groups present in the wool will be ionised since the pH of dye baths are close to the isoelectric point of wool.

5.3 Characterisation of unaged model textiles – Results and discussion

Iron and copper ions can also bind to amine and carboxylic acid functionalities present in wool and silk; in the cuticle of wool these are present as iso-dipeptides. Silk contains 2 – 3 times more carboxylic acid groups than amino groups (Robson 1998) than wool though it contains fewer carboxylic acid and amino groups than wool (Broadbent 2001). However, this coupled with the lack of a hydrophobic cuticle, could explain the greater concentration of iron in the silk than in the wool. In addition, the variations seen could also be affected by differences in relative quantities of textiles during dyeing (while the length of the textiles being dyed was often similar, the mass was not), and variations in weave, thickness, and surface morphology of analysed textiles. Further detail on the binding of iron-tannate dye complexes, tannic acid, and metal ions to the fibres is discussed in Chapter 4.

5.3.2.3 Surface pH

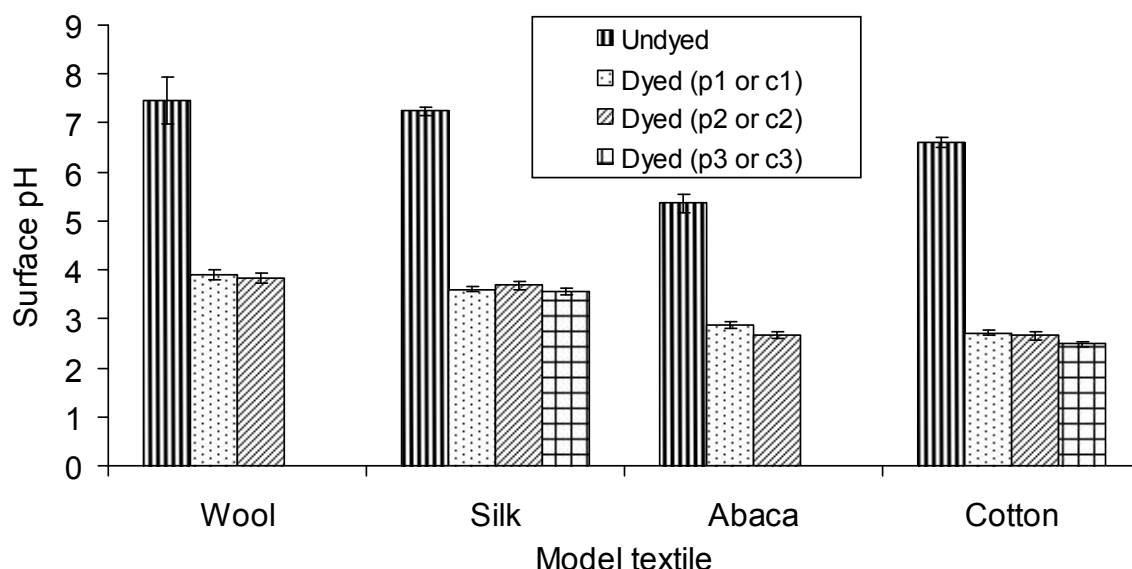


Figure 5.14 The effect of dyeings on the surface pH of the model textiles

The rate of acid hydrolysis of an organic material is highly dependent on its pH. For example, the rate of hydrolysis of cellulose in paper increases 10-fold for every single unit decrease in pH (Whitmore 2011). As discussed in Chapter 4 (Section 4.1.6), iron-tannate dyes are highly acidic and so it follows that the application of iron-tannate dyes to textiles can cause a significant decrease in the pH of the textiles and consequently accelerates the rate of acid hydrolysis. The dyed model textiles (pH 2.65 – 3.91) were between ~2.5 and ~4 pH units lower than the undyed equivalents (pH 5.36 – 7.46) (Table 5.5 and Figure 5.14). There was no significant difference between the pH of samples of the same textile type that had been dyed with the different dye formulations. Simultaneously dyed textiles,

5.3 Characterisation of unaged model textiles – Results and discussion

for example, abaca and cotton in the c1 dyebaths and silk and wool in the p1 dyebaths, resulted in comparable surface pH despite being of different pH before dyeing, e.g. Ac1, Ac2 compared with Cc1, Cc2, respectively. The surface pH of the textiles was found to be relatively uniform with the largest variation in surface pH being +/- 6.52% (WU) and the least being +/-1.28% (SU).

Table 5.5 The effect of dye application on the breaking load, extension, and surface pH of the model textiles

Model textile ^a	Breaking load (N)			Extension (%)			Surface pH		
	Mean	SD	C.V.	Mean	SD	C.V.	Mean	SD	C.V.
WU	ND ^b	ND	ND	ND	ND	ND	7.5	0.5	6.5
Wp1	ND	ND	ND	ND	ND	ND	3.9	0.1	2.5
Wp2	ND	ND	ND	ND	ND	ND	3.8	0.1	2.8
SU	70.2	4.9	6.9	28.2	1.7	6.1	7.2	0.1	1.3
Sp1	62.9	4.9	7.8	25.0	2.6	10.6	3.6	0.1	1.7
Sp2	56.4	2.5	4.5	22.9	1.7	7.6	3.7	0.1	2.3
Sp3	55.3	3.8	6.9	22.6	1.6	7.3	3.6	0.1	1.8
AU	239.9	43.1	18.0	3.9	0.5	13.0	5.4	0.2	3.4
Ac1	105.9	18.3	17.3	2.1	0.3	16.2	2.9	0.1	2.4
Ac2	130.1	24.8	19.0	2.5	0.5	19.2	2.7	0.1	3.0
CU	73.2	7.7	10.5	10.5	1.1	10.7	6.6	0.1	1.6
Cc1	68.3	5.3	7.7	6.9	0.7	10.5	2.7	0.1	2.3
Cc2	51.0	4.8	9.5	9.2	1.3	13.9	2.7	0.1	2.8
Cc3	45.7	8.6	18.9	10.2	1.9	18.3	2.5	0.0	1.4

Note for Table 5.5:

- a. See Table 5.2;
- b. Not done.

This observed consistently large increase in acidity of the textiles due to dye application occurred despite post-dyeing rinsing in which it was intended that the majority if not all soluble acids and metal ions were removed from the model textiles. Only the acids (not weak acids) that are extractable, i.e. that are able to move to the pH electrode surface, are being measured by pH measurement (Smith 2011). Non-extractable acids such as carboxylic acids attached to cellulose (Smith 2011) and possibly also acidic groups in tannic acid or iron-tannate complexes that are bound to the fibres are not measured. Consequently, the increased acidity in the dyed textiles is likely to be due to remaining soluble acidic compounds in the textiles such as tannic acid and iron-tannate complexes that are not bound to fibres.

5.3.2.4 Tensile testing

Tensile testing of the model textiles before accelerated ageing is important for the evaluation of changes in textile strength and extensibility during accelerated ageing and also for understanding the effect of the dyeing procedure on the integrity of the textiles.

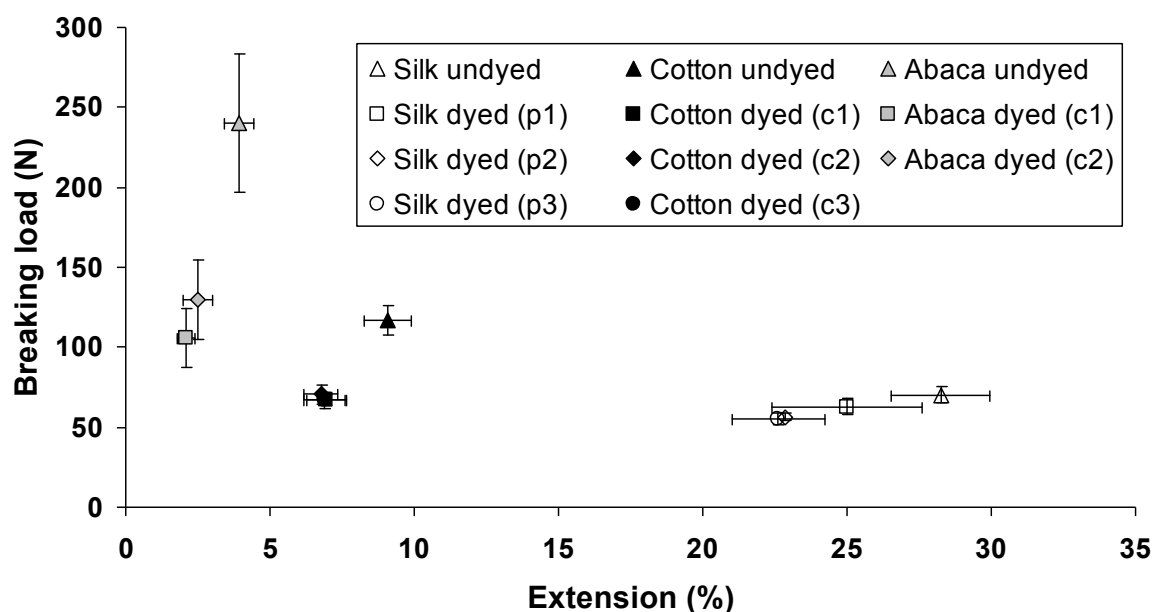


Figure 5.15 The effect of dyeing methodology on the strength and extensibility of the model textiles

Generally, the application of the dyes caused statistically significant weakening of the textile, even before any accelerated ageing had occurred (Figure 5.15 and Table 5.5). It has been postulated that the majority of strength loss seen in iron-tannate dyed textiles arises from the harsh dye application conditions and not subsequent accelerated degradation since sufficient washing of the dyed textiles would remove the water-soluble acid and metal ion catalysts from the textile (Hofenk de Graaff 2002). In this study, there was a significant decrease in breaking load of the p2, p3 dyed silk compared to the undyed silk. However, the difference between p1 and undyed was less clear. For abaca and cotton, application of all of the dyes resulted in a significant loss of strength and extensibility; the dyeing of abaca caused the greatest strength loss of all the model textiles. Wool was not tensile tested due to its strength since it slipped in the jaws of the tensile tester under the conditions used.

5.3.3.5 Colour measurement

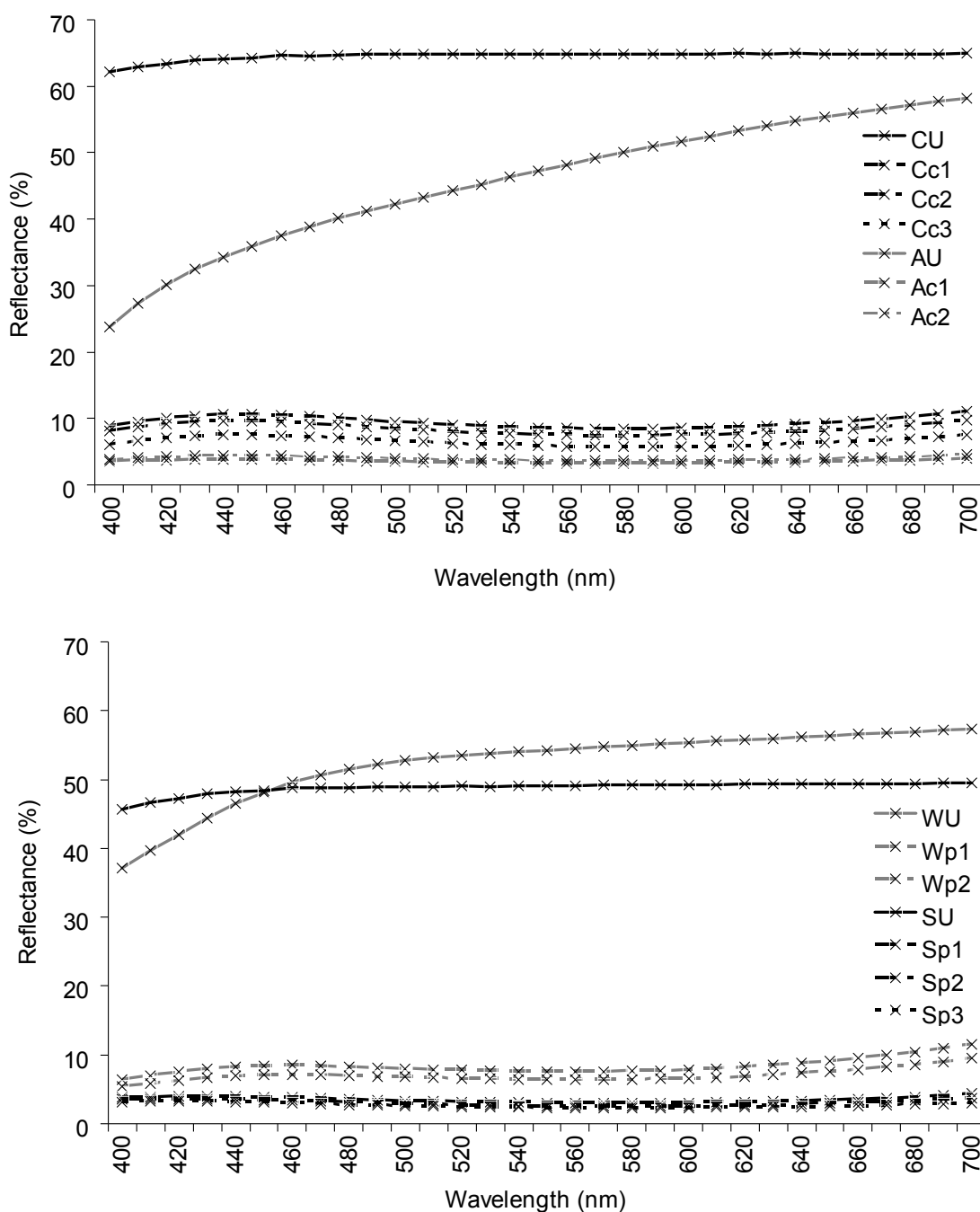


Figure 5.16 The effect of dye application on the reflectance spectra of the cellulosic (upper) and proteinaceous (lower) model textiles

The reflectance spectra in Figure 5.16 correlate well with those reported in a study on model iron gall ink documents (Sistach, Gibert and Areal 1999) and traditionally dyed New Zealand Flax (*Phormium tenax*) (Te Kanawa, Thomsen, Smith, Miller, Andary and Cardon 1999). They demonstrate the strong absorption of visible light, particularly in the 550-700 nm region, that is due primarily to the reversible light-induced charge-transfer in iron-tannate complexes (Krekel 1999). As can be seen in Table 5.6 the obvious change in

5.3 Characterisation of unaged model textiles – Results and discussion

colour due to dye application is primarily due to a large decrease in lightness ($-\Delta L^*$) in addition to small increases in typically, blueness ($-\Delta b^*$) and redness (Δa^*).

Table 5.6 The effect of dye application on the colour of the model textiles

Model textile	Colour measurement			Variation in colour throughout textile ^b (ΔE_{00}^*)	Change in colour due to dye application			
	L^*	a^*	b^*		ΔE_{00}^{*c}	ΔL^{*d}	Δa^{*d}	Δb^{*d}
WU	78.39 (0.39) ^a	-1.06 (0.04)	6.67 (0.24)	0.68	0.00	0.00 (0.78) ^e	0.00 (0.08)	0.00 (0.48)
Wp1	33.53 (1.03)	1.31 (0.04)	-1.11 (0.12)	1.68	42.52	-44.85 (1.42)	2.33 (0.08)	-7.70 (0.36)
Wp2	31.03 (0.79)	0.93 (0.07)	-1.05 (0.18)	1.30	45.84	-47.54 (1.18)	1.99 (0.11)	-7.59 (0.42)
SU	75.36 (0.36)	-0.20 (0.02)	0.97 (0.12)	0.58	0.00	0.00 (0.72)	0.00 (0.04)	0.00 (0.24)
Sp1	20.75 (0.37)	1.46 (0.03)	-3.90 (0.09)	0.55	54.5	-54.88 (0.73)	1.63 (0.05)	-4.97 (0.21)
Sp2	18.76 (0.30)	1.61 (0.03)	-4.37 (0.07)	0.44	55.68	-56.66 (0.66)	1.77 (0.05)	-5.31 (0.19)
Sp3	17.79 (0.20)	1.38 (0.03)	-4.09 (0.07)	0.31	56.38	-57.91 (0.56)	1.54 (0.05)	-5.20 (0.19)
AU	74.25 (1.66)	1.91 (0.41)	13.56 (1.09)	2.92	0.00	0.00 (3.32)	0.00 (0.82)	0.00 (2.18)
Ac1	21.66 (0.75)	0.56 (0.05)	-2.22 (0.12)	1.09	53.67	-52.84 (2.41)	-1.34 (0.46)	-15.91 (1.21)
Ac2	23.34 (0.83)	0.50 (0.04)	-2.65 (0.17)	1.24	52.54	-51.13 (2.49)	-1.42 (0.45)	-16.31 (1.26)
CU	84.31 (0.51)	-0.26 (0.02)	0.67 (0.09)	0.70	0.00	0.00 (1.02)	0.00 (0.04)	0.00 (0.18)
Cc1	35.7 (0.91)	0.70 (0.06)	-4.33 (0.15)	1.54	42.92	-48.57 (1.42)	0.91 (0.08)	-4.94 (0.24)
Cc2	33.58 (0.50)	0.80 (0.04)	-4.89 (0.12)	0.84	45.52	-50.71 (1.01)	1.00 (0.06)	-5.50 (0.21)
Cc3	29.61 (1.01)	0.57 (0.05)	-4.62 (0.13)	1.58	50.45	-54.69 (1.52)	0.77 (0.07)	-5.23 (0.22)

Notes for Table 5.6:

- Standard deviations of mean data are in parentheses;
- The colour difference (calculated using the CIE2000 colour difference formula) between the mean CIEL*a*b* values – the corresponding SD values and the mean CIEL*a*b* values + the corresponding SD values i.e. the 68.27% of the areas of each model textile analysed are within this ΔE_{00}^* of each other;
- Calculated using the CIE2000 colour difference formula;
- Calculated by subtracting the colour parameter of the undyed sample from that of the dyed sample;
- Standard deviations calculated by addition of the standard deviation of each value used in the calculation of the change in colour parameter. The SD for ΔE_{00}^* has not been calculated due to the complicated nature of the CIE2000 formula.

The colouration of the model textiles is increasingly homogenous (i.e. decreasing variation in colour throughout the textile) with decreasing ΔE_{00}^* (Column 4 of Table 5.6). As hoped, variations in colouration across the model textiles are generally low and imperceptible

5.3 Characterisation of unaged model textiles – Results and discussion

since ΔE_{00}^* is generally < 1.7 (Reissland and Cowan 2002). Only AU ($\Delta E_{00}^* = 2.92$) and Wp1 ($\Delta E_{00}^* = 1.68$) have a variation in colour that is perceptible being ≥ 1.7 . The high colour variation across AU will be noticeable by the majority of people as it is close to the value of 3 (Gilchrist and Nobbs 1999; Kolar, Strlic and Pihlar 2006). This is likely to be due in part to the loose weave of the textile and the high contrast between the pale coloured fibre bundles and black velvet on which it was measured (despite attempts to reduce this effect by measuring two layers of abaca textile at once). For the silk and abaca textiles the colour of the dyed textiles was more homogenous than the undyed. The dyed silk model textiles showed the least colour variation of all the model materials with all silk model textiles having a $\Delta E_{00}^* < 1$ and with Sp3 showing the least variation in colour of all of the model textiles ($\Delta E_{00}^* = 0.31$). Of the dyed cotton textiles, dye formulation 2 resulted in the most level dyeing with $\Delta E_{00}^* < 1$.

5.3.3.6 GPC-MALLS

Table 5.7 The effect of dye application on the average molecular weight and carbonyl content of cotton

Sample	DP _n	Average molecular weight			% polymer content in				Theoretical amount of reducing end groups (oxidised groups) (μmol/g)	Overall carbonyl content (μmol/g) ^a
		M _n ^a (kg/mol)	M _w ^a (kg/mol)	PDI	DP<100	DP100-200	DP200-2000	DP>2000		
CU	3164	513	1037	2	0	0	12	88	2 (2)	4
Cc1	1051	170	439	3	0	2	57	42	6 (15)	21
Cc2	1072	174	477	3	0	1	56	42	6 (18)	24
Cc3	902	146	486	3	1	2	57	40	7 (27)	34

Note for Table 5.7:

a. The standard deviation of the carbonyl content is $<5\%$, while that of M_w is $\sim 5\%$, and that of M_n is $\sim 10\%$. These are based on long-term analyses of standard pulps (Potthast, Henniges and Banik 2008).

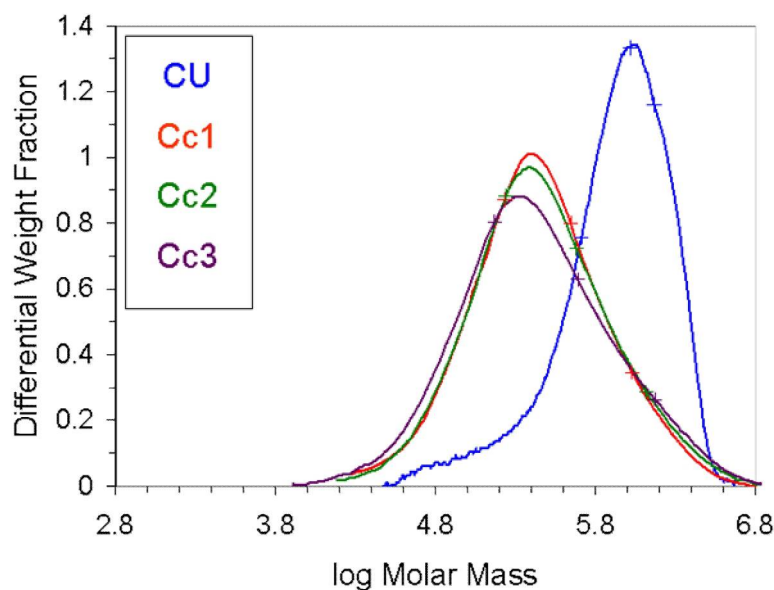


Figure 5.17 The effect of the application of different dye formulations on the molar mass distribution of the cotton substrate

The application of the iron-tannate dye formulations 1-3 caused a great decrease in the average molecular weight and DP_n of the cellulose in the cotton samples, an increase in PDI, and a significant increase in overall carbonyl content (Table 5.7 and Figure 5.17). A loss of at least 65% in M_n (and therefore DP_n also) and 53% in M_w occurred on dye application. This is due to hydrolysis which causes depolymerisation of the cellulose, thus increasing the PDI (i.e. broadening the range of molecular weights of the polymer chains present in the sample (Malawer 1995)) and increasing the proportion of polymers with lower DP (particularly those with DP200-2000) at the expense of those with DP>2000. The significantly lower surface pH of the dyed cotton samples (all between pH 2.5-2.7) compared to the undyed cotton (pH 6.6) supports the hypothesis of acid hydrolysis occurring, especially as in paper at least, the rate of acid hydrolysis increases ten-fold with each pH unit decrease (Zou, Uesaka and Gurnagul 1996b; Whitmore 2011). Consequently it can be expected that the rate of hydrolysis in the dyed textiles is 1000 times greater than that in the undyed. The depolymerisation that occurred due to dye application is reflected in the tensile testing data, particularly of the cotton weft, which shows that all of the dye formulations caused a statistically significant decrease in breaking load and in all but one case (Cc3 weft was lower but not statistically significantly lower than the undyed sample) in extension also. The overall carbonyl content of the textiles increased more than 5 times (over 8 times for c3) following the application of the dyes. Some of this increase was due

5.3 Characterisation of unaged model textiles – Results and discussion

to acid hydrolysis (REGs) however, more was due to oxidation. Oxidation consistently contributed to the overall carbonyl content at least twice as much as hydrolysis.

The different dye formulations caused no significant difference in the extent of depolymerisation, as indicated by molecular weight, molecular weight distribution, and REG carbonyl content. This was supported by the lack of significant difference in tensile properties between the differently dyed cotton textiles. However, dye formulation 3 appears to have caused greater oxidation of the cotton than the other dye formulations, almost twice as much as occurred in Cc1 on dye application. This correlates well with the higher iron content in Cc3 (at least 20% more) compared to Cc1 or Cc2 as determined using XRF. A very small increase in oxidation was observed in Cc2 compared to Cc1 which may be due to the presence of copper sulphate in addition to iron sulphate. This was observed with iron gall inks with and without copper on paper. The copper containing ink led to more oxidation but similar levels of hydrolysis of the paper substrate (Potthast, Henniges and Banik 2008).

5.3.3.7 EPR

Based on spectral intensities, it was observed that only environmental levels (under 10 μM) of iron and copper were present in the undyed model textiles (Figure 5.18). Undyed abaca also contained manganese. Quantitative evaluation of the metal ion content in the undyed model textiles was not undertaken due to the low levels of metal ions present.

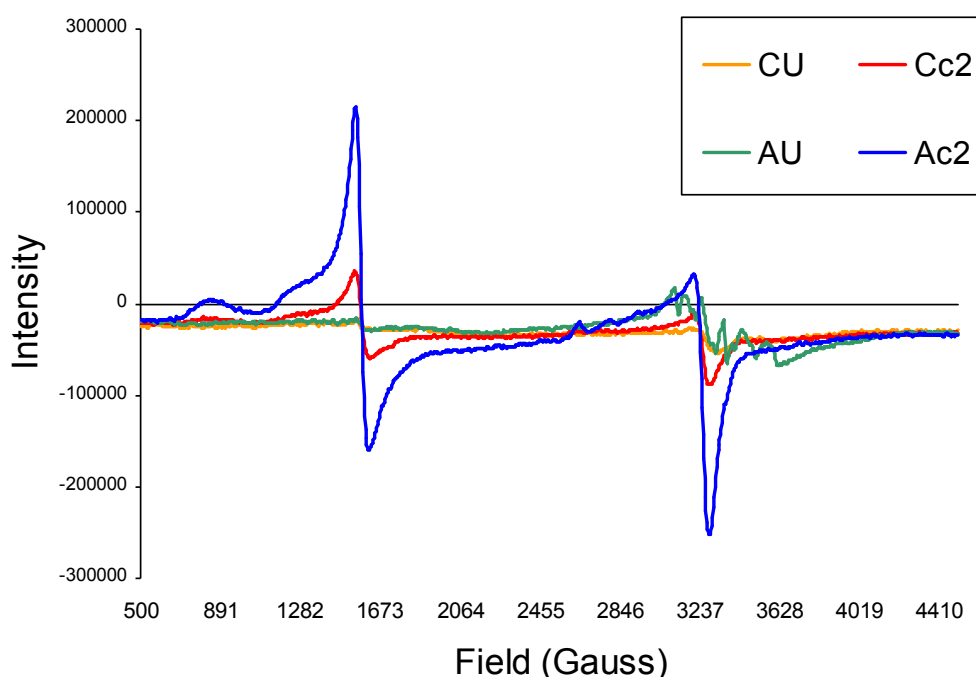


Figure 5.18 First derivative EPR spectra of c2 dyed and undyed cotton and abaca

Table 5.8 The changes in iron(III), copper(II), and radical content in the model textiles following dye application

Model textile	Relative integral (%)			Iron (%)	
	Iron(III) ^a	Cu(II) ^b	Radicals ^c	Bound	Unbound
CU	ND ^d	ND	23	ND	ND
Cc1	35	ND	46	32	68
Cc2	7	100	0	0	100
Cc3	7	ND	55	100	0
AU	ND	ND	224	ND	ND
Ac1	39	ND	90	88	12
Ac2	28	717	71	100	0
SU	ND	ND	43	ND	ND
Sp1	46	ND	115	43	57
Sp2	102	1398	92	47	53
Sp3	117	ND	232	58	42
WU	ND	ND	44	ND	ND
Wp1	26	ND	100	3	97
Wp2	21	1497	34	0	100

Notes for Table 5.8:

- Relative to Ac1 2s which was analysed at the same time;
- Relative to Cc2;
- Relative to Wp1;
- Not done because only environmental levels of iron or copper detected.

The model dyes introduced iron(III) ions (and Cu(II) ions in c2/p2 dye formulations) to the textiles (Table 5.8). The most iron(III) out of all the model textiles was introduced to the silk using the p2 and p3 dye formulations and the least to the cotton using c2 and c3 dye formulations. A weak positive correlation exists between the total iron content (determined using XRF), and the relative Fe(III) content determined using EPR exists (Figure 5.19). This suggests that at the time of analysis (around two years after production of the model textiles), there is no constant Fe(II):Fe(III) ratio for all materials.

5.3 Characterisation of unaged model textiles – Results and discussion

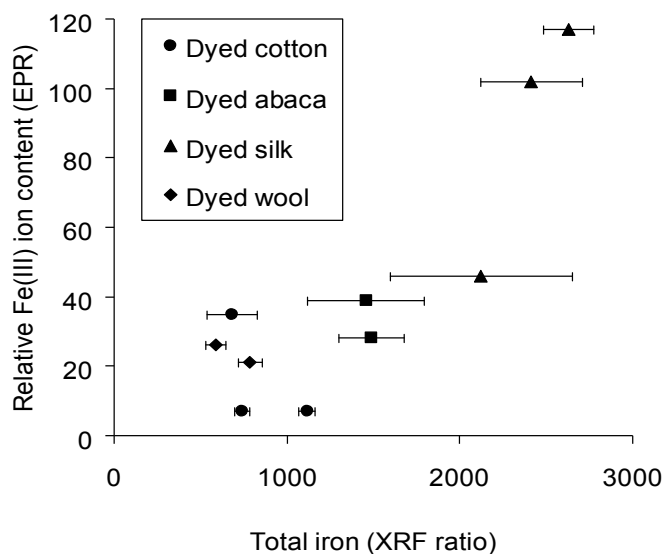


Figure 5.19 Comparison between the total iron content (ratio determined using XRF) and the relative Fe(III) ion content (determined using EPR) in the dyed unaged model textiles

The different dyes resulted in similar levels of bound Fe(III) in the abaca, silk, and wool textiles while the levels in cotton varied from 0 – 100%. Typically, dyed abaca (88% minimum) contained the greatest proportion of octahedrally bound (O_h) iron while dyed wool contained the least (3% maximum). The proportion of bound Fe(III) in the dyed silk varied around the 50% (43-58%).

Precise ligand identification is not possible with EPR however the types of signal observed are typically, though not exclusively, associated with oxygen ligands. These ligands were bound to the iron(III) ions to form octahedral (O_h) complexes. Tetrahedral (T_d) complexes may also exist but this could not be verified because the signals from the unbound and T_d bound iron overlap. These results are consistent with the presence of iron(III)-gallate/tannate/pyrogallol complexes in iron gall inks and iron tannate dyes as discussed in Chapter 4 (Section 4.1.2) and with the binding of iron(III) ions to carboxyl or hydroxyl groups in the textile fibres. Octahedrally coordinated iron(III) ions in iron(III):gallate/tannate/pyrogallol complexes have been proposed and evidenced in iron gall ink e.g. the 2:2 complex with 4 water molecules filling the final four coordination sites as suggested by Krekel (Krekel 1999) and the 1:1 hexagonal iron(III):gallic acid framework proposed by Wunderlich (Wunderlich 1991) in which one iron is bound to four different gallic acids. In a study into the mechanism of formation of 1:2 and 1:3 iron(III):gallate complexes from 1:1 complexes, the iron(III) ions in all of these complexes were presented as octahedrally coordinated with the 1:2 complex capable of cis and trans

5.3 Characterisation of unaged model textiles – Results and discussion

formations (Qureshi and Kazmi 1994). However, the iron(III) in both the 1:2 and 2:2 complexes have been presented as tetrahedral complexes (Darbour 1980; Delamare and Repoux 2001).

The Cu(II) ion concentration was lowest in Cc2 (100% relative integral normalised for mass) and greatest in Wp2 (1497% relative integral). The cellulosic and proteinaceous textiles were dyed using different formulations. The difference in Cu(II) content between Wp2 and Sp2 was significantly smaller than the difference in Cu(II) content between Cc2 and Ac2. These trends are mirrored in the XRF data of the dyed model textiles however the XRF data suggests that the total copper content of Ac2 and Wp2 are similar which is not the case in the EPR data. This could be due to variation in Cu(II) content in the fibres or due the existence of Cu(I) which is EPR-inactive.

The g and A values suggest that the copper is surrounded by oxygen ligands which may originate from tannic acid or oxygen-donor atoms on the cellulose, hemicellulose, keratin, and fibroin chains within the fibres. There are no iron-copper complexes present in any of the samples and the Cu(II) complexes are expected to be tetrahedral since there is no indication of octahedral complexes.

Radicals were present in all the model textiles except Cc2. Excepting abaca, the quantity of radicals typically increased following textile dyeing. Both c1 and c2 dye formulations caused the radical content in abaca to decrease. As with all of the analyses of the model textiles the low quantity of radicals makes identification of radical type difficult. However, based on line shape and g values it is likely that the radicals are semiquinones and similar phenolic compounds such as lignin derivatives, tannates, and gallates. This is consistent with the presence of iron(III)-tannate or gallate complexes, since it is possible that the tannic acids can be oxidised whilst bound to iron(III) ions, while excess gallic and tannic acids can also be oxidised (Hynes and O'Coinceanainn 2001; Andrade Jr., Dalvi, Silva Jr., Lopes, Alonso and Hermes-Lima 2005; Andrade Jr., Ginani, Lopes, Dutra, Alonso and Hermes-Lima 2006). The formation of semi-quinones from phenols and an excess of iron(III) ions is discussed in Chapter 4 (Scheme 4.2).

In summary, significant levels of iron(III) and copper(II) (c2/p2 dyed textiles only) were detected in all of the dyed model textiles using EPR. EPR data suggests that the iron(III) ions are being bound in octahedral complexes by oxygen ligands which is in agreement

5.4 Characterisation of c1 and p1 dyed model textiles during accelerated ageing – Results and discussion

with the numerous iron(III):gallate/tannate complexes previously identified in iron gall ink. Only environmental levels of metal ions were detected in the undyed textiles. Radicals were present in all undyed and dyed model textiles (except Cc2) before accelerated ageing and are likely to be semi-quinones or similar phenol-based radicals. This is also consistent with the presence of iron-tannate dyes.

5.4 Characterisation of c1 and p1 dyed model textiles during accelerated ageing – Results and discussion

5.4.1 Surface pH

Table 5.9 Effect of accelerated ageing (80°C and 58% RH) on the surface pH of the p1 and c1 dyed model textiles

Model textile	Ageing period (weeks) ^a	Surface pH					
		Undyed			Dyed (c1 or p1)		
		Mean	SD	CV(%)	Mean	SD	CV(%)
Abaca	0	5.4	0.2	3.4	2.9	0.1	2.4
	1	6.2	0.2	2.5	2.9	0.1	4.3
	2	6.1	0.0	0.6	2.8	0.1	4.4
	3	5.9	0.1	1.8	2.7	0.1	4.9
	4	5.7	0.1	1.3	2.6	0.1	3.4
Cotton	0	6.6	0.1	1.6	2.7	0.1	2.3
	1	6.5	0.1	1.9	3.3	0.1	2.3
	2	6.4	0.0	0.5	3.1	0.1	3.5
	3	6.1	0.2	3.6	3.1	0.2	5.5
	4	6.5	0.1	1.4	3.2	0.0	0.4
Silk	0	7.2	0.1	1.3	3.6	0.1	1.7
	1	7.4	0.1	1.5	3.6	0.0	0.7
	2	7.4	0.1	1.2	3.5	0.0	1.0
	3	7.2	0.1	1.2	3.4	0.1	2.1
	4	7.2	0.1	1.3	3.4	0.0	0.9
Wool	0	7.5	0.5	6.5	3.9	0.1	2.5
	1	7.5	0.1	1.9	3.6	0.1	1.8
	2	7.3	0.1	1.7	3.6	0.0	0.9
	3	7.2	0.1	0.8	3.6	0.2	6.7
	4	7.2	0.1	1.5	3.3	0.0	0.7

Note for Table 5.9:

a. The unaged sample data were acquired separately from the aged sample data.

Overall a decrease in pH occurred with oxidation. Acid groups are formed throughout the ageing of the organic material with a small increase in surface acidity, with increasing exposure to 80°C and 58% RH, occurring in both the undyed and p1/c1 dyed model textiles tested (Table 5.9).

5.4 Characterisation of c1 and p1 dyed model textiles during accelerated ageing – Results and discussion

There are small statistically significant discrepancies between the surface pH of some of the unaged and aged materials. In particular, the 1 week aged AU sample is 0.8 pH units higher than the unaged AU sample, and the 1 week aged Cc1 sample is 0.6 pH units higher than the unaged. The reasons for these differences are uncertain but variations could have arisen due to difficulties encountered with the water absorption properties of the textiles.

5.4.2 Colour measurement

Table 5.10 Changes in overall colour (ΔE_{00}^*), colour coordinates, breaking load (N), and extension (%) of substitute textiles during accelerated ageing (80°C and 58% RH)

Sample	Extent of ageing (weeks)	Difference in colour (aged versus unaged) ^a				Mean tensile properties	
		ΔE_{00}^*	ΔL^*	Δa^*	Δb^*	Breaking load (N)	Extension (%)
WU	0	0.00	0.00	0.00	0.00	ND ^b	ND
	1	1.14	0.05	-0.40	1.38	ND	ND
	2	1.33	0.32	-0.48	1.58	ND	ND
	3	1.75	0.17	-0.61	2.16	ND	ND
	4	2.44	-0.22	-0.72	3.17	ND	ND
SU	0	0.00	0.00	0.00	0.00	70.2 (4.9) ^c	28.2 (1.7) ^c
	1	1.04	-0.06	-0.32	1.00	64.2 (4.4)	25.2 (0.8)
	2	1.57	0.00	-0.44	1.54	65.5 (4.8)	24.9 (2.5)
	3	2.16	-0.48	-0.54	2.17	62.3 (4.7)	24.8 (2.7)
	4	2.59	-0.40	-0.57	2.70	61.6 (4.3)	21.7 (2.1)
AU	0	0.00	0.00	0.00	0.00	239.9 (43.1)	3.9 (0.5)
	1	2.39	-2.17	0.67	2.78	255.5 (38.1)	3.7 (0.5)
	2	3.08	-2.82	1.05	3.43	262.8 (47.3)	3.8 (0.5)
	3	3.03	-1.63	1.39	4.22	250.0 (40.3)	3.9 (0.6)
	4	3.95	-2.64	1.76	5.29	248.8 (28.9)	3.5 (0.5)
CU	0	0.00	0.00	0.00	0.00	117.1 (9.2)	9.1 (0.8)
	1	0.62	-0.15	-0.10	0.61	101.9 (15.7)	8.2 (1.0)
	2	1.20	0.06	-0.06	1.26	107.2 (11.6)	8.2 (0.7)
	3	1.52	-0.84	-0.07	1.48	107.1 (8.3)	8.6 (0.5)
	4	1.82	-0.28	-0.06	1.92	108.2 (11.0)	8.1 (0.5)
Wp1	0	0.00	0.00	0.00	0.00	ND	ND
	1	ND	ND	ND	ND	ND	ND
	2	2.74	-0.50	-0.39	2.73	ND	ND
	3	3.64	0.42	-0.46	3.70	ND	ND
	4	5.70	3.33	-0.62	5.21	ND	ND
Sp1	0	0.00	0.00	0.00	0.00	62.9 (4.9)	25.0 (2.6)
	1	1.07	-0.61	-0.17	1.13	55.6 (6.1)	19.7 (1.4)
	2	1.78	-0.31	-0.30	1.98	46.0 (3.7)	14.5 (0.7)
	3	2.15	0.25	-0.41	2.37	34.2 (9.4)	13.2 (1.5)
	4	3.27	2.02	-0.39	3.24	33.2 (6.1)	10.1 (1.8)
Ac1	0	0.00	0.00	0.00	0.00	105.9 (18.3)	2.1 (0.3)
	1	3.04	0.24	0.11	3.17	14.6 (4.9)	1.8 (0.4)
	2	4.54	-0.37	0.63	4.64	6.5 (1.9)	1.0 (0.3)
	3	5.33	-0.68	1.20	5.34	ND ^d	ND ^d
	4	4.96	-2.00	1.08	4.75	ND ^d	ND ^d
Cc1	0	0.00	0.00	0.00	0.00	68.3 (5.3)	6.9 (0.7)
	1	7.35	-4.23	0.30	6.92	29.5 (3.9)	4.9 (0.6)
	2	10.49	-4.68	1.29	10.55	13.0 (0.4)	3.7 (0.6)
	3	12.15	-5.71	2.29	12.24	7.7 (1.1)	3.5 (0.2)
	4	13.24	-6.72	3.02	13.22	6.2 (0.7)	3.5 (0.2)

Notes for Table 5.10:

5.4 Characterisation of c1 and p1 dyed model textiles during accelerated ageing – Results and discussion

- The CIELAB coordinates (SCE/100) of the unaged model textiles are presented in Table 5.3;
- Not done;
- Standard deviations of mean data are in parentheses ;
- Not done because the samples were too brittle to be prepared for analysis.

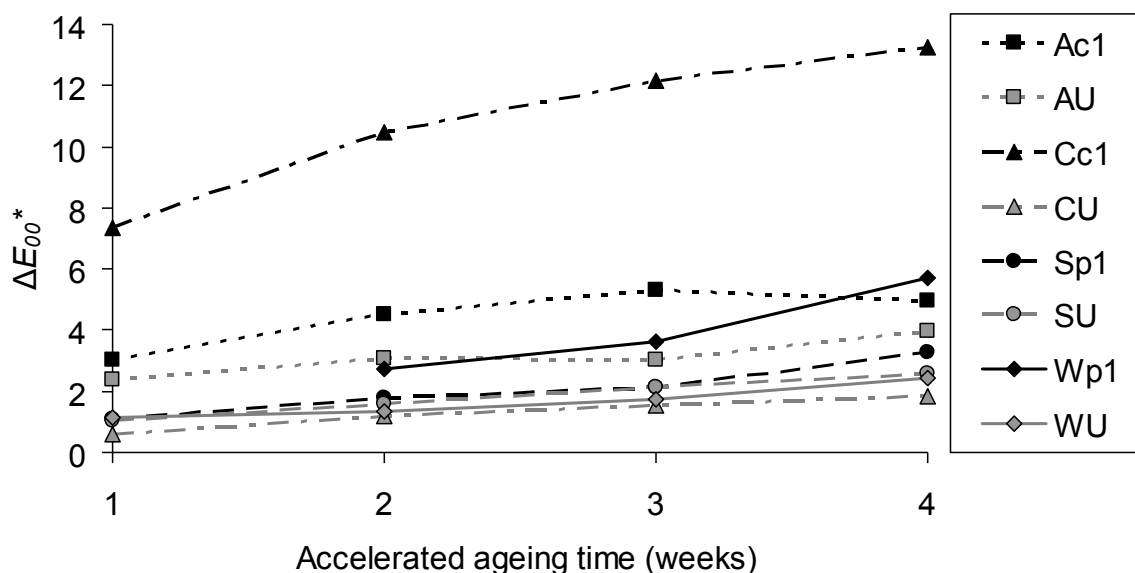


Figure 5.20 The colour change (ΔE_{00}^*) of the undyed and p1/c1 dyed model textiles during 4 weeks of accelerated ageing (80°C and 58% RH)

There was little overall change in colour of the undyed textiles after 4 weeks of ageing; abaca shows the most colour change with a ΔE_{00}^* value of 3.95 after 4 weeks of ageing (Figure 5.20 and Table 5.10). A slight yellowing ($+\Delta b^*$) occurred with all of the undyed textiles during ageing but this was less than that seen in the dyed equivalents (Table 5.10).

The dyed textiles changed colour more than the undyed equivalents during ageing and the dyed cotton textiles changed colour significantly more ($\Delta E_{00}^* = 13.2$) than the other dyed textiles ($\Delta E_{00}^* < 6$). Observable colour changes i.e. $\Delta E_{00}^* > 1.7$ occurred within 1 week of ageing for the dyed cellulosic textiles and within 2 weeks of ageing for the proteinaceous textiles. All of the dyed textiles increased in redness ($+\Delta a^*$ with a greater reflectance of 600-700 nm light) and yellowness ($+\Delta b^*$ and a greater reflectance of 560-600 nm light) with ageing resulting in browner coloured samples. The dyed cotton showed particularly large increases in redness after 4 weeks of ageing. These colour changes correspond to the breakdown of the blue-black iron-tannate complex with thermal ageing into coloured degradation products as described in Chapter 4 (Section 4.1.5.1).

5.4.3 Tensile testing

The presence of unbound iron ions either from the dyeing process or breakdown of the iron-tannate dye complex, as well as acids in the model textiles is expected to weaken the textiles during accelerated ageing. Tensile testing allows an objective assessment of the strength of the model textiles.

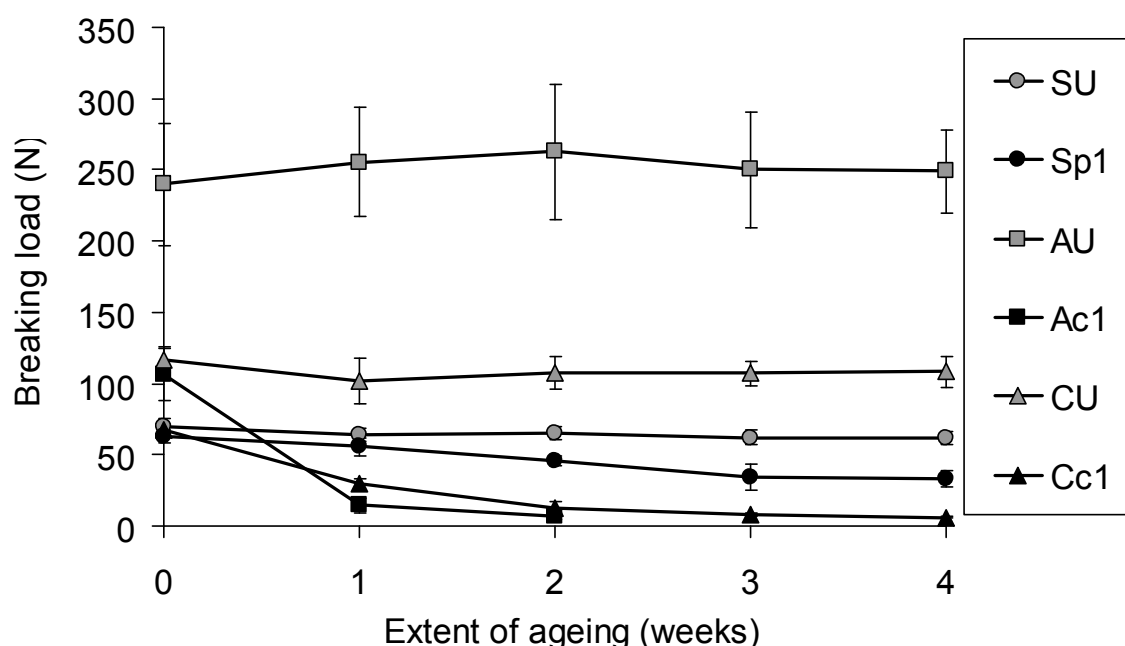


Figure 5.21 The changing breaking load (N) of the model textiles for 0, 1, 2, 3 and 4 weeks accelerated aged (80°C and 58% RH)

Little or no change in breaking load and extension was seen in the undyed materials during ageing. However, a significant decrease in the breaking load and extension occurred after two weeks of ageing at 80°C and 58% RH for dyed silk (Sp1) and after one week of ageing for dyed abaca and cotton (Ac1 and Cc1) (Figure 5.21 and Table 5.10). The rate of loss of extensibility was greatest with the dyed silk which had a significantly larger extension when unaged than either the cotton or abaca. However, the rate of loss of breaking load of dyed silk was similar to that of cotton and that projected for abaca, particularly after 2 weeks of ageing. The dyed abaca had an initially faster rate of loss of breaking load than the dyed cotton and overall, weakened and embrittled more than the Cc1. This is congruent with the greater presence of non-cellulosic, less crystalline components such as hemicellulose and lignin (Sun, Fang, Goodwin, Lawther and Bolton 1998; Hsieh 2007), and the higher iron content (Table 5.4 – XRF ratios) in abaca compared to cotton. Beyond two weeks of ageing the dyed abaca had become too weak for tensile testing.

5.4.4 EPR

Table 5.11 The changing iron(III) content and environment and radical content in the c1/p1 dye formulation dyed model textiles during accelerated ageing (80°C and 58% RH)

Model textile	Extent of ageing at 80°C and 58% RH (weeks)	Iron(III)				Radical relative integral (%) ^c
		Types of environment ^a	Relative integral (%) ^b	Bound (%) ^b	Unbound (%) ^b	
Cc1	0	0	35	32	68	46
	1	Distorted O _h	45	32	68	55
	2	Distorted O _h	59	42	58	68
	4	Distorted O _h	33	42	58	133
Ac1	0	0	39	88	12	90
	1	Distorted O _h	76	62	38	191
	2	Distorted O _h	100	48	52	234
	4	Distorted O _h	78	59	41	299
Sp1	0	0	46	43	57	115
	1	Distorted O _h	109	38	62	138
	2	Distorted O _h	107	42	58	119
	3	ND	132	44	56	134
Wp1	4	Distorted O _h	135	44	56	124
	0	0	26	3	97	100
	1	0	29	7	93	162
	2	0	25	22	78	138
CU	4	0	33	22	78	223
	0	ND	ND	ND	ND	23
	1	ND	ND	ND	ND	ND
	2	ND	ND	ND	ND	70
AU	4	ND	ND	ND	ND	98
	0	ND	ND	ND	ND	224
	1	ND	ND	ND	ND	ND
	2	ND	ND	ND	ND	188
SU	4	ND	ND	ND	ND	397
	0	ND	ND	ND	ND	43
	1	ND	ND	ND	ND	ND
	2	ND	ND	ND	ND	52
WU	3	ND	ND	ND	ND	ND
	4	ND	ND	ND	ND	78
	0	ND	ND	ND	ND	44
	1	ND	ND	ND	ND	ND
	2	ND	ND	ND	ND	37
	4	ND	ND	ND	ND	69

Notes for Table 5.11:

a. Other than tetrahedral (T_d) complexes and/or unbound iron;

b. Relative to Ac1 2s;

c. Relative to Wp1. The radicals present were semiquinone or phenol based but accurate identification is difficult due to the low content.

Only environmental levels (under 10 µM) of iron and copper were detected in the undyed model textiles consequently relative integrals for the metal ion content of the undyed model textiles were not calculated. Abaca also contained manganese. Immediate observation of the spectra for the undyed abaca identified that the levels of iron and copper remained the same throughout four weeks of ageing while the ‘visible’ manganese content decreased. Two oxidation states of manganese are EPR active (2+, 4+) however it is very

difficult to detect the 4+ state. Consequently, the manganese detected is thought to be in the 2+ oxidation state and the decrease in concentration of this ion is likely due to its oxidation to non-EPR active oxidation states such as 3+. Therefore, there is no “background chemistry” in the undyed textiles that is causing significant degradation after four weeks of ageing. Any accelerated degradation seen in the dyed textiles compared to the undyed can therefore be attributed to the presence of the iron/dye.

Sp1 contains significantly more iron(III) ions but similar levels of radicals to simultaneously dyed Wp1 (Table 5.11). Ac1 typically contains more iron(III) ions than simultaneously dyed Cc1 and significantly more radicals.

Overall, the radical content in the undyed model textiles increased with ageing and were of semi-quinone or phenol radical type. The low radical content makes determination of any changes to speciation difficult and unreliable. The radical content in the dyed cotton, abaca, and wool increased with age while that in the dyed silk remained fairly constant. Interestingly, the radical content in AU was typically greater than that in the dyed equivalent, Ac1, while for all other textiles the undyed sample had lower radical content than the dyed.

While there was no change in the quantity or speciation of the ferric ions with ageing of Wp1, there was a significant change in the quantity of bound iron(III) by 2 weeks of ageing. This new ratio of bound:unbound iron(III) remained constant for the following 2 weeks of ageing. Since there was no increase in the quantity of iron(III) with ageing these results suggest that complexation of unbound ferric ions occurred with ageing and/or that a complex mixture of reactions occurred that resulted in the effect described. The radical content in Wp1 generally increased throughout ageing.

By 1 week of ageing of Sp1 an increase in the quantity of ferric ions had occurred. Subsequent ageing caused further increases but to a lesser extent than that in the first week of ageing. No significant change in the ratio of bound:unbound ferric ion occurred during the ageing of Sp1 (Figure 5.22). This suggests that bound and unbound ferrous ions which are EPR-inactive were being oxidised to ferric ions at a similar rate to each other. This increase suggests that the Fenton reaction occurred. Consequently, hydroxyl radicals may have been formed but as they are highly reactive they have too short a lifetime to be

5.4 Characterisation of c1 and p1 dyed model textiles during accelerated ageing – Results and discussion

detected by EPR. As the radicals propagate, more stable radicals such as semi-quinone radicals can be formed which can be detected by EPR. However, for Sp1 the radical content remained fairly stable with ageing.

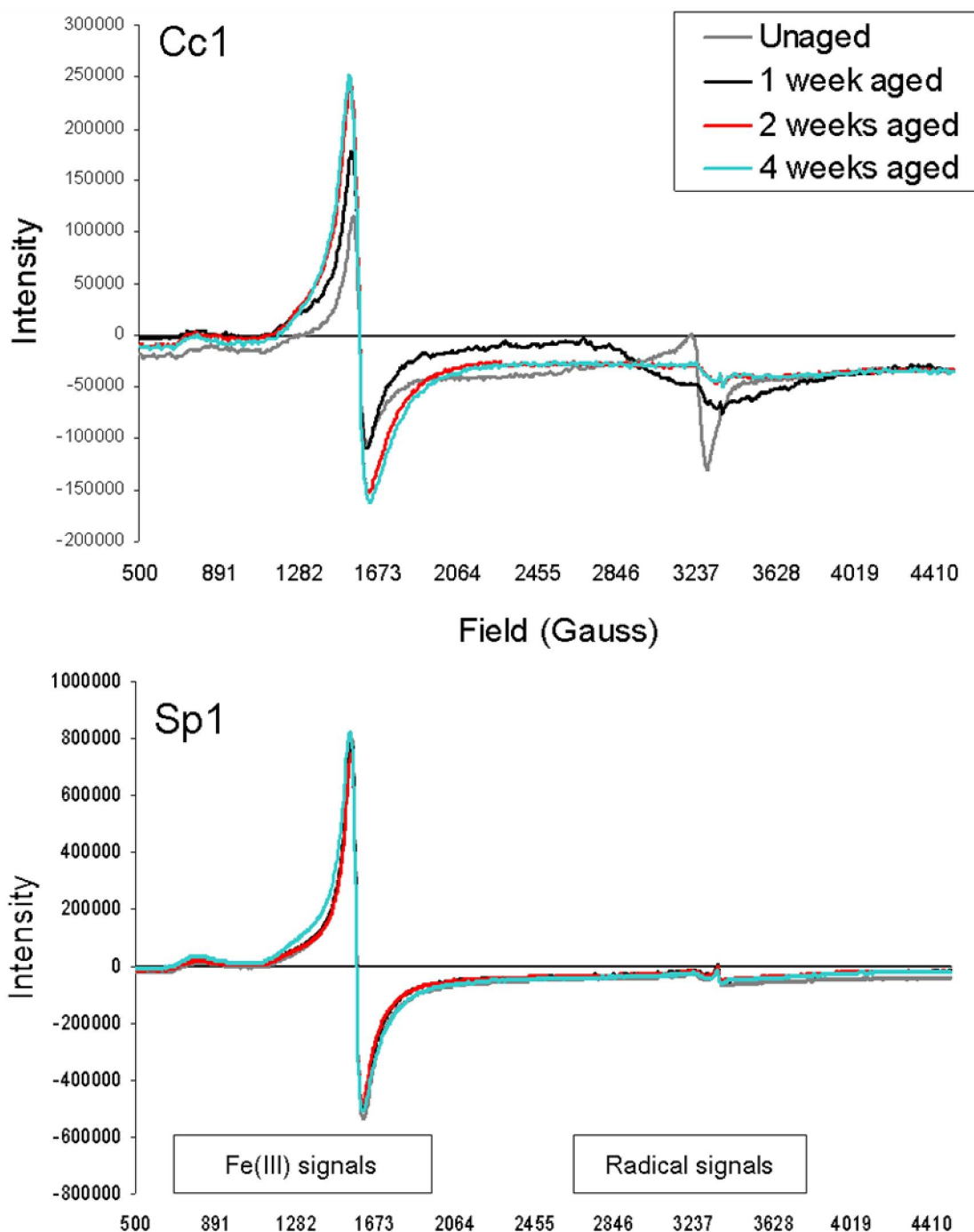


Figure 5.22 The changes in iron(III) and radical content in Cc1 (upper) and Sp1 (down) during accelerated ageing (80°C and 58% RH) for 0, 1, 2, and 4 weeks. NB: the unaged Cc1 and Sp1 sample was analysed separately from the aged samples but under the same experimental conditions

5.4 Characterisation of c1 and p1 dyed model textiles during accelerated ageing – Results and discussion

The ferric ion content in Cc1 increased during the first and second weeks of ageing but decreased by the fourth week of ageing (Table 5.11 and Figure 5.22). A continual increase in radical content occurred in Cc1 during ageing with the largest change (per week) occurring after between 2 and 4 weeks of ageing. By two weeks of ageing an increase in the proportion of bound iron(III) occurred which remained constant over the next two weeks of ageing. These trends suggest that oxidation of iron(II) ions (particularly bound iron(II)) to iron(III) ions occurred, particularly after 1 week of ageing.

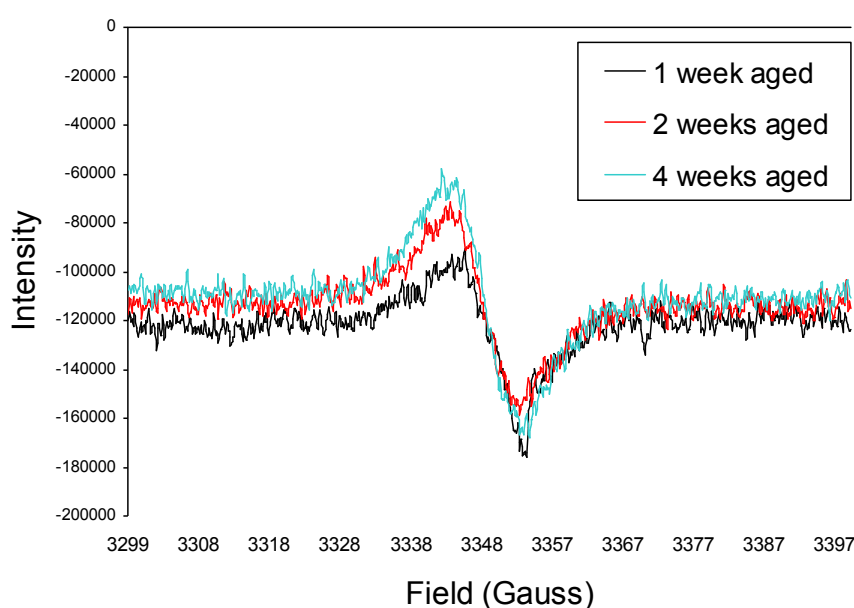


Figure 5.23 The changing radical content in Ac1 with accelerated ageing (80°C and 58% RH) for 1, 2, and 4 weeks

The relative quantity of bound iron(III) decreased slightly over the four weeks of ageing of Ac1. Over the same time the total quantity of iron(III) and radicals increased (Table 5.11 and Figure 5.23). The increase in radical content was particularly high, resulting in the highest radical content of all the model textiles during ageing. Overall, these trends suggest that oxidation of potentially bound and unbound ferrous ions occurred, possibly by the Fenton reaction, during accelerated ageing. It is likely that iron(III)-tannate dye complexes broke down during ageing since Ac1 became browner with age (spectrophotometry data characterises this). Such a breakdown could occur via an acid-catalysed process (Sistach, Gibert and Areal 1999) in which iron(III) ions and coloured polyphenol degradation products are released (via phenoxyl radicals). Oxidation of polyphenols by oxygen, or iron(III) ions, forms quinones via EPR-detectable semi-quinone radicals. This can occur in acid conditions such as those present in iron-tannate dyed textiles and could explain the

5.4 Characterisation of c1 and p1 dyed model textiles during accelerated ageing – Results and discussion

observations seen with Ac1 during ageing. Examination of the spectra suggests that the complex in Ac1 1s is different to that in Ac1 and that the same shift occurs with the 2 week aged Cc3. This could be due to iron(III) catalysed decarboxylation of gallic acids to give iron(III) pyrogallol complexes (Krekel 1999).

Since only environmental levels of metal ions were detected in the undyed model textiles and remained constant throughout accelerated ageing, any changes in properties and composition of the dyed model textile equivalents during accelerated ageing is due to the presence of the iron-tannate dye. The quantity of radicals increased in all of the dyed model textiles during ageing but the trends in iron(III) content and bound:unbound iron(III) ratios varied. Radical producing mechanisms occurred in the dyed model textiles and in some cases, most notably Ac1 and Sp1, an increase in iron(III) ions was also seen, suggesting that the Fenton reaction was occurring in the dyed model textiles during ageing. The proportion of bound iron(III) increased in all but the abaca dyed textiles for which it decreased during ageing.

5.4.5 GPC-MALLS

Table 5.12 The change in average molecular weight and molecular weight distribution of CU and Cc1 with accelerated ageing (80°C and 58% RH)

Model textile	Ageing period (weeks)	DP _n	Average molecular weight		PDI	% polymer content in			
			M _n (kg/mol)	M _w (kg/mol)		DP<100	DP100-200	DP200-2000	DP>2000
CU ^a	0	3164	513	1037	2	0	0	12	88
	1	ND ^c	ND	ND	ND	ND	ND	ND	ND
	2	3286	532	878	2	0	0	12	88
	3	ND	ND	ND	ND	ND	ND	ND	ND
	4	2843	461	859	2	0	0	59	41
Cc1 ^a	0	1051	170	439	3	0	2	57	42
	1	369	60	313	5	5	7	64	24
	2	209	34	205	6	10	12	63	15
	3	ND	ND	ND	ND	ND	ND	ND	ND
	4	203	33	180	5	12	16	59	14
Cc1 ^b	0	565	92	469	5	3	5	57	35
	1	243	39	238	6	9	10	63	19
	2	189	31	248	8	11	13	59	17
	3	223	36	265	7	10	14	61	15
	4	215	35	223	6	10	15	60	16

Notes for Table 5.12:

a. Samples analysed in same batch;

5.4 Characterisation of c1 and p1 dyed model textiles during accelerated ageing – Results and discussion

- b. Sample analysed in different batch to those in note 'a';
c. Not done.

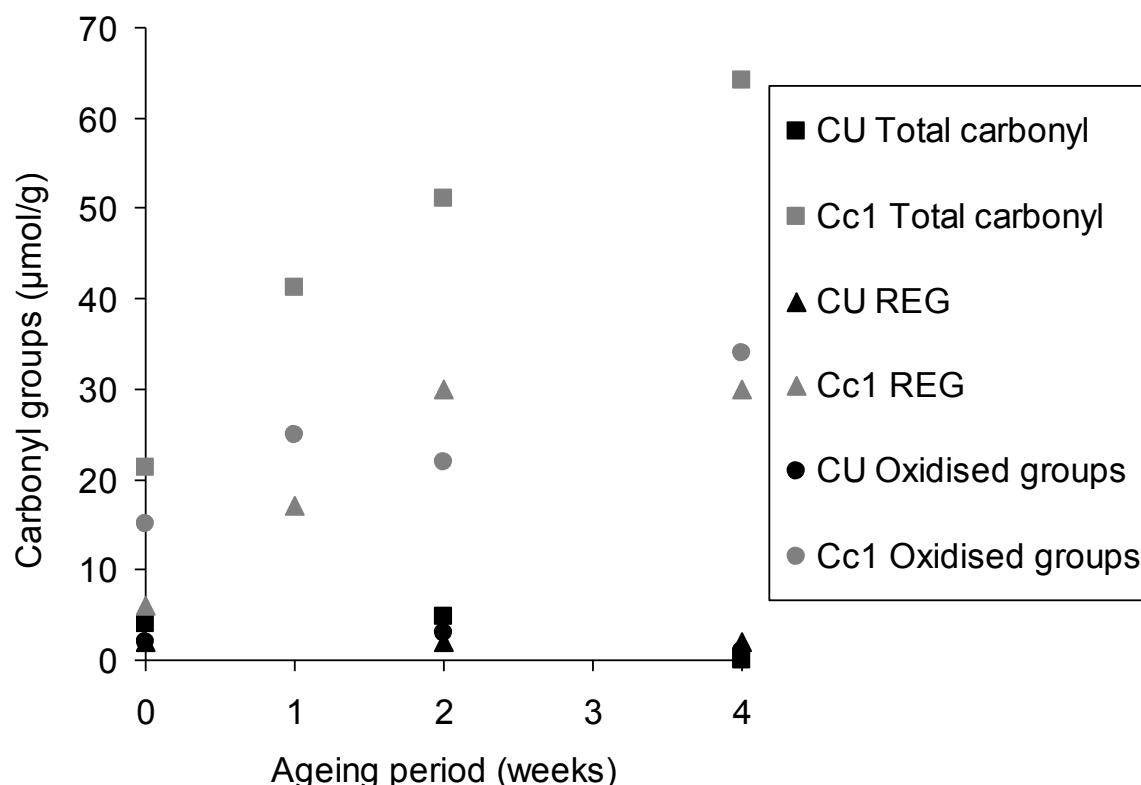


Figure 5.24 The changing carbonyl content and theoretical carbonyl content due to oxidation in CU and Cc1 during accelerated ageing (80°C and 58% RH)

After four weeks of accelerated ageing (80°C and 58% RH) a small decrease in average molecular weight and DP_n of CU occurred but this was not statistically significant. Changes in carbonyl content were less clear but by four weeks of ageing there was a small increase in REGs suggesting that some depolymerisation had occurred (Figure 5.24). This was corroborated by the molecular weight distribution, particularly the significant increase in % of polymers with DP between 200 and 2000 and corresponding decrease in % of polymers with $DP > 2000$ by four weeks of ageing. The depolymerisation was low enough to impart a negligible effect on the tensile properties of the textiles. Based on non-REG carbonyl content, some oxidation also occurred in CU during ageing. Since carbonyl groups are chromophores when part of larger conjugated systems (Timar-Balazsy and Eastop 1998), the small increase in carbonyl content by 4 weeks of ageing was mirrored by a small increase in yellowness that results in a small but visually observable colour difference of $\Delta E_{00}^* = 1.82$.

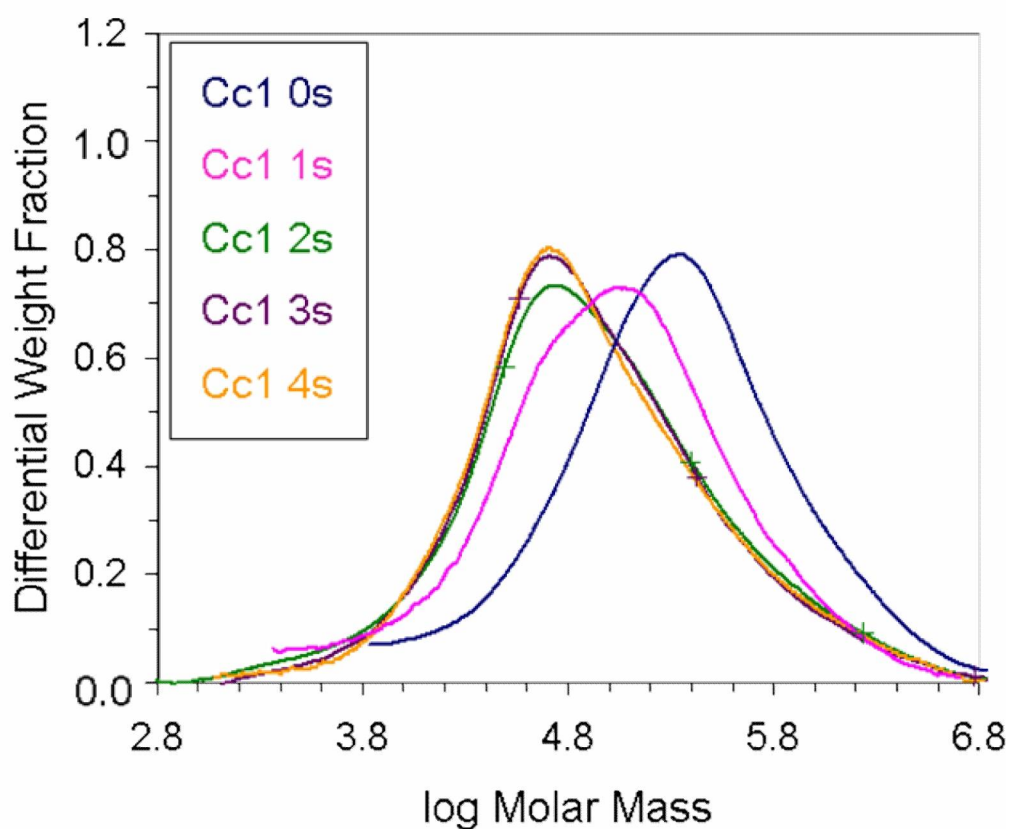


Figure 5.25 The change in molar mass distribution of cellulose in Cc1 with accelerated ageing (80°C and 58% RH)

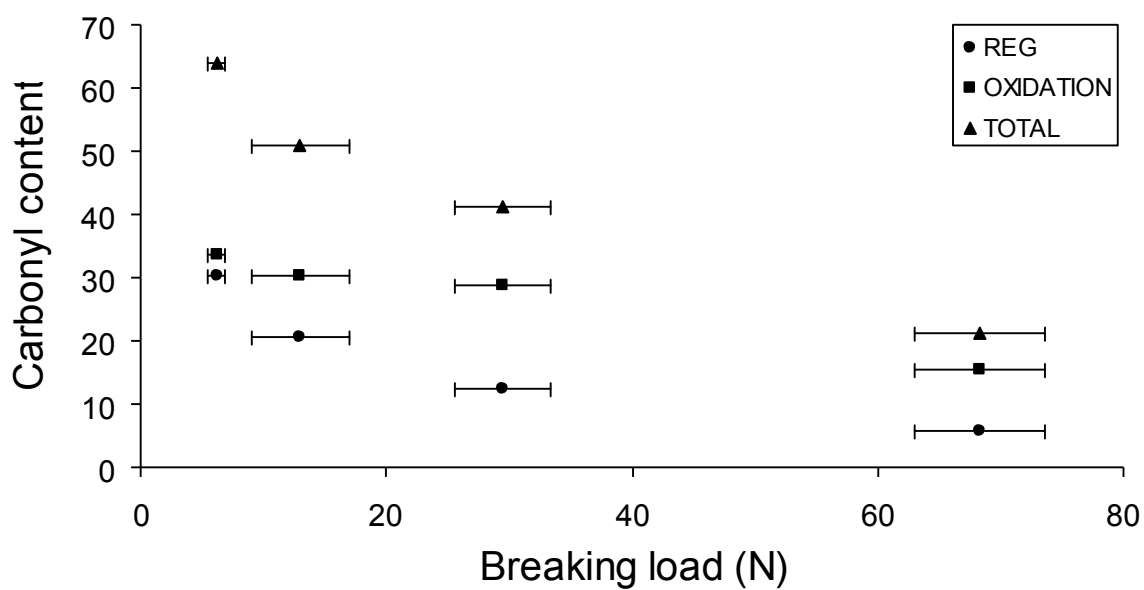


Figure 5.26 The negative correlation between breaking load and carbonyl content of samples during ageing

In contrast, in both batches of Cc1 samples, significant depolymerisation occurred after 1 week of ageing, as demonstrated by the significant loss of average molecular weight, DP_n , increase in PDI, and increase in the proportion of lower molecular weight polymers ($DP < 200$) (Table 5.12 and Figure 5.25). The initially fast rate of depolymerisation was significantly slowed in the second week of ageing and further slowed by the fourth week so that results from weeks 2 and 4 of ageing are similar. This trend was mirrored in the tensile properties of the samples during ageing. Calculation of the REG content suggests that the majority of carbonyl groups in the unaged sample are due to oxidation rather than acid hydrolysis but that by the end of the ageing the contribution from both degradation mechanisms was similar. The rate of oxidation was particularly rapid in the first and second week of ageing and fell off sharply after 2 weeks of ageing. While the rate of acid hydrolysis is also most rapid in the first two weeks of ageing it continues after two weeks at a greater rate than oxidation. As demonstrated in Figure 5.26 a negative correlation exists between the extent of strength loss and acid hydrolysis (REG content). However, as ageing progresses the rate of strength loss becomes lower than the rate of acid hydrolysis and the two factors are no longer related as they initially were. This is due to the decrease in quantity of cellulose chains in amorphous regions that link two crystalline regions. Scission of these cellulose chains (in the amorphous regions) causes a significant decrease in polymer strength per chain scission. Eventually, the quantity of broken chains is greater than the quantity of unbroken chains. Hydrolysis then results primarily in the breaking of amorphous cellulose chains that link to one or no crystalline regions. Such breaks do not cause a significant decrease in tensile strength per chain breakage but still form an REG group per scission (Whitmore 2011). While the rate of strength loss of Cc1 was decreasing with ageing, the quantity of carbonyl groups continued to increase until by four weeks of ageing the carbonyl content has tripled to $64.1 \mu\text{mol/g}$. The overall increasing carbonyl content also correlated well with the increasing yellow and red discolouration of the dyed cotton with age which by four weeks of ageing has led to a ΔE_{00}^* of 13.24. These trends were confirmed in the second batch of samples also in Table 5.12 and are comparable with those seen in model paper and model iron gall ink on paper samples (Potthast, Henniges and Banik 2008).

5.4.6 SEM

As is visible from Figures 5.26 and 5.27 there were no observable differences between the surfaces of the c1/p1 dyed 4 week aged model textiles and the unaged equivalents. The greater abrasion to the surface of the unaged silk compared to the aged silk is due to an error in sampling rather than an effect of dyeing. Due to the method of dyeing on the Winch machine some areas of the wool and silk textiles were abraded more than others as they moved against the metal of the machine. Investigation of the broken ends of the fibres formed during tensile testing was not undertaken but may show a difference due to accelerated ageing as increasing brittleness may lead to “cleaner” breaks of the fibres.

5.4 Characterisation of c1 and p1 dyed model textiles during accelerated ageing – Results and discussion

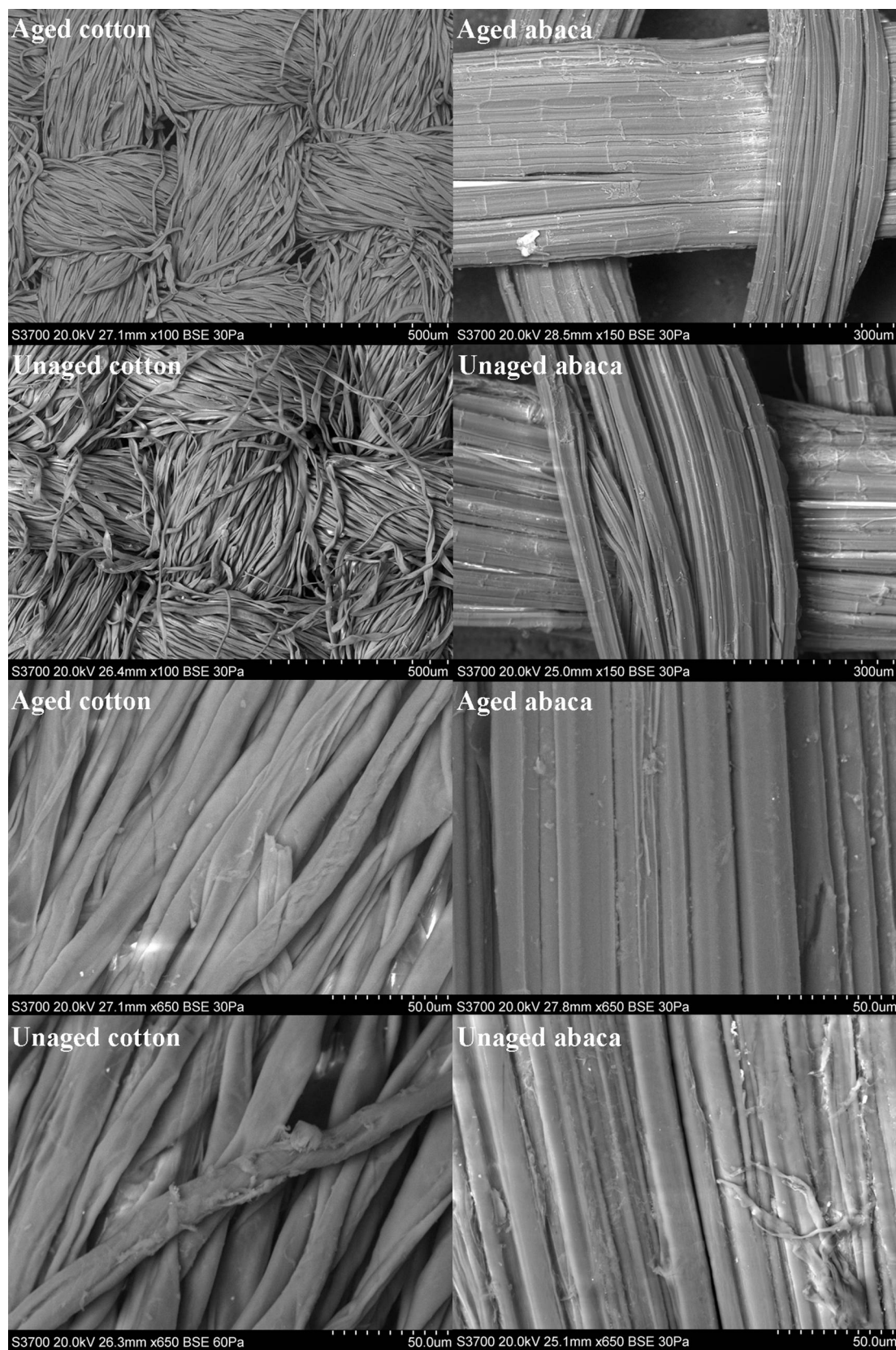


Figure 5.27 SEM micrographs of 4 week aged (80°C and 58% RH) and unaged Cc1 and Acl samples at $\times 100$ or $\times 150$ and $\times 650$ magnifications

5.4 Characterisation of c1 and p1 dyed model textiles during accelerated ageing – Results and discussion

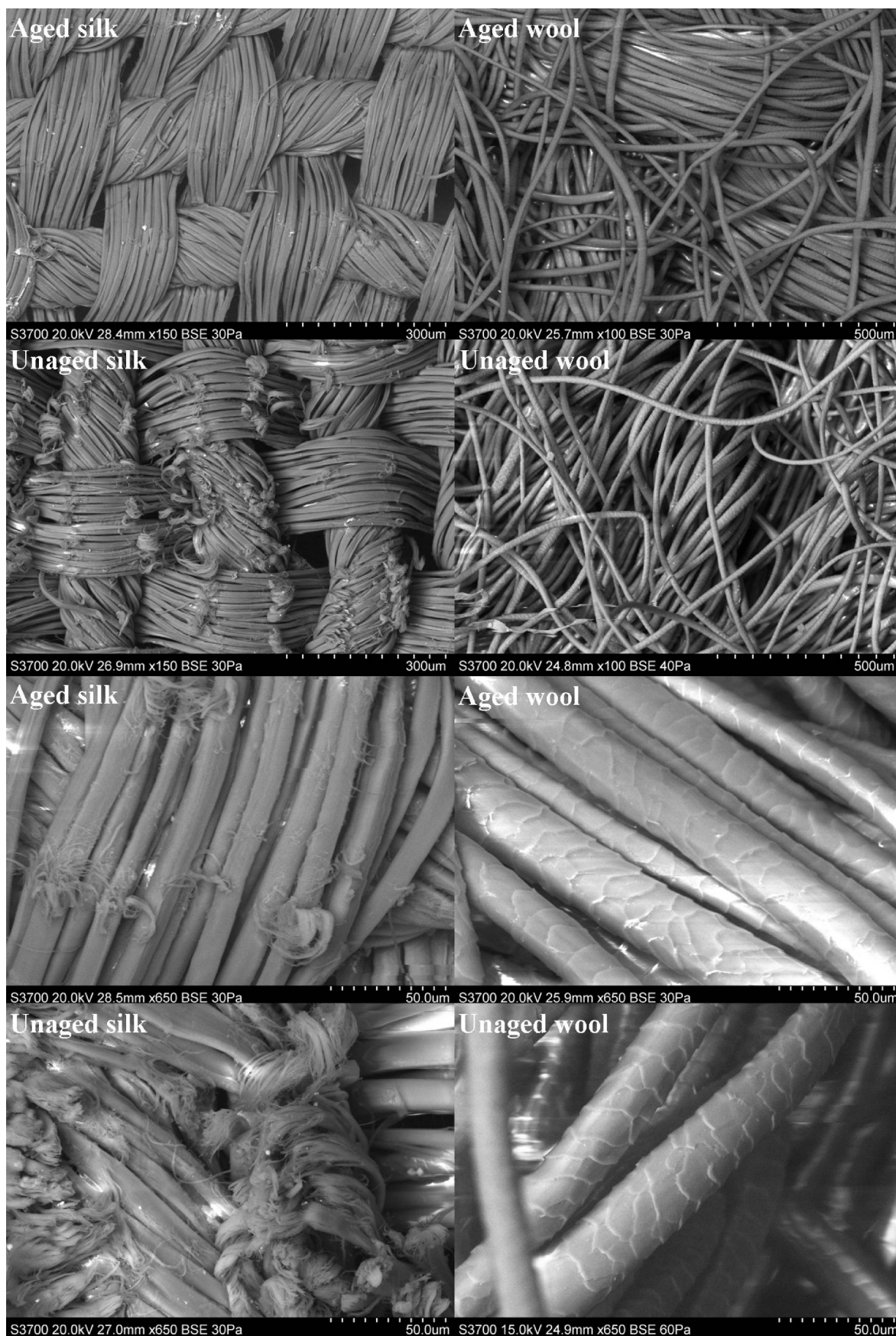


Figure 5.28 SEM micrographs of 4 week aged (80°C and 58% RH) and unaged Sp1 and Wp1 samples at $\times 100$ or $\times 150$ and $\times 650$ magnifications

5.5 Effect of dye type on textile stability – Results and discussion**5.5.1 Colour measurement**

Table 5.13 Changes in overall colour and colour coordinates of the cotton and silk model textiles due to accelerated ageing (70°C and 65% RH) for up to 39 days

Model textile	Ageing period (days)	ΔE_{00}^*	ΔL^*	Δa^*	Δb^*
CU	14	2.02	-0.84	-0.19	2.10
	21	2.83	-0.78	-0.21	3.07
	28	3.40	-1.12	-0.18	3.73
	35	3.92	-1.23	-0.15	4.36
Cc1	14	6.32	0.41	0.59	6.85
	21	7.99	0.60	1.06	8.93
	28	9.59	0.99	1.66	10.93
	35	11.12	2.01	2.63	12.85
Cc2	14	6.98	1.82	0.29	7.40
	21	9.34	3.33	0.80	10.07
	28	12.41	5.73	1.89	13.53
	35	14.82	7.06	3.21	16.64
Cc3	14	8.12	2.60	0.59	8.49
	21	9.68	3.72	1.19	10.26
	28	11.72	4.86	2.17	12.84
	35	13.52	5.90	3.39	15.05
SU	14	3.38	-0.37	-0.71	3.67
	21	4.12	-0.25	-0.80	4.64
	28	5.11	-0.62	-0.83	5.93
	39	5.53	-1.13	-0.69	6.52
Sp1	14	1.13	-0.19	-0.12	1.27
	21	1.36	-0.24	-0.20	1.50
	28	1.57	-0.21	-0.25	1.72
	39	1.85	-0.38	-0.26	2.02
Sp2	14	1.27	0.40	-0.14	1.41
	21	1.61	0.95	-0.24	1.64
	28	1.82	0.57	-0.33	1.97
	39	2.06	0.44	-0.36	2.25
Sp3	14	1.29	0.62	-0.28	1.34
	21	1.57	0.72	-0.41	1.61
	28	1.82	0.82	-0.45	1.87
	39	2.02	0.81	-0.52	2.06

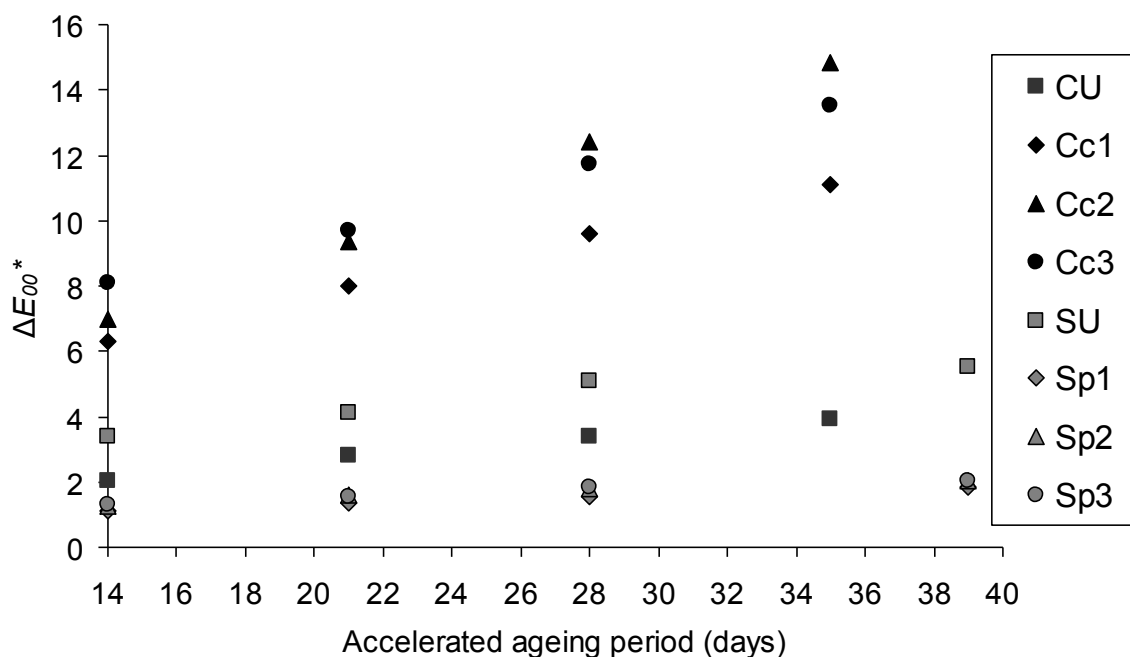


Figure 5.29 The effect of dye formulation type on the extent of colour change (ΔE_{00}^*) in cotton and silk model textiles during accelerated ageing (70°C and 65% RH)

The undyed silk showed a greater change in colour due to accelerated ageing than the dyed silk textiles (Table 5.13 and Figure 5.29). After 14 days of ageing the discolouration seen in the undyed silk was greater than that seen in the dyed silks after 39 days of ageing. As with all the silk textiles, a small darkening ($-\Delta L^*$) of SU occurred with ageing, however the main cause for the overall colour change (ΔE_{00}^*) was due to increasing yellowness ($+b^*$). The greater discolouration that is observed in SU compared to the dyed equivalents suggests that the presence of the dye formulations masks the discolouration of the silk occurring during humid thermal ageing.

Increasing yellowness ($+\Delta b^*$) is also the main contributor to the overall change in colour of the cotton samples though significant increases in ΔL^* and Δa^* also occurred. Unlike the silk textiles, the dyed cotton textiles showed significantly more change in colour than the undyed cotton textile. Discolouration in CU after 35 days of ageing is less than that seen in 14 days in the dyed cotton textiles and between 3 and 4 times less than that seen in the dyed cotton textiles after 35 days of ageing. This suggests that the iron-tannate dyes greatly accelerate the discolouration of the cotton under humid, thermal ageing conditions.

In all cases the rate of discolouration was most rapid at the start of the ageing process

5.5 Effect of dye type on textile stability – Results and discussion

leading to the extent of discolouration in the 14 day aged samples being typically equal to or greater than half of the discolouration seen after 35 or 39 days (cotton and silk textiles, respectively).

The different dyes caused little difference in the extent of discolouration of the silk during ageing. However, the following consistent trend in the extent of discolouration was observable: $Sp3=Sp2>Sp1$ i.e. the intentionally added impurities caused greater degradation than the 'pure' dye formulation 1 which was produced from iron sulphate and purified and unpurified tannic acids alone.

By 14 days of ageing the c1 and c2 dye formulations had caused similar extents of discolouration in cotton while c3 had caused greater discolouration. By 21 days of ageing dye formulations c2 and c3 caused and continued to cause greater discolouration than dye formulation c1. This trend was also present in the yellowing of the samples. While Cc3 initially caused greater discolouration in cotton than Cc2, after 21 days of ageing Cc2 caused the greatest colour change.

These results suggest that the inclusion of copper(II) sulphate in addition to iron(II) sulphate or the use of a natural tannin extract rather than purified and non-purified tannic acids caused a slight increase in textile discolouration, i.e. increases the rate of reactions that form chromophoric groups that absorb light in the visible region. Aldehyde groups are chromophoric groups that absorb light in the visible region when part of larger conjugated systems (Timar-Balazsy and Eastop 1998). They are responsible for the yellowing in undyed cotton. The quantity of aldehyde groups increases with the oxidation of alcohol groups and, in cotton, with the hydrolysis of the cellulose which form one new reducing end group per chain scission. The copper ions in c2 and p2 can increase the rate of oxidation (Strlic, Selih and Kolar 2006; Potthast, Henniges and Banik 2008). The use of natural gall extract in c3 may have increased the rate of acid hydrolysis by introducing a larger number of tannins and tannic acids than was introduced using tannic acid in c1 and p1. The phenolic hydroxyl groups of tannins are acidic and therefore an increased quantity in the textile could increase the rate of acid hydrolysis. If these groups are weak acids or strong acids that are unable to diffuse to the surface pH electrode during testing, such an increase in tannin content would have little or no effect on the pH of the samples. This would explain why there was little difference between the surface pH of the model textiles

dyed with different model dye types. Changes in colour during ageing also arise from the breakdown of the dye complex into coloured degradation products. The high acidity of the dyed cotton samples (frequently the most acidic of all the model dyed textiles) could have caused higher levels of iron-tannate dye complex breakdown than in the other dyed textiles, thus explaining the significant increase in discolouration seen in the dyed cotton textiles compared to the undyed. Cc3 was very slightly but statistically significantly more acidic than the other dyed cotton textiles which may have contributed to Cc3 discolouring faster than the other cotton dyed textiles. Interestingly further oxidation of aldehyde groups produces carboxylic acid groups which are not chromophores. Consequently, the rate of discolouration caused by oxidation could decrease with the oxidation of the aldehydes to carboxylic acids. This may explain why c2 has greater discolouration than c3 after 21 days of ageing.

The decrease in yellowing of the silk with the presence of the dye suggests that the sites that become chromophores on oxidation are unavailable for oxidation. Possibly these are involved with the binding of the iron-tannate dye to the fibres. Alternatively the dye is filtering the UV and limiting chromophore formation.

In summary, the application of dyes to cotton caused a significant increase in discolouration on ageing but caused a relative decrease in discolouration of silk. The inclusion of copper ions and natural tannin extracts increased the rate of discolouration of both cotton and silk to a small extent, very small in the case of silk. Dye formulation 3 caused the greatest discolouration in the silk and initially in the cotton however, after 21 days dye formulation 2 caused the greatest discolouration in silk. The dye 1 formulations which involved the use of iron(II) sulphate and tannic acid extracts caused the least discolouration of all the dye formulations.

5.5 Effect of dye type on textile stability – Results and discussion

5.5.2 Tensile testing

Table 5.14 The effect of dye type on the tensile properties of cotton and silk after accelerated ageing (70°C and 65% RH)

Extent of ageing (days)	Model textile	Yarn direction	Cotton				Silk			
			Breaking load (N)		Extension (%)		Breaking load (N)		Extension (%)	
			Mean	SD	Mean	SD	Mean	SD	Mean	SD
0	U	Warp	131.9	9.7	13.6	1.0	62.7	2.9	54.5	10.3
		Wefit	80.2	15.3	28.8	2.7				
	c1 or p1 ^a	Warp	82.5	12.0	10.9	1.9	54.1	5.6	38.7	1.7
		Wefit	58.3	8.6	20.9	3.4				
	c2 or p2	Warp	84.4	5.5	10.4	0.9	57.9	6.8	42.1	8.8
		Wefit	66.5	4.3	17.2	1.4				
	c3 or p3	Warp	71.0	1.6	8.5	0.3	58.5	6.9	36.0	3.8
		Wefit	47.9	7.1	15.0	1.4				
14	U	Warp	122.6	3.8	14.3	2.5	63.0	12.6	45.2	4.4
		Wefit	67.2	6.7	29.5	1.8				
	c1 or p1	Warp	16.0	1.4	12.9	14.2	45.4	8.3	34.2	6.8
		Wefit	10.7	0.6	16.4	12.9				
	c2 or p2	Warp	14.2	0.9	6.1	6.4	44.9	7.0	30.2	4.5
		Wefit	9.1	1.1	18.9	9.0				
	c3 or p3	Warp	11.7	0.5	3.4	0.4	43.7	7.2	24.4	5.7
		Wefit	7.9	0.8	25.1	22.3				
21	U	Warp	123.1	11.5	13.6	1.4	65.9	9.9	52.5	8.5
		Wefit	62.6	13.1	29.0	3.9				
	c1 or p1	Warp	10.8	0.2	8.2	7.5	48.1	3.8	31.3	3.7
		Wefit	6.3	0.5	14.0	10.0				
	c2 or p2	Warp	8.9	0.7	10.0	7.0	39.2	6.9	24.6	1.9
		Wefit	6.0	0.5	10.2	7.8				
	c3 or p3	Warp	6.8	0.8	5.4	4.2	40.0	7.6	23.2	3.2
		Wefit	4.8	1.2	10.0	5.8				
28	U	Warp	114.1	7.6	12.4	2.2	55.0	8.2	39.1	2.7
		Wefit	85.6	9.4	28.2	1.8				
	c1 or p1	Warp	7.8	0.9	7.6	6.5	38.0	7.6	29.9	7.2
		Wefit	4.2	0.7	15.9	8.3				
	c2 or p2	Warp	6.3	0.4	5.1	3.9	38.6	6.7	20.8	2.7
		Wefit	3.4	0.6	17.2	8.7				
	c3 or p3	Warp	5.5	0.2	3.2	0.1	35.7	7.3	18.9	3.0
		Wefit	3.4	0.6	19.4	9.3				
35 or 39 ^b	U	Warp	122.9	10.4	12.1	1.6	62.4	13.4	44.1	8.9
		Wefit	81.6	22.6	27.9	4.1				
	c1 or p1	Warp	5.8	0.2	3.4	0.2	34.4	4.6	26.5	5.8
		Wefit	3.0	0.1	16.7	7.6				
	c2 or p2	Warp	4.8	0.2	3.8	0.2	31.6	4.9	28.0	7.5
		Wefit	3.4	0.3	14.9	7.2				
	c3 or p3	Warp	4.3	0.3	3.4	0.5	31.0	2.9	21.9	11.9
		Wefit	2.7	0.3	14.2	7.1				

Notes for Table 5.14:

a. c1 for cotton and p1 for silk;

b. 35 days for cotton and 39 days for silk. Note also that due to a malfunction in the environmental chamber, the 39 day aged silk samples are thought to have remained damp but at room temperature for 3 weeks and 2 days.

5.5 Effect of dye type on textile stability – Results and discussion

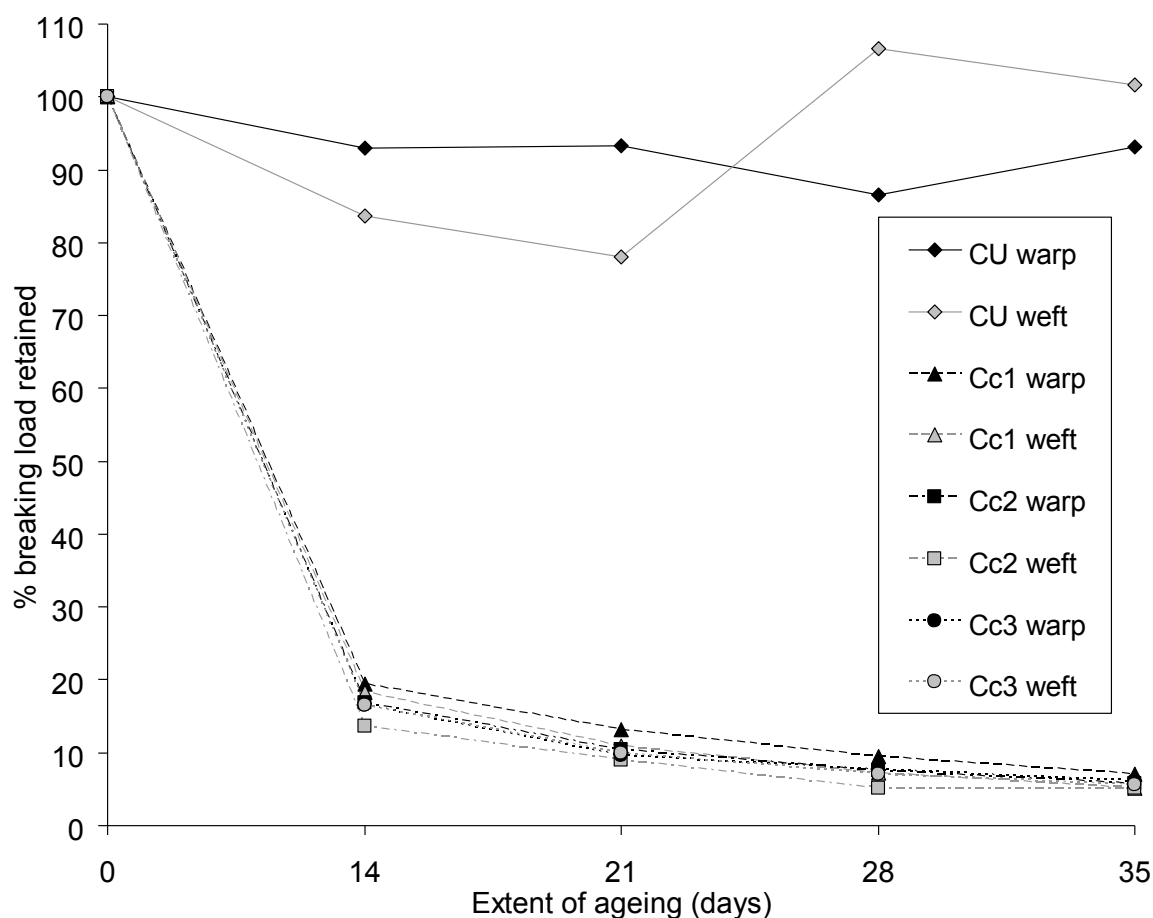


Figure 5.30 The effect of dye type on the breaking load of cotton warp and weft as a % breaking load retained during accelerated ageing (70°C and 65% RH)

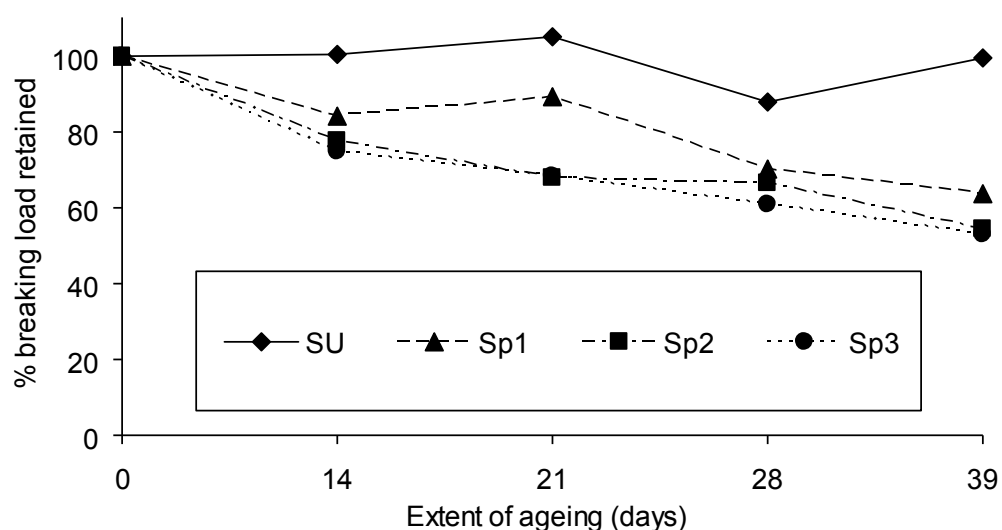


Figure 5.31 The effect of dye type on the breaking load of silk as a % breaking load retained during accelerated ageing (70°C and 65% RH)

From Figures 5.28 and 5.29 and Table 5.14 it is clear that the presence of iron tannate dye formulations 1 to 3 cause a significant decrease in tensile properties of cotton and silk after

5.5 Effect of dye type on textile stability – Results and discussion

35 days of accelerated ageing for cotton and 39 days for silk. Negligible change in breaking load occurred to the undyed cotton and silk during these periods of ageing. The most dramatic decrease in breaking load was seen in the cotton dyed textiles which lost approximately 80% of their tensile strength after 14 days of ageing and approximately 90% by 21 days. In contrast, after 39 days of ageing the dyed silk samples have lost between 35% and 45% of their strength, retaining over half of their strength. The decrease in breaking load of the dyed cotton samples levelled off by 21 days of ageing but there is no indication that the decrease in breaking load in the dyed silk samples was levelling off. In future studies it would be interesting to extend the ageing period to determine when a plateau of breaking load occurs in silk. This was attempted in this study but the malfunction in the environmental chamber curtailed the experiment. Note that due to different dye formulations, the trends in the cellulosic textiles to those in the silk should not be directly compared.

Based on warp cotton data c3 resulted in the most degradation while c1 resulted in the least. The differences in the breaking load of the cotton warp due to c1 and c2 was often statistically insignificant though the mean data consistently showed c1 as causing the least decrease in breaking load. Based on weft cotton data, there are no consistently statistically significant differences in breaking load due to the different dye types. At 0 and 35 days of ageing Cc2 had a small but statistically significant greater breaking load (weft) than Cc3 (i.e. c2: 66.5 ± 4.3 N and c3: 47.9 ± 7.1 N at 0 days of ageing and c2: 3.4 ± 0.3 N and c3: 2.7 ± 0.3 N at 35 days of ageing). But at 14 day of ageing Cc1 had the statistically significant greater breaking load (weft) than Cc3 (c1: 10.7 ± 0.6 N and c3: 7.9 ± 0.8 N) and at 21 and 28 days of ageing there were no statistically significant differences in the breaking load weft data. However, based on mean data alone the trends identified in the warp data continue. There were no statistically significant differences between the breaking load of the differently dyed silks during ageing though based on % retention of breaking load (Figure 5.31) p1 appears to have caused the least degradation of the proteinaceous dyes. Overall this suggests that the addition of copper ions to the c2 and p2

5.6 Overall discussion

dye formulations may have caused a small increase in the rate of degradation. Additionally the use of natural tannin extract rather than pre-prepared tannic acid extracts may have increased the rate of degradation slightly, possibly by introducing more tannic acid than present in the other dyes.

There was a consistently significant difference between the breaking load of the warp and weft of the same sample. The warp had a consistently greater breaking load than the weft even after 35 days of ageing when there was only a 1 to 3N difference. However the extension of the weft was consistently though not always statistically significantly higher than the extension of the warp throughout ageing. It is unclear if there was continued decrease in extension of the cotton weft with age but a significant decrease in the extension of the cotton warp with age is clear.

5.6 Overall discussion

5.6.1 *Homogeneity of the dyeing*

The variation in iron distribution throughout the textiles was greatest in p1/c1 dyed textiles (a maximum from 25% variation from the mean) and least in p3/c3 dyed textiles (below 10% variation of the mean). The latter can be considered to be relatively uniform and has been achieved in model iron-gall ink on paper studies (Kolar, Strlic and Pihlar 2006). Based on EPR and bathophenanthroline test results, some of these iron ions exists as unbound iron ions (ferric and ferrous). The surface pH of the model textiles was also found to be relatively uniform with standard deviations ranging between 6.5 and 1.3%. Low standard deviations in the CIE L*, a*, b* values were also obtained suggesting relatively even dyeing had occurred.

5.6.2 *Stability to thermal ageing*

The presence of the model iron-tannate dyes (c1 and p1) significantly destabilised the textiles with respect to thermal ageing. No significant change in tensile properties occurred to the undyed textiles on ageing and only low levels of colour and pH change occurred. However, in the dyed cotton, abaca, and silk textiles significant loss of breaking load and extension had occurred. The increasing carbonyl content, decreasing average molecular weight, and increasing quantity of lower molecular weight polymers in the dyed cotton samples during ageing explains the decreasing breaking load with ageing and strongly suggests that hydrolysis was occurring. The significant loss of tensile properties on ageing

5.6 Overall discussion

in the dyed textiles correlates well with their low surface pH prior to ageing. This supports the hypothesis that acid hydrolysis, is a major degradation mechanism in these iron-tannate dyed materials. The presence of radicals in the dyed cotton, abaca, and silk textiles prior to ageing and the increase in radical content, frequent increase in iron(III) content, and increase carbonyl groups (beyond that expected by acid hydrolysis (cotton analysed only)) strongly suggests that oxidation and the Fenton reaction occurred during the degradation of these textiles. In addition to the significant loss of tensile properties with the presence of iron from the iron-tannate dyes, the increases in ferric ion quantity with age supports the theory that iron-catalysed oxidation occurred. Significant discolouration, an overall browning due to increased yellowness and redness, also occurred with the dyed textiles which is congruent with the breakdown of the iron-tannate complex with thermal ageing. This may have contributed to the increase in semi-quinone radicals and possibly also to the increase in ferric ions that occurs with the ageing of all dyed textiles except the wool.

The wool dyed textile showed the least degradation of all the model textiles during ageing. Tensile properties were unable to be assessed due to the strength of the 10 mm textile strips being used. It also contained the least quantity of iron ions which were distributed in the external cuticle rather than the internal core of the fibres. Any catalysed degradation in the cuticle would have little effect on the tensile properties of the fibre which are a result of the core of the fibre. The dyed cotton, abaca, and silk had detectable levels of iron throughout the fibres and therefore the degradation that did occur would affect the tensile properties of the fibres, as has been seen. EPR analysis also suggests that no radicals were present in the unaged or aged wool samples, unlike in the samples of the other textiles.

While all of the variations of dye formulations resulted in similar levels of loss of tensile strength in the cotton and silk samples, it appears fairly consistent that dye formulation 1 (c1 and p1) caused the least degradation while dye formulation 3 (c3 and p3) caused the most. These differences are small and sometimes statistically insignificant.

5.6.3 Comparison of iron-gall ink and iron-tannate dye data

The application of iron-tannate dyes or iron gall inks to organic substrates are known to result in predominantly acidic materials (Daniels 1999b; Kolar, Stolfa, Strlic, Pompe, Pihlar, Budnar, Simcic and Reissland 2006; Pullan and Baldwin 2008) with significant levels of iron ions (Budnar, Simcic, Ursic, Rupnik and Pelicon 2006) which are of black,

5.7 Conclusions

brown, or grey colouration with a strong absorption of red light (Sistach, Gibert and Areal 1999; Te Kanawa, Thomsen, Smith, Miller, Andary and Cardon 1999; Neevel 2006). It is important for the model textiles to replicate these characteristics in order for them to degrade in a similar manner to historic iron-tannate dyed objects and this has been validated in Section 5.3. Additionally, accelerated ageing of the c1/p1 dyed abaca, the c1, c2, c3 dyed cotton, and p1, p2, p3 dyed silk textiles has shown discolouration consistent with the breakdown of the iron-tannate complexes, and a significant decrease in tensile properties as has been known for hundreds of years to occur to iron-tannate dyed objects. Iron-catalysed oxidation and acid-catalysed hydrolysis have been evidenced. Since the samples were aged using elevated conditions it is possible that the proportion of degradation occurring by these two degradation mechanisms may be different to those experienced during natural ageing. Nevertheless the important conclusions with the iron-tannate dyed model textiles produced in this study was that they do undergo catalysed loss of breaking load and extension similar to that observed in many historic iron-tannate dyed materials.

5.7 Conclusions

The iron-tannate dyed model textiles produced for this project have been investigated for their colour, pH, and metal ion uniformity and their stability to thermal ageing, i.e. their ability to fulfil aims 'a'-'c' for the model dyes developed in this project. All of the dyed model textiles were suitably uniform in their colour, metal ion distribution, and surface pH for the needs of this project thereby fulfilling aim 'a'. The application of the dye was found to significantly decrease the breaking load and extension of the dyed cotton, abaca, and silk textiles tested. The dyes also introduced significant quantities of iron which, based on EPR and bathophenanthroline test results, included unbound iron, i.e. an excess of iron as required for the model dyes to be a success (aim 'b'). The dyed cotton, abaca, and silk model textiles were found to degrade significantly faster than the undyed equivalents with thermal ageing and also showed discolouration consistent with the breakdown of the iron-tannate dyed complex. EPR and GPC-MALLs data confirm that metal-catalysed oxidation and acid hydrolysis are the major degradation mechanisms occurring in these iron-tannate dyed model textiles. These model textiles have therefore fulfilled aims 'a'-'c' stated at the start of this chapter. Comparison with iron-tannate dyed British Museum objects is still needed in order to ascertain the success of the model dyes at fulfilling the remaining untested aim ('d'); this will be tested in Chapter 6. The dyed wool textiles did not undergo substantial degradation within the timeframe and under the conditions used and

5.7 Conclusions

consequently are not valid substitutes for this research. This is likely to be due to the lack of iron ions within the strength-giving cortical core of the wool fibres. Improved dye diffusion into the core may have occurred with the use of a higher temperature during the dyeing process. Finally these model textiles may be regarded as useful substitutes for other research into accelerated degradation based on heat and humidity and that different analytical methods for assessment of degradation may be necessary e.g. yarn testing rather than tensile testing strips of fabric, will be needed.

6 IRON-TANNATE DYED CULTURAL HERITAGE

The British Museum houses a vast collection of cultural heritage from around the world which it aims to protect for future generations. An unknown quantity of this collection of objects contains iron-tannate dyes. In order for the validity of the model iron-tannate dyed textiles as substitutes for historic iron-tannate dyed materials to be ascertained it was important to identify some authentic iron-tannate dyed objects within the British Museum's collection. This involved an initial collaboration between conservators, curators, and conservation scientists. With Pippa Cruickshank and Dr. Marei Hacke, visits to a variety of departments at the British Museum were organised during which black organic materials showing signs of accelerated degradation were identified, and if possible, sampled for analysis. Methods of identifying the likelihood of an object containing iron-tannate dye have been described in Section 4.4 and have been based on a knowledge of the method of production, colour, condition of the object, and analysis for unusually high iron content and tannin content. In this chapter the results of analysis of a variety of objects (including some from the British Museum) using one or more of the following techniques are reported: spectrophotometry, bathophenanthroline testing, surface pH, XRF, EPR, GPC-MALLS, and SEM-EDX. Comparison of these results with those of aged model dyed textiles clarifies if the model textiles behave similarly to iron-tannate dyed cultural heritage, thereby fulfilling the only remaining unconfirmed aim of the model textiles (as detailed in Chapter 5). In addition, within this chapter a selection of objects which are thought to be iron-tannate dyed are described.

6.1 Experimental





6.1.1 *Historic samples*

Samples analysed in this chapter include: samples from Islamic carpets at the Museum of Islamic Art which were provided by Anna Beselin (senior textile conservator); samples from several carpets (mainly Axminster carpets) that were obtained with Heather Tetley (carpet conservator) on a visit to The Tetley Workshop Carpet & Tapestry Conservation Studio, Saltram House (National Trust property), and the Axminster Factory in November 2010; British Museum objects; pieces of piú piú and Maori cloak from the Horniman Museum which were supplied by Louise Bacon (Head of Collections Conservation and Care); and finally, a modern piú piú which is owned by Dr Vincent Daniels. Additionally an aged sample (48 hours, conditions unstated) of modern iron-tannate dyed model raffia that was produced by Mark Sandy (Camberwell College of Arts) (Sandy and Bacon 2008)

6.1 Experimental

has been analysed alongside an unaged undyed sample. Where possible, images of the objects analysed are presented in Table 6.1.

Table 6.1 Images^a, British Museum (or other) registration numbers, and descriptions of the objects analysed in this chapter

	
<p>6371</p> <p>Egyptian basket with black dyed detail. The poor condition of this basket includes losses to the black dyed areas which are thought to be iron-tannate dyed. XRF analysis of similar baskets has been reported by Wills and Hacke (Wills and Hacke 2007).</p>	<p>H290 9C</p> <p>Woven black and cream striped African textile. Labelled as a woven grass mat possibly acquired around 1928. Part of the British Museum's handling collection.</p>
	
<p>Am1937,0617.1</p> <p>North American skin bag which showed severe degradation. The image opposite is of the bag after conservation to stabilise the structure of the bag. The method of conservation has been published (Cruikshank, Daniels and King 2009).</p>	<p>1881,0802.48 P+E</p> <p>Gorget/breast-plate/back-plate made of leather, textile, and metal.</p>

6.1 Experimental



Horniman Museum samples provided by Louise Bacon

Broken piu piu and Maori cloak pieces made from New Zealand flax (*Phormium tenax*). The dyed areas of the objects are very brittle and weak. These dyed fibres have broken to leave undyed areas with brown tufts of dyed fibres at both ends and piles of small fibres and brown dust.



Owned by Dr Vincent Daniels

Modern Maori piu piu made with traditional methods as detailed by Daniels (Daniels 1995). This is made from New Zealand flax (*Phormium tenax*) which is iron-tannate dyed in selected areas using iron-rich mud and local tannin sources.



Asia 1981,0808.225

Japanese ceremonial "Hina doll" hair can be made from iron-tannate dyed silk known as Suga-fiber (Sato and Okubayashi 2010). Many Hina dolls such as this one suffer from fragile hair that is easily broken.



SLM2105, Af,SLMisc2105

Woven textile, possibly of banana fibre, from Madagascar, Africa. Previously owned by a Queen of Madagascar. 1753 acquisition. The black warp is degrading, showing multiple losses, while the coloured warp remains intact.

6.1 Experimental



Oc1904,-282, Oc1904C3.282

Micronesian loin cloth of abaca fibre (confirmed by Dr Caroline Cartwright at the British Museum). Fine weave with dark brown, light brown, and red/brown colouration. The fringe at end is stiff and brittle and significant losses have occurred in the dark brown areas of the cloth.



1906-0524-8, Oc1906,0524.8

Finely woven black, white, red, and yellow belt that is reported to have been worn by a chief "Tol". The yarn has been confirmed by Dr Caroline Cartwright at the British Museum to be abaca. There are losses to the black dyed loose ends of the belt. From Oceania.



H288 5J

Woven African textile with tufts of black/brown and yellow fibres incorporated into the weave. This object is part of the British Museum's handling collection. The faintness of the diamond and line pattern suggests some losses, particularly to the black/brown areas, have occurred.



Coins & Medals handling collection at the British Museum

Kuba cloths such as this one are raffia textiles with cut-pile embroidery produced by the Kuba peoples in the Democratic Republic of Congo. They are a status symbol displayed at funeral ceremonies and collected by men of high rank and chiefs.

6.1 Experimental



H279

African woven textile with tufts of black dyed fibre incorporated into the weave similar to a Kuba cloth. A strip of material which is part of the British Museum's handling collection. Some losses to the black dyed areas have occurred.



Af1818,1114.23, PRN: EAF88

A 19th century Adinkra made in Ghana from hand woven cotton strips whip stitched together. Iron-tannate dye of coal tar consistency was made for Adinkra by boiling 'Badie' tree bark with iron slag ('Etia') for several hours. Carved calabash stamps were used to apply the dye. Adinkra rolled up for storage (upper image) and reverse of Adinkra showing loss and discolouration (lower image).



Oc4253, Oc1866C1.4253, and Oc1866E6.54

Decorated tiputa (poncho) from Niue Island. It is made from tapa, bark cloth and painted with sienna and dark brown/black dyes.



Oc9954A, Oc1876C1.19954, Oc1876C1118.7, and Oc1876E6.63

Barkcloth two layer garment (possibly mourning dress) from Cook Island. The lower red/brown layer is soft and pliable but the upper black cut layer is brittle and easily lost.

6.1 Experimental



Am1933,1216.3

Border of an Andean textile embroidered with birds.



Am1933,1216.4

Embroidered Andean textile depicting flying mythical figures each with a staff.



Am1934.0714.2

Embroidered Andean textile with chess-board arrangement. Each design depicts a supernatural figure holding a staff in either hand.



Am1934.0714.8 a (upper) and b (lower)

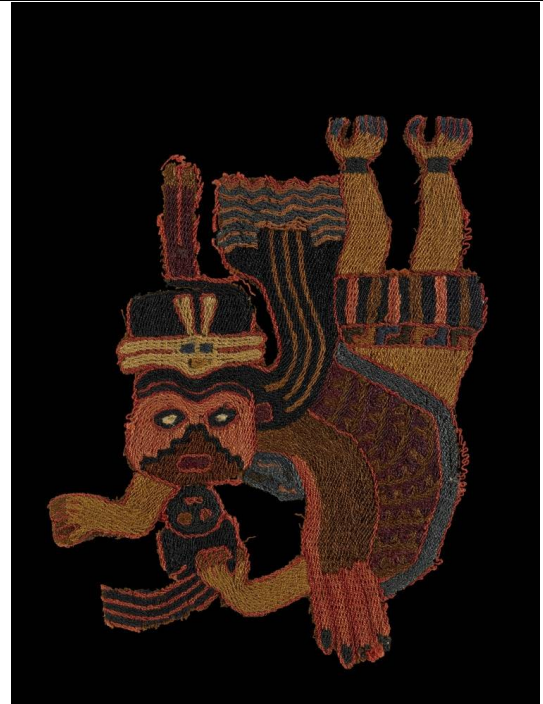
Embroidered Andean textile depicting a seated zoomorphic figure with numerous appendages terminating in trophy heads with flowing hair.

6.1 Experimental



Am1933,1216.1

Embroidered Andean textile fringed fragment with 'flying' figures. The figures have multiple serpentine appendages sprouting from heads and holding trophy heads.



Am1954,05.565

Embroidered Andean textile motif of flying supernatural winged figure holding a trophy head by the hair in one hand.



1881,0802.158

The black velvet and red felt lining of an Islamic steel helmet. The helmet is made of steel and almost hemispherical with raised bands of repousse flowers and foliate scrolls.



6.1 Experimental



Am1954,05.555

A fringed Andean textile with embroidered various creatures and two intertwined serpentine figures through the design.



Af1936_1211_5

Machine woven stamped Adinkra cloth from Africa.



M4-S-22 37129

Black and beige strip of Egyptian woven textile.



M4-S-22 37119

Black textile with white pattern with many losses.



No number

Horse chainmail with black lining fabric in poor condition.

6.1 Experimental



Af1938,1004.13

African mask that was acquired by the British Museum in 1938 and is made of wood and vegetable fibres.



1979,Af,1,2397

African mask with black dyed raffia that is currently on display in The Sainsbury Galleries (Room 25) at the British Museum.



21789

Coptic textile with cream and dark brown areas. Areas of the brown are missing in places. Loose fibre taken



43369

Black and cream Egyptian textile.

6.1 Experimental



As2005,0727.1.o

The original 19th century textile body of this Akali Sikh turban (pictured) is now too weak to display the metal ornaments. The cotton textile contains iron-tannate dye. A replica textile has been made to enable display of the metal ornaments (Pullan and Baldwin 2008).



1957,As11,9

Rattan basketry Apatani rain cape with black palm fibres from India.



As1957,11.10


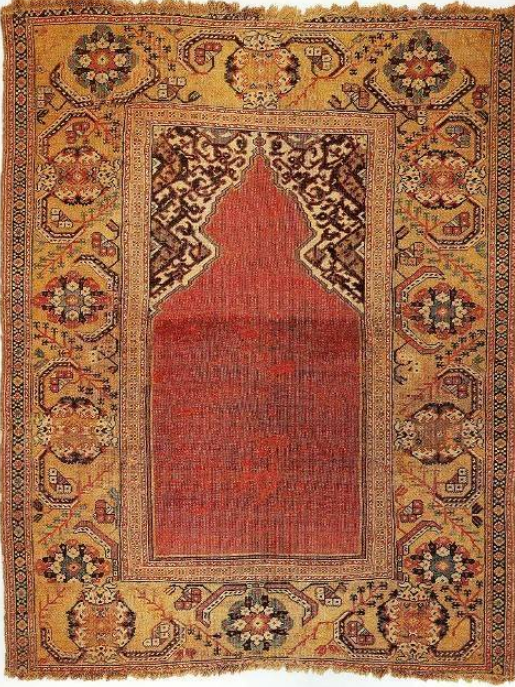

Rattan basketry rain hat with black palm fibres, patterned bamboo slivers, triangles of plaited rattan and leaves.



1909,5,19,8

Printing brush with blackened tip which is very brittle.

6.1 Experimental

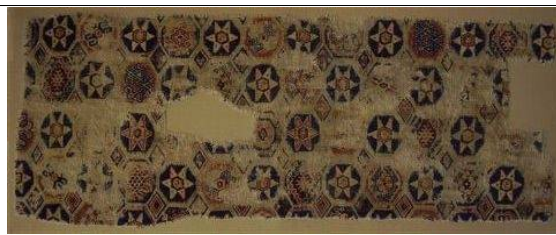
 <p>No number</p> <p>Thailand Siam Royal Cypher Medal, 1926</p>	<p>Objects analysed with no image:</p> <p>The British Museum No number - 19th Century banana fibre belt from the Caroline Islands. The method of conservation of this belt has been published (Cruickshank and Morgan 2011).</p> <p>OA+7279 - Brown fragile velvet of a saddle from Asia.</p> <p>The Museum of Islamic Art, Berlin I.0007/62 – Islamic carpet I. 0041/70 – Islamic carpet KGM1875,111 – Islamic carpet</p>
 <p>KGM1875,197 (Museum of Islamic Art, Berlin)</p> <p>Islamic carpet.</p>	 <p>I.5526 (Museum of Islamic Art, Berlin)</p> <p>Islamic carpet.</p>

6.1 Experimental



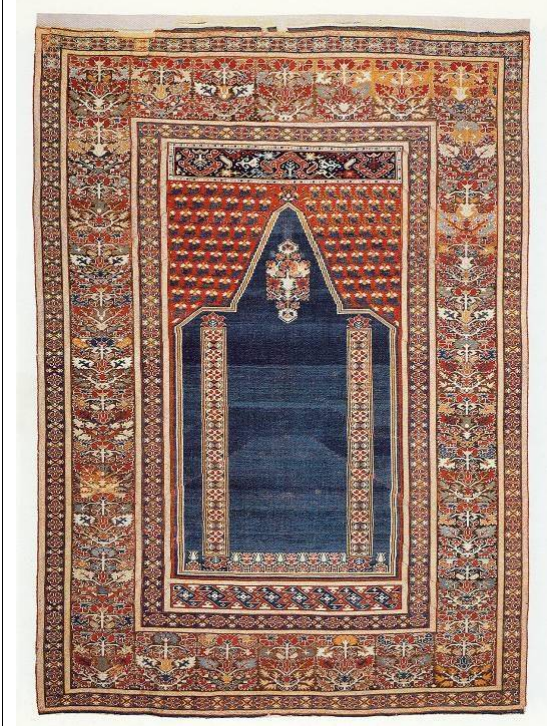
KGM1885,248a (Museum of Islamic Art, Berlin)

Islamic carpet.



KGM1900,55A (Museum of Islamic Art, Berlin)

Islamic carpet.



I.0001/64 (Museum of Islamic Art, Berlin)

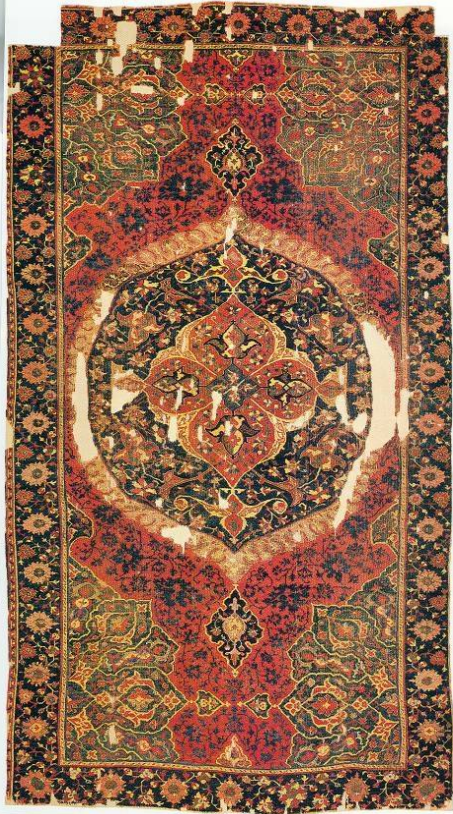
Islamic carpet.



I.0072/62 (Museum of Islamic Art, Berlin)

Islamic carpet.

6.1 Experimental



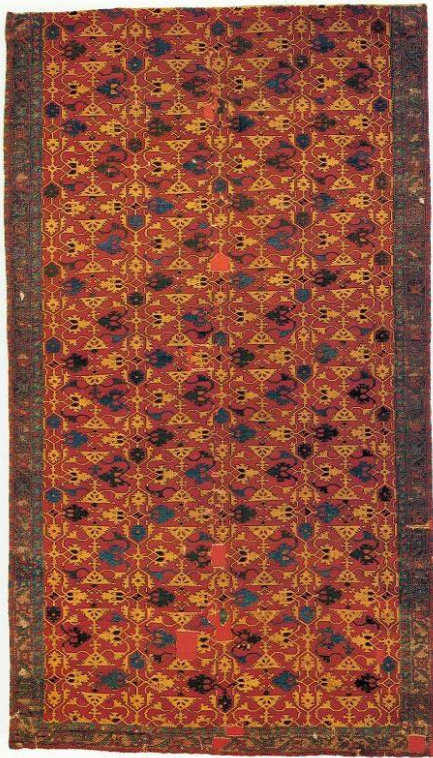
KGM1880,919 (Museum of Islamic Art, Berlin)

Islamic carpet.



KGM1882,703 (Museum of Islamic Art, Berlin)

Islamic carpet.



KGM1882,707 (Museum of Islamic Art, Berlin)

Islamic carpet.



KGM1883,522 (Museum of Islamic Art, Berlin)

Islamic carpet.

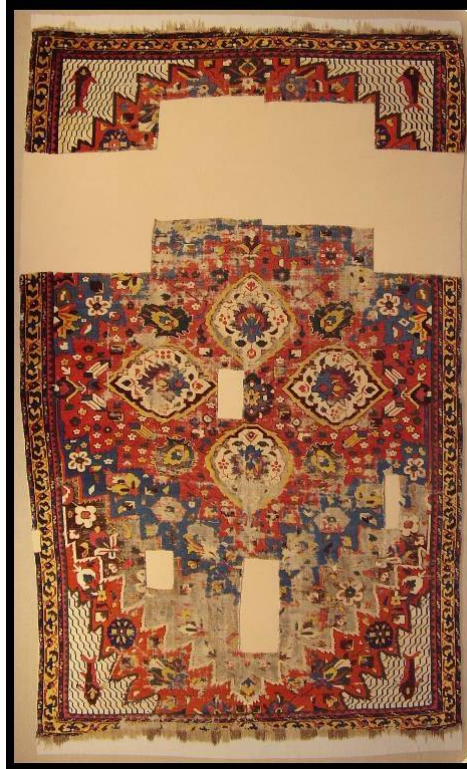
6.1 Experimental

25



KGM1885,247 (Museum of Islamic Art, Berlin)

Islamic carpet.



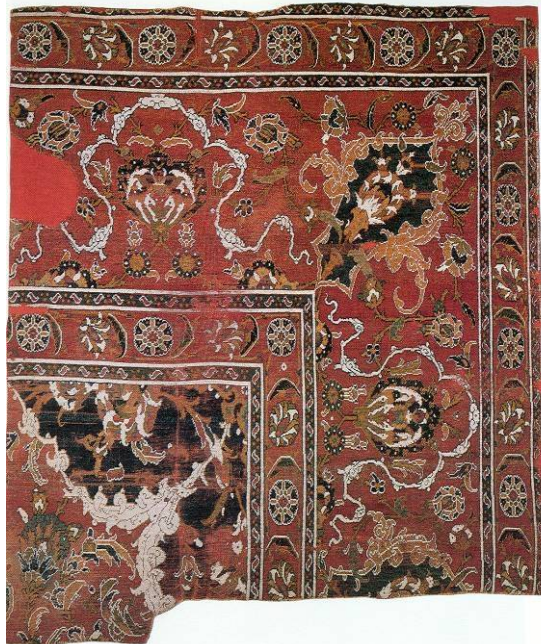
KGM1885,248a. (Museum of Islamic Art, Berlin)

Islamic carpet.



KGM1886,500 (Museum of Islamic Art, Berlin)

Islamic carpet.



KGM1889,150 (Museum of Islamic Art, Berlin)

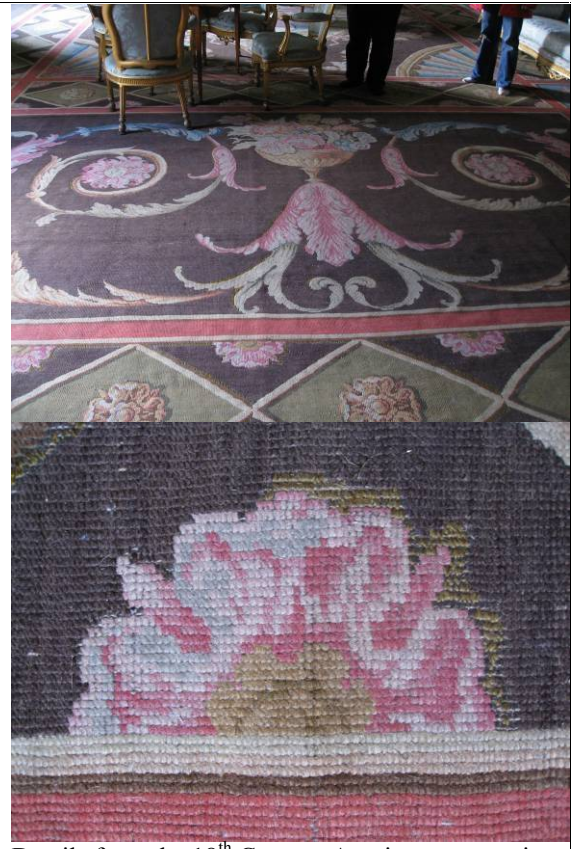
Islamic carpet.

6.1 Experimental



The Tetley Workshop Job number: TC920D3

18th Century Axminster carpet being conserved at The Tetley Workshop in November 2010 (top) and an image showing severe losses of the black/brown wool (below).



Details from the 18th Century Axminster carpet in the Saloon of Saltram House, National Trust.



Detail from the 18th Century Axminster carpet in the dining room of Saltram House, National Trust.

Notes for Table 6.1:

- a. all images of British Museum objects are © Trustees of the British Museum and all of objects from the Museum of Islamic Art, Berlin are © National Museums in Berlin, the Museum of Islamic Art.

6.1 Experimental

6.1.2 *Analytical techniques*

The experimental methods used to characterise historic iron-tannate dyed objects are detailed below. The methods used to analyse model textiles with which the results of the historic objects are compared are detailed in Section 5.2.

6.1.2.1 XRF

A Bruker ArtTax μ -XRF spectrometer with a molybdenum X-ray tube and ArtTax 4.9 software was used for semi-quantitative analysis of the areas of historic samples that may have been iron-tannate dyed. Where possible, analysis of equivalent undyed material was undertaken for comparison with the dyed region. Small samples such as a few short strands from some objects including those provided by Anna Beselin (Islamic carpet samples) and Heather Tetley (Axminster carpet samples) were adhered to a carbon tab on filter paper for analysis while other objects such as the piu piu belonging to Dr Vincent Daniels and various objects from the British Museum's handling collection were analysed in situ. The XRF spectra were obtained over 400 s, using a 0.65 mm collimator, 50 kV, 500 μ A, and a He purged atmosphere or over 100 s, using a 1.5 mm collimator and air atmosphere. Elemental peak areas were divided by the Compton peak area and multiplied by 1000 to give the XRF ratio values that are reported in Appendix 6. These XRF ratios are therefore unaffected by the use of different lifetimes and collimators during analysis. The different types of materials being analysed and their different surface morphologies which may interact differently with the incident X-rays during analysis is likely to make direct comparison of XRF ratios in different samples inappropriate and unreliable. Consequently, the iron content of the analysed objects was categorised as follows to enable a more reliable assessment of the relative magnitude of iron content of the objects analysed: '-' for ratios of 30 or less for which it is expected that the object is not iron-tannate dyed; '+' for ratios of 31-200 which indicates that the object is potentially iron-tannate dyed if it is also black, grey, or brown; '++' for ratios of 201-500; '+++' for ratios of 501-3000; and '++++' for ratios > 3000 which indicate the greatest likelihood of the object being iron-tannate dyed if it is also black, grey, or brown. These levels were based around the background ('-') and iron-tannate dye related ('+++') iron XRF ratios of the model textiles.

6.1 Experimental

6.1.2.2 Colour measurement

Spectrophotometric and colorimetric data of historic iron-tannate dyed materials were collected as described in Section 5.2.4.2 from up to 3 randomly selected areas of sample as sample size allowed.

6.1.2.3 Bathophenanthroline testing

The same method as described in Section 5.2.3 was used to test the iron(III) and iron(II) content of a selection of historic samples using bathophenanthroline paper.

6.1.2.4 EPR

The same experimental conditions were used to analyse the historic materials as are described in Section 5.2.6 except that an unweighed piece of each sample was used rather than three randomly selected yarns of known mass. Consequently, the results for the historic materials are qualitative only.

6.1.2.5 GPC-MALLS

Two historic samples were analysed using the same method of GPC-MALLS as detailed in Section 5.2.8.

6.1.2.6 Surface pH testing

The surface acidity of a selection of historic samples was analysed using the method detailed in Section 5.2.2 except that between one and four analyses of each historic material were made depending on sample size.

6.1.2.7 SEM-EDX

BSE imaging of the surfaces of a selection of historic and modern iron-tannate dyed organic materials was undertaken using a Hitachi VP-SEM S-3700N (30Pa) operated at 20 kV and an approximate 12.5 mm working distance. Images were taken of representative areas of each sample at $\times 25$, $\times 150$, and $\times 500$ (sometimes of two separate areas). Elemental analyses of surface deposits on the samples were collected in 50 s using an Oxford Instruments energy dispersive X-ray analyser and INCA software. The data from these analyses are qualitative only due to the lack of a calibration method for these materials.

6.2 Results and Discussion

When comparing historic iron-tannate dyed materials with the model iron-tannate dyed textiles from this project it is important to remember that it is highly unlikely the results will be exactly the same. Even when comparing a historic iron-tannate dyed cotton sample with the dyed cotton model textiles from this project, there will be variations in material type, dye type, storage conditions, treatment history, and handling in addition to differences due to natural ageing compared to accelerated ageing. The lack of knowledge regarding the history of the historic object (storage, treatment, usage), particularly prior to acquisition by the British Museum, means that even if the dyed textile was replicated perfectly, exactly the same extent of degradation may not be achieved with either natural or accelerated ageing. Consequently, when comparing the model textiles of this project with historic examples, if the properties of the model textiles are in the vicinity of those of the historic textiles then they are considered a valid substitute for historic materials in the stabilisation studies of this project.

6.2.1 XRF

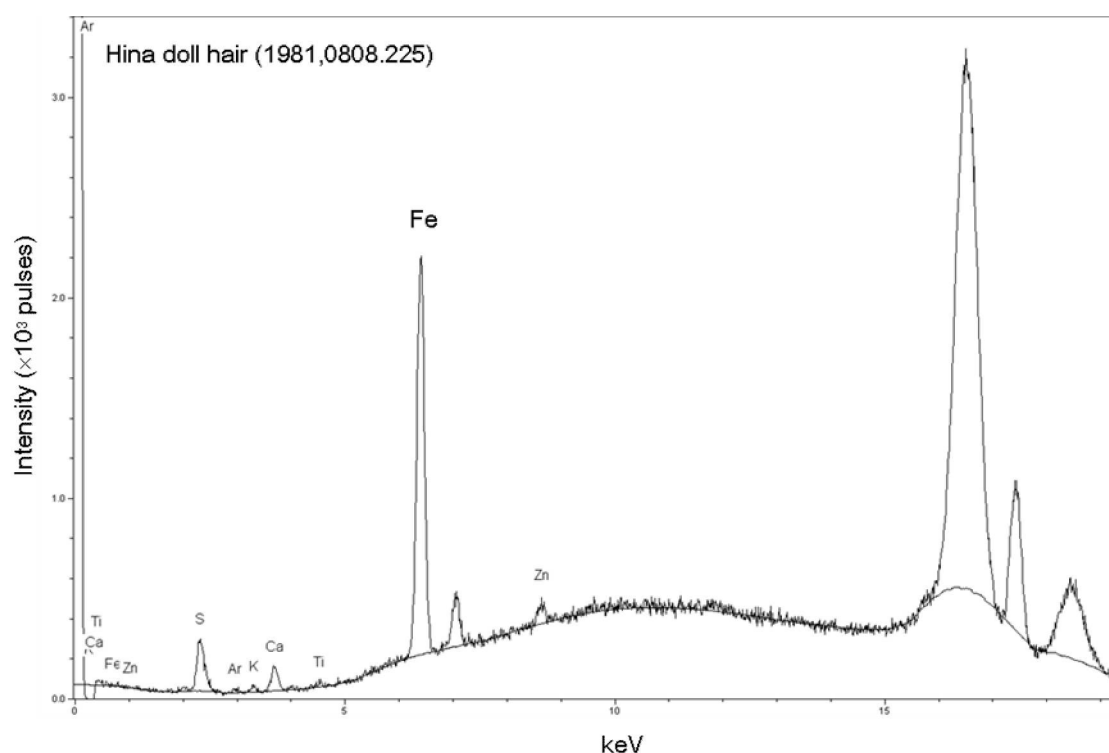


Figure 6.1 XRF spectrum of silk hair from a Hina doll in the British Museum's collection

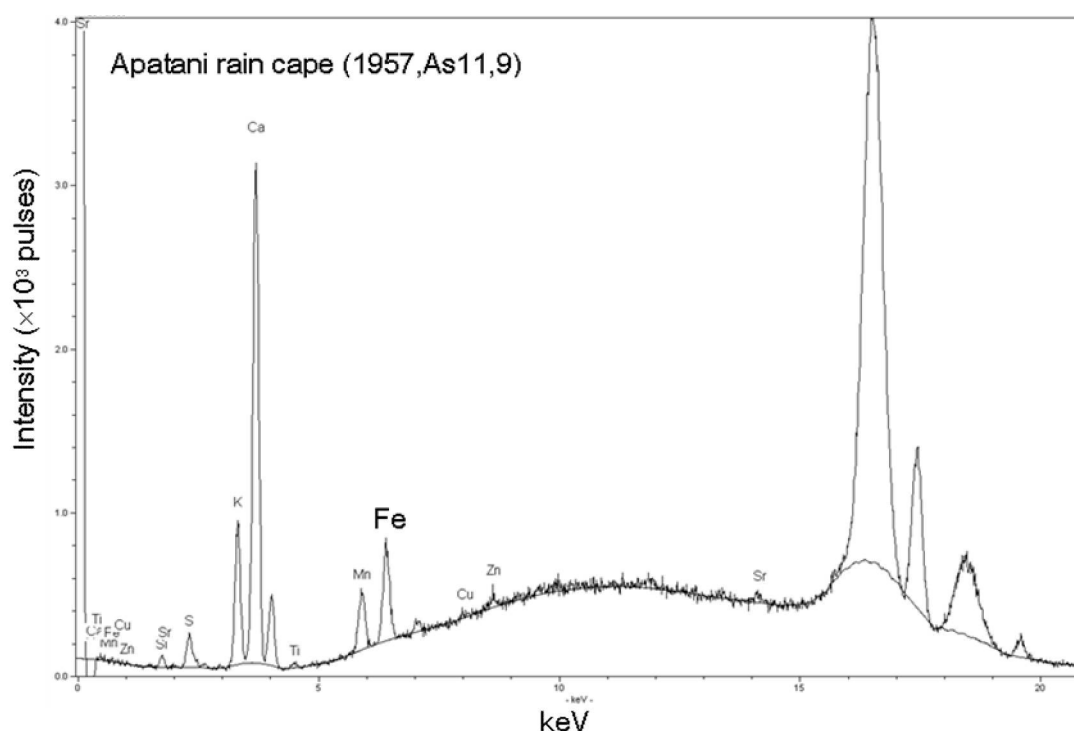


Figure 6.2 XRF spectrum of a cellulosic sample from an Apatani rain cape in the British Museum's collection

All of the model iron-tannate dyed textiles from this project have an iron level of '+++'. Consequently, objects containing black, grey, or brown dyed areas with iron levels of '+++ or greater are highly likely to be iron-tannate dyed. Examples of such objects include the Akali Sikh turban (2005,0727.1) (Pullan and Baldwin 2008), the 19th century banana belt (no registration number) (Cruickshank and Morgan 2011), and the 6371 Egyptian basket, other iron-tannate dyed example of which have been identified (Wills and Hacke 2007) (Table 6.2). Additionally, objects such as the modern and historic piu piu which are known to be iron-tannate dyed due to the method of colouration being well documented had comparable or higher levels of iron than the dyed model textiles. Black, brown, or grey areas of objects that had an iron level of '++' e.g. the Japanese hina doll (1981,0808.225) (Figure 6.1), the original wool from the Axminster carpet (TC920D3), and the Islamic carpets (KGM1886,500, KGM1875,111, and I.0072/62) are likely to be iron-tannate dyed. Those that had iron levels of '+' may be iron-tannate dyed but it is most likely that they are if they are also in poor physical condition i.e. brittle and weak, for example the Apatani rain cape (1957,As11,9) (Figure 6.2) and striped textile from Madagascar (Af,SLMisc2105). Objects with an iron level of '-' e.g. many of the samples from the Axminster carpets, contemporary wool used in modern Axminster carpets, and

6.2 Results and Discussion

restauration wool used in the conservation of carpets at The Tetley Workshop, are not considered to be iron-tannate dyed as they had iron levels comparable to background iron levels in the undyed model textiles.

Significant levels of copper were also identified in some of the samples (Table in Appendix 6), most notably: the beige areas of the Kuba cloth from the C&M handling collection, the light brown samples of Am1933,1216.4 (an Andean textile), the lining of an Islamic helmet (1881,0802.158), black lining of horse chain mail (no registration number), and the brown wool from Islamic carpet I.5526. The copper XRF ratios of the p2 and c2 model textiles ranged from 83 to 371. The model textiles therefore have similar and in some cases lower copper content than the historic examples stated above.

Following the XRF results, a selection of objects that are likely to be iron-tannate dyed were analysed using spectrophotometry, surface pH testing, bathophenanthroline testing, SEM-EDX, EPR, and GPC-MALLS.

6.2 Results and Discussion

Table 6.2 Semi-quantitative XRF analysis of iron in black or brown areas of British Museum and other objects

British Museum registration number	Name	Iron XRF concentration ^a	Other registration number	Name	Iron XRF concentration ^a
1881,0802.48 P+E	Gorget/breast-plate/back-plate	++++	NA	Model iron-tannate dye precipitate	++++
1909,5,19,8	Printing brush	++	NA	Model iron-tannate dyed raffia	+++
1957,As11,9	Black Apatani rain cape	+	NA	Historic piu piu	++++
1979,Af,1,2397	African mask	+	NA	Modern piu piu	+++
1981,0808.225	Hina doll hair	++	<i>Museum of Islamic Art carpet samples (supplied by Anna Beselin)</i>		
6317	Egyptian basket	+++	I.0007/62	Islamic carpet	+++
21789	Coptic textile	-	KGM1880,919	Islamic carpet	+++
43369	Black and cream Egyptian textile	+	KGM1882,707	Islamic carpet	+++
Af1938,1004.13	African mask	++	I. 5526	Islamic carpet	+++
No number	Horse chain mail with black lining	+++	KGM1900,55A	Islamic carpet	++
M4-S-22 37119	Black and white textile	+	KGM1885,248a	Islamic carpet	+++
M4-S-22 37129	Black and beige strip of woven textile	+	I.0072/62	Islamic carpet	++
OA+7279	Saddle	+++	KGM1882,703	Islamic carpet	++
Thailand Siam Royal Cypher Medal 1926	Medal	+	KGM1875,197	Islamic carpet	+++
Af1818,1114.23	Adinkra (mourning cloth)	+++	I. 0001/64	Islamic carpet	++
1881,0802.158	Islamic steel helmet (lining)	+++	I. 0041/70	Islamic carpet	++
1904_282	Loin cloth of banana or hibiscus fibre	++	KGM1886,500	Islamic carpet	++
1906-0524-8, Oc1906,0524.8	Belt worn by a chief "Tol"	+++	KGM1875,111	Islamic carpet	++
1936_1211_5	Machine woven adinkra cloth	++	KGM1883,522	Islamic carpet	-
Am1937,0617.1	North American skin bag	++++	KGM1885,247	Islamic carpet	-
Am1933,1216.3	Andean textile	-	KGM1889,150	Islamic carpet	-
Am1933,1216.4	Andean textile	+	<i>Axminster carpet samples obtained on visit to Tetley Studios, Saltram House, and the Axminster Factory</i>		
Am1934,0714.2	Andean textile	+	TC920D3	Axminster carpet in Tetley Studio (original wool)	++
Am1934,0714.8	Andean textile	+	TC920D3	Axminster carpet in Tetley Studio (restoration wool)	-
H279	African woven textile	+++	NA	Appletons brown groundings 584 dyed wool used in carpet conservation	-
H288 5J	African woven textile	+++	NA	Axminster carpet from Saloon of Saltram House (original wool)	-
H290 9C	African woven textile	++++	NA	Axminster carpet from Saloon of Saltram House	+
As1957,11.10 (from the C&M handling collection)	Kuba cloth	+++	NA	Axminster carpet from Saloon of Saltram House (restoration wool)	-
Oc4253, Oc1866C1.4253, and Oc1866E6.54	Decorated tiputa (poncho) made from tapa, bark cloth.	+	NA	Axminster carpet from Saloon of Saltram House	-
Oc9954A, Oc1876C1.19954, Oc1876C1118.7, and Oc1876E6.63	Barkcloth two layer garment (possibly mourning dress)	+++	NA	Axminster carpet from the dining room at Saltram House	-
SLM2105, 1. Af,SLMisc2105	Colourful striped woven textile from Madagascar	+	NA	Axminster carpet from the dining room at Saltram House	-
2005,0727.1	Akali Sikh turban	+++	NA	Axminster carpet from Saloon of Saltram House	-
No number	19th Century banana fibre belt from the Caroline Islands	++++	NA	Wool from Axminster Factory	-

Note for Table 6.2:

6.2 Results and Discussion

- a. Categories of iron content were determined from XRF ratios as followed: ‘-’ for ratios of 30 or less; ‘+’ for ratios of 31-200; ‘++’ for ratios of 201-500; ‘+++’ for ratios of 501-3000; and ‘++++’ for ratios > 3000. These levels were based around the iron XRF ratios of the model textiles.

6.2.2 Spectrophotometry

All of the historic materials tested show the broad absorption of visible wavelengths that is seen in iron-tannate dyed textiles, particularly aged textiles. Increased reflectance in the red region of the visible spectrum with age has been demonstrated with the chemically similar iron gall inks on paper (Sistach, Gibert and Areal 1999) and traditionally dyed New Zealand flax (Te Kanawa, Thomsen, Smith, Miller, Andary and Cardon 1999) and is associated with the breakdown of the iron-tannate complex and formation of brown degradation products (Section 4.1.5). It also occurs with the dyed cellulosic model textiles on ageing, as demonstrated in Figure 6.3. It is clear from these reflectance spectra that the four week aged Cc1 and Ac1 rather than the unaged Cc1 and Ac1 are the most similar to the reflectance spectra of the dyed iron-tannate dyed objects analysed. This suggests that the iron-tannate dyed model textiles discolour similarly to the historic iron-tannate dyed objects with age.

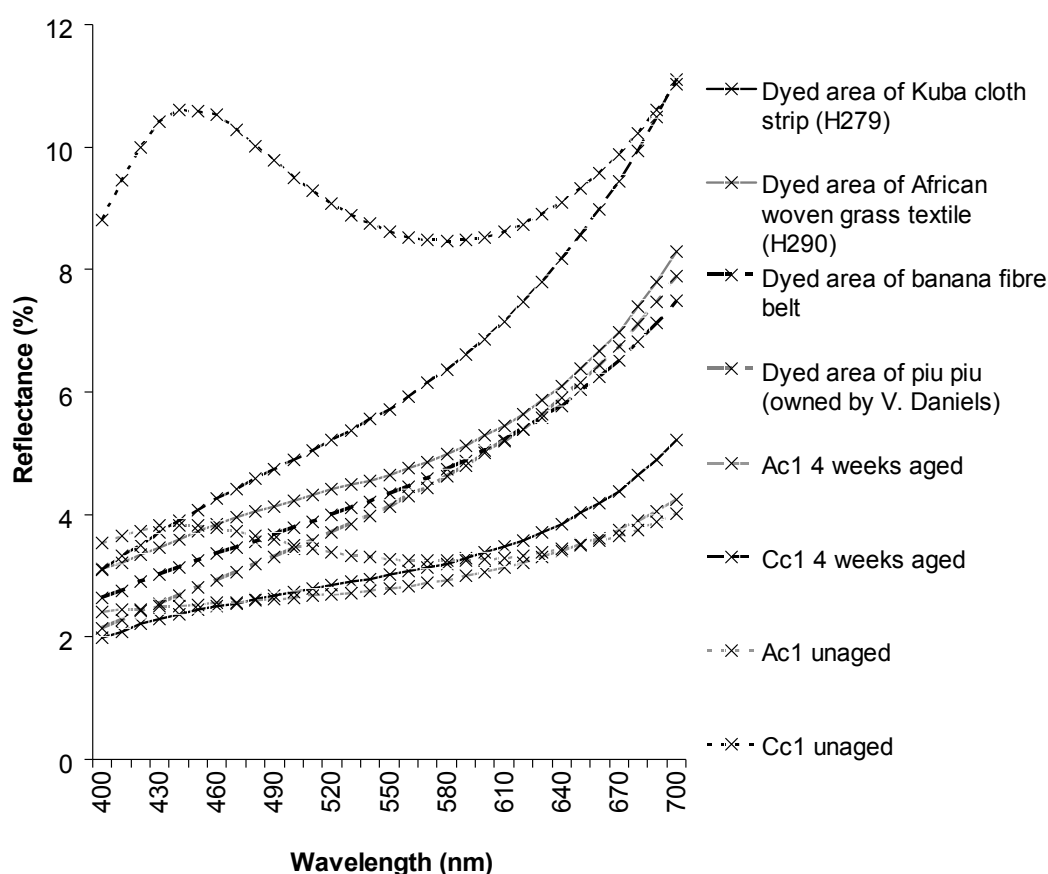


Figure 6.3 Reflectance spectra of iron-tannate dyed cultural heritage compared to aged (80°C and 58% RH) and unaged model textiles

6.2.3 Bathophenanthroline testing

The dyed areas of the historic objects analysed contained unbound iron while the undyed samples contained undetectable or only slightly detectable levels of unbound iron (Table 6.3). In many cases, significant quantities of unbound ferric as well as ferrous ions were present. Unbound iron ions were present in the dyed cellulosic model textiles to a similar extent as in the dyed historic materials (based on the colour chart (Vuori and Tse 2005a)). The large difference in colour between the different categories on the colour chart prevents further detailed comparison between the samples.

Table 6.3 Results of bathophenanthroline testing and XRF on a selection of historic iron-tannate dyed cellulosic materials and cellulosic model textiles

Historic/model textiles	Sample	Dyed/undyed	Unbound iron content (ppm) ^b		Total iron content (XRF ratio)
			Fe ²⁺	Fe ²⁺ and Fe ³⁺	Mean (SD) ^c
Historic	Piu piu/Maori cloak ^a	Dyed	10	25	5924
	H279 9C	Dyed	10	10	767
		Undyed	<1	<1	418
	H290 9C	Dyed	10	10	2844
		Undyed	0	0	74
	H288 9C	Dyed	<1	10	542
		Undyed	0	<1	204
Model iron-tannate dyed textile	CU	Undyed	0	0	15 (1)
	Cc1	Dyed	10	10	683 (145)
	Cc2	Dyed	0	10	742 (41)
	Cc3	Dyed	10	10	1115 (44)
	AU	Undyed	0	0	24 (5)
	Ac1	Dyed	10	25	1459 (338)
	Ac2	Dyed	1	10	1490 (190)

Notes for Table 6.3:

a. From the Horniman Museum's collection. The sample was provided by Louise Bacon;

b. Estimated content of unbound iron ions based on the bathophenanthroline test paper and colour chart (Vuori and Tse 2005a);

c. Mean ratio with standard deviation in parentheses if more than one area was analysed.

6.2 Results and Discussion

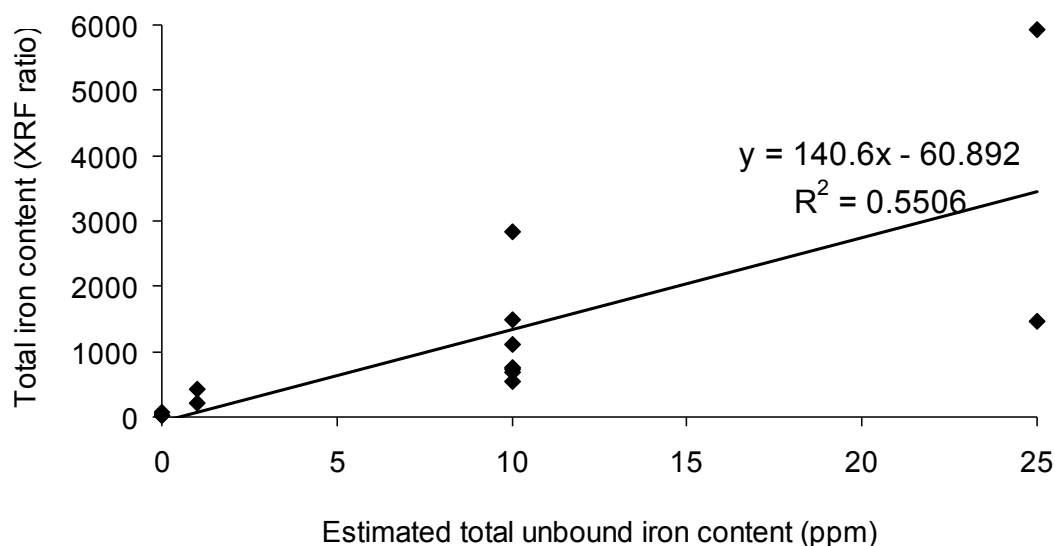


Figure 6.4 The correlation between XRF and bathophenanthroline test data of historic iron-tannate dyed and undyed textiles and model iron-tannate dyed and undyed cellulosic textiles

Comparison of the bathophenanthroline data with the XRF ratios suggests a positive correlation between total unbound iron content and total iron content within the sample. This correlation can be calculated using the formula of the best fit line in Figure 6.4 but this is a relatively unreliable calculation since there is only a 55% probability of calculating the correct answer. This unreliability may be due to: the subjectiveness of the bathophenanthroline test; natural variation iron content throughout the model textiles; changes in unbound iron content due to sample age, or washing or treatment of the sample; and the low resolution of the test which could for example, result in samples with unbound iron levels of 5 – 18 ppm being grouped together at 10 ppm.

Since the quantity of bound iron is not calculated in these techniques, a ratio of bound to unbound iron cannot be determined. EPR may prove more useful in this type of analysis.

6.2.4 EPR

The historic textiles tested were taken from a heavily degraded piu piu or Maori cloak samples that were supplied by Louise Bacon from the Horniman Museum; raffia from an African mask (1979 Af1.2397); and lining fabric (unknown fibre type) from horse armour. The first two samples are most similar to the dyed abaca samples from this project due to the higher non-cellulosic content compared to cotton.

6.2 Results and Discussion

In both the historic textiles and the model textiles, iron was detected bound in an octahedral environment as well as unbound and/or in a tetrahedral environment (indistinguishable) (Figure 6.5). The radicals present were also of similar type and indicate the presence of semiquinones and related compounds e.g. phenolics such as tannates, gallates, and lignin derivatives. Therefore it appears that the model textiles are comparable to the historic iron-tannate dyed objects in terms of the type of iron(III) binding and type of radicals present.

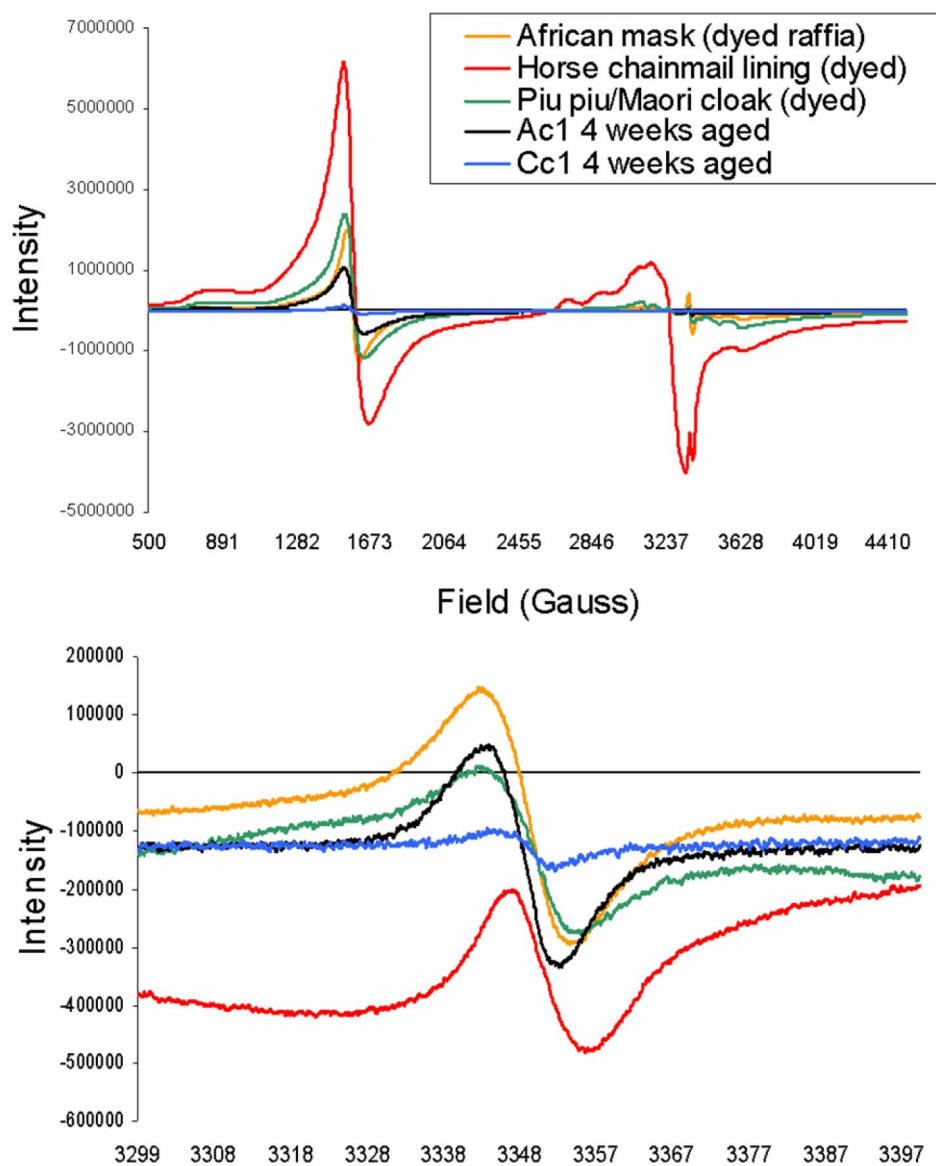


Figure 6.5 EPR spectra (upper image) of historic iron-tannate dyed materials and accelerated aged (80°C, 58% RH) Ac1 and Cc1 model textiles with close-up of the radical section of the spectra (lower image)

6.2.5 GPC-MALLS

Both historic samples were very fragile and low quantities of the materials led to noisy spectra (Figure 6.6). Consequently the molecular weight distribution of these samples was not included in Table 6.4 as they were thought to be unreliable. Significant acid hydrolysis has occurred in the historic samples which is demonstrated not only by the low M_n and high PDI (indicative of extensive depolymerisation), but also by the high carbonyl content, particularly the REG content. The turban sample was tested for surface pH and identified as being of pH 3.4 \pm 0.0. This acidity will have contributed to continued degradation of the material by acid hydrolysis and metal ion catalysed oxidation.

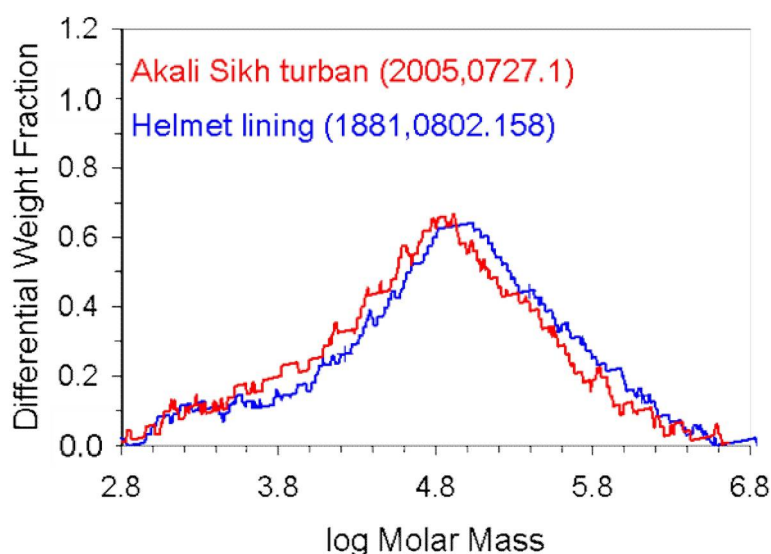


Figure 6.6 The molar mass distribution of two historic cotton samples from the British Museum

Table 6.4 Molecular weight and carbonyl content of samples from two British Museum objects compared to a severely degraded dyed cotton model textile sample

Sample	DP _n	Average molecular weight		PDI	Theoretical amount of reducing end groups (oxidised groups) (μmol/g)	Overall carbonyl content (μmol/g)
		M _n (kg/mol)	M _w (kg/mol)			
Ccl unaged	565	92	469	5	11 (10)	20
Ccl 3s	223	36	265	7	28 (22)	50
Ccl 4s	215	35	223	6	29 (46)	74
Turban	86	14	187	13	72 (-7.5)	64
Helmet	102	17	244	15	61 (-6)	54

6.2 Results and Discussion

The carbonyl content of both objects is comparable to the carbonyl content of 3 or 4 week aged (80°C and 58% RH) Cc1 from this project. However based on the REG calculation the historic textiles have undergone primarily hydrolysis while oxidation has contributed significantly to the degradation of the model textiles (particularly by 4 weeks of ageing). Based on these results, their significantly lower molecular weights and significantly larger quantity of low molecular weight molecules, which cause an increase in PDI, it is likely that the historic textiles were weaker than the four week aged model textile.

6.2.6 Surface pH testing

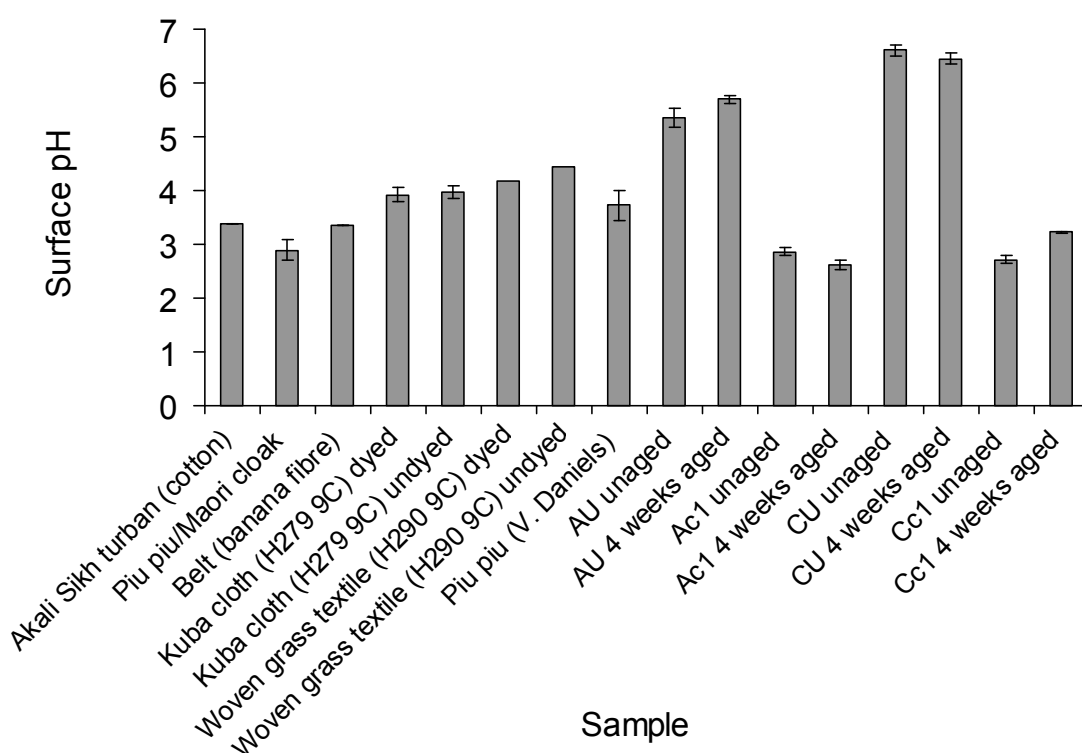


Figure 6.7 Comparison between the surface pH of some historic iron-tannate dyed materials and aged and unaged cellulosic model textiles. The piu piu/Moari cloak samples were provided by Louise Bacon from the Horniman Museum.

Dyed and undyed areas of the same object were analysed when available for direct comparison. However in several cases the form of the sample e.g. the curved surface of an undyed area of piu piu or Maori cloak made reliable analysis with the surface pH electrode impossible. For those objects that did have undyed and dyed areas analysed, the pH of each was similar, unlike with the undyed and dyed model textiles. This similarity may be due to

contamination from the dyed material of the same object or from handling of the objects, or be due to the production method.

The surface pH values of aged and unaged cellulosic model textiles have been illustrated in Figure 6.7 in order to compare with the cellulosic historic materials analysed. It was not expected that the model textiles would have the same pH as historic materials of similar or same material type, since the formulation of the dyes is unknown and likely to be different to those used for the model textiles. Additionally, the history of the storage and treatment of these objects is unknown. The washing of an object could have removed much of its acidity giving a surface pH that is greater than it would have been had it not been washed. Consequently, the fact that the dyed model textiles are typically within 1.5 pH units of the surface pH of historic materials of similar or same material type is sufficient for the model textiles to be classed as having similar pH properties to historic British Museum iron-tannate dyed objects. In this study the dyed model textiles were more acidic than the dyed historic materials.

6.2.7 SEM-EDX

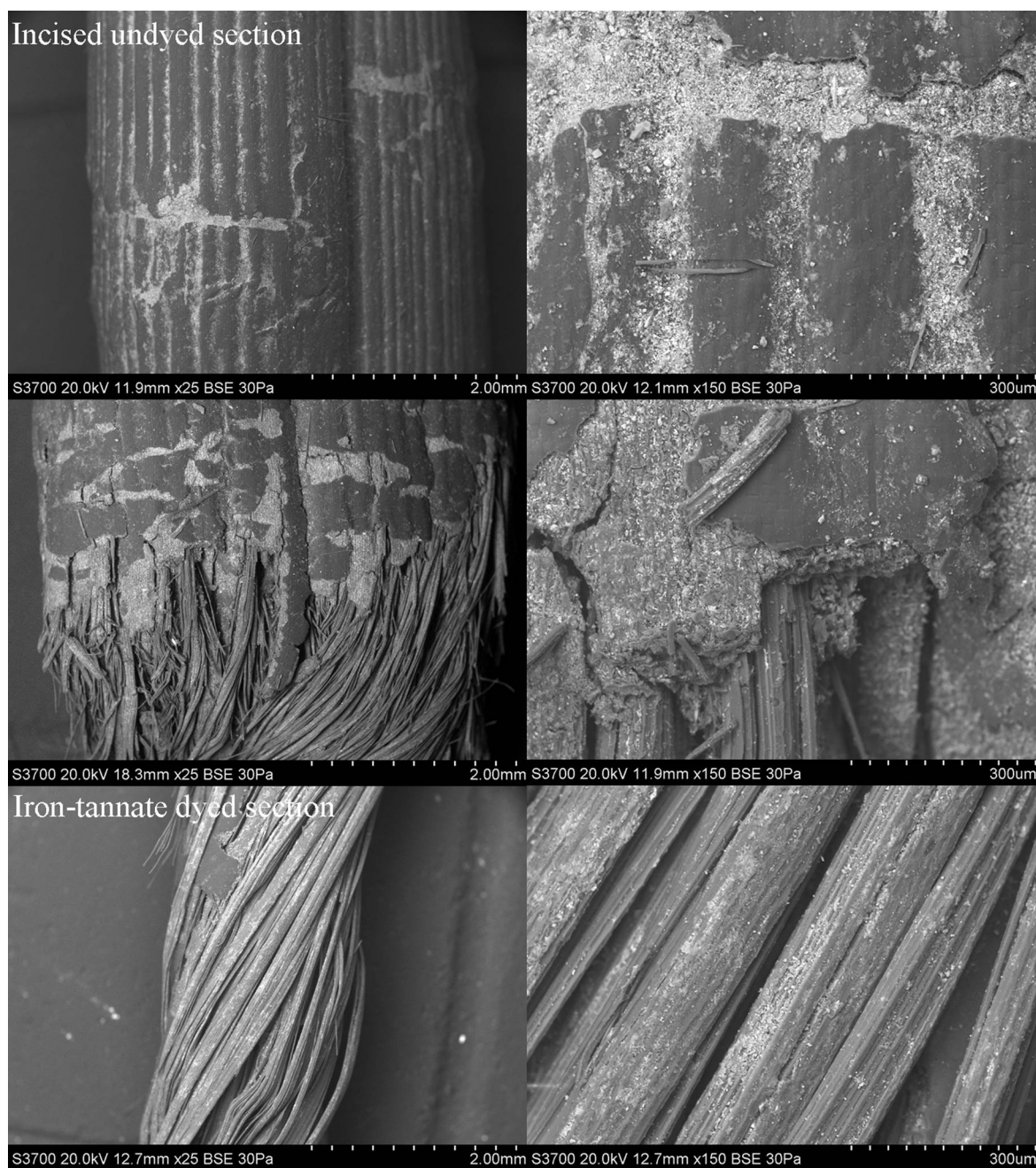


Figure 6.8 SEM micrographs at $\times 25$ and $\times 150$ magnifications of undyed and dyed sections of a broken piece of historic New Zealand flax piupiu or Maori cloak from the Horniman Museum (provided by Louise Bacon)

6.2 Results and Discussion

Analysis of the surface of the New Zealand flax showed that the undyed region (the upper and middle micrographs in Figure 6.8) had fewer higher atomic mass deposits (white appearance on the micrographs) than the dyed region. EDX analysis of these deposits (Figure 6.9) confirms their high iron content which, when the fact that the dyed areas are brown and the iron-tannate dye production method is known (Daniels 1995), is congruent with the deposits being iron-tannate dye complexes. The areas with the least iron-rich deposits (iron-tannate dye) have a smooth surface that covers fibrous material (Figure 6.10). This is the hydrophobic outer layer of the New Zealand flax leaf that prevents dye uptake by the fibrous material. When this layer is broken and/or removed e.g. in the incision shown in the upper images of Figure 6.8 or the transition between the undyed and dyed regions in the middle images, iron-tannate dye is taken up by the fibres. In these regions other elements (Si, S, Ca, K, Mg, Al, and P) were also present which may be due to the fibre structure and to the use of iron-rich mud during the dyeing process. The fibre bundles of the abaca model textiles are similar to the fibres beneath the smooth outer layer of these New Zealand flax pieces of *piu piu*. The hydrophobic outer layer of abaca was removed during processing to form the woven fabric (Section 3.4.2).

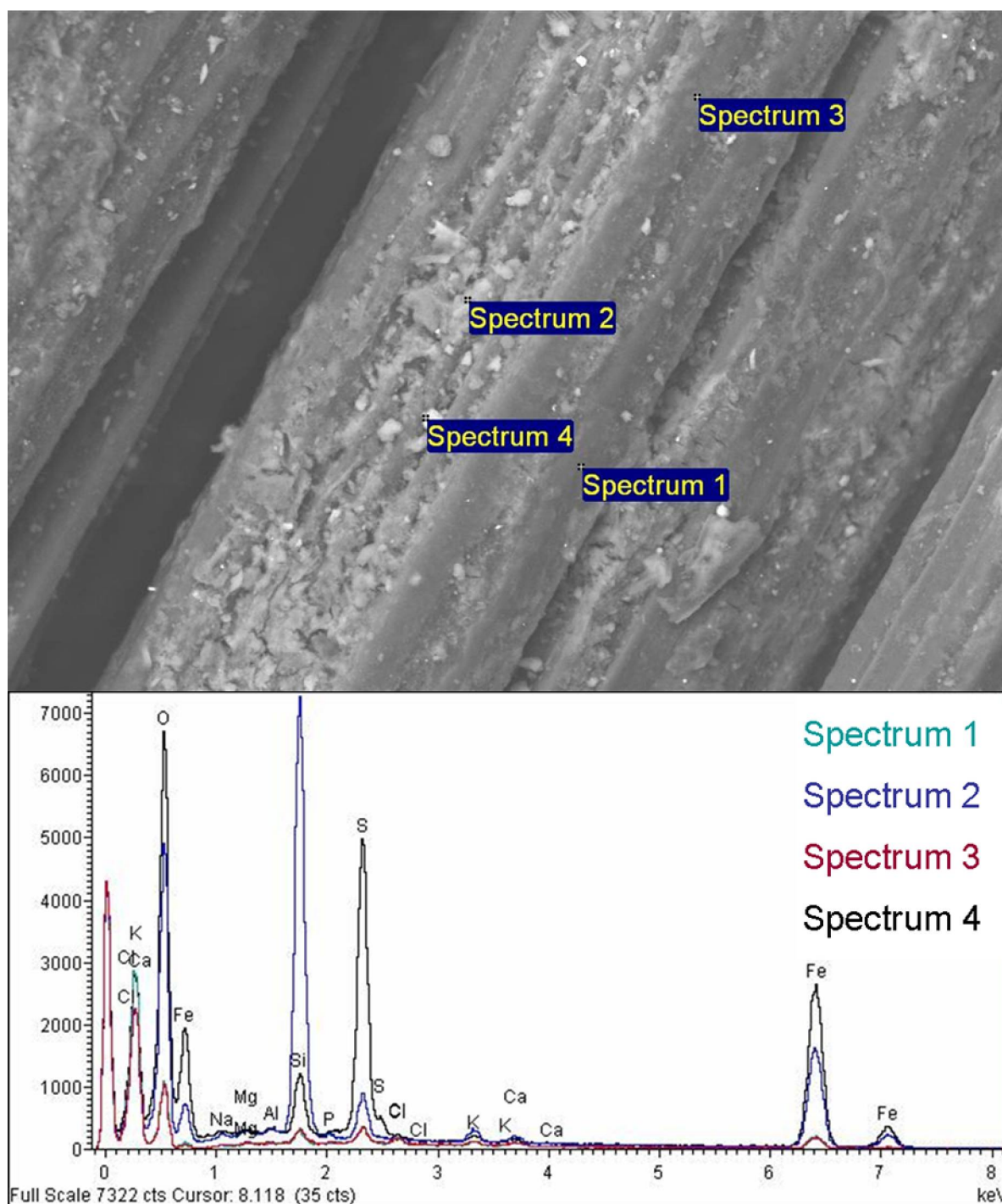


Figure 6.9 SEM micrograph at $\times 500$ magnification and EDX spectrum of the surface of a dyed section of piupiu or Maori cloak. Samples provided by Louise Bacon from the Horniman Museum.

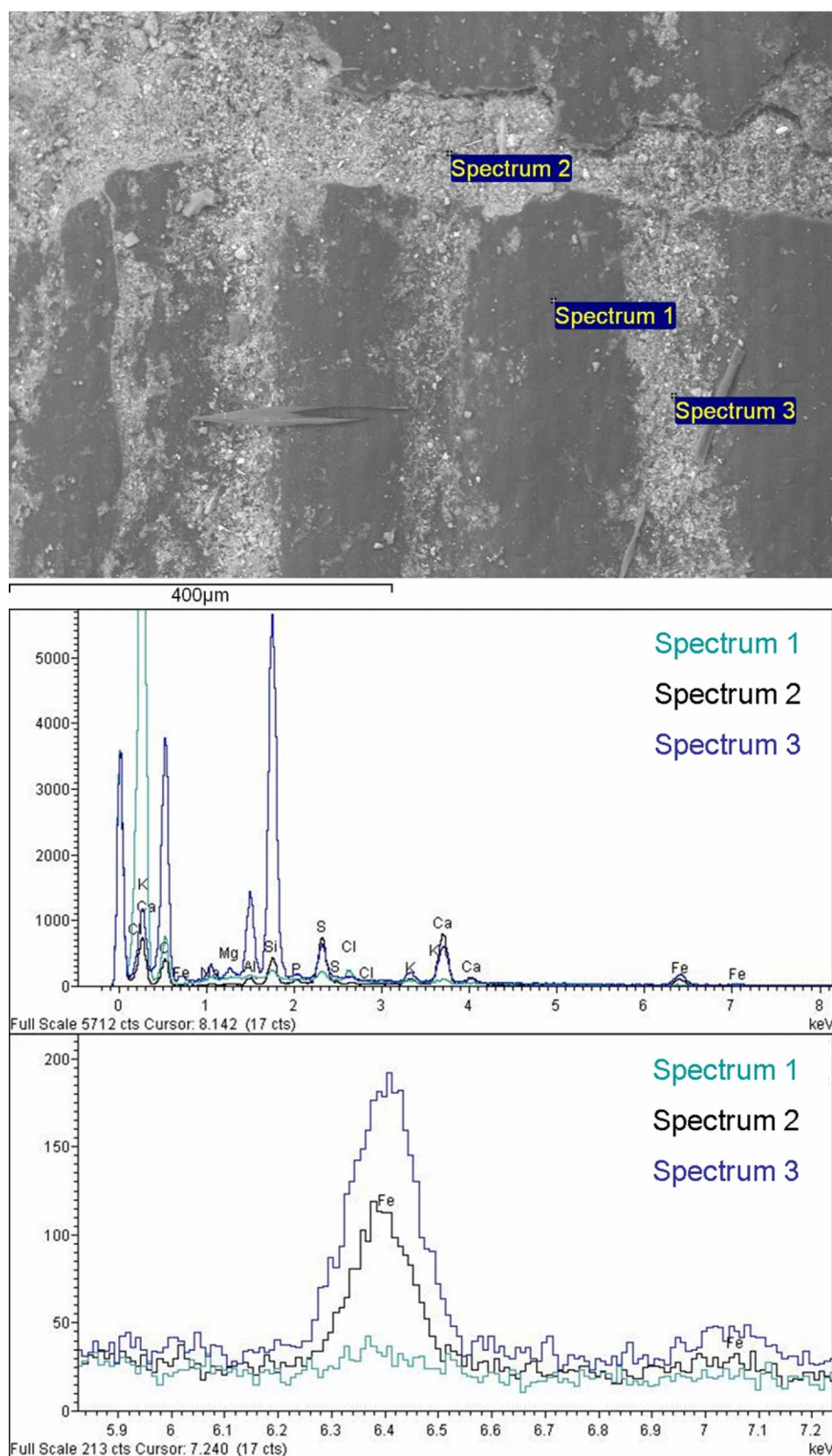


Figure 6.10 SEM micrograph and XRF spectra of point analyses of the surface of an incised undyed section of pui pui or Maori cloak at $\times 150$ magnification. Samples provided by Louise Bacon from the Horniman Museum.

6.2 Results and Discussion

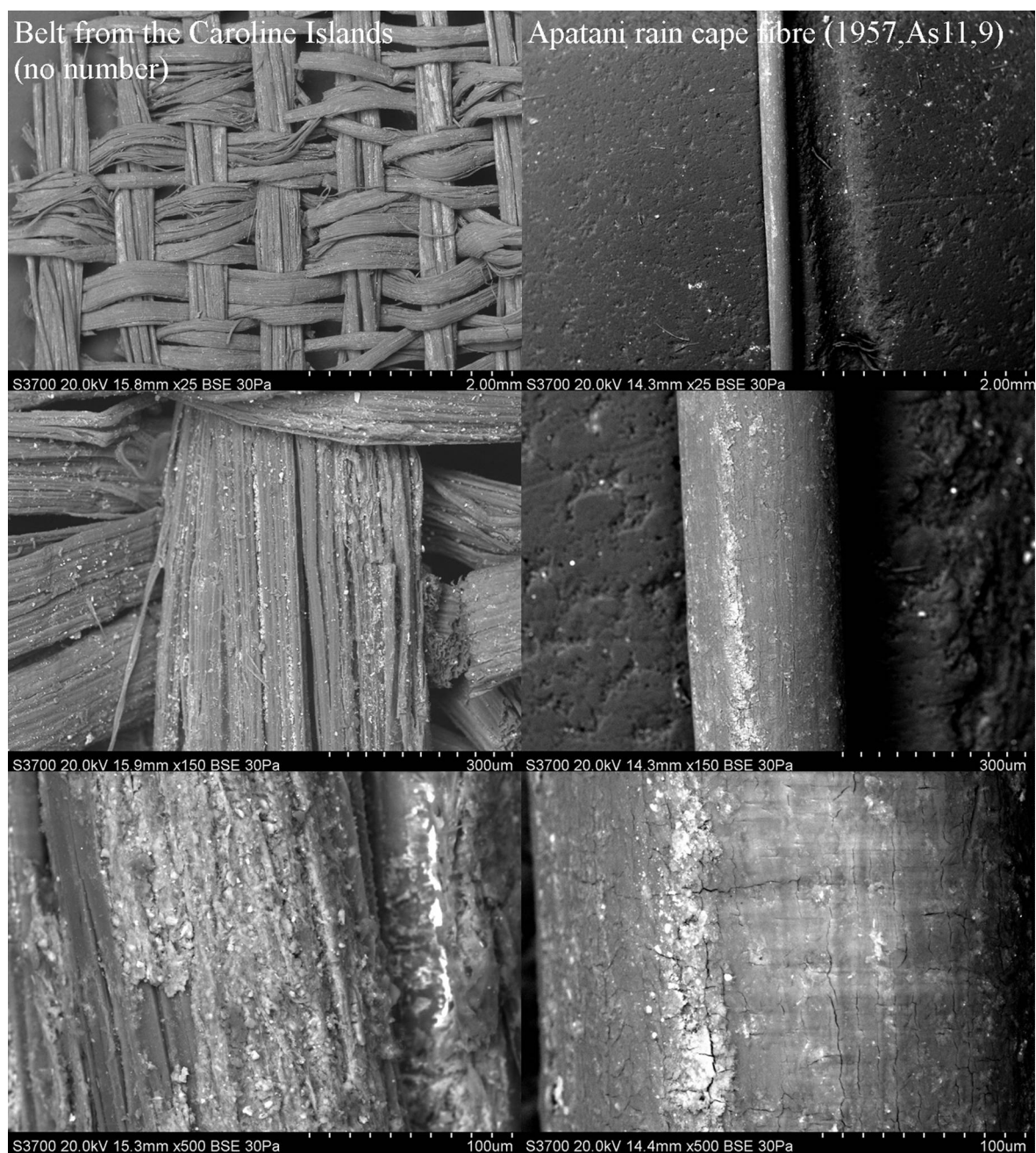


Figure 6.11 SEM micrographs of black coloured samples from a fragile banana fibre belt from the Caroline Islands (19th Century) and a fragile Apatani rain cape from the British Museum's collection

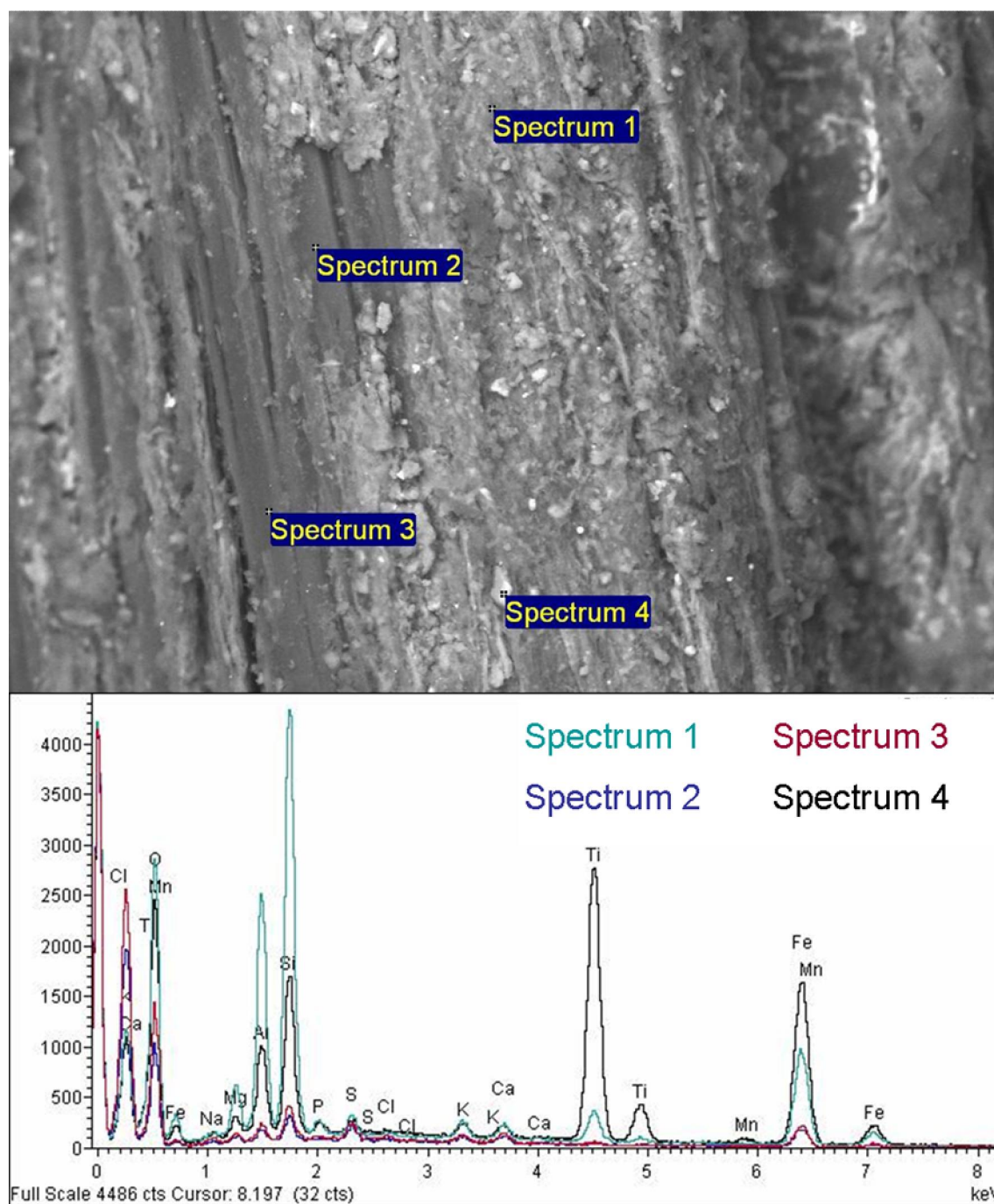


Figure 6.12 SEM micrograph and EDX spectrum of a dyed fibre from a black dyed 19th Century belt from the Caroline Islands (no registration number)

Iron-rich surface deposits were present on the fibre from the fragile black dyed belt from Oceania (Figures 6.11 and 6.12). Areas without surface deposits also contained iron but to a lesser extent than that detected in the surface deposits. The surface deposits also contained significant levels of Al, Si, and Ti, with lower levels of P, S, K, Ca, Mg, and Mn which may have arisen from the deposition of clay particles during an iron-rich mud

6.2 Results and Discussion

dyeing process. As this fibre is also abaca the SEM micrographs of the historic material are similar to those of the model iron-tannate dyed abaca (Section 5.4.6).

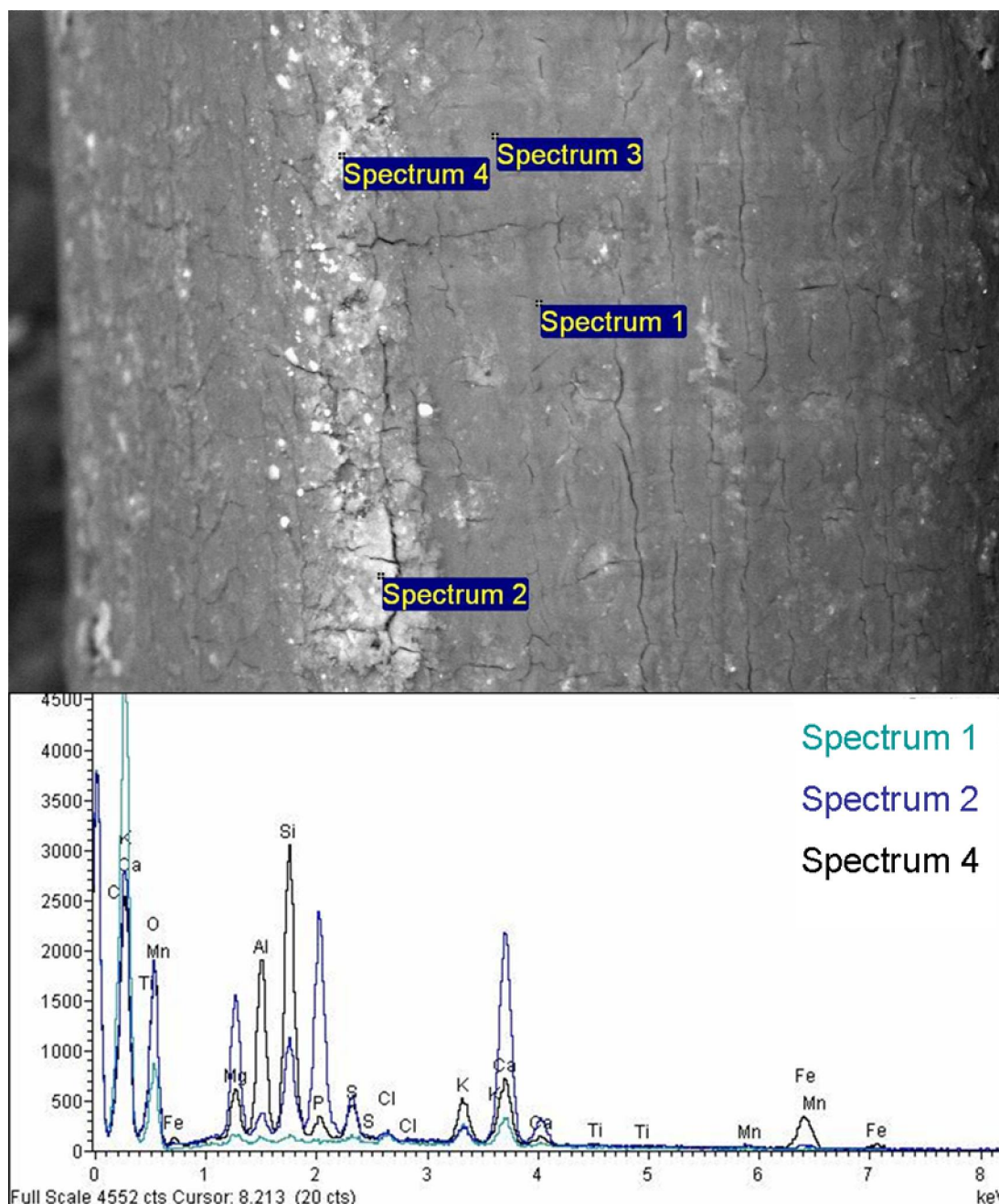


Figure 6.13 SEM micrograph at $\times 500$ magnification and EDX spectrum of a cellulosic fibres from an Apatani rain cape (1957,As11,9)

The fibres from the Apatani rain cape have minimal surface deposits (Figures 6.11 and 6.13). Where there are no surface deposits, negligible iron content was identified. Analysis of two areas in a long area of deposit identified areas of low and high iron content. The area low in iron content contained significant quantities of Mg, Si, P, S, and Ca with lower

6.2 Results and Discussion

levels of Cl, Al, and K. The area with the most iron content (Spectrum 4) also contained high levels of Si, and Al, with lower levels of Mg, P, S, K, and Ca.

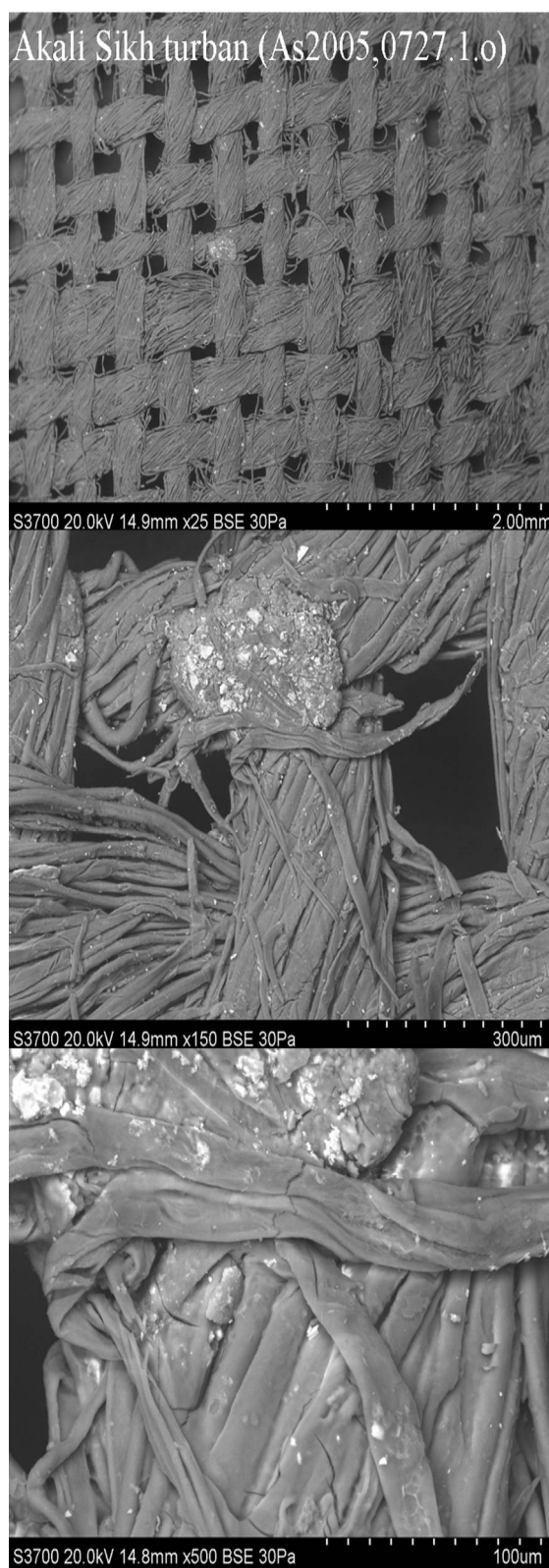


Figure 6.14 SEM micrographs at $\times 25$, $\times 150$, and $\times 500$ magnification of a piece of fragile iron-tannate dyed cotton from an Akali Sikh turban (As2005,0727.1.o)

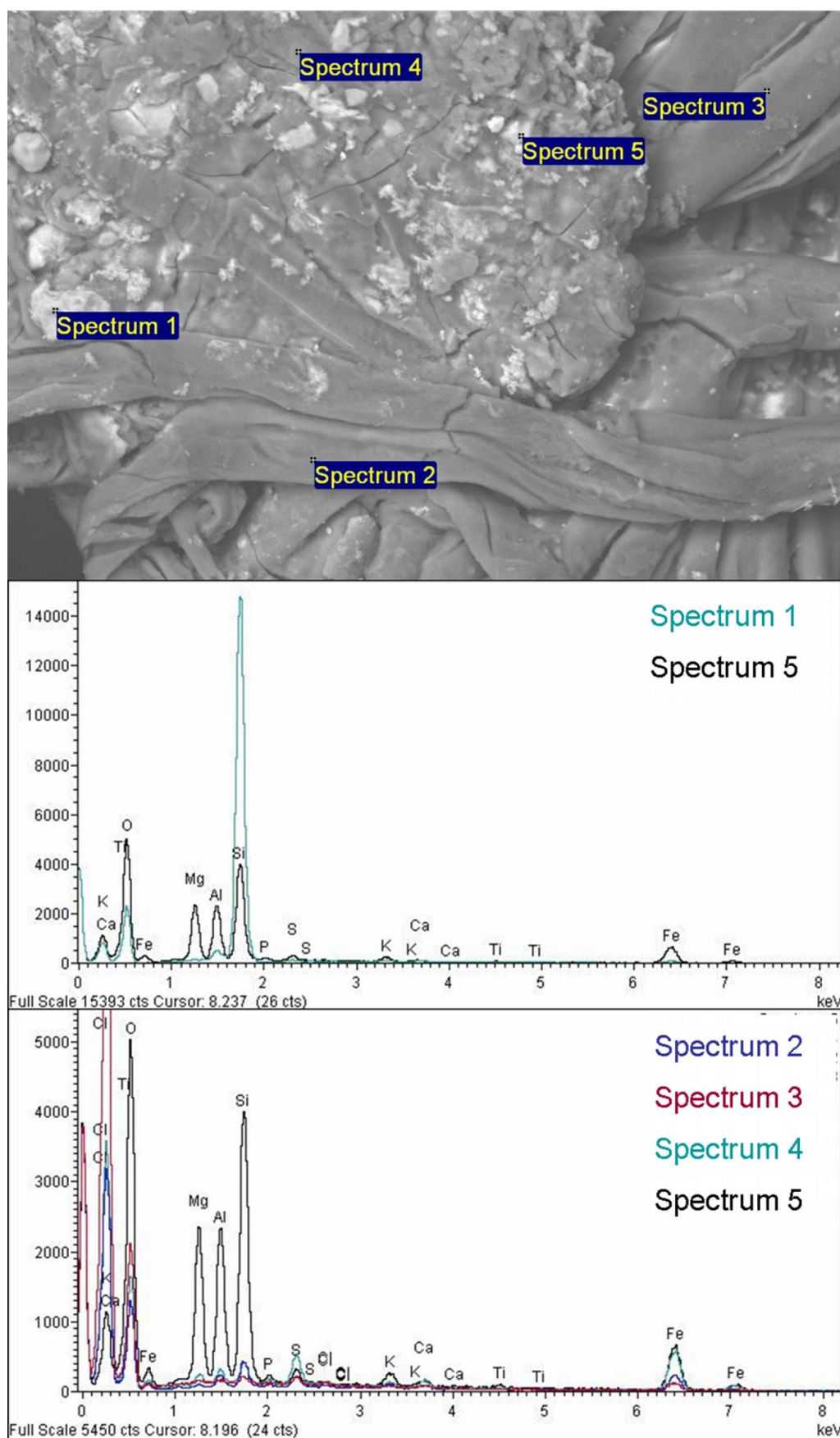


Figure 6.15 SEM micrograph $\times 500$ magnification and EDX spectra of a section of dyed Akali Sikh turban (As2005,0727.1.o)

6.2 Results and Discussion

The cotton fibres of the fragile iron-tannate dyed cotton of the Akali Sikh turban contained many surface breaks which may be indicative of the fragile nature of the fibres (Figure 6.14). The aged cotton model textile (Cc1 4s) in Section 5.4.6 did not have these surface breaks but based on the DP values determined using GPC-MALLS (Table 6.3) the aged cotton sample had a DP over twice as large as the turban. In the historic Akali Sikh turban, areas of cotton fibre without surface deposits were found to contain significant levels of iron (Figure 6.15). Analysis of various areas within a large surface deposit show that there are silicon-rich deposits with negligible iron content as well as those that include significant levels of iron. More iron was identified in the areas of the large surface deposit compared to the areas of fibres without deposits. Si, Mg, and Al were particularly prevalent in an iron-rich area on the large surface deposit. Lower levels of P, S, K, Ca, and Ti were also detected in this and some other regions.

6.2 Results and Discussion

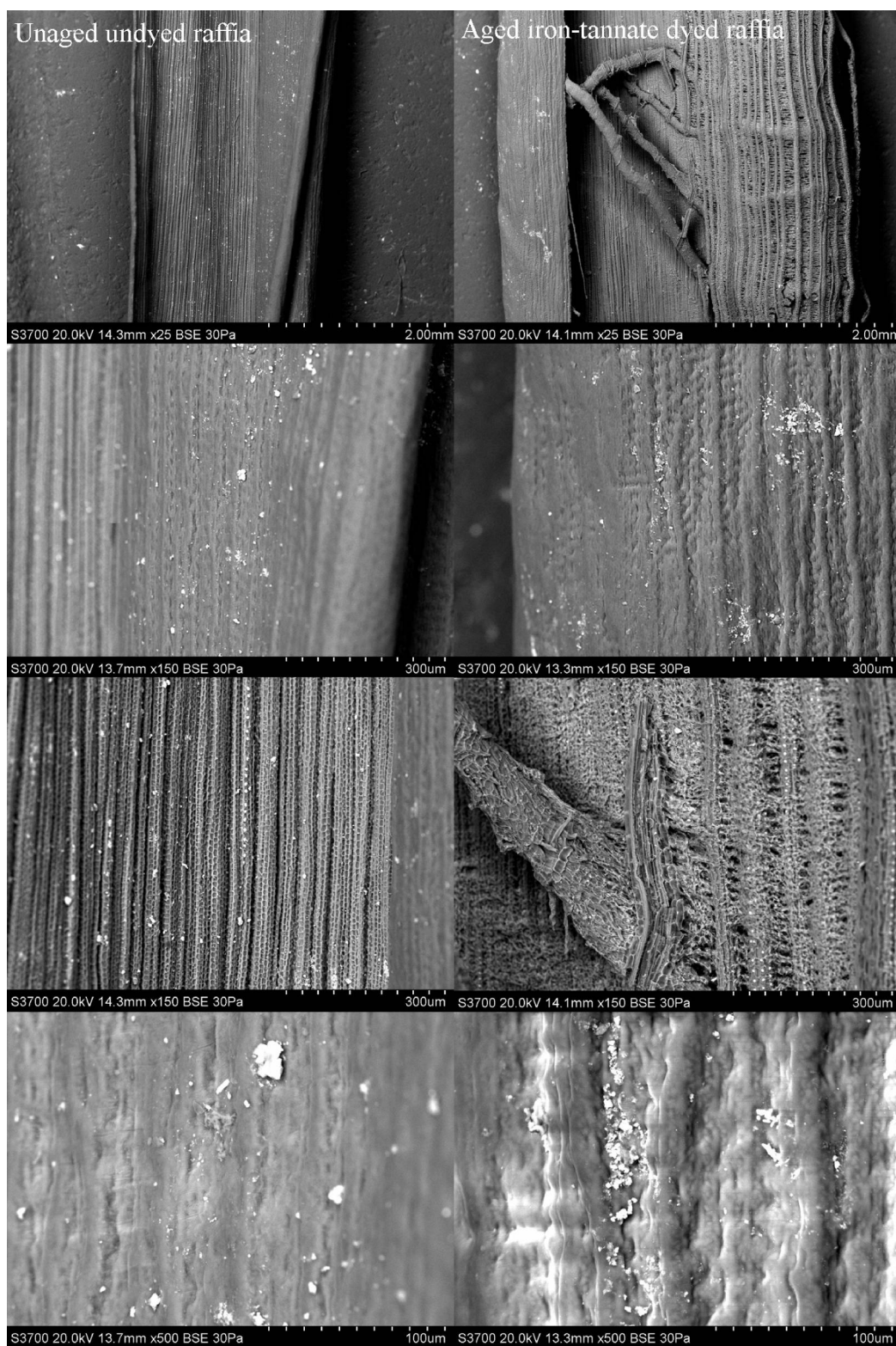


Figure 6.16 SEM micrographs at $\times 25$, $\times 150$, and $\times 500$ magnifications of unaged undyed raffia (left) and accelerated aged iron-tannate dyed raffia that was produced and supplied by Mark Sandy (Camberwell College of Arts)

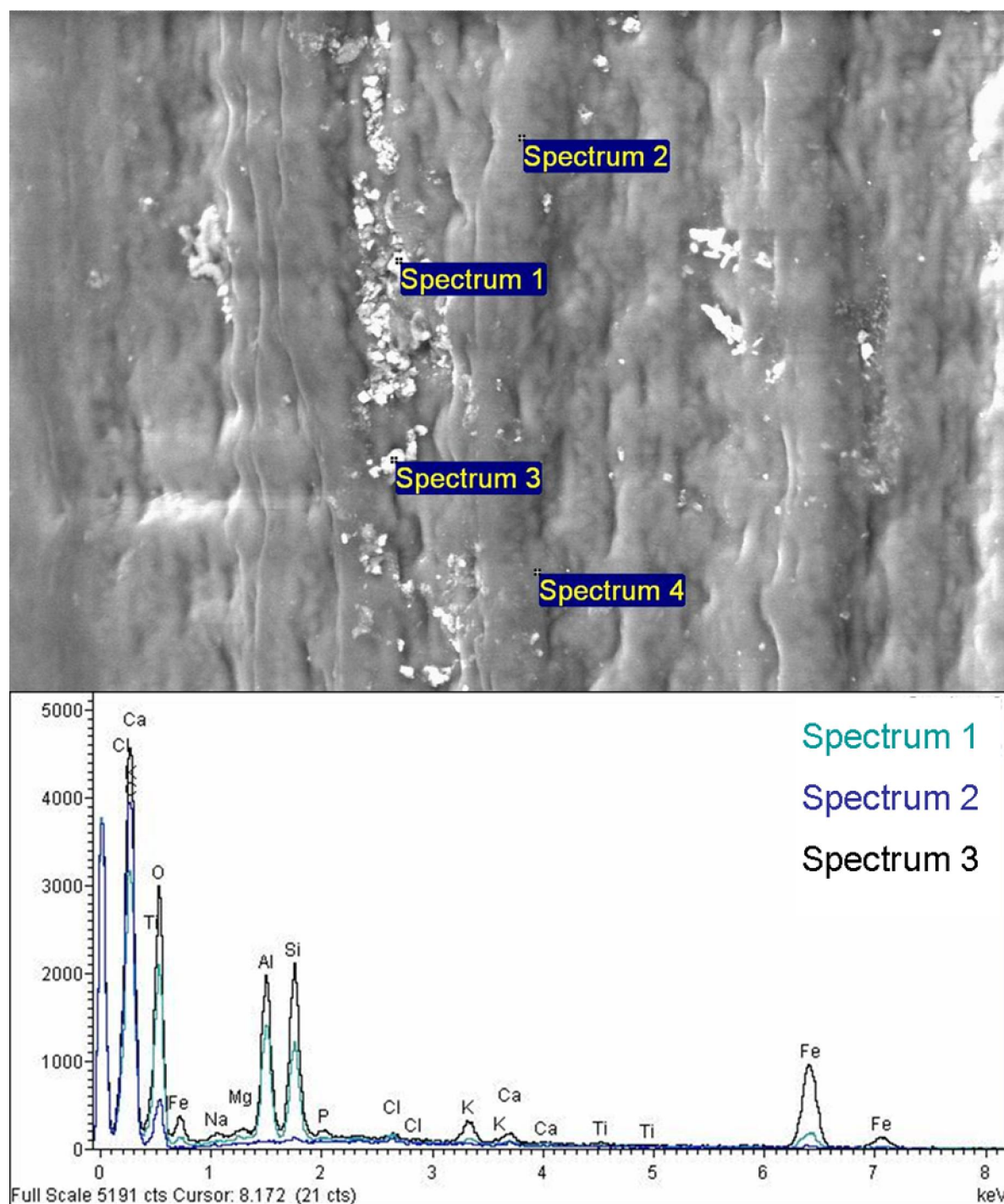


Figure 6.17 SEM micrograph at $\times 500$ magnification and EDX spectrum of an iron-tannate dyed aged raffia sample produced by Mark Sandy (Camberwell College of Arts)

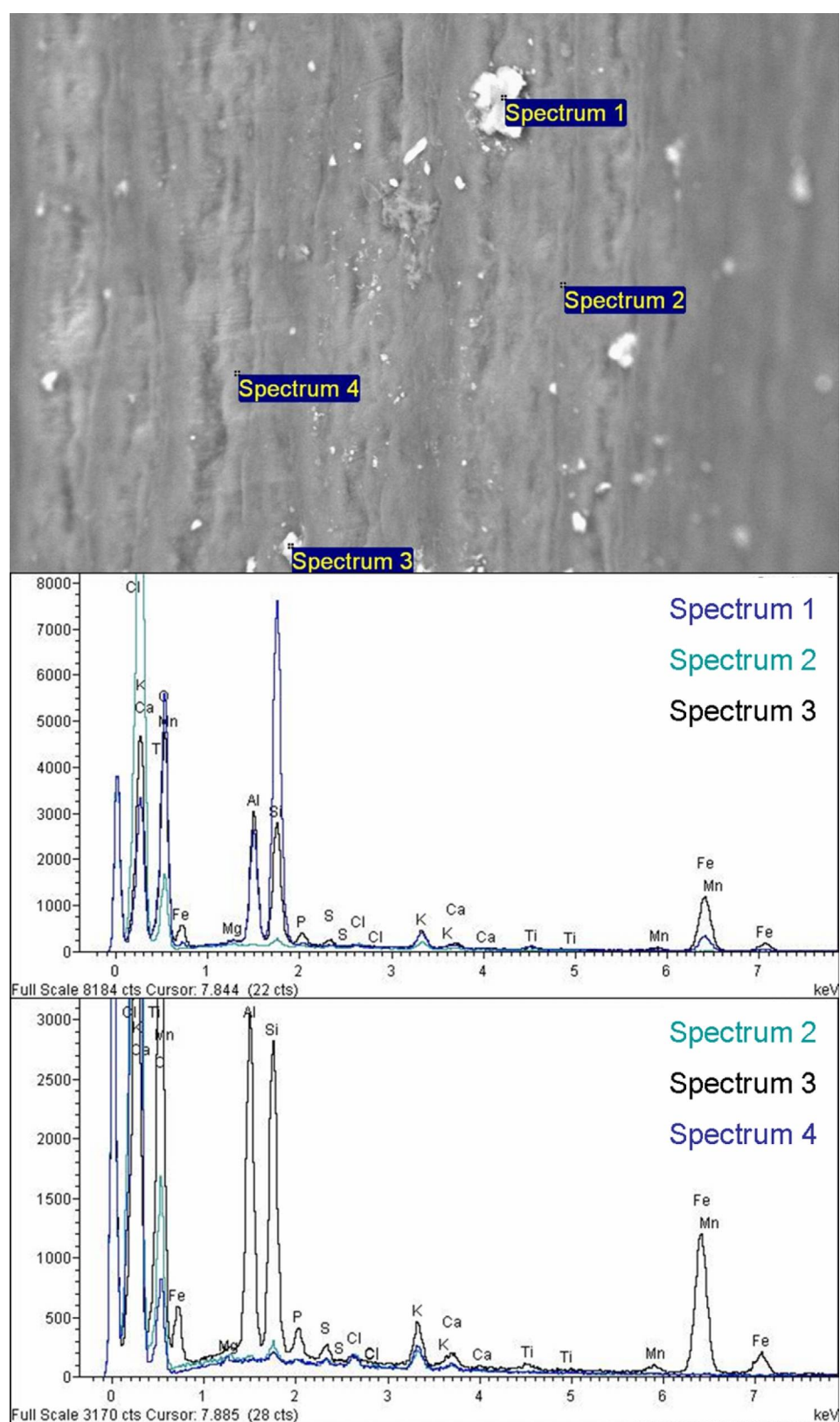


Figure 6.18 SEM micrograph $\times 500$ magnification and EDX spectra of an unaged undyed raffia sample provided by Mark Sandy (Camberwell College of Arts)

6.3 Conclusions

Slight differences in the surface appearance of the accelerated aged iron-tannate dyed raffia and the unaged undyed raffia are apparent at the $\times 500$ magnification (Figure 6.16).

However this may be due to natural variation in the surface topography and so further analysis is needed to determine how significant this difference is. The iron-tannate dyed raffia contained iron-rich surface deposits while areas without surface deposits contained particularly low quantities of iron. Al and Si were also present in significant quantities in the surface deposits as well as lower levels of Mg, P, K, and Ca (Figure 6.17). These elements were also present in surface deposits on the undyed raffia that was also provided by Mark Sandy (Figure 6.18). An iron-rich surface particle was also identified on the surface of the undyed raffia however this is likely to be a surface contaminant, possibly from the dyed raffia with which it was stored, since the areas of undyed raffia without surface deposits contained no iron.

Overall, iron-tannate dyed fibres from historic materials typically contained detectable levels of iron in surface deposits and in areas of the fibre without surface deposits. Undyed equivalents also contained surface deposits, some rich in iron, but the areas without surface deposits typically had negligible levels of iron. These trends were also present in model iron-tannate dyed and undyed raffia provided by Mark Sandy and the dyed (c3/p3) cotton and silk model textiles as reported in Chapter 5.

6.3 Conclusions

Based on surface pH, reflectance spectra, bathophenanthroline testing, and XRF the cellulosic dyed model textiles, particularly the four week aged samples (80°C and 58% RH) are comparable to the historic iron-tannate dyed material analysed in this chapter. All of the samples had an acidic surface pH (typically within 1.5 pH units of each other), typically contained significantly higher quantities of iron than undyed equivalent areas (XRF), had similar reflectance spectra (aged model textiles cf. historic materials), and had similar levels of unbound iron (detected using bathophenanthroline test paper). The iron content in the model dyed textiles was similar to and in many cases higher than that in the historic samples analysed. Using SEM-EDX it was identified that iron-rich surface deposits were present on many of the dyed historic materials analysed and that iron was detectable in areas of dyed samples without surface deposits. This was also identified in the Cc3 and Sp3 model textiles. Undyed equivalent historic materials often contained iron-

6.3 Conclusions

containing surface deposits but there was no iron detected in areas without deposits. GPC-MALLS identified that the two historic samples analysed were more degraded than the four week aged Cc1 (80°C and 58% RH) and that potentially acid hydrolysis had played a more significant role in the natural ageing of the historic samples than in the accelerated degradation of the model textiles. EPR identified that the model textiles contained iron(III) ions in similar chemical environments to the historic materials as well as similar types of radicals.

The dyed model textiles have fulfilled the remaining project aim in that they have similar properties to and behave similarly on ageing to historic British Museum objects that are highly likely to be iron-tannate dyed. Consequently, the dyed cotton, abaca, and silk textiles are valid substitutes for historic iron-tannate dyed samples in the stabilisation studies of this PhD project.

7 ACCELERATED AGEING

Accelerated ageing involves exposing material to elevated conditions (temperature, relative humidity (RH), light, oxygen, pollutants) in a climate chamber for a specific period of time in order to accelerate the rate of degradation of the material.

Accelerated ageing is used in textile and paper studies in 3 ways (Erhardt and Mecklenburg 1995; Porck 2000):

1. Simulation studies. Accelerated ageing is used to study the long-term behaviour of a material and to study its degradation mechanisms in order to validate its usage as a substitute for naturally aged material in comparison studies. Degradation indicators such as pH, colour, degree of polymerisation (DP) or strength are used to quantify the extent of degradation occurring in the samples during accelerated ageing thus identifying the effect they have on the rate of degradation. This aids understanding of the factors affecting the stability of a material during natural ageing (Calvini and Gorassini 2006). Additionally, when the accelerated ageing conditions simulate in the model materials the degradation that occurs due to natural ageing, the use of model materials as substitutes for historic materials can be validated. This allows more extensive and reliable testing to occur than would be possible with historic material since there is likely to be much more material available for use that is of known composition and for which the production, storage, and treatment history is also known;

2. Comparison studies. Accelerated ageing is used to degrade treated model materials to determine the effect of the treatments on the permanence of the material. Analysis for degradation indicators such as textile strength, colour, and acidity before and after ageing provides a quantitative understanding of the efficacy of the treatments tested and enables identification of the most successful treatments. While quantitative data is obtained about the degradation of the materials tested, Bansa (Bansa 2002) recommends that the data acquired from accelerated ageing of materials be only used comparatively rather than quantitatively;

3. Arrhenius tests. Accelerated ageing can also be used to predict lifetimes of materials at ambient conditions. In these studies it is assumed that the rate of each degradation reaction that contributes to the overall rate of degradation of a material is accelerated by the same factor when one or more environmental conditions are altered. However, as will be discussed later, this may not be true. The Arrhenius equation has been found to be

7.1 Aims

applicable to the ageing of paper under conditions ranging from 60-100°C and 2-100% RH (Zou, Uesaka and Gurnagul 1996a) and to give good predictions of lignin-free paper permanence if all factors affecting the pre-exponential factor are kept the same in both natural and accelerated ageing conditions (Zou, Uesaka and Gurnagul 1996b). However, at best the predictive results of Arrhenius are estimates (Zou, Uesaka and Gurnagul 1996a; Porck 2000) and the high unreliability of predicted lifetimes for materials obtained using accelerated ageing has made some authors advise that accelerated ageing not be used for lifetime prediction at all (Bansa 2002; Calvinini and Gorassini 2006).

7.1 Aims

In this project, accelerated ageing procedures were required for two purposes:

1. *Simulation studies*. Investigation into the mechanism of degradation of iron-tannate dyed model textiles and the validation of the model textiles for use as substitutes for historic material in the stabilisation studies in this project (see Chapters 5 and 6);
2. *Comparison studies*. To identify the efficacy of a range of stabilisation treatments for iron-tannate dyed textiles in Treatment Tests 1 and 2.

In this chapter investigations were undertaken to determine the most suitable temperature, RH, and periods of ageing to achieve significant and measurable signs of degradation within 6 weeks, as necessitated by the timeframe of the project. These conditions were subsequently used in Treatment Test 1 to age treated and untreated cotton and silk samples in a comparison study to determine the most successful treatments to use in Treatment Test 2. The results from this chapter also affected the choice of accelerated ageing conditions used in Treatment Test 2 for accelerated ageing of model textiles before and after treatment application. Importantly, the ageing conditions must simulate degradation as closely as possible to that produced during natural ageing conditions to ensure that the degradation that occurs is comparable to that which will occur through natural ageing.

7.2 Accelerated ageing theory

During natural ageing a material is exposed to a variety of environmental conditions that are based around room temperature and which often fluctuate during the lifetime of the material. The ageing of a material is a complex process of multiple reactions (Erhardt and Mecklenburg 1995) including hydrolysis, oxidation, and thermal degradation (Porck 2000). Hydrolysis cleaves the polymer chains, weakening the material at a rate that is temperature, pH, and moisture dependent. During oxidation cross-links, carbonyl groups, and acidic carboxyl groups are formed, increasing brittleness, discolouration, and acidity. The rate of

7.2 Accelerated ageing theory

oxidation is primarily oxygen dependent. During thermal degradation atomic vibrations cause bonds to break, weakening the material at a rate that is temperature dependent. During accelerated ageing the aim is to accelerate the rates of all of the degradation reactions present in a material by the same extent, thereby resulting in the attainment of the same types and relative quantities of degradation products as occurs during natural ageing but in a significantly shorter timeframe.

7.2.1 Rates of reaction

The rate of degradation of a material at a given temperature and RH can be calculated by monitoring the change in a property of the material (chemical, mechanical/physical, or optical) during ageing and plotting this change against the change in time. The gradient of such a plot is the rate constant, k , of the reaction. Physical properties such as tensile strength are often used to determine rates of degradation however chemical properties such as DP, are better indicators of degradation (Zou, Uesaka and Gurnagul 1996a). This is because unlike the chemical indicators, there is potentially a non-linear correlation between the loss of physical properties of a material with ageing and a chemical change.

Additionally the rate constants determined using different physical properties as indicators of degradation can produce different rates of degradation for the same material. Changes in chemical properties can occur before changes in the physical properties that are influenced by these chemical changes become apparent (Feller 1994). Finally and usefully for historic materials in particular, the assessment of chemical properties often requires smaller samples than are needed to assess physical properties (Feller 1994). However, Feller (Feller 1994) notes that it is important to identify the correlation between the chemical factor being tested and the degradation reaction to which it might be an indicator and also, to the change in physical indicators of the degradation. Consequently a mixture of both chemical and physical analyses may be the “best” investigative approach when studying the degradation of a material.

Calvini and Gorassini (Calvini and Gorassini 2006) advise that the number of scissions occurring in a material during ageing is the most important factor to be monitored and that this can be estimated after calculation of the DP by using the following equation:

$$S = \left(\frac{DP^o}{DP} \right) - 1 \quad \text{Equation 7.1}$$

7.2 Accelerated ageing theory

Where S is the average number of scissions per chain, DP° is the initial DP, and DP is the final DP. In this equation, the viscosity-average DP (DP_v) which is closer to the weight-averaged DP (DP_w) than the number-average DP (DP_n) (Sharples 1954), is used since the DP_n that is meant to be used is difficult to calculate. Note that a widely used assumption is that $DP_v = 2DP_n$ (Whitmore and Bogaard 1994).

Ideally accelerated ageing should be employed at least until the levelling-off DP (LODP) has been reached in order for comparison between rates of different reactions or the assessment of the most successful stabilisation treatment to be accurate (Feller 1994; Calvini and Gorassini 2006); the LODP of paper is generally considered to be between 150 and 250 (Shroff and Stannett 1985; Feller 1994; Zou, Uesaka and Gurnagul 1996a; Emsley, Ali and Heywood 2000) since all mechanical strength is lost below 250 (Shroff and Stannett 1985). In doing so, whether the kinetics of the reactions follows a 1-exponential or S-shaped path will be determined. Typically for accelerated ageing studies the 1-exponential path characteristic of a single first-order reaction is assumed however this is incorrect for important reactions in paper degradation which have been found to follow S-shaped kinetic paths (Bicchieri and Pepa 1996; Bogaard and Whitmore 2001; Zervos and Moropoulou 2005; Calvini and Gorassini 2006).

7.2.1.1 The Arrhenius equation

The effect of temperature on the rate constant (k) of a reaction can be described by the Arrhenius equation (Equation 7.2):

$$k = Ae^{-\frac{E_a}{RT}} \quad \text{Equation 7.2}$$

Where A is the pre-exponential factor or frequency factor which is specific to a reaction and which is affected by factors other than temperature (e.g. light, material source, RH, acidity, pollutants, impurities/additives (Begin and Kaminska 2002)). The units of A vary depending on the order of the reaction (s^{-1} for first order reactions) and are the same as that of the rate constant. A represents the total number of collisions between reactants that can occur in a reaction (successful and unsuccessful). E_a is the activation energy of the reaction ($J\ mol^{-1}$) which is mainly affected by the mechanism (Calvini and Gorassini 2006), R is the universal gas constant ($8.314\ JK^{-1}mol^{-1}$), and T is the absolute temperature (K). The $\exp(-E_a/RT)$ term of the Arrhenius equation gives the probability of each collision being

7.2 Accelerated ageing theory

successful so that the rate constant, k , represents the number of successful collisions between reactants i.e. those with enough energy and in the correct orientation to react. The activation energy of the overall degradation reaction involved in model iron gall ink on paper was calculated to be $142 \pm 20 \text{ kJ mol}^{-1}$, using viscometric DP data, and to range between 138 and $150 \pm 20 \text{ kJ mol}^{-1}$ for those that were treated (Kolar, Strlic, Balazic, Smodis, Malesic and Sala 2006). Activation energies ranging from 104 to 113 kJ mol^{-1} were identified for the degradation of three types of bleached chemical pulps (Zou, Uesaka and Gurnagul 1996a) and activation energy of 113 kJ mol^{-1} is typical of hydrolysis reactions in paper (Calvini and Gorassini 2006). Often the pre-exponential factor and the rate constants calculated in experiments (A' and k' respectively) are dependent on the concentration of reagents unlike A and k (Erhardt and Mecklenburg 1995). Often the concentration of reagents affects the rate of the reaction. Consequently, the rate constants at the start of the reaction are used in Arrhenius tests since the concentrations of reagents are regarded as constant early in the reaction when they are large enough for the changes in concentration to be negligible. The determination of A' and k' rather than A and k occurs when the reactions involved in the degradation process are too complicated for the roles of the chemicals present to be understood; this prevents the concentration of the reagents from being factored out of A' and k' . In such cases it must be remembered that the calculated pre-exponential factor and rate of reaction is concentration dependent and therefore can be affected by the environmental conditions such as moisture content if water is a reactant in a reaction (Erhardt and Mecklenburg 1995). Zou, Uesaka, and Gurnagul (Zou, Uesaka and Gurnagul 1996a) report that the frequency factor (pre-exponential factor) indicates the frequency of collision of the reagents and is therefore dependent on factors such as concentration of hydrogen ions and water (depending on the reaction studied) which affect this. They showed experimentally that the moisture content and acidity of paper significantly affect the rate of paper degradation and that high moisture contents increase the effect of acidity on the degradation rate.

In order to determine the activation energy and pre-exponential factor of a reaction, the rates of reaction of a material at multiple temperatures but with all other environmental factors the same must be ascertained. Then, a plot of $\ln(k)$ against $1/T$ or $1/RT$ can be produced which can be used to determine the activation energy (from the gradient) and pre-exponential factor (from the y-intercept) of a reaction.

$$\ln k = \ln A - \frac{E_a}{RT} \quad \text{Equation 7.3}$$

If the reaction follows the Arrhenius equation then the plot will be linear. The rate of degradation of this material under natural ageing conditions can be estimated by extrapolation of this plot to lower temperatures (Erhardt and Mecklenburg 1995; Zou, Uesaka and Gurnagul 1996a). Alternatively, by calculating the length of time, d , it takes to age a material to the same extent at a variety of different elevated temperatures, a plot of $\ln(d)$ against $1/T$ can be made. Extrapolation of the gradient to lower temperatures than those tested gives an estimation of the time it will take to degrade the tested material to the same extent at a lower temperature e.g. that used in a store room (Porck 2000). These are methods of Arrhenius testing.

As mentioned previously, the ageing of a material is a complex process of multiple reactions (Erhardt and Mecklenburg 1995). If properties of a material that are affected by n multiple degradation reactions are monitored at different temperatures rather than properties that are affected by just one, then the rate of degradation of the material will be proportional to the sum of the n rates of the individual reactions. A plot of $\ln(k_{total})$ against $1/RT$ will identify the average activation energy of the n reactions occurring and $\ln(A_1 + A_2 + \dots A_n)$. The average activation energy is weighted by the rates of each reaction and can be significantly different from the activation energy of each individual reaction (Erhardt and Mecklenburg 1995; Zou, Uesaka and Gurnagul 1996a).

While research by Zou, Uesaka, and Gurnagul (Zou, Uesaka and Gurnagul 1996b) into the comparability of accelerated and natural ageing results of lignin-free paper suggests that a good lifetime prediction can be made (if factors affecting the pre-exponential factors of each reaction are kept the same in both ageing situations), serious doubts regarding the validity of the Arrhenius equation to predict the lifetime of a material do exist (Porck 2000; Bansa 2002; Strlic, Kolar and Pihlar 2005; Zervos and Moropoulou 2005). At best Arrhenius testing is regarded as providing an estimate as there is a high level of uncertainty involved (Porck 2000; Strlic, Kolar and Pihlar 2005). However, it is advised by some authors (Bansa 2002; Calvini and Gorassini 2006) that accelerated ageing be not used for lifetime prediction since the huge variation in predicted lifetime values when the typical error of 5% is incorporated into the calculation makes a reliable prediction impossible (Begin and Kaminska 2002; Calvini and Gorassini 2006). Additionally the estimation is based on temperature alone and does not consider effects of other environmental conditions, or that the activation energy at lower temperature can differ

from that at higher temperature due to different reactions occurring or predominating (Bansa 2002; Begin and Kaminska 2002; Calvini and Gorassini 2006).

7.2.2 *Methods of accelerated ageing*

During accelerated ageing the temperature, relative humidity, light, and atmospheric composition can be controlled. Which factors are varied or made constant depends on the facilities available and the aim of the study. In this study the temperature, light, and RH will be controlled. The samples will be aged in the dark by accelerated ageing in the environmental chamber since British Museum objects are stored in the dark unless on display. The temperature and RH will be controlled by the environmental chamber. However, where suitable temperature can also be controlled by constant-temperature baths (BS 6288-3:1996/ISO 5630-3:1996 1996) and RH can also be controlled by using saturated salt solutions in an enclosed environment (Greenspan 1977; Baranski, Dutka, Dziembaj, Konieczna-Molenda and Lagan 2004).

Both dynamic (cycling) (Neevel 1995; Neevel 2002) and stable RH (Kolar, Mozir, Strlic, Ceres, Conte, Mirruzzo, Steemers and de Bruin 2008) methods have been used during accelerated ageing of iron gall ink on paper samples. Cycling the relative humidity is thought to more accurately simulate natural ageing (Strlic, Kolar and Pihlar 2005) and at constant temperature has been found to cause greater degradation to individual sheets of paper than stable relative humidity during ageing (Shahani 1995). However, when stacked, these conditions bring about similar extents of degradation. This is thought to be due to the greater exposure of the single sheet compared to those within the stack to the fluctuating environmental conditions whereas only the surfaces of the stacks are exposed to the same fluctuation.

The method of exposure of the samples to these elevated conditions i.e. their arrangement in the chamber, also varies depending on the types of samples being aged and the equipment available. Paper for example can be aged in stacks or as single sheets and it has been found that when aged in stacks paper degrades faster than when aged as single sheets (Shahani 1995). This is because unlike with a single sheet, volatile organic compounds (VOCs) such as acidic compounds, that can accelerate the degradation of the substrate, are retained within a stack. This trapping of VOCs and their migration through the stack to an open surface enables them to degrade the substrate (Bulow, Begin, Carter and Burns 2000; Carter, Begin and Grattan 2000; Calvini, Gorassini and Merlani 2007). This explains the continually decreasing rate of strength loss of the paper in stacks compared to the constant

rate that occurred in the ageing of the single sheets (Shahani 1995). Iron gall ink, and therefore it is likely iron-tannate dye also, has been found to accelerate the rate of formation of VOCs (Havermans and de Feber 1999), thus ageing samples in stacks could be important in this project. In order to retain moisture and VOCs in a method other than the stacking of samples, methods involving sealing small samples of material in glass tubes have been used (Begin and Kaminska 2002; Zervos and Moropoulou 2005; BS ISO 5630-5:2008 2008; Nilsson, Vilaplana, Karlsson, Bjurman and Iversen 2010).

7.2.3 Natural ageing versus accelerated ageing

For the results of accelerated ageing to be most useful they need to be comparable to the results of natural ageing, but produced in a significantly shorter timeframe. With no universally agreed set of conditions for the accelerated ageing of organic materials in conservation, a large variety of conditions have been and are in use by researchers. Interestingly, Bansa (Bansa 2002) suggests that the conditions themselves are not as important as how the data is used, e.g. that it is used for comparative studies only and that any relative change that is identified must be identified in more than one set of samples before it can be considered significant. Whitmore also suggests that so long as some mobile water is present in the paper in order to promote hydrolysis (i.e. temperatures above 100°C and RH that are very low should not be used), the exact choice of environmental conditions during the accelerated ageing of paper is not critical (Whitmore and Bogaard 1994; Whitmore 2011). Since acid hydrolysis is also an important degradation pathway for textiles and particularly iron-tannate dyed textiles, the use of moist-thermal ageing is important for this research.

There have been few comparisons between samples aged naturally and artificially, partly due to the difficulties of setting up such an experiment (Wilson and Parks 1980; Porck 2000). However there have been a few examples where a particular batch of paper has been studied over numerous years. One such example is a study in which 36 year old (naturally aged) papers were analysed and the results compared to those obtained following accelerated ageing (100°C for 3 days) of the original samples in 1937 (Wilson and Parks 1980). Some of the papers compared well with the accelerated aged equivalents when tear resistance, folding endurance, and chemical characteristics were considered. Another study in which 22 year old lignin-free paper was re-tested and compared with previous test results confirmed that accelerated ageing was suitable for the prediction of natural ageing results of such material (Zou, Uesaka and Gurnagul 1996b). More recently a detailed study into accelerated ageing conditions that most replicate the condition of historic undyed silk

7.2 Accelerated ageing theory

samples has been undertaken using modern undyed silk (Nilsson, Vilaplana, Karlsson, Bjurman and Iversen 2010). Of all the conditions tested the dry thermal ageing (125°C) produced mechanical and chemical (FTIR, SEC, and tensile testing) results that were the most comparable to those in historic samples. In such conditions there is unlikely to be enough moisture present to facilitate hydrolysis reactions. A project involving the chemical and physical analysis of identical books that are stored in multiple nationally significant libraries over time is underway which will aid understanding of the effects of different environmental conditions and handling on the condition of books

(<http://www.bl.uk/aboutus/stratpolprog/ccare/projects/mellonfoundation/identicalbooks.pdf>

). A study of the degradation products of accelerated aged custom made papers compared with naturally aged papers suggests that ageing the papers in stacks and sealed glass tubes resulted in the most comparable degradation to that achieved naturally (Begin and Kaminska 2002).

As mentioned previously, all of the reactions involved in the degradation of a material combine to give an overall rate of reaction. However, each reaction has its own activation energy, which may differ from that of other reactions and may affect the changes in rate of reaction with changes in temperature. Based on the Arrhenius equation, different activation energies would result in different increases in the rates of different reactions with the same increase in temperature. Reactions with lower activation energies are less sensitive to changes in temperature than reactions with higher activation energy (Erhardt and Mecklenburg 1995). Additionally, each of the reactions involved in the overall degradation of a material may be affected by environmental conditions such as moisture and pH to different extents. Consequently, when environmental conditions are altered, the rate of each reaction may increase by different quantities. This can cause the overall ratio of degradation reactions and their degradation products to alter. Thus, the degradation caused by accelerated ageing may differ to that caused by natural ageing.

Paper ageing studies by Erhardt and Mecklenburg (Erhardt and Mecklenburg 1995) suggest that the ratio of rates of degradation reactions is not altered by changes in temperature but is altered (non-linearly) by changes in relative humidity. Consequently, it is suggested (Erhardt and Mecklenburg 1995; Porck 2000) that accelerated ageing of samples for future comparison with naturally aged samples should be aged using the same relative humidity as that in the natural ageing environment. However, under the RH range used (60-90°C and 30-80% RH) the changes in degradation due to variations in RH are noted as being small and likely to be comparable within variations in degradation that

7.2 Accelerated ageing theory

could occur during natural ageing due to natural variation in environmental conditions (Erhardt and Mecklenburg 1995). Therefore, in paper, and possibly also in textiles, the use of such conditions within these limits should produce accelerated ageing results that are comparable to those produced over a longer time using natural ageing conditions. The presence of non-cellulosic components such as lignin and hemicellulose, could alter the ageing process of the material which may decrease the range of environmental conditions which produce comparable results to natural ageing (Erhardt and Mecklenburg 1995).

In contrast to the above where the use of the same RH as used in natural ageing is advised, other authors (Zou, Uesaka and Gurnagul 1996a; Porck 2000) advise that it is the moisture content in the air and consequently the moisture content in the material that it is most important to maintain. It was found that the correlation between extent of degradation and RH was non-linear (s-shaped) over a wide range of RH values (Zou, Uesaka and Gurnagul 1996a; Baranski, Dutka, Dziembaj, Konieczna-Molenda and Lagan 2004). This was similar to the correlation between the moisture content of paper and the RH of the air (adsorption isotherm) since adsorption of moisture from the air is the general cause of moisture content in a material (Feller 1994; Zou, Uesaka and Gurnagul 1996a). Following experimental confirmation it has been recommended (Zou, Uesaka and Gurnagul 1996a) that a RH of 25-75% be used in accelerated ageing studies as during this range, the variation in moisture content in a material with change in RH is lowest. In his comprehensive review of accelerated ageing (photochemical and thermal), Feller (Feller 1994) reports that it is the air in immediate contact with a material in addition to the material's temperature that controls the moisture content in the object. The recommendation to use the same RH during accelerated ageing as occurs during natural ageing (Erhardt and Mecklenburg 1995; Porck 2000) potentially conflicts with the recommendations to maintain the moisture content. This is because the moisture content of an environment differs with changing RH at a set temperature and also with the same RH at different temperatures. This occurs because the RH is a measure of the moisture content (partial pressure of water vapour) in an environment divided by the maximum moisture content the environment will hold at a given temperature (saturated vapour pressure). The saturated vapour pressure increases with temperature and so if the temperature is increased but the RH stays the same there will be an increase in total moisture content in the environment and therefore also in the material. To maintain the same quantity of water in the air and therefore in the material, the relative humidity would have to decrease with increasing temperature

7.3 Accelerated ageing methods in use

7.3.1 *Conditions used*

Industrial standards, for example the ISO standards (BS 6388-2:1987/ISO 5630-4:1986 1987, 1986; BS 6388-1:1991/ISO 5630-1:1991 1991; BS 6288-3:1996/ISO 5630-3:1996 1996; BS ISO 5630-5:2008 2008; BS ISO 5630-6:2009 2009) referenced here, are available for accelerated ageing of paper and board. These use moist thermal ageing 80°C and 65% RH, or dry thermal ageing (100°C, 105°C, 120°C, or 150°C). A range of ASTM standards for accelerated ageing were withdrawn without succession in 2011. If used, standards are usually used with slight variations (Bansa 2002). Additionally, a wide variety of accelerated ageing conditions have been used on organic materials including iron gall ink on paper and iron-tannate dyed textiles. Many of the wide variety of conditions used in paper conservation have been summarised by several authors (Porck 2000; Bansa 2002). The following is a list of the many though no doubt not all, ageing conditions that have also been used in iron gall ink and iron-tannate dye research. Sandy and Bacon (Sandy and Bacon 2008) used 65% RH and 80°C for 120 hours to age iron-tannate dyed raffia. Kim and Wyeth (Kim and Wyeth 2009) conditioned silk using dry thermal ageing at 125°C, and moist thermal ageing at 100°C and 100% RH and 80°C maintained by a small volume of a 20:80 mole ratio of glycerol-water mixture was used to age New Zealand flax treated with a zinc alginate (Te Kanawa, Smith, Fenton, Miller and Dunford 2002; Te Kanawa and Smith 2009). 70% RH and 70°C with and without Xe light ageing was used to identify the effect of different historical processing methods on the stability of silk (Garside and Wyeth 2009; Garside, Wyeth and Zhang 2010b). 65% RH and 80°C were being used in the development of a non-aqueous antioxidant treatment for iron gall ink on paper (Kolar, Mozir, Strlic, Ceres, Conte, Mirruzzo, Steemers and de Bruin 2008). During the development of the phytate treatment 50% RH and 70°C were used for three days to pre-age iron gall ink on paper before final ageing of treated samples using a cycling relative humidity between 35% and 80% every 3 hours at 90°C (Neevel 1995; Neevel 2002). The latter set of conditions for the same or different cycling humidity time frame has been used by other researchers (Eusman 2002; Potthast, Henniges and Banik 2008). Light ageing has also been used on organic materials. Silk was exposed to sunlight equivalent ageing (25 MJ/m² over one day) in air over 20 days for analysis by a range of techniques (Kim and Wyeth 2009).

7.3.2 Discussion of suitability of conditions for this research

While the relative rates of reactions in paper have been found to remain similar with increasing temperature (Erhardt and Mecklenburg 1995), the most reliable results from accelerated ageing will be obtained using conditions as close to those in natural ageing as possible. Additionally, under natural ageing conditions, hydrolysis is one of the main degradation pathways for iron-gall inked paper and for iron-tannate dyed textiles, partly due to the high acidity of the iron-tannate ink/dye. The high dependence of the rate of acid hydrolysis on water and the need to degrade the model textiles in as similar way to natural ageing as possible suggests that dry thermal ageing in which the relative humidity is between 1 and 5 %, is unsuitable for this project. Since the extent of degradation varies non-linearly with increasing RH (Erhardt and Mecklenburg 1995), a relative humidity closer to that in natural ageing will be required. Based on results by Erhardt and Mecklenburg (Erhardt and Mecklenburg 1995) for paper, a RH between 30 and 80% at a temperature between 60 and 90°C could result in degradation within the natural variation expected due to variation in environmental conditions during natural ageing. The use of an RH equal to that occurring in natural ageing was also advised (Erhardt and Mecklenburg 1995; Porck 2000) and at the British Museum, the desirable RH and temperature for the storage and display of organic objects including objects of mixed composition, is 40-55% with a daily variation of $\leq \pm 5$ and 16-20°C with $\leq \pm 2$ daily variation; although the acceptable levels are slightly broader at 40-60% RH and 16-25°C (Saunders 2006). However, as previously discussed, maintaining similar moisture content during accelerated and natural ageing may be more pertinent (Feller 1994; Zou, Uesaka and Gurnagul 1996a) in which case a lower RH than that used in storage may be necessary. Zou, Uesaka, and Gurnagul advised that the use of an RH between 25 and 75% would be the most useful because the moisture content in paper varies the least in this range (Zou, Uesaka and Gurnagul 1996a). This range includes RH values higher and lower than those used in stores at the British Museum and consequently, the use of an RH in this range could be the best balance between the two theories (RH vs moisture content).

Light ageing was of interest in this project however, the majority of iron-tannate dyed museum objects that would be treated with a treatment developed in this project would be stored in the dark. Some may be exhibited but due to being classed as very sensitive to light degradation this would involve display under UV-filtered light at 50 lux for no more than one year in ten (Reissland and Cowan 2002; Saunders 2006). Consequently the effect of light on the treated and untreated model textiles is not as important as the effect of temperature and relative humidity and is therefore not studied in this project. Temperature

7.3 Accelerated ageing methods in use

and humidity ageing in the dark is most suitable for this project. Determining the exact conditions of these needed including whether cycling/dynamic or stable RH is most suitable to fulfil the aims of the accelerated ageing process is the focus of the following experiments.

7.4 Experimental method

7.4.1 *Model textiles used*

Dyed (p1/c1) and undyed cotton, abaca, wool, and silk were used in these preliminary ageing tests.

7.4.2 *Equipment used*

The environmental chambers used were a WK3-180/40 chamber (A) at Camberwell College of Arts, a Sanyo Gallenkamp SEC185 (BR185/RO) (B) at the British Museum, and a Sanyo Gallenkamp Environmental Chamber (reference 8291) (C) at The National Gallery, London.

7.4.3 *Conditions investigated*

Five sets of conditions (Table 7.1) were investigated. Condition 3 was chosen for its use in the development of the calcium phytate treatment (Neevel 1995; Neevel 2002). Conditions 1 and 4 were chosen because they were lower in temperature than condition 3. Conditions 2 and 5 were chosen to compare with conditions 1 and 4, respectively, due to different relative humidities. The relative humidity in condition 5 was chosen to be the mid-point between the extreme relative humidities used in condition 4. In some tests the samples were stacked and in others they were suspended from racks in the chamber using unbleached linen thread or clips on metal wires. Two stacks were used in conditions 4 and 5, one for dyed samples and one for undyed. These were moved to different locations in the chamber during ageing to counter uneven temperature and RH distribution but the order of samples in the stack was kept the same.

7.3 Accelerated ageing methods in use

Table 7.1 Accelerated ageing conditions tested

Condition number	Temperature (°C)	Relative Humidity (%)	Stacked or suspended	Exposure time (weeks)	Estimated equivalent exposure time at 20°C (weeks) ¹	Environmental chamber used
1	75	35-80 every 3 hours	Suspended	4	8192 (approx 157.5 years)	A
2	75	75	Suspended	9	18432 (approx 354.5 years)	B
3	90	35-80 every 3 hours	Suspended	3	49152 (approx 945.2 years)	C
4	80	35-80 every 3 hours	Stacked	4	16384 (approx 315.1 years)	C
5	80	58	Stacked	4	16384 (approx 315.1 years)	C

Notes for Table 7.1:

1. The equivalence of these ageing conditions to natural ageing can be loosely estimated using the following approximation: the rate of reaction doubles for every 5°C increase in temperature. The effects of environmental conditions other than temperature are not considered in this approximation, and it is assumed that a linear relationship exists between the natural log of the rate of reaction and the inverse of the temperature. The approximation above is most accurate for reactions with an activation energy of around 105 kJ (25 kcal) (Erhardt and Mecklenburg 1995). The major reactions occurring in paper during degradation have activation energies between 83-125 kJ (20-30 kcal), higher than the activation energies (42-63 kJ (10-15 kcal)) to which the widely used rule of thumb that the rate of reaction doubles for every 10°C increase in temperature relates. Since the activation energy of accelerated aged model iron gall ink on paper samples was calculated to be 142 +/- 20 kJ mol⁻¹ (~34 +/- 5 kcal) (Kolar, Strlic, Balazic, Smodis, Malesic and Sala 2006) it is possible that the activation energies of the major degradation reactions of the cellulosic iron-tannate dyed textiles will also be greater than 83-125 kJ (20-30 kcal). This will mean that the estimation of a doubling of rate with 5°C will underestimate the length of time of natural ageing that will give equivalent results since the rate will change more than twice per each 5°C increase in temperature. An example of the calculation involved in the estimation of the number of years that the ageing at elevated temperature is equivalent to at 20°C (T₁) is below:

For 4 weeks of accelerated ageing at 75°C (T₂):

1. Difference in temperatures: T₂ - T₁ = 75 - 20 = 55°C;
2. Number of 5°C increased in temperature difference: 55/5 = 11;
3. Difference in rate at T₂ compared to T₁ when rate doubles for every 5°C increase: 2¹¹ = 2048 i.e. at T₂ the rate of reaction is 2048 times greater than that at T₁ as a rough estimate;
4. Length of time at 20°C that is equivalent to 4 weeks at 75°C: 2048 × 4 = 8192 weeks;
5. Convert weeks into years (52 weeks per year): 8192/52 = 157.5 years.

7.4.4 Analytical methods

Samples aged using conditions 1-3 were analysed using handling tests only while those aged using conditions 4 and 5 were analysed with tensile testing, spectrophotometry, surface pH, and GPC-MALLS.

7.4.4.1 Subjective handling tests

Samples aged with conditions 1-3 were tested after each week of ageing and assessed manually for strength by tearing an area of each sample. This subjective analysis was made as objective as possible through consistency in the person analysing the sample. Samples were not retained for each week so comparison between weeks was made through observations from the previous week. A code was devised to indicate obvious differences in sample strength during ageing. This form of analysis was able to indicate whether the dyed model textiles degraded faster than the undyed equivalents and whether this occurred within one or two months.

When performed, colour change was also assessed as objectively as possible by consistency of person analysing the samples and use of a well-lit area and white background when making judgements.

Note that comparisons between samples aged for the same length of time using different conditions were not directly compared as they were undertaken in different locations and/or at different times.

7.4.4.2 Tensile testing

Tensile testing of the cotton, silk, and abaca samples aged using 80°C and either stable RH (58%) or cycling RH (35-80% every 3 hours) was performed as described in Section 5.2.5.1. An error in preparation of the textiles for ageing meant that the direction of warp was not noted on the cotton for which the warp and weft were not easily discernable. Based on the resulting data it appears that during analysis, a mixture of warp and weft directions were tested unintentionally. From the data it is clear that for CU the stable aged samples were all warp but weeks 1 and 4 of the cycling aged samples were weft while weeks 2 and 3 were warp. The direction of yarns tested in the Cc1 textiles is unclear as after 1 week of ageing in either condition the breaking load and extension had decreased to below the levels in both warp and weft yarns. Also the dyeing of the textiles resulted in warp and weft yarns of similar crimp levels and after 3 and 4 weeks of ageing the textiles can be so weak that the textile breaks before a yarn can be extracted from the textile.

7.5 Results and discussion

Exponential trend lines were used for the extension and breaking load data presented in Figures 7.2 and 7.1, respectively.

7.4.4.3 Colorimetry

The colour of the samples aged using 80°C and either stable (58%) or cycling RH (35-80% every 3 hours) was analysed as described in Section 5.2.4.2. Exponential trend lines were used for the ΔE_{00}^* data in Figures 7.3 and 7.4 while linear trend lines were used for other colorimetry data.

7.4.4.4 Surface pH

The surface pH of samples aged using 80°C and either stable (58%) or cycling RH (35-80% every 3 hours) was analysed as described in Section 5.2.2 except that three analyses per sample rather than ten were made on randomly selected locations of each sample and an average calculated.

7.4.4.5 GPC-MALLS

The molar mass distribution, molecular weights, DP, and carbonyl content of the samples during accelerated ageing by either the stable or cycling RH conditions were determined as described in Section 5.28.

7.5 Results and discussion

7.5.1 *Subjective handling tests*

There were three aims to these subjective handling tests for which subjective rather than objective testing was sufficient. Firstly, these tests were intended to give a quick indication of which environmental conditions would produce a noticeable decrease in strength of the model textiles by four weeks of ageing. Secondly, these tests would identify which of the conditions tested or which conditions can be recommended for use in Treatment Test 1. Thirdly, the final aim of these tests was to ascertain if the model dyes did accelerate the degradation of the model textiles since prior to these tests this was unknown.

7.5 Results and discussion

Table 7.2 The effect of different accelerated ageing conditions on the strength and colour of the model textiles as determined using subjective testing

Condition	Model textile	Extent of Accelerated Ageing (weeks)								
		1	2	3	4	5	6	7	8	9
75°C 35-80% RH every 3 hours Suspended Chamber A	CU ^b									
	Cc1		T	T+	T++					
	AU									
	Ac1		T	T+++	T+++					
	SU									
	Sp1		T	T	T+					
75°C 75% Suspended Chamber B	WU									
	Wp1									
	CU									
	Cc1	T	T+	T++	T++	T++	T++	T++	T+++	T+++
	AU									T
	Ac1	T+	T++	T+++	T+++	T+++	T _C	T _C	T _C	T _C
90°C 35-80% RH every 3 hours Suspended Chamber C^a	SU									
	Sp1							T	T	T+
	WU									
	Wp1									
	CU									
	Cc1	T, D	T+++, D+	T+++						
80°C 35-80% RH every 3 hours Stacked Chamber C^c	AU									
	Ac1	T	T+++	T _C						
	SU									
	Sp1	T	T+	T++						
	WU									
	Wp1		D							
80°C 58% RH Stacked Chamber C^c	CU			D	D					
	Cc1	D, T	D+, T++	D+, T+++	D++, T+++					
	AU									
	Ac1	D, T++	D+, T+++	D+, T+++	D++, T _C					
	SU									
	Sp1	T	D, T+	D, T+	D, T+					
80°C 58% RH Stacked Chamber C^c	WU									
	Wp1		D	D+	D+					
	CU									
	Cc1	D, T+	D+, T++	D++, T++	D++, T+++					
	AU									
	Ac1	D, T+++	D+, T+++	D++, T _C	D++, T _C					
80°C 58% RH Stacked Chamber C^c	SU									
	Sp1	D, T	D, T	D, T	D, T					
	WU	D	D	D	D					
	Wp1	D	D	D+?	D+					

Notes for Table 7.2:

- a. A malfunction in the chamber caused the samples to be wetted and the colour from the dyed samples to run;
- b. Abbreviations used: C = cotton, A = abaca, S = silk, W = wool, U = undyed, c1/p1 = model textile dyed with dye formulation 1, T = tears but possibly difficult to do or just in one direction, T+ = tears in both directions or easily, T++ = very easy to tear but fibres don't break when bent, T+++ = fibres break when bent, TC = crumbles when handled, D = slight discolouration, D+ = noticeable discolouration, D++ = severe discolouration. Note that tearing was monitored for all samples but discolouration was only monitored in some cases;
- c. Dr. David Pegg at the National Gallery commented that the environmental chamber struggled to attain the 80% RH during the cycle. Consequently, the average RH experienced by samples in the cycling RH programme (condition 4) will be lower than the 58% RH used for comparison in the stable RH programme (condition 5).

7.5 Results and discussion

It is clear from Table 7.2 that all of the accelerated ageing conditions used caused a loss in strength to the c1/p1 dyed cotton, abaca, and silk textiles by 7 weeks of ageing at the most. Wp1 did not reach a “tearable” state after any of the ageing conditions which was most likely to be due to the lack of unbound iron ions within the core of the wool fibres. This was confirmed using SEM-EDX and is detailed along with further discussion in Section 5.3.2. The undyed textiles showed no discernable strength loss with ageing. Consequently, the project established that the c1/p1 dye formulations were found to accelerate the degradation of the cotton, abaca, and silk textiles.

The cotton and abaca dyed textiles weakened significantly faster than the silk dyed textiles typically showing more significant strength loss within 1 week of ageing using conditions 2-5 than was seen in Sp1. Consequently, to achieve a similar extent of degradation in all of the dyed textiles (except wool) either different conditions or different lengths of exposure are required for the cellulosic textiles compared to the proteinaceous textiles. Alternatively, the same conditions and extents of exposure could be used for both textile types with the acceptance that significantly different stages of degradation will be reached.

Comparison between the results from conditions 1 and 3 gives the most reliable indication of the effect of temperature on the degradation rates of the model textiles since these methods (cycling RH, suspended samples) were the most similar out of all the conditions tested. This comparison showed that increasing the temperature from 75°C to 90°C and maintaining the same cycling RH caused substantially faster degradation in the dyed cotton, abaca, and silk textiles. This conclusion is expected based on reaction theory.

The effect of cycling or stable RH on the degradation of the model textiles is best evaluated by comparing the results from conditions 4 and 5 since in these conditions only the RH conditions are altered. From these results the stable RH may have caused slightly greater degradation than the cycling RH for the dyed abaca. The trend for the dyed cotton is less clear while for the dyed silk cycling the RH caused slightly greater degradation than maintaining a stable RH. Objective analysis using tensile testing was used to clarify whether either of the ageing methods caused more degradation than the other. It is possible that the average RH experienced by the samples in condition 4 was lower than the expected 58% that was used for comparison in condition 5, since the chamber may have struggled to reach 80% RH during the ageing process. This could have resulted in the rates of moisture-sensitive reactions such as hydrolysis, occurring at a faster rate in the stable RH aged samples than in the cycling RH aged samples. In conditions 1 and 2 the RH and

7.5 Results and discussion

ageing chamber used are the only factors varied. Here the stable RH conditions caused faster degradation to the dyed cotton, abaca, and silk textiles than the cycling RH conditions. However, this may be due to the fact that the 75% RH in condition 2 is greater than the average RH (58%) experienced by the samples under cycling RH. Interestingly Sp1 lost strength faster under the cycling RH of condition 1 than under the stable RH of condition 2. This may be an effect of using a different chamber or a discrepancy arising from the subjective handling method.

The effect of stacking the samples rather than suspending them cannot be accurately ascertained since no two sets of conditions had all other factors the same. The closest conditions for comparison are conditions 1 and 5 where a 5°C in temperature difference also exists. As discussed previously this temperature difference could cause an approximate doubling of the reaction rates (Erhardt and Mecklenburg 1995). Certainly, the dyed model textiles, except wool, degraded at a faster rate when stacked in condition 5 (80 °C) than when suspended in condition 1 (75 °C). Part of this effect may have been due to the retention of volatile organic compounds (VOCs) within the stack rather than the release of these VOCs into the environment as has been observed in paper samples (Shahani 1995; Baranski, Lagan and Lojewski 2005).

7.5.2 Tensile testing

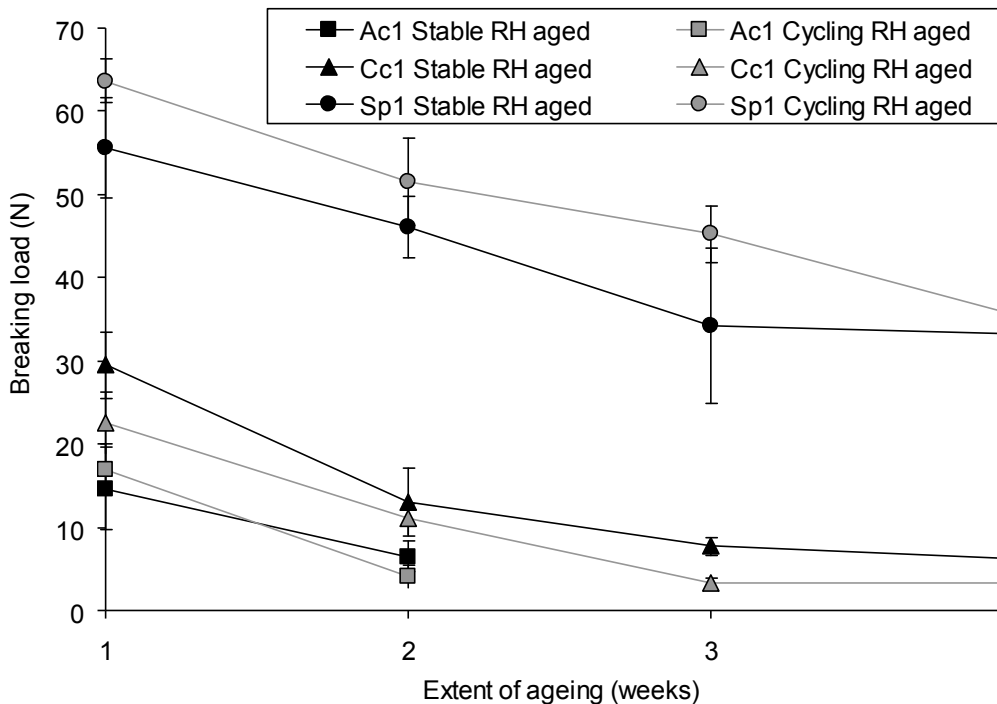


Figure 7.1 The effect of stable and cycling RH ageing on the breaking load of dyed model textiles

7.5 Results and discussion

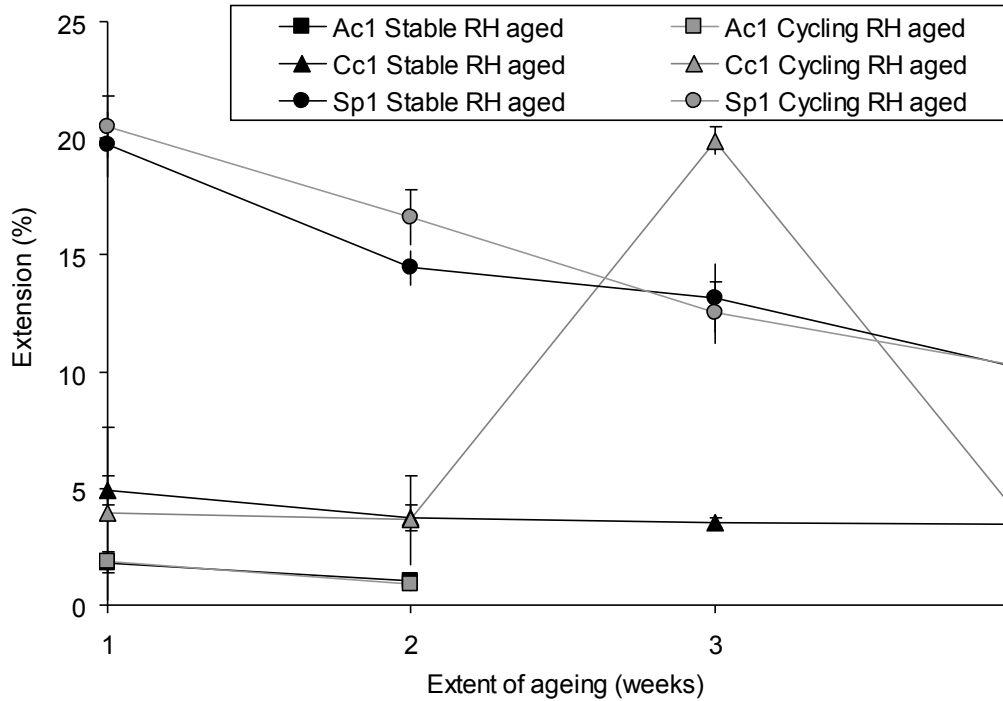


Figure 7.2 The effect of using cycling and stable RH during accelerated ageing on the extension of the dyed and undyed model textiles

The effect of cycling RH on the loss of breaking load and extension of Ac1 and Sp1 during ageing is statistically insignificant (Table 7.3 and Figures 7.1 and 7.2) with both ageing methods showing a similar decrease per textile with age. No significant decrease in breaking load or difference due to ageing method was seen with any undyed textile. The effect of cycling RH on the loss of breaking load of Cc1 is a little more complicated. Initially the difference in breaking load between cycling RH aged and stable RH aged Cc1 was insignificant but after 4 weeks of ageing the cycling RH aged sample was weaker (3.2 ± 0.4 N) than the stable RH aged sample (6.2 ± 0.7 N). No significant difference in extension of Cc1 occurred during ageing with the different RH conditions. The cause of the unusually high extension of Cc1 aged for 3 weeks using the cycling RH is uncertain but was consistent throughout the ten strips of textile tested.

Table 7.3 The effect of using cycling and stable RH during accelerated ageing on the breaking load and extension of the dyed and undyed model textiles

Textile	Tensile testing parameter	Statistics	Accelerated ageing method	DYED (p1 or c1)				UNDYED			
				Extent of accelerated ageing (weeks)				Extent of accelerated ageing (weeks)			
				1	2	3	4	1	2	3	4
ABACA	Breaking load (N)		s	14.6	6.5	-	-	255.5	262.8	250	248.8
		Mean	c	17	4.1	-	-	-	225.7	-	222.2
			s	4.9	1.9	-	-	38.1	47.3	40.3	28.9
		SD ^a	c	3.1	1.4	-	-	-	41.8	-	26.4
			s	33.8	28.7	-	-	14.9	18	16.1	11.6
		CV ^b	c	18.4	34.2	-	-	-	18.5	-	11.9
	Extension (%)		s	1.8	1	-	-	3.7	3.8	3.9	3.5
		Mean	c	1.8	0.9	-	-	-	3.9	-	3.9
			s	0.4	0.3	-	-	0.5	0.5	0.6	0.5
		SD ^a	c	0.4	0.3	-	-	-	0.5	-	0.5
			s	22	31.1	-	-	12.3	13.4	15.2	12.9
		CV ^b	c	23.7	34.9	-	-	-	12.9	-	12.2
COTTON	Breaking load (N)		s	29.5	13	7.7	6.2	101.9	107.2	107.1	108.2
		Mean	c	22.6	11	3.4	3.2	82.7	96.2	92.3	78.7
			s	3.9	4	1.1	0.7	15.7	11.6	8.3	11
		SD ^a	c	3.7	1.9	0.6	0.4	11.7	13	11.6	7.2
			s	13.4	31.1	14.1	11.5	15.4	10.8	7.8	10.2
		CV ^b	c	16.4	17.3	17.8	12	14.2	13.5	12.6	9.1
	Extension (%)		s	4.9	3.7	3.5	3.5	8.2	8.2	8.6	8.1
		Mean	c	3.9	3.6	19.9 ^c	3.9	11.2	8.4	9	11.8
			s	0.6	0.6	0.2	0.2	1	0.7	0.5	0.5
		SD ^a	c	0.4	0.3	2.1	0.7	1.4	0.8	1.2	1.3
			s	12.8	14.9	5.9	6.4	11.9	8.1	6	6.3
		CV ^b	c	10.8	7.6	10.6	18.6	12.3	9.1	12.8	10.8
SILK	Breaking load (N)		s	55.6	46	34.2	33.2	64.2	65.5	62.3	61.6
		Mean	c	63.7	51.6	45.2	35.5	67.5	62.1	62.2	61.6
			s	6.1	3.7	9.4	6.1	4.4	4.8	4.7	4.3
		SD ^a	c	2.7	5.3	3.4	2.6	3.6	5.6	3.8	2.5
			s	10.9	8	27.5	18.3	6.8	7.3	7.5	6.9
		CV ^b	c	4.2	10.2	7.5	7.3	5.3	8.9	6.1	4.1
	Extension (%)		s	19.7	14.5	13.2	10.1	25.2	24.9	24.8	21.7
		Mean	c	20.5	16.6	12.5	10.2	24.2	24.1	21.8	22.1
			s	1.4	0.7	1.5	1.8	0.8	2.5	2.7	2.1
		SD ^a	c	1.3	1.2	1.3	0.9	1.2	1	1.4	1.5
			s	7.1	4.9	11	17.9	3	10	10.9	9.6
		CV ^b	c	6.3	7	10.2	9	5.1	4.1	6.4	7

Notes for Table 7.3:

- a. Standard deviation;
- b. Coefficient of variation;
- c. 19.9% is unusually high but is correct.

7.5.3 Colorimetry

7.5.3.1 Undyed textiles

Table 7.4 The change in colour of the undyed model textiles after accelerated ageing with stable and cycling RH methods

Change in colour parameter compared to unaged sample	Sample (approximate error) ^a	Ageing method	Ageing period (weeks)			
			1	2	3	4
ΔE_{00}^*	CU	s	0.62	1.20	1.52	1.82
		c	0.92	1.13	1.80	1.78
	AU	s	2.39	3.08	3.03	3.95
		c	ND ^b	3.55	ND	5.01
	SU	s	1.04	1.57	2.16	2.59
		c	1.33	1.70	1.97	2.18
	WU	s	1.14	1.33	1.75	2.44
		c	1.90	2.04	2.37	2.87
ΔL^*	CU (1.02)	s	-0.15	0.06	-0.84	-0.28
		c	0.27	0.06	-0.15	-0.34
	AU (3.32)	s	-2.17	-2.82	-1.63	-2.64
		c	ND	-3.57	ND	-4.05
	SU (0.72)	s	-0.06	0.00	-0.48	-0.40
		c	0.43	0.20	0.14	0.22
	WU (0.78)	s	0.05	0.32	0.17	-0.22
		c	-0.11	0.58	0.44	-0.65
Δa^*	CU (0.04)	s	-0.10	-0.06	-0.07	-0.06
		c	-0.07	-0.12	-0.11	-0.15
	AU (0.82)	s	0.67	1.05	1.39	1.76
		c	ND	1.06	ND	1.90
	SU (0.04)	s	-0.32	-0.44	-0.54	-0.57
		c	-0.36	-0.46	-0.54	-0.57
	WU (0.08)	s	-0.40	-0.48	-0.61	-0.72
		c	-0.58	-0.71	-0.75	-0.77
Δb^*	CU (0.18)	s	0.61	1.26	1.48	1.92
		c	0.93	1.18	1.91	1.86
	AU (2.18)	s	2.78	3.43	4.22	5.29
		c	ND	3.58	ND	6.40
	SU (0.24)	s	1.00	1.54	2.17	2.70
		c	1.27	1.69	1.98	2.20
	WU (0.48)	s	1.38	1.58	2.16	3.17
		c	2.41	2.49	3.01	3.75

Notes for Table 7.4:

- Since ΔL^* , Δa^* , and Δb^* are calculated by subtracting the colour parameter before ageing from that after ageing, the error can be approximated by adding together the standard deviation of each value. The standard deviations used in these calculations are those calculated in Chapter 5 when characterising the uniformity of the unaged textile colouration. SCI/100 data was used to calculate these errors while SCE/100 data is used in the CIE2000 calculations. There was little difference between the SCI/100 and SCE/100 data;
- Not done.

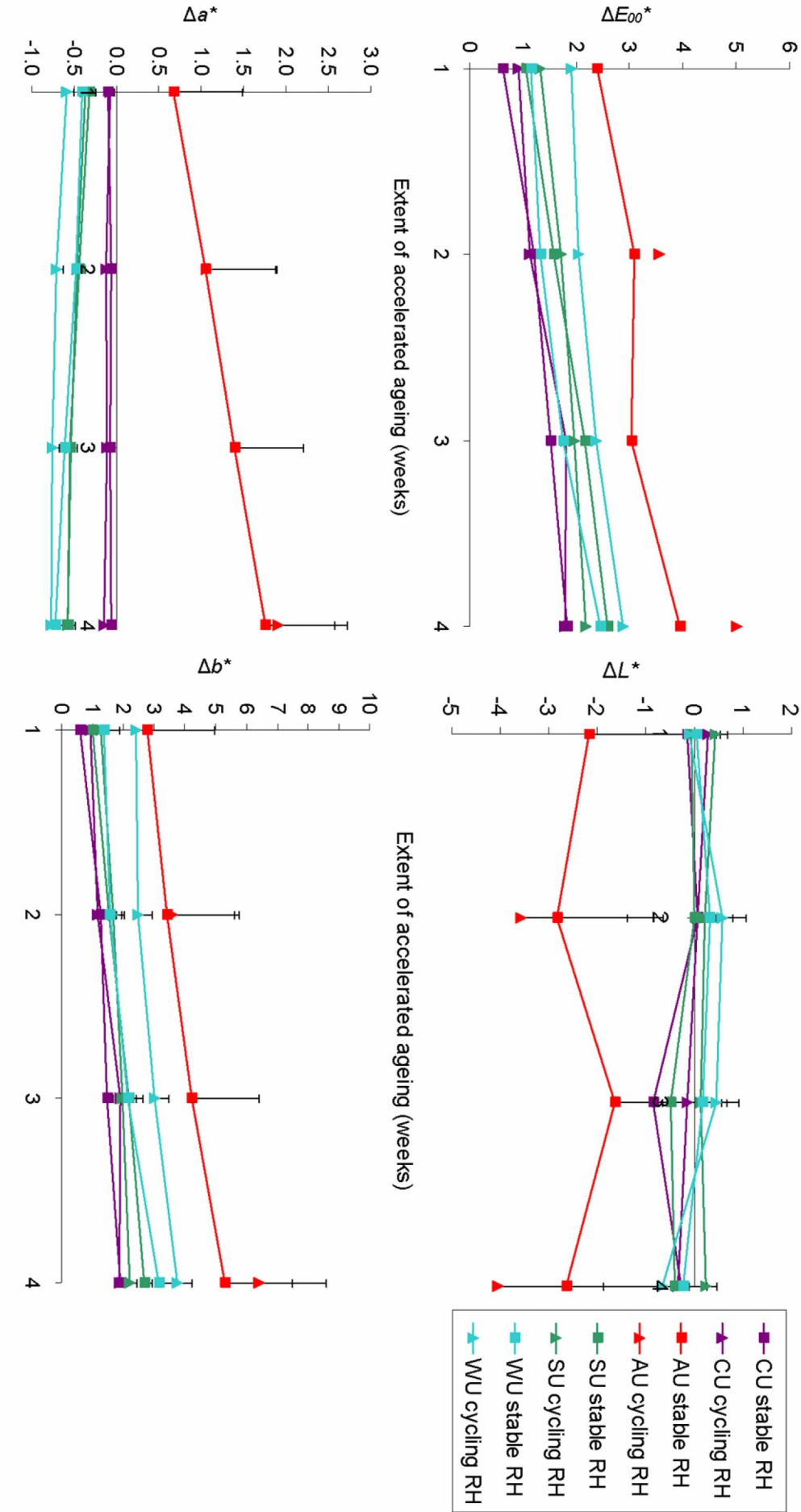


Figure 7.3 The change in colour of the undyed model textiles due to accelerated ageing using cycling and stable RH

7.5 Results and discussion

All undyed textiles showed a colour change (ΔE_{00}^*) greater than 1.6 after 4 weeks of ageing in either condition (Table 7.4 and Figure 7.3). For CU and SU the difference between cycling and stable RH conditions was small and inconsistent with extent of ageing. For AU and WU cycling RH conditions caused consistently greater colour change than stable RH conditions. The difference in colour change between samples aged using different methods is greatest with AU ($\Delta E_{00}^* = 2.06$). No consistent trends in the variation of ΔL^* , Δa^* , or Δb^* with ageing method was apparent.

There was no significant difference in ΔL^* between cycling and stable RH ageing of any of the undyed model textiles.

After 4 weeks of ageing, a small but significant decrease in Δa^* was seen for cycling RH aged CU compared to stable RH aged CU. For the first 2 weeks of ageing cycling RH caused greater Δa^* (more negative) in WU than stable RH ageing, but by the 3rd week the difference between ageing conditions was insignificant. AU and SU show no significant difference in Δa^* with age.

By 4 weeks of ageing SU shows greater Δb^* with stable RH than with cycling RH conditions. CU, AU, shows no consistently significant change in Δb^* due to ageing method. Cycling RH caused a greater Δb^* than stable ageing for 1 week only, after which, differences in Δb^* due to ageing method were insignificant.

7.5.3.2 Dyed textiles

Table 7.5 The change in colour of the dyed (p1 and c1) model textiles after accelerated ageing with stable and cycling RH methods

Change in colour parameter compared to unaged sample	Sample (approximate error) ^a	Ageing method	Extent of ageing (weeks)			
			1	2	3	4
ΔE_{00}^*	Cc1	s	7.35	10.49	12.15	13.24
		c	7.80	10.54	12.40	14.53
	Ac1	s	3.04	4.54	5.33	4.96
		c	2.86	5.52	7.68	8.09
	Sp1	s	1.07	1.78	2.15	3.27
		c	1.54	1.89	2.25	2.65
	Wp1	s	ND ^b	2.74	3.64	5.70
		c	ND	3.38	4.00	5.30
ΔL^*	Cc1 (2.02)	s	-4.23	-4.68	-5.71	-6.72
		c	-5.76	-7.17	-3.69	-5.26
	Ac1 (1.50)	s	0.24	-0.37	-0.68	-2.00
		c	0.30	1.59	1.65	1.57
	Sp1 (0.40)	s	-0.61	-0.31	0.25	2.02
		c	-0.49	-0.51	-0.66	-0.27
	Wp1 (2.06)	s	ND	-0.50	0.42	3.33
		c	ND	-0.10	0.37	-0.57
Δa^*	Cc1 (0.10)	s	0.30	1.29	2.29	3.02
		c	0.49	1.26	2.30	4.19
	Ac1 (0.10)	s	0.11	0.63	1.20	1.08
		c	0.03	0.67	1.83	2.46
	Sp1 (0.06)	s	-0.17	-0.30	-0.41	-0.39
		c	-0.15	-0.32	-0.38	-0.47
	Wp1 (0.08)	s	ND	-0.39	-0.46	-0.62
		c	ND	-0.43	-0.53	-0.60
Δb^*	Cc1 (0.26)	s	6.92	10.55	12.24	13.22
		c	6.69	9.45	13.29	15.51
	Ac1 (0.24)	s	3.17	4.64	5.34	4.75
		c	2.99	5.59	7.87	8.13
	Sp1 (0.14)	s	1.13	1.98	2.37	3.24
		c	1.71	2.07	2.45	2.90
	Wp1 (0.24)	s	ND	2.73	3.70	5.21
		c	ND	3.44	4.09	5.56

Notes for Table 7.5:

- Since ΔL^* , Δa^* , and Δb^* are calculated by subtracting the colour parameter before ageing from that after ageing, the error can be approximated by adding together the standard deviation of each value. The standard deviations used in these calculations are those calculated in Chapter 5 when characterising the uniformity of the unaged textile colouration. SCI/100 data was used to calculate these errors while SCE/100 data is used in the CIE2000 calculations. There was little difference between the SCI/100 and SCE/100 data;
- Not done.

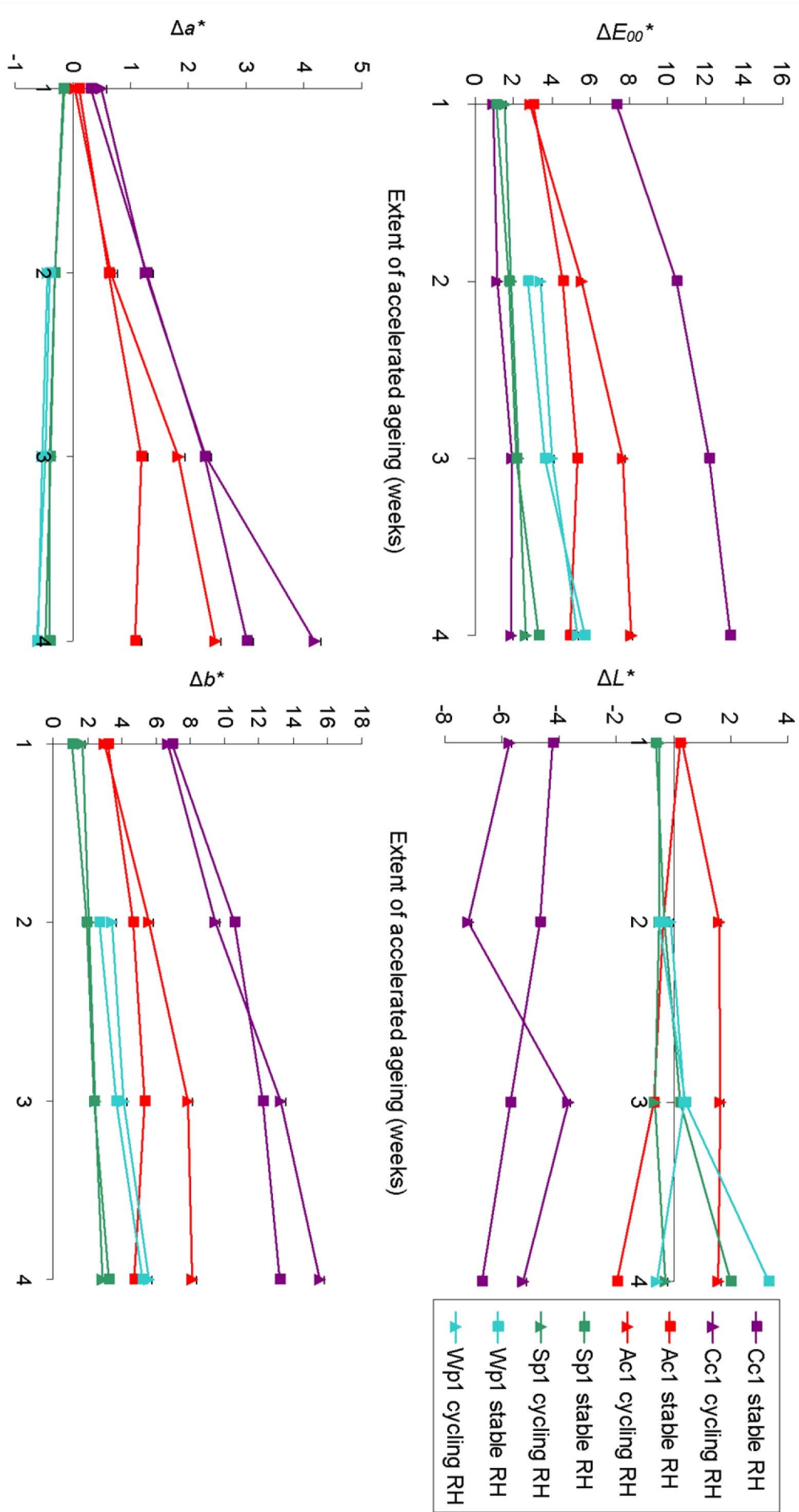


Figure 7.4 The change in colour of the dyed (p1/c1) model textiles due to accelerated ageing using cycling and stable RH

7.5 Results and discussion

Cycling RH conditions produced colour change (ΔE_{00}^*) in Cc1 that was consistently, though only slightly, greater than for stable RH conditions (Table 7.5 and Figure 7.4). For Ac1 cycling RH caused significantly greater colour change than for stable RH conditions with a difference in ΔE_{00}^* of 3.13 after 4 weeks of ageing. In contrast, after 4 weeks of ageing Sp1 and Wp1 aged with stable RH showed the most colour change despite stable ageing causing the least colour change for the first 3 weeks of ageing.

No significant difference in lightness (ΔL^*) of the samples due to accelerated ageing method was seen with Cc1, Ac1, or Wp1. However, after 4 weeks of ageing, the stable RH aged Sp1 was significantly lighter than the cycling RH aged Sp1.

Cycling RH caused significantly greater reddening ($+\Delta a^*$) of Ac1 after 1 week of ageing and of Cc1 after 3 weeks of ageing than the stable RH conditions. No significant change in redness (Δa^*) was seen in Sp1 or Wp1 samples due to accelerated ageing method.

By 3 and 4 weeks of ageing cycling RH conditions had caused significantly greater yellowing ($+\Delta b^*$) than the stable RH conditions despite stable RH conditions causing the largest yellowing at 2 weeks of ageing. For Ac1 cycling RH caused the larger yellowing ($+\Delta b^*$) of the two methods from week 2 of ageing. For Sp1 the trend in which condition caused the greatest Δb^* is less consistent; cycling RH caused the greatest significant Δb^* at 1 week of ageing but stable RH caused the greatest significant Δb^* after 4 weeks of ageing. In between there was no statistically significant difference between ageing methods. For Wp1 the difference in Δb^* due accelerated ageing method was generally insignificant.

7.5.4 Surface pH

Table 7.6 The surface pH of the dyed and undyed model textiles after accelerated ageing with stable and cycling RH methods

Textile	Surface pH	Accelerated ageing method	Accelerated ageing period (weeks)							
			DYED (c1 or p1)				UNDYED			
			1	2	3	4	1	2	3	4
ABACA	Mean	s	2.9	2.8	2.7	2.6	6.2	6.1	5.9	5.7
		c	3.4	2.9	2.5	2.5	-	5.6	-	5.4
	SD ^a	s	0.1	0.1	0.1	0.1	0.2	0.0	0.1	0.1
		c	0.0	0.1	0.1	0.2	-	0.2	-	0.0
	CV ^b	s	4.3	4.4	4.9	3.4	2.5	0.6	1.8	1.3
		c	0.3	2.2	2.6	5.9	-	3.3	-	0.6
COTTON	Mean	s	3.3	3.1	3.1	3.2	6.5	6.4	6.1	6.5
		c	3.5	3.5	3.0	2.8	6.4	6.0	6.1	6.2
	SD ^a	s	0.1	0.1	0.2	0.0	0.1	0.0	0.2	0.1
		c	0.1	0.2	0.1	0.1	0.1	0.4	0.1	0.1
	CV ^b	s	2.3	3.5	5.5	0.4	1.9	0.5	3.6	1.4
		c	3.8	6.2	4.3	2.4	1.6	6.3	2.0	1.5
SILK	Mean	s	3.6	3.5	3.4	3.4	7.4	7.4	7.2	7.2
		c	3.9	3.7	3.8	3.5	7.5	7.1	7.1	7.0
	SD ^a	s	0.0	0.0	0.1	0.0	0.1	0.1	0.1	0.1
		c	0.2	0.0	0.1	0.1	0.2	0.2	0.1	0.3
	CV ^b	s	0.7	1.0	2.1	0.9	1.5	1.2	1.2	1.3
		c	4.6	0.8	3.2	2.5	2.3	3.0	0.9	4.3
WOOL	Mean	s	3.6	3.6	3.6	3.3	7.5	7.3	7.2	7.2
		c	-	3.5	3.4	3.4	7.0	7.0	7.1	6.8
	SD ^a	s	0.1	0.0	0.2	0.0	0.1	0.1	0.1	0.1
		c	-	0.1	0.0	0.2	0.1	0.1	0.1	0.1
	CV ^b	s	1.8	0.9	6.7	0.7	1.9	1.7	0.8	1.5
		c	-	2.3	1.3	4.7	0.8	1.8	1.0	1.5

Notes for Table 7.6:

- a. Standard deviation;
- b. Coefficient of variation.

7.5 Results and discussion

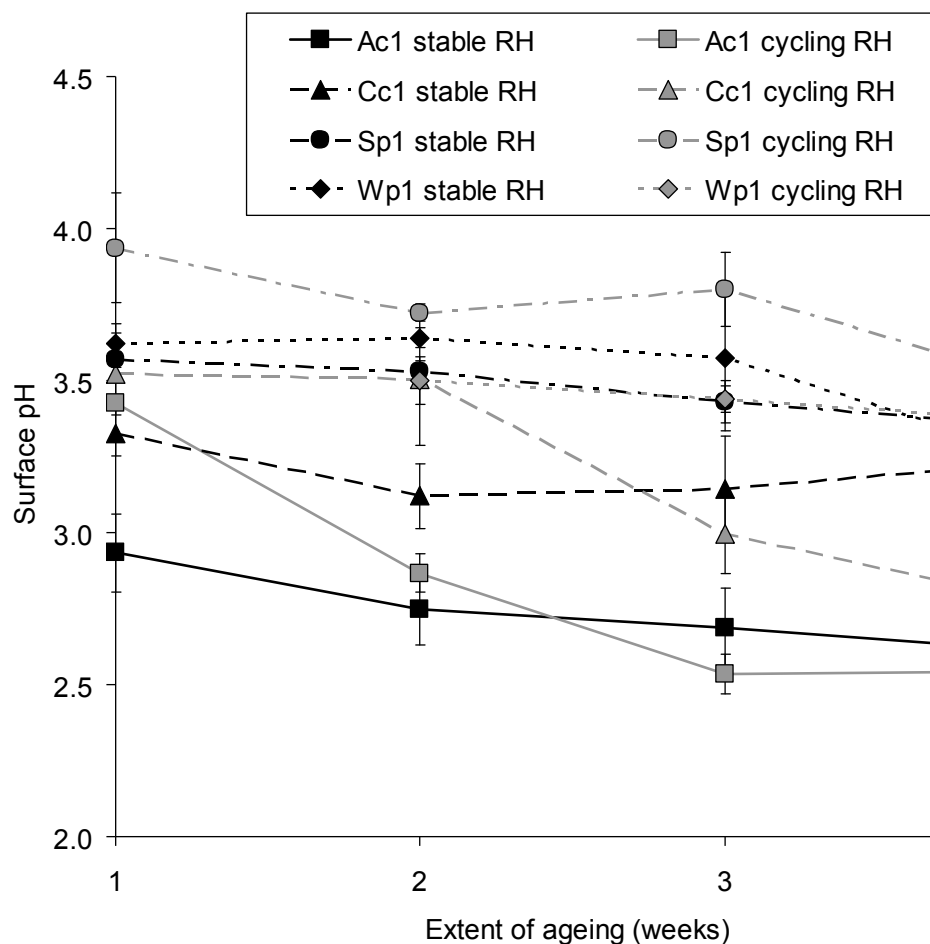


Figure 7.5 The variation in surface pH of c1 and p1 dyed model textiles with different accelerated ageing methods

The undyed model textiles showed no significant changes in surface pH with either accelerated ageing method (Table 7.6 and Figure 7.5). The dyed model textiles generally showed little if any significant change in surface pH on ageing. For Cc1, Ac1, and Sp1 the change in surface pH due to cycling RH accelerated ageing conditions was typically greater than that produced with the stable RH conditions but often not statistically significant.

7.5.5 GPC-MALLS

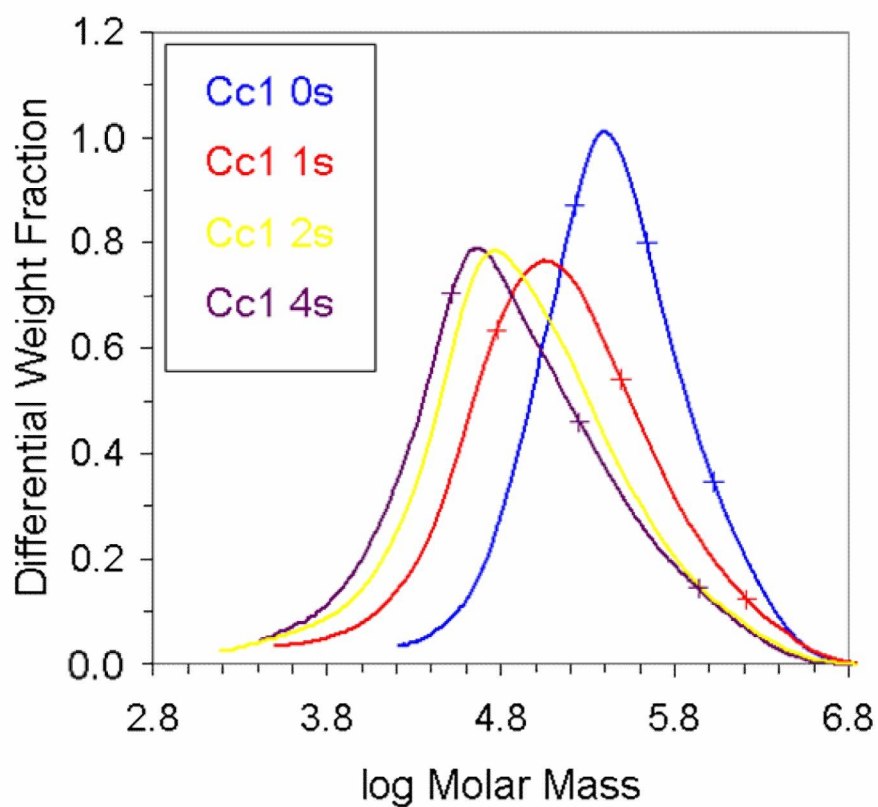


Figure 7.6 The changing molar mass distribution of Cc1 during accelerated ageing with stable RH (80°C, 58% RH)

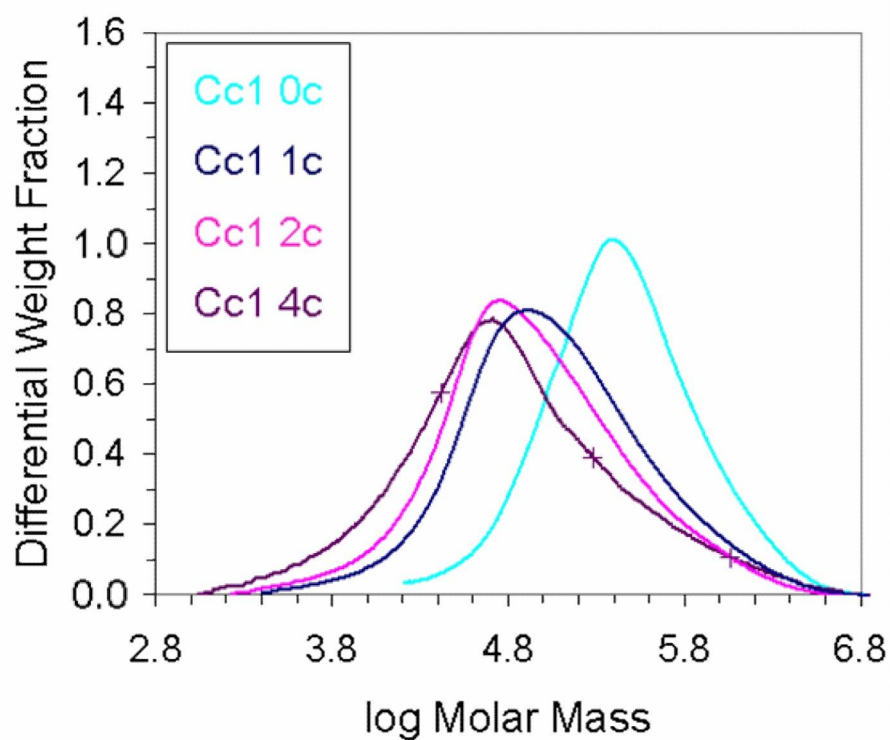


Figure 7.7 The changing molar mass distribution of Cc1 during accelerated ageing with cycling RH (80°C, 35-80% RH)

7.5 Results and discussion

Table 7.7 The effect of different accelerated ageing methods on the molecular weight and PDI of CU and Cc1 model textiles

Model textile	Extent of ageing (weeks)	Stable or cycling RH ^a	DP _n	Average molecular weight		PDI	% polymer content in			
				M _n (kg/mol)	M _w (kg/mol)		DP<100	DP100-200	DP200-2000	DP>2000
CU	0		3164	513	1037	2	0	0	12	88
	2	S	3286	532	878	2	0	0	12	88
	2	C	3238	525	1053	2	0	0	13	87
	4	S	2843	461	859	2	0	0	17	84
	4	C	2875	466	829	2	0	0	15	85
Cc1	0		1051	170	439	3	0	2	57	42
	1	S	369	60	313	5	5	7	64	24
	1	C	351	57	244	4	5	9	68	19
	2	S	209	34	205	6	10	12	63	15
	2	C	256	42	189	5	7	12	66	14
	4	S	203	33	180	6	12	16	59	14
	4	C	161	26	191	7	15	16	56	14

Notes for Table 7.7:

- a. 's' is used to denote the use of stable RH in accelerated ageing, 80°C, 58% RH. 'c' is used to denote the use of cycling RH in accelerated ageing, 80°C, 35-80% RH every 3 hours (35-80-35 in 6 hours).

Table 7.8 The effect of different accelerated ageing methods on the carbonyl content of CU and Cc1 model textiles

Model textile	Extent of ageing (weeks)	Stable or cycling RH ^a	Theoretical amount of reducing end groups (oxidised groups) (μmol/g)	Overall carbonyl content (μmol/g)
CU ^a	0		2 (2)	4
	2	S	2 (3)	5
	2	C	2 (2)	4
	4	S	2 (2)	4
	4	C	2 (2)	4
Cc1	0		6 (15)	21
	1	S	17 (24)	41
	1	C	18 (25)	42
	2	S	30 (22)	51
	2	C	24 (28)	52
	4	S	30 (34)	64
	4	C	38 (37)	75

Notes for Table 7.8:

- a. 's' is used to denote the use of stable RH in accelerated ageing, 80°C, 58% RH. 'c' is used to denote the use of cycling RH in accelerated ageing, 80°C, 35-80% RH every 3 hours (35-80-35 in 6 hours).

7.6 Choice of accelerated ageing conditions for use in Treatment Test 1 (Chapter 9)
The results in Tables 7.7 and 7.8 indicate that the different accelerated ageing methods produced comparable results in CU by four weeks of ageing. This resulted in a similar lack of change in tensile properties and similarly low levels of discolouration of CU during ageing.

Small differences between the average molecular weights and PDI of the differently aged dyed (Cc1) samples exist after two and four weeks of ageing (Table 7.7). These suggest that after two weeks of ageing the stable RH aged samples were slightly more degraded than the cycling RH aged samples but that by four weeks of ageing, the cycling RH aged samples were the most degraded. This correlates well with tensile testing data of the samples which showed that by four weeks of ageing the cycling RH aged sample was weaker than the stable RH aged sample. By four weeks of ageing the carbonyl content in the cycling RH aged dyed sample was greater than that in the stable RH aged dyed sample. Calculation of approximate REG content suggests that after two weeks of ageing the stable RH aged Cc1 sample had undergone more hydrolysis and less oxidation than the cycling aged sample but that by four weeks the cycling aged sample had undergone more hydrolysis and oxidation. Colorimetry of the dyed samples during ageing showed that the cycling aged sample discoloured more than the stable RH aged sample throughout the study by a small amount.

7.6 Choice of accelerated ageing conditions for use in Treatment Test 1 (Chapter 9)

In order for the results of accelerated ageing to be comparable to those of natural ageing, the elevated conditions used need to be as close as possible to those used in natural ageing, whilst also producing the required level of degradation within a short time (a maximum of 6 weeks for this project). These accelerated ageing studies have identified that the conditions used with temperatures of 75°C, 80°C, and 90°C can produce significant strength loss within 7 weeks in all but the undyed textiles and dyed wool textiles. The particularly fast strength loss that occurred in Cc1 and Ac1 at 90°C is possibly too rapid for use in this project as it may cause subtle physical and chemical trends to be missed.

Based on these tests little difference in sample degradation occurs through the use of cycling RH rather than stable RH. Any small statistically significant differences that do occur indicate that cycling RH produces slightly greater degradation than the stable RH. This may be due to the expected increase in stress exerted on the fibres through their continual expansion and contraction with the continual fluctuations in moisture content in the atmosphere. Consequently either cycling RH or stable RH could be used with similar

7.6 Choice of accelerated ageing conditions for use in Treatment Test 1 (Chapter 9)
effect in Treatment Test 1. However, as with higher temperatures, the use of a cycling RH cycle increases the demands on the equipment and increases the risk of malfunction of the environmental chamber. One such malfunction occurred during these tests. It is therefore more sustainable to use lower temperatures and stable RH and to thus minimise the chances that the environmental chambers will malfunction during the test. Additionally, since ideally British Museum objects are stored in stable RH environments it follows that the use of a stable rather than cycling RH will cause the degradation in the samples after treatment to be more representative of that expected during the natural ageing of British Museum objects after treatment. Conversely, the use of cycling RH may better simulate the natural degradation that British Museum objects underwent prior to being acquired by the British Museum. Cycling RH could therefore be most suitable when pre-ageing model textiles in Treatment Test 2 to simulate the condition of historic objects prior to treatment application.

The need for a standard set of conditions to be used by researchers to enable the acquisition of comparable results has been highlighted (Porck 2000; Banik 2009) and suggests that it would be useful if the conditions used in Treatment Test 1 were comparable to those used in studies into either iron-tannate dyed textiles or iron gall ink on paper. Of the many conditions used, the use of 80°C and 65% RH looks most suitable as it has been used in research into a non-aqueous treatment for iron-gall ink on paper (Kolar, Mozir, Strlic, Ceres, Conte, Mirruzzo, Steemers and de Bruin 2008) and is close to the conditions used in condition 5 of these tests (80°C and 58% RH) which caused significant degradation to dyed cotton, abaca, and silk within the timeframe needed. These conditions also fall within the range (RH between 30 and 80% at a temperature between 60 and 90°C) that Erhardt and Mecklenburg (Erhardt and Mecklenburg 1995) proposed would result in pure cellulose of comparable degradation to naturally aged paper since variation in the condition of naturally aged paper will result due to fluctuations in the natural ageing conditions over time. The RH is however greater than that which the British Museum objects are exposed to and therefore does not comply with the suggestion that the same RH as that used in natural ageing be used in accelerated ageing (Erhardt and Mecklenburg 1995; Porck 2000). The need for a standard set of conditions to be used by researchers also suggests that both the proteinaceous and cellulosic materials should be aged using the same conditions for different lengths of time rather than using different conditions for the same length of time. Based on the results from condition 5 in these tests, the dyed cellulosic textiles should show significant degradation in 2 weeks of ageing at 80°C and 65% RH without being too weak to handle and test mechanically. Between 4 and 6 weeks of ageing can be used for

7.7 Natural ageing studies

the proteinaceous textiles though it is expected that the dyed wool will show no significant degradation. Due to the quantity of samples to be aged, ageing samples in stacks rather than individually (e.g. laid flat or suspended) will be necessary. However, accelerated ageing of stacks of paper have been found to simulate natural ageing better than paper aged individually (Begin and Kaminska 2002).

7.7 Natural ageing studies

A range of real-time ageing tests of SU, CU, Sp3, and Cc3 have been prepared with Dr Marei Hacke and Pippa Cruickshank at the British Museum. Unaged samples of the textiles that are untreated and those that are treated with the T292-260, MP30/2CB30, and ME30 treatments that are used in Treatment Test 1 are being framed in conservation grade mounting board in preparation for placement in an exhibition case in the British Museum. Two other sets of framed samples are in production one of which will be placed in dark storage at Blythe House (a storage facility for British Museum objects) and the other in a lit uncontrolled environment. Pippa Cruickshank and Dr Marei Hacke will monitor the samples during ageing using spectrophotometry, viscometry (cotton only), and potentially micro-pH testing.

7.8 Conclusions

The subjective and objective analyses of accelerated aged model textiles confirmed that iron-tannate dye formulation 1 accelerates the degradation of cotton, abaca, and silk but not of wool. The causes of the latter are explained in Chapter 4. The accelerated ageing tests showed that if there was any statistically significant difference, cycling RH caused faster degradation than stable RH to the dyed cotton, abaca, and silk. However the differences were small. The tests also indicated the capabilities and limitations of the environmental chambers available which affected the choice of ageing conditions to be used. The use of a stable RH, a temperature below 90°C, and ideally, conditions that had been used in other iron-tannate dye or iron gall ink research resulted in the decision to use 80°C and 65% RH on the cotton and silk textiles in Treatment Test 1. All of the model textiles will experience the same conditions during ageing but the silk textiles will be aged for four weeks while the cotton textiles will be aged for two weeks in order to gain the best results from each material. Finally, real-time ageing studies of model textiles from this project have been discussed and initiated.

8 STABILISATION TREATMENTS FOR IRON-TANNATE DYED TEXTILES

Having validated the use of the model iron-tannate dyed textiles as substitutes for historic material in stabilisation treatment studies, a strategy to determine which chemicals and solvents will be tested was needed. This chapter provides a literature review of relevant stabilisation treatments, based upon which a range chemicals and solvents was chosen. The reagents' properties and experimentation with treatment combinations for further investigation are presented here.

8.1 Conservation strategies

Through conservation we seek to preserve for the benefit of future generations objects from the past for their information and meaning. Conservation encompasses preventive conservation, remedial (interventive) conservation, and restoration. In preventive conservation the environment e.g. conditions of storage, transportation, and handling, and the environmental conditions, of the object is altered to prevent further degradation to the object. Unlike in preventive conservation where the object is usually treated as part of a group, in remedial conservation the object is usually treated individually and is altered either physically or chemically or both to arrest degradation reactions and stabilise the object's structure. Restoration involves the altering of an object that has already lost part of its function or meaning e.g. through degradation or previous alteration, to improve its appreciation and facilitate its use and understanding (Caple 2000; ICOM-CC 2008). In this project, non-aqueous chemical remedial conservation treatments are investigated, using accelerated ageing, for their ability to slow down the rate of degradation of iron-tannate dyed organic materials.

8.2 Theory of stabilisation

As discussed in Chapter 4 iron-tannate dyed organic materials become weak, brittle, and often discolour at a faster rate than undyed equivalents. A treatment will ideally conserve the structural integrity and appearance of an object to extend the object's useful lifetime. This can be achieved by chemical and physical means using preventive and remedial conservation methods. For example, for well-preserved chintzes incorporating iron-tannate dyed outlines in the pattern, it has been recommended that only the preventive conservation measures of low light levels and stable temperature and RH be used (Hofenk de Graaff 2002). Strong and flexible objects (i.e. at low risk of mechanical damage) can also be stabilised with chemical remedial conservation treatments involving deacidifiers and antioxidants since acid hydrolysis and metal-catalysed oxidation are the major degradation mechanisms of the iron-tannate dyed organic materials. Such remedial

8.2 Theory of stabilisation

conservation treatments alone will be of little benefit to a significantly weakened object since much of the degradation that these treatments prevent has already occurred (Pullan and Baldwin 2008; Strlic, Csefalvayova, Kolar, Menart, Kosek, Barry, Higgitt and Cassar 2010). Physical remedial conservation such as consolidants with or without chemical stabilisation treatments or attaching a support fabric to a material can be used to strengthen significantly weakened objects that are at high risk of mechanical damage. Examples of physical remedial conservation on objects containing iron-tannate dye include the lining of a fragile banana fibre belt (Cruickshank and Morgan 2011), and stabilisation of a Great Lakes iron-tannate dyed skin pouch (Cruickshank, Daniels and King 2009). The need for a chemical remedial conservation treatment becomes particularly apparent when objects such as the iron-tannate dyed cotton of an Akali Sikh turban are retired from 'active museum service' and their continued degradation accepted because they are too fragile for even consolidation to be of benefit (Pullan and Baldwin 2008).

The following sections discuss the use of antioxidants, deacidifiers, and consolidants on historic and model iron gall ink and iron-tannate dyed samples. A summary of such research has been published (Kolar and Strlic 2006).

8.2.1 *Antioxidants*

Antioxidants can be divided into two main categories: chain breaking antioxidants (Scott 1993c) and preventive antioxidants (Al-Malaika 1993). Chain breaking antioxidants are radical scavengers that produce stable products on reaction with the radicals that propagate the oxidative chain reaction. Preventive antioxidants prevent the formation of radicals for example by using metal ion chelators or peroxide decomposers (Scott 1993c; Kolar, Malesic and Strlic 2005). The combination of different types of antioxidant at once can produce powerful synergistic effects, e.g. between ascorbic acid and α -tocopherol (Scott 1985; Scott 1993a; Hras, Hadolin, Knez and Bauman 2000). In antioxidants that have multiple antioxidative functions, auto-synergism between these functions can occur (Scott 1985). Gallic acid (Kolar, Malesic and Strlic 2005) and tannic acid (Andrade Jr., Ginani, Lopes, Dutra, Alonso and Hermes-Lima 2006) for example can scavenge radicals and chelate iron ions while iodide ions are radical scavengers and peroxide decomposers (Bray and Liebafsky 1931; Kolar and Strlic 2006).

Examples of antioxidants that have been investigated for their ability to stabilise iron-gall inked paper and iron-tannate dyed objects are discussed below. Of these, myo-inositol hexaphosphate (phytic acid) (Neevel 2002; Kolar, Mozir, Strlic, de Bruin, Pihlar and

Steemers 2007), Tinuvin 770 (bis(2,2,6,6-tetramethyl-4-piperidiny) sebacate) (Kolar, Malesic and Strlic 2005), tetrabutylammonium chloride (TBACl) or bromide (TBABr) (Malesic, Kolar, Strlic and Polanc 2005), NNNN-tetrakis(2-pyridylmethyl)ethylenediamine (TPEN) (Cude 2010), 1-ethyl-3-methylimidazolium Bromide (EMIMBr), and 1-butyl-2,3-dimethylimidazolium bromide (BDMIMBr) (Kolar, Mozir, Balazic, Strlic, Ceres, Conte, Mirruzzo, Steemers and De Bruin 2008) have been shown to be particularly effective at slowing down the degradation of iron gall ink on paper.

8.2.1.1 Metal ion chelators

A range of metal ion chelators have been investigated in iron gall ink research, most notably phytate which has been developed to a point where its usage on cultural heritage objects as the calcium or magnesium phytate/calcium bicarbonate treatment has been accepted (Neevel 2002). More information about the phytate treatment is presented in Section 8.2.2. Other metal ion chelators studied in either synthetic Fenton-like systems¹, model iron gall inked papers, or iron-tannate dyed materials include tannins, diethylenetriaminepentaacetate (DTPA), desferrioxamine methanesulphonate (desferal), ethylenediaminetetraacetic acid (EDTA), citric acid, acetylacetone, dibenzoylmethane, TPEN, and cysteine (Bulska, Wagner and Sawicki 2001; Smith, Te Kanawa, Miller and Fenton 2001; Strlic, Kolar and Pihlar 2001; Wagner and Bulska 2003; Cude 2010; Sato, Okubayashi and Sato 2011).

To be a successful antioxidant the chelator needs to bind to the iron or other metal ion to produce an inert, colourless complex that is preferably soluble (and over a wide pH range) so that complexed and uncomplexed metal can be removed from the sample during treatment. Additionally, it must not breakdown the iron-tannate complex or be detrimental to the stability of the support (Bulska, Wagner and Sawicki 2001; Wagner and Bulska 2003). DTPA, phytate, and desferal showed antioxidant properties (increasing in the order given) at 20°C (Strlic, Kolar and Pihlar 2001). Based on their iron ion extraction abilities from iron gall inked and non-inked papers, DTPA (pH 9), desferal (pH 8), and potassium-magnesium phytate (pH 7) were viewed as the most successful treatments of those tested

¹ Synthetic Fenton-like systems such as the *N,N'*-(5-nitro, 1,3-phenylene)-bisglutaramide (NPG) hydroxylation assay that has been used in iron gall ink research can be aqueous systems in which the Fenton reaction can be studied. The NPG hydroxylation assay is a simpler model system than a real cellulose system (e.g. paper with ink) and so the effects of different factors on the production of radicals and efficacy of antioxidants can be determined more easily yet are expected to be applicable to the real cellulose systems in which water is present for the chemical reactions to occur (Malesic, J., J. Kolar, M. Strlic and S. Polanc (2006). "The influence of halide and pseudo-halide antioxidants in Fenton-like reaction schemes." *Acta Chim. Slov.* **53**: 450-456.).

8.2 Theory of stabilisation

(Wagner and Bulska 2003). Accelerated ageing studies of these or comparable samples are needed to confirm the long-term success of these treatments. DTPA was viewed as particularly successful since it is likely to be neutral for cellulose as it is already used in the paper industry and it could potentially bind other reactive metal ions such as copper and manganese as well as iron. Additionally, by applying the treatment at this pH a subsequent deacidification treatment is not necessary² and it can be applied in a water/alcohol solvent (though a second application is needed as increasing the alcohol content decreases the extraction abilities of the ligands) (Wagner and Bulska 2003). The high alkalinity of this treatment (pH 9) is of concern since iron-tannate complexes can break down at pH > 8.0 (Krekel 1999). This was not considered within the paper but may not have been a problem due to the short immersion times tested (maximum of 20 minutes). While desferal was found to be successful at extracting iron ions from paper (Wagner and Bulska 2003), it is reported to have broken down the iron gall complex, causing a weakening of the colour of the iron gall ink after 30 minutes of immersion (Bulska, Wagner and Sawicki 2001). Consequently, potentially only the potassium-magnesium phytate (pH 7) is of benefit to iron-tannate dyed textiles. The acetylacetone and dibenzoylmethane also studied by these authors were found to not fulfil the pre-defined aims of a conservation treatment for iron gall inked paper because iron-dibenzoylmethane complexes were coloured and not easily removed from the paper, and acetylacetone gave unsatisfactory extents of iron ion extraction (Bulska, Wagner and Sawicki 2001)

EDTA and citric acid showed pro-oxidant effects by promoting the production of hydroxyl radicals (Strlic, Kolar and Pihlar 2001). EDTA is used in conservation in the bleaching of paper and to remove iron ions from paper (Burgess 1991). However, it is unsuitable for use on iron gall ink as it can breakdown the iron(III) tannate complexes in which the iron(III) is inert and insoluble and bind them in soluble, catalytically active EDTA complexes, thus increasing the quantity of reactive iron ions present in the system (South and Miller 1998). EDTA binds iron ions in all six binding sites but due to the small size of EDTA a seventh site is made available with which iron can participate in the Fenton reaction (Graf and Eaton 1990; Engelmann, Bobier, Hiatt and Cheng 2003). Citric acid is an important natural antioxidant that is widely used in the food industry as it strongly chelates metal ions such as iron ions using its carboxyl and hydroxyl groups (Hras, Hadolin, Knez and Bauman

² No pH data of the treated papers was published to support this. Consequently, there is no evidence to suggest that lower pH conditions during chelate application do not deacidify the paper to a suitable (unstated) extent. In view of the high alkalinity of pH 9 and the potential discolouration to iron gall ink and alkaline hydrolysis that may be able to occur, a lower pH with slightly lower iron ion extraction ability might be preferable.

8.2 Theory of stabilisation

2000). However, references noted by Strlic, Kolar, and Pihlar (Strlic, Kolar and Pihlar 2001) show that iron(III)-citrate complexes are catalytically active complexes that are more soluble than iron(III) ions and in the case of iron(II)-citrate, are more reactive than the iron(II) ions. Photo-degradation of iron(III)-citrate complexes is particularly rapid and forms iron(II) ions and peroxide (Faust and Zepp 1993). Additionally, the presence of an α -hydroxyl group in citric acid may increase hydroxyl radical formation via the Fenton reaction as has occurred with a range of other α -hydroxyl acids (Ali and Konishi 1998).

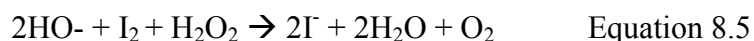
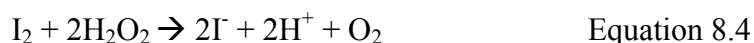
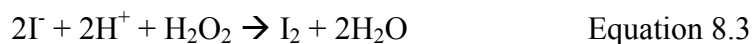
Cysteine in the lower concentration tested was shown to stabilise iron-tannate dyed silk, sometimes to a greater extent than phytate (Sato, Okubayashi and Sato 2011). As well as being a metal ion chelator due to the thiol group, cysteine also quenches hydrogen peroxide (Sato, Okubayashi and Sato 2011). The higher concentration of cysteine was not an effective stabiliser possibly due to interaction between cysteine molecules.

The application of tannins, in this case aqueous *hinau* extract, to iron-tannate dyed *Phormium tenax*, was shown to significantly inhibit the degradation of the substrate. This effect is due to iron(III) ions binding more strongly to the catechol groups of tannin than to the carboxylic acid groups in the substrate so that when the tannin is applied, the iron(III) ions transfer from carboxylic acid groups to the catechol groups. This prevents iron(III)-catalysed decarboxylation of the carboxylic acid groups which produces radicals that can weaken the fibre and cause the dye to fade. It also improves the colour of the substrate, taking it back to a colour closer to the original, and is an original component of the material, unlike the other antioxidants under investigation (Smith, Te Kanawa, Miller and Fenton 2001).

TPEN is a derivative of EDTA that is able to strongly chelate divalent metal ions including iron(II), copper(II), manganese(II), and zinc(II) ions and is soluble in aqueous and a range of non-aqueous solvents including ethanol. As well as being a metal ion chelator it can act as a radical scavenger at concentrations of $7.5 \mu\text{molL}^{-1}$ and it has been shown to provide comparable stabilisation to phytate on iron gall inked paper when applied in water. However, the iron(II)-TPEN complex is bright yellow and TPEN is amber coloured (Cude 2010). While the iron-TPEN complex was soluble in water and so removed from the paper samples in this study, its solubility in non-aqueous solvents has not yet been tested.

8.2.1.2 Peroxide decomposers

Halides such as iodide and bromide act as peroxide decomposers when under acidic conditions, and radical scavengers and have been investigated in an NPG hydroxylation assay and on paper (with and without iron gall ink) with a variety of associated cations e.g. potassium, imidazolium, tetrabutylammonium, and tetraethylammonium cations (Malesic, Kolar, Strlic and Polanc 2006; Ceres, Conte, Mirruzzo, Kolar and Strlic 2008; Kolar, Mozir, Balazic, Strlic, Ceres, Conte, Mirruzzo, Steemers and De Bruin 2008). Halides are of particular interest as antioxidants for conservation because their stabilisation properties are independent of the metal ion present and some of the compounds, e.g. imidazolium bromides and some ammonium bromides, can be dissolved in and have been tested in non-aqueous solvents such as ethanol or dichloromethane (Malesic, Kolar, Strlic and Polanc 2005; Ceres, Conte, Mirruzzo, Kolar and Strlic 2008; Kolar, Mozir, Balazic, Strlic, Ceres, Conte, Mirruzzo, Steemers and De Bruin 2008). Indeed in one study the imidazolium bromides tested were more successful as antioxidants and at retaining the colour of iron gall inked paper in ethanol than in water (Ceres, Conte, Mirruzzo, Kolar and Strlic 2008). The antioxidant activity of halide and pseudo-halide anions is demonstrated in Equations 8.1 – 8.5 and has been found to increase in the following order in an NPG hydroxylation assay: $\text{Br}^- \leq \text{SCN}^- < \text{I}^-$ (Malesic, Kolar, Strlic and Polanc 2006). Additionally, when tested on paper with iron gall ink TBACl (tetrabutylammonium chloride) was found to give slightly better stabilisation results than TBABr (tetrabutylammonium bromide) (both in dichloromethane) (Malesic, Kolar, Strlic and Polanc 2005).



In neutral solution iodide ions react with hydroxyl radicals to give $\cdot\text{I}_2^-$ (Equations 8.1 and 8.2). At low acidity Equations 8.3 and 8.4 “cycle”. In alkaline conditions iodide ions do not react with hydrogen peroxide but reaction between iodine and hydrogen peroxide (Equation 8.5) is very rapid.

In the same study it was found that quaternary ammonium bromide antioxidant efficiency increased with increasing aliphatic chain length thus TBABr was one of the most

8.2 Theory of stabilisation

successful out of those tested (Malesic, Kolar, Strlic and Polanc 2005; Malesic, Kolar, Strlic and Polanc 2006). This is possibly due to the increasing hydroxyl radical scavenging ability outweighing the decreasing rate of peroxide decomposition with increasing chain length. TBABr has recently been used to successfully stabilise model iron gall inked papers by interleaving the papers with paper treated with TBABr and calcium carbonate, conditioning the stack at 65% or 90%, and subsequently applying pressure to the stack to improve contact, thereby improving chemical transfer between the papers (Malesic, Kolar and Balazic Fabjan 2012). More research is needed before this method can be confirmed suitable for use on historic materials.

Alkylimidazolium halides which act as peroxide decomposers and radical scavengers have also been tested (Ceres, Conte, Mirruzzo, Kolar and Strlic 2008; Kolar, Mozir, Balazic, Strlic, Ceres, Conte, Mirruzzo, Steemers and De Bruin 2008). Imidazolium-based ionic liquids are non-volatile and thought at present to be environmentally friendly however there is limited toxicity information currently available (Kolar, Mozir, Balazic, Strlic, Ceres, Conte, Mirruzzo, Steemers and De Bruin 2008). Also, evidence (Ebner, Schiehser, Potthast and Rosenau 2008) suggests that butylmethylimidazolium ionic liquids are not as inert with respect to cellulose as previously thought. The observed binding between the ionic liquid and cellulose reducing end groups however may not be of importance for conservation purposes since the effect was small and mainly of concern for applications such as medicine, where minor impurities can cause problems. When a range of imidazolium halides (mainly bromide) were tested on iron gall inked paper against phytate (magnesium and calcium) and TBABr, EMIMBr and BDMIMBr (both soluble in ethanol) were found to be the most successful (Kolar, Mozir, Balazic, Strlic, Ceres, Conte, Mirruzzo, Steemers and De Bruin 2008).

8.2.1.3 Radical scavengers

TBABr, alkylimidazolium bromides, and tannic acid are previously mentioned antioxidants that are also radical scavengers. Additionally Tinuvin 770 and BHT have been used in iron gall ink research. Tinuvin 770 is a hindered amine light stabiliser (HALS) which is soluble in dichloromethane and which was shown to be an effective stabiliser of iron gall inked paper (Kolar, Malesic and Strlic 2005). It is particularly effective against photo-oxidation (Mills and White 1994). Oxidation of the amine group of Tinuvin 770 results in a nitroxyl radical which scavenges alkyl radicals. A cyclic process is initiated in which the nitroxyl radical is regenerated unless it is broken down by side reactions (Chakraborty and Scott 1980).

8.2 Theory of stabilisation

BHT (butylated hydroxyl toluene, 2,6-di-tert-butyl-4-methylphenol) is a hindered phenol radical scavenger that is soluble in ethanol. It has been shown to be an effective stabiliser of paper with (Kolar, Strlic, Novak and Pihlar 1998) and without iron gall ink, particularly when used with a deacidifier (Havlinova, Minarikova, Hanus, Jancovicova and Szaboova 2007). The mechanism of antioxidant ability of BHT is presented by Scott (Scott 1993a) and involves oxidation of BHT to form a hindered aryloxy (ArO^\bullet) radical. The bulky *tert*-alkyl groups in the ortho positions of BHT sterically hinder reactions involving the aryloxy radical and the radical can delocalise into the aromatic ring thus increasing the stability of the radical. Subsequent reaction can result in a quinone or a quinone methide which is yellow and could therefore discolour a treated object with age (Mills and White 1994). Such compounds can also act as antioxidants but unlike for Tinuvin 770, BHT is not regenerated. Hindered phenols are good stabilisers of thermal autoxidation but poor stabilisers in light (Mills and White 1994).

8.2.1.4 Efficacy of antioxidants

Antioxidants can show both pro- and antioxidant activity depending on factors such as concentration (Engelmann, Bobier, Hiatt and Cheng 2003; Malesic, Kolar, Strlic and Polanc 2006), ratios of the concentrations of antioxidant (Engelmann, Bobier, Hiatt and Cheng 2003), temperature (Strlic, Kolar and Pihlar 2001), and/or on the substance they are intended to protect (Aruoma, Murcia, Butler and Halliwell 1993). For example: when the ratio of gallic acid and ferric ions is greater than 2 gallic acid acts as an antioxidant while for ratios lower than 2 it acts as a pro-oxidant (Strlic, Radovic, Kolar and Pihlar 2002); DTPA is a pro-oxidant at 80°C but antioxidant at 20°C (Strlic, Kolar and Pihlar 2001); and, gallic acid shows antioxidant properties towards lipids but prooxidative properties towards DNA and carbohydrates under the test conditions used (Aruoma, Murcia, Butler and Halliwell 1993).

8.2.2 Deacidifiers

The aim of deacidification is to permanently neutralise existing acidity and leave an evenly distributed alkaline reserve in order to neutralise future acidity. Criteria for ideal deacidifiers for paper have been published (Wittekind 1994; Cedzova, Gallova and Katuscak 2006) which also mention that the chemicals used must not: adversely affect any components (e.g. inks, or book bindings) of the object; change the appearance of the object; or change the brightness of the paper. Additionally, the treatment must: leave the paper with a pH between 7 and 8.5 and an alkaline reserve of 2% of earth alkaline carbonate, be safe for users, produce permanent results, and be applicable to all paper types. Ideally the

8.2 Theory of stabilisation

deacidification will also strengthen the paper (Cedzova, Gallova and Katuscak 2006).

Deacidification in addition to the application of antioxidants has been recommended (Hofenk de Graaff 2002) and proven essential for the long term stability of iron gall inked objects (Havlinova, Minarikova, Hanus, Jancovicova and Szaboova 2007).

Many deacidification treatments have been evaluated on paper as is demonstrated by the lists of patents that have been published (Cedzova, Gallova and Katuscak 2006). A comprehensive review of aqueous and non-aqueous deacidification methods has been published (Baty, Maitland, Minter, Hubbe and Jordan-Mowery 2010) as well as a comprehensive review of the mechanisms behind the main aqueous deacidification methods used in paper conservation (Smith 2011). In this section, the deacidification treatments that have been used on iron gall inked or iron tannate dyed materials will be discussed.

The neutralisation of acids involves the formation of neutral salts that do not dissociate in water. While hydrogen ions as well as ions of sodium, aluminium, and potassium can dissociate from carboxylate anions in water, ions of calcium and magnesium do not (Smith 2011). Consequently, hydroxides, carbonates, and hydrogen carbonates of calcium and magnesium are often used in deacidification. The ability of these compounds to leave calcium or magnesium carbonate alkaline reserves in the treated material is discussed below.

Calcium or magnesium carbonates or bicarbonates are commonly used to deacidify paper. The low solubility of alkali earth carbonates in water requires that CO_2 be introduced into the aqueous solution in order to lower the pH of the solution and that low temperatures be used to increase the solubility of the carbonate. For solutions with calcium carbonate, atmospheric levels of CO_2 lower the pH of the solution down to around pH 8.3 from the pH 10 it would be with pure solution of the alkali carbonate, due to the formation of carbonic acid (H_2CO_3). Replacing the air above the solution with CO_2 increases the quantity of absorbed CO_2 and can take the pH of the solution down further (to pH 3.9 for calcium carbonate). The pH of calcium bicarbonate deacidification treatment solutions is often around pH 6 while for magnesium bicarbonate solutions it is around pH 7. During immersion of the sample in the acidic treatment solution ion exchange occurs which forms calcium (or magnesium) salts of accessible acid groups. Subsequently, the sample is air-dried and small white particles of alkali carbonate are precipitated within the structure of the sample. Uneven accumulation of precipitate at the evaporation surface of the sample

8.2 Theory of stabilisation

(‘gritting’) can occur at particularly high concentrations of solution and can be observable as hazy areas on dark samples. This is an undesirable side effect which can be eliminated by drying the sample slowly and using solutions with concentrations that are lower than the maximum. While the application solution was acidic or neutral, once dried, the sample is alkaline due to the alkali carbonate deposits. Due to the presence of absorbed water in organic samples, a small quantity of alkali carbonate will be dissociated. Alkali carbonates are stronger bases than water because they are formed from a strong base (alkali hydroxide) and weak acid (carbonic acid), and so the carbonate anions can take a hydrogen ion from water to produce a bicarbonate anion and a hydroxide ion. The hydroxide ions cause the pH of residual water in a sample containing alkali carbonate to be alkaline (pH 8.3 for calcium carbonate and pH 9.2 for magnesium carbonate). The higher alkalinity of samples treated with magnesium rather than calcium-based deacidifiers has been shown to cause lower extents of stabilisation and cause discolouration (yellowing) of various papers and pulps as well as the fading of iron gall inks (Kolar and Novak 1996; Bansa 1998; Reissland 1999). Consequently it was recommended that magnesium carbonate not be used for the treatment of iron gall inked paper (Reissland 1999) with calcium bicarbonate being the preferred deacidifier in a study into the efficacy of the phytate treatment on iron gall inked paper (Neevel 2002). The hydroxide ions can diffuse through the organic substrate and neutralise hydrogen or hydronium ions. The alkali cation can also bind to the counter-anions of acids. In the case of sulphuric acid, calcium carbonate would result in the formation of calcium sulphate which has low solubility and is white (Smith 2011).

The acidity of the alkali bicarbonate solutions makes this a useful deacidification method for materials with alkali sensitive components such as iron-tannate complexes. Deacidification of wool or silk using alkaline solutions is not recommended due to their sensitivity to alkali (Hofenk de Graaff 2002). Magnesium bicarbonate has been shown to stabilise samples of iron-tannate dyed silk and was particularly effective when combined with either phytate or cysteine (Sato, Okubayashi and Sato 2011). Additionally, the mildly acidic or neutral solution of the alkali bicarbonate causes lower swelling and lower levels of extraction of smaller compounds than in alkaline solution. This is because in alkaline solution compounds with dissociable acid groups acquire a negative charge which causes increased attraction between these compounds and water molecules and cations, thus increasing the swelling of the fibres, and causes negatively charged smaller, mobile molecules to be repelled from the fixed, negatively charged fibres. These smaller compounds are therefore more easily removed from the sample of organic fibres in alkaline solution than acidic or neutral solution (Smith 2011). While solutions of a pH of 8.5 or above are best to

8.2 Theory of stabilisation

maximise cotton fibre swelling and the removal of compounds that are soluble in alkaline environments, to minimise damage to alkaline-sensitive materials a pH between 7.5 and 8 is preferred (Smith 2011). To prevent damage to iron gall inks on paper, Reissland (Reissland 1999) recommends using a treatment that has a pH between 5 and ca. 8.5 during application and that causes a pH in the same range after treatment. Krekel (Krekel 1999) noted that above pH 8 the black complex of iron gall ink breaks down. The use of calcium hydroxide to deacidify iron gall inked paper and leave a calcium carbonate reserve is therefore not advisable due to the alkaline pH of the solution (up to pH 12 depending on concentration used) (Reissland 2001). However, for old yarns of iron-tannate dyed New Zealand flax that are particularly acidic, Daniels (Daniels 1999a) found that multiple applications of magnesium bicarbonate (formed from magnesium hydroxide and CO₂) were required. While browning of modern iron-tannate dyed New Zealand flax was observed, deacidification of old yarns caused much less discolouration and even darkened some samples. Consequently, in particularly acidic cases, the more alkaline treatments that are unsuitable for iron gall inked paper may be suitable for use on iron-tannate dyed materials.

Non-aqueous methods of introducing magnesium carbonate into iron gall inked or iron-tannate dyed samples includes the use of magnesium ethoxide in ethanol (Kolar, Malesic and Strlic 2005) and methyl magnesium carbonate in methanol (Daniels 1999a). When deposited magnesium ethoxide reacts with water in the paper to form magnesium hydroxide and ethanol. The ethanol evaporates and the magnesium hydroxide reacts with atmospheric carbon dioxide to form magnesium carbonate and water (Wittekind 1994). More recently nano-particles of calcium hydroxide have been dispersed in isopropanol to successfully deacidify iron gall inked paper (Sequeira, Casanova and Cabrita 2006).

Some metal ion chelating antioxidants have been investigated for their ability to raise the pH of the paper to a suitable level during antioxidant application to make subsequent deacidification unnecessary (Wagner and Bulska 2003). In this case DTPA applied at pH 9 was found to be the most successful however, as discussed with the alkali carbonate solutions, this pH could damage alkaline-sensitive materials such as iron-tannate complexes which can breakdown at pH >8.0 (Krekel 1999).

8.2.3 Calcium phytate treatment



Figure 8.1 The treatment of iron gall inked documents during a visit to the Zeeuws Archief, Middelburg, The Netherlands in 2007

The calcium phytate/calcium bicarbonate treatment was developed following investigation into a range of phytate/bicarbonate combinations, to combat oxidation and acid hydrolysis in iron gall inked documents (Neevel 1995; Neevel 2002). Its usage on iron-tannate dyed textiles as well as iron gall inked paper has been suggested (Barker 2002). Sodium phytate and magnesium bicarbonate has been shown to be an effective stabiliser of modern iron-tannate dyed New Zealand flax (Daniels 1999a), phytate and magnesium bicarbonate has been applied to historic material (Cull 2007).

The ability of this treatment to decelerate these reactions has been demonstrated through the observation of stabilised carbonyl content and molecular weight of cellulose in iron gall ink samples during accelerated ageing (Henniges and Potthast 2008). The calcium phytate/calcium bicarbonate treatment applied in a 50:50 water:alcohol solvent has also been shown to be innocuous to the paper support based on chemical, mechanical, and optical tests (Botti, Mantovani and Ruggiero 2005). The phytate ligand makes catalytically active iron ions catalytically inactive by occupying all coordination sites on the iron ions and by enforcing one oxidation state (iron(III)) on the ion thus preventing it from redox cycling. Both of these factors prevent the iron ions from participating in the Fenton reaction and producing radicals (Graf and Eaton 1990). Additionally, the water-solubility of the iron(III) phytate complexes³ enables much of the catalytic iron ions to be removed during the treatment application (Neevel 2002).

³ The solubility of metal ion-phytate complexes decreases with increasing number of metal ions per phytate, e.g. monoferric-phytate complexes are highly soluble while tetraferic-phytate complexes are insoluble Graf, E. and J. W. Eaton (1990). "Antioxidant functions of phytic acid." *Free Radical Biology & Medicine* 8: 61-69.

8.2 Theory of stabilisation

Calcium or magnesium carbonate is combined with phytic acid in the treatment in addition to ammonia when necessary, to raise the pH of the solution from 2.9 to between pH 5.5 and 6 (thereby improving the solubility of the iron-phytate complexes since this increases with increasing pH) (Neevel 2002). The use of magnesium phytate rather than calcium phytate has been recommended since unlike for calcium phytate, the production of an aqueous solution of magnesium phytate does not require the use of ammonia to raise the pH of the solution in order to improve solubility of the iron(III)-phytate complex. As well as lowering the health risks associated with the treatment the magnesium phytate solutions produce similarly successful stabilisation results to the calcium phytate solutions (Kolar, Mozir, Strlic, de Bruin, Pihlar and Steemers 2007).

A drawback to the use of phytate is that it is metal-specific. It only forms catalytically inert complexes with iron. Consequently, other catalytically active metal ions such as copper(II), which are often present in iron gall ink, and likely also in iron-tannate dyed, organic materials are not made inert (Budnar, Simcic, Ursic, Rupnik and Pelicon 2006). While usually in significantly lower levels than iron ions (Wagner, Bulska, Hulanicki, Heck and Ortnier 2001) some of these ions can catalyse oxidation to a similar and even greater extent than iron depending on the pH of the environment. For example, copper(II) ions can be more catalytically active than iron(II) or iron(III) ions at pH > 7.7 (Selih, Strlic and Kolar 2004; Strlic, Selih and Kolar 2006). Additionally, when bound in phytate complexes, the activity of copper(II) is increased (Smolis and Strlic 2003; Kolar and Strlic 2006).

The use of phytate ligands to stabilise substrates against oxidation needs to be followed by deacidification so that the pH of the substrate is raised sufficiently to decelerate acid hydrolysis and so that an alkaline reserve can be left to combat future acidity (Wagner and Bulska 2003; Havlinova, Minarikova, Hanus, Jancovicova and Szaboova 2007; Rouchon, Durocher, Pellizzi and Stordiau-Pallot 2009). As previously discussed calcium bicarbonate is the preferred deacidifier (Neevel 2002).

Attempts at producing a successful phytate-based non-aqueous treatment have been unsuccessful (Neevel 2002). However, calcium phytate has been applied to iron gall inked paper in a 50:50 water:alcohol solvent with or without subsequent aqueous deacidification using calcium bicarbonate (Botti, Mantovani and Ruggiero 2005) following the recommendation from Reissland (Reissland 2001). The use of this water:alcohol solvent has many benefits including: more uniform extraction of compounds from the ink line; supposed greater penetration of the chemical into the fibres due to a lowering of surface

8.2 Theory of stabilisation

tension of the solution; and limiting migration of coloured and non-coloured degradation products throughout the paper. Also, a range of derivatives of D-*myo*-inositol have been found to have similar stabilisation properties to phytate, but have the potential to be developed for non-aqueous solvents by conversion of the hydroxyl groups present into groups soluble in non-aqueous solvents (Kolar and Strlic 2006; Sala, Kolar, Strlic and Kocevar 2006).

8.2.4 Consolidants

Consolidants are not investigated in this research project, however, a brief overview is given here to highlight the difference in approach between a consolidation and a chemical stabilisation treatment as terminology can sometimes be confused. Consolidants are applied to strengthen materials by holding together friable, fragmented, or splintered regions of an object with a binder. Consolidants can be applied to the entire object or localised areas and usually cause a stiffening of flexible material. Ideally, sufficient consolidant needs to be applied to suitably strengthen the material without affecting its appearance (e.g. darkness and gloss of the surface) (Florian, Kronkright and Norton 1990). Reviews of consolidants used in the conservation of textiles (Timar-Balazsy and Eastop 1998) and artifacts made from plant materials (Florian, Kronkright and Norton 1990) have been published. A range of consolidants including Klucel G (a hydroxylpropyl cellulose), Finori (a polysaccharide derived from seaweed), and a range of alginates have been evaluated for their ability to consolidate iron-tannate dyed Maori textiles sufficiently whilst maintaining the appearance of the object (Te Kanawa, Smith, Fenton, Miller and Dunford 2002). Of these chemicals, the alginates with divalent metal ions such as zinc were found to be the most successful and zinc alginate has subsequently been used to consolidate an historic piupiu (traditional Maori waist garment) (Te Kanawa and Smith 2009). Polyethylene glycol has been used to consolidate model iron-tannate dyed silk (Sato and Okubayashi 2010) and New Zealand flax (Daniels 1998), while glycerol (Daniels 1998) and Klucel G with methyl magnesium carbonate (Daniels 1998) have also been used on New Zealand flax.

8.2.5 Solvents – Aqueous vs non-aqueous

Aqueous and non-aqueous solvents have been used in the treatment of iron gall ink and iron-tannate dyed organic materials and each have associated benefits and risks. Water is the solvent required for the calcium phytate/calcium bicarbonate treatment. While the chemical stabilisation afforded by this treatment has resulted in its acceptance and use in conservation studios there are drawbacks to the use of water that can make it an unsuitable

8.2 Theory of stabilisation

treatment for particular objects. Water is a polar solvent and as such it can swell polar fibres such as cellulose, and dissolve polar compounds. In paper without the presence of water-sensitive inks, water is the solvent of choice as it positively affects paper by reactivating hydrogen bonding between cellulose chains (Rouchon, Durocher, Pellizzi and Stordiau-Pallot 2009). The swelling of fibres improves the penetration of the treatment chemicals into the fibres, however, for particularly degraded fibres such as those that have undergone cross-linking due to oxidation, the fibres have become more hydrophobic. Consequently, the swelling of the fibres can cause mechanical damage including cracking between regions of greater and lesser hydrophobicity (Reissland 2001). The ability of water to dissolve polar compounds can be useful as it can cause the removal of soluble catalysts (e.g. acid and/or metal ions) and degradation products from paper. Indeed part of the success of the calcium phytate treatment is thought to be due to the removal of soluble iron ions and iron phytate complexes during treatment application (Neevel 2002). However, these soluble coloured and uncoloured ions and compounds (e.g. degradation products) can also migrate into adjacent areas of the object, thereby increasing the risk of discolouration ('bleeding') and accelerated degradation in these areas (Reissland 2001). Other disadvantages of water include the long drying time required, the risk of changes to the surface appearance and dimensions of the substrate, and changes in colour of the ink and overall object (Malesic, Kolar, Strlic and Polanc 2005; Baty, Maitland, Minter, Hubbe and Jordan-Mowery 2010; Bruckle 2011a). Additionally, the use of water may be unsuitable for objects that contain water-sensitive materials such as metals in composite objects or some dyes and pigments. Furthermore, large and 3D objects could be physically damaged or misshapen if wetted with water (Daniels 1999a).

The effects of using non-aqueous solvents rather than water particularly depend on the polarity of the solvent. Alcohols are polar protic (can donate a proton) non-aqueous solvents, though they are significantly less polar than water (Lichtblau and Anders 2006). Polar aprotic solvents include e.g. acetone and dimethylformamide. Non-polar solvents are always aprotic and include e.g. heptane and dichloromethane. Decreasing the polarity of the solvent in a treatment solution will cause a decrease in the swelling of polar fibres and in the extraction of polar compounds. The former could cause a decrease in the efficacy of the treatments as the chemicals may not be distributed as far into the fibres as they are with water. This was suggested as the reason behind methyl magnesium carbonate in methanol being a less successful deacidifier for iron-tannate dyed New Zealand flax than magnesium bicarbonate in water (Daniels 1999a). However in one study in which several ammonium bromides were applied to iron gall inked paper in both water and dichloromethane,

8.2 Theory of stabilisation

comparable results were obtained (Malesic, Kolar, Strlic and Polanc 2005). In another study the stabilisation effect of nano-particles of calcium hydroxide suspended in isopropanol was less than that in water but so was the colour change to the iron gall ink (Sequeira, Casanova and Cabrita 2006). Solutions of pure alcohol or mixtures of >66% alcohol and <33% water have been shown to cause no or only minor observable migration of coloured compounds in iron gall inked paper, while mixtures of lower alcohol content caused increased migration compared to water. This increase arises from the presence of sufficient water to dissolve the coloured compounds but insufficient water to remove them from the surface of the paper and the presence of a less polar solvent than water that is also unable to remove them from the surface of the paper (Rouchon, Durocher, Pellizzi and Stordiau-Pallot 2009). Additionally, increasing the alcohol contribution to the solvent decreased the extent of iron ion migration from iron gall inked paper (Wagner and Bulska 2003). Drawbacks to the use of non-aqueous solvents can include the solvation of coloured compounds that are not water soluble (e.g. non-polar dyes) (Reissland, van Gulik and de la Chapelle 2006) and the health risks of the solvents e.g. methanol which is highly flammable and toxic to humans. A more detailed description of the issues that could arise due to treatment application has been published (Reissland, van Gulik and de la Chapelle 2006).

8.2.6 Conclusions

Since oxidation and acid hydrolysis are the major degradation mechanisms of iron-tannate dyed organic materials a stabilisation treatment will ideally involve antioxidants and deacidifiers. Antioxidants with an efficiency that is independent of the type of metal ions will be preferable since ions other than iron are present in iron-tannate dyes and can be catalytically active also. Many of the undesirable side-effects of using water as the solvent in the treatment of iron gall ink documents can be overcome by using a non-aqueous solvent. A similar situation is likely to exist for iron-tannate dyed organic materials and with extra issues that arise from the potentially large and composite nature of some of the iron-tannate dyed objects in the British Museum, the need for a non-aqueous stabilisation treatment as an alternative to the aqueous calcium or magnesium carbonate/calcium bicarbonate treatment is apparent.

8.3 Chemicals for experimentation

The chemicals and solvents that were chosen to be investigated in this project are presented in Table 8.1. The reasons for the choice of the chemicals, their structures (Figure 8.2 – 8.3) and reactivity are presented in this section.

Table 8.1 Antioxidants, deacidifiers and solvents under investigation in this project

Stabilisation role	Chemical/Solvent	IUPAC nomenclature	Chemical abbreviation
Radical scavenging antioxidant	(+)-alpha-Tocopherol	(2R)-2,5,7,8-tetramethyl-2-[(4R,8R)-4,8,12-trimethyltridecyl]-3,4-dihydrochromen-6-ol	AT
	1-ethyl-3-methylimidazolium bromide	1-ethyl-3-methylimidazolium bromide	EBR
	Irganox 1135	Benzenepropanoic acid, 3,5-bis (1,1-dimethyl-ethyl)-4-hydroxy-.C7-C9 branched alkyl esters	I1135
	Irganox 1425	1:1-Combination of calcium-bis (((3,5-bis(1,1-dimethylethyl)-4-hydroxyphenyl)methyl)-ethylphosphonate) and polyethylene-wax	I1425
	Tinuvin 144	Bis (1,2,2,6,6-pentamethyl-4-piperidinyl)-[[3,5-bis(1,1-dimethylethyl)-4-hydroxyphenyl]methyl]butylmalonate	T144
	Tinuvin 292	Bis(1,2,2,6,6-pentamethyl-4-piperidinyl)-sebacate and 1-(methyl)-8-(1,2,2,6,6-pentamethyl-4-piperidyl sebacate	T292
Metal ion chelating antioxidant	Phytic acid	(1r,2R,3S,4s,5R,6S)-cyclohexane-1,2,3,4,5,6-hexayl hexakis[dihydrogen (phosphate)]	PA
	Etidronic acid	1-hydroxyethane 1,1-diphosphonic acid	EA
	Melaneze	Synthetic melanin	M
Deacidifier	Magnesium ethoxide	Magnesium ethanolate	ME
Solvent	Ethanol (100%)	Ethyl alcohol	EtOH
	Industrial methylated spirits	Ethyl alcohol (denatured)	IMS
	Tetrachloroethylene	1,1,2,2-tetrachloroethene	T
	n-Hexane	n-Hexane	H
	Cyclosiloxane D5 (GreenEarth)	2,2,4,4,6,6,8,8,10,10-decamethyl-1,3,5,7,9,2,4,6,8,10-pentaoxapentasilcane	GE

8.3.1 Antioxidants

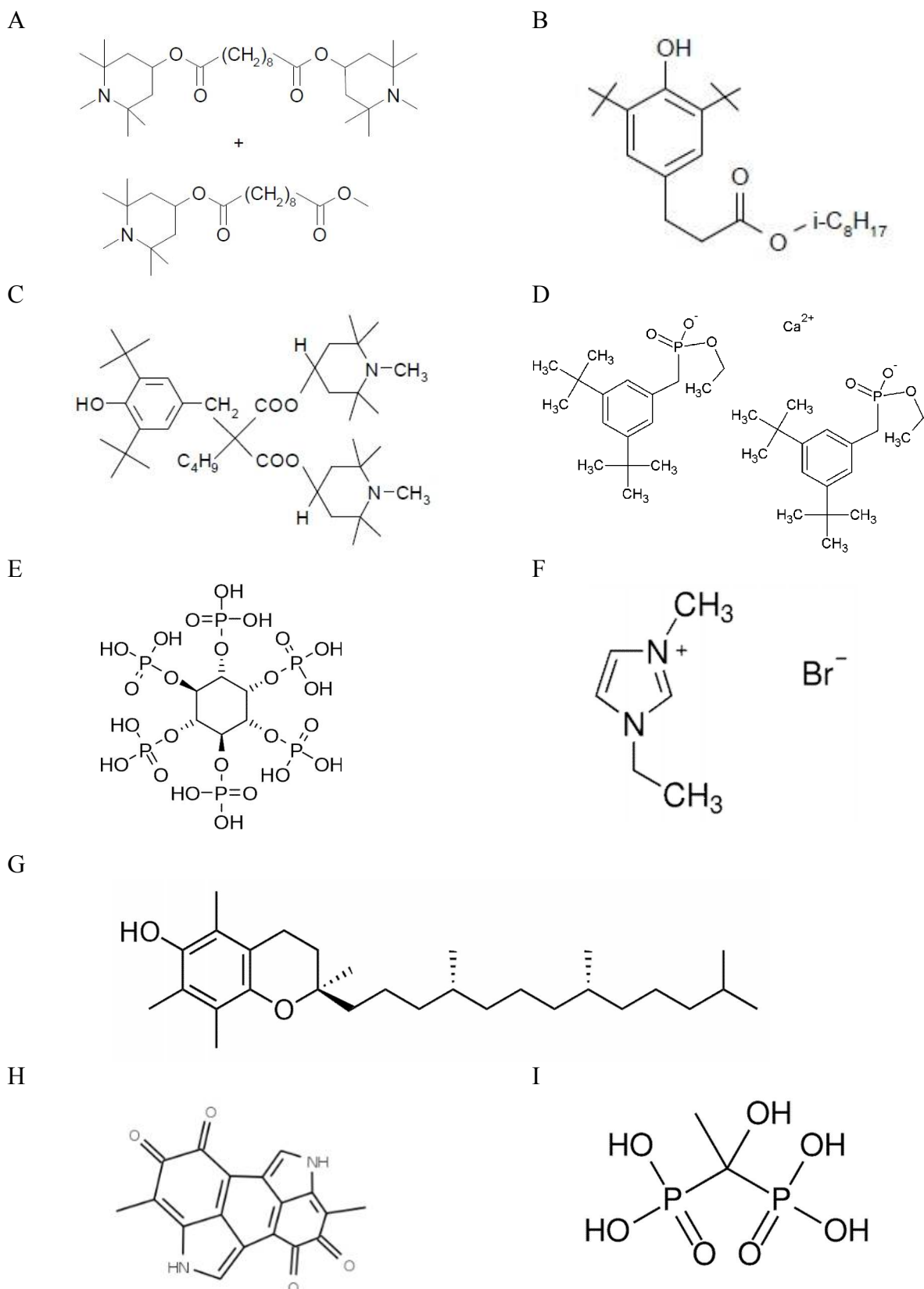


Figure 8.2 The chemical structures of antioxidants used in this project. A: Tinuvin 292 (Top: Bis(1,2,2,6,6-pentamethyl-4-piperidyl)-sebacate, Bottom: 1-(methyl)-8-(1,2,2,6,6-pentamethyl-4-piperidyl) sebacate), B: Irganox 1135, C: Tinuvin 144, D: Irganox 1425, E: phytic acid, F: 1-ethyl-3-methylimidazolium bromide, G: (+)- α -tocopherol, H: Synthetic melanin, I: etidronic acid.

8.3.1.1 Tinuvin 292

Tinuvin 292 (Bis(1,2,2,6,6-pentamethyl-4-piperidiny)-sebacate and 1-(methyl)-8-(1,2,2,6,6-pentamethyl-4-piperidyl sebacate) (M_w 508.8 g mol^{-1} and 369.6 g mol^{-1} , respectively) was supplied by Chris Addie at Ciba (Ciba Speciality Chemicals Ltd 2000) which is now part of BTC. Tinuvin 292 is a slightly yellow liquid hindered amine light stabiliser (radical scavenger) that is miscible in a variety of non-aqueous solvents but not in water. It was developed for a wide range of coatings including paints and varnishes (Ciba Speciality Chemicals Ltd 2000) and is used in conservation to stabilise varnishes in UV-filtered environments (filter cut-on wavelength of at least 400 nm) (de la Rie 1988; de la Rie and McGlinchey 1989; Mills and White 1994). Since objects stored and exhibited within the British Museum will be exposed to UV-filtered conditions and due to its miscibility in a wide range of non-aqueous solvents, Tinuvin 292 is of particular interest in this project. Concentrations of up to 3% (by weight of coating resin solids) are recommended (Ciba Speciality Chemicals Ltd 2000) and in an article by de la Rie that was referenced by Mills and White (Mills and White 1994), the use of 3% Tinuvin 292 in dammar varnishes is estimated to give the varnish film a useful lifetime of over 100 years under UV-filtered conditions. Tinuvin 292 is an irritant as it may cause sensitisation of skin, and is dangerous for the environment, being very toxic for aquatic organisms.

8.3.1.2 Tinuvin 144

Tinuvin 144 (Bis (1,2,2,6,6-pentamethyl-4-piperidiny)-[[3,5-bis(1,1-dimethylethyl)-4-hydroxyphenyl]methyl]butylmalonate) (M_w 685 g mol^{-1}) was supplied by Chris Addie at Ciba (Ciba Speciality Chemicals Ltd). It is a white/slightly yellow powdered hindered amine light stabiliser (radical scavenger) which also incorporates a sterically hindered phenol. Tinuvin 144 is effectively insoluble in water at 20°C and has low solubility in a range of non-aqueous solvents e.g. 10 g per 100 g of butylacetate and 2.5 g per 100 g of butanol (Ciba Speciality Chemicals Ltd). Developed for use in coatings, concentrations of up to 3% (of weight of binder solid) are recommended (Ciba Speciality Chemicals Ltd) as well as combination with a UV absorber for maximum effect. A UV absorber is unlikely to be necessary for the treatment of objects which will be stored in the UV-filtered environments of the British Museum. Tinuvin 144 is an irritant and harmful to the environment.

8.3.1.3 Irganox 1135

Irganox 1135 (Benzenepropanoic acid, 3,5-bis (1,1-dimethyl-ethyl)-4-hydroxy-.C7-C9 branched alkyl esters) (M_w 390 g mol^{-1}) is a colourless/slightly yellow liquid hindered

8.3 Chemicals for experimentation

phenol that was supplied by Chris Addie at Ciba. It is used to stabilise polymers by scavenging radicals and thus preventing the formation of peroxides. It is soluble in non-aqueous solvents such as methanol and dichloromethane (> 50% w/w) but not in water (< 0.01% w/w) (Ciba Speciality Chemicals Ltd 2004). Irganox 1135 is a derivative of butylated hydroxytoluene (BHT) which has been discussed previously in the chapter since it has been used in iron gall ink research (Havlinova, Minarikova, Hanus, Jancovicova and Szaboova 2007). Irganox 1135 is potentially dangerous for the aquatic environment, as it may cause long-term adverse effects.

8.3.1.4 Irganox 1425

Irganox 1425 is a 1:1-combination of calcium-bis (((3,5-bis(1,1-dimethylethyl)-4-hydroxyphenyl)methyl)-ethylphosphonate) and polyethylene-wax that was supplied by Chris Addie at Ciba. It has multiple roles including (trans)-esterification catalyst, property modifier, and antioxidant against thermal degradation. It is a light stable white free-flowing powder with M_w 695 gmol^{-1} which has low solubility in water and ethanol (<0.024 % w/w) at 20°C. Concentrations of up to 0.1% are advised for use as a stabiliser (BASF 2010). If it is soluble in a polar solvent the calcium ions could neutralise acids in iron-tannate dyed textiles and the sterically hindered aromatic ring could act as a radical scavenger while the phosphonate group could bind to metal ions such as iron(II) or iron(III). Irganox 1425 is an irritant that necessitates the use of personal protection equipment including respiratory equipment during its use.

8.3.1.5 1-ethyl-3-methylimidazolium bromide (EBr)

As previously mentioned, EBr is a radical scavenger and under acidic conditions, a peroxide decomposer, due to the bromide ion. The imidazolium cation is thought to contribute to the efficiency of the system due to its affinity for cellulose (in much higher concentrations than those used in iron gall ink research imidazolium can dissolve cellulose) (Ceres, Conte, Mirruzzo, Kolar and Strlic 2008). The EBr for this project was supplied by Sigma-Aldrich as a fine white powder with M_w 191.07 gmol^{-1} . It was chosen for use in this project due to its success as a non-aqueous antioxidant treatment (0.03 mol L^{-1} in ethanol) in conjunction with magnesium ethoxide (0.05 mol L^{-1} in ethanol) on iron gall inked paper (Kolar, Mozir, Balazic, Strlic, Ceres, Conte, Mirruzzo, Steemers and De Bruin 2008). It has also been used successfully on its own (0.3 mol L^{-1} in ethanol) (Ceres, Conte, Mirruzzo, Kolar and Strlic 2008). As it has yet to be applied to iron-tannate dyed textiles it will be particularly interesting to view its success in this project. EBr is moisture sensitive so it needs to be stored under nitrogen atmosphere and is an irritant for the eyes, skin, and

respiratory system. Consequently, personal protective equipment including eye and respiratory protection was needed when using EBr.

8.3.1.6 (+)- α -tocopherol

(+)- α -tocopherol ((2R)-2,5,7,8-tetramethyl-2-[(4R,8R)-4,8,12-trimethyltridecyl]-3,4-dihydrochromen-6-ol) ($430.71 \text{ g mol}^{-1}$) is an important natural antioxidant that is also known as vitamin E. It is a clear, light yellow, viscous liquid. (+)- α -tocopherol is a radical scavenger as the hydrogen radical can be abstracted from (+)- α -tocopherol to produce an aryloxyl radical. Unless this radical is reduced back to (+)- α -tocopherol e.g. by a labile hydrogen in ascorbic acid, the (+)- α -tocopherol is irreversibly destroyed as α -tocopheroquinone is formed (Scott 1993a; Rezk, Haenen, van der Vijgh and Bast 2004). In some environments this quinone can also act as an antioxidant (Scott 1985). (+)- α -tocopherol is not hazardous but requires storage in cool, dry, well-ventilated place at preferably -20°C . By requiring such a low temperature for storage, there is concern that the antioxidant abilities of this chemical under ambient conditions will be different from those under accelerated ageing conditions of 80°C for example and that therefore, accelerated ageing will not accurately indicate the efficacy of this treatment at stabilising iron-tannate dyed textiles.

8.3.1.7 Magnesium phytate

Phytic acid ((1r,2R,3S,4s,5R,6S)-cyclohexane-1,2,3,4,5,6-hexayl hexakis[dihydrogen (phosphate)]) ($660.04 \text{ g mol}^{-1}$) was purchased as an ~40% aqueous solution (w/w) from Sigma-Aldrich. It was combined with magnesium carbonate hydrate ($\text{MgCO}_3 \cdot x\text{H}_2\text{O}$, Mw (anhydrous) 84.31 g mol^{-1}), a white powder also from Sigma-Aldrich, to produce magnesium phytate. Magnesium phytate rather than calcium phytate was used due to the equivalent results and lower health risk (Kolar, Mozir, Strlic, de Bruin, Pihlar and Steemers 2007). As previously discussed, the phytate is a metal ion chelator that forms stable, white, unreactive complexes with iron(II) and iron(III) ions (Graf and Eaton 1990). The *scyllo*-form of the phytate has all phosphate groups in the equatorial position, while the *myo*-form which is used here has one phosphate group in the axial position. This and the two adjacent phosphonate groups can bind iron(II) ions tightly and more successfully the *scyllo*-form (Neevel 2002). Various phytate salts have been used on iron-tannate dyed materials such as silk (Sato, Okubayashi and Sato 2011) and New Zealand flax yarns (Daniels 1999a). It will be of interest to assess the success of this aqueous treatment on a wider range of iron-tannate dyed materials (cotton, abaca, wool, and silk) that are woven

and in either good condition (unaged) or weak condition (aged). Phytic acid is an irritant to the eyes, skin, and respiratory system. Magnesium carbonate hydrate is not hazardous.

8.3.1.8 Etidronic acid

Etidronic acid (1-hydroxyethan-1,1-diphosphonic acid, HEDP) monohydrate ($224.04 \text{ g mol}^{-1}$) was supplied as a liquid by Sigma-Aldrich. It is a preventive antioxidant that strongly binds to metal ions such as iron(III) and aluminium(III) using its phosphonate groups. A 2:3 Fe(III):etidronic acid complex has been suggested in oxygenated solutions (Airey, Armstrong and Handyside 1988). Diphosphonic acids such as etidronic acid are highly hydrophilic and have high thermostability and low toxicity due to the P-C-P bond. They are also flexible and mobile which enables them to chelate with many ionic radii (Gumienna-Kontecka, Silvagni, Lipinski, Lecouvey, Marincola, Crisponi, Nurchi, Leroux and Kozlowski 2002). If it dissolved in non-aqueous solvent etidronic acid could be an alternative chelating agent to phytate. Etidronic acid is an irritant that can cause serious damage to eyes so the use of eye protection among other personal protective equipment is necessary when using this acid.

8.3.1.9 Melaneze (Synthetic melanin)

Melaneze is a natural biomelanin with CAS number 8049-97-6 and Mw $318.28 \text{ g mol}^{-1}$. It is used in cosmetics and is a chelating agent and radical scavenger (LookChem.com 2008). Melaneze was supplied as a dark brown water soluble powder by Dass Chahal from Croda. Melaneze is a non-hazardous substance however dust formation must be avoided as there is a risk of dust explosion.

8.3.2 Deacidifiers

8.3.2.1 Calcium bicarbonate (calcium hydrogencarbonate)

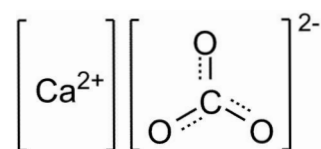


Figure 8.3 The chemical structure of calcium carbonate.

Water soluble calcium bicarbonate ($\text{Ca}(\text{HCO}_3)_2$) ($\text{Mw } 162.11 \text{ g mol}^{-1}$) was produced by bubbling CO_2 through a dispersion of calcium carbonate in water. Calcium carbonate ($\text{Mw } 100.09 \text{ g mol}^{-1}$) is a fine white powder that was supplied by Sigma-Aldrich. Aqueous calcium bicarbonate solution is the deacidification treatment that is applied following the

8.4 Solvents for experimentation

application of phytate salts to iron gall inked paper (Neevel 2002; Kolar, Mozir, Strlic, de Bruin, Pihlar and Steemers 2007). Calcium carbonate is an irritant of the skin and respiratory system and can cause serious damage to eyes.

8.3.2.2 Magnesium ethoxide

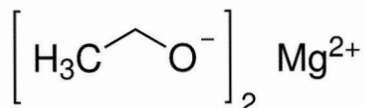


Figure 8.4 The chemical structure of magnesium ethoxide

Magnesium ethoxide (magnesium ethanolate, 98%) ($114.43 \text{ g mol}^{-1}$) is a non-aqueous deacidifier that has been used on iron gall inked paper in ethanol (0.05 mol L^{-1}) (Kolar, Mozir, Balazic, Strlic, Ceres, Conte, Mirruzzo, Steemers and De Bruin 2008). It was supplied by Sigma-Aldrich as a white/light grey powder. As previously mentioned, magnesium ethoxide reacts with water and subsequently carbon dioxide in the air to form magnesium carbonate (Wittekind 1994). Magnesium ethoxide however is moisture sensitive as it reacts violently with water. It is also an irritant (particularly for the eyes) and is highly flammable. Consequently it should be stored under nitrogen when not in use and suitable protective clothing should be worn when using it.

8.4 Solvents for experimentation

A range of non-aqueous solvents of differing polarity were chosen to increase the probability that all of the antioxidants would dissolve in at least one of the solvents tested to enable their use in this research. The solvents chosen are detailed below and their chemical structures are presented in Figure 8.5.

8.4.1 *Ethanol (100% ethyl alcohol) and IMS (ethyl alcohol denatured)*

These non-aqueous polar protic solvents are frequently used in conservation and were supplied by VWR. Ethanol ($\text{Mw } 46.07 \text{ g mol}^{-1}$) has a boiling point of 78°C and IMS of $77-78^\circ\text{C}$ and thus they evaporate rapidly at room temperature. Ethanol has been used in the deacidification of iron gall inked paper using magnesium ethoxide (Kolar, Mozir, Balazic, Strlic, Ceres, Conte, Mirruzzo, Steemers and De Bruin 2008). Both ethanol and IMS are highly flammable and IMS is harmful particularly when inhaled. IMS is frequently used by conservators during practical work and consequently was selected for use in this project as an alternative to ethanol. IMS is also known as IDA (Industrial Denatured Alcohol).

8.4.2 *Tetrachloroethylene (1,1,2,2-tetrachloroethene)*

Tetrachloroethylene (Mw 165.85 g mol⁻¹) is a non-polar non-aqueous organic solvent with a boiling point of 121°C that has been used in the dry cleaning industry (Ballard and Baer 1989). It was supplied by VWR. As it is a halogenated compound it requires disposal with other halogenated waste. It is toxic to aquatic organisms and is harmful particularly if inhaled. It must therefore be used under extraction. Additionally, tetrachloroethylene should not have contact with alkali hydroxides.

8.4.3 *n-Hexane*

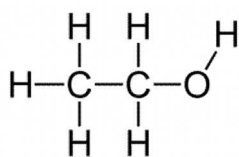
n-Hexane (hexane) (Mw 86.18 g mol⁻¹) is a non-polar organic solvent with a boiling point of 69°C, that was supplied by VWR. It is a highly flammable irritant that is toxic to aquatic organisms and harmful if inhaled. Consequently, any usage of n-hexane needs to be done under extraction.

8.4.4 *Cyclosiloxane D5*

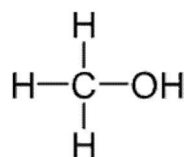
Cyclosiloxane D5 also known as silbione pentamer D5 (2,2,4,4,6,6,8,8,10,10-decamethyl-1,3,5,7,9,2,4,6,8,10-pentaoxapentasilcane) has a trade name of GreenEarth[®] and was kindly supplied by Tim Grice at Johnson Cleaners UK Ltd. It is a non-oily siloxane fluid (Mw 370.77 g mol⁻¹) that has a boiling point of 210°C and is currently used as an environmentally friendly dry cleaning agent at Johnson Cleaners. Of concern with this solvent is the evaporation rate since during the drycleaning process heated air is used to evaporate the solvent (Grice 2010) and this may not be an acceptable or practical option for the treatment of cultural heritage. Cyclosiloxane D5 is reported to not interact with textiles, thereby retaining the shape and colour of the textiles. This may mean that any chemicals it dissolves will not be deposited within the fibres as would occur with polar solvents; however the presence of moisture in the fibres could transfer chemicals deposited on the fibre surface into the fibres. It is a non-toxic, environmentally friendly fluid that decomposes to silicon dioxide, carbon dioxide, and water (Silicones Environmental Health and Safety Council of North America 2008; GreenEarth Cleaning LLC 2010).

8.5 Solvent-model textile compatibility

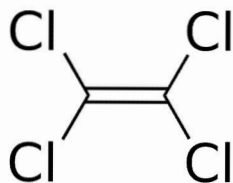
A



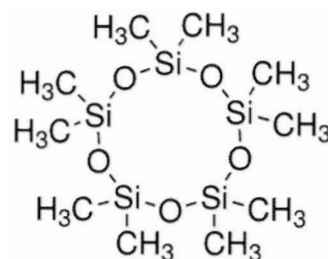
B



C



D



E

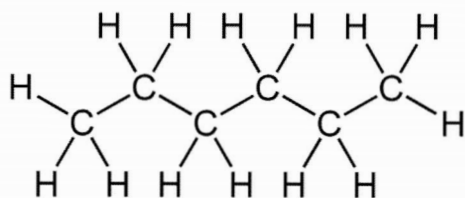


Figure 8.5 Chemical structures of the solvents used in this project. A: ethanol, B: IMS includes a small percentage of methanol (depicted) as well as ethanol, C: tetrachloroethylene, D: cyclosiloxane D5, E: hexane.

8.5 Solvent-model textile compatibility

In order to decide the combinations of solvents and chemicals that would be used in the stabilisation treatment studies, the suitability of the solvents for use on cotton and silk (solvent-textile compatibility), and their ability to dissolve the chosen chemicals (solvent-chemical compatibility) was required. In this section the compatibility of the solvents and model textiles is assessed.

8.5.1 Experimental Method

An experiment was devised to determine if any of the solvents resulted in adverse effects to dyed (c3 and p3) and undyed cotton and silk textiles during immersion. Small pieces ($< 5 \times 5$ cm) of dyed cotton and silk were immersed for 5, 15, and 30 minutes in either IMS, tetrachloroethylene, n-Hexane, cyclosiloxane D5, or water. Ethanol was not used in this test since IMS is predominantly ethanol in composition. Undyed cotton and silk samples were immersed for 30 minutes. On removal from the solvent, the 5 and 15 minute immersed samples were hung to dry in a fume hood. After 30 minutes immersion two of

8.5 Solvent-model textile compatibility

each sample were removed; one was hung to dry while the other was laid flat on paper towel to dry. Excess solvent was removed from the samples by blotting with paper towel prior to drying. Undyed cotton and silk samples were immersed together in 400 ml of solvent while dyed cotton and silk samples were immersed separately, each in 300 ml of solvent. Approximate drying times of the samples in the fume hoods were noted. Note that the considerable airflow due to extraction was present to aid drying which may not be present in a conservation studio or fume room. Colorimetry, microscopy, and SEM were used to ascertain any changes in colour or surface appearance due to the solvent.

Solvent toxicity, ease of use, cost, and evaporation rate in addition to extent of dye running into the solvent, and colour and handle of the dried samples were used to determine an order of preference of solvent use in the treatments.

8.5.2 Analytical techniques

8.5.2.1 Colorimetry

Colorimetric data was collected as described in Section 5.2.4 and a single thickness of each sample was analysed in five randomly selected locations to calculate average L^* , a^* , and b^* . Colour differences (ΔE_{00}^* , ΔL^* , Δa^* , Δb^*) between samples immersed and not immersed in solvent, were calculated from SCE/100 data using the CIE2000 formula. The error in the subtraction calculation of ΔL^* , Δa^* , and Δb^* due to the natural variation in colour for Cc3 is approximately the sum of the standard deviation for the model textile and is presented in Table 8.2. The error in the ΔE_{00}^* values due to variation in colour of the dyed textiles was not calculated.

Table 8.2 Error values in changes in colour parameters for the model textiles

Model textile	Standard deviation			Error in subtraction result		
	L^*	a^*	b^*	ΔL^*	Δa^*	Δb^*
SU	0.36	0.02	0.12	0.72	0.04	0.24
Sp3	0.20	0.03	0.07	0.40	0.06	0.14
CU	0.51	0.02	0.09	1.02	0.04	0.18
Cc3	1.01	0.05	0.13	2.02	0.10	0.26

8.5.2.2 Microscopy

A Leica MZ8 microscope with Leica DFC500 camera, Intralux 5000 light source, and Adobe CS2 software was used to inspect the surface of dyed (c3 and p3) cotton and silk textiles. Consistently significant changes in surface structure or deposits due to immersion in solvent for 30 minutes were noted and untreated equivalent samples were analysed for

comparison. Undyed samples were not tested because it was very difficult to see any surface characteristics due to the whiteness of the textiles.

8.5.2.3 SEM

Using a Hitachi Variable Pressure SEM at the following conditions: 30 Pa, 20 kV, and 13.1 mm working distance, small pieces of sample were viewed and imaged under magnification ($\times 50$, $\times 150$, $\times 650$, and $\times 500$). The sample surface was investigated for consistently significant alterations in surface deposits (type and quantity) and fibre condition on cotton and silk dyed (c3 and p3) and undyed samples immersed for 30 minutes in solvent and those not immersed.

8.5.3 Results and discussion

8.5.3.1 General observation

Table 8.3 General observations during immersion and drying of dyed model textiles in a variety of solvents

Solvent	Dye (c3 or p3) transfer to		Approximate time to	
	Solvent ¹	Blotting paper 1	Wet sample (minutes) ²	Evaporate (hours)
Water	C3: +++	C3: +++	Cc3: up to 30	1/2
IMS	C3: +	C3: +	I	1/6
Ethanol	N	N	I	1/4
Cyclosiloxane D5	N	N	I	24
n-Hexane	C3: +	N	I	1/6
Tetrachloroethylene	C3: +	N	I	1/3

Notes for Table 8.3:

1. Classification of c3 or p3 dye transfer to the solvent during immersion or blotting paper after immersion:

- N No transfer
- + Slight transfer
- ++ Moderate transfer
- +++ Considerable transfer;

2. 'I' is for immediate wetting out of the textile sample in the solvent.

All solvents except cyclosiloxane D5 evaporated from the textiles within 20 minutes of suspension in the fume hood (Table 8.3). Of these, hexane, and IMS were the fastest, taking a maximum of 10 minutes to fully evaporate. Cyclosiloxane D5 took at least 24 hours to fully evaporate though the samples were “touch dry” in 30 minutes. It was clear that cyclosiloxane D5 was still present when the sample saturated various areas on paper. After 24 hours the cyclosiloxane D5 samples did not saturate paper on contact. The evaporation rates are approximate and depend on the quantity of solvent on the sample when it was hung or laid to dry, the environmental conditions, and the volatility of the solvent. The volatility of cyclosiloxane D5 is low as it has a very high boiling point

8.5 Solvent-model textile compatibility

(210°C). In the dry cleaning industry heat is used to fully evaporate the cyclosiloxane D5. This is unlikely to be possible to historic textiles for practical and ethical reasons.

All but the dyed cotton in water wetted out immediately or within 5 seconds. Fast or immediate wetting out of the textile is important as it ensures that the stabilising chemical can be in contact with all of the fibres throughout the textile. In some cases such as cyclosiloxane D5 which is a relatively large molecule, the solvent may not be successful in getting the treatment into the interior of the fibres due to their size. However, if the chemical is water soluble, the unbound water present in the fibres could transport the chemicals deeper into the fibre.

Table 8.4 Hazards of the solvents determined by MSDS

Solvent	Flammable	Harmful	Dangerous for the environment	Use under extraction	Supply	Other notes
Water	N	N	N	N	In lab	
IMS	Y	Y (because of methane)	N	Y	VWR/Sigma Aldrich etc	
Ethanol	Y	N	N	Y	VWR/Sigma Aldrich etc	
Cyclosiloxane D5	N	N	N	N	Johnson Cleaners Ltd (for this study)	Drip tray essential due to slow evaporation and extreme slippiness on hard surfaces
n-Hexane	Y (explosive vapour/air mixture)	Y (toxic for reproduction)	Y	Y	VWR/Sigma Aldrich etc	
Tetrachloroethylene	N	Y (likely carcinogen)	Y	Y	VWR/Sigma Aldrich etc	

Hexane and tetrachloroethylene are the most toxic of the solvents tested and if possible they won't be used in subsequent research. Hexane is also flammable and explosive which makes its usage more complicated for safety reasons. Ethanol and IMS are both flammable and IMS harmful, so these solvents must be used under extraction. In the UK, IMS is more commonly used than ethanol in conservation. Cyclosiloxane D5 is non-toxic, non-flammable, and non-harmful and consequently, like water, can be used without extraction. However it is "slippy" when spilt and for this research it has been kindly donated by Tim Grice at Johnson Cleaners. A supply chain for wider use in conservation is not currently in place and costs have not been ascertained.

8.5.3.2 Colorimetry

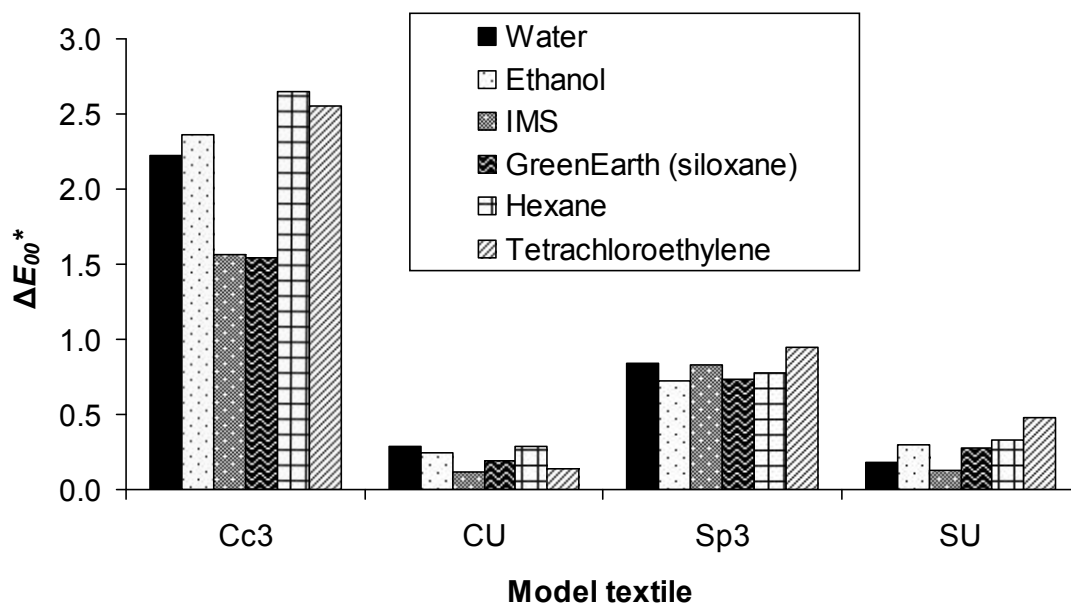


Figure 8.6 The change in colour of unaged cotton and silk model textiles due to 30 minute immersion in different solvents.

Table 8.5 The change in colour parameters of unaged cotton and silk model textiles due to 30 minute immersion in different solvents

Model textile	Solvent	ΔE_{00}^*	ΔL^*	Δa^*	Δb^*
Cc3	Ethanol	2.36	-1.58	-0.06	2.35
	Cyclosiloxane D5	1.54	0.03	-0.24	1.78
	Hexane	2.65	-2.16	0.07	2.39
	Water	2.22	-2.11	-0.22	1.77
	IMS	1.56	0.17	-0.22	1.80
	Tetrachloroethylene	2.56	-1.14	0.19	2.71
CU	Ethanol	0.24	-0.20	-0.01	0.21
	Cyclosiloxane D5	0.20	0.12	-0.04	0.18
	Hexane	0.28	0.28	-0.02	0.22
	Water	0.29	0.44	0.01	-0.01
	IMS	0.12	-0.09	-0.03	0.10
	Tetrachloroethylene	0.14	-0.14	-0.02	0.11
Sp3	Ethanol	0.72	0.68	-0.21	0.59
	Cyclosiloxane D5	0.74	0.94	-0.17	0.37
	Hexane	0.77	0.96	-0.20	0.39
	Water	0.84	1.04	-0.22	0.44
	IMS	0.83	1.09	-0.14	0.40
	Tetrachloroethylene	0.95	1.23	-0.11	0.52
SU	Ethanol	0.29	0.32	-0.05	0.17
	Cyclosiloxane D5	0.28	0.22	-0.04	0.23
	Hexane	0.33	0.30	-0.07	0.23
	Water	0.19	-0.20	-0.05	0.10
	IMS	0.13	-0.09	-0.02	0.11
	Tetrachloroethylene	0.48	0.59	-0.03	0.22

Minimal and unobservable colour change was seen in the undyed cotton and silk ($\Delta E_{00}^* < 0.5$), and the dyed silk ($\Delta E_{00}^* < 1$). IMS and cyclosiloxane D5 caused the least and

unobservable colour change to Cc3 of all the solvents after 30 minutes of immersion (approximately $\Delta E_{00}^* \times 1.5$). The remaining solvents caused a colour change of $\Delta E_{00}^* > 2.3$ which is observable to the human eye. Generally the more noticeable colour changes in Cc3 due to immersion in solvent (Figure 8.6 and Table 8.5) correlates well to dye loss into the solvent or onto the paper towel during blotting observed during the experiment (Table 8.3). Ethanol and IMS are exceptions to this correlation since colorimetry suggests there was greater colour change to the sample immersed in ethanol than in IMS but dye loss during immersion was only noted with IMS.

8.5.3.3 Microscopy

Ideally any solvent used in a conservation treatment should not adversely affect the textile being treated. Microscopy was used to ascertain if any of the solvents tested caused consistently significant changes in textile structure and/or surface deposits after 30 minutes of sample immersion. No significant variations between the immersed and non-immersed samples were noted but the surface of each textile varied slightly across the sample with respect to quantity of surface deposits, loose fibres, areas of abrasion, and gaps in the weave. These variations were related to the dyeing process.

The non-aqueous solvents caused no observable changes to the textile surface when observed under microscopy.

8.5.3.4 SEM

SEM allows the surface topography of the model textiles to be characterised at a micro scale. Since the condition of textiles on the micro-level affects the condition on the macro-level it is important to identify if solvent immersion caused any structural changes on the micro-level which are at present undetectable with macro-observational techniques. No consistently significant changes were found between samples immersed in solvent and those not immersed. There were possibly more deposits of similar density to the silk present on Sp3 hexane-immersed sample which were of random but rounded shape than on other Sp3 or any SU textiles. These deposits were not analysed for composition but their atomic number contrast compared to that of the silk fibres suggests they are of similar density to the silk fibres and therefore not metal-based.

The only change observed using SEM which may be of significance is the presence of randomly shaped and rounded deposits of similar density to the silk fibres in the hexane-immersed Sp3 sample on which they were observed.

8.5.4 Conclusions

Based on all of these results the most preferred solvent for use in this project is cyclosiloxane D5 because it is the least toxic and most environmentally friendly of all the non-aqueous solvents tested and had no effect on the colour or surface appearance of the textiles. The next preference is IMS or ethanol since these are widely used in conservation studios and are the least toxic of the remaining solvents. Following this is tetrachloroethylene and then hexane as tetrachloroethylene is marginally safer to use than hexane and both caused observable colour change to the iron-tannate dyed model textiles during immersion. Additionally, hexane may have caused the deposition of low atomic mass precipitates on the surface of the dyed silk.

8.6 Solvent-chemical combinations

8.6.1 Experimental method

A small quantity of chemical (<1 g) was added to 50 ml or 10 ml of solvent and stirred to identify if it dissolved. The chemicals were dissolved in the solvents in the order of most preferred (see Section 7.5.4) until dissolution occurred. The ability of the chemicals to dissolve in pure ethanol was not tested since IMS is predominantly ethanol. If the chemical dissolved in a solvent, larger quantities were added until saturation point was reached or a specific quantity had been added. These specific quantities varied with each chemical and were calculated to produce 50 ml solutions of concentrations which were calculated at the time of experimentation, to be the maximum concentration required for the treatment of the large textile samples in the treatment stage of the project.

8.6.2 Results and discussion

The preferred non-aqueous solvent, cyclosiloxane D5, dissolved (+)- α -tocopherol, Tinuvin 292, and Irganox 1135 (Table 8.6). IMS dissolved 1-ethyl-3-methylimidazolium bromide, phytic acid, etidronic acid, and magnesium ethoxide. It is expected that ethanol will also dissolve these chemicals. Tetrachloroethylene will be used for Tinuvin 144 while hexane, the least preferred solvent due to its toxicity and flammability, will not be used at all. Neither melaneze nor Irganox 1425 dissolved in any of the solvents tested and so were not used in this project.

8.7 Treatment concentrations

Table 8.6 The compatibility of the chemicals with the solvents

Chemical	Non-aqueous solvent ¹	Total quantity dissolved (g) in 50 ml	Concentration (M)
(+)-alpha-Tocopherol	Cyclosiloxane D5	58.79	2.73
1-ethyl-3-methylimidazolium bromide	IMS	26.08	2.73
Irganox 1135	Cyclosiloxane D5	2.70	0.14
Irganox 1425	None	-	-
Tinuvin 144	Tetrachloroethylene	0.41	0.01
Tinuvin 292	Cyclosiloxane D5	0.41	0.01
Phytic acid (40% solution in water)	IMS	13.10	0.16
Etidronic acid	IMS	1.78	0.16
Melaneze	None	-	-
Magnesium ethoxide	IMS	Unknown ²	Unknown

Notes for Table 8.6:

1. Least toxic non-aqueous solvent that the chemical dissolves in.

2. Magnesium ethoxide is hygroscopic. Some dissolved in IMS but the quantity is unknown because the extent of magnesium ethoxide decomposition during the experiment is unknown. Ethanol rather than IMS could also be used since IMS is mainly composed of ethanol.

8.7 Treatment concentrations

The concentrations of the chemicals in the treatment solutions is important since, as previously discussed, some antioxidants can act as pro-oxidants at certain concentrations. Since 1-ethyl-3-methylimidazolium bromide, calcium bicarbonate, magnesium phytate, and magnesium ethoxide had been used in iron gall ink research, the quoted mass of chemical per gram of material was used as a guide and scaled up according to the masses of the model textiles in this project. As the volume of treatment solution was set to 300 ml for practical reasons, slight deviations in the concentrations of the chemicals used occurred from those quoted in the literature. For Tinuvin 292, Tinuvin144, and Irganox 1135 the recommended concentrations provided by Ciba or BASF were used as a guide. For example, 2% by weight of coating resin solids for Tinuvin 292 was interpreted as 2% by mass of textile being treated. As etidronic acid had not been used previously in iron gall ink research and had no recommendations for use from the supplier, the concentrations of phytic acid (another metal ion chelator) were used as a guide. For (+)- α -tocopherol the recommended concentration of Tinuvin 144 was used as a guide since both scavenge radicals via a substituted phenol group.

As with all of the treatment chemicals, a range of concentrations were used based around the guide values. A 3% solution by weight of solvent of Tinuvin 292, Tinuvin 144, and Irganox 1135 and a 2.3% solution by weight of solvent of (+)- α -tocopherol were also

8.7 Treatment concentrations

chosen. Consequently, the treatment concentrations that are tested in the next chapter are presented in Table 8.7.

Table 8.7. Chemical concentrations used in Treatment Test 1 (Chapter 9)

Chemical	Solvent	ME ~30% textile weight ^a	Chemical mass in 300 ml of solvent as approximate % textile weight ^b	Concentration, M	
				Dyed ^c	Undyed ^c
<i>Antioxidants</i>					
AT	GE	Y	2.00	0.00052	0.00047
			3.00	0.00078	0.00070
			6.00	0.00155	0.00141
			6.00	0.00157	0.00141
AT ^d	GE		200.00	0.05146	0.05146
EA	IMS	Y	0.40	0.00019	0.00017
			0.40	0.00019	0.00017
			2.00	0.00097	0.00087
			4.00	0.00195	0.00174
		Y	4.00	0.00195	0.00174
EBR	EtOH		6.00	0.00335	0.00300
			30.00	0.01675	0.01500
			60.00	0.03350	0.03001
II135	GE	Y (in IMS)	2.00	0.00057	0.00051
			3.00	0.00086	0.00077
			6.00	0.00172	0.00154
			43.00	0.01229	0.01229
		Y (in IMS)	43.00	0.01229	0.01229
PA	IMS	Y (in IMS)	3.00	0.00047	0.00044
			15.00	0.00243	0.00219
			30.00	0.00486	0.00438
			30.00	0.00487	0.00436
T144	T	Y	2.00	0.00033	0.00029
			3.00	0.00049	0.00044
			6.00	0.00098	0.00088
			6.00	0.00099	0.00088
			450.00	0.07282	0.07282
T292	GE	Y	2.00	0.00025	0.00023
			3.00	0.00038	0.00034
			6.00	0.00077	0.00069
			6.00	0.00077	0.00069
			260.00	0.03277	0.03277
PA (MP)	Water		5.00	0.00098	0.00044
			15.00	0.00244	0.00218
			30.00	0.00487	0.00436
MC	Water		0.82	0.00108	0.00107
			4.66	0.00617	0.00562
			9.37	0.01241	0.01125
<i>Deacidifier</i>					
ME	EtOH		6.00	0.00558	0.00502
			30.00	0.02793	0.02496
			60.00	0.05603	0.05000

Notes for Table 8.7:

a. Y (yes) means a separate application of ME30 was made to a treated sample;

8.8 Conclusions

- b. Combination of these values and the chemical abbreviation form the treatment codes referred to from now on e.g. AT200. IMS is included in the treatment code when used with PA to highlight the use of non-aqueous solvent. The magnesium phytate and calcium bicarbonate treatment is noted as MPx/2CBx, where 'x' is the mass of PA(MP) as percentage of textile weight;
- c. In some cases, concentrations for undyed and dyed textiles vary because of differing textile masses so that the mass of chemical per mass of textile is equal. In other cases the concentration is independent of textile mass;
- d. A very small piece of undyed textile was added to the dyed sample treatment bath rather than treating 10 cm x 15 cm undyed samples separately due to insufficient quantity of solvent.

8.8 Conclusions

A range of chemicals and solvents were selected for use in this project. Through compatibility testing of the chemicals and model textiles with the solvents, and consideration of the practicality and toxicity when using the solvents, the combinations of chemicals and solvents that constitute a treatment were established. The method of calculation of the concentrations to be used was explained. Cyclosiloxane D5 will be used in this project to apply (+)- α -tocopherol, Tinuvin 292, and Irganox 1135 to model textiles. IMS or ethanol will be used to apply 1-ethyl-3-methylimidazolium bromide, phytic acid, etidronic acid, and magnesium ethoxide to the samples while tetrachloroethylene will be used to apply Tinuvin 144.

9 STABILISATION TREATMENT TEST 1 – UNAGED COTTON AND SILK

9.1 Experimental Method**9.1.1 Treatment solutions**

Based on the results from the preliminary tests (Chapter 8), a variety of chemical concentrations and combinations (Table 9.1), were selected to be applied to the cotton and silk model textile samples. Where available, published precedents or manufacturer guidelines were used to choose the treatment concentrations for study (Kolar, Mozir, Strlic, de Bruin, Pihlar and Steemers 2007; Kolar, Mozir, Strlic, Ceres, Conte, Mirruzzo, Steemers and de Bruin 2008). Where unavailable, the choice of chemical concentration was influenced by the concentrations used for chemicals in similar stabilisation roles, e.g. radical scavengers. All concentrations were calculated with respect to the mass of fabric being treated so that the mass of chemical per mass of textile remained the same for sample comparability. The concentrations for the dyed and undyed samples differed due to the dyed samples containing the dye/mordant system.

The control treatment involved the initial application of a magnesium phytate (MP) solution followed by two consecutive applications of calcium bicarbonate (CB). Each solution was applied once the sample had dried following the previous treatment application. MP was produced by combining magnesium carbonate hydrate (MC) and phytic acid (40% aqueous solution (w/w)) (PA(MP)) in reverse osmosis water. MC was added until the solution was within the pH 4-6.5 range used during the testing of this treatment on iron gall ink on paper and close to the pH 5.8-6.0 range that was identified as showing optimal stabilisation performance (Kolar, Mozir, Strlic, de Bruin, Pihlar and Steemers 2007). Under experimental conditions the pH of the MP treatment solutions ranged from pH 5.70 to 5.82 and was checked using a Hanna Instruments HI2210 pH meter with HI1131 probe and separate temperature sensor. The CB solutions were produced as described by Kolar J, Mozir A, Strlic M, de Bruin G, Pihlar B, Steemers T (Kolar, Mozir, Strlic, de Bruin, Pihlar and Steemers 2007) but using 26.6832 g of calcium carbonate in 7.2 L of deionised water through which CO₂ was bubbled overnight.

9.1 Experimental method

Table 9.1 The concentrations of the treatment solutions used in Treatment Test 1

Chemical	Solvent	ME ~30% textile weight ^a	Chemical mass in 300 ml of solvent as approximate % textile weight ^b	Concentration, M	
				Dyed ^c	Undyed ^c
<i>Antioxidants</i>					
AT	GE	Y	2.00	0.00052	0.00047
			3.00	0.00078	0.00070
			6.00	0.00155	0.00141
			6.00	0.00157	0.00141
AT ^d	GE		200.00	0.05146	0.05146
EA	IMS	Y	0.40	0.00019	0.00017
			0.40	0.00019	0.00017
			2.00	0.00097	0.00087
			4.00	0.00195	0.00174
		Y	4.00	0.00195	0.00174
EBR	EtOH		6.00	0.00335	0.00300
			30.00	0.01675	0.01500
			60.00	0.03350	0.03001
I1135	GE		2.00	0.00057	0.00051
			3.00	0.00086	0.00077
			6.00	0.00172	0.00154
			43.00	0.01229	0.01229
		Y (in IMS)	43.00	0.01229	0.01229
PA	IMS	Y (in IMS)	3.00	0.00047	0.00044
			15.00	0.00243	0.00219
			30.00	0.00486	0.00438
			30.00	0.00487	0.00436
T144	T	Y	2.00	0.00033	0.00029
			3.00	0.00049	0.00044
			6.00	0.00098	0.00088
			6.00	0.00099	0.00088
			450.00	0.07282	0.07282
T292	GE	Y	2.00	0.00025	0.00023
			3.00	0.00038	0.00034
			6.00	0.00077	0.00069
			6.00	0.00077	0.00069
			260.00	0.03277	0.03277
PA (MP)	Water		5.00	0.00098	0.00044
			15.00	0.00244	0.00218
			30.00	0.00487	0.00436
MC	Water		0.82	0.00108	0.00107
			4.66	0.00617	0.00562
			9.37	0.01241	0.01125
<i>Deacidifier</i>					
ME	EtOH		6.00	0.00558	0.00502
			30.00	0.02793	0.02496
			60.00	0.05603	0.05000

Notes for Table 9.1:

a. Y (yes) means a separate application of ME30 was made to a treated sample;

b. Combination of these values and the chemical abbreviation form the treatment codes referred to from now on e.g. AT200. IMS is included in the treatment code when used with PA to highlight the use of non-aqueous solvent. The magnesium phytate and calcium bicarbonate treatment is noted as MPx/2CBx, where 'x' is the mass of PA(MP) as percentage of textile weight. If the chemical abbreviation ends in a number a hyphen will be used to separate it from the concentration code e.g. T292-260;

9.1 Experimental method

- c. In some cases, concentrations for undyed and dyed textiles vary because of differing textile masses; the mass of chemical per mass of textile is equal. In other cases the concentration is independent of textile mass;
- d. A small piece of undyed textile was added to the dyed sample treatment bath rather than treating 10 cm x 15 cm undyed samples separately due to insufficient quantity of solvent.

9.1.2 *Treatment application*

Samples of dyed (c3 and p3) and undyed cotton and silk model textiles (15 × 10 cm) were used in all tests. The samples were immersed in 300 ml of treatment solution for 30 minutes and were hung to dry in the fume cupboard. Cross-contamination of dye was eliminated through separate treatment of dyed and undyed samples except for the AT200 test.

9.1.3 *Accelerated ageing*

Following treatment application, the treated samples and the untreated control samples were labelled and cut into three 10 × 5 cm pieces. One of these pieces of each model textile was accelerated aged in a Sanyo Gallenkamp Environmental Chamber (reference 8291) at the National Gallery, London at 80°C and 65% RH. After two weeks of ageing the cotton samples were cut in half and one 5 × 5 cm piece of each two week aged sample was removed for analysis. The remaining piece was aged for a further two weeks before removal for analysis along with the four week aged silk. These ageing conditions were identified as suitable in previous studies (Chapter 7). The cotton and silk samples were stacked together on pieces of Munktell CXD pHoton Aqua Forte High Wet Strength absorbent paper (90 g/m²). Undyed and dyed samples were stacked separately to minimise transfer of iron ions and dye between samples during accelerated ageing. Plastic tubing was used to gently hold the samples in place as otherwise the airflow through the chamber caused them to move (Figure 9.1). An untreated sample of each model textile tested was included.



Figure 9.1 Cotton and silk dyed (c3 and p3) and undyed treated samples prepared for accelerated ageing

9.1.4 Analysis

9.1.4.1 Micro-pH testing

The pH of the treated and untreated dyed cotton and silk samples was determined before and after accelerated ageing. Samples EA50, EA100 and EA100/ME50 were aged with untreated sample U-b and the rest of the samples were aged with untreated sample U.

The small size (5×5 cm) of the two week aged cotton samples and the requirement for sample material for other destructive analyses such as viscometry necessitated the use of micro-pH analysis rather than alternative methods such as surface pH testing or hot or cold extraction techniques based one of several standards (ASTM D778-97 2002; BS EN ISO 3071:2006 2006). A method of micro-pH testing which was an adaptation of methods described in literature (Strlic, Kolar, Kocar, Drnovsek, Selih, Susic and Pihlar 2004; Vuori and Tse 2005b) was developed after small-scale testing. For micro-pH analysis 3 mg of sample was soaked overnight in 150 μ l of deionised water (Vuori and Tse 2005b). The fibres were wetted out before leaving to soak overnight. Soaking overnight was necessary for accurate pH measurements as alkali-earth metal carbonates had been used in some treatments. The low solubility of these carbonates necessitated a longer soaking time for equilibration and an accurate pH reading to occur (Strlic, Kolar, Kocar, Drnovsek, Selih, Susic and Pihlar 2004).

9.1 Experimental method

A Mettler Toledo InLab® micro-pH electrode, separate temperature probe, and Hanna Instruments HI2210 pH meter were used to determine the stabilised pH values of each solution. The electrode was calibrated using pH 7 and pH 4 buffer solutions and rinsed in deionised water between readings. Three analyses of each sample were obtained and an average calculated. Prior to analysis, the soaked fibres were removed from the solution to ensure no fibres made contact with the electrode.

9.1.4.2 Colorimetry

Colorimetric data was collected as described in Sections 5.2.4 and 5.2.4.2. Colour differences (ΔE_{00}^* , ΔL^* , Δa^* , Δb^*) between aged treated and unaged treated samples, and samples immersed and not immersed in solvent, were calculated from SCE/100 data using the CIE2000 formula (Equation 2.1).

Analysis of all of the aged treated dyed (Sp3) and undyed (SU) silk samples was undertaken after tensile testing in which the samples were prepared into 1 cm wide strips. With the medium aperture (MAV) measuring over 1 cm in diameter it was decided that the use of small aperture (SAV) would be more accurate. Calculation of the changes in colour parameters have been calculated from MAV data for the unaged treated samples and SAV data for the aged treated samples, unless otherwise stated, using SCE/100 data and the CIE2000 formula. As the software settings were altered accordingly, the use of SAV or MAV should produce statistically similar results of the same sample.

The error in the results due to the variation in colour of the textiles for the ΔL^* , Δa^* , and Δb^* values was found to be approximately twice the standard deviation in CIE L^* , a^* , and b^* values (Table 9.2), respectively as determined in the homogeneity characterisation tests in Chapter 5 (Table 5.6). Note that the standard deviations for 30 analyses per model textile were noted for SCE/100 data only. The data used in the evaluation of the effect of treatment application on fabric colour was the SCE/100 data but the difference between the two types of data is small.

9.1 Experimental method

Table 9.2 Approximate error in the colorimetric data due to variation in model textile colour prior to treatment or accelerated ageing

Model textile	Mean			Standard deviation			Approximate error in		
	L^*	a^*	b^*	L^*	a^*	b^*	ΔL^*	Δa^*	Δb^*
CU	84.31	-0.26	0.67	0.51	0.02	0.09	1.02	0.04	0.18
Cc3	29.61	0.57	-4.62	1.01	0.05	0.13	2.02	0.1	0.26
SU	75.36	-0.2	0.97	0.36	0.02	0.12	0.72	0.04	0.24
Sp3	17.79	1.38	-4.09	0.2	0.03	0.07	0.4	0.06	0.14

Calculation of the error in ΔE_{00}^* data due to natural colour variation of the model textiles has not been calculated due to the complicated nature of the CIE2000 calculation.

9.1.4.3 Subjective handling tests (Cc1)

The aged dyed samples were assessed by comparing treated samples (T) with the aged untreated sample (U). The subjective handling tests were always conducted in a well-lit area by the same experienced person (British Museum object conservator Pippa Cruickshank) for consistency and accuracy. The PhD investigator was also present to confer and take notes.

Strength was assessed by gently pulling individual fibres apart, folding and pressing a corner of the sample until it broke or four folds was reached, and folding and rolling a fibre together between fingers to see if it broke.

Surface rub resistance was assessed by rubbing the sample gently between the thumb and forefinger and judging the quantity of dark fibres left on the nitrile rubber glove.

Colour was assessed by visually comparing the aged treated samples next to an aged untreated control sample and was supported by colorimetric and spectrophotometric analysis to obtain an objective measure of colour changes.

Classification of treated (T) and untreated (U) samples followed a five point scale:

- T exhibits poorer property retention than U.
- 0 No difference between T and U.
- + T exhibits slightly better property retention than U.
- ++ T exhibits better property retention than U.
- +++ T exhibits markedly better property retention than U.

9.1.4.4 Tensile testing

Untreated and treated dyed silk samples that had been aged for four weeks at 80°C and 65% RH were tested in the weft direction as detailed in Section 5.2.5.1 using between three and five strips per sample (as sample size allowed). Cotton fabric was not tensile tested due to insufficient material and the need for other analysis, and also because the most successful treatments at impeding strength loss and brittleness during accelerated ageing were easily identified using the handling tests.

9.1.4.5 Viscometry

20-35 mg of aged cotton samples were defibrillated in water and dissolved in cupri-ethylenediamine (CED) solution (20 ml, 0.5 M) as described in BS ISO 5351:2010 (BS ISO 5351:2010 2010). Using a thermostatic water bath both the solutions and capillary-tube viscometer were maintained at 25.0 \pm 0.1°C. One repeat of each sample was made. A shear rate of 456 \pm 61 s⁻¹ was used and, using equation 1, the viscosity ratio was 1.30 \pm 0.18. The time for the solution to pass through a set volume (between two markers) was measured manually with a stopwatch.

The time for the solutions and the blank (CED and water only) to pass between two marks on the capillary-tube viscometer was recorded with the mass of sample. It was assumed that the textile contained 5% water from the atmosphere. The intrinsic viscosity number ($[\eta]$) was calculated using equation 1 and the Wetzel-Elliot-Martin's equation. The average molecular weight of the polymer was calculated using the Mark-Houwink-Sakurada equation and the average DP was calculated using the Evans and Wallis equation (Equation 9.2) (Kolar, Strlic and Pihlar 2006).

$$\frac{t}{t_0} = \frac{\eta}{\eta_0} \quad \text{Equation 9.1}$$

Where t and t_0 are the efflux times of the polymer solution and solvent, respectively, and η/η_0 is the viscosity ratio.

$$\text{DP}^{0.85} = 1.1 \cdot [\eta] \quad \text{Equation 9.2}$$

9.1.4.6 SEM-EDX

A selection of treated dyed cotton and silk samples (unaged) were analysed using SEM-EDX to identify if the application of the selected treatments had caused obvious and consistent changes in surface appearance of the textiles. BSE images at $\times 25$, $\times 100$, $\times 250$ magnification and EDX spectra were collected as described in Section 5.2.7.2 Unaged (Cc3 and Sp3 samples).

9.1.4.7 EPR spectroscopy

Electron paramagnetic resonance (EPR) spectroscopy was used to investigate quantitatively the types and quantities of radicals and iron(III) present in a selection of aged and unaged treated samples. The method used is detailed in Section 5.2.6.

9.1.4.8 GPC-MALLS

GPC-MALLS was used to determine the average molecular weight, carbonyl content, molar mass distribution, and DP of treated and untreated, aged and unaged cotton samples using the method detailed in Section 5.2.8.

9.2 The effect of treatment application on the model textiles – Results and discussion**9.2.1 Micro-pH testing**

Table 9.3 The effect of treatment application on the colour and pH of Cc3 and the colour of CU

Treatment code	pH of Cc3	Change in pH of Cc3	Change in colour of Cc3				Change in colour of CU			
	Average pH (SD)	$\Delta\text{pH}^{\text{a}}$ (SD ^b)	ΔE_{00}^*	ΔL_c^*	Δa_c^*	Δb_c^*	ΔE_{00}^*	ΔL_c^*	Δa_c^*	Δb_c^*
U	3.7 (0.0)	0.0 (0.0)	-	-	-	-	-	-	-	-
U ^d	3.7 (0.0)	0.0 (0.0)	-	-	-	-	-	-	-	-
ME6	4.1 (0.1)	0.4 (0.1)	1.8	1.6	0.2	1.4	0.2	0.2	0.0	0.1
ME30	5.4 (0.0)	1.7 (0.0)	3.5	0.2	1.0	3.4	0.6	0.8	-0.1	0.2
ME60	7.4 (0.2)	3.7 (0.2)	4.4	1.6	1.1	4.3	0.6	0.9	-0.1	0.2
ME60/IMS	5.9 (0.1)	2.2 (0.1)	3.8	-0.3	1.2	3.7	0.6	0.9	-0.1	0.1
EA0.4	4.1 (0.0)	0.4 (0.1)	4.0	4.4	-0.1	2.4	0.4	0.6	0.0	-0.1
EA0.4/ME30	5.1 (0.2)	1.4 (0.2)	3.0	1.7	0.5	2.8	0.5	0.8	0.0	0.0
EA2 ^d	3.9 (0.0)	0.2 (0.1)	1.3	1.2	-0.2	1.0	0.2	0.0	0.1	-0.1
EA4 ^d	3.9 (0.0)	0.2 (0.1)	2.6	2.8	-0.2	1.6	0.5	-0.7	0.1	-0.2
EA4/ME30 ^d	5.2 (0.2)	1.5 (0.3)	4.8	-3.2	1.8	3.3	0.3	0.1	-0.1	0.3
EBR6	4.0 (0.1)	0.3 (0.1)	1.4	-1.7	0.3	0.5	0.0	0.0	0.0	0.0
EBR30	4.0 (0.0)	0.3 (0.0)	1.9	-1.8	0.6	1.2	0.1	-0.1	0.0	0.1
EBR60	3.8 (0.0)	0.1 (0.0)	1.7	-1.2	0.6	1.3	0.3	0.5	0.0	0.1
EBR60/IMS	3.8 (0.1)	0.1 (0.1)	1.2	-0.9	0.5	0.8	0.4	0.6	-0.1	0.2
T144-2	4.0 (0.0)	0.3 (0.1)	1.4	-1.8	0.2	-0.2	0.1	-0.2	0.0	-0.1
T144-3	3.9 (0.0)	0.2 (0.0)	0.7	-0.9	0.2	0.1	0.1	0.1	0.0	-0.1
T144-6	4.0 (0.0)	0.3 (0.0)	1.8	-2.3	0.2	-0.3	0.2	0.3	0.0	-0.1
T144-6/ME30	4.9 (0.1)	1.2 (0.1)	3.1	0.7	0.7	3.1	0.5	0.8	0.0	0.2
T144-450	5.3 (0.1)	1.6 (0.1)	1.3	-1.6	0.0	0.5	1.9	-2.8	0.0	0.3
T292-2	4.0 (0.0)	0.2 (0.0)	0.2	-0.2	0.1	-0.1	0.4	0.6	0.0	0.0
T292-3	3.9 (0.0)	0.2 (0.0)	0.2	0.1	0.1	0.0	0.1	0.2	0.0	0.1
T292-6	3.9 (0.0)	0.2 (0.1)	0.7	-0.7	0.2	0.1	0.2	0.3	0.0	0.1
T292-6/ME30	4.4 (0.0)	0.7 (0.0)	2.4	-0.4	0.5	2.5	0.3	0.3	-0.1	0.2
T292-260	6.9 (0.1)	3.2 (0.0)	2.1	-2.7	0.1	0.7	1.0	-1.4	0.1	0.4
AT2	3.9 (0.1)	0.2 (0.1)	0.3	0.3	0.1	0.2	0.3	0.5	-0.1	0.1
AT3	4.0 (0.0)	0.3 (0.0)	0.5	0.3	0.1	0.5	0.5	0.7	-0.1	0.1
AT6	4.0 (0.0)	0.3 (0.1)	0.8	1.1	0.0	0.1	0.4	0.5	-0.1	0.2
AT6/ME30	5.0 (0.1)	1.3 (0.1)	2.8	0.4	0.6	2.9	0.7	1.0	0.0	0.2
AT200	3.9 (0.0)	0.2 (0.0)	1.4	-1.7	0.0	0.5	1.1	-1.3	0.0	0.7
PA10/IMS/ME30	4.9 (0.1)	1.2 (0.2)	3.6	1.5	0.8	3.5	0.5	0.7	0.0	0.0
PA10ME60/IMS	4.5 (0.0)	0.8 (0.0)	1.6	-0.1	0.5	1.5	0.2	0.1	0.0	-0.2
PA10MC15/IMS	4.3 (0.1)	0.5 (0.1)	2.2	1.5	0.3	2.1	0.2	0.0	0.1	-0.2
PA5/IMS	3.9 (0.1)	0.2 (0.1)	0.7	0.7	0.1	0.6	0.3	0.5	0.0	-0.2
PA15/IMS	3.9 (0.0)	0.2 (0.0)	1.8	2.0	-0.1	0.9	0.4	0.3	0.0	-0.3
PA30/IMS	3.7 (0.1)	0.0 (0.1)	4.7	5.5	-0.2	1.9	0.3	0.2	0.0	-0.2
PA30/IMS/ME30	4.2 (0.0)	0.5 (0.1)	2.3	1.0	0.6	2.2	0.4	0.4	0.0	-0.2
MP5/2CB5	4.9 (0.1)	1.2 (0.1)	3.4	-3.4	1.2	1.5	0.5	0.6	0.0	-0.2
MP15/2CB15	5.6 (0.1)	1.9 (0.1)	6.2	-4.8	2.6	3.6	0.6	0.9	0.0	-0.3
MP30/2CB30	6.2 (0.1)	2.5 (0.1)	7.3	-4.3	3.5	5.1	0.6	0.7	0.0	-0.3
I1135-2	3.7 (0.1)	0.0 (0.1)	0.7	0.8	0.0	0.0	0.4	0.5	-0.1	-0.1
I1135-3	3.9 (0.0)	0.1 (0.0)	1.0	1.3	0.0	0.0	0.2	0.3	-0.1	0.1
I1135-6	3.7 (0.1)	0.0 (0.1)	0.4	0.5	0.0	0.0	0.1	0.1	0.0	0.0
I1135-43	3.8 (0.1)	0.1 (0.1)	1.4	-1.8	0.2	0.0	0.5	-0.7	0.0	0.1
I1135-43/ME30	5.0 (0.0)	1.3 (0.1)	2.9	-3.4	0.7	1.1	0.4	0.5	-0.1	0.1

Notes for Table 9.3:

a. Change in pH = pH(treated) – pH(untreated);

b. SD = SD(treated) + SD(untreated);

9.2 The effect of treatment application on the model textiles – Results and discussion

- c. Change in colour parameter = parameter(treated) – parameter(untreated) e.g. $L^*(\text{treated}) - L^*(\text{untreated})$;
- d. Undyed for comparison with EA4, EA2, EA4/ME30 only and vice versa.

The application of treatments without deacidifier such as ME or MC caused little change in the pH of the cotton samples (< 0.4 pH units) (Table 9.3). With a deacidifier present, the change in pH was generally greater than that seen in the equivalent samples without deacidifier and ranged between 0.4 pH units (ME6) and 3.7 pH units (ME60). A feature of the successful application of a deacidifier will be the neutralisation of acid present in the sample and deposition of a residue capable of neutralising future acidity (alkaline reserve) until it has been fully neutralised (Smith 2011). Interestingly, T292-260 (3.22 pH units change) and T144-450 (1.63 pH units change) caused a greater pH change on application without deacidifier than with. This may be due to the hindered amine groups in their structures which are presumably still able to assist in the neutralisation of acidity. However, if as is the case with ammonia, these amines are weak bases, problems may arise during ageing since acidic rather than neutral salts will be formed on reaction with strong acids (e.g. sulphuric acid which is a possible byproduct of the dyeing procedure) (Smith 2011). After treatment application the samples with the highest pH and therefore those most likely to experience the least depolymerisation with ageing are the ME60 (pH = 7.4 ± 0.2), T292-260 (pH = 6.9 ± 0.1), and MP30/2CB30 (pH = 6.2 ± 0.1) treated dyed cotton samples. T144-450, MP15/2CB15, ME30, ME60/IMS and several antioxidants combined with ME caused a final textile pH > 5 .

Of the treated dyed silk samples that were analysed for their pH, ME60 (pH 6.9 ± 0.0) raised the pH of the silk the greatest (Table 9.4). MP30/2CB30 and MP15/2CB15 also raised the pH of Sp3 to above pH 6. T292 caused no statistically significant change in pH in Sp3 after ageing. All of the analysed EBR treated samples resulted in over 1 pH unit lower than the untreated sample. This may be an error. Micro-pH testing was stopped prematurely based on these results and concerns that the treatments may have contaminated the electrode during the previous analyses (cotton dyed aged and silk dyed aged samples) resulting in inaccurate results and long calibration times during this study. The potential unreliability of the silk pH data makes comparison with the cotton pH data unsuitable.

9.2 The effect of treatment application on the model textiles – Results and discussion

Table 9.4 The effect of treatment application on the pH and colour of Sp3 and the colour of SU

Treatment code	pH of Sp3	Change in pH of Sp3	Change in colour of Sp3				Change in colour of SU			
	Average pH (SD) ^a	ΔpH^b (SD) ^a	ΔE_{00}^*	ΔL_c^*	Δa_c^*	Δb_c^*	ΔE_{00}^*	ΔL_c^*	Δa_c^*	Δb_c^*
U	4.4 (0.1)	0.0 (0.2)	-	-	-	-	-	-	-	-
U ^d	-	-	-	-	-	-	-	-	-	-
ME6	5.2 (0.3)	0.8 (0.5)	3.4	4.1	-0.4	2.1	0.3	-0.3	-0.1	0.2
ME30	5.9 (0.1)	1.5 (0.2)	5.0	6.8	-0.6	1.8	0.6	0.7	-0.1	0.3
ME60	7.5 (0.0)	3.1 (0.1)	5.4	7.4	-0.6	1.5	1.4	1.8	-0.2	0.4
ME60/IMS	6.9 (0.0)	2.5 (0.2)	5.2	7.3	-0.6	0.0	1.0	1.3	-0.1	0.0
EA0.4	-	-	2.8	3.3	-0.5	1.8	0.6	0.7	0.0	-0.2
EA0.4/ME30	-	-	3.8	4.8	-0.5	2.0	0.6	0.7	-0.1	0.2
EA2 ^d	-	-	0.7	0.3	-0.2	0.8	0.2	0.1	0.0	0.2
EA4 ^d	-	-	0.8	0.0	-0.2	0.9	0.1	-0.1	0.0	0.1
EA4/ME30 ^d	-	-	3.5	4.7	-0.4	1.6	0.4	0.4	-0.1	0.3
EBR6	3.1 (0.2)	-1.3 (0.3)	0.2	0.1	-0.1	0.1	0.6	-0.9	0.0	0.0
EBR30	2.6 (0.1)	-1.8 (0.2)	0.4	-0.3	-0.1	0.4	0.8	-1.0	0.0	0.0
EBR60	2.9 (0.1)	-1.5 (0.2)	0.5	0.0	-0.1	0.5	0.6	-0.9	0.0	0.0
EBR60/IMS	-	-	0.3	0.4	-0.1	0.2	0.4	0.2	-0.1	0.3
T144-2	-	-	0.5	-0.4	0.0	-0.5	0.2	-0.3	0.0	0.0
T144-3	-	-	0.5	-0.3	-0.1	-0.5	0.2	-0.2	0.0	0.1
T144-6	-	-	0.5	-0.4	-0.1	-0.5	0.1	-0.1	0.0	0.0
T144-6/ME30	-	-	4.2	5.3	-0.5	2.2	0.6	0.7	-0.1	0.3
T144-450	-	-	3.1	-3.9	-0.7	1.6	3.0	-4.1	-0.1	0.2
T292-2	4.5 (0.1)	0.1 (0.2)	0.5	-0.4	-0.1	-0.5	0.0	0.0	0.0	0.0
T292-3	4.4 (0.0)	0.0 (0.1)	0.5	-0.5	-0.1	-0.4	0.1	0.1	0.0	0.0
T292-6	2.9 (0.1)	-1.5 (0.2)	0.6	-0.5	-0.1	-0.4	0.1	0.1	0.0	0.0
T292-6/ME30	4.4 (0.3)	0.0 (0.4)	3.9	5.0	-0.5	2.1	0.6	0.9	0.0	0.1
T292-260	5.1 (0.7)	0.7 (0.8)	2.4	-3.5	-0.3	0.8	2.2	-2.9	0.0	0.4
AT2	-	-	0.2	0.3	-0.1	0.1	0.1	0.1	0.0	0.0
AT3	-	-	0.2	0.2	-0.1	0.1	0.1	0.1	0.0	0.1
AT6	-	-	0.3	0.4	-0.1	0.1	0.2	0.0	-0.1	0.2
AT6/ME30	-	-	4.1	5.2	-0.5	2.1	0.8	1.0	-0.1	0.5
AT200	-	-	2.2	-3.2	-0.3	0.7	1.6	-1.8	-0.1	0.9
PA10/IMS/ME30	-	-	4.2	5.6	-0.6	1.8	0.8	1.0	-0.1	0.1
PA10ME60/IMS ^e	-	-	1.2	1.4	-0.4	-0.3	0.2	0.2	-0.1	-0.1
PA10MC15/IMS	-	-	0.9	-1.3	-0.2	-0.2	0.3	0.0	-0.1	-0.3
PA5/IMS	-	-	0.6	-0.8	-0.1	-0.2	0.4	-0.1	-0.1	0.3
PA15/IMS	-	-	0.7	-1.0	-0.1	-0.2	0.5	0.6	-0.1	-0.2
PA30/IMS	-	-	0.7	-1.0	-0.1	-0.2	0.5	0.6	-0.2	-0.2
PA30/IMS/ME30	-	-	1.5	2.0	-0.4	0.2	1.1	1.6	-0.1	-0.1
MP5/2CB5	5.6 (0.1)	1.2 (0.2)	1.0	-1.5	-0.2	0.2	0.3	0.1	0.0	-0.3
MP15/2CB15	6.1 (0.1)	1.7 (0.2)	1.0	-1.2	-0.1	0.6	1.5	1.9	-0.1	-0.6
MP30/2CB30	6.4 (0.0)	2.0 (0.1)	1.5	-1.6	-0.1	1.2	2.2	3.1	-0.2	-0.4
I1135-2	-	-	0.4	-0.4	-0.1	-0.3	0.6	0.3	-0.1	0.6
I1135-3	-	-	0.5	-0.6	-0.1	-0.3	0.5	0.2	-0.1	0.5
I1135-6	-	-	0.5	-0.5	-0.1	-0.3	0.4	0.2	-0.1	0.4
I1135-43	-	-	0.7	-1.0	-0.1	0.0	0.2	0.1	0.0	0.2
I1135-43/ME30	-	-	3.6	5.1	-0.4	0.4	0.5	0.5	-0.1	0.4

Notes for Table 9.4:

- Change in pH = pH(treated) – pH(untreated);
- SD = SD(treated) + SD(untreated);

9.2 The effect of treatment application on the model textiles – Results and discussion

- c. Change in colour parameter = parameter(treated) – parameter(untreated) e.g. $L^*(\text{treated}) - L^*(\text{untreated})$;
- d. Undyed for comparison with EA4, EA2, EA4/ME30 only and vice versa;
- e. This sample had some powdery residue on the surface. The side with the least powdery residue was analysed as it was thought that the residue may be a direct result of the application method (immersion) rather than the treatment. It is highly unlikely that immersion will be used by conservators to treat iron-tannate dyed objects.

9.2.2 Colorimetry

A conservation treatment needs to have minimal adverse effects on the object to which it is applied. A noticeable undesirable change in colour of the object due to application of the treatment would be an adverse effect. The immediate brightening of paper by treatment application is viewed as a desirable colour change (Bruckle 2011a). For iron-tannate dyed textiles however, if anything, a darkening of the textile would be most desirable as it enhances the intended colour of the object. In this research a colour change of $\Delta E_{00}^* = 1.7$ is viewed as ‘just perceptible’ (BS EN 20105-A02:1995/ISO 105-A02:1993 1995, 1993; Reissland and Cowan 2002). Since the non-aqueous solvents used in this study result in minimal colour change to the samples when used alone (Chapter 8), any colour change seen on treatment application must be due to the presence of antioxidant or deacidifier and also the application method. In this study the model textiles were immersed in treatment solution for 30 minutes. Despite the fact that this is unlikely to be the method of application to historic objects, particularly fragile ones, analysis of colour changes to samples following treatment application by immersion is still pertinent to this study as it will identify if any treatments are likely to cause colour changes by other application methods also. Consequently, the change in colour of the model textiles due to treatment application has been calculated (Tables 9.3 and 9.4). The colour coordinates (SCE/100) of the standards are presented in Table 5.3.

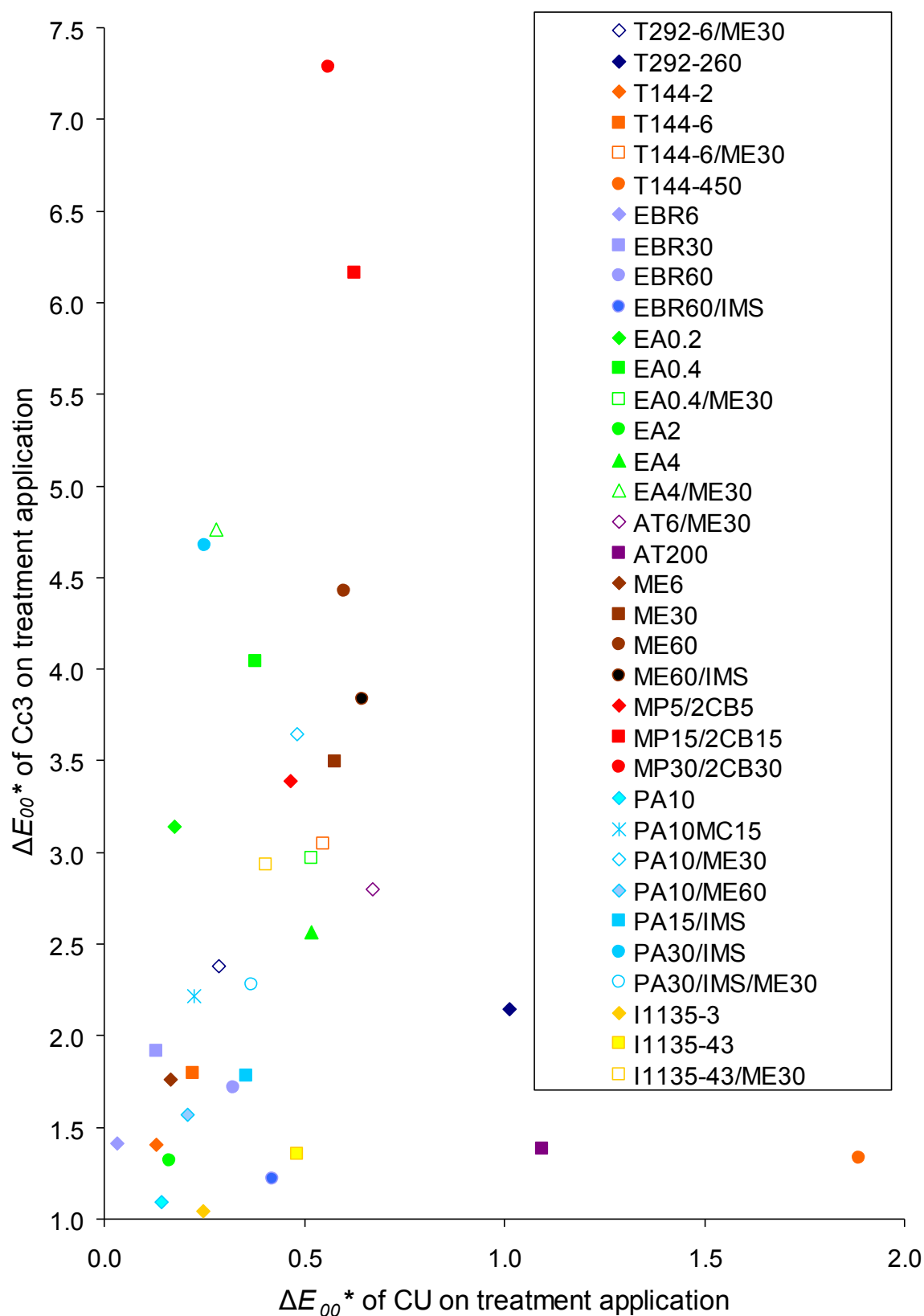


Figure 9.2 Change in colour (ΔE_{00}^*) of dyed and undyed cotton due to treatment application (for colour changes in Cc3 textiles >1)

For all treatments excepting T144-450, treatment applications to Cc3 caused greater changes in colour than when applied to CU (Table 9.3 and Figure 9.2). This could be due

9.2 The effect of treatment application on the model textiles – Results and discussion to the stability of the dye complex with respect to the treatments. Although breakdown of the dye complex can occur in alkaline and acid conditions to give brown degradation products. Generally the treatments which caused the greatest colour change in Cc3 included ME ($\Delta E_{00}^* = 1.8$ to 4.4) or one of the MPx/2CBx (where $x = 5, 15$, or 30 , and $\Delta E_{00}^* = 3.4$ to 7.3) treatments. These samples increased in redness ($+\Delta a^*$) and yellowness ($+\Delta b^*$) following treatment application, significantly more than the other treated samples. This could indicate that iron-tannate dye complexes have been broken down to form brown degradation products as previously mentioned, particularly as these treatments raised the pH of the textiles significantly on application (Table 9.3). The MPx/2CBx samples also appear to have significantly darkened on treatment application ($-\Delta L^*$) unlike the ME treated samples which either barely changed or lightened a little. PA30/IMS, EA0.4, EA0.2, T292-260, and ME in combination with some antioxidants e.g. T144-6, also caused $\Delta E_{00}^* > 2$ when applied to Cc3. EBR30, T144-6, PA15/IMS, and EBR60 were treatments without ME which caused a ΔE_{00}^* between 1.7 and 2 .

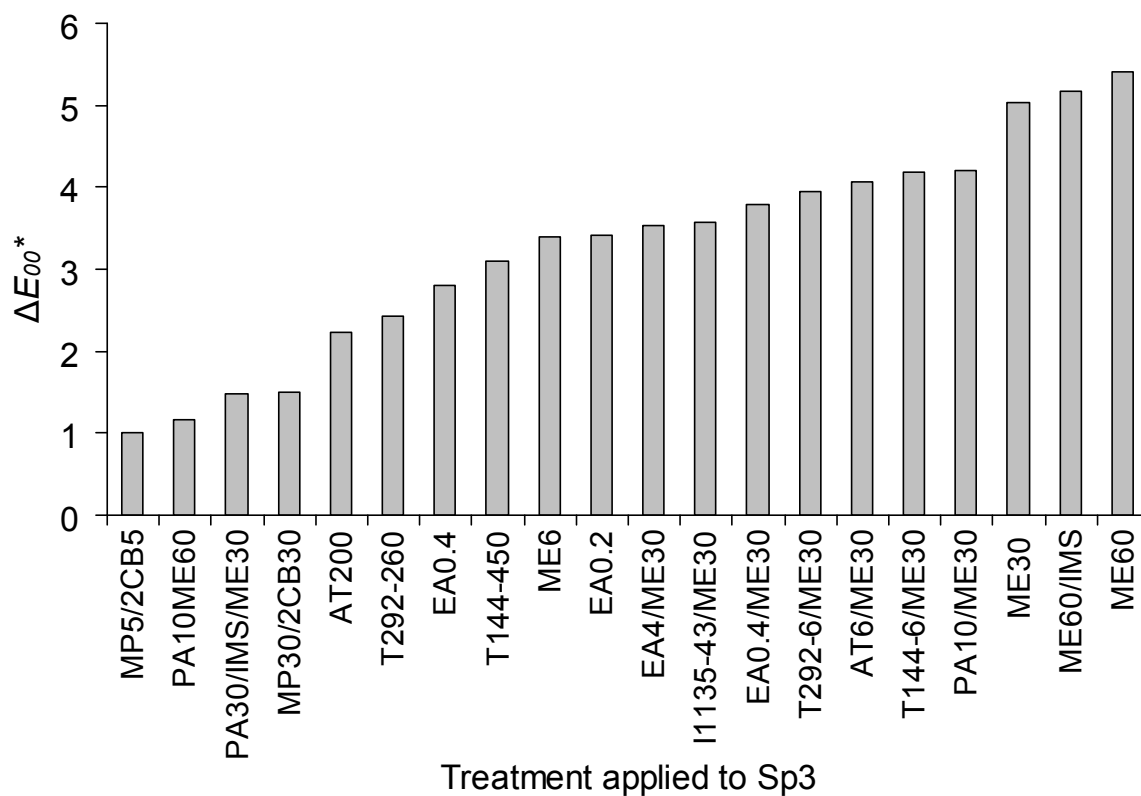
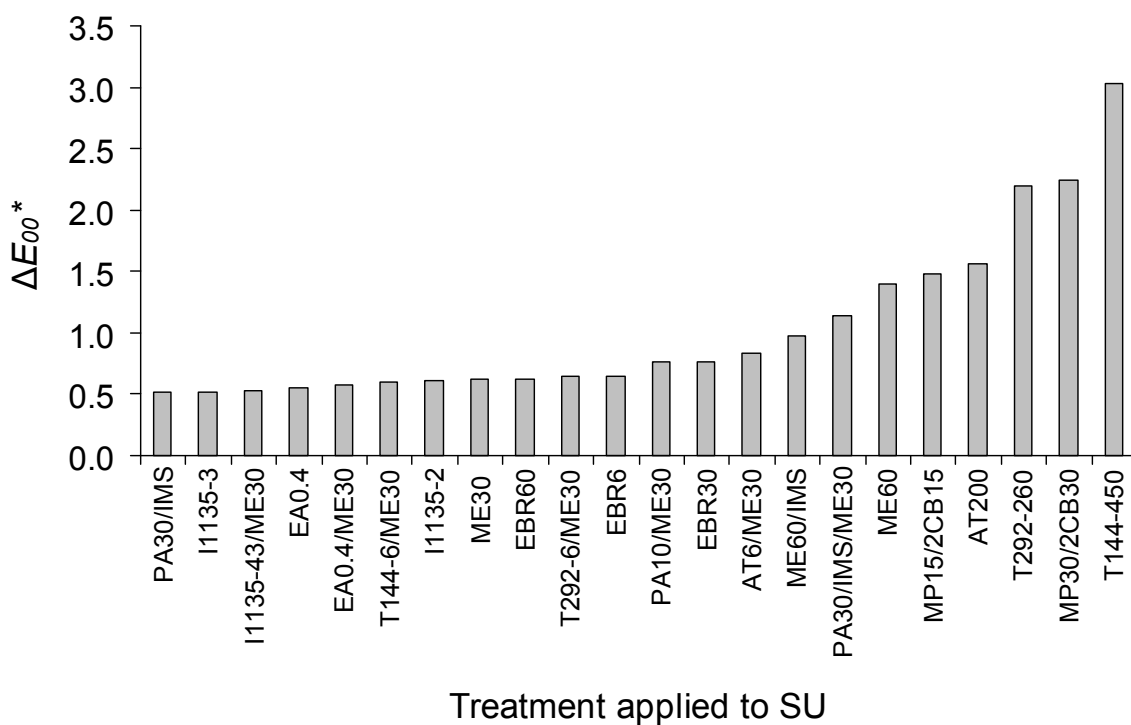
There is little correlation between concentration of treatment solution and the resulting colour change of the sample upon treatment application. In some cases such as for the MPx/2CBx treatments a clear increase in ΔE_{00}^* occurs with increasing concentration. However with the majority of the model textiles there is no consistent rise in ΔE_{00}^* with treatment concentration. It is possible that a correlation does occur but that the error in the results, which at present is uncalculated for ΔE_{00}^* , due to the complicated nature of the CIE2000 formula, that is incurred through the natural variation in colour of the model textiles prior to treatment application has “masked” this trend. Also, uneven treatment application may have occurred due to the immersion method of application used. The noticeably larger colour change in Cc3 caused by treatment with EA0.2, and EA0.4 when compared to higher concentrations of the same chemical, e.g. EA2, may be due to variations in the natural colouration of the model textile.

In CU (Table 9.3) the greatest colour changes occurred with the highest concentrations of T144, AT, and T292. However, only the T144 resulted in a colour change greater than 1.7 which is ‘just perceptible’ (BS EN 20105-A02:1995/ISO 105-A02:1993 1995, 1993; Reissland and Cowan 2002). Despite causing some of the largest changes in colour in CU, T144-450 and AT200 caused a colour change of less than 1.5 in Cc3 while T292-260 caused a more noticeable colour change of 2.15 in Cc3 upon application. In Cc3 the MP30/2CB30 and MP15/2CB15 caused the greatest overall colour changes of all the treatments (7.29 and 6.16 , respectively).

The change in L^* upon treatment application to the cotton samples is greatest in the Cc3 rather than CU textiles. The change in lightness ranged from -4.8 to 5.5 for Cc3 and -2.8 to 1 for CU. As was seen with the overall change in colour, T144-450, T292-260, and AT200, caused the greatest change in L^* (darkening with ΔL^* ranging between -1.3 and -2.8). In Cc3 the MPx/2CBx treatments darkened the samples the most while PA30/IMS, EA0.2, EA0.4, EA4, and PA15/IMS lightened the samples the most, causing ΔL^* between 2.0 and 5.5. The approximate error of ± 1.02 for CU, and ± 2.02 for Cc3 mean that many of the differences in ΔL^* due to different treatments are insignificant. As a result, no consistent significant trends between the change in lightness and concentration have been identified.

The approximate error in Δa^* is 0.1 for Cc3 and 0.02 for CU. Even with these errors it is clear that in Cc3 the inclusion of ME in a treatment with an antioxidant causes a significant increase in redness ($+\Delta a^*$). Indeed, the only treatments which caused a Δa^* of between 0.3 to 3.5 are treated with ME, with or without an antioxidant, with MPx/2CBx, or with EBR. The remaining treatments caused relatively small changes in redness ($\Delta a^* = -0.2$ to 0.3). While there are no consistent trends in CU samples with respect to the change in redness (Δa^* ranges from -0.8 to 0.8), there is generally an overall increase in redness of Cc3 as the treatment concentration increases. Also, EA caused a decrease in redness while T292 caused an increase in redness upon application.

Greater change in yellowness-blueness Δb^* occurred on treatment application to Cc3 samples (between -0.32 and 5.13) than for treatment application to CU samples (between -0.32 and 0.71). All of the treatments that caused an increase in yellowness of $\Delta b^* > 0.75$ in Cc3 textiles included one or more of the following treatments: MPx/2CBx, ME, PA, EA, and EBR. MP30/2CB30 caused the greatest increase in yellowness of Cc3 samples of all the treatments with ME60 the second greatest. T144-6, followed by T144-2, caused the greatest decrease in yellowness of Cc3 upon application. I1135 treatments caused the least change in yellowness of Cc3 upon application. In the CU samples, the highest concentrations of AT, T292, and T144 caused the greatest yellowing ($\Delta b^* > 0.29$) followed by treatments containing ME ($\Delta b^* > 0.16$). MPx/2CBx, PA, and EA generally caused the greatest decrease in yellowness on application to CU ($\Delta b^* < -0.16$).

Figure 9.3 The effect of treatment application on the colour of Sp3 (for $\Delta E_{00}^* > 1$)Figure 9.4 The effect of treatment application on the colour of SU (for $\Delta E_{00}^* > 0.5$)

As shown in Figure 9.3 and Table 9.4, ME60 caused the greatest overall change in colour to Sp3 of all the treatments on application ($\Delta E_{00}^* = 5.42$). ME was present in all treatments

9.2 The effect of treatment application on the model textiles – Results and discussion that caused a $\Delta E_{00}^* > 3.54$ in Sp3. Other treatments that resulted in overall colour change observable to the human eye (>1.7) but without the use of ME, included: EA, and the highest concentrations of T144, T292, and AT. The lowest colour change was seen with lower concentrations of AT such as AT3 (0.19), EBR, and PA. However, treatments involving ME caused colour changes of less than 1.4 in SU while the highest concentrations of T144, MPx/2CBx, and T292 caused colour changes observable to the human eye when applied to SU. AT200 caused $\Delta E_{00}^* > 1.56$.

All treatments that caused a change in lightness of Sp3 of $\Delta L^* > 4.69$ on application included ME. EA, AT, and EBR treatments generally caused the least change in lightness of the Sp3 textiles ($\Delta L^* = -0.3$ to 0.4). The highest concentrations of T144, T292, AT, and MPx/2CBx caused the greatest darkening of Sp3 textiles on application (< -1). For SU samples, the highest concentrations of T144, T292, and AT as well as various concentrations of EBR resulted in $\Delta L^* < -1$, while MP30/2CB30 caused the greatest lightening of SU (3.07). MP15/2CB15 followed by treatments including ME, were the next treatments to cause the most lightening of SU samples on application.

The range of change in redness (Δa^*) was lower for SU (-0.20 to -0.01) than for Sp3 (-0.73 to -0.05). The greatest Δa^* to Sp3 samples on treatment application occurred with the highest concentration of T144 (-0.73) followed by treatments involving ME, or in some cases, EA. AT200 and T292-260 also caused significant change in Δa^* (-0.34 , and -0.29 , respectively). The greatest change in Δa^* in SU occurred with the MP30/2CB30 treatment, closely followed by ME60. In addition to these, treatments which caused a $\Delta a^* < -0.10$ included various concentrations of PA, AT, I1135, and EBR100 (-0.11).

Treatments with ME caused the greatest increase in yellowness ($+\Delta b^*$) of all the treatments ($\Delta b^* > 2$). EBR, PA, EA, T292-260, and MPx/2CBx also caused a $\Delta b^* > 1$ on application to Sp3. Generally the lower concentrations of T144, T292, and I1135 caused the greatest decrease in yellowness of the Sp3 samples on application ($\Delta b^* = -5.4$ to -3.0). Of the treatments applied to SU AT200 caused the greatest increase in yellowness (0.89) followed by treatments including I1135, ME, and T292-260 (0.40). MPx/2CBx caused a decrease in yellowness of SU on application as well as various treatments involving PA and some involving EA. However the trends are not as clear as with the Sp3 treated textiles.

9.2.3 SEM-EDX

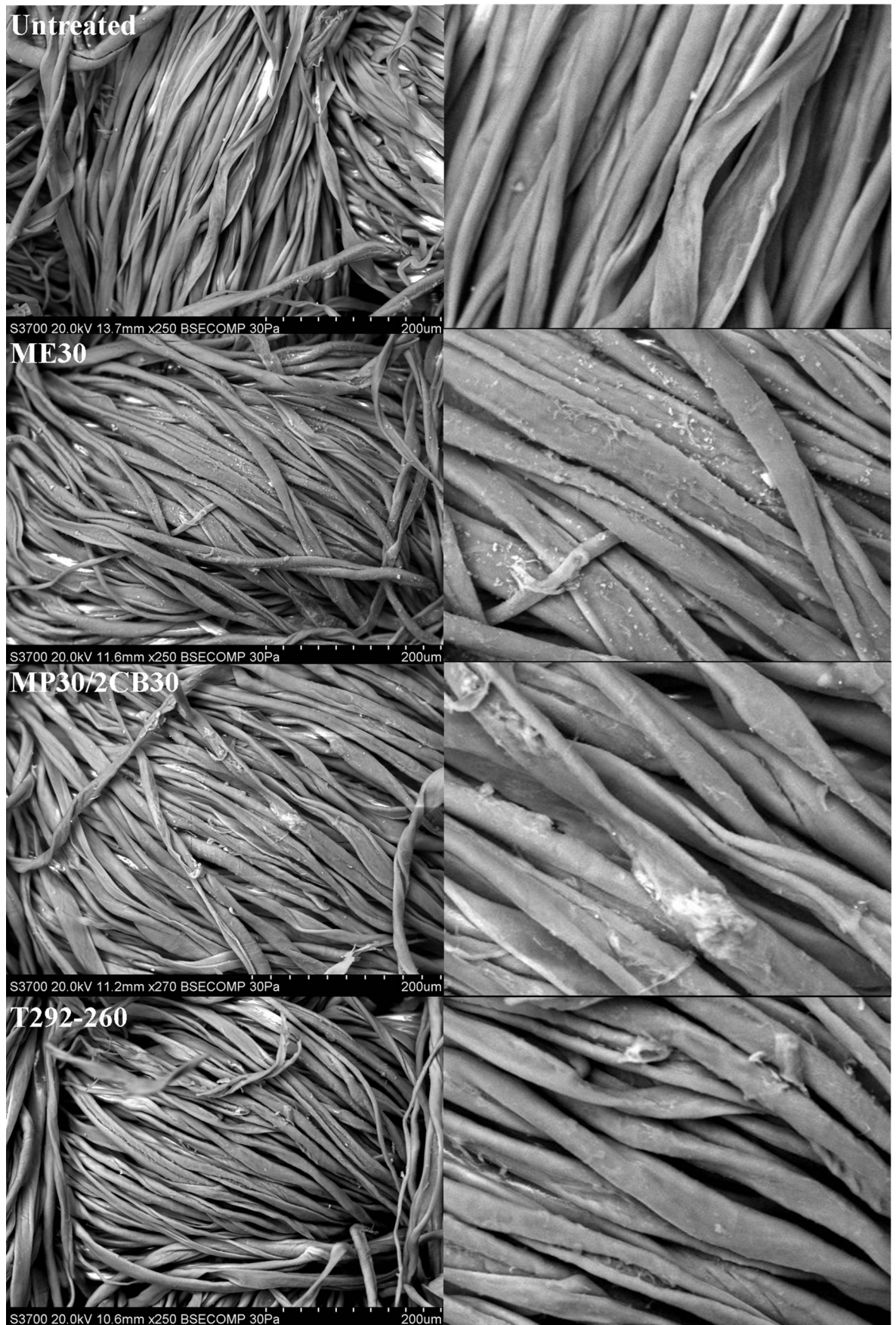


Figure 9.5 SEM micrographs at $\times 250$ magnification (left) and enlarged sections (right) of untreated and treated Cc3 before accelerated ageing

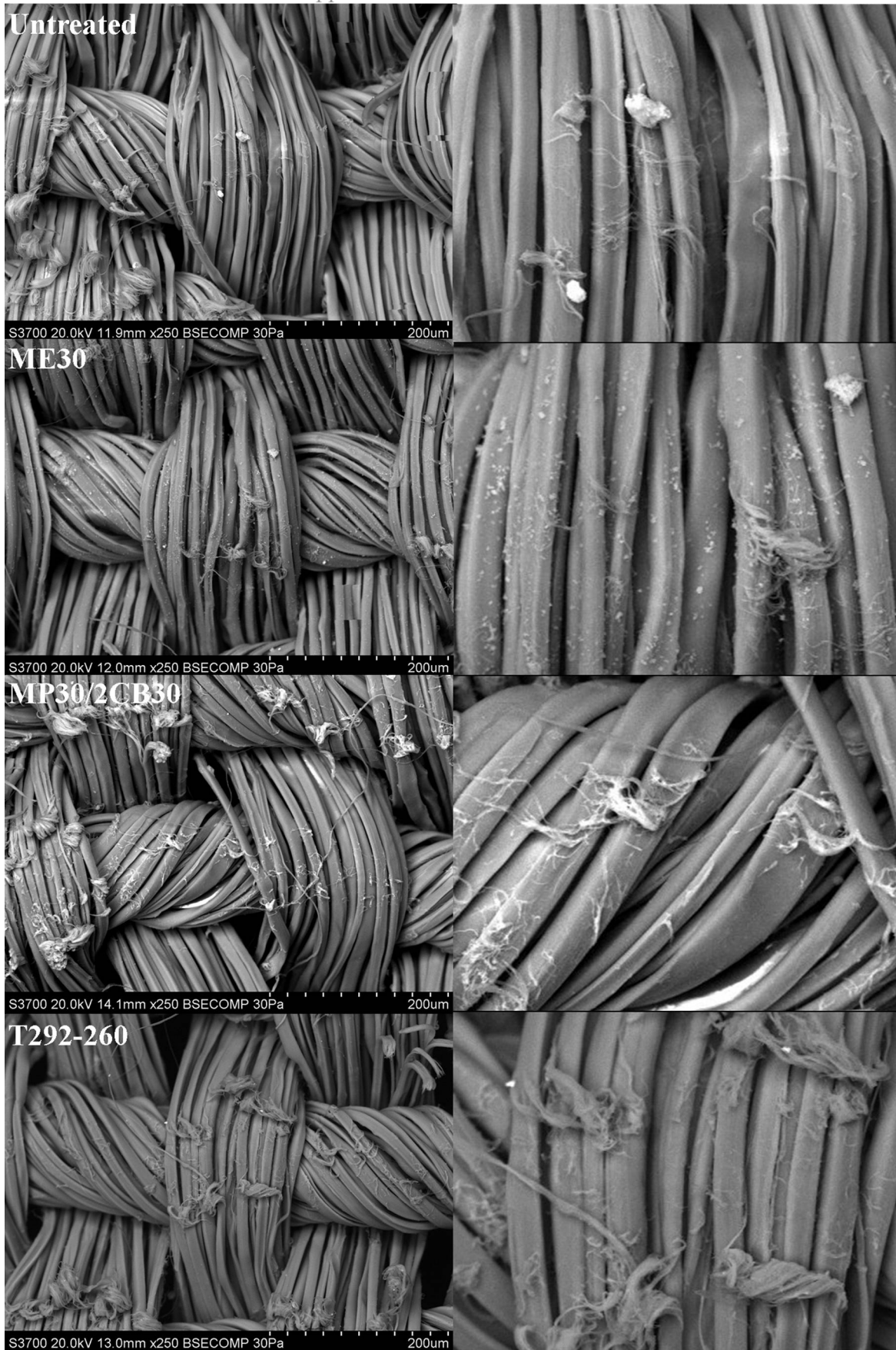


Figure 9.6 SEM micrographs at $\times 250$ magnification (left) and enlarged sections (right) of untreated and treated Sp3 before accelerated ageing

9.2 The effect of treatment application on the model textiles – Results and discussion
The surfaces of Cc3 and Sp3 samples that had been treated with MP30/2CB30, T292-6/ME30, ME30, and T292-260 as well as untreated samples were inspected using SEM-EDX to establish if the treatment application caused any consistently significant changes in surface topography.

The only consistently significant changes were obtained using ME30 (Figures 9.5 to 9.7) and T292-6/ME30 (Figure 9.8) treatment solutions. In all of these samples an increase in small magnesium rich deposits was observed on the fibre surfaces. This was particularly apparent on the ME30 treated samples. These deposits can be attributed to the magnesium ethoxide used in the treatment. Indeed, the deacidification afforded to the textile sample by ME30 is due to the deposition of magnesium carbonate; however, unlike in the calcium bicarbonate treated sample in which calcium carbonate will be deposited, a consistently greater extent of deposition occurred with the ME30. This may have arisen due to the low solubility of the magnesium ethoxide and that the treatment solution was not filtered prior to use (the undissolved ME had settled at the bottom of the beaker to give a relatively clear solution above which was used as the treatment solution). Filtering of the solution prior to application to the textiles may result in fewer surface deposits than are present in these samples. The other treatments may cause some surface deposits but if they did they were not present throughout and to a noticeable level.

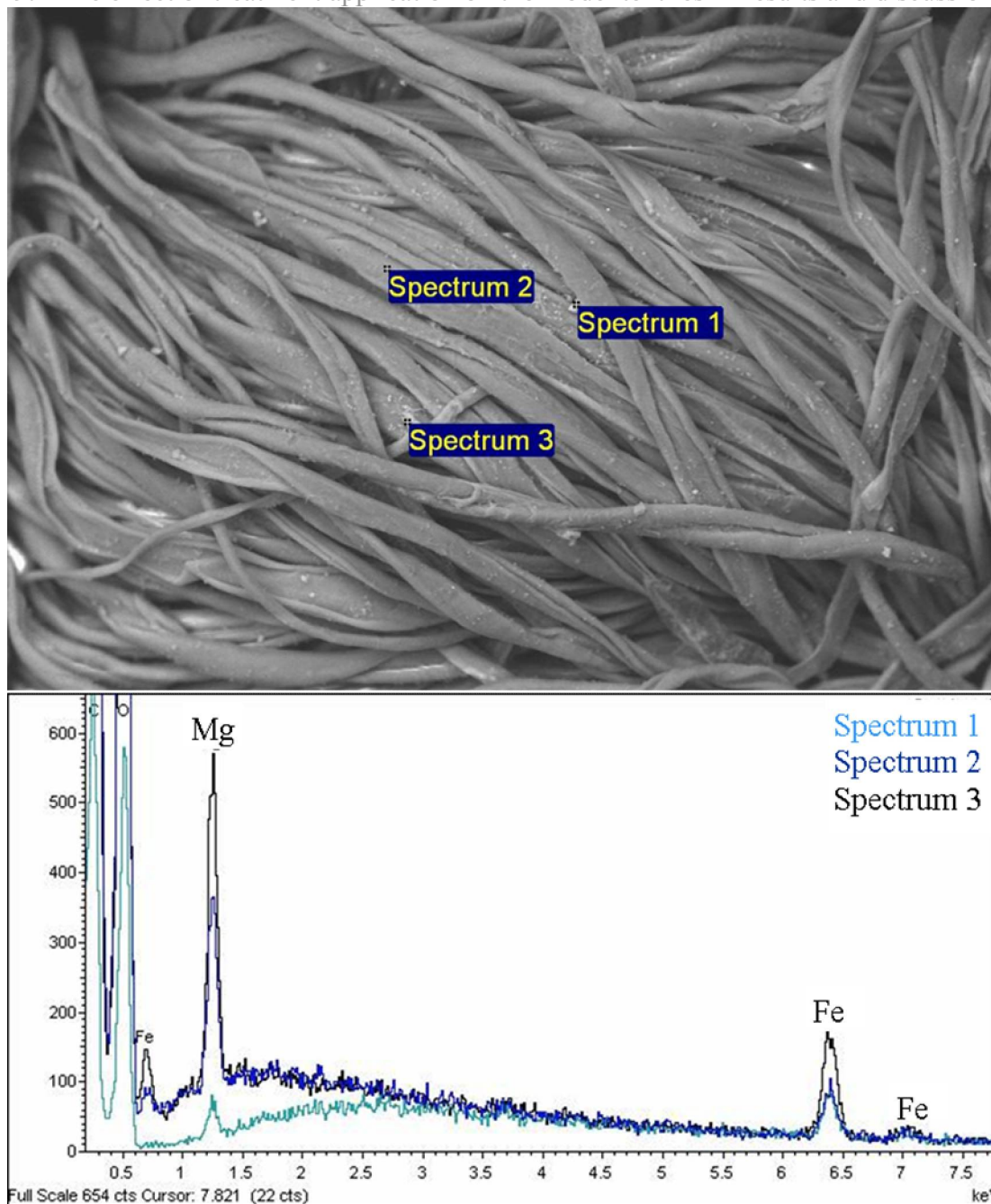


Figure 9.7 SEM micrograph and EDX spectrum of the Cc3 sample following immersion in the ME30 treatment solution for 30 minutes

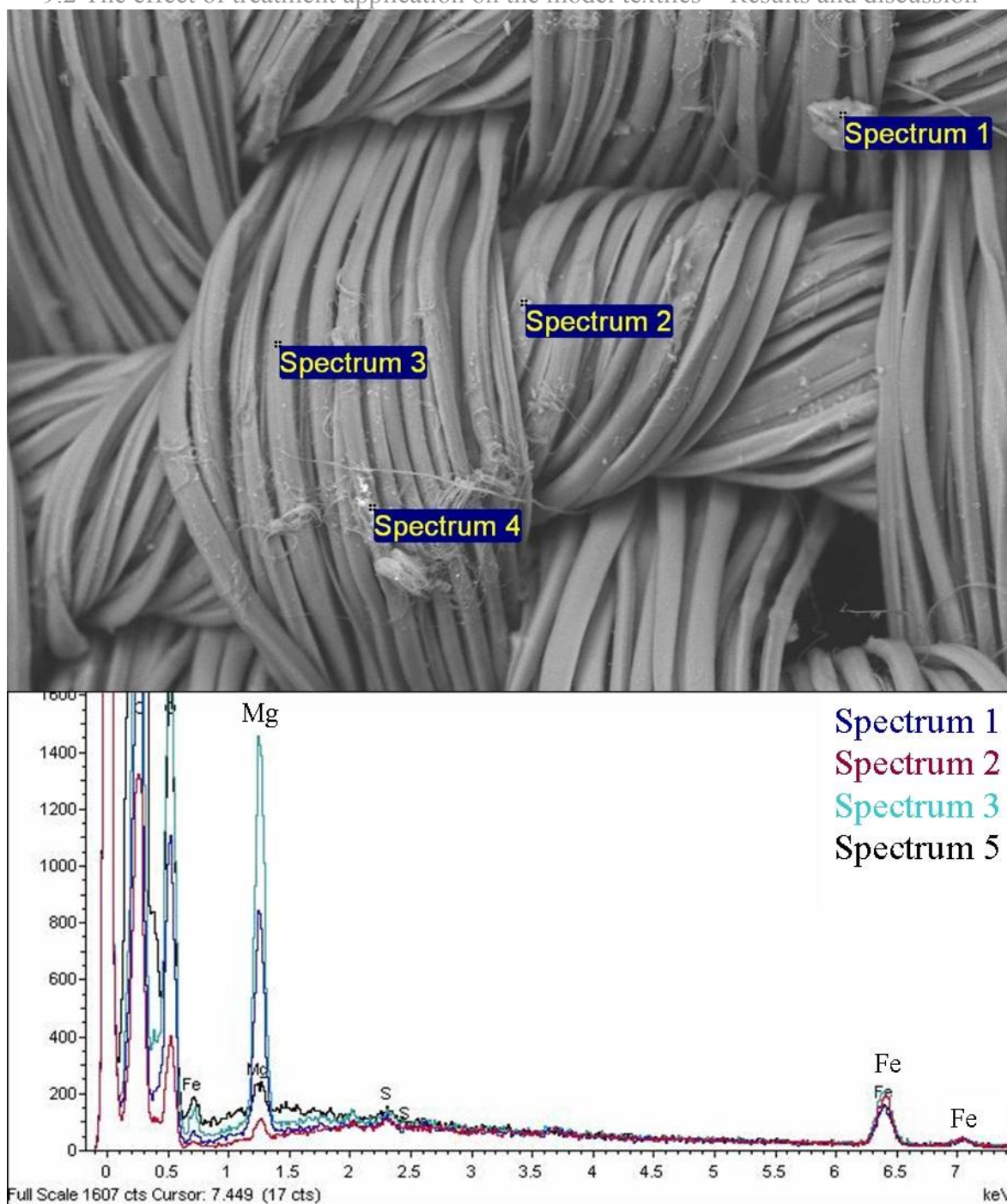


Figure 9.8 SEM micrograph and EDX spectrum of surface deposits on Sp3 yarns treated with T292-6/ME30

9.2.4 GPC-MALLS

Table 9.5 The effect of the application of a selection of treatments to Cc3 on the GPC-MALLS molecular weight, carbonyl content, polydispersity index, and molecular weight distribution

Treated Cc3 sample	Solvent	DP _n	Average molecular weight		PDI	% polymer content in				Theoretical amount of reducing end groups (oxidised groups) (μmol/g)	Overall carbonyl content (μmol/g)
			M _n (kg/mol)	M _w (kg/mol)		DP<100	DP100-200	DP200-2000	DP>2000		
Untreated Cc3	None	902	146	486	3	1	2	57	40	7 (27)	34
MP30/2CB30	Water	1035	168	467	3	0	1	57	41	6 (11)	17
T292-260	Cyclohexane-D5	658	107	431	4	2	4	55	39	9 (22)	31
ME30	Ethanol	829	134	559	4	1	3	55	41	7 (27)	34

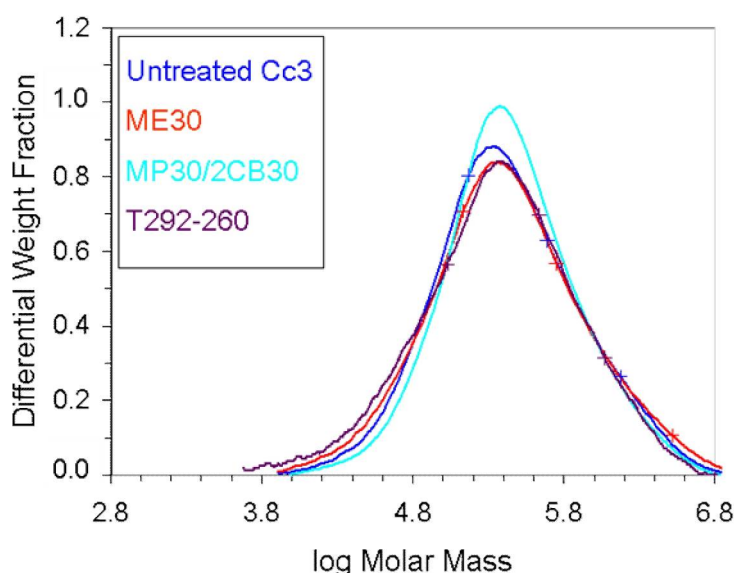


Figure 9.9 The effect of treatment application on the molar mass distribution of the cellulose in Cc3

The application of the treatments had little effect on the molecular weight distribution, PDI, and quantity of REGs of the Cc3 samples when compared to the untreated equivalent (Table 9.5 and Figure 9.9). This suggests that little or no acid hydrolysis occurred on and following treatment application. This correlates well with the raised pH of the treated samples compared to the untreated sample; for example, the MP30/2CB30 treated sample had a micro-pH of 6.20 \pm 0.06 which is significantly greater than the 3.71 \pm 0.02 of the untreated sample. However, the MP30/2CB30 treatment caused an apparent increase in M_n and DP_n, and decrease in the overall quantity of carbonyl groups, mainly those due to oxidation. The removal of low molecular weight molecules such as mono- and

9.2 The effect of treatment application on the model textiles – Results and discussion
oligosaccharides, hydroxyl acids, and sugar acids is thought to occur during aqueous washing of aged paper (Uchida, Inaba and Kijima 2007). The removal of low molecular weight carbonyl-containing molecules from some of a selection of historic textiles due to washing has been demonstrated through the increased Mw and decreased carbonyl content of the samples after washing in water (Henniges, Bjerregaard, Ludwig and Potthast 2011). Similar processes could have occurred in Cc3 during aqueous treatment application. Exactly how these losses occur is still unknown since the low molecular weight molecules are still too large to be soluble. Possibly the molecules are broken off from larger, damaged polymers during the treatment application (Henniges 2012). An alternative explanation lies in the time between treatment application and GPC-MALLS analysis in which oxidation could occur due to the presence of the dye. The apparent decrease in carbonyl groups arising from oxidation in the MP30/2CB30 treated sample could be due to an increase in the stability of Cc3 to oxidation during storage before analysis. This could occur since the phytic acid in the MP30/2CB30 treatment chelates with the iron(II) and iron(III) ions, preventing it from participating in oxidation (Neevel 2002). A lack of similar chelation in the untreated and differently treated samples would result in the comparable levels of carbonyl groups during storage (due to oxidation) that are seen.

The M_n and DP_n of the T292-260 treated sample is significantly lower than that of the other samples and the Mw is significantly lower than that of all but the MP30/2CB30 sample. In addition there is a slightly higher PDI and % of polymers with a $DP < 200$ than in the other samples. This suggests that treatment application has caused an increase in the number of low molecular weight molecules thus increasing the PDI. Potentially this could be due to slightly greater depolymerisation occurring in this sample compared to the others either due to the treatment application or due to natural variation in the model textile. Since the micro-pH of this sample was pH 6.93 \pm 0.11, it is possible that some alkaline ‘peeling’ reactions have occurred. These would increase the quantity of molecules with $DP < 200$ whilst retaining the quantity of molecules with high DP. The rate of alkaline degradation increased 10 times with each increase of 1 pH unit and can be a major degradation pathway for deacidified materials (Whitmore 2011).

The application of ME30 to Cc3 caused negligible change M_n and DP_n , or carbonyl content of the textile though a significant increase in Mw is seen and the PDI is slightly higher than many samples. The increase in PDI is supported by the slight increase in % polymers with $DP < 200$. The low average molecular mass (114.43 u i.e. $114.43 \text{ g mol}^{-1}$) of ME makes it highly unlikely that it will affect the molar mass of Cc3. Consequently, these results

9.2 The effect of treatment application on the model textiles – Results and discussion suggest that chain scission has occurred. The resulting micro-pH of the sample was pH 5.40 +/- 0.03 suggests that alkaline degradation may not have occurred as it may have done for the T292-260 sample.

9.2.5 EPR spectroscopy

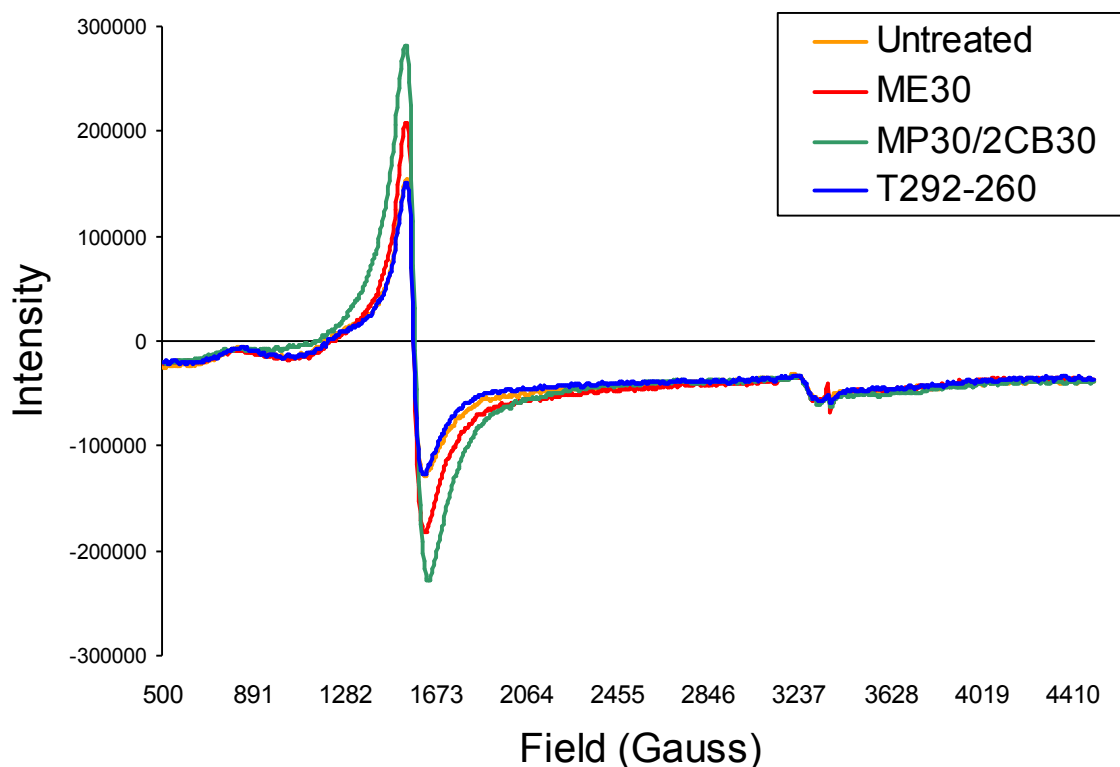


Figure 9.10 The effect of treatment application on the EPR spectrum of Cc3

Table 9.6 The effect of dye application to Cc3 on the iron(III) ion content, ratio of bound and unbound iron(III) ions and radical content.

Treatment	Relative iron(III) ratio ^a	Iron (%)		Radical relative integral (%) ^b
		Bound	Unbound	
None	51	100	0	54
T292-260	66	100	0	74
MP30/2CB30	100	24	76	35
ME30	90	48	52	177

Notes for Table 9.6:

- Normalised for mass and acquired approximately 13 months after treatment application;
- Normalised for mass and acquired approximately 22 months after treatment application using the same samples as analysed for the relative iron(III) ratio.

Since the treated samples were analysed between 13 and 22 months after treatment application, the results of these samples reflect changes due to natural ageing as well as treatment application. Additionally, the data presented, particularly the bound/unbound

9.3 The effect of the treatments on the stability of the model textiles during accelerated ageing – Results and discussion
values have an unknown level of associated error from variations in the model textiles, and consequently any trends here would need further investigation to confirm their reliability.

Comparison of the untreated fabric with the treated samples indicated some interesting effects for example T292-260 produced no change in the proportion of bound iron and only slightly increased the radical and iron(III) content (Table 9.6 and Figure 9.10). ME30 and MP30/2CB30 however caused an approximate doubling of the relative iron(III) ratio suggesting that oxidation of iron(II) ions has occurred. The phytate ligand in the MP30/2CB30 treatment binds preferentially to iron(III) ions rather than iron(II) ions and once bound prevents the cycling of iron oxidation states (Graf and Eaton 1990). This could explain the increase in iron(III) content in the MP30/2CB30 treated sample and the decrease in radicals observed since the binding prevents free radical formation. However an associated increase in the proportion of bound iron(III) ions was not observed. As with the MP30/2CB30 treated sample the proportion of bound iron(III) decreased in the ME treated sample compared to the untreated which may signify the breakdown of iron-tannate dye complexes. The radical content greatly increased with the presence of deacidifier ME30.

In summary, the application of MP30/2CB30 and ME30 to Cc3 significantly decreased the proportion of bound iron(III) suggesting the breakdown of iron-tannate dyed complexes or oxidation of iron(II) ions. A large increase in radical content occurred in the ME30 treated sample after 22 months of natural ageing. T292-260 caused the least change the iron(III) and radical content of Cc3.

9.3 The effect of the treatments on the stability of the model textiles during accelerated ageing – Results and discussion

9.3.1 *Micro-pH testing*

Issues with the reliability and the incomplete nature of the pH results for the unaged treated Sp3 samples limit the evaluation possible. Comparison of the aged treated Sp3 data is possible with the unaged untreated or aged untreated samples only. However, for the cotton samples it is also possible to compare the aged treated samples with the unaged treated samples, thereby evaluating the direct effect of the treatment during accelerated ageing.

9.3 The effect of the treatments on the stability of the model textiles during accelerated ageing – Results and discussion

Table 9.7 The change in pH upon accelerated ageing of unaged and aged Cc3 fabrics

Treatment code	Unaged samples		Aged samples		ΔpH^a	Total error (standard deviation) ^b
	Average pH	SD	Average pH	SD		
U	3.71	0.02	3.34	0.06	-0.37	0.04
U ^c	3.69	0.04	3.56	0.16	-0.14	0.12
ME6	4.11	0.10	3.39	0.08	-0.72	-0.02
ME30	5.40	0.03	4.37	0.16	-1.03	0.14
ME60	7.39	0.21	5.82	0.21	-1.57	0.00
ME60/IMS	5.91	0.07	4.39	0.14	-1.52	0.08
EA0.4	4.11	0.05	3.61	0.07	-0.50	0.02
EA0.4/ME30	5.07	0.16	4.45	0.15	-0.62	0.00
EA2 ^c	3.90	0.04	3.61	0.04	-0.29	0.01
EA4 ^c	3.86	0.02	3.90	0.03	0.05	0.01
EA4/ME30 ^c	5.15	0.23	4.05	0.03	-1.10	-0.20
EBR6	3.97	0.08	3.79	0.02	-0.18	-0.06
EBR30	4.00	0.01	3.97	0.01	-0.02	0.00
EBR60	3.85	0.03	4.13	0.01	0.28	-0.02
EBR60/IMS	3.79	0.06	4.48	0.20	0.69	0.14
T144-2	4.03	0.04	3.65	0.03	-0.38	0.00
T144-3	3.93	0.03	3.67	0.03	-0.27	0.01
T144-6	3.98	0.02	3.60	0.03	-0.38	0.01
T144-6/ME30	4.89	0.07	4.08	0.05	-0.81	-0.02
T144-450	5.34	0.06	4.37	0.07	-0.97	0.02
T292-2	3.96	0.01	3.39	0.10	-0.57	0.10
T292-3	3.94	0.03	3.45	0.06	-0.49	0.03
T292-6	3.87	0.04	3.37	0.07	-0.50	0.03
T292-6/ME30	4.39	0.01	3.36	0.03	-1.04	0.02
T292-260	6.93	0.11	5.04	0.05	-1.89	-0.06
AT2	3.89	0.06	3.53	0.04	-0.36	-0.02
AT3	3.99	0.01	3.48	0.02	-0.51	0.01
AT6	4.04	0.04	3.53	0.02	-0.50	-0.02
AT6/ME30	4.98	0.13	3.90	0.03	-1.07	-0.10
AT200	3.90	0.02	3.58	0.05	-0.32	0.03
PA10/IMS/ME30	4.89	0.14	4.34	0.16	-0.55	0.02
PA10ME60/IMS	4.52	0.03	4.29	0.18	-0.23	0.16
PA10MC15/IMS	4.25	0.10	4.07	0.23	-0.18	0.13
PA5/IMS	3.87	0.06	3.58	0.18	-0.30	0.13
PA5/IMS	3.69	0.04	3.80	0.08	0.11	0.05
PA10/IMS	3.79	0.04	3.71	0.24	-0.08	0.20
PA15/IMS	3.86	0.02	4.00	0.14	0.14	0.12
PA30/IMS	3.69	0.06	3.89	0.10	0.21	0.04
PA30/IMS/ME30	4.18	0.03	4.43	0.09	0.25	0.06
MP5/2CB5	4.87	0.07	4.14	0.04	-0.73	-0.03
MP15/2CB15	5.62	0.07	4.99	0.08	-0.63	0.01
MP30/2CB30	6.20	0.06	5.75	0.14	-0.45	0.08
I1135-2	3.74	0.07	3.55	0.15	-0.19	0.07
I1135-3	3.85	0.02	3.42	0.12	-0.43	0.10
I1135-6	3.74	0.05	3.57	0.07	-0.17	0.02
I1135-43	3.81	0.05	3.67	0.15	-0.14	0.10
I1135-43/ME30	4.97	0.05	4.22	0.17	-0.74	0.13

Notes for Table 9.7:

- Aged pH value - unaged pH value = difference in pH due to ageing. Negative values mean the sample became more acidic on ageing;
- Aged SD value + unaged SD value = total error based on SD values;
- Undyed for comparison with EA4, EA2, EA4/ME30 only and vice versa.

9.3 The effect of the treatments on the stability of the model textiles during accelerated ageing – Results and discussion

Almost all of the samples that are treated with deacidifier have resulted in a decrease in the pH of Cc3 of between 0.62 and 1.89 pH units after accelerated ageing (Table 9.7). Also in this range are the T292-260 and T144-450. These samples, along with all of the deacidified samples also resulted in the most change in pH upon treatment application (before accelerated ageing). The greater change in pH in these treated samples could be an effect of the higher initial pH since each decrease in pH by one pH unit is indicative of a ten-fold increase in hydrogen ion concentration. Therefore, changes in hydrogen ion concentration will cause a larger change in pH when the sample is initially at higher pH than when it is at lower pH. MP30/2CB30 treated sample has the highest pH of all the samples after ageing (pH 5.75 +/- 0.14) followed by the T292-260 treated sample (pH 5.04 +/- 0.05) and generally, treatments involving ME30 and an antioxidant caused the aged samples to have a greater pH than the samples treated with antioxidant alone. Excepting the T292-260 treatment, all other T292 treatments resulted in samples after ageing with the lowest pH, which was comparable to the untreated sample after ageing. Unusually EBR appears to have caused an increase in pH of Cc3 (i.e. become less acidic) with age, and this trend increases with increasing EBR concentration.

The pH of the untreated Sp3 sample decreased by 3.6 pH units during the four weeks of accelerated ageing (Table 9.9). The Sp3 samples that had been treated with EBR, EA, I1135, PA, AT, and the lower concentrations of T144, and T292 had a similar pH after ageing to the untreated equivalent. Samples treated with a combination of ME30 and an antioxidant retained a higher pH than the samples treated with the antioxidant alone. All samples treated with ME alone had a pH after ageing that was larger than the pH of the untreated aged sample. The highest pH was seen with the ME60 treated sample (pH 5.7). ME30, ME60/IMS, MP30/2CB30, MP15/2CB15, PA10/ME30, and T144-450 treated aged Sp3 samples also have a pH > 4.5. The pH of T292-6/ME30 and T292-260 are close to this (pH 4.4 and 4.2, respectively).

9.3.2 Subjective handling tests

The condition of many of the treated Cc3 samples after two weeks of accelerated ageing was degraded sufficiently for handling tests to be able to easily and reliably assess which treatments were the most successful. The handling tests were unsuitable for use on the Sp3 treated samples even after four weeks of ageing due to their relatively good condition. Four week aged cotton samples were generally too weak to give useful results even by the handling testing or tensile testing and so have not been analysed.

9.3 The effect of the treatments on the stability of the model textiles during accelerated ageing – Results and discussion

Table 9.8 The effect of the treatments on the handle, colour, and DP of the treated Cc3 textiles after accelerated ageing (2 weeks at 80°C and 65% RH)

Treatment code	Handling test				Viscometry	
	Strength ^a	Surface rub	Colour ^a	Overall ^a	Average DP	SD
U (unaged)	ND ^c	ND ^c	ND ^c	ND ^c	1140.2	12.5
U	0	0	0	0	221.0	11.1
U ^b	0	0	0	0	239.0	0.4
ME6	+	0	+	+	255.6	0.1
ME30	++	++	++	++	473.8	58.8
ME60	++	+++	+++	+++	675.6	11.4
ME60/IMS	++	+++	+++	+++	476.2	10.2
EA0.4	+	+	0	+	292.1	3.4
EA0.4/ME30	++	++	+	++	308.9	- ^c
EA2 ^b	+	+	0	0	247.7	2.4
EA4 ^b	++	++	+	++	322.7	0.2
EA4/ME30 ^b	++	++	+	++	327.9	4.1
EBR6	-	-	+	0	230.0	5.3
EBR30	+	0	++	+	220.4	27.6
EBR60	+	0	++	+	234.8	1.3
EBR60/IMS	0	0	++	0	233.4	6.0
T144-2	+	+	+	+	224.4	22.4
T144-3	++	+	+	+	237.3	19.2
T144-6	++	+	+	+	239.3	6.5
T144-6/ME30	+++	+++	++	+++	334.4	5.8
T144-450	++	++	+	++	318.8	2.3
T292-2	+	0	+	+	261.0	13.1
T292-3	+	0	+	+	233.2	4.8
T292-6	+	0	0	0	234.1	3.1
T292-6/ME30	++	++	++	++	275.7	29.7
T292-260	+++	+++	+++	+++	913.7	21.1
AT2	0/+	+	0	+	235.6	0.6
AT3	+	+	0	+	236.3	0.1
AT6	+	+	0	+	224.4	3.1
AT6/ME30	++	++	++	++	324.5	16.1
AT200	++	++	+	++	225.1	13.8
PA10/IMS/ME30	+++	+++	++	+++	357.0	13.4
PA10ME60/IMS	++	++	+	++	296.7	4.0
PA10MC15/IMS	++	++	+	++	295.7	1.2
PA5/IMS	0	+	0	0	231.9	2.9
PA15/IMS	+	++	0	+	261.5	2.9
PA30/IMS	++	++	-	++	300.9	4.0
PA30/IMS/ME30	+++	++	0	+++	386.0	5.3
MP5/2CB5	+++	+++	+	+++	410.7	11.7
MP15/2CB15	+++	+++	++	+++	669.0	8.7
MP30/2CB30	+++	+++	++	+++	788.8	0.6
I1135-2	+	++	0	+	240.5	4.2
I1135-3	+	++	0	+	214.3	8.9
I1135-6	+	++	0	+	213.0	5.7
I1135-43	0	+	0	0	219.5	- ^c
I1135-43/ME30	+	++	0	+	267.5	0.4

Notes for Table 9.8:

a. Classification of treated (T) and untreated (U) samples followed a five point scale:

- T exhibits poorer property retention than U.
- 0 No difference between T and U.
- +
- ++ T exhibits slightly better property retention than U.
- +++ T exhibits better property retention than U.
- ++++ T exhibits markedly better property retention than U;

b. Undyed for comparison with EA4, EA2, EA4/ME30 only and vice versa;

c. Not done;

d. No SD because only one analysis of this sample was undertaken.

9.3 The effect of the treatments on the stability of the model textiles during accelerated ageing – Results and discussion

The treatments which offered the greatest retention of strength properties of Cc3 after accelerated ageing were the MPx/2CBx, PA10/IMS/ME30, PA30/IMS/ME30, T292-260, and T144-6/ME30 treatments (Table 9.8). EBR and I1135 showed the least success at retaining the strength of Cc3 after ageing. Higher concentrations of T292, T144, and AT show promise but were not the best. The trends in surface rub resistance properties were similar to the strength retention properties except that ME60 and I1135 (various concentrations) were better at surface rub resistance retention than at strength retention while EBR and the lower concentrations of the T292 treatments were worse.

I1135 changed colour similar to the untreated sample while T292, EBR, ME, and MPx/2CBx treated samples resulted in Cc3 samples of noticeably different colour to the untreated. Colorimetry has been used to objectively ascertain the exact change in colour of the samples (Section 9.3.6).

9.3.3 Viscometry (*Cc3 only*)

Viscometry allows the calculation of an average degree of polymerisation (DP) of a polymeric sample. Acid hydrolysis and oxidation lead to the breakdown of polymer chains and therefore a lowering of DP with increasing degradation. There is a point when the polymers are so degraded that the object has low mechanical strength and is easily damaged through handling. For paper, this has been reported as being between 250 and 300 (Shroff and Stannett 1985), or 400 (Strlic, Csefalvayova, Kolar, Menart, Kosek, Barry, Higgitt and Cassar 2010). An effective stabilisation treatment will inhibit the rate of chain scission and extend the time it takes for all mechanical strength to be lost. Based on the average DP of the treated Cc3 textiles after accelerated ageing it is clear that T292-260 was the most successful non-aqueous treatment (Table 9.8). MPx/2CBx and ME were also successful causing average DP > 400. In the region DP 300 – 400, ME30 features predominantly in combination with antioxidants. EA4, T144-450, and PA30 were also present in this region. Based on the viscometry results, I1135, AT, and EBR had little stabilising effect on the Cc3 textiles during accelerated ageing.

9.3 The effect of the treatments on the stability of the model textiles during accelerated ageing – Results and discussion

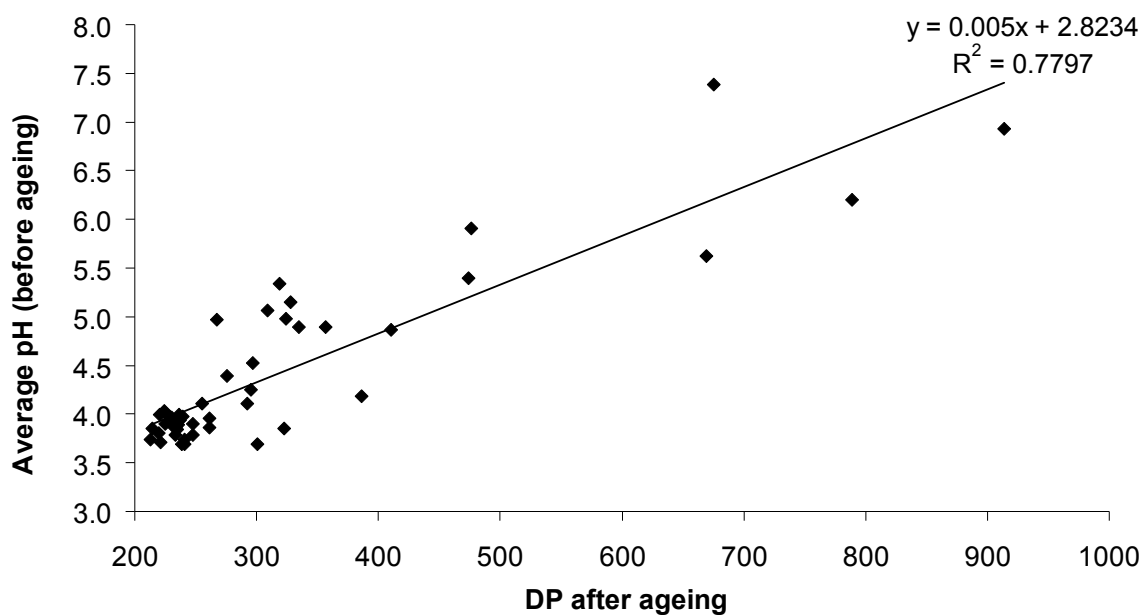


Figure 9.11 Correlation between the pH of treated Cc3 textiles before accelerated ageing (2 weeks at 80°C and 65% RH) and the resulting DP after ageing

Figure 9.11 clearly shows a good ($R^2 = 0.78$) positive correlation between the average pH of the treated sample before ageing and the DP after ageing i.e. the greater the acidity of the sample before ageing the greater the extent of depolymerisation during ageing and consequently the lower the resulting DP. It is assumed that application of treatments did not affect the DP of the textile before accelerated ageing and that all of the samples started at the same DP before treatment. Therefore, any differences in the change in DP on ageing have occurred due to the presence of the treatment. The highest concentrations of MPx/2CBx, ME, and T292 resulted in pH values for Cc3 of between 6 and 7 and stabilised the textiles to give the greatest average DP values of all the treatments. This correlates well with the handling test results (Table 9.8).

9.3.4 Tensile testing

Tensile testing was used to objectively assess the change in tensile properties of the treated Sp3 samples after accelerated ageing because the handling tests devised for the aged treated Cc3 samples were unsuitable for the Sp3 samples.

Generally the inclusion of ME with an antioxidant caused greater strength retention of Sp3 after ageing than without the ME (Table 9.9 and Figure 9.12). Additionally, from Figure 9.12 it is clear that MP30/2CB30, MP15/2CB15, ME60, and T292-260 are the most successful treatments, causing retention of at least 50% of the Sp3 breaking load after

9.3 The effect of the treatments on the stability of the model textiles during accelerated ageing – Results and discussion

ageing. EBR and some of the lowest concentrations of AT treatments were the least successful at retaining the strength of Sp3 textiles upon ageing. Due to the errors in the breaking load data it is unclear as to whether the success of the treatment increases with concentration.

Trends in the extension properties of the treated Sp3 samples after ageing are unclear due to the variable and often large standard deviation in the data (Figure 9.12).

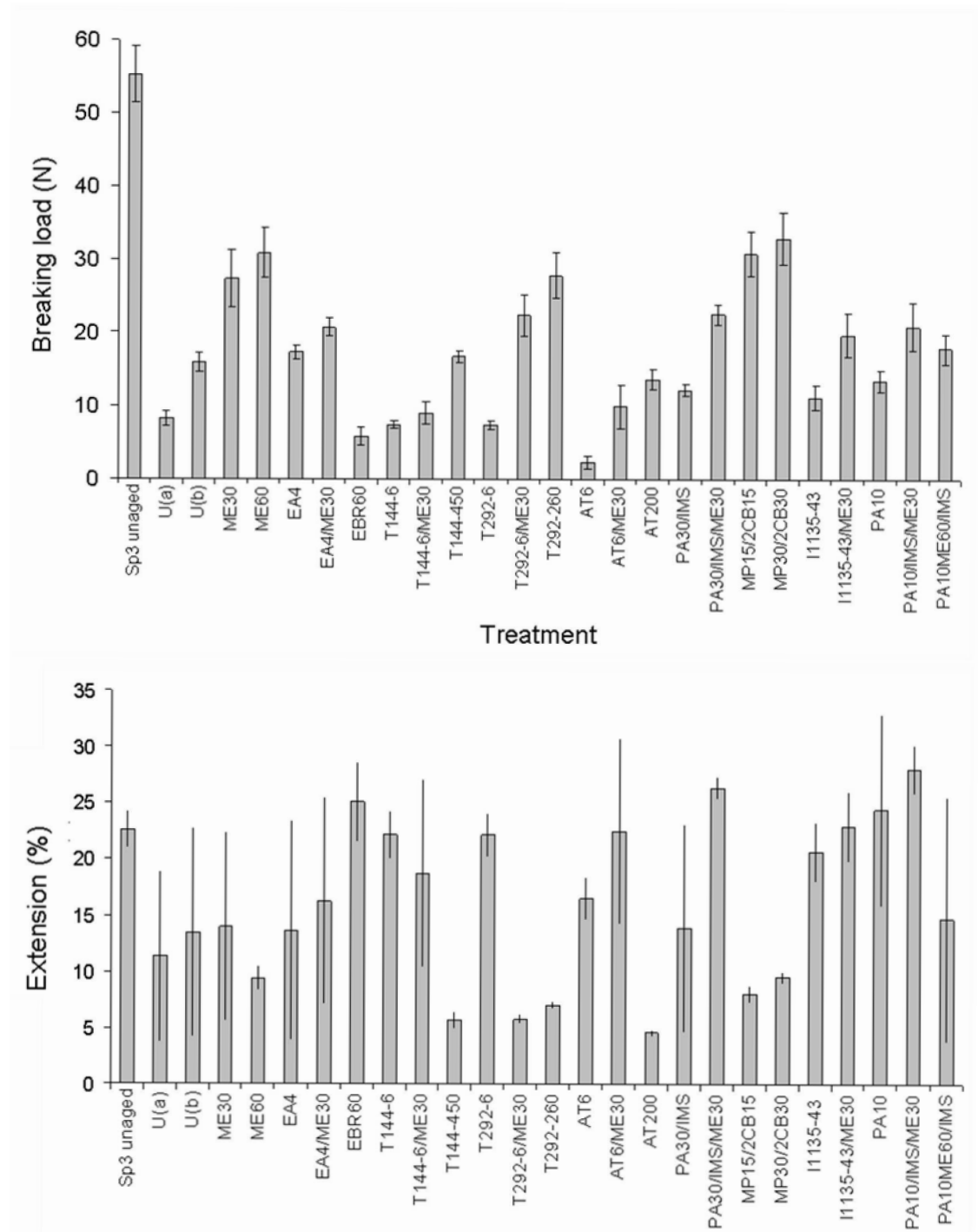


Figure 9.12 The breaking load (N) and extension (%) of treated and untreated Sp3 model textiles after accelerated ageing

9.3 The effect of the treatments on the stability of the model textiles during accelerated ageing – Results and discussion

Table 9.9 Breaking load and extension of treated and untreated of Sp3 after accelerated ageing (4 weeks at 80°C and 65% RH)

Treatment code	Micro-pH		Breaking load (N)			Extension (%)		
	Mean	SD ^a	Mean	SD ^a	CV ^b	Mean	SD ^a	CV ^b
<i>Sp3 unaged</i>	7.2	0.2	55.3	3.8	6.9	22.6	1.6	7.3
U	3.6	0.1	8.3	1.0	12.6	11.4	7.6	66.7
U ^c	4.1	0.0	15.9	1.3	7.9	13.5	9.3	69.0
ME6	4.1	0.0	14.9	1.4	9.2	13.8	10.6	76.7
ME30	5.2	0.0	27.3	4.0	14.5	14.0	8.4	59.9
ME60	5.7	0.0	30.8	3.4	11.2	9.4	1.1	11.2
ME60/IMS	4.9	0.2	12.2	2.0	16.1	25.9	7.9	30.6
EA0.4	3.6	0.0	17.9	0.5	2.8	4.9	0.9	18.2
EA0.4/ME30	4.5	0.0	15.0	2.3	15.4	17.0	11.8	69.3
EA2 ^c	4.2	0.0	17.5	0.1	0.5	22.2	1.9	8.5
EA4 ^c	4.2	0.1	17.3	0.9	5.0	13.6	9.7	71.4
EA4/ME30 ^c	4.3	0.1	20.7	1.2	5.8	16.3	9.1	56.2
EBR6	3.7	0.0	6.8	1.2	17.9	25.4	3.9	15.2
EBR30	3.5	0.0	7.5	1.3	17.2	15.4	11.0	71.2
EBR60	3.4	0.0	5.9	1.2	20.6	25.1	3.5	13.9
EBR60/IMS	3.5	0.0	2.2	1.1	49.8	16.3	3.3	20.0
T144-2	3.8	0.0	7.2	1.1	14.8	14.4	7.9	55.2
T144-3	3.8	0.0	6.5	0.8	12.1	14.1	7.3	52.1
T144-6	3.7	0.0	7.4	0.5	6.8	22.1	2.1	9.3
T144-6/ME30	4.1	0.1	9.1	1.5	16.2	18.7	8.4	44.6
T144-450	4.6	0.1	16.7	0.7	4.2	5.7	0.7	12.9
T292-2	4.0	0.2	12.0	0.5	4.2	11.9	7.4	62.7
T292-3	3.9	0.1	10.0	2.3	23.3	23.4	1.1	4.8
T292-6	3.8	0.0	7.4	0.6	8.7	22.1	1.9	8.7
T292-6/ME30	4.4	0.1	22.3	2.8	12.6	5.8	0.4	6.8
T292-260	4.2	0.0	27.8	3.1	11.0	7.0	0.3	4.0
AT2	3.7	0.0	6.1	1.5	24.7	21.9	3.8	17.5
AT3	3.7	0.0	6.3	1.0	15.7	15.1	9.7	64.6
AT6	3.2	0.0	2.3	0.8	35.8	16.5	1.8	11.1
AT6/ME30	4.4	0.1	10.0	3.0	30.6	22.5	8.2	36.5
AT200	3.9	0.0	13.7	1.4	10.3	4.6	0.3	6.0
PA10	3.7	0.0	13.5	1.5	10.8	24.5	8.5	34.7
PA10/IMS/ME30	4.7	0.0	20.8	3.3	15.6	28.1	2.1	7.4
PA10ME60/IMS	4.2	0.0	17.8	2.0	11.3	14.7	10.8	73.7
PA10MC15/IMS	3.7	0.0	13.0	0.6	4.9	6.0	1.0	17.0
PA5/IMS	3.6	0.0	9.0	1.3	14.2	6.8	1.8	26.7
PA15/IMS	3.6	0.0	12.4	1.2	10.0	23.5	0.6	2.7
PA30/IMS	3.6	0.0	12.3	0.8	6.5	13.9	9.3	66.7
PA30/IMS/ME30	4.3	0.0	22.5	1.4	6.2	26.4	1.0	3.9
MP5/2CB5	4.3	0.0	25.5	1.7	6.7	6.3	0.5	7.2
MP15/2CB15	4.7	0.0	30.8	3.1	10.0	8.0	0.8	9.8
MP30/2CB30	4.9	0.0	32.9	3.6	10.9	9.6	0.5	5.2
I1135-2	3.7	0.0	7.8	0.3	4.3	20.5	4.2	20.6
I1135-3	3.7	0.0	12.3	1.3	10.8	21.6	1.3	6.2
I1135-6	3.7	0.1	10.7	0.7	6.4	19.8	1.5	7.7
I1135-43	3.7	0.1	11.2	1.7	15.2	20.7	2.6	12.4
I1135-43/ME30	4.2	0.0	19.6	3.0	15.3	23.0	3.1	13.6

Notes for Table 9.9:

- Standard deviation;
- Coefficient of variation;
- For comparison with EA2, EA4 and EA4/ME30.

9.3.5 EPR spectroscopy

Table 9.10 The effect of accelerated ageing on the iron(III) ion and radical content of the model textiles

Treatment	Extent of ageing (weeks)	Relative iron(III) ratio ^a	Aged/unaged	Iron (%)		Radical relative integral (%) ^b
				Bound	Unbound	
None	0	51		100	0	54
	2	162	3.18	46	54	57
T292-260	0	66		100	0	74
	2	185	2.82	40	60	51
MP30/2CB30	0	100		24	76	35
	2	69	0.69	33	67	47
ME30	0	90		48	52	177
	2	133	1.48	46	54	104

Notes for Table 9.10:

- Normalised for mass and acquired approximately 13 months after treatment application for unaged samples and 12 months after accelerated ageing of aged samples;
- Normalised for mass and acquired approximately 22 months after treatment application for unaged samples and 21 months after accelerated ageing of aged samples. The same samples were used for radical content analysis as analysed for the relative iron(III) ratio.

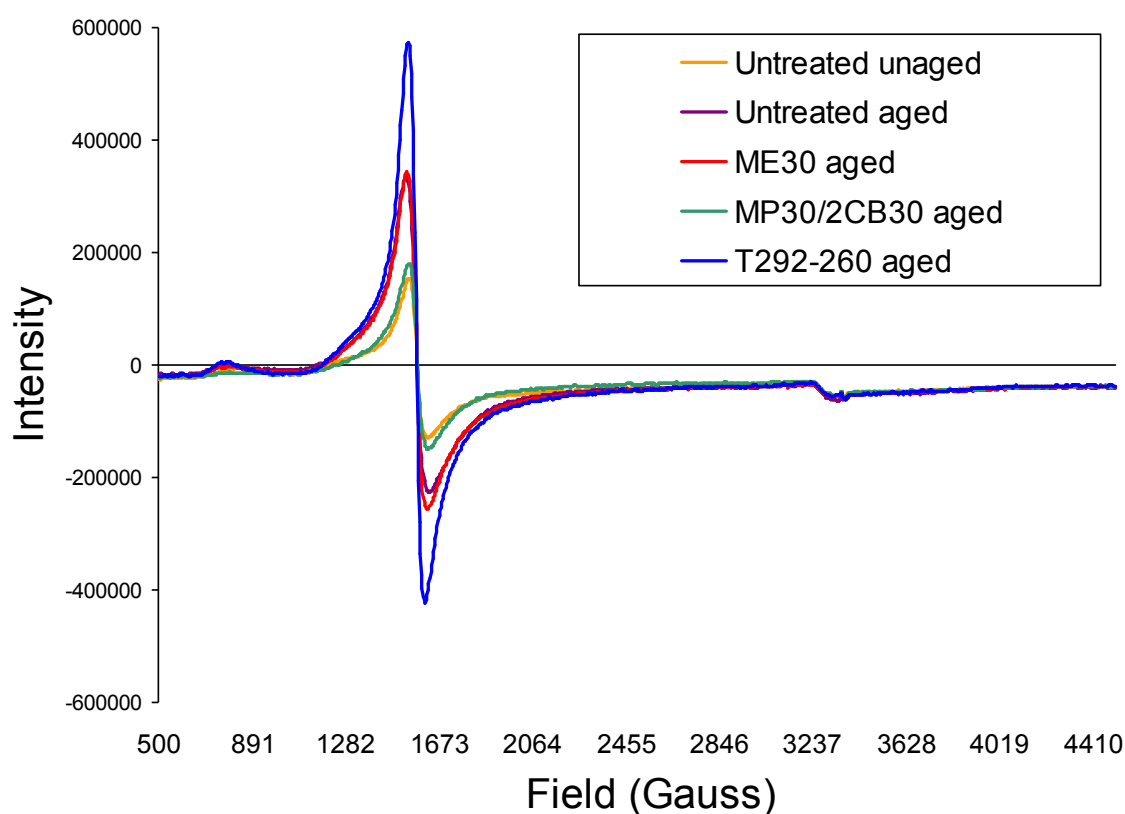


Figure 9.13 The first-derivative EPR spectra of treated aged Cc3 samples

The untreated Cc3 showed a significant increase in the quantity of iron(III) ions and a decrease in the proportion of bound iron(III) with ageing (Table 9.10 and Figure 9.13).

9.3 The effect of the treatments on the stability of the model textiles during accelerated ageing – Results and discussion

This is consistent with the oxidation of iron(II) ions and the breakdown of iron(III) complexes that led to a change in colour as determined by colorimetry. Negligible change in the radical content occurred in the untreated Cc3 on ageing which may suggest that the radicals are propagating without significant overall formation or termination. T292-260 resulted in similar changes in iron(III) content and proportion of bound iron(III) to the untreated sample. There was also a slight decrease in radical content with ageing which may be a result of the antioxidant nature of the T292. The changes in the ME30 and MP30/2CB30 treated samples were generally lower than those in the untreated or T292-260 treated samples. The radical content of the ME30 treated sample decreased significantly with ageing and was still almost double the radical content in the untreated sample. There was little change in the proportion of bound iron(III) ions but an increase in total iron(III) occurred. MP30/2CB30 showed a slight increase in radical content with ageing along with a slight increase in the proportion of bound iron(III) ions.

In summary, the use of T292-260 led to similar changes in the proportion of bound iron(III) ions as seen in the untreated sample. The ME30 treated samples contained significantly more radicals than the untreated samples both before and after ageing. MP30/2CB30 potentially caused a decrease in iron(III) content with ageing and little effect on radical quantity or proportion of bound iron(III).

9.3.6 Colorimetry

By comparing data from the same sample when aged and unaged the errors due to variations in dye application have been essentially eliminated and the effect of the treatment application on colour is removed. Consequently, the data in Tables 9.9, 9.10, and 9.11 reflect the ability of the treatment application to retain the original colour of the treated sample. Colour-retention can occur by the treatments slowing down the rates of reactions such as oxidation and acid hydrolysis that cause coloured degradation products.

9.3 The effect of the treatments on the stability of the model textiles during accelerated ageing – Results and discussion

Table 9.11 Change in colour of Cc3 samples after accelerated ageing (80°C and 65% RH) for 2 and 4 weeks as determined using colorimetry

Treatment	ΔE_{00}^{*a}		ΔL^{*a}		Δa^{*a}		Δb^{*a}	
	2 weeks	4 weeks	2 weeks	4 weeks	2 weeks	4 weeks	2 weeks	4 weeks
U	10.82	12.91	1.37	-1.93	1.15	3.99	12.15	14.36
U ^b	10.81	13.01	0.96	0.89	1.45	3.63	12.13	14.78
ME6	9.07	11.53	-1.93	-5.11	1.13	3.37	9.90	11.93
ME30	6.07	10.39	-3.05	-1.04	-0.17	3.45	6.03	11.93
ME60	5.68	10.40	-4.44	-0.37	-0.18	3.28	4.88	12.48
ME60/IMS	5.44	10.14	-2.81	-0.17	-0.35	2.87	5.31	11.91
EA0.4	8.97	12.65	-1.53	-2.96	1.59	4.70	9.89	14.16
EA0.4/ME30	7.52	10.88	1.79	0.84	-0.10	3.25	8.07	12.39
EA2	9.78	12.98	-2.30	0.98	1.88	4.20	10.56	14.74
EA4	9.48	11.29	-4.65	-2.50	2.00	3.41	9.44	12.27
EA4/ME30	7.51	12.94	2.01	7.97	0.11	2.69	8.21	13.82
EBR6	8.61	11.01	-0.88	-2.58	0.71	2.92	9.44	11.93
EBR30	5.71	10.78	-1.10	1.91	0.05	2.21	6.07	12.09
EBR60	5.05	8.41	-2.03	0.30	0.15	0.79	5.16	9.28
EBR60/IMS	5.41	8.34	-0.93	0.23	0.06	0.60	5.80	9.16
T144-2	10.21	15.03	-0.10	2.50	1.01	5.00	11.43	17.47
T144-3	10.45	13.15	0.52	-1.57	1.28	4.37	11.73	14.73
T144-6	10.87	14.19	1.15	1.02	1.21	4.62	12.22	16.31
T144-6/ME30	6.66	12.61	-1.61	0.98	0.19	4.94	7.14	14.91
T144-450	9.67	16.46	-0.02	4.63	0.85	6.21	10.77	19.41
T292-2	9.89	13.16	0.16	-0.63	1.36	3.83	10.97	14.97
T292-3	9.96	13.70	-1.81	-0.05	1.16	4.28	10.97	15.72
T292-6	10.17	13.35	0.44	-0.87	1.03	4.32	11.38	15.16
T292-6/ME30	7.42	10.72	-0.49	-3.77	0.38	3.76	8.14	11.31
T292-260	7.18	16.44	-2.35	10.83	1.64	3.34	7.24	16.79
AT2	10.47	13.02	0.30	-3.58	1.23	4.40	11.76	14.10
AT3	10.62	14.93	0.79	0.27	1.28	5.64	11.97	17.47
AT6	10.85	15.56	0.11	-0.08	1.30	5.88	12.25	18.34
AT6/ME30	6.81	13.94	-1.73	2.44	0.17	5.86	7.28	16.66
AT200	10.76	13.38	-0.32	-3.18	1.62	5.18	12.13	14.45
PA10/IMS/ME30	6.42	9.82	-3.07	-2.15	0.33	3.10	6.51	10.99
PA10ME60/IMS	8.94	11.87	0.55	0.23	0.98	3.53	9.94	13.57
PA10MC15/IMS	8.55	10.00	-0.94	-3.08	1.25	2.72	9.44	10.68
PA5/IMS a	9.85	14.28	-1.35	-1.28	1.42	5.44	10.89	16.36
PA5/IMS b	9.86	14.55	-1.57	-1.24	1.40	5.69	10.88	16.72
PA10/IMS	9.53	13.47	-0.20	-0.67	1.50	5.09	10.57	15.26
PA15/IMS	10.00	13.13	-0.43	-2.34	1.57	4.66	11.15	14.59
PA30/IMS	9.32	11.70	-1.84	-4.65	1.95	4.13	10.34	12.31
PA30/IMS/ME30	8.50	12.14	-0.06	0.85	1.09	3.70	9.39	13.94
MP5/2CB5	7.95	10.04	2.83	1.70	-0.43	1.49	8.29	11.31
MP15/2CB15	6.91	9.24	4.17	5.34	-1.64	-0.36	6.11	9.41
MP30/2CB30	6.04	7.51	3.37	4.50	-2.55	-1.97	4.43	6.65
I1135-2	10.62	13.37	-0.57	-4.16	1.44	4.54	11.91	14.38
I1135-3	10.73	14.38	-0.86	-3.35	1.43	5.29	12.04	15.94
I1135-6	10.74	15.98	-0.72	0.12	1.24	6.26	12.08	18.90
I1135-43	10.78	14.94	1.36	0.47	1.26	5.60	12.09	17.29
I1135-43/ME30	9.76	15.55	2.86	4.47	0.61	6.07	10.67	18.30

Notes for Table 9.11:

- Change in colour parameter = parameter(aged treated) – parameter(unaged treated) e.g. L^* (aged treated) – L^* (unaged treated);
- Undyed for comparison with EA4, EA2, EA4/ME30 only and vice versa.

9.3 The effect of the treatments on the stability of the model textiles during accelerated ageing – Results and discussion

Table 9.12 Change in colour of CU samples after accelerated ageing (80°C and 65% RH) for 2 and 4 weeks as determined using colorimetry

Treatment	ΔE_{00}^{*a}		ΔL^{*a}		Δa^{*a}		Δb^{*a}	
	2 weeks	4 weeks	2 weeks	4 weeks	2 weeks	4 weeks	2 weeks	4 weeks
U	1.72	2.16	0.01	-0.42	-0.15	-0.07	1.81	2.30
U ^b	1.61	2.25	-0.45	-0.79	-0.05	-0.07	1.68	2.35
ME6	1.45	2.23	-0.82	-1.22	-0.05	-0.07	1.42	2.23
ME30	1.55	2.39	-1.05	-1.31	-0.11	-0.15	1.47	2.41
ME60	1.48	2.20	-0.70	-0.93	-0.14	-0.18	1.49	2.27
ME60/IMS	1.71	3.15	-0.56	-1.23	-0.16	-0.11	1.77	3.35
EA0.4	3.46	7.06	-1.50	-3.93	-0.01	0.85	3.64	7.67
EA0.4/ME30	2.93	6.34	-1.79	-3.20	-0.05	0.26	2.91	7.02
EA2	1.81	8.97	-0.79	-10.75	-0.15	0.56	1.81	5.50
EA4	1.90	7.73	0.30	-8.66	-0.19	0.63	1.98	5.41
EA4/ME30	1.52	9.93	0.09	-11.93	0.00	1.02	1.62	5.99
EBR6	1.26	2.25	0.02	-0.50	-0.08	-0.04	1.32	2.39
EBR30	1.25	2.07	0.50	-0.56	-0.07	-0.04	1.27	2.19
EBR60	1.69	2.72	-0.54	-0.94	-0.10	-0.05	1.75	2.89
EBR60/IMS	1.58	3.04	-0.40	-1.44	-0.07	0.02	1.66	3.18
T144-2	1.48	2.39	-0.48	-0.11	-0.05	-0.06	1.52	2.57
T144-3	1.51	2.11	-0.26	-0.75	-0.06	-0.08	1.58	2.19
T144-6	1.59	2.47	-0.54	-0.41	-0.10	-0.13	1.63	2.64
T144-6/ME30	2.47	3.73	-1.36	-1.50	-0.20	-0.17	2.48	4.03
T144-450	2.00	2.61	2.39	2.20	-0.15	-0.09	1.25	2.33
T292-2	2.10	3.22	-1.27	-1.35	-0.08	0.02	2.05	3.40
T292-3	2.10	3.50	-1.06	-1.03	-0.10	-0.12	2.12	3.80
T292-6	1.84	2.62	-1.17	-0.85	-0.08	-0.05	1.77	2.78
T292-6/ME30	2.48	3.36	-1.90	-1.47	-0.18	-0.08	2.29	3.56
T292-260	1.87	4.30	-0.46	-0.24	-0.10	-0.20	1.99	4.94
AT2	2.53	4.15	-0.98	-1.89	-0.19	-0.19	2.64	4.43
AT3	2.27	3.55	-0.84	-1.49	-0.12	-0.14	2.37	3.79
AT6	2.05	3.16	-0.69	-1.23	-0.07	-0.11	2.15	3.36
AT6/ME30	2.87	4.21	-1.31	-2.28	-0.20	0.01	2.99	4.43
AT200	7.31	9.26	-1.52	-2.97	-1.70	-1.41	8.76	11.78
PA10/IMS/ME30	2.22	3.58	-1.36	-1.73	0.03	0.00	2.17	3.75
PA10ME60/IMS	1.70	2.40	-0.38	-0.40	-0.12	-0.18	1.76	2.54
PA10MC15/IMS	2.45	4.03	-0.13	-1.01	-0.12	-0.06	2.62	4.41
PA5/IMS a	2.11	3.68	-0.97	-1.41	-0.15	-0.08	2.12	3.91
PA5/IMS b	2.06	4.14	-0.61	-1.53	-0.13	-0.01	2.13	4.46
PA10/IMS	3.12	6.22	-0.95	-2.83	-0.02	0.58	3.32	6.85
PA15/IMS	5.00	9.86	-2.09	-6.54	0.27	1.88	5.40	10.64
PA30/IMS	10.83	17.38	-8.51	-17.02	2.49	4.77	10.88	15.48
PA30/IMS/ME30	1.70	2.36	-0.91	-0.90	-0.07	-0.12	1.66	2.43
MP5/2CB5	1.83	2.53	-0.66	-1.09	-0.11	-0.10	1.86	2.59
MP15/2CB15	1.64	2.12	-0.69	-0.90	-0.08	-0.11	1.64	2.15
MP30/2CB30	1.82	2.41	-0.40	-0.80	-0.12	-0.12	1.89	2.49
I1135-2	2.13	3.28	-0.83	-0.85	-0.02	-0.06	2.19	3.54
I1135-3	1.86	3.40	-0.33	-1.25	-0.06	-0.12	1.98	3.65
I1135-6	1.67	2.79	-0.27	-0.90	-0.07	-0.12	1.76	2.96
I1135-43	1.72	3.16	0.27	-0.21	-0.13	-0.24	1.81	3.47
I1135-43/ME30	2.10	3.55	-0.72	-1.43	-0.15	-0.10	2.20	3.81

Notes for Table 9.12:

- Change in colour parameter = parameter(aged treated) – parameter(unaged treated) e.g. L^* (aged treated) – L^* (unaged treated);
- Undyed for comparison with EA4, EA2, EA4/ME30 only and vice versa.

9.3 The effect of the treatments on the stability of the model textiles during accelerated ageing – Results and discussion

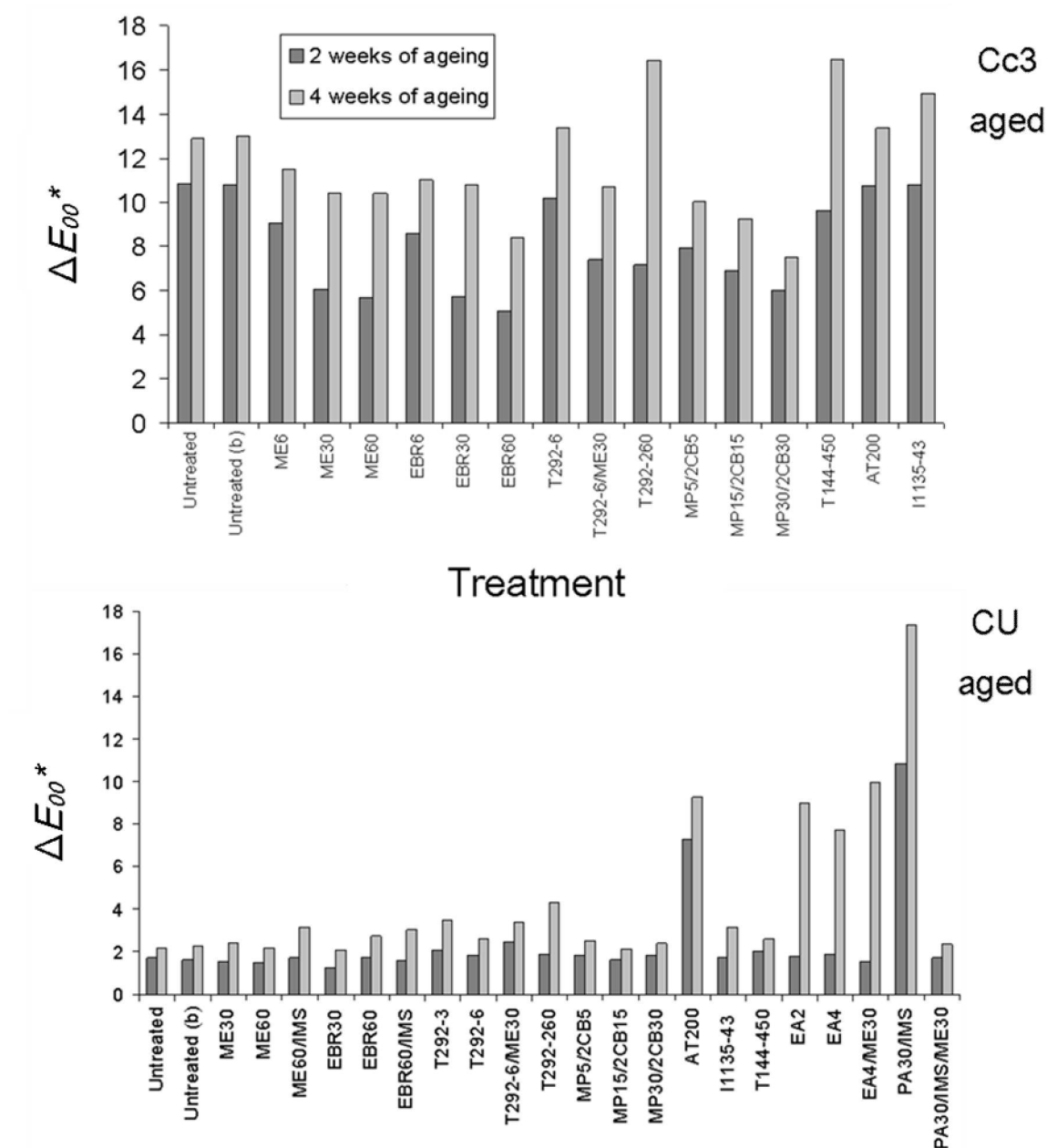


Figure 9.14 The change in colour of a selection of treated Cc3 (upper) and CU (lower) samples following 2 and 4 weeks of accelerated ageing (80°C and 65% RH)

9.3 The effect of the treatments on the stability of the model textiles during accelerated ageing – Results and discussion

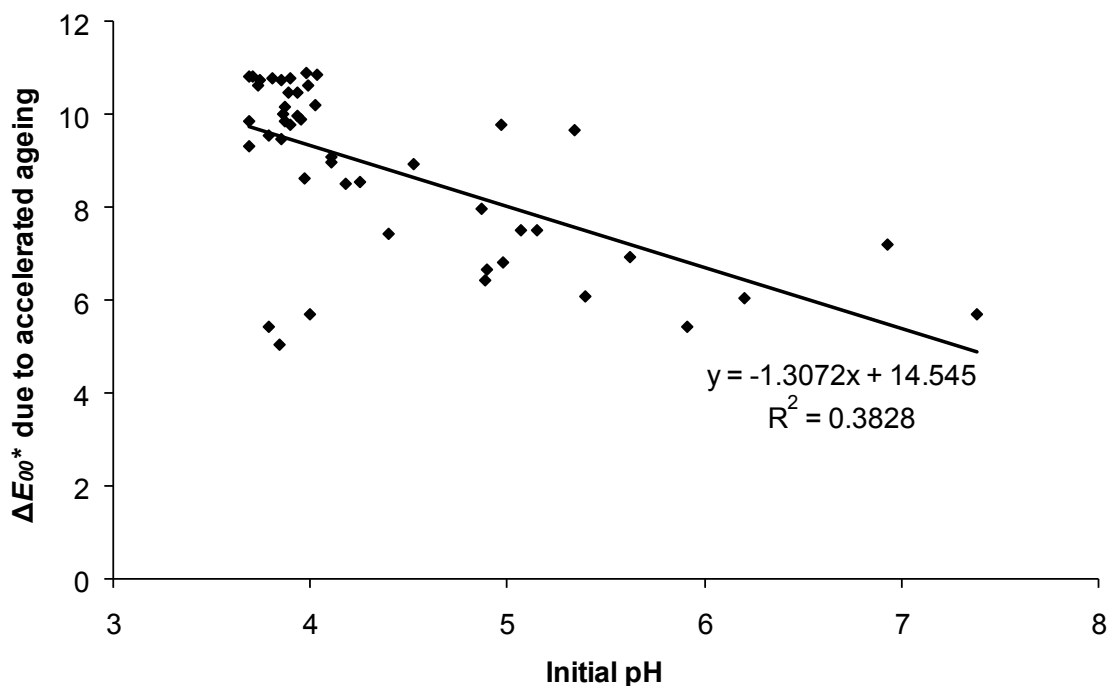


Figure 9.15 The correlation between initial pH and the change in overall colour of treated Cc3 during accelerated ageing (80°C and 65% RH)

Increases in lightness ($+\Delta L^*$), redness ($+\Delta a^*$), and yellowness ($+\Delta b^*$) of the Cc3 treated samples occurs with ageing (Table 9.11 and Figure 9.14). These result in the overall increase in colour change (ΔE_{00}^*) that is seen with ageing. There is a low ($R^2 = 0.3828$) negative correlation between the overall colour change due to accelerated ageing and the initial pH of the textiles as seen in Figure 9.15. This suggests that generally greater discolouration occurs during ageing to samples of lower initial pH.

The majority of discolouration that occurred to the untreated and treated Cc3 textiles on accelerated ageing occurred in the first 2 weeks of ageing. This discolouration was observable in all cases and ranged from $\Delta E_{00}^* = 5.05$ to 10.87 after 2 weeks of ageing and from $\Delta E_{00}^* = 7.51$ to 16.46 after 4 weeks. It is clear that T144, I1135, PA, AT, and the lower concentrations of T292 had little or no beneficial effect on the colour of the dyed textile during accelerated ageing since the overall change in colour of these treated Cc3 samples after 2 and 4 weeks of ageing was comparable to the untreated sample treatments ($\Delta E_{00}^* = 10.82$ and 12.91, respectively). After four weeks of ageing many of the T144, AT, and I1135 treated samples showed greater discolouration than the untreated equivalent. EA and PA treated samples were often less discoloured than the untreated sample after 2 weeks of ageing but comparable to it after 4 weeks of ageing. The MPx/2CBx, ME30,

9.3 The effect of the treatments on the stability of the model textiles during accelerated ageing – Results and discussion

ME60, EBR30, and EBR 60 treated samples changed colour less than the untreated sample after both 2 and 4 weeks of ageing and are therefore the most successful at sample colour-retention. Increasing concentration of these chemicals consistently resulted in decreasing magnitudes of sample discolouration, i.e. improved colour-retention properties. EBR60 in both ethanol ($\Delta E_{00}^* = 5.05$ and 8.41) and IMS ($\Delta E_{00}^* = 5.41$ and 8.34) and MP30/2CB30 ($\Delta E_{00}^* = 6.04$ and 7.51) were particularly effective at retaining the original colour of the samples after 2 and 4 weeks, respectively. The use of ME alone, particularly ME60 ($\Delta E_{00}^* = 5.68$ and 10.40), stabilised the colour of the samples by 2 two weeks of ageing to a similar extent as EBR60. By four weeks of ageing EBR60 was more successful than ME60 at colour-retention though discolouration of the ME60 treated sample was still less than in the untreated sample. The combination of ME30 with antioxidants consistently lowered the extent of discolouration of the sample after 2 weeks of ageing compared to the samples treated with antioxidant alone or the untreated equivalent. This trend continued after 4 weeks of ageing with some of the treatments such as T292 and T144. Interestingly, both T292-6/ME30 and T292-260 treated samples discoloured by a similar amount ($\Delta E_{00}^* = 7.42$ and 7.18 , respectively) after 2 weeks of ageing but by 4 weeks of ageing the T292-260 treated sample had discoloured significantly more than the T292-6/ME30 treated sample ($\Delta E_{00}^* = 16.44$ and 7.42 , respectively) and was one of the top two treated samples showing the greatest discolouration after 4 weeks of ageing. This suggests that the combination of T292-260 and ME30 could be particularly good at slowing the rate of discolouration of the iron-tannate dyed cotton samples.

After 2 and 4 weeks of ageing the change in colour of the untreated CU samples is low and only slightly visible, being close to $\Delta E_{00}^* = 1.7$ (Table 9.12 and Figure 9.14). Generally the treated samples showed similarly low levels of discolouration after 2 weeks of ageing.

ME, EBR, and T144 treated samples typically discoloured similarly to or less than the untreated CU sample after both 2 and 4 weeks of ageing. MPx/2CBx treated samples discoloured comparably or slightly more than the untreated CU sample after 2 and 4 weeks of ageing. PA, AT, and EA (particularly the lowest concentrations) treated samples typically discoloured more than the untreated CU samples after both 2 and 4 weeks of ageing. Some of these samples (particularly those involving EA or PA) were discoloured by significant amounts after 4 weeks of ageing, reaching $\Delta E_{00}^* > 5$. AT200 ($\Delta E_{00}^* = 7.31$ and 9.26) and PA30/IMS ($\Delta E_{00}^* = 10.83$ and 17.38) treated samples discoloured the most during 2 and 4 weeks of ageing, respectively. The dramatic increase in discolouration was

9.3 The effect of the treatments on the stability of the model textiles during accelerated ageing – Results and discussion

predominantly due to significant yellowing in the AT200 treated sample and a darkening and yellowing of the PA30/IMS treated sample. T292 and I1135 treated samples discoloured similarly throughout the accelerated ageing procedure and only slightly more than the MPx/2CBx. The T292-260 treated sample was an exception to this ($\Delta E_{00}^* = 4.30$ after 4 weeks of ageing). The use of ME30 with antioxidants typically caused a small increase in discolouration when compared with the samples treated with antioxidants only. A significant exception to this was for the PA30/ME30 treated sample which showed comparable discolouration to the untreated sample after both 2 and 4 weeks of ageing despite the use of PA30 alone causing significant and high discolouration.

All of the treated dyed silk samples changed colour by a noticeable amount (i.e. $\Delta E_{00}^* > 1.7$) ranging from $\Delta E_{00}^* = 2.52$ to 5.32 (Table 9.13 and Figure 9.16). While some of the treated Sp3 samples changed colour more than the untreated equivalent, the majority changed colour less. Treatments that resulted in Sp3 colour changes $\Delta E_{00}^* < 3.50$ include several treatments involving EA or EBR, several antioxidants when combined with ME30, T292-260, and T144-450. Increasing concentration of ME and PA caused increasing colour change with ageing which was mainly due to increase in yellowness (b^*). The ME60/IMS treated Sp3 sample showed the greatest discolouration of the Sp3 samples ($\Delta E_{00}^* = 5.32$) which was greater than the untreated equivalent ($\Delta E_{00}^* = 4.74$). In contrast, T292, EBR, and I1135 treated samples consistently showed decreasing discolouration with increasing treatment concentration. The highest concentration of T292 and EBR caused similar levels of discolouration ($\Delta E_{00}^* \sim 3.2$) while that of I1134 caused a higher discolouration ($\Delta E_{00}^* = 4.35$). The MP15/2CB15 and MP30/2CB30 treated samples were slightly more discoloured after ageing ($\Delta E_{00}^* 3.61$ and 3.60 , respectively) than the T292-260 and EBR60 samples. T144, EA, and AT treated samples showed an increase in discolouration with increasing concentration on ageing until the highest concentration was used. The Sp3 samples treated with the highest concentration of T144 and AT produced less discolouration than the lowest concentration. The use of ME with an antioxidant generally resulted in greater colour retention of the Sp3 samples. While for I1135-43 this stabilisation was negligible, for T292-6 it was significant, causing a difference in $\Delta E_{00}^* > 1$. The T292-6/ME30 treated sample discoloured less with age than the T292-260 treated sample.

9.3 The effect of the treatments on the stability of the model textiles during accelerated ageing – Results and discussion

Table 9.13 The effect of accelerated ageing (4 weeks at 80°C and 65% RH) on the colour of treated and untreated dyed (Sp3) and undyed (SU) silk samples

Treatment	Sp3				SU			
	ΔE_{00}^{*a}	ΔL^{*a}	Δa^{*a}	Δb^{*a}	ΔE_{00}^{*a}	ΔL^{*a}	Δa^{*a}	Δb^{*a}
U	4.74	2.48	-0.89	4.71	3.55	-0.49	-0.79	3.80
U ^b	3.74	1.27	-1.08	3.77	4.75	-1.62	-0.65	5.23
ME6	2.69	-2.74	-0.48	1.91	3.31	0.33	-0.80	3.54
ME30	4.28	-5.29	-0.20	2.23	3.22	-0.92	-0.72	3.39
ME60	4.67	-5.45	0.05	2.79	3.36	-2.84	-0.50	2.89
ME60/IMS	5.32	-5.31	-0.10	4.13	3.38	-1.33	-0.71	3.47
T144-2	4.30	2.30	-0.94	4.32	3.54	-0.29	-0.77	3.81
T144-3	4.59	2.29	-0.82	4.69	3.18	0.08	-0.72	3.40
T144-6	4.72	2.34	-0.81	4.83	3.25	-0.27	-0.73	3.45
T144-6/ME30	2.95	-3.02	-0.41	2.10	3.12	-1.07	-0.75	3.21
T144-450	3.40	2.47	-0.20	3.16	4.87	4.46	-0.92	3.83
AT2	3.87	1.73	-0.90	3.89	4.10	-0.12	-0.74	4.56
AT3	4.08	1.39	-0.81	4.23	3.89	-0.36	-0.75	4.28
AT6	4.77	2.24	-0.71	4.84	3.84	-0.50	-0.71	4.24
AT6/ME30	3.15	-3.48	-0.42	2.04	3.55	-1.18	-0.72	3.81
AT200	3.62	1.94	-0.63	3.57	6.29	-0.75	-1.24	7.63
EA0.4	2.71	-1.50	-0.30	2.63	5.10	-1.87	-0.73	5.57
EA0.4/ME30	3.08	-3.31	-0.32	2.12	4.56	-1.71	-0.70	4.99
EA2	3.26	2.39	-0.78	2.90	15.61	-18.30	0.84	5.76
EA4	2.97	1.67	-0.78	2.80	11.70	-13.46	0.69	5.75
EA4/ME30	2.52	-2.18	-0.64	1.98	11.80	-13.87	0.62	5.29
T292-2	5.24	3.37	-0.86	5.09	5.06	-1.28	-0.75	5.68
T292-3	4.11	2.39	-0.72	4.12	4.46	-0.98	-0.68	4.97
T292-6	4.50	2.37	-0.79	4.57	4.42	-0.61	-0.65	4.98
T292-6/ME30	3.05	-3.33	-0.39	2.03	3.68	-1.45	-0.77	3.82
T292-260	3.26	2.33	-0.37	3.09	5.55	1.10	-0.78	6.50
MP5/2CB5	3.88	2.93	-0.66	3.59	4.74	-0.49	-0.88	5.27
MP15/2CB15	3.61	2.96	-0.63	3.20	4.37	-0.64	-0.81	4.71
MP30/2CB30	3.60	3.31	-0.57	2.96	3.84	-0.75	-0.75	4.11
PA5/IMS a	4.14	1.93	-0.70	4.20	4.79	-1.00	-0.61	5.39
PA5/IMS b	4.11	1.91	-0.71	4.16	4.41	-0.58	-0.62	4.95
PA10/IMS	4.16	2.07	-0.70	4.19	4.82	-0.63	-0.79	5.38
PA15/IMS	4.46	2.54	-0.78	4.43	5.55	-1.35	-0.79	6.30
PA30/IMS	4.47	2.79	-0.75	4.37	7.88	-1.75	-0.71	9.62
PA30/IMS/ME30	4.67	2.38	-0.45	4.86	3.95	-1.37	-0.71	4.20
PA10/IMS/ME30	3.58	-3.89	-0.19	2.45	3.77	-1.50	-0.62	3.99
PA10MC15/IMS	4.80	3.45	-0.52	4.57	4.37	-0.95	-0.74	4.77
PA10ME60/IMS	4.10	1.12	-0.38	4.44	3.58	-0.87	-0.62	3.85
I1135-2	5.10	2.33	-0.75	5.24	3.51	-0.29	-0.72	3.90
I1135-3	4.59	2.01	-0.82	4.73	3.36	-0.32	-0.69	3.71
I1135-6	4.46	1.75	-0.83	4.63	3.21	-0.59	-0.70	3.46
I1135-43	4.35	1.95	-0.80	4.45	2.99	-0.01	-0.72	3.17
I1135-43/ME30	4.34	-3.11	-0.41	4.05	3.21	-0.32	-0.74	3.47
EBR6	4.04	1.98	-0.79	4.05	3.31	-0.27	-0.67	3.57
EBR30	3.40	1.44	-0.75	3.45	3.89	-0.48	-0.68	4.27
EBR60	3.23	1.19	-0.78	3.28	5.21	-1.13	-0.76	5.92
EBR60/IMS	3.46	1.28	-0.75	3.57	5.16	-1.35	-0.71	5.91

Notes for Table 9.13:

- Change in colour parameter = parameter(aged treated) – parameter(unaged treated) e.g. L^* (aged treated) – L^* (unaged treated);
- Undyed for comparison with EA4, EA2, EA4/ME30 only and vice versa.

9.3 The effect of the treatments on the stability of the model textiles during accelerated ageing – Results and discussion

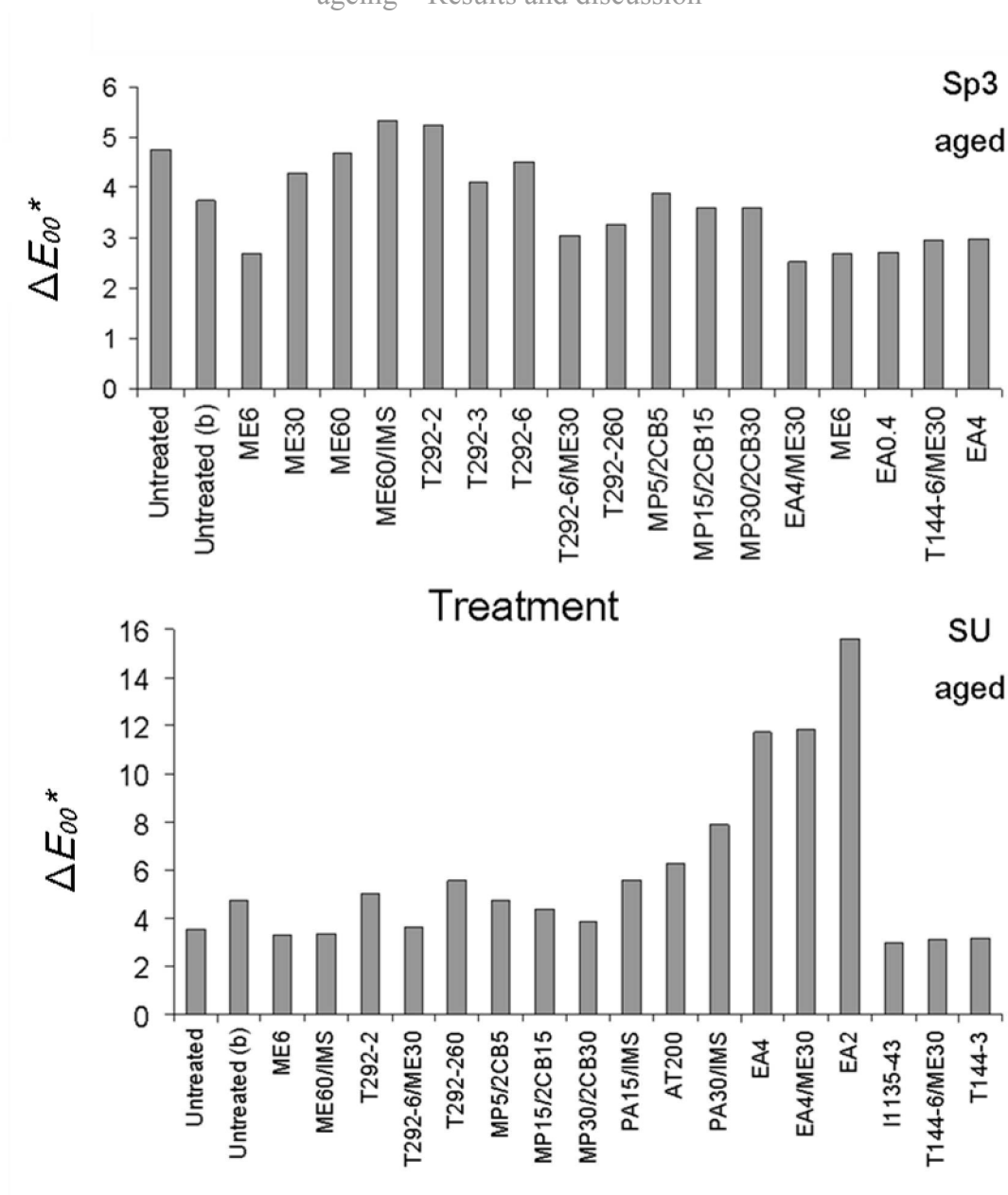


Figure 9.16 The change in colour of a selection of treated Sp3 (upper) and SU (lower) samples following 4 weeks of accelerated ageing (80°C and 65% RH)

The trends in ΔE_{00}^* of the silk textiles are mainly due to similar changes in trends in increasing yellowness ($+\Delta b^*$). Lightness of the samples also varies similarly in some cases (e.g. EBR treated Sp3 samples) but the trends were not always consistent (e.g. the I1135 treated Sp3 samples). While the majority of samples lightened ($-\Delta L^*$) with age the ME treated samples darkened considerably ($-\Delta L^*$). Of all the colour parameters the least change on ageing occurred in the redness (Δa^*) which was almost always negative indicating a decrease in redness.

9.3 The effect of the treatments on the stability of the model textiles during accelerated ageing – Results and discussion

In contrast to the dyed silk treated samples, the undyed silk treated samples mainly discoloured more than the untreated equivalent and over a larger range ($\Delta E_{00}^* = 2.99$ to 15.60) (Table 9.13 and Figure 9.16). Treatments involving I1135, T144, and ME frequently showed less discolouration ($\Delta E_{00}^* = 2.99$ to 3.54) of SU than no treatment ($\Delta E_{00}^* = 3.55$). Generally treatments involving ME in addition to an antioxidant resulted in less discolouration of the sample during ageing. This is particularly evident when ME30 was combined with PA30. The following treatments caused $\Delta E_{00}^* > 10$: EA4, EA4/ME30, and EA2. The significant colour change arises from a significant darkening of the samples on ageing and increase in redness (other samples show a decrease in redness). This may be due to the acidic nature of the treatment which will accelerate acid hydrolysis and the formation of small coloured molecules. However the same treatments on the dyed silk caused some of the smallest colour changes to the sample during ageing. A repeat test of this treatment on these samples would help identify if the large discolouration seen in the SU was a consistent trend. Treatments involving PA also caused significant discolouration ($\Delta E_{00}^* = 4.41$ to 7.88). While increasing the concentration of T292 caused a consistent decrease in the extent of discolouration of Sp3 after ageing, in SU T292-260 breaks this trend by causing greater discolouration to SU ($\Delta E_{00}^* = 5.55$) than the lowest concentration ($\Delta E_{00}^* = 5.06$). However, by combining T292-6 with ME30 the discolouration of SU is effectively lowered by $\Delta E_{00}^* > 1$ (when compared with the T292-6 treated SU sample). Consequently, a combination of T292-260 with ME30 may be more successful at retaining the colour of SU during ageing than T292-260 alone. Increasing the concentration of the MPx/2CBx treatment resulted in decreasing discolouration to the treated SU sample. The MP30/2CB30 treated SU sample was discoloured ($\Delta E_{00}^* = 3.84$) only slightly more than the T292-6/ME30 treated sample ($\Delta E_{00}^* = 3.68$).

As with the Sp3 treated samples there is a close correlation between the change in ΔE_{00}^* and the change in Δb^* in the SU treated samples. EA4, EA4/ME30, and EA2 are exceptions to this as previously discussed. T144-450 is also an exception which has arisen due to a significant lightening of the sample ($\Delta L^* = 4.46$) during ageing compared to the generally low levels of darkening ($\Delta L^* < -1$).

Frequently the discolouration that occurred to treated SU samples was equivalent to or greater than the discolouration to the similarly treated Sp3 samples. I1135 treated samples are typically an exception to this as are usually one or two samples of each treatment.

9.3.7 GPC-MALLS

Table 9.14 Effect of treatments on the molecular weight, molecular weight distribution, and polydispersity index of Cc3 textiles during accelerated ageing (2 weeks at 80°C and 65% RH)

Treatment (weeks of ageing)	DP _n	Average molecular weight		PDI	% polymer content in			
		M _n (kg/mol)	M _w (kg/mol)		DP<100	DP100-200	DP200-2000	DP>2000
Untreated (0)	902	146	486	3	1	2	57	40
Untreated (2)	197	32	151	4	12	16	60	12
MP30/2CB30 (0)	1035	168	467	3	0	1	57	41
MP30/2CB30 (2)	604	98	293	3	1	4	69	26
MP30/2CB30 (2) ^a	572	93	274	3	1	4	72	22
MP15/2CB15 (2) ^a	219	35	215	6	8	8	67	17
ME30 (0)	829	134	559	4	1	3	55	41
ME30 (2)	350	57	255	5	5	8	65	22
ME60 (2) ^a	382	62	234	4	4	7	72	18
T292-260 (0)	658	107	431	4	2	4	55	39
T292-260 (2)	645	105	259	2	1	3	71	24
T292-260 (2) ^a	327	53	228	4	5	8	69	19
T292-6/ME30 (2)	345	56	190	3	5	9	70	16
T292-6 (2)	194	31	141	4	12	15	62	11
EBR60 (2)	106	17	64	4	21	20	58	1

Note for Table 9.14:

- a. From a different batch to the other samples and so caution must be taken when comparing data between batches.

The difference in values between separate analysis batches of the same sample (Table 9.14 and Figure 9.17) e.g. MP30/2CB30 and T292-260 may arise from variations in dye and/or treatment application. Due to these differences only samples from the same analysis batch will be compared to ensure reliability of the evaluation.

T292-260, ME30, and MP30/2CB30 decreased the extent of depolymerisation in Cc3 to a similar extent (Table 9.14). Based on the greater quantity of low molecular weight molecules (DP<200), the ME30 treatment may be viewed as slightly less successful than the others. This correlates well with the slightly more acidic nature of the ME30 treated sample (pH 5.4 +/- 0.0) compared to the T292-260 and MP30/2CB30 treated samples (pH 6.9 +/- 0.1 and pH 6.2 +/- 0.2, respectively) prior to ageing. These treatments caused some of the least acidic samples of all the treatments with significantly greater pH values than the untreated sample (pH 3.7 +/- 0.0). The retention of high molecular weight molecules explains why these three samples were judged in handling tests to be some of the most successful at retaining the strength of the dyed cotton during ageing. The ME30 treated

9.3 The effect of the treatments on the stability of the model textiles during accelerated ageing – Results and discussion

sample was judged in the handling tests to be weaker than the MP30/2CB30 and T292-260 treated samples.

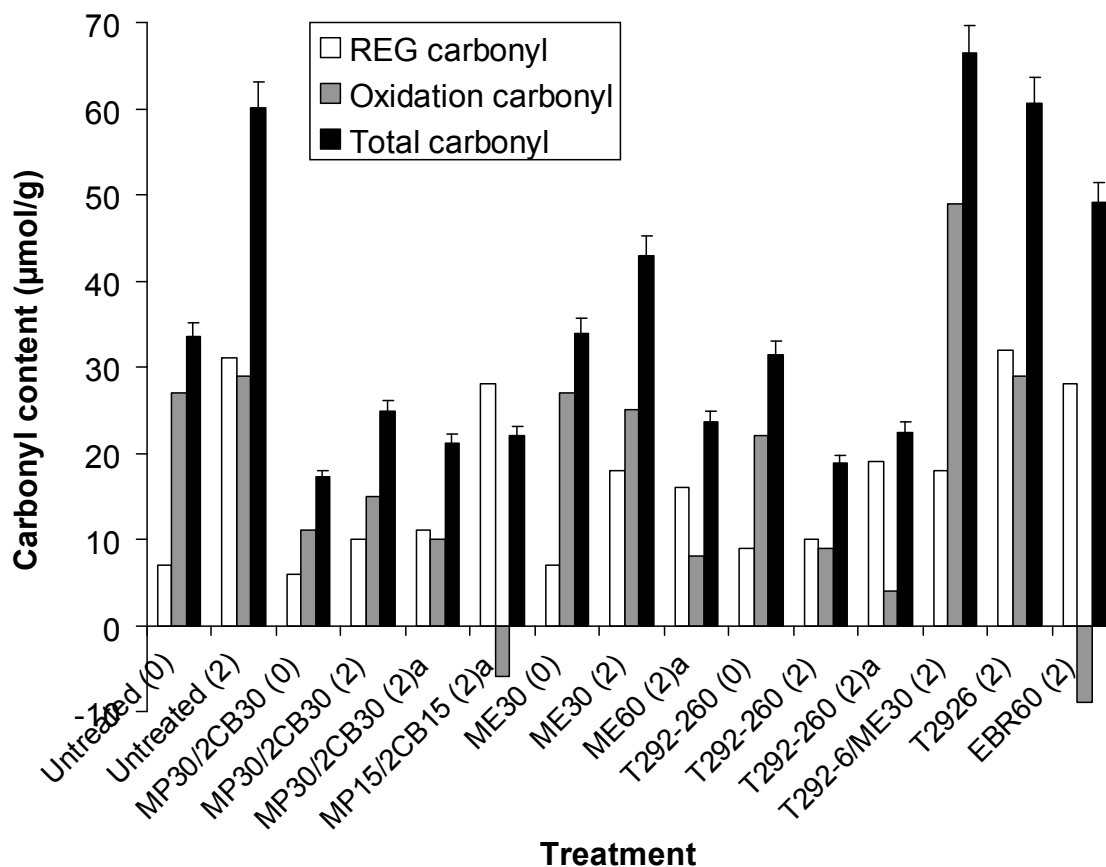


Figure 9.17 The carbonyl content of unaged (0) and two week aged (2) treated and untreated Cc3 textiles determined using GPC-MALLS in two batches one of which is denoted by ‘a’

The T292-260, ME30, and MP30/2CB30 treatments decreased the rate of carbonyl group formation by 30% and 70% (compared to the untreated sample) (Figure 9.17). The main cause of the increase in carbonyl groups of the untreated sample is due to hydrolysis. Only a small increase is attributed to oxidation. Unlike in the T292-260 treated sample in which the carbonyl content decreased by approximately 40% with ageing, the carbonyl content in the ME30 and MP30/2CB30 treated samples increased by approximately 25% and 30%, respectively with ageing. Interestingly, the increase in carbonyl groups for the ME30 treated sample with ageing was due to increasing depolymerisation (REGs) while both oxidation and depolymerisation contributed to the small increase in carbonyl content of the MP30/2CB30 treated sample with ageing. Comparison with the untreated sample suggests that MP30/2CB30 had little effect on the extent of oxidation in Cc3 during ageing but significantly decreased the extent of hydrolysis. It has been suggested that the aqueous

9.3 The effect of the treatments on the stability of the model textiles during accelerated ageing – Results and discussion

nature of this treatment contributes to the success of this treatment through the removal of soluble low molecular weight molecules (e.g. sulphuric acid) and soluble metal ions (Neevel 2002; Rouchon, Pellizzi, Duranton, Vanmeert and Janssens 2011). The GPC-MALLS results suggest that the deacidifier is the main cause of the stabilising properties of this treatment to Cc3. This compares well with recent research into the stabilisation of iron gall ink in which deacidification of paper samples treated with calcium phytate was identified as being vital to the long-term success of the treatment (Rouchon, Pellizzi, Duranton, Vanmeert and Janssens 2011). The unexpected decrease in carbonyl content of the T292-260 treated sample compared to that in the untreated sample with ageing was confirmed in a second analysis of the sample and may be due to the oxidation of the REGs and other carbonyl groups to acid groups since acid groups are not detected with this method. It is unlikely that acid or alkaline hydrolysis has occurred to a significant extent since neither an increase in lower molecular weight molecules or carbonyl content occurred on ageing.

Based on the results in Table 9.13, T2926 had no stabilising effect on the Cc3 during ageing, giving comparable results to the untreated sample after 2 weeks of ageing (80°C, 65% RH). Consequently, the stabilising ability of T2926/ME30 with respect to depolymerisation was due to the presence of ME30. The T2926/ME30 treatment caused similar, possibly slightly larger, levels of depolymerisation to the ME30 treatment but a much greater extent of oxidation based on the theoretical non-REG carbonyl content. Interestingly the T292-260 treatment resulted in the lowering of carbonyl groups with ageing, including those due to oxidation. Excepting the effect on oxidation, these results correlate well with the differences in acidity of the treated samples before ageing: the untreated sample before ageing (pH 3.7 +/- 0.0); T2926 sample (pH 3.9 +/- 0.0); T2926/ME30 (pH 4.4 +/- 0.0); and ME30 sample (pH 5.4 +/- 0.0). The fact that T292-260 was a successful stabiliser of the Cc3 with respect to acid hydrolysis while the lower concentration in the T2926 treatment was not, demonstrates the importance of concentration in the effectiveness of antioxidants (Section 8.2.1.4). The results are also supported by those from the handling tests since the T2926 treatment was assessed as being less successful at retaining the strength of the dyed cotton than the T292-260, ME30, and MP30/2CB30 treatments when compared with the untreated aged sample.

9.3 The effect of the treatments on the stability of the model textiles during accelerated ageing – Results and discussion

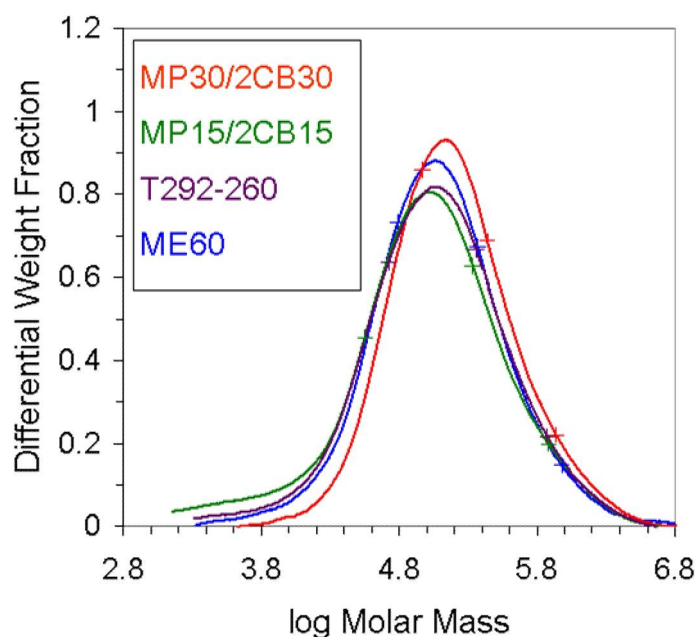


Figure 9.18 The effect of treatments on the molar mass distribution of cellulose in Cc3 after two weeks of ageing (80°C and 65% RH)

While the ME60 treatment results cannot be reliably compared with the ME30 treatment results due to the samples being in separate batches it can be compared to the other samples in its batch. In doing so it is clear that the ME60 treatment resulted in comparable if not slightly greater stabilisation of the dyed cotton during ageing than the T292-260 treatment (Figure 9.18). This correlates well with the slightly greater pH of the ME60 treated sample (pH 7.5 \pm 0.2) compared to the T292-260 treated sample (pH 6.9 \pm 0.1). In the handling tests, the ME60 treated sample was thought to have retained the strength of the dyed textile slightly less than the T292-260 but have resulted in comparable surface rub resistance of the textile. Similar levels of hydrolysis appear to have occurred in these samples on ageing (based on estimated REG content) but a slightly greater extent of oxidation may have occurred in the ME60 treated sample.

EBR60 was the least successful treatment of those tested at stabilising the dyed cotton during ageing as it underwent greater depolymerisation than the untreated sample. Only 1.25% of polymers with a DP > 2000 remained after ageing (a tenth of the % resulting from no treatment) and approximately double the % of molecules with DP < 100 occurred in the treated sample after ageing compared to the untreated. This again corresponds to the low pH of the treated sample before ageing (pH 3.8 \pm 0.0), which was comparable to that of the untreated sample (pH 3.7 \pm 0.0). While a significant increase in carbonyl content occurred in the EBR60 treated sample, it appeared to be less than that in the untreated

9.3 The effect of the treatments on the stability of the model textiles during accelerated ageing – Results and discussion

sample despite the significantly greater depolymerisation. Estimated REG content suggests that hydrolysis was the major degradation mechanism. A negative value was calculated for the quantity of carbonyl groups arising from oxidation. However, due to the precision of the M_n determination this may simply indicate that no oxidation occurred.

MP15/2CB15 showed similar carbonyl content to the higher concentration (MP30/2CB30) but resulted in greater depolymerisation as expected from a lower concentration of metal ion chelator and deacidifier. The depolymerisation was still less than that seen in the untreated sample and the carbonyl content was still significantly less than seen in the untreated sample. Again a negative value of carbonyl content due to oxidation has been calculated which may suggest that hydrolysis was the major degradation pathway and that no oxidation occurred.

Discolouration arises from the formation of chromophores in the sample. Aldehydes can be precursors of chromophores for example, they can be part of large conjugated systems that absorb visible light and thus cause discolouration of the sample. When only the magnitude of changes in CIE2000 colour parameter and carbonyl content on ageing are considered, i.e. the direction, positive or negative, of the change is not considered, there is a good correlation between the extent of discolouration (ΔE_{00}^*) and change in carbonyl content during ageing.

From Figure 9.19 it is clear that a positive trend exists between increasing yellowness of the treated samples with age and increasing overall carbonyl content.

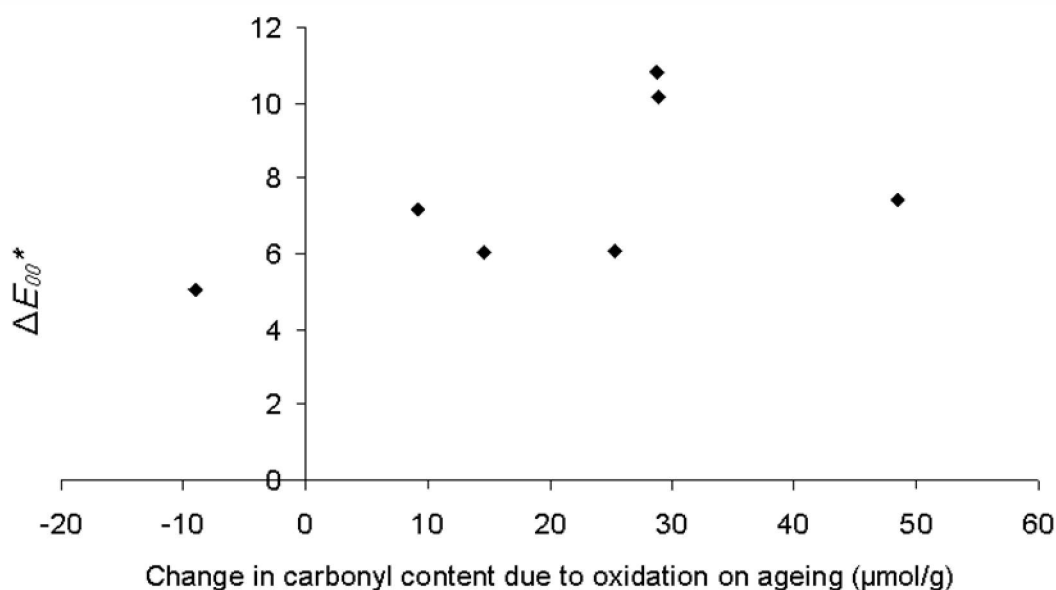


Figure 9.19 Correlation between overall change in colour (ΔE_{00}^*) with overall change in carbonyl content in treated samples with ageing¹

9.4 The technical merits of the most successful treatments

The application of treatments involving a deacidifier (CB or ME), or T292-260, and T144-450 caused the greatest increase in pH of the Cc3 textiles (CU and SU were not analysed). Of the treated Sp3 samples that were analysed, ME and MPx/2CBx raised the pH the most while T292 caused no significant difference to the pH. The application of the aqueous MPx/2CBx and non-aqueous ME treatments caused the greatest change in colour of the Cc3 textiles. An increase in redness was most notably seen with the ME treatments and is likely to be due to the high alkalinity of the treatment which could cause the breakdown of the iron-tannate dye complexes and formation of brown degradation products. Magnesium-rich surface deposits were also identified on ME30 and T292-6/ME30 treated Cc3 and Sp3 samples using SEM-EDX. The presence of these deposits is likely due to the low solubility of the ME in ethanol and the fact that the solution was not filtered before use. In future, filtering of these solutions may be beneficial. Consistently significant differences in the surfaces of the MPx/2CBx and T292-260 treated samples were not identified. The use of lower concentrations of ME could reduce the discolouration seen on application. The same

¹ The change in carbonyl content has been calculated by subtracting the carbonyl content of the unaged sample from the aged sample. Four samples have both of these data. Three samples didn't have the initial carbonyl content and so the initial carbonyl content of the untreated sample was used in the calculation. For the samples treated with non-aqueous treatments this is a suitable substitution as the carbonyl content of several unaged non-aqueous treated samples had comparable carbonyl content to the unaged untreated sample. The use of aqueous treatment (MP/2CB treatments) causes a decrease in carbonyl content which would make substitution of unknown initial carbonyl contents with that of the untreated sample unreliable. The change in carbonyl content during ageing of the MP15/2CB15 sample was therefore not calculated.

9.5 Fulfilment of the aims of the treatment

applies to T144-450, T292-260, AT200 which caused observable discolouration to Sp3 and SU on application.

Based on the analyses of the dyed cotton and silk textiles following accelerated ageing it is clear that the aqueous MPx/2CBx treatment is a very successful antioxidant and deacidification treatment. It impedes the rates of acid hydrolysis and oxidation, thereby retaining more polymer chains of high DP and forming fewer carbonyl groups compared to those treated with less successful treatments. These results are demonstrated on a macro level as good strength retention of the textile and relatively good colour-retention, respectively. Of the non-aqueous treatments investigated those including ME, T292-260, T144-450, and antioxidants in combination the ME30 e.g. T144-6/ME30, PA10/ME30, and PA30/ME30 show potential based on the handling tests. However, ME and T292-260 show the most potential when tensile test, viscometry, and GPC-MALLS results are also considered. Some drawbacks to these treatments exist based on the colorimetry data. T292-260 was found to impart relatively good colour-retention of Cc3 after two weeks of ageing but after four weeks of ageing the discolouration was greater than that seen in the untreated equivalent. It is possible that combination of T292 at this or a slightly lower concentration with the deacidifier ME could result in lowered discolouration during ageing since this trend was observed with T292-6/ME30 and T292-6. Additionally, yellowing of the undyed textiles occurred after ageing which was most notable on SU and caused a $\Delta E_{00}^* = 5.55$ after four weeks of ageing. This was not the highest discolouration of undyed textiles seen on ageing and was within $\Delta E_{00}^* = 2$ of the majority of the other treatments including the MPx/2CBx treatments. EBR and I1135 offered little, if any, strength-retention properties. EBR60 was however the most successful treatment for colour retention of Cc3 and performed well on CU and Sp3 also. On SU EBR60 resulted in similar colour change to T292-260. I1135 showed good colour-retention for the undyed textiles but was not as successful as EBR on the dyed textiles.

9.5 Fulfilment of the aims of the treatment

Any successful treatment developed in this project should be non-aqueous and preventive, i.e. not a consolidant, and it should significantly impede the rate of degradation of iron-tannate dyed textiles. T292, particularly T292-260 and ME were the most successful non-aqueous treatments in this study based on strength-retention properties. EBR was the most successful treatment based on colour-retention properties.

9.6 Conclusions

Additionally, the treatment should have minimal effect on textile handle and colour and if possible, be non-toxic, and easy to apply to large or three-dimensional objects that may be made of composite materials using readily available chemicals, solvents and equipment. Consequently, the hazardous nature of ME (a highly flammable irritant that reacts violently with water), its low solubility in ethanol or IMS both of which require extraction during usage and are highly flammable, the discolouration it causes to iron-tannate dyed cotton and silk on application as well as the presence of surface deposits on the textile fibres after application makes ME less favourable for use despite it being one of the best strength-retention treatments tested. T292 dissolves in non-toxic cyclosiloxane D5 though the logistics of acquiring the solvent and its cost have not been investigated at present. It can also dissolve in IMS which is already used in conservation studios and is used in the EBR treatments. T292 is an irritant and dangerous for the environment (very toxic to aquatic organisms) while EBR is also an irritant. Based on these factors and the limited number of non-aqueous treatments that will be tested on pre-aged cotton, abaca, wool, and silk dyed (c2, c3, p2, and p3) and undyed textiles in Treatment Test 2, ME will not be investigated further in this study. Instead, T292 will be investigated at the same concentration as used here and a higher one, as well as in combination with EBR. The EBR will be applied separately when T292 is dissolved in cyclosiloxane D5 but simultaneously when T292 is dissolved in IMS. MP/2CB will also be used as a control.

9.6 Conclusions

The effect of the application and subsequent accelerated ageing, of a range of non-aqueous treatments to dyed (c3 and p3) and undyed cotton and silk samples has been investigated using pH testing, SEM-EDX, spectrophotometry, tensile testing, handling tests, viscometry, and EPR spectroscopy. The pH of the treated textiles prior to accelerated ageing was found to correlate well with the tensile strength, DP, overall colour change, and handling test results of the samples after accelerated ageing. The change in carbonyl content of Cc3 treated samples during ageing also correlated well with the overall colour change. The T292 treatment at the highest concentration tested was found to be as successful as the aqueous MP/2CB treatment in maintaining the strength of the textile samples during ageing. It had little if any effect on the proportion of bound iron(III) ions but caused a decrease in radical content. ME was also highly successful when used on its own and also gave improved stabilisation properties to antioxidants when used in combination with them. EPR spectroscopy identified that the ME30 treated Cc3 sample contained significantly more radicals before and after ageing than the untreated equivalent. However both T292 and ME have some deficiencies regarding colour change of the dyed and undyed materials

9.6 Conclusions

on application and after ageing. EBR was particularly good at colour-retention but not at strength-retention. The technical merits of the most successful treatments with respect to the aims of the project have been discussed and have initiated further investigations of T292 and EBR in the Stabilisation Treatment Test 2 (Chapter 10).

10 STABILISATION TREATMENT TEST 2 – PRE-AGED MODEL TEXTILES

In Treatment Test 2 undyed and dyed (c2, c3, p2, and p3) model textiles of cotton, abaca, wool, and silk were pre-aged (accelerated aged before treatment application) using dark, thermal accelerated ageing before being treated with one of five treatments. These treatments were chosen based on the results of Stabilisation Treatment Test 1 (Chapter 9). The effect of immersion in a range of solvents for 30 minutes on the colour, surface, and integrity of the most delicate textiles was investigated. Additionally, the effect of treatment application on the colour of the model textiles was ascertained using colorimetry. After treatment application the samples were subjected to further accelerated ageing. Due to a malfunction of the environmental chamber at the National Gallery during accelerated ageing of half of the treated samples colour leakage and an unknown extent of treatment transferral occurred between samples. Consequently these samples were assumed to be compromised and not suitable for further study. The remaining half were successfully accelerated aged in an environmental chamber at Camberwell College of Arts however due to the damage to the other half of the treated samples there were no remaining pre-aged samples to tensile test for comparison with the twice aged samples.

Before Treatment Test 2 could be started two experiments needed to be performed. The first was to determine the highest concentration of Tinuvin 292 (T292) to be used in Treatment Test 2 and the second was to determine the effect of solvents on fragile aged model textiles.

10.1 Determination of the highest concentration of T292 to be used in Stabilisation Treatment Test 2

10.1.1 *Experimental method*

Small pieces of undyed and dyed (p3) silk were immersed together for 30 minutes in 50 ml of T292 solution. Cyclosiloxane D5 (Greenearth, GE) or IMS were used as the solvent. A range of concentrations of T292 (3, 6, 8, 10, 15, and 18% of approximate weight of the solvent) were tested. The samples were blotted dry on tissue paper and hung to dry in a fume cupboard. After 24 hours, observations were made as to the solubility of the T292 in the solvents, the colour of solutions, and the handle of the dried textiles. These subjective analyses were made as objective as possible by comparing treated and untreated samples side by side in a well lit environment by the same assessor. This was a suitable level of accuracy for the results required.

Table 10.1 The concentrations of T292 solutions tested on Sp3 samples

Approximate concentration (% weight of 50 ml GE)	Solvent	Concentration (M)	Mass in 50 ml
3	GE	0.033	1.447
6	GE	0.066	2.912
8	GE	0.088	3.886
10	GE	0.109	4.779
15	GE	0.168	7.369
18 ^a	IMS	0.192	8.458

Note for Table 10.1:

a. based on weight of GE rather than IMS.

10.1.2 Results and discussion

The T292 dissolved in both GE and IMS to give clear and colourless solutions for all concentrations tested.

No observable colour transfer from the dyed silk to the undyed silk occurred in the treatment solutions and none of the treated samples were stiff after drying. The surfaces of the treated samples were possibly slightly greasy. This may be due to the T292 which is a liquid at room temperature or may signify that the GE had not fully evaporated. The extent of greasiness of sample surfaces was difficult to distinguish. Increasing the concentration of T292 resulted in a slight observable darkening of the dyed silk suggesting the concentrating of the antioxidant in or on the fibre.

10.1.3 Summary

The highest and lowest concentrations of T292 tested here will be used in GE in Treatment Test 2 and have treatment codes of T292-3 and T292-15, respectively. Additionally, T292-3 will be dissolved in IMS as part of another treatment.

10.2 Effect of solvent immersion on the conditions of fragile pre-aged model textiles

10.2.1 Experimental

Pre-aged (4 weeks at 80°C and 35-80% RH (every three hours)), dye formulation 1 dyed cotton and abaca were conditioned to 20°C and 41 +/- 3% RH (Hanwell ml-4000) and cut into small pieces and weighed. Two of three pieces of each textile were immersed for 30 minutes in 150 ml of each of the solvents tested (deionised water, IMS, and GE). The remaining pieces were left dry and untreated for comparison. After air drying, the samples were reweighed under similar conditions to those before immersion.

10.2 Effect of solvent immersion on the conditions of fragile pre-aged model textiles

During immersion any loss of fibres or dye from the samples were noted. Approximate times for the samples to wet out and to dry were also noted.

10.2.1.1 Microscopy and SEM-EDX analysis

The surfaces of all of the samples were inspected using microscopy at $\times 5$ magnification in order to ascertain any consistently significant differences in appearance. Small pieces of sample (approximately 1×2 cm) that appeared representative of the whole were adhered at one end to aluminium tape and placed flat on a stand in preparation for SEM-EDX. SEM micrographs were collected using the conditions described in Section 5.2.7.2 (Unaged p1/c1 dyed model textiles). INCA software was used to identify the elemental composition of areas and points of samples using 100 s lifetime, 0-20 keV range, and 2K channels. Three separate areas of each sample were analysed and a BSE image documented of one representative area.

10.2.1.2 GPC-MALLS

The fragile aged Cc1 samples that were immersed in different solvents and dried were analysed as described in Section 5.2.8.

10.2.1.3 XRF of GE-immersed samples

Several months after the immersion tests a selection of GE-immersed cotton and abaca samples were analysed using XRF in order to identify if any GE still remained. The samples were analysed in one layer on two pieces of Whatman filter paper that were supported so that the paper with the sample was suspended over air. Identification of unusually large Si peaks would be indicative of GE remaining in concentrations that are detectable using XRF. Helium purging was used to enable detection of elements of low atomic mass, including Si. X-ray spectra were taken using an ArtTax μ -XRF spectrometer with molybdenum X-ray tube, Artax3 software, and the following settings: 0.65 mm collimator, 400 s lifetime, 50 kV, 500 μ A. Bayes deconvolution was used by the software to calculate elemental peak areas. Elemental XRF ratios were calculated using Equation 5.1 (Section 5.2.1).

10.2.2 Results and discussion**10.2.2.1 General observations and SEM-EDX**

Table 10.2 Effects of solvent immersion on colour and weight of pre-aged cotton and abaca samples, observation of wetting out and drying times, and indication of which samples were analysed with SEM-EDX

Dyed (c1) aged ^a textile	Sample number	Solvent	Observations from solvent immersion test				% weight loss	Fewer iron-rich surface deposits than un-immersed sample ^d
			Wets out immediately	Drying time	Colour loss	Fibre loss		
Cotton	1a	- ^b	-	-	-	-	0.0	-
	1b	H ₂ O	N - Takes a while. Took longer than abaca to wet out.	Next day	Y	Most losses seen here; possibly affected by increased manipulation necessary to wet out samples	3.3	Y
	1c						3.2	ND
Abaca	1a	-	-	-	-	-	0.0	-
	1b	H ₂ O	N - Takes a while	Next day	Y	Most losses seen here; possibly affected by increased manipulation necessary to wet out samples	8.9	Y
	1c						9.8	ND
Cotton	2a	-	-	-	-	-	0.3 ^e	ND
	2b	GE	Y	Touch dry next day ^b	N	Small fibres lost	0.4	N
	2c						0.8	ND
Abaca	2a	-	-	-	-	-	0.0	ND
	2b	GE	Y	Touch dry next day ^c	N	Small fibres lost	0.1	N
	2c						0.1	ND
Cotton	3a	-	-	-	-	-	0.2	ND
	3b	IMS	Y	30 mins	N	Small fibres lost	0.6	N
	3c						0.9	ND
Abaca	3a	-	-	-	-	-	0.0	ND
	3b	IMS	Y	30 mins	N	Small fibres lost	0.2	N
	3c						0.2	ND

Notes for Table 10.2:

- 4 weeks at 80°C and 35-80% RH (every three hours);
- Sample left dry and un-immersed;
- Takes longer than 1 day to be fully dry. If only touch dry or wet the sample saturates the surface of any absorbent material it comes into contact with leaving “greasy” marks that should disappear as the GE evaporates;
- Consistently significant differences in quantity of iron-rich particles were identified using SEM-EDX. Areas of treated samples were compared to the cotton 1a and abaca 1a un-immersed samples. ND denotes that these samples were not analysed;
- Loss of fibres during handling due to the brittleness and fragility of the sample.

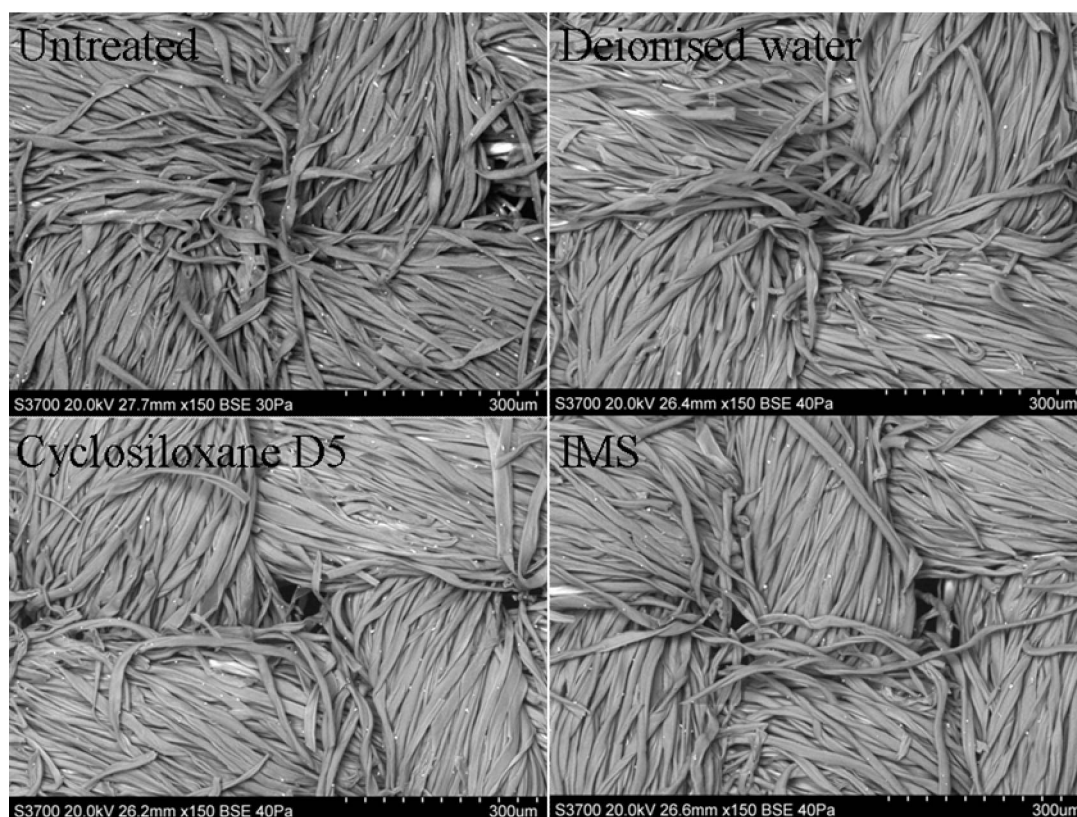


Figure 10.1 SEM micrographs of untreated pre-aged dyed (c1) cotton and pre-aged dyed (c1) cotton that has been immersed for 30 minutes in deionised water, cyclosiloxane D5, or IMS

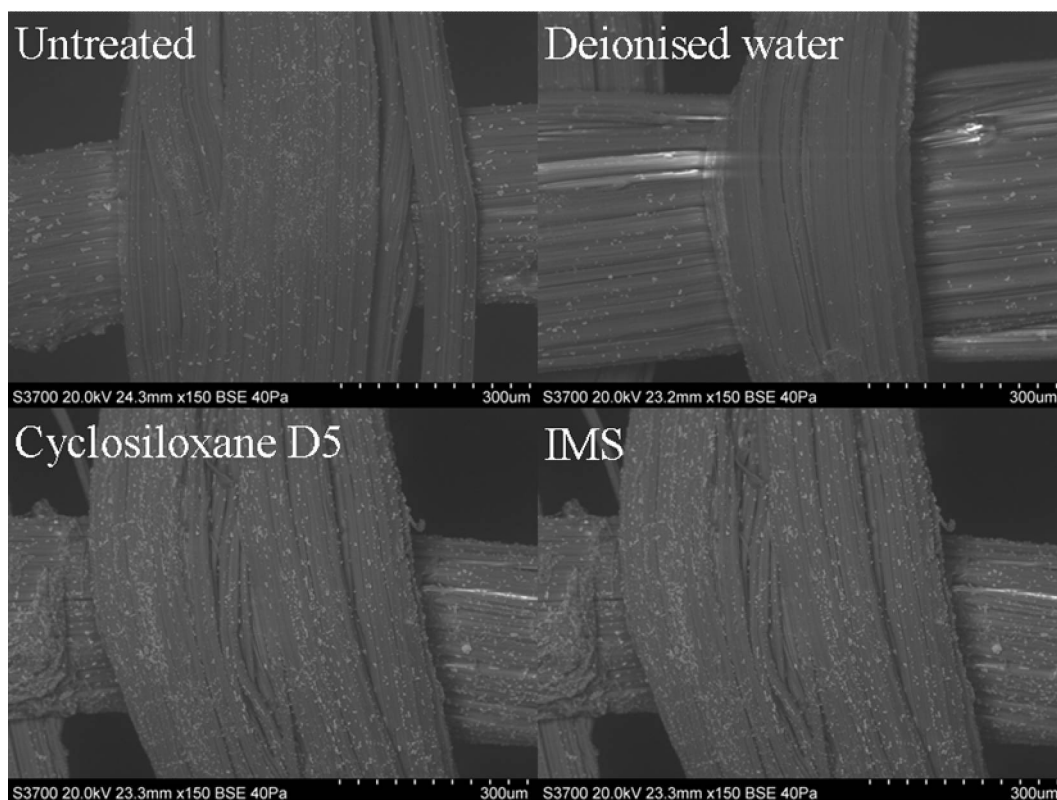


Figure 10.2 SEM micrographs of untreated pre-aged dyed (c1) abaca and pre-aged dyed (c1) abaca that has been immersed for 30 minutes in deionised water, cyclosiloxane D5, or IMS

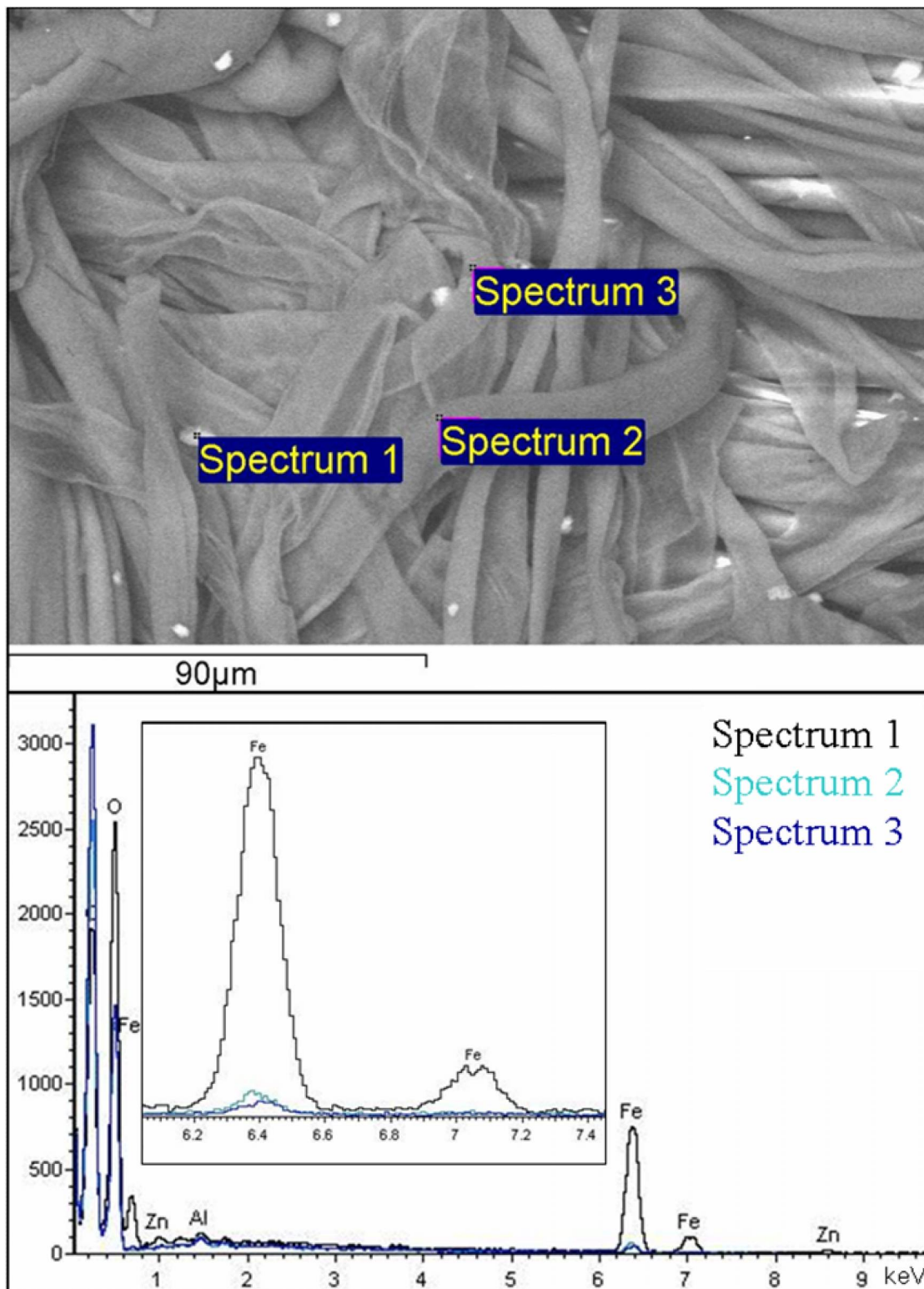


Figure 10.3 SEM micrograph and EDX spectrum of the surface deposits on un-immersed pre-aged dyed cotton. In spectra 1 and 3 a point and an area, respectively, with surface deposits are analysed. In spectrum 2 an area without surface deposits is analysed.

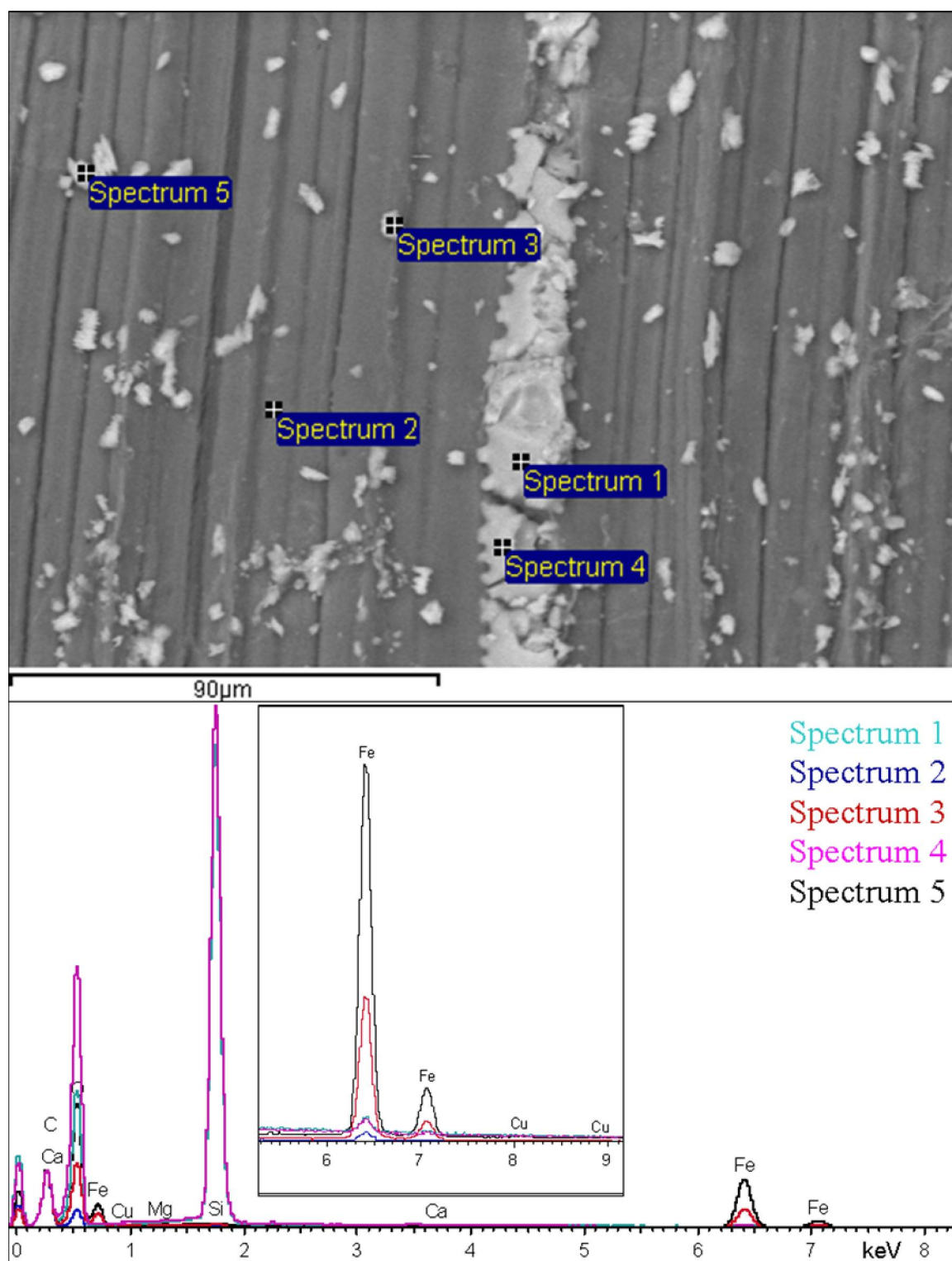


Figure 10.4 SEM micrograph and EDX spectrum of the surface deposits on un-immersed pre-aged dyed abaca. Spectra 1 and 4 are of phytoliths (silicon plant bodies) that are naturally present in abaca.

During immersion there was noticeable dye loss from the samples immersed in the deionised water (Table 10.2). While there was no observable difference between the surfaces of the samples when using microscopy, a difference which supports this dye loss

10.2 Effect of solvent immersion on the conditions of fragile pre-aged model textiles was seen with SEM¹. In the BSE images (Figures 10.1 and 10.2) noticeably fewer surface particles are present in the deionised water-immersed samples than the other samples. The white appearance of these particles is due to the mass/density of the particles being greater than the density of the textile yarns/fibre bundles. In these iron-tannate dyed model textiles, the “white” surface deposits were frequently rich in iron (determined using SEM-EDX analysis, Figures 10.3 and 10.4) and as demonstrated in Chapter 5, are a consequence of the dyeing process. Consequently, the dye that was lost from the deionised water-immersed textiles came, at least to some extent, from the surface of the textiles. A study to quantify the difference in surface particle concentration between samples was not undertaken but while there was little difference between the concentration of particles in the un-immersed, GE-immersed, and IMS-immersed samples, the difference between these and the deionised water-immersed samples was significant.

Fibres were lost in all solvents however the greatest loss occurred in the deionised water (% weight loss in Table 10.2). It is not known if this trend on sample loss was purely an effect of swelling of the fibres due to the water or due to handling, or both.

The samples wet out instantly in the GE and IMS but it took many minutes for them to wet out in the deionised water (Table 10.2). In fact, rather than sinking like the other samples, the cotton floated during the 30 minutes of the test. This could be a problem for the application of aqueous treatments to iron-tannate dyed textiles by, for example, spraying, unless the inclusion of additives in the treatment solution enables faster wetting out of the textile.

Table 10.3 Si content in GE immersed samples determined using XRF

Pre-aged ^a model textile	Solvent	Si XRF ratio ^b
Ac1	H ₂ O	3.1
Cc1	GE	0.2
Cc1	GE	0.0
Ac1	GE	0.1
Ac1	GE	2.0

Notes for Table 10.3:

- 4 weeks at 80°C and 35-80% RH (every three hours)
- (Si peak area/Compton peak area)×1000

¹ The difference in quantity of surface deposits was most noticeable at the lower magnifications of those used. Consequently Figures 10.1 and 10.2 include the micrographs at ×150 magnification rather than ×650 magnification.

10.2 Effect of solvent immersion on the conditions of fragile pre-aged model textiles

The IMS evaporated very quickly, within 30 minutes, while the deionised water and GE-immersed samples generally dried overnight (Table 10.2). The GE can take longer than one day to evaporate fully, though it often looks as though it is fully evaporated much sooner. Many months after immersion XRF results for Si suggested that no GE remained in the samples (Table 10.3). Heat is used to evaporate the GE when it is used in the dry cleaning industry (Grice 2010), however this may not be suitable or feasible for cultural heritage objects. A possible issue arising from rapid evaporation such as that seen with IMS is damage to the fibres due to rapid fibre contraction. In addition, it is possible that the treatment chemical will not be distributed within the fibres as successfully as with water which takes longer to evaporate and therefore has more time to move into the fibres. The cyclosiloxane D5 of GE is a large molecule compared to water or ethanol (the primary component of IMS), and consequently any treatment dissolved in GE may not reach the centre of the fibres being treated due to the size of the cyclosiloxane-D5 molecules. However water present in the fibres may enable diffusion of the treatment further into the fibres from the location at which the GE deposited it.

For health and safety reasons, tests involving IMS were performed in a fume cupboard, unlike the testing with the other solvents. A treatment which used IMS would therefore need to be performed with suitable extraction which could be difficult for larger objects, unless a fume room is available.

10.2.2.2. GPC-MALLS

Table 10.4 Changes in molecular weight, polydispersity index, and carbonyl content in aged (4 weeks aged at 80°C and 35-80% RH cycling every 3 hours) and fragile Cc1 due to immersion in solvents

Solvent	DP _n	Average molecular weight		PDI	% polymer content in				Theoretical amount of reducing end groups (oxidised groups) (μmol/g)	Overall carbonyl content (μmol/g)
		M _n (kg/mol)	M _w (kg/mol)		DP<100	DP100-200	DP200-2000	DP>2000		
None	95	15	126	8	20	15	56	9	65 (12)	77
H ₂ O	268	43	87	2	7	13	79	2	23 (40)	63
GE	278	45	98	2	6	13	78	3	22 (41)	63
IMS	112	18	84	5	18	18	60	4	55 (24)	79

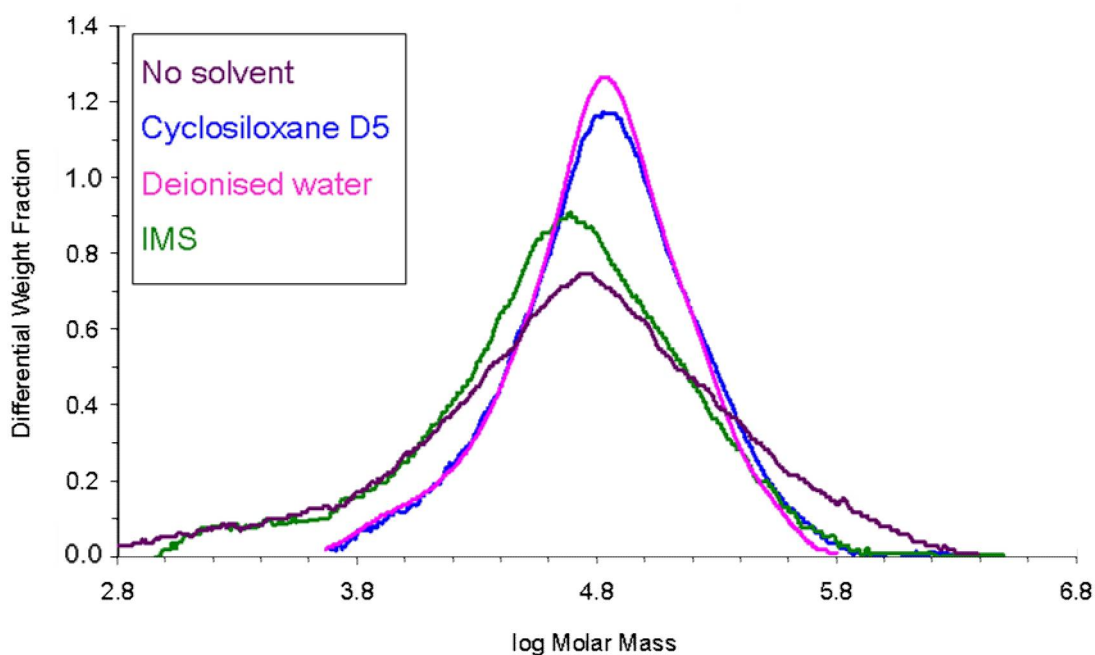


Figure 10.5 The effect of solvent immersion on the molar mass distribution of fragile Cc1 (4 weeks aged at 80°C and 35-80% RH)

Immersion of the fragile dyed cotton sample in water and cyclosiloxane D5 produced a similar change in molar mass distribution (Figure 10.5), similar increase in number average molecular weight (M_n) and DP_n , and decrease in M_w and carbonyl content (Table 10.4). The REG content decreases comparably and the non-REG content (i.e. due to oxidation) increases comparably following immersion in the water and GE compared to no immersion. Increasing M_n and decreasing carbonyl content has also been seen following the washing of historic textiles in water and suggests that low molecular weight carbonyl-containing molecules were removed from the samples during immersion (Henniges, Bjerregaard, Ludwig and Potthast 2011). However in the same study, washing of modern European cotton samples (less than 100 years old) that were in good condition in water for 2 hours caused a decrease in M_w and an increase in carbonyl content i.e. depolymerisation, that was not attributable to experimental error (Henniges, Bjerregaard, Ludwig and Potthast 2011). IMS retained more of the low molecular weight molecules in the model textile sample than the other solvents. This is confirmed by the similar carbonyl content compared with the un-immersed sample though there is a greater quantity of carbonyl groups in the IMS-immersed sample that are attributed to oxidation.

10.2.3 Summary

It is apparent that there are advantages and disadvantages for the use of the solvents tested in treatment applications to weak iron-tannate dyed cultural heritage materials exist for all

of the solvents tested. Loss of material occurred with all the solvents, and even an untreated sample, due to the fragile nature of the samples but it was most prevalent with immersion in deionised water. GPC-MALLS identified that both deionised water and GE caused the loss of low MW molecules. This was confirmed by the decrease in carbonyl content and increase in M_n . IMS had little effect on the carbonyl content and M_n of the fragile aged cotton. Deionised water caused noticeable dye loss to the dyed textiles during immersion, the effect of which was observable at high magnification using VP SEM-EDX. Additionally the slow rate of wetting out of the fragile dyed material in deionised water could cause problems during treatment application. No dye loss or noticeable changes occurred to the surfaces of the IMS or GE immersed samples and both solvents caused rapid or instantaneous wetting out of the samples. However, treatments with IMS require the use of fume extraction which may not be practical for large objects, and the fast evaporation, while useful in terms of a rapid drying time, may cause damage to the weak fibres by rapid swelling and contraction. GE has a significantly longer evaporation time which could be decreased through the use of heat. However this may not be suitable or practical for use on cultural heritage objects. Potentially a combination of solvents such as IMS and water, or IMS and GE may be of use and further investigation of this is needed.

10.3 Treatment Test 2

10.3.1 *Experimental method*

10.3.1.1 Accelerated ageing

Before treatment application (pre-ageing)

Six pieces each of approximately 10 × 15 cm of undyed and dyed (c2, c3, p2, and p3) model textiles of cotton, abaca, wool, and silk were pre-aged (1 week for cellulosic and 4 weeks for proteinaceous samples) at 80°C and 60-80% RH in a Sanyo Gallenkamp Environmental Chamber at the National Gallery, London. Initially the RH was programmed to be 60% but after three days of ageing of the wool and silk this was changed to be 65% since these conditions are used by other researchers in the iron-tannate dye/iron gall ink research field. 65% RH was achieved for at least 2 weeks during the ageing of the wool and silk. However blockages in the drainage of the chamber meant that the RH fluctuated between 65 and 75% RH for at most 1 week of the ageing of the wool and silk, and then between 70-80% for the last week of ageing of wool and silk. This week was also the 1 week of ageing of the cotton and abaca. The samples were stacked by material type i.e. cotton or silk for example, with paper (Munktell CXD pHoton Aqua Forte High Wet Strength absorbent paper, 90 gsm) throughout the stacks to separate

samples of different dye types. Six pieces of each model textile tested was aged to enable application of five treatments whilst retaining one of each material untreated. During pre-ageing the cotton and silk were stacked as c3 or p3, c2 or p2, U with the undyed on the top of the stack and c3 or p3 at the bottom, while the abaca and wool were stacked as c2 or p2, U with the U at the top of the stack.

After treatment application

Accelerated ageing of the treated samples occurred for one week at 70°C and 65% RH. Half of the treated pre-aged samples were prepared for accelerated ageing. The first half was compromised during a malfunction in the environmental chamber at the National Gallery. The second half was then aged in a WK3-180/40 environmental chamber at Camberwell College of Arts. Dyed and undyed textiles were stacked separately and according to treatment type with paper (Munktell CXD pHoton Aqua Forte High Wet Strength absorbent paper, 90 gsm) separating the layers of different model textile types. Cotton tying tape was used to secure the paper and textiles into individual bundles. The sample order in stack was as follows (from bottom to top): wool, silk, abaca, cotton. Within the silk and cotton sections the model textiles were stacked (from the bottom to the top): p3 or c3 then p2 or c2. The wool and abaca sections had p2 or c2 only. All bundles were aged on the same shelf and in six piles, one for each treatment (including untreated). The dyed sample bundles were aged on top of the undyed sample bundles of the same treatment.

10.3.1.2 Treatment application

The samples were immersed in 300 ml of treatment solution for 30 minutes in a plastic tray. Two samples (cotton and silk or wool and abaca of the same dye type) were treated in each tray so that 5 pairs of samples required treatment (Cc3 and Sp3, Cc2 and Sp2, CU and SU, Ac2 and Wp2, and AU and WU). Treatment solutions were prepared at one concentration in 1.5 l quantities and divided into 5 trays for the treatment application. Consequently while the treatment concentration was the same for all materials, the ratio of treatment mass to textile mass differed. After immersion the samples were blotted on paper towel to remove excess solution before being hung to dry, often in a fume cupboard, before further treatment applications or analysis. Paper clips were used to attach the samples to cotton tying tape. A small amount of damage occurred to the samples due snagging of the textiles on the paperclips or the formation of rust marks on textiles (WU sample set C, EBR in IMS

10.3 Treatment test 2

sample before T292 application). Once dry the samples were put into labelled brown paper envelopes.

The concentrations of the treatment solutions are presented in Table 10.5. The concentrations used in treatments B, C, D, and E were equal to those used in Treatment Test 1 however the mass of textile being treated was not the same. The samples were not weighed prior to treatment application and so an accurate measure of the concentration of treatment per mass of textile cannot be calculated. An approximate mass of textiles based on the maximum dimensions of the samples (10 × 15 cm) has been determined after the completion of Treatment Test 2 using data for unaged untreated model textiles. The minimum concentration per mass of textile is therefore also presented in Table 10.5 and differs per pair of model textiles. Note that in Treatment Test 1 the concentrations of treatment solutions were altered to account for differences in masses of the textiles being treated at one time.

Table 10.5 Treatment application conditions for pre-aged model textiles

Set	Chemical	Solvent	Chemical concentration (M)	Chemical mass (g) per 1.5 L	Mass of chemical as % of textile mass						
					CU and SU ^a	Cc2 and Sp2 ^a	Cc3 and Sp3 ^a	AU and WU ^a	Ac2 and Wp2 ^a	Mean	SD
A	None	None									
B	MC (MP)	H ₂ O	0.012	1.480	10	10	10	6	5	8	2
	PA (MP)	H ₂ O	0.002	1.938	13	13	13	8	6	10	3
	CB ^b	H ₂ O	0.037	9.070	63	59	59	36	30	49	13
C	EBR	IMS	0.033	9.600	66	62	62	38	31	52	14
	T292	GE	0.033	43.280	298	279	279	173	142	234	64
D	EBR	IMS	0.033	9.600	66	62	62	38	31	52	14
	T292	IMS	0.033	43.280	298	279	279	173	142	234	64
E	T292	GE	0.033	43.212	298	279	279	173	142	234	64
F	T292	GE	0.163	215.000	1483	1387	1387	860	705	1164	318

Notes for Table 10.5:

- Abbreviations used: cotton (C), abaca (A), wool (W), and silk (S), dye formulation 2 and 3 for cellulosic textiles (c2 and c3), dye formulation 2 and 3 for proteinaceous textiles (p2 and p3), PA (phytic acid), CB (calcium bicarbonate), MC (magnesium carbonate), MP (magnesium phytate), EBR (1-ethyl-3-methylimidazolium bromide), T292 (Tinuvin 292), IMS (industrial methylated spirit), H₂O for deionised water, and GE (cyclosiloxane-D5);
- The data for calcium bicarbonate was estimated by assuming that all of the calcium carbonate that was added to water with CO₂ bubbling through it was converted into calcium bicarbonate. A 1:1 molar ratio between the two chemicals therefore exists and so by calculating the number of moles of calcium carbonate used, the number of moles and the mass, of calcium bicarbonate in 1.5 L was calculated.

Set A remained untreated. Set B (treatment code: MP/2CB) was treated first with a magnesium phytate (MP) solution that was produced by combining magnesium carbonate hydrate (MC) and phytic acid (PA) in water. The source of phytic acid was a ~40% (w/w) solution in water. 4.84 g of the ~40% solution was combined with 1.48 g of MC. The mass

10.3 Treatment test 2

of pure PA is assumed to be 40% of that of the ~40% solution and is noted in Table 10.5. The pH of the MP solution was checked using a Hanna Instruments HI2210 pH meter with HI1131 probe and separate temperature sensor and was determined to be pH 5.71. This was within the pH 4-6.5 range used during the testing of this treatment on iron gall ink on paper and close to the pH 5.8-6.0 range that was identified as showing optimal stabilisation abilities (Kolar, Mozir, Strlic, de Bruin, Pihlar and Steemers 2007). During the application of MP to wool, 4 ml of IMS was added to aid wetting out of the textile. Calcium bicarbonate (CB) was prepared overnight in a pressurised cylinder by bubbling carbon dioxide through 16.8 g of calcium carbonate in 4.5 L of water. The same concentration was used as in Treatment Test 1 and this was approximately 3 times greater than that used in the research into iron gall ink (Kolar, Mozir, Strlic, de Bruin, Pihlar and Steemers 2007) because approximately 3 times more textile mass was being treated per litre than paper mass per litre in the iron gall ink treatment research. Dried samples that had been treated with the MP solution were then treated with two successive applications of CB. No IMS was used to aid wetting out of the wool textiles in these treatment applications however the wool only wet out once it was “scrunched a bit” by hand. Clearly this would not be done to historic materials!

In set C (treatment code: EBR/T292-3) the EBR was applied first to the textiles in IMS. Once these were dry, the T292 was applied to the textiles in GE. In set D (treatment code: EBRT292-3) the treatment chemicals were applied together in the same solution with the same mass of each chemical as was used in set C. In set D IMS was used as the solvent. The use of IMS meant that the samples dried within a few hours but the cotton samples were thought to be a little stiff. For comparison with sets C and D, set E was produced in which only T292 in GE was applied. Finally, in set F a significantly larger quantity of T292 was used in GE.

In set E (treatment code: T292-3)² and set F (treatment code: T292-15) the textiles were treated with a single application of T292 at the appropriate concentration in GE.

Following treatment application and drying the samples were placed in labelled envelopes for storage. Envelopes for treatments D – F showed significant patches where the paper was saturated and darker than usual. Envelope C showed a lesser amount which may have

² The use of the % of solvent mass (3 and 15) rather than the % mass of chemical as % of textile mass (235 ± 64 and 1164 ± 318) has been used in the treatment codes for simplicity.

transferred from the other envelopes. This saturation could be an indication that the GE had not fully evaporated (for E and F) and/or that the surface of the samples was “oily” from the T292 that was present in treatments C-F and which is a liquid at room temperature.

10.3.1.3 Analytical methods for treated samples before accelerated ageing

Handling tests

Following treatment application and drying the treated pre-aged model textiles were assessed for observable changes in colour and handle (surface texture and stiffness) when compared to the untreated equivalent. Pippa Cruickshank, an object conservator at the British Museum, assisted in this assessment, making this analysis as objective and well informed as possible. The abaca was too brittle to be handled and so was assessed for colour change only. Cotton was assessed for handle only since noticeable variation in colour of the cotton sample arising from the pre-ageing process made assessment of variations in colour due to treatment unreliable. Stiffness was assessed by gently folding the samples backwards and forwards while the surface texture was assessed through gently rubbing the samples between thumb and forefinger.

Colorimetry

Colorimetric data was collected over 5 areas per sample as detailed in Section 5.2.4.

Surface pH

A Mettler Toledo InLab surface pH electrode attached to Hanna Instruments HI2210 pH Meter was used to assess the surface pH of the treated dyed samples. Three small pieces of textile were cut from each sample for analysis, each just large enough to cover the pH electrode surface. The pieces were analysed on a clean glass sheet and an average pH and standard deviation per sample were calculated. On each piece, one drop of reverse osmosis purified water from a glass pipette was added and the electrode placed on top. When possible the electrode surface was not placed in direct contact with the textile surface, as advised by Tse (Tse 2007), so that the surface pH rather than a mixture of surface and bulk pH was detected. However, with the majority of the samples this was not possible due to their absorbency which caused immediate dissipation of the water on application rather than allowing the water to remain as a drop on the surface of the textile. On the very absorbent samples the pH was noted after 30 seconds while on less-absorbent samples the pH was recorded once it had stabilised or at 10 minutes, whichever occurred first. The first

of the three samples acted as a guide for the time to expect before recording the pH of the following two analyses of the same sample. The electrode was rinsed with reverse osmosis water in between readings and the glass surface wiped with paper towel.

Prior to analysis glassware was rinsed 8 times with reverse osmosis water to reduce the risk of contamination of the water. Calibration of the electrode was performed using pH 7.01 and pH 4.01 buffer solutions prior to analysis and once more during the analysis to maintain accurate readings. The pH of the water and of a water drop on the surface of the glass was recorded prior to sample analysis.

10.3.1.4 Analytical methods for treated samples after 1 week of accelerated ageing (70°C and 65% RH)

Tensile testing

Treated and untreated cotton, abaca, and silk model textiles were tested as described in Section 5.2.5.1 except that a 10 mm gauge length was used and between 3 and 10 strips were analysed per sample direction (as sample size allowed). Where possible both directions of the cotton textiles were tested and warp or weft directions assigned following evaluation of the results using data from known warp or weft directions as a guide. The strips had been conditioned overnight to 65 \pm 4% RH and 20 \pm 2°C.

Colorimetry

The same conditions were used to analyse the colour of the treated samples prior to and following accelerated ageing as were used to analyse the samples prior to treatment application (Section 10.3.1.3). By directly analysing the samples that were to be aged and comparing the data of the sample before and after ageing, error due to natural variation in dye and treatment distribution has been effectively eliminated.

10.3.2 Results and discussion - Treated pre-aged samples before accelerated ageing

10.3.2.1 Subjective handling tests

Increasing the concentration of T292 resulted in the dyed silk becoming increasingly greasy in surface texture and increasingly dark in colour compared to the untreated. T292-15 resulted in the greasiest and darkest silk and wool. Apart from this treatment, wool showed no noticeable change in colour or handle. T292-15, EBR/T292-3, and EBRT292-3 caused slight but acceptable stiffening of cotton. No changes in colour of abaca due to treatment application were noted though it was difficult to judge accurately due to the

loose weave of the textile. MP/2CB resulted in no consistent changes in handle or colour of the textiles.

The undyed textiles were assessed for colour change only and only silk treated with T292-15 was found to differ noticeably, in this case it was yellower than the untreated.

10.3.2.2 Colorimetry

It is important for a treatment to cause minimal colour change to a sample on application. Consequently, colorimetry was used to objectively quantify the colour change in the model textiles due to treatment application (Table 10.6). The overall change in colour (ΔE_{00}^*) is presented in Figure 10.6. The colorimetric data are as free as possible from error arising from uneven textile colouration since the same sample was analysed before and after treatment application. A ΔE_{00}^* that is equal to or greater than 1.7 indicates a colour difference that is ‘just perceptible’ (Reissland and Cowan 2002) when the fastness grades in ISO 105-A02 (BS EN 20105-A02:1995/ISO 105-A02:1993 1995, 1993) are used as a guide.

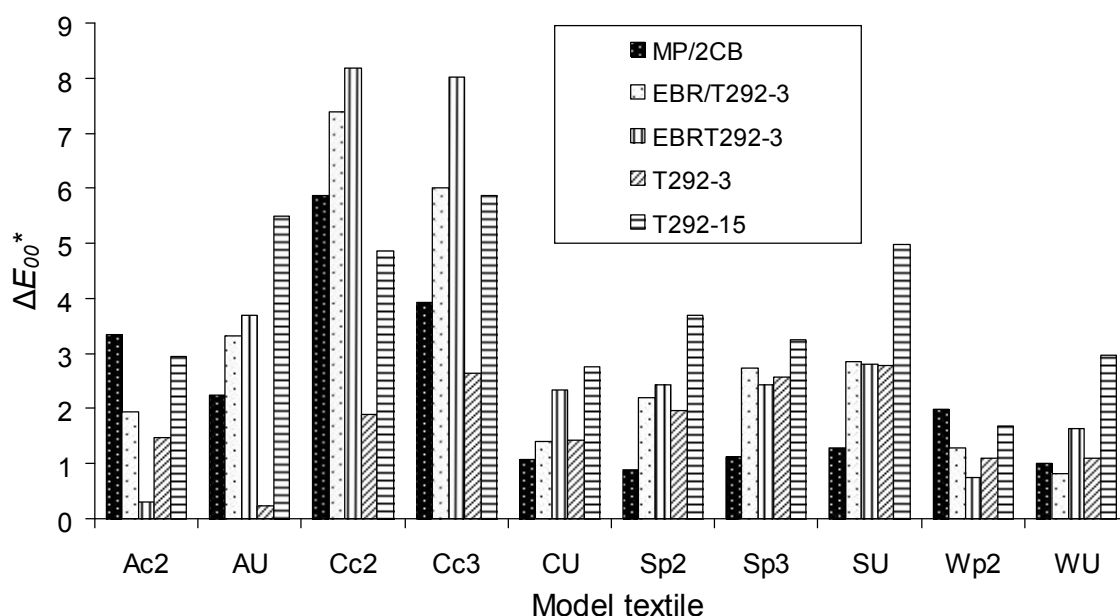


Figure 10.6 Colour change in pre-aged model textiles due to treatment application

Overall the change in colour (ΔE_{00}^*) of the samples varied from 0.2 to 8.2 depending on the treatment applications (Figure 10.6). Over two-thirds of the samples showed an observable colour change on treatment application. All of the treatments caused observable colour change to some if not all textile samples and the most colour change due to

10.3 Treatment test 2

treatment application occurred on the dyed cotton textiles. Treatment application typically caused a decrease in lightness and yellowness of the textiles (Figures 10.7 and 10.9, respectively) and an increase in redness of the model textiles (Figure 10.8).

The change in colour due to the application of treatments to model textiles shows few consistent trends, however a few trends have been identified, each with some exceptions.

Based on ΔE_{00}^* values the highest concentration of T292 caused the greatest colour change in the majority of the model textiles. It darkened the textiles it was applied to (Figure 10.7) and caused small but significant changes in a^* and b^* (Figures 10.8 and 10.9).

The application of MP/2CB often imparted the least changes in overall colour appearance to the model textiles (ΔE_{00}^*) (Figure 10.6). It generally caused the least darkening, in some cases even caused lightening (Figure 10.7), of the samples and generally increased the redness (a^*) of the samples (Figure 10.8). Of all the treatments, it caused the most change in b^* for the cellulosic materials and the least for the proteinaceous (Figure 10.9).

EBRT292-3 and EBR/T292-3 caused frequently large changes in the overall colour (ΔE_{00}^*) and lightness (ΔL^*) of the model textiles on application. Often the difference in colour change due to application of EBRT292-3 and EBR/T292-3 to a particular model textile was small and the greatest difference was in the Δa^* values for Cc2 and Cc3.

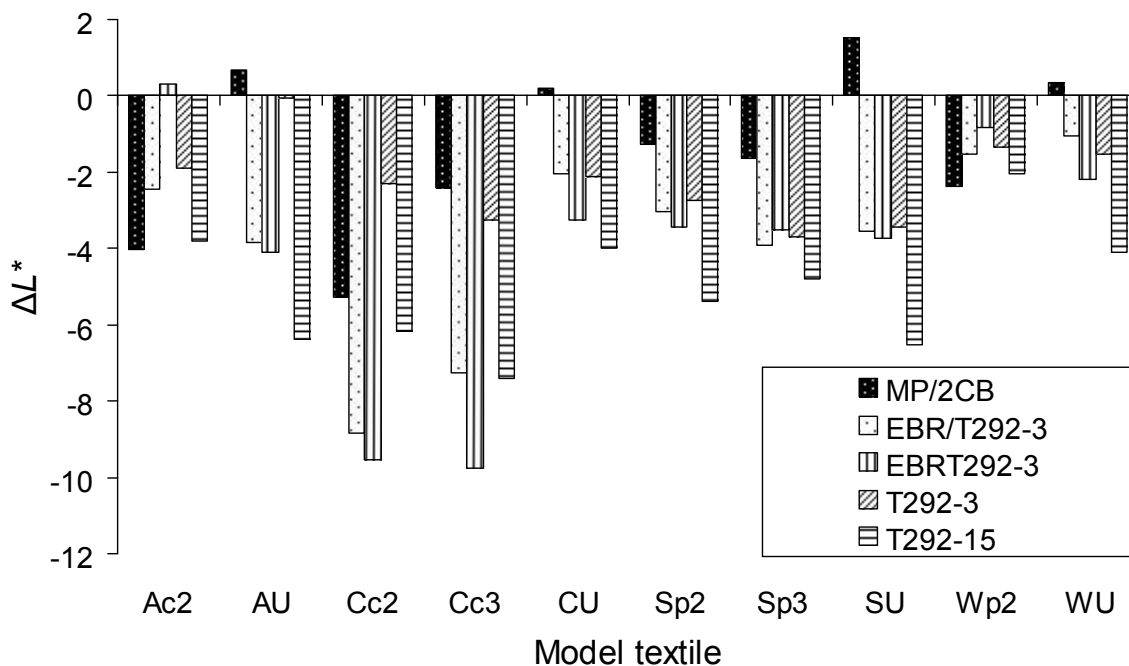


Figure 10.7 The change in lightness of samples due to treatment application

Table 10.6 Colour change in pre-aged model textiles due to treatment application

Model textile	Treatment code	ΔE_{00}^*	ΔL^*	Δa^*	Δb^*
Ac2	MP/2CB	3.3	-4.0	1.0	-1.2
	EBR/T292-3	1.9	-2.4	0.2	-0.9
	EBRT292-3	0.3	0.3	0.1	-0.1
	T292-3	1.5	-1.9	-0.1	-0.6
	T292-15	2.9	-3.8	-0.3	-1.3
AU	MP/2CB	2.2	0.7	-0.9	2.8
	EBR/T292-3	3.3	-3.8	0.0	1.9
	EBRT292-3	3.7	-4.1	0.4	2.4
	T292-3	0.2	-0.1	0.0	-0.4
	T292-15	5.5	-6.4	0.3	0.8
Cc2	MP/2CB	5.9	-5.3	3.0	1.2
	EBR/T292-3	7.4	-8.8	1.0	-2.1
	EBRT292-3	8.2	-9.5	1.7	-2.0
	T292-3	1.9	-2.3	0.0	-0.1
	T292-15	4.9	-6.2	0.2	-0.4
Cc3	MP/2CB	3.9	-2.4	2.4	1.8
	EBR/T292-3	6.0	-7.2	0.3	-2.5
	EBRT292-3	8.0	-9.8	1.1	-2.8
	T292-3	2.6	-3.3	0.1	-0.7
	T292-15	5.9	-7.4	0.1	-1.7
CU	MP/2CB	1.1	0.2	0.3	-1.1
	EBR/T292-3	1.4	-2.0	0.2	0.2
	EBRT292-3	2.3	-3.2	0.2	0.9
	T292-3	1.4	-2.1	0.1	0.0
	T292-15	2.8	-4.0	0.1	0.7
Sp2	MP/2CB	0.9	-1.3	0.1	0.0
	EBR/T292-3	2.2	-3.0	0.0	0.8
	EBRT292-3	2.4	-3.4	0.0	0.7
	T292-3	2.0	-2.7	-0.1	0.6
	T292-15	3.7	-5.4	-0.4	0.5
Sp3	MP/2CB	1.1	-1.6	0.0	0.0
	EBR/T292-3	2.7	-3.9	0.0	0.7
	EBRT292-3	2.4	-3.5	0.0	0.6
	T292-3	2.6	-3.7	0.0	0.6
	T292-15	3.2	-4.8	-0.1	0.5
SU	MP/2CB	1.3	1.5	0.2	-0.7
	EBR/T292-3	2.8	-3.5	0.0	1.4
	EBRT292-3	2.8	-3.7	0.0	0.5
	T292-3	2.8	-3.5	0.0	1.3
	T292-15	5.0	-6.5	-0.1	0.8
Wp2	MP/2CB	2.0	-2.4	0.0	-0.7
	EBR/T292-3	1.3	-1.5	0.2	0.1
	EBRT292-3	0.8	-0.8	0.1	-0.3
	T292-3	1.1	-1.3	0.1	0.0
	T292-15	1.7	-2.0	0.0	-0.4
WU	MP/2CB	1.0	0.4	0.4	-1.2
	EBR/T292-3	0.8	-1.1	0.2	0.3
	EBRT292-3	1.6	-2.2	0.2	0.5
	T292-3	1.1	-1.5	0.2	0.0
	T292-15	3.0	-4.1	0.2	0.0

10.3 Treatment test 2

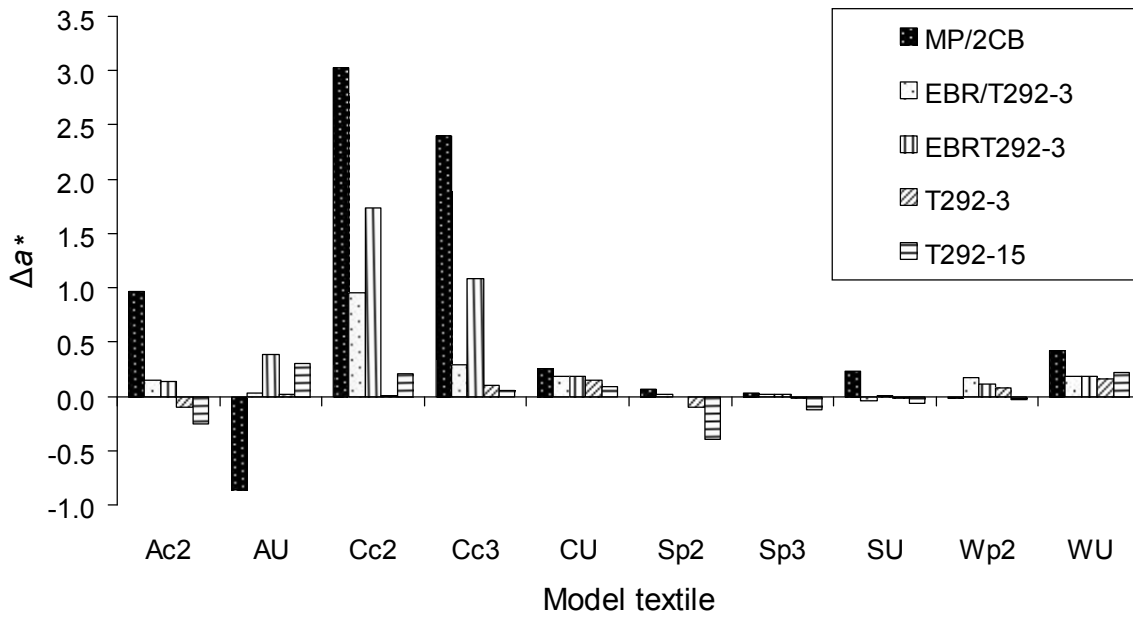


Figure 10.8 The change in redness ($+\Delta a^*$) and greenness ($-\Delta a^*$) of samples due to treatment application

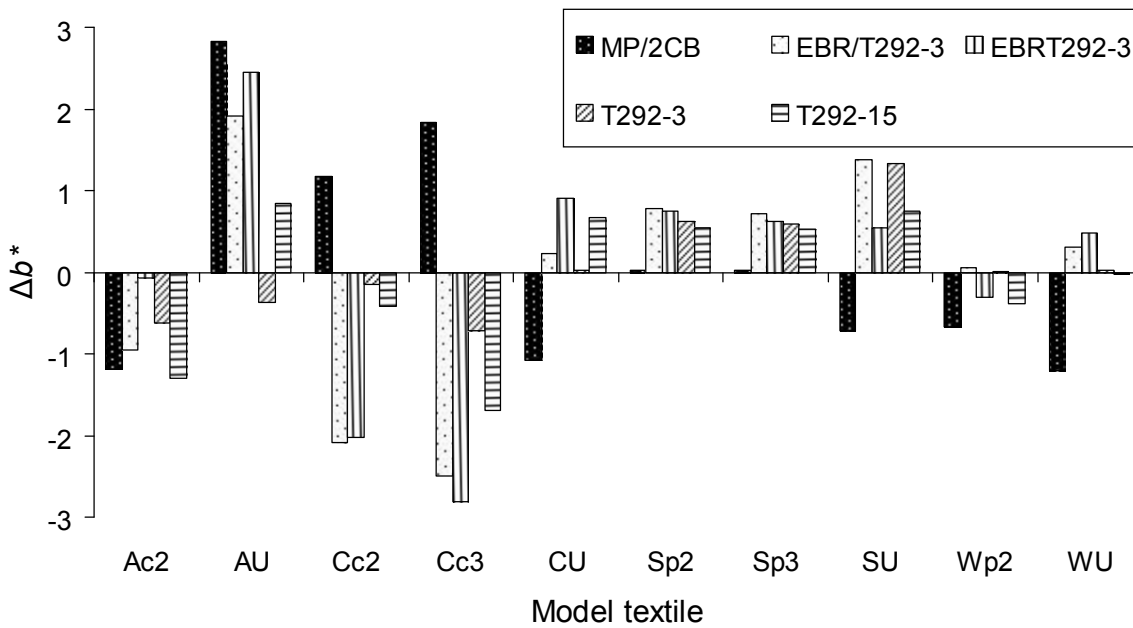


Figure 10.9 The change in blueness ($-\Delta b^*$) and yellowness ($+\Delta b^*$) of samples due to treatment application

10.3.2.3 Surface pH

The cotton and silk dyed textiles were treated together in the same treatment solutions while the abaca and wool samples were treated together separately. Consequently, the surface pH results of the cotton and silk samples are similar (Table 10.7). The silk samples were typically slightly less acidic than the equivalently treated cotton. The surface pH of the equivalently treated abaca and wool samples are less close to one-another than the cotton and silk samples, and wool often has the higher pH after 30 s extraction (Table 10.7). However, close correlation in the surface pH of similarly treated samples was observed between samples of the same textile type i.e. proteinaceous or cellulosic. Clearly the variations in % mass of treatment chemical per mass of textile that are reported in Table 10.5 had no significant effect on the resulting surface pH of the samples.

While the surface pH method may not be as reproducible as hoped due to problems associated with the absorption properties of the textiles, the results are reliable enough to show that all of the treatments increased the pH of the samples by at least 1 pH unit. The treatments involving T292 caused the greatest pH increase. These treatments also changed the water absorption properties of the textiles since they caused the textiles to wet out instantly when the drop of water was added whereas on the untreated and MP/2CB treated samples the water remained in a drop on the surface before the electrode was placed on it. In just 30 seconds the samples treated with T292 indicated a surface pH typically greater than 7 and in many cases greater than pH 8.

Table 10.7 Surface pH of a selection of treated and untreated pre-aged samples prior to accelerated ageing

Textile	Treatment	Sample code	Average pH	SD
Cc2	Untreated ^a	Cc2 A	3.1	0.2
	MP/2CB ^a	Cc2 B	6.0	0.1
	EBR/T292-3	Cc2 C	7.7	0.2
	EBRT292-3	Cc2 D	7.3	0.2
	T292-3	Cc2 E	7.3	0.1
	T292-15	Cc2 F	8.1	0.1
Cc3	Untreated ^a	Cc3 A	3.4	0.1
	MP/2CB ^a	Cc3 B	6.2	0.3
	EBR/T292-3	Cc3 C	7.7	0.0
	EBRT292-3	Cc3 D	6.3	0.8
	T292-3	Cc3 E	6.7	0.5
	T292-15	Cc3 F	7.9	0.1
Ac2	Untreated ^a	Ac2 A	3.0	0.2
	MP/2CB ^a	Ac2 B	6.2	0.4
	EBR/T292-3	Ac2 C	7.7	0.2
	EBRT292-3	Ac2 D	7.7	0.1
	T292-3	Ac2 E	7.6	0.4
	T292-15	Ac2 F	7.7	0.4
Sp2	Untreated ^a	Sp2 A	4.1	0.1
	MP/2CB ^a	Sp2 B	5.5	0.1
	EBR/T292-3	Sp2 C	8.0	0.1
	EBRT292-3	Sp2 D	7.9	0.0
	T292-3	Sp2 E	8.5	0.1
	T292-15	Sp2 F	8.5	0.0
Sp3	Untreated ^a	Sp3 A	4.5	0.1
	MP/2CB ^a	Sp3 B	5.6	0.1
	EBR/T292-3	Sp3 C	7.9	0.0
	EBRT292-3	Sp3 D	7.8	0.0
	T292-3	Sp3 E	8.5	0.0
	T292-15	Sp3 F	8.4	0.1
Wp2	Untreated ^a	Wp2 A	4.0	0.1
	MP/2CB ^a	Wp2 B	5.6	0.1
	EBR/T292-3	Wp2 C	7.9	0.1
	EBRT292-3	Wp2 D	8.3	0.1
	T292-3	Wp2 E	8.8	0.2
	T292-15	Wp2 F	8.7	0.2

Note for Table 10.7:

- a. Length of extraction between 30 s and 10 min. The rest of the samples were extracted for 30 s.

10.3.3 Results and discussion - Treated pre-aged samples after accelerated ageing

10.3.3.1 Colorimetry

Assessment of colour change with ageing of the model textiles has proven a useful indicator of the extent of degradation that has occurred in the samples due to accelerated ageing. Consequently colorimetry has been used here to objectively determine changes in the colour of the treated samples following accelerated ageing. Since the calculation of the colour change in a sample involved data describing the colour of the same sample before and after ageing, any deviation in colour change from the untreated equivalent indicates a direct effect of the treatment on the extent of degradation of the textile. A ΔE_{00}^* lower than that for the equivalent untreated sample suggests that the treatment has decreased the rate of degradation processes that cause the production of or breakdown of coloured compounds. A result such as this suggests that the treatment is successful at protecting the textile from degradation.

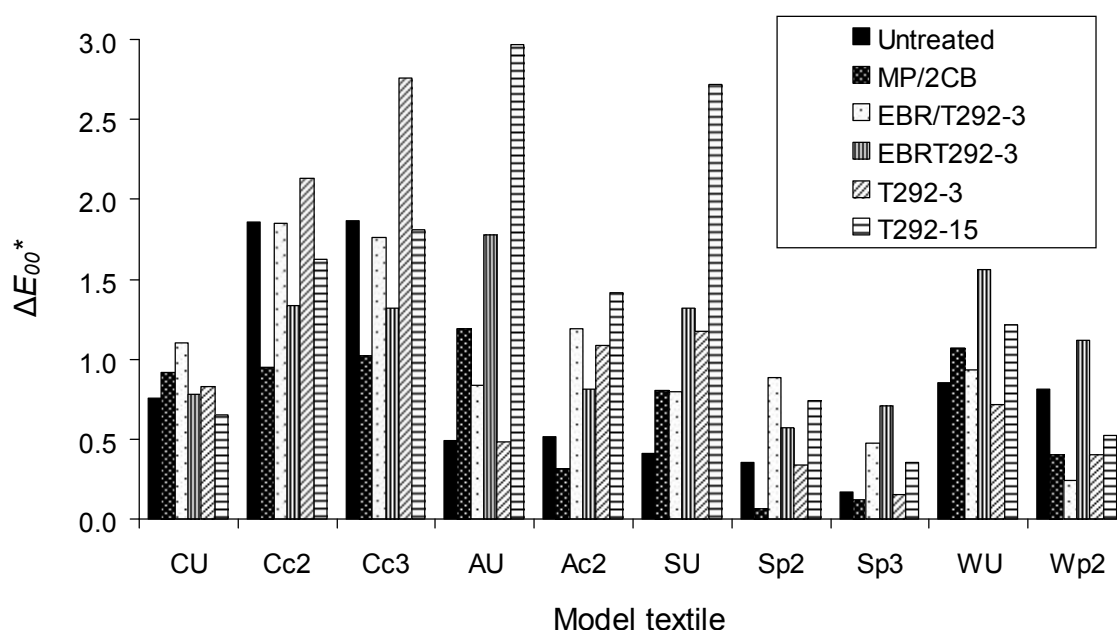


Figure 10.10 The effect of the treatments on the discolouration of pre-aged model textile samples during accelerated ageing (1 week at 70°C and 65% RH)

10.3 Treatment test 2

Table 10.8 The effect of treatments on the discolouration of the pre-aged model textiles during accelerated ageing (1 week at 70°C and 65% RH)

Model textile	Treatment code	ΔE_{00}^*	ΔL^*	Δa^*	Δb^*
CU	Untreated	0.8	-0.5	0.0	0.8
Cc2	Untreated	1.9	-2.0	0.5	0.8
Cc3	Untreated	1.9	-1.4	0.9	1.1
AU	Untreated	0.5	0.0	0.2	0.7
Ac2	Untreated	0.5	-0.3	0.3	0.3
SU	Untreated	0.4	0.3	-0.1	0.4
Sp2	Untreated	0.4	-0.5	0.0	0.1
Sp3	Untreated	0.2	-0.2	0.0	0.1
WU	Untreated	0.9	0.4	-0.1	1.2
Wp2	Untreated	0.8	-0.9	0.0	0.4
CU	MP/2CB	0.9	-0.2	-0.1	1.0
Cc2	MP/2CB	0.9	0.5	-0.5	0.4
Cc3	MP/2CB	1.0	1.1	-0.2	0.6
AU	MP/2CB	1.2	-0.3	0.3	1.7
Ac2	MP/2CB	0.3	0.1	-0.2	-0.1
SU	MP/2CB	0.8	-0.1	-0.2	0.9
Sp2	MP/2CB	0.1	0.0	0.0	0.1
Sp3	MP/2CB	0.1	-0.1	0.1	0.1
WU	MP/2CB	1.1	-0.3	-0.2	1.5
Wp2	MP/2CB	0.4	-0.3	0.0	0.4
CU	EBR/T292-3	1.1	-1.0	0.0	1.0
Cc2	EBR/T292-3	1.9	-1.3	0.9	1.5
Cc3	EBR/T292-3	1.8	-1.5	0.9	1.0
AU	EBR/T292-3	0.8	0.8	0.3	-0.6
Ac2	EBR/T292-3	1.2	-1.3	0.1	-0.8
SU	EBR/T292-3	0.8	0.7	-0.1	0.7
Sp2	EBR/T292-3	0.9	1.2	0.1	0.3
Sp3	EBR/T292-3	0.5	0.7	0.0	0.0
WU	EBR/T292-3	0.9	-0.8	-0.1	1.1
Wp2	EBR/T292-3	0.2	-0.1	0.0	0.3
CU	EBRT292-3	0.8	0.2	0.0	0.9
Cc2	EBRT292-3	1.3	0.4	0.6	1.4
Cc3	EBRT292-3	1.3	0.2	0.7	1.2
AU	EBRT292-3	1.8	2.0	0.2	-1.1
Ac2	EBRT292-3	0.8	-0.8	0.2	-0.5
SU	EBRT292-3	1.3	1.6	0.0	0.6
Sp2	EBRT292-3	0.6	0.7	0.1	0.3
Sp3	EBRT292-3	0.7	1.0	0.1	0.3
WU	EBRT292-3	1.6	-1.8	0.0	1.2
Wp2	EBRT292-3	1.1	-1.3	0.1	0.5
CU	T292-3	0.8	-0.4	0.0	0.9
Cc2	T292-3	2.1	-1.6	0.9	1.4
Cc3	T292-3	2.8	-2.6	1.3	1.1
AU	T292-3	0.5	-0.2	-0.1	-0.7
Ac2	T292-3	1.1	-1.2	0.3	-0.5
SU	T292-3	1.2	1.5	0.0	0.5
Sp2	T292-3	0.3	-0.3	0.1	0.3
Sp3	T292-3	0.2	0.0	0.0	0.1
WU	T292-3	0.7	-0.3	-0.1	1.0
Wp2	T292-3	0.4	-0.2	0.1	0.5
CU	T292-15	0.7	0.1	0.1	0.8
Cc2	T292-15	1.6	-1.1	0.7	1.2
Cc3	T292-15	1.8	-1.5	0.9	0.8
AU	T292-15	3.0	3.3	-0.1	0.1
Ac2	T292-15	1.4	-1.4	0.2	-1.1
SU	T292-15	2.7	3.5	0.0	0.5
Sp2	T292-15	0.7	0.9	0.2	0.3
Sp3	T292-15	0.4	0.4	0.2	0.0
WU	T292-15	1.2	-0.2	-0.2	1.8
Wp2	T292-15	0.5	-0.5	0.1	0.4

10.3 Treatment test 2

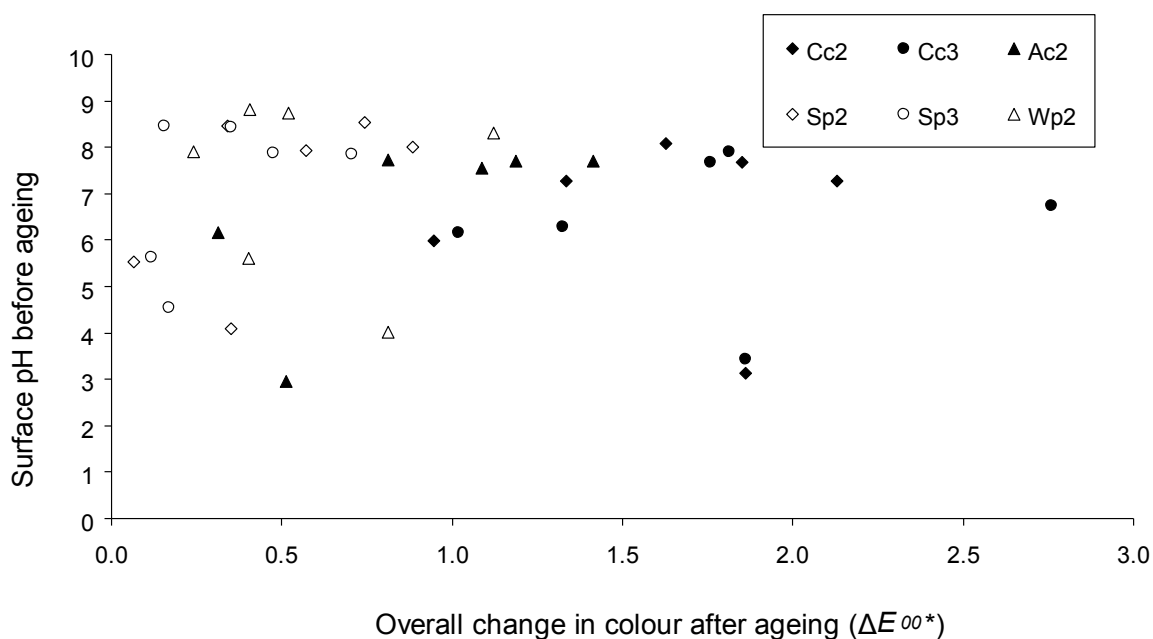


Figure 10.11 Correlation between surface pH of pre-aged samples and overall colour change (ΔE_{00}^*) after further accelerated ageing (1 week at 70°C and 65% RH) for dyed textiles

Figures 10.10, 10.12, 10.13, and 10.15, show that there are few consistent trends in the effects of the treatments on the extent of discolouration to the model textiles during accelerated ageing. There was also little correlation between overall colour change and surface pH prior to accelerated ageing for the proteinaceous textiles (W and S) (Figure 10.11). This may be due to the need for longer ageing times before significant trends occur. The cellulosic samples (C and A) however show a typically positive correlation between overall colour change and initial surface pH with the more alkaline samples suffering greater discolouration during accelerated ageing possibly due to breakdown of the dye complex (Section 4.1.5). The overall colour change for the majority of the samples is less than $\Delta E_{00}^*=1.7$ and so imperceptible or barely perceptible at most (Figure 10.10).

Except for the cotton samples which showed the opposite, the undyed textiles generally showed more discolouration per treatment than the dyed textiles. The cellulosic textiles typically discoloured more than the proteinaceous textiles and are the major type of material with $\Delta E_{00}^* > 1.7$. For CU, Sp2, Sp3, and Wp2 the majority of the treated samples as well as the untreated samples showed a colour change of less than $\Delta E_{00}^*=1$. Generally the cotton dyed textiles discoloured more than the abaca equivalents and frequently the wool textiles discoloured more than the silk.

10.3 Treatment test 2

MP/2CB consistently caused the undyed textiles to change colour more than the untreated equivalents on ageing and the dyed textiles to change colour less than the untreated equivalents. In many cases the MP/2CB treated aged samples showed the least discolouration with ageing. Excepting Wp2, the EBR/T292-3 treatments demonstrated little ability at colour-retention as the treated samples showed equal or greater discolouration on ageing than the untreated equivalents. The combination of the two chemicals in one treatment solution did not improve the effectiveness of the treatment as EBRT292-3 caused greater discolouration to the majority of samples compared to no treatment (Cc2 and Cc3 were the exceptions). In all of the wool samples and most of the silk samples the presence of EBRT292-3 caused greater discolouration to the samples than no treatment or treatment with EBR/T292-3 with ageing. However in the cotton samples the EBR/T292-3 treated samples showed more discolouration than the EBRT292-3 treated alone samples. AU also followed this trend while Ac2 showed the opposite. Neither T292-3 nor T292-15 stabilised the samples with respect to colour-loss. The T292-3 treated cotton, abaca, and silk samples generally resulted in comparable or greater discolouration than the untreated equivalents while T292-3 treated wool showed less discolouration than the untreated after ageing. The use of a greater concentration of T292 in T292-15 resulted in samples that showed greater discolouration than the T292-3 and untreated samples in all cases except the cotton model textiles where less discolouration occurred. Little correlation exists between the surface pH of the treated textiles and the overall change in colour after ageing in this study (Figure 10.11), particularly for the proteinaceous dyed textiles. A small trend for increasing discolouration with initial surface pH occurs for the cellulosic textiles.

The inclusion of EBR100 in the EBR/T292-3 and EBRT292-3 treatments did not cause a consistently lower change in colour of the textiles than the T292-3 treatment. Only in Cc2 and Cc3 was the inclusion of EBR100 beneficial in the retention of colour of the samples.

10.3 Treatment test 2

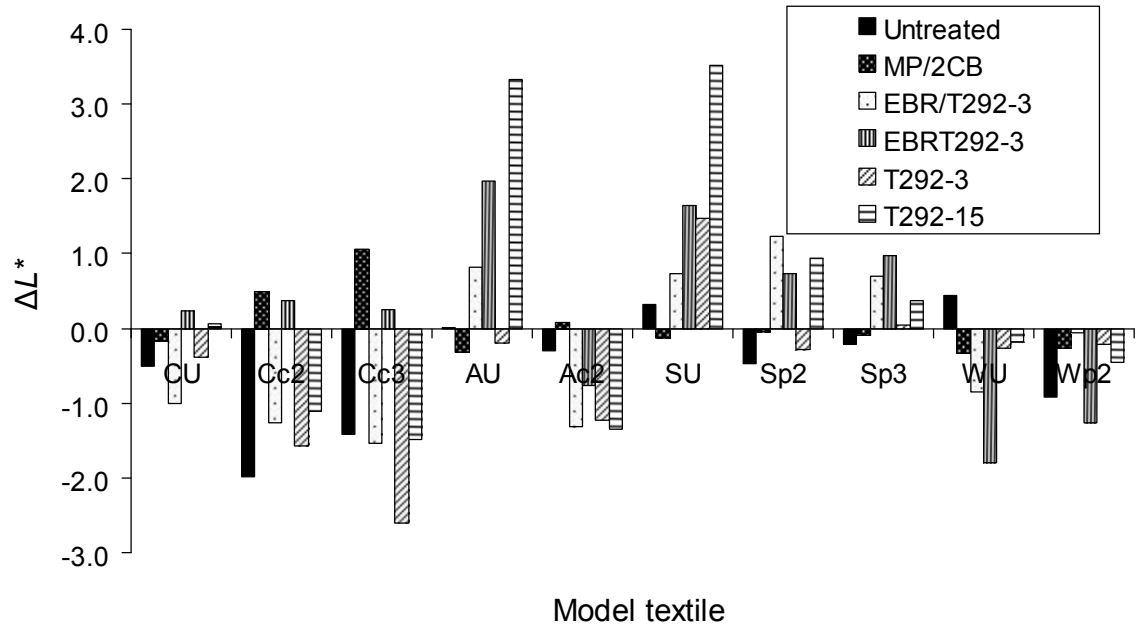


Figure 10.12 The change in lightness of the pre-aged treated samples due to the treatment on accelerated ageing

Often accelerated ageing of the treated and untreated samples caused a darkening of the colour (Table 10.8 and Figure 10.12). Exceptions to this predominantly occur with T292 treated AU and silk textiles.

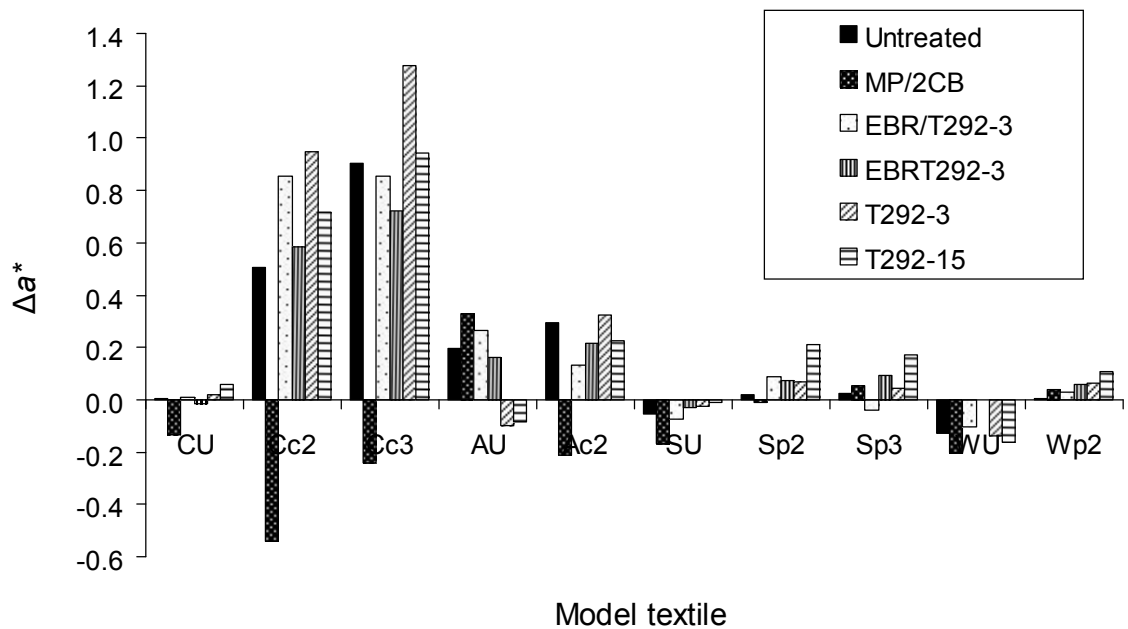


Figure 10.13 The change in redness ($+\Delta a^*$) and greenness ($-\Delta a^*$) of treated and untreated pre-aged samples following accelerated ageing

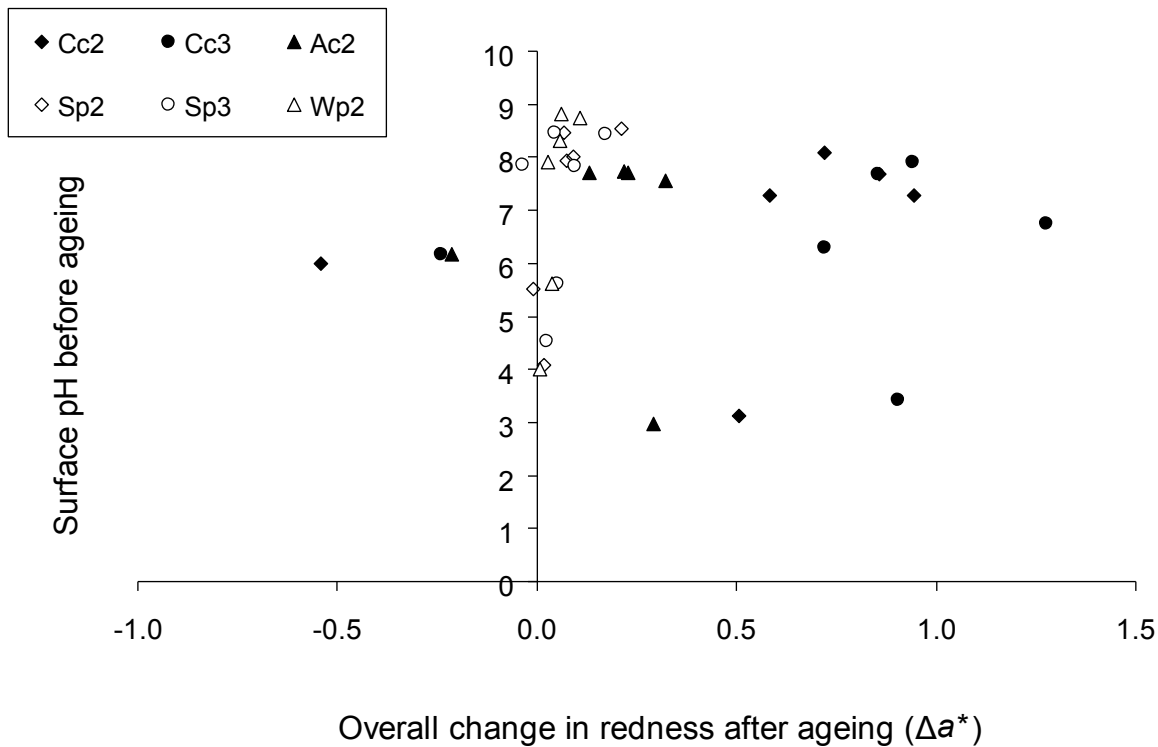


Figure 10.14 Correlation between surface pH of pre-aged samples and change in redness ($+\Delta a$) after further accelerated ageing (1 week at 70°C and 65% RH) for dyed textiles

Excepting the Cc2 and Cc3, the changes in the redness of the samples on ageing were small, being typically lower than 0.4 in magnitude (Figure 10.13). The dyed treated textiles generally showed an increase in redness with ageing, particularly Cc2 and Cc3, for which a positive correlation between the change in redness and initial surface pH can be seen in Figure 10.14. For the proteinaceous textiles there was little correlation between the change in redness and the surface pH (Figure 10.14). As previously discussed, this may be due to the need for a longer ageing period before significant trends occur. Significantly lower changes in redness occurred for the undyed textiles compared to the dyed equivalents. Negligible change in redness occurred in the untreated silk textiles and Wp2. While the treatments involving T292 caused similar or greater increase in redness in the cotton samples than in the equivalent untreated samples the MP/2CB caused a decrease in redness. Excepting Ac2, the use of the T292-3 or T292-15 caused greater increase in redness than no treatment.

10.3 Treatment test 2

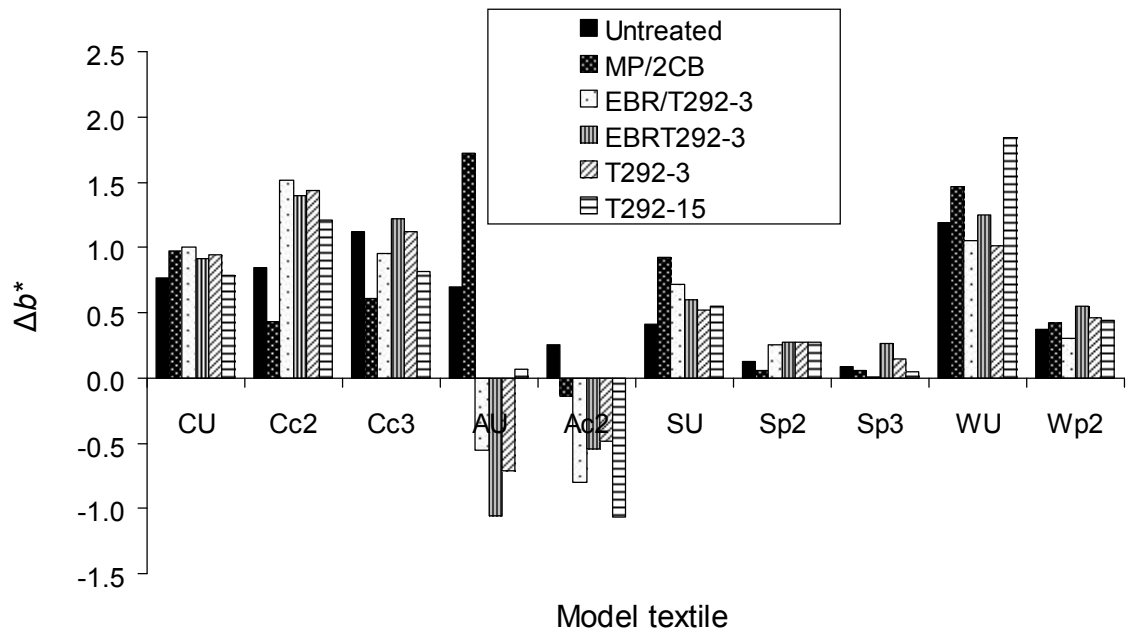


Figure 10.15 The change in blueness ($-\Delta b^*$) and yellowness ($+\Delta b^*$) of treated and untreated pre-aged samples following accelerated ageing

Except for the majority of abaca samples, the effect of accelerated ageing was to increase the yellowness of the textiles (Figure 10.15). The greatest increases in yellowness were often in the cotton samples or WU and the least are often in the dyed silk textiles. The four treatments involving T292 typically caused a comparable or greater change (positive or negative) in yellowness of the textiles than no treatment during ageing. In Cc2 and Cc3 MP/2CB caused the least change in yellowness of all the treatments.

10.3.3.2 Tensile testing

The effects of the treatments on the breaking load and extension properties of the pre-aged model textiles during ageing are presented in Table 10.9 and Figure 10.16. Only three samples show statistically significant differences from the untreated sample (Sp3 T292-315SOL (extension), Ac2 EBRT292-3 (extension), Cc2 (weft) EBRT292-3 (breaking load), and none of these form a consistent trend. A slight improvement in retention of breaking load was noted for all silk samples treated with EBRT292-3, however, the differences were still within the standard deviation of other samples and further testing would be necessary to confirm if this trend is statistically significant.

10.3 Treatment test 2

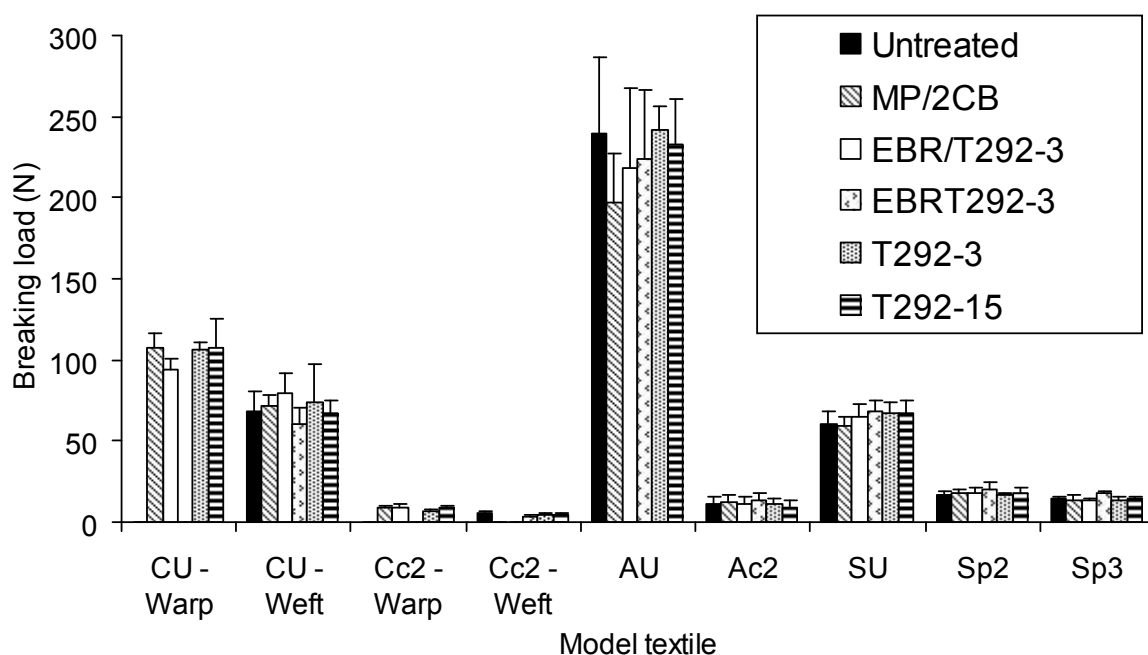


Figure 10.16 The effect of treatments on the breaking load of the model textiles after accelerated ageing

It is possible that a longer period of ageing would have resulted in statistically significant differences between treated and untreated samples because the rate of degradation progressively decreases after the first week of ageing (as determined in accelerated ageing studies of the model textiles). Consequently, while in Treatment Test 1 2 weeks of ageing at 80°C and 65% RH produced significant degradation to previously unaged cellulosic textiles, in this study, the pre-aged nature of the textiles and the lower temperature during ageing means that the extent of degradation (i.e. strength-loss) that will occur in 1 week is less than that with the new, unaged materials. In Treatment Test 1 the silk was aged for 4 weeks after treatment. Consequently the 1 week of ageing and lower temperature used during ageing will have also caused significantly less degradation than seen in Treatment Test 1. A longer period of ageing was not used as there was concern that the untreated cellulosic samples would be too weak to prepare for tensile testing after 1 week of ageing at 70°C and 65% RH.

Table 10.9 The effect of treatments on the breaking load and extension properties of the model textiles after accelerated ageing

Model textile	Treatment code	Breaking load (N)		Extension (%)	
		Average	SD	Average	SD
CU - Warp	Untreated	ND ^a	ND	ND	ND
	MP/2CB	107.10	9.20	26.46	2.32
	EBR/T292-3	93.51	7.02	23.26	3.62
	EBRT292-3	ND	ND	ND	ND
	T292-3	106.60	4.32	21.50	4.05
	T292-15	108.00	16.95	23.20	4.37
CU - Weft	Untreated	68.71	11.39	34.55	8.24
	MP/2CB	71.20	7.15	31.96	4.18
	EBR/T292-3	79.69	11.61	34.04	6.14
	EBRT292-3	59.93	10.55	33.28	9.70
	T292-3	73.33	24.27	35.00	14.02
	T292-15	66.97	7.84	36.83	13.29
Cc2 - Warp	Untreated	ND	ND	ND	ND
	MP/2CB	9.11	1.50	11.20	7.49
	EBR/T292-3	9.33	1.32	8.99	2.93
	EBRT292-3	ND	ND	ND	ND
	T292-3	6.47	1.54	9.49	4.16
	T292-15	9.28	0.84	7.43	1.18
Cc2 - Weft	Untreated	5.75	0.94	39.55	18.30
	MP/2CB	ND	ND	ND	ND
	EBR/T292-3	ND	ND	ND	ND
	EBRT292-3	3.61	0.78	26.35	2.24
	T292-3	4.88	0.44	31.06	6.90
	T292-15	4.44	0.86	24.50	8.58
AU	Untreated	239.90	46.36	10.64	1.26
	MP/2CB	197.30	30.43	11.76	1.57
	EBR/T292-3	218.30	48.77	11.92	1.61
	EBRT292-3	224.40	42.52	10.59	1.21
	T292-3	241.40	14.96	12.94	1.34
	T292-15	232.90	27.91	11.82	1.94
Ac2	Untreated	11.56	4.05	2.58	0.54
	MP/2CB	12.01	4.65	2.61	0.75
	EBR/T292-3	11.29	4.73	2.29	0.43
	EBRT292-3	13.40	4.41	1.63	0.34
	T292-3	10.80	3.66	2.56	0.48
	T292-15	9.51	3.58	1.93	0.69
SU	Untreated	59.89	8.40	52.00	10.47
	MP/2CB	59.30	5.52	50.29	9.39
	EBR/T292-3	64.85	7.65	55.73	7.60
	EBRT292-3	68.33	6.65	57.81	7.03
	T292-3	67.51	6.44	53.97	3.87
	T292-15	67.65	6.94	61.23	11.57
Sp2	Untreated	16.53	1.95	71.44	22.28
	MP/2CB	17.85	2.44	57.30	34.92
	EBR/T292-3	17.71	4.07	48.75	27.92
	EBRT292-3	20.31	3.87	37.32	17.99
	T292-3	16.71	1.60	38.50	26.58
	T292-15	17.98	2.94	31.70	11.17
Sp3	Untreated	14.02	2.19	58.98	20.94
	MP/2CB	13.43	3.33	49.36	21.82
	EBR/T292-3	13.36	1.75	42.08	24.94
	EBRT292-3	17.40	1.91	34.47	20.26
	T292-3	13.24	2.44	57.62	28.33
	T292-15	14.02	1.41	27.94	4.19

Notes for Table 10.9:

a. Not done.

10.3.4 *Identification of most successful treatments*

The 1 week of ageing used in this study was insufficient to cause consistently significant differences in tensile properties of the treated samples compared to the untreated equivalents. Few consistent trends exist in the effect of the treatments on the textile colour following ageing. The most significant trend is that the aqueous MP/2CB decreased the extent of discolouration of the dyed textiles more than any other treatment. The other treatments frequently had no effect on the colour of the textile with ageing or caused greater discolouration. The inclusion of EBR with T292 did not cause any significant difference in the colour of the textiles after ageing compared to the equivalent T292 treated samples. With a greater extent of accelerated ageing trends are likely to become clearer, more pronounced and therefore more reliable. Since the accelerated ageing results cannot be used to determine the most successful treatments the results for the effect of treatment application and solvent application on the textiles must be used to indicate which treatments are most promising. Based on the results from the solvent tests treatments involving non-aqueous solvents, particularly IMS, it appears that the solvents caused lower loss of dye, fibres, and, in the case of IMS, low M_n molecules, than water. GE is more environmentally friendly than IMS and does not require the use of fume extraction during use but it takes a significantly longer time to evaporate than IMS, particularly when heat is not employed. Possibly a combination of GE and IMS therefore would be of use in further studies. Both of these solvents wet out the textiles faster than water.

Based on the results from the application of the treatments to the model textiles it is clear that all of the treatments, but particularly the non-aqueous treatments that include T292, tested show promise due to the increase in surface pH that the treatment imparts to the textile. This increase in pH that is assumed to also occur within the textile, though to possibly a lesser extent, will slow down the rate of acid hydrolysis. However, care must be taken to ensure that the textile does not become too alkaline since this can cause the breakdown of the iron-tannate dye complex which will cause changes in colour to the textile and can also accelerate alkaline hydrolysis. A possible indication of dye discolouration with increasing initial surface pH occurred with the cellulosic dyed textiles when considering the overall colour change, and particularly the change in redness, after ageing and the initial surface pH (Figures 10. 11 and 10.14). The breakdown of the iron-tannate complexes in iron gall ink in both acid and alkaline environments is why Reissland (Reissland 2001) recommends that alkaline treatments have a pH no greater than 8.5 and that the treated iron gall inked paper have a pH between 5 and 8.5.

T292 is promising as a non-aqueous treatment chemical but more investigation needs to be made to determine if the “greasiness” imparted to storage envelopes was due to T292 or un-evaporated GE. If due to T292 the point at which this becomes undesirable needs to be determined. A “greasy” residue on the surface of the textile may attract dirt which is undesirable. The majority of the non-aqueous treatments used in this study also caused an immediate and perceptible colour change to all of the model textiles. The highest concentration of T292 often caused the greatest colour change in a model textile. A darkening of the dyed textiles often occurred. Treatments involving T292 caused yellowing of the undyed abaca, cotton, and silk, particularly. However, lower concentrations may still be suitable. Additionally, the increase in hygroscopicity that the T292 treatment imparted to the textiles may make the textile fibres more responsive to moisture content in the atmosphere. This could result in the fibres being more responsive to fluctuating environmental conditions and possibly more susceptible to damage through moisture-related expansion and contraction than in the less hygroscopic fibres. Further testing is needed to determine if this does have a negative impact on the stability of the textiles.

In Treatment Test 1 the beneficial impact of T292 and MP/2CB on the stability of dyed cotton and silk textiles after two and four weeks of ageing (80°C, 65% RH) was clear. In this study, the effect of the selected treatments was less clear after one week of ageing at a lower temperature (70°C, 65% RH). If a longer ageing period had been used in this study it is possible that differences in the stabilising properties of the different treatments would become apparent. However, it is also possible that none of the treatments would have been successful since they are not consolidants and the textiles to which they were applied were pre-aged and weak. For cultural heritage objects that are at high risk of mechanical damage during handling due to their weakness, consolidation treatments rather than deacidification and antioxidant treatments may be the best stabilisation treatment option. This has been suggested for iron gall ink on paper drawings (Strlic, Csefalvayova, Kolar, Menart, Kosek, Barry, Higgitt and Cassar 2010) in a study in which a DP of 400 was used as a classification for paper objects of ‘high risk of mechanical damage’. Future research into stabilisation treatments for iron-tannate dyed textiles could involve the combination of antioxidants and deacidifiers with consolidants for textiles that are showing signs of mechanical weakness. Additionally, a study to determine when a developed stabilisation treatment should be applied to iron-tannate dyed textiles is necessary to ensure the most benefit is gained from the treatment.

10.3.5 *Summary*

Perceptible and often large colour changes occurred to the textiles on application of the treatments. The highest concentration of T292 caused the greatest colour change in many of the textiles. Yellowing of the undyed textiles occurred with the non-aqueous treatments due to T292. Significant increase in surface pH occurred to the textiles following treatment application. The treatments including T292 caused large changes, particularly the highest concentration of T292. The highest concentration of T292 caused a noticeable “greasiness” to the surface of the silk and wool.

Accelerated ageing resulted in changes in tensile properties of the textiles that were statistically insignificant. Few trends in spectrophotometry data also occurred. These suggest that only the aqueous MP/2CB treatment was successful at slowing down the discolouration that occurs in the untreated samples. The non-aqueous treatments either had no stabilisation effect on the colour change of the textiles on ageing or caused slightly greater discolouration. A longer period of accelerated ageing may have caused statistically significant changes to become apparent and is needed before a judgement can be made on which treatment is most successful at stabilising the textiles.

10.4 Conclusions

Using pre-aged model textiles, a range of treatments have been tested for their effectiveness in stabilising already fragile cultural heritage materials. The results of the ageing experiments are inconclusive since statistically significant differences in tensile properties did not occur in the time frame used. In future studies a longer period of ageing should be used on similarly pre-aged textiles. In studying the effect of solvents on fragile iron-tannate dyed textiles it was found that immersion in water resulted in undesirable effects such as dye loss and a greater extent of fibre loss. Less of these effects occurred with the non-aqueous solvents confirming the need for a non-aqueous stabilisation treatment to be developed. The treatments tested included the most successful non-aqueous strength-retaining antioxidant from Treatment Test 1 with the most successful colour-retaining treatment. Their solubility in the same solvent, IMS, opens great possibilities for a treatment that retains both strength and colour of iron-tannate dyed textiles. The combination of IMS and GE solvents is also an area for further study as it may result in a more environmentally friendly and less harmful solvent that dries faster than GE and slower than IMS alone. The latter could decrease stress on the fragile fibres through slower expansion and contraction rates. T292 is still a potentially useful stabilisation treatment

10.4 Conclusions

particularly as it can significantly raise the pH of the acidic iron-tannate dyed textiles, however, there are some issues that need further investigation including possible “greasy” surface residue and yellowing of undyed textiles.

11 CONCLUSIONS AND FURTHER WORK

11.1 Conclusions

Many conclusions have been derived from this research study and how they address the three aims of the project is discussed below.

11.1.1 Model iron-tannate dyed textiles

The method of developing model iron-tannate dyed textiles based on knowledge from the literature research and subsequent experimentation has been shown to be effective in this project. Through analysis (colour, pH, XRF, GPC-MALLS, EPR, tensile testing) of the model textiles before and after ageing and comparison where possible with results from historic materials, the cotton, abaca, and silk model textiles have been validated for use as substitutes for historic iron-tannate dyed organic materials. The decision to create dyes based around the key ingredients of iron sulphate and tannic acid rather than recreating specific historical dye formulations has been successful. The inclusion of copper (II) ions in dye formulations c2/p2 and the use of natural tannin extracts in dye formulations c3/p3 caused slightly greater degradation in terms of strength loss and discolouration than the combination of iron(II) ions and tannic acids (c1/p1). For example, after 28 days of ageing (70°C and 65% RH) both Cc2 and Cc3 had lost approximately 92% of their breaking load and exhibited colour changes of $\Delta E_{00}^* = 12.4$ and 11.7, respectively while Cc1 had lost approximately 90% of its breaking load and exhibited a colour change of $\Delta E_{00}^* = 9.6$. Sp2 and Sp3 lost approximately 94% of their breaking load and exhibited a colour change of approximately $\Delta E_{00}^* = 2.0$ compared to the 93% and $\Delta E_{00}^* = 1.9$ of Sp1 after 39 days of ageing at 70°C and 65% RH. Using SEM-EDX of cross-sections of the dyed wool fibres it was apparent that the wool had been ring dyed only which is the likely cause of the lack of strength loss seen in these textiles during ageing. The use of a higher temperature during the dyeing process would have improved dye penetration into the fibre core and the subsequent dye-catalysed degradation would have caused similar strength loss to that observed with the other fibres.

11.1.2 Accelerated ageing

Following the assessment of a range of possible accelerated ageing conditions (all without light) 80°C and 65% RH were chosen for use in the treatment tests, in part due to the usage of these conditions in previous iron gall ink research. More importantly however, these conditions were close to the 80°C and 58% RH that caused measurable strength-loss and discolouration in 1-4 weeks of exposure to the dye formulation 1 dyed cotton (81% decrease in breaking load and $\Delta E_{00}^* = 10.49$ by 2 weeks of ageing), abaca (94% decrease

11.1 Conclusions

in breaking load and $\Delta E_{00}^* = 4.54$ by 2 weeks of ageing), and silk (47% decrease in breaking load and $\Delta E_{00}^* = 3.27$ by 4 weeks of ageing), as required by one of the three aims of the project. Consequently the model iron-tannate dyes were shown to accelerate the degradation of these substrates. As previously discussed the dyed wool textiles did not lose strength during accelerated ageing however longer ageing times and/or more extreme ageing conditions may have resulted in a measurable change. Alternatively the analysis of yarns rather than woven textiles may have identified degradation on a smaller scale to that in the other dyed model textiles. 70°C and 65% RH were used in a range of tests that were performed later in the project to decrease the stress on the environmental chambers which had undergone several malfunctions throughout the project.

The use of cycling rather than stable RH conditions in accelerated ageing tests caused little if any statistically significant differences in the property changes occurring in the samples. For example, after 4 weeks of ageing cycling RH led to a breaking load and colour change (ΔE_{00}^*) of 3.2 ± 0.4 N and 14.5, respectively for Cc1 while stable RH led to a breaking load and colour change (ΔE_{00}^*) of 6.2 ± 0.7 N and 13.2, respectively. Also after 4 weeks of ageing cycling RH led to a breaking load and colour change (ΔE_{00}^*) of 35.5 ± 2.6 N and 2.7, respectively for Sp1 while stable RH led to a breaking load and colour change (ΔE_{00}^*) of 33.2 ± 6.1 N and 3.3, respectively. Due to the increased stress that the cycling conditions put on the environmental chambers available for this study, stable RH conditions were chosen for this project.

11.1.3 Treatments

The hindered amine light stabiliser Tinuvin 292, non-aqueous deacidifier magnesium ethoxide, and aqueous iron gall inked paper stabilisation treatment magnesium phytate/calcium bicarbonate all imparted significant stabilisation to the cotton and silk model textiles that were tested (particularly the higher concentrations). The DP_n of the 2 week aged treated Cc3 textiles was 645, 350, 604, and 197 for T292-260, ME30, MP30/2CB30, and untreated aged samples respectively. The breaking load of the Sp3 samples treated with the highest concentrations of the above chemicals decreased by 40-50% after 4 weeks of ageing compared to the 85% decrease of the untreated. However, all these have caused significant colour changes e.g. on application to Cc3 and after 2 weeks of ageing: ME60 (4.4 and 5.68); T292-260 (2.1 and 7.2); MP30/2CB30 (7.3 and 6.0); and untreated (N/A, 10.8) and on application to Sp3 and after 4 weeks of ageing: ME60 (5.4 and 4.7); T292-260 (2.4 and 3.3); MP30/2CB30 (1.5 and 3.6); and untreated (N/A, 4.74).

11.1 Conclusions

Nevertheless, optimisation could help to minimise these colour changes particularly those on application and accordingly these treatments should be considered for further study. The lack of strength-retention afforded by the 1-ethyl-3-methylimidazolium bromide (Cc3: $DP_n = 106$ after 2 weeks of ageing; Sp3: approximately 89% loss of breaking load by 4 weeks of ageing) was surprising as it has been highlighted as a potential new stabilisation method for iron gall inked paper with and without magnesium ethoxide. It was however the most successful treatment of those tested at colour-retention with only a colour difference of 5.1 for Cc3 (2 week ageing) compared to the untreated equivalent's 10.8, and 3.2 for Sp3 (4 week aged) compared to the untreated equivalent's 4.7. Therefore in future studies, it would be interesting to combine this chemical with magnesium ethoxide, Tinuvin 292, or other chemicals capable of retaining the strength of iron-tannate dyed textiles during ageing. Etidronic acid and Tinuvin 144 could also be of further interest, however the use of the hazardous tetrachloroethylene as a solvent for Tinuvin 144 makes Tinuvin 144 a less favoured option for optimisation. A deacidifier would be needed with etidronic acid. Since the concentration of antioxidants can greatly affect their pro- and antioxidant properties some of the other chemicals tested in this project may still be of use at different concentrations. Cyclosiloxane D5 and IMS have been effective solvents in these studies and future work could investigate mixtures of the solvents to decrease the toxicity and drying time of the treatments.

The aqueous magnesium phytate/calcium bicarbonate treatment has been shown to be an effective stabiliser on the cotton and silk dyed textiles. It may be suitable in some cases for use on iron-tannate dyed organic materials when they are in good condition and particularly if a water/alcohol mixture is used to reduce dye loss. The damaging effects of water to fragile iron-tannate dyed materials were demonstrated in the preliminary experiments of Treatment Test 2 to be greater than those occurring with cyclosiloxane D5 or IMS.

It is now evident that remedial stabilisation treatments need to be applied when the textiles are still strong in order to slow down their degradation. Application to objects that are already weak and at risk of mechanical damage is expected to be of little benefit. This was tested in Treatment Test 2 but the results were inconclusive and ideally need further evaluation.

11.2 Original contributions to knowledge

There have been many original contributions to the field of conservation science derived from this study and these are detailed below:

11.2.1 *Model iron-tannate dyed textiles*

The model textiles for this project were chosen to expand our knowledge of the effect of iron-tannate dyes on the substrates they colour. It was identified in the literature that there was a significant body of research into understanding the degradation mechanisms of and the stabilisation methods for iron gall ink on paper made from cotton fibres. This was useful for this project due to the chemical similarity of iron gall ink and iron-tannate dye. However, very little research has been published on these areas for iron-tannate dyed materials and the studies that were available were published on New Zealand flax, raffia, and silk yarns, none of which were in the form of woven fabric. Therefore the scale of production of the model textiles for this project is unprecedented (~80 m² dyed textile produced) and required the use of industrial dyeing equipment. This has usefully resulted in the creation of a materials resource that can provide the platform on which to continue this research. The use of these woven cotton, abaca, silk, and wool model textiles in this project has provided original contributions to this field including assessing the effect of iron-tannate dyes on both cellulosic and proteinaceous woven materials, and the effect of a range of antioxidants and deacidifiers on the stability of the model textiles.

11.2.2 *Analytical techniques*

EPR has rarely been applied to cultural heritage materials and certainly not as an innovative quantitative probe for iron-tannate dyed cultural heritage or model textiles in order to determine the presence and type of radicals and EPR-active metal ion species present. Additionally as the sample was recoverable the use of EPR in the field of conservation could be expanded to further study other degradation mechanisms in historic textiles.

GPC-MALLS had been used to study the efficacy of the phytate treatment on iron gall inked paper. An original contribution has been made through the use of this technique on the iron-tannate dyed model textiles. Just as with the iron gall inked paper it has confirmed the ability of the magnesium phytate/calcium bicarbonate treatment to stabilise the iron-tannate dyes as well as aiding in the knowledge of the degradation of the model textiles, the effect of immersion in different solvents, and the effect of accelerated ageing.

11.2 Original contributions to knowledge

Little has been published on identification methods for iron-tannate dyes. Analysis of a range of objects from the British Museum's collection has shown the usefulness but also the limitations of using XRF to identify the presence of the dye. XRF is an essentially non-destructive surface analytical technique which is useful in the analysis of cultural heritage. The XRF results however are expected to be affected by the structure of the surface and at present there is a lack of standards available to make XRF a quantitative technique for iron-tannate dyed organic materials. Other techniques such as atomic absorption spectrometry may be more suitable for quantitative analysis but the destruction of the sample is not ideal and the analytical instruments are unlikely to be available in the majority of conservation or even conservation science departments. Bathophenanthroline test papers can be useful on cellulosic materials but are not effective on proteinaceous textiles. From the results of this PhD it is advisable to decide if an object is highly likely to be iron-tannate dyed based on its iron content (higher than background level using XRF, bathophenanthroline testing, or other method), condition (weak, brittle), history of production (if known), and colour (black, grey, or brown). Identifying the presence of tannins as well as iron, e.g. using HPLC, would be the most accurate method of determining if an object is iron-tannate dyed.

11.2.3 Antioxidant and deacidifiers for iron-tannate dyed organic materials

The aqueous magnesium phytate/calcium bicarbonate treatment is an improvement on the calcium phytate/calcium bicarbonate treatment that has been accepted for use on iron gall inked cultural heritage. It has rarely been applied to iron-tannate dyed textile materials and when it has, usually yarns or fibre bundles have been treated rather than woven materials. Consequently the use of this treatment and analysis of its efficiency on the woven dyed model textiles in this study is an original contribution to this field, as is the testing of the non-aqueous treatments, a few of which had also been used on iron gall inked paper.

11.2.4 The study of a range of historic objects at the British Museum

Samples from historic objects at the British Museum and the Museum of Islamic Art, Berlin as well as several Axminster carpets have been analysed using XRF. Consideration of their colour, and condition as well as iron content has led to the identification of a range of objects that are highly likely to contain iron-tannate dyes. This information will aid decisions regarding the most beneficial storage, exhibition, and treatment conditions.

11.3 Retrospective changes to this project

Having completed the project it is apparent with hindsight that various aspects could have been approached differently. These include:

1. Weighing the samples before and after treatment application in a conditioned environment to determine how much treatment chemical was taken up by the sample;
2. Measure the pH of samples by cold extraction rather than surface pH testing and remove CO₂ from the water used in the tests;
3. Study the dyed wool samples through tensile testing of the woollen yarns and more detailed investigation of changes to the surface of the fibres using SEM;
4. Use longer accelerated ageing times, particularly for the silk and wool model textiles to monitor their degradation preferably to the end of their useful lifetime;
5. Investigate the ends of broken yarns using SEM to determine if changes in the breaks occur with increasing age of the textiles;
6. Use SEM to investigate changes in the surface of the model textiles with accelerated ageing. This was planned but due to time limitations was not achieved in the project;
7. Analyse textiles as close to the time of treatment application or completion of accelerated ageing as possible to limit error introduced through degradation that could occur on storage;
8. Consistently analyse the same sample before and after treatment application or accelerated ageing to eliminate error due to natural variations between samples. In Treatment Test 2 this method was used but it was not used prior to this;
9. Use higher concentrations of etidronic acid than used in this study and combining 1-ethyl-3-methylimidazolium bromide with magnesium ethoxide as has been used on iron gall inked paper.

11.4 Further work

11.4.1 *Optimisation of treatments*

There are still challenges (e.g. discolouration) with the successful treatments from this research that would need to be resolved before the treatments could be applied to historic objects. Additionally, it would be interesting to further investigate combinations of different chemicals to see if synergistic effects occur that could further improve the efficiency of the chemicals. In particular, the effects of etidronic acid (at higher concentrations than used in this project) combined with a deacidifier, the combination of 1-ethyl-3-methylimidazolium bromide with magnesium ethoxide as has been used in iron

gall ink research and/or Tinuvin 292, TPEN which is a chemical that has shown promise on iron gall inked paper in water but which is soluble in non-aqueous solvents, and tannins which are applied in water which would be of interest to investigate further.

11.4.2 *Application method investigation*

A study to determine the most effective method of applying an optimised non-aqueous treatment to model textiles is necessary before application of the treatment to an historic object can occur. The application method would need to be easy to use and acquire for conservation studios and cause no physical damage to the object during treatment application or drying. Collaboration with conservators and curators would be of great benefit in this study since their opinions on acceptable levels of risk to the objects will be invaluable. A reapplication programme may be needed if the treatments involve chemicals that are used up during the stabilisation process.

11.4.3 *Light ageing of the dyed model textiles*

In this research only dark ageing of the model textiles has been undertaken. This is suitable for the consideration of the stability of treated model textiles stored or exhibited within a museum environment however, prior to acquisition by the museum the object may have been exposed to light. It would therefore be beneficial to determine the effect of light on the stability of the dyed model textiles to aid in the understanding of the catalytic degradation that is caused by the dye.

11.4.4 *Lifetime ageing studies of iron-tannate dyed cultural heritage*

The initiation of or continuation of analysis of iron-tannate dyed model textiles and cultural heritage over many years will enable the validity of the current thinking of the degradation of iron-tannate dyed organic materials to be established. By monitoring objects within a museum environment the most damaging degradation mechanisms in that environment can be identified and treatment options adapted if necessary.

11.4.5 *Use longer accelerated ageing times*

Accelerated ageing of the iron-tannate dyed model textiles from this study for longer than 4 weeks and using a variety of conditions would further improve understanding of the degradation of these materials.

11.4.6 *Application to a modern iron-tannate dyed textile*

Once a treatment has been developed and fully optimised it would be beneficial for it to be applied to a modern iron-tannate dyed textile (e.g. bogolanfini or piu piu) and to monitor the condition of this during natural and accelerated ageing before accepting the treatment for use on cultural heritage materials.

11.4.7 *Determination of acceptable levels of change to an object during treatment*

For a treatment to be accepted in the conservation community it will need to cause minimal adverse changes to the objects. Exactly what constitutes as a minimal and acceptable level of change to an object during treatment is at present uncertain. A method of achieving such information would be to hold a workshop in which conservators, conservation scientists, and curators are asked their views on acceptability of a range of variations in textile properties e.g. colour and handle, that arise during treatment application. These could be quantitatively analysed e.g. using colorimetry for colour change, and an approximate level of acceptable change in these properties determined.

11.4.8 *Methods of iron-tannate dye identification*

For a stabilisation treatment involving antioxidant and deacidifier to be of most benefit it should be applied when the object is still strong. Therefore it is important to identify the presence of iron-tannate dyes before significant degradation has occurred. The identification of rapid, preferably low technology methods of identification that either already exist or could be developed would be beneficial. At present the bathophenanthroline tests are used by some conservators but this analysis does not provide positive results on iron-tannate dyed wool and silk. In this study it was considered that objects were iron-tannate dyed if their method of production was known to involve the combination of iron ions and tannins. If the method of production was unknown it was considered that objects were highly likely to be iron-tannate dyed if they were black, grey, or brown, if they had unusually high iron content, and particularly if they were in poor condition (i.e. weak and brittle).

11.4.9 *Further investigation into iron-tannate dyed objects in the British Museum's collection*

A study aimed at locating iron-tannate dyed objects within the British Museum's collection, assessing their condition, and identifying the organic material that is dyed would enable better informed decisions regarding the preservation and conservation of iron-tannate dyed objects at the British Museum to be made than can be made at present. By identifying the

11.4 Further work

location of objects of similar material type and condition, more time-efficient treatments such as bulk treatment can be considered. Additionally, since the stated material type of many of the iron-tannate dyed British Museum objects mentioned in Chapter 6 was informed by curatorial information which can be inaccurate or misleading, it is recommended that separate analytical testing to confirm the material types occurs.

REFERENCES

- Airey, K., R. D. Armstrong and T. Handyside (1988). "The use of molybdates combined with etidronic acid as corrosion inhibitors for iron." Corrosion Science **28**(5): 449-460.
- Ali, M. A. and T. Konishi (1998). "Enhancement of hydroxyl radical generation in the Fenton reaction by alpha-hydroxy acid." IUBMB Life **46**(1): 137-145.
- Alliance Technical Sales Inc (2012). A guide to pH measurement - the theory and practice of laboratory pH applications, Alliance Technical Sales Inc.
- Al-Malaika, S. (1993). Autoxidation. Atmospheric oxidation and antioxidants. G. Scott. Amsterdam, Elsevier Science Publishers B.V. **1**: 45-82.
- Andrade Jr., R. G., L. T. Dalvi, J. M. C. Silva Jr., G. K. B. Lopes, A. Alonso and M. Hermes-Lima (2005). "The antioxidant effect of tannic acid on the in vitro copper-mediated formation of free radicals." Archives of Biochemistry and Biophysics **437**: 1-9.
- Andrade Jr., R. G., J. S. Ginani, G. K. B. Lopes, F. Dutra, A. Alonso and M. Hermes-Lima (2006). "Tannic acid inhibits in vitro iron-dependent free radical formation." Biochimie **88**: 1287-1296.
- Anonymous (1898). "Black Silks." Textile Colorist **20**(237): 287-288.
- Armecin, R. B. and F. M. Gabon (2008). "Biomass, organic carbon and mineral matter contents of abaca (*Musa textilis* Nee) at different stages of growth." Industrial Crops and Products **28**: 340-345.
- Arts Council England (2010). Cultural capital: A manifesto for the future.
- Aruoma, O. I., A. Murcia, J. Butler and B. Halliwell (1993). "Evaluation of the antioxidant and prooxidant actions of gallic acid and its derivatives." Journal of Agricultural and Food Chemistry **41**: 1880-1885.
- Aspland, J. R. (1997). Textile dyeing and coloration. Triangle Park, American Association of Textile Chemists and Colorists.
- ASTM D778-97 (2002). Standard test methods for hydrogen ion concentration (pH) of paper extracts (hot-extraction and cold-extraction procedures), ASTM International.
- ASTM D1795-96 (2001). Standard test method for intrinsic viscosity of cellulose, ASTM International.
- ASTM D2165-94 (2000). Standard test method for pH of aqueous extracts of wool and similar animal fibers, ASTM International.
- ASTM D5034-95 (2001). Standard test methods for breaking force and elongation of textiles fabric (grab method), ASTM International.
- ASTM D5035-95 (2003). Standard test methods for breaking force and elongation of textiles fabric (strip method), ASTM International.
- ASTM D5804-97 (2002). Standard test methods for zero-span tensile strength ("Dry zero-span tensile"), ASTM International.
- ASTM D6188-97 (2008). Standard test method for viscosity of cellulose by cuprammonium ball fall, ASTM International.
- Atkins, P. and J. de Paula (2002a). Processes at solid surfaces. Atkins' Physical Chemistry. Oxford, Oxford University Press: 977-1012.
- Atkins, P. and J. de Paula (2002b). Atkins' physical chemistry. Oxford, Oxford University Press.
- Atkins, P. and J. de Paula (2002c). Spectroscopy 3: magnetic resonance. Atkins' physical chemistry. Oxford, Oxford University Press: 579-627.
- Attanasio, D., D. Capitani, C. Federici, M. Paci and A. L. Segre (1995a). Electron paramagnetic resonance and ^1H and ^{13}C NMR study of paper. Multidimensional spectroscopy of polymers ACS Symposium Series 598. M. W. Urban and T. Provder. Washington, DC, American Chemical Society: 333-353.

References

- Attanasio, D., D. Capitani, C. Federici and A. L. Segre (1995b). "Electron spin resonance study of paper samples dating from the XV to the XVIII century." Archaeometry **37**: 377-384.
- Ayed, N. and A. Alatrache (1997/1998). Traditional recipes for natural dyeing of wool in the south of Tunisia. Dyes in History and Archaeology 16/17, Lyons, 11-12 December 1997 and Greenwich, 26-27 November 1998, Lyons and Greenwich, Archetype Publications.
- Bacci, M., A. Casini, C. Cucci, M. Picollo, B. Radicati and M. Vervat (2003). "Non-invasive spectroscopic measurements on the Il ritratto della figliastra by Giovanni Fattori: Identification of pigments and colorimetric analysis." Journal of Cultural Heritage **4**(4): 329-336.
- Baird, H. C. (1850). The dyer and colour maker's companion. Philadelphia, Henry C. Baird.
- Balla, J., T. Kiss and R. F. Jameson (1992). "Copper(II)-catalyzed oxidation of catechol by molecular oxygen in aqueous solution." Inorganic Chemistry **31**(1): 58-62.
- Ballard, M. and N. S. Baer (1989). "Conservation I: Halogenated hydrocarbons dry-cleaning solvent." The International Journal of Museum Management and Curatorship **8**(3): 336-341.
- Bancroft, E. (1813). Philosophy of permanent colours. London, T. Cadell and W. Davies. **2**: 338-486.
- Banik, G. (2009). "Scientific conservation: Transfer of scientific research on ink corrosion to conservation practice - does it take place?" Restaurator **30**: 131-146.
- Banik, G. (2011). Dissociation of water: Acids and bases. Paper and Water: A guide for conservators. G. Banik and I. Bruckle. London, Butterworth-Heinemann: 57-80.
- Banwell, C. N. and E. M. McCash (1994). Spin resonance spectroscopy. Fundamentals of molecular spectroscopy. Maidenhead, McGraw-Hill Publishing Company: 199-257.
- Bansa, H. (1998). "Aqueous deacidification - with calcium or with magnesium?" Restaurator **19**: 1-40.
- Bansa, H. (2002). "Accelerated ageing of paper: Some ideas on its practical benefit." Restaurator **23**(2): 106-117.
- Baranski, A., D. Dutka, R. Dziembaj, A. Konieczna-Molenda and J. M. Lagan (2004). "Effect of relative humidity on the degradation rate of cellulose: Methodology studies." Restaurator **25**(1): 68-74.
- Baranski, A., J. M. Lagan and T. Lojewski (2005). Acid-catalysed degradation. Ageing and stabilisation of paper. M. Strlic and J. Kolar. Ljubljana, CIP: 93-109.
- Bardet, M., G. Gerbaud, L. Le Pape, S. Hediger, Q. K. Tr  n and N. Boumlil (2009). "Nuclear magnetic resonance and electron paramagnetic resonance as analytical tools to investigate structural features of archaeological leathers." Analytical Chemistry **81**: 1505-1511.
- Barker, K. (2002). Iron gall and the textile conservator, Philadelphia, North American Textile Conservation Conference 2002.
- BASF (2010). Irganox[®] 1425.
- Batra, S. K. (1998a). Other long vegetable fibers. Handbook of Fiber Chemistry. M. Lewin and E. M. Pearce. New York, Marcel Dekker, Inc. **15**: 505-575.
- Batra, S. K. and A. J. Turner (1998b). The structure of textile fibres. Plant fibre and processing: A handbook. C. Jarman. Rugby, Intermediate Technology Publications: 32.
- Baty, J. W., C. Maitland, W. Minter, M. A. Hubbe and S. K. Jordan-Mowery (2010). "Deacidification for the conservation and preservation of paper-based works: A review." BioResources **5**(3): 1955-2023.
- Begin, P. L. and E. Kaminska (2002). "Thermal accelerated ageing test method development." Restaurator **23**(2): 89-105.
- Bendak, A., W. M. Raslan and M. Salama (2008). "Treatment of wool with metal salts and their effects on its properties." Journal of Natural Fibres **5**(3): 251-269.

References

- Bereck, A. (1990). Bleaching of pigmented fibres using copper salt catalysts. 8th International Wool Textile Research Conference, Christchurch New Zealand, Wool Research Organisation of New Zealand (Inc.).
- Bhattacharya, S. D. and A. K. Shah (2000). "Metal ion effect on dyeing of wool fabric with catechu." Journal of the Society of Dyers and Colourists **116**: 10-12.
- Bicchieri, M. and S. Pepa (1996). "The degradation of cellulose with ferric and cupric ions in a low-acid medium." Restaurator **17**: 165-183.
- Bicchieri, M., M. Monti, G. Piantanida and A. Sodo (2008). "All that is iron-ink is not always iron-gall!" Journal of Raman Spectroscopy **39**(8): 1074-1078.
- Bicchieri, M., M. Monti, G. Piantanida, F. Pinzari, S. Iannuccelli, S. Sotgiu and L. Tireni (2012). "The Indian drawings of the poet Cesare Pascarella: non-destructive analyses and conservation treatments." Analytical and Bioanalytical Chemistry **402**(4): 1517-1528.
- Billmeyer, F. W. and M. Saltzman (1966). Principles of color technology. London, Interscience Publishers.
- Bird, C. L. (1972). The theory and practice of wool dyeing. Bradford, The Society of Dyers and Colourists.
- Bird, F. J. (1876). The dyer's hand-book. Manchester, John Heywood.
- Bogaard, J. and P. M. Whitmore (2001). "Effects of dilute calcium washing treatments on paper." Journal of the American Institute for Conservation **40**(2): 105-123.
- Booth, J. E. (1968). Principles of textile testing - An introduction to physical methods of testing textile fibres, yarns and fabrics. London, Butterworths.
- Bors, W., C. Michel and K. Stettmaier (2000). "Electron paramagnetic resonance studies of radical species of proanthocyanidins and gallate esters." Archives of Biochemistry and Biophysics **374**(2): 347-355.
- Botti, L., O. Mantovani and D. Ruggiero (2005). "Calcium phytate treatment of corrosion caused by iron gall inks: Effects on paper." Restaurator **26**(1): 44-62.
- Boutaine, J. L., B. David and C. Dudley (2006). Chapter 1 The modern museum. Physical Techniques in the Study of Art, Archaeology and Cultural Heritage, Elsevier. **1**: 1-39.
- Brady, P. R. (1990). Penetration pathways of dyes into natural protein fibres. 8th International Wool Textile Research Conference, Christchurch New Zealand, Wool Research Organisation of New Zealand (Inc.).
- Bray, W. C. and H. A. Liebhafsky (1931). "Reactions involving hydrogen peroxide, iodine and iodate ion. I. Introduction." Journal of American Chemical Society **53**: 38-44.
- Brilli, M., L. Conti, F. Giustini, M. Occhiuzzi, P. Pensabene and M. De Nuccio (2011). "Determining the provenance of black limestone artifacts using petrography, isotopes and EPR techniques: the case of the monument of Bocco." Journal of Archaeological Science **38**(6): 1377-1384.
- Broadbent, A. D. (2001). Basic principles of textile coloration. Bradford, Society of Dyers and Colourists.
- Bruckle, I. (2011). Structure and properties of dry and wet paper. Paper and Water: A guide for conservators. G. Banik and I. Bruckle. London, Butterworth-Heinemann: 81-119.
- Bruckle, I. (2011a). Aqueous treatment in context. Paper and Water: A guide for conservators. G. Banik and I. Bruckle. London, Butterworth-Heinemann: 419-436.
- Bruker AXS. (2012). "What is a Handheld XRF spectrometer and how can it help you?" Retrieved 12/06/12, 2012, from <http://www.bruker-axs.com/xrf-basics.html>.
- Bruker Nano GmbH. (2012, 12/06/12). "ARTAX - Portable μ -XRF spectrometer." from http://www.bruker-axs.com/fileadmin/user_upload/pdf_pool/BAXS/Technical%20Documents/Product_s_BrukerNano/Product_Info_uXRF/Bro_artax_8p_en_rev1_1_lowres.pdf.

References

- BrukerAXS. (2009, 22/09/09). "ARTAX - Ideal for valuable objects: non-destructive chemical analysis on the spot." Bruker AXS Retrieved 22/09, 2009, from <http://www.bruker-axs.de/artax.html>.
- Brunello, F. (1973). The Classical Period. The Art of Dyeing. Vicenza, Neri Pozza Editore: 87-116.
- BS 6288-3:1996/ISO 5630-3:1996 (1996). BS 6288-3:1996, ISO 5630-3:1996 Accelerated ageing for paper and board - Part 3: Method for moist heat treatment at 80°C and 65% relative humidity London, British Standards Institution.
- BS 6388-1:1991/ISO 5630-1:1991 (1991). BS 6388-1:1991, ISO 5630-1:1991 Accelerated ageing of paper and board - Part 1: Method for dry heat treatment at 105°C. London, British Standards Institution.
- BS 6388-2:1987/ISO 5630-4:1986 (1987, 1986). BS 6388-2:1987, ISO 5630-4:1986 Accelerated ageing of paper and board - Part 2: Method for dry heat treatment at 120°C or 150°C. London, British Standards Institution.
- BS EN 20105-A02:1995/ISO 105-A02:1993 (1995, 1993). BS EN 20105-A02:1995, ISO 105-A02:1993 Textiles. Tests for colour fastness. Grey scale for assessing change in colour. British Standards Online.
- BS EN ISO 1974:2012 (2012). Paper. Determination of tearing resistance. Elmendorf method, British Standards Institution.
- BS EN ISO 2758:2003 (2002). Paper. Determination of bursting strength, British Standards Institution.
- BS EN ISO 3071:2006 (2006). BS EN ISO 3071:2006 Textiles - Determination of pH of aqueous extract. London, British Standards Institution.
- BS ISO 5351:2010 (2010). Pulps - Determination of limiting viscosity number in cupri-ethylenediamine (CED) solution, ISO.
- BS ISO 5630-5:2008 (2008). BS ISO 5630-5:2008 Paper and board - Accelerated ageing Part 5: Exposure to elevated temperature at 100°C. London, British Standards Institution.
- BS ISO 5630-6:2009 (2009). BS ISO 5630-6:2009 Paper and board - Accelerated ageing Part 6: Exposure to atmospheric pollution (nitrogen dioxide) London, British Standards Institution.
- BS ISO 5626:1993 (1994). Paper. Determination of folding endurance, British Standards Institution.
- BS ISO 15361:2000 (2001). Pulps. Determination of zero-span tensile strength, wet or dry, British Standards Institution.
- Budnar, M., J. Simcic, M. Ursic, Z. Rupnik and P. Pelicon (2006). Transition metals in historical documents, determined by In-Air PIXE. Iron Gall Inks: On Manufacture, Characterisation, Degradation and Stabilisation. M. Strlic and J. Kolar. Ljubljana, National and University Library: 141-146.
- Bulow, A., P. Begin, H. Carter and T. Burns (2000). "Migration of volatile compounds through stacked sheets of paper during accelerated ageing part II: Variable temperature studies." Restaurator **21**(4): 187-203.
- Bulska, E., B. Wagner and M. G. Sawicki (2001). "Investigation of complexation and solid-liquid extraction of iron from paper by UV/VIS and Atomic Absorption Spectrometry." Microchimica Acta **136**(1): 61-66.
- Burgess, H. (1991). "The use of chelating agents in conservation treatments." The Paper Conservator **15**: 36-44.
- Burkinshaw, S. M. and N. Kumar (2008). "A tannic acid/ferrous sulfate aftertreatment for dyed nylon 6,6." Dyes and Pigments **79**: 48-53.
- Calvini, P. and A. Gorassini (2002). "The degrading action of iron and copper on paper: A FTIR-deconvolution analysis." Restaurator **23**(4): 205-221.
- Calvini, P. and A. Gorassini (2006). "On the rate of paper degradation: Lessons from the past." Restaurator **27**(4): 275-290.

References

- Calvini, P., A. Gorassini and A. L. Merlani (2007). "Autocatalytic degradation of cellulose paper in sealed vessels." Restaurator **28**(1): 47-54.
- Caple, C. (2000). Conservation skills: Judgement, method and decision making. London, Routledge.
- Capitani, D., V. Di Tullio and N. Proietti (2012). "Nuclear magnetic resonance to characterize and monitor cultural heritage." Progress in Nuclear Magnetic Resonance Spectroscopy **64**(0): 29-69.
- Capitani, D., M. C. Emanuele, A. Segre, C. Fanelli, A. A. Fabbri, D. Attanasio, B. Focher and G. Capretti (1998). "Early detection of enzymatic attack on paper by NMR relaxometry, EPR spectroscopy and X-Ray powder spectra." Nordic Pulp and Paper Research Journal **13**(2): 95-100.
- Cardon, D. (1990). Black dyes for wool in Mediterranean textile centres: an example of the chemical relevance of guild regulations. Dyes in History and Archaeology, York.
- Cardon, D. (2007). Natural dyes: Sources, tradition, technology and science. London, Archetype Publications Ltd.
- Carter, H., P. Begin and D. Grattan (2000). "Migration of volatile compounds through stacked sheets of paper during accelerated ageing - Part 1: Acid migration at 90° C." Restaurator **21**(2): 77-84.
- Cedzova, M., I. Gallova and S. Katuscak (2006). "Patents for paper deacidification." Restaurator **27**: 35-45.
- Ceres, G., V. Conte, V. Mirruzzo, J. Kolar and M. Strlic (2008). "Imidazolium-based ionic liquids for the efficient treatment of iron gall inked papers." ChemSusChem **1**: 921-926.
- Chakraborty, K. B. and G. Scott (1980). "Mechanisms of antioxidant action-behaviour of hindered piperidines during photo-oxidation of polypropylene." Polymer **21**(3): 252-253.
- Chamberlain, G. J. and R. R. Coupe (1961). "Testing the surface pH of paper." Printing Technology: 7-21.
- Chen, W. X., S. F. Lu, Y. Y. Yao, Y. Pan and Z. Q. Shen (2005). "Copper(II)-Silk fibroin complex fibers as air-purifying materials for removing ammonia." Textile Research Journal **75**(4): 326-330.
- Christie, R. M. (2001). Colour Chemistry. Cambridge, The Royal Society of Chemistry.
- Church, J. S., G. L. Corino and A. L. Woodhead (1998). "The effects of stretching on wool fibres as monitored by FT-Raman spectroscopy." Journal of Molecular Structure **440**(1-3): 15-23.
- Ciba Speciality Chemicals Ltd Ciba® TINUVIN® 144 - Light stabiliser.
- Ciba Speciality Chemicals Ltd (2000). Ciba™ TINUVIN® 292.
- Ciba Speciality Chemicals Ltd (2004). Ciba® IRGANOX® 1135.
- Cook, J. G. (1993a). Natural fibres of vegetable origin. Handbook of Textile Fibres I. Natural Fibres. Durham, Merrow Publishing Co. LTD: 3-78.
- Cook, J. G. (1993b). Natural fibres of animal origin. Handbook of Textile Fibres I. Natural Fibres. Durham, Merrow Publishing Co. LTD: 79-165.
- Cook, J. R. and B. E. Fleischfresser (1984). "Sorption of water-soluble anionic polymers by wool." Textile Research Journal **54**: 441-446.
- Cruickshank, P., V. D. Daniels and J. King (2009). "A Great Lakes pouch: black-dyed skin with porcupine quillwork." British Museum Technical Research Bulletin **3**: 63-72.
- Cruickshank, P. and H. Morgan (2011). Lining a banana fibre belt - a cool vacuum table technique. Readings in Conservation. Changing views of textile conservation. M. M. Brooks and D. D. Eastop. Los Angeles, The Getty Conservation Institute: 501-511.
- Cruz, B. H., J. M. Diaz-Cruz, C. Arino, R. Tauler and M. Esteban (2000). "Multivariate curve resolution of polarographic data applied to the study of copper-binding ability of tannic acid." Analytica Chimica Acta **424**: 203-209.

References

- Csefalvayova, L., B. Havlinova, M. Ceppan and Z. Jakubikova (2007). "The influence of iron gall ink on paper ageing." Restaurator **28**(2): 129-139.
- Cude, A. (2010). TPEN: A treatment for iron gall ink. Department of Art. Kingston, Ontario, Queen's University. **Master's of Art Conservation**: 75.
- Cull, D. (2007). "Conserving Harakeke at The Royal Albert Memorial Museum and Art Gallery." ICON News **11**: 45-47.
- D1795-96(2007)e1, A. (2007). Standard test method for intrinsic viscosity of cellulose, ASTM International.
- Daniels, V. (1995). Maori Black Mud Dyeing of Phormium Tenax Fibre, York, Textiles Research Associates.
- Daniels, V. D. (1997, 1998). Degradation of Artefacts caused by Iron-Containing Dyes. Dyes in History and Archaeology 16/17, Lyons, 11-12 December 1997 and Greenwich, 26-27 November 1998, Lyon and Greenwich, Archetype Publications Ltd.
- Daniels, V. D. (1998). 1998/23 The conservation of black dyed *Phormium Tenax*. Part 3: Mechanical Properties. London, The British Museum.
- Daniels, V. D. (2000). The Chemistry of Iron Gall Ink. The Iron Gall Ink Meeting - First triennial conservation conference. A. J. E. Brown. Newcastle upon Tyne, Conservation of Fine Art, University of Northumbria: 31-36.
- Daniels, V. D. (1996). "The Chemistry of Paper." Chemical Society Reviews **25**: 179-186.
- Daniels, V. D. (1999a). Stabilisation treatments for black-dyed New Zealand flax. ICOM-CC 12th triennial meeting 29 August - 3 September 1999. J. Bridgland. Lyon, James & James. **II**: 579-584.
- Daniels, V. (1999b). "Factors affecting the deterioration of the cellulosic fibres in black-dyed New Zealand flax (Phormium Tenax)." Studies in Conservation **44**(2): 73-85.
- Darbour, M. (1980). Les encres métallogalliques. Étude de la dégradation de l'acide gallique et analyse du complexe ferrogallique., Université de Paris VI. **PhD**.
- Darbour, M., S. Bonnassies and F. Flieder (1981). Les encres métallogalliques. Étude de la dégradation de l'acide gallique et analyse du complexe ferrogallique. ICOM-CC 6th Triennial Meeting, Los Angeles, USA, ICOM-CC.
- de Feber, M. A. P. C., J. B. G. A. Havermans and P. Defize (2000). "Iron-gall ink corrosion: A compound-effect study." Restaurator **21**(4): 204-212.
- Delamare, F. and M. Repoux (2001). Studying dyes by Time of Flight Secondary Ion Mass Spectrometry. Dyes in History and Archaeology 20, Amsterdam, Archetype Publications.
- de la Rie, E. R. (1988). "Polymer stabilizers. A survey with reference to possible applications in the conservation field." Studies in Conservation **33**(1): 9-22.
- de la Rie, E. R. and C. W. McGlinchey (1989). "Stabilized dammar picture varnish." Studies in Conservation **34**(3): 137-146.
- Del Rio, J. C. and A. Gutierrez (2006). "Chemical composition of abaca (*musa textilis*) leaf fibers used for manufacturing of high quality paper pulps." Journal of Agricultural and Food Chemistry **54**: 4600-4610.
- Del Rio, J. C., A. Gutierrez, I. M. Rodriguez, D. Ibarra and A. T. Martinez (2007). "Composition of non-woody plant lignins and cinnamic acids by Py-GC/MS, Py/TMAH and FT-IR." Journal of Analytical and Applied Pyrolysis **79**(1-2): 39-46.
- Deo, H. T. and B. K. Desai (1999). "Dyeing of cotton and jute with tea as a natural dye." Journal of the Society of Dyers and Colourists **115**: 224-227.
- Donne, J. B. (1973). "Bogolanfini: A Mud-Painted Cloth from Mali." Man **8**(1): 104-107.
- Dussubieux, L., D. Naedel, R. Cunningham and H. Alden (2005). Accuracy, precision and investigation: mordant analysis on antique textile by various methods. ICOM-CC 14th Triennial Meeting, The Hague 12-16 September 2005, The Hague, James and James.

References

- Ebner, G., S. Schiehser, A. Potthast and T. Rosenau (2008). "Side reaction of cellulose with common 1-alkyl-3-methylimidazolium-based ionic liquid." Tetrahedron Letters **49**: 7322-7324.
- El-Shishtawy, R. and M. M. Kamel (2002). "Iron complexed acid mordant dyes and their application on nylon 6 and wool." Chem. Eng. Technol. **25**(8): 849-853.
- Emerson Process Management (2010). Application data sheet 43-002/rev.C: The theory of pH measurement, Rosemount Analytical Inc.
- Emsley, A. M., M. Ali and R. J. Heywood (2000). "A size exclusion chromatography study of cellulose degradation." Polymer **41**(24): 8513-8521.
- Emsley, J. (1998). The Elements. Oxford, Clarendon Press.
- Engelmann, M. D., R. T. Bobier, T. Hiatt and I. F. Cheng (2003). "Variability of the Fenton reaction characteristics of the EDTA, DTPA, and citrate complexes of iron." BioMetals **16**(4): 519-527.
- Erhardt, D. and M. F. Mecklenburg (1995). "Accelerated vs natural aging: Effect of aging conditions on the aging process of cellulose." Materials Issues in Art and Archaeology IV **352**: 247-270.
- Eusman, E. (2002). Effects of aqueous treatment on iron-gall ink - Monitoring iron migration with the iron(II) indicator test. The Broad Spectrum - Studies in the materials, techniques and conservation of color on paper. H. K. Stratis and B. Salvesen. London, Archetype Publications: 122-127.
- Falcao, L. and M. E. M. Araujo (2011). "Tannins characterisation in new and historic vegetable tanned leathers fibres by spot tests." Journal of Cultural Heritage **12**: 149-156.
- Fan, L. T., M. M. Gharpuray and Y.-H. Lee (1987). Cellulose hydrolysis. Berlin, Springer-Verlag.
- FAO UN. (2009). "Natural Fibres - Abaca." Retrieved 29/07/09, 2009, from <http://www.naturalfibres2009.org/en/fibres/abaca.html>.
- FAO/CFC/UNIDO/FIDA (c2004). ABACA: Improvement of fiber extraction and identification of higher yielding varieties - Final technical report CFC/FIGHF/09: 1-69.
- Feller, R. L., S. B. Lee and J. Bogaard (1986). The kinetics of cellulose deterioration. Historic textiles and paper materials I - Conservation and characterization. H. Needles, L. and S. H. Zeronian. Washington, DC, American Chemical Society: 329-347.
- Feller, R. L. (1994). Accelerated aging: Photochemical and thermal aspects, The J. Paul Getty Trust.
- Fellers, C., T. Iversen, T. Lindstrom, T. Nilsson and M. Rigdahl (1989). Ageing/degradation of Paper - A literature survey. Rapport (FoU-projektet for papperskonservering (Sweden)). Stockholm, FoU-projektet for papperskonservering.
- Fenech, A., M. Strlic, I. Degano and M. Cassar (2010). "Stability of chromogenic colour prints in polluted indoor environments." Polymer Degradation and Stability **95**(12): 2481-2485.
- Findlay, M. (1989). Four Black-Dyed Silk Textiles of the Late 17th Century. Dyes in History and Archaeology 8, Paisley, Textile Research Associates, York.
- Florian, M.-L. E., D. P. Kronkright and R. E. Norton (1990). The conservation of artifacts made from plant materials. Marina del Rey, The Getty Conservation Institute.
- Fonteneau Tamime, C. and P. Viallier (2000). "A new kinetic model for wool dyeing." Journal of the Society of Dyers and Colourists **116**: 116-120.
- Forbes, R. J. (1956). Studies in Ancient Technology. Leiden, E. J. Brill.
- Frausto-Reyes, C., M. Ortiz-Morales, J. M. Bujdud-Perez, G. E. Magana-Cota and R. Mejia-Falcon (2009). "Raman spectroscopy for the identification of pigments and

References

- color measurement in Dugès watercolors." Spectrochimica Acta Part A: Molecular and Biomolecular Spectroscopy **74**(5): 1275-1279.
- Frazier, R. A., E. R. Deaville, R. J. Green, E. Stringano, I. Willoughby, J. Plant and I. Mueller-Harvey (2010). "Interactions of tea tannins and condensed tannins with proteins." Journal of Pharmaceutical and Biomedical Analysis **51**: 490-495.
- Fukatsu, K. (1988). "Formation of Copper(II):Wool Keratin Complexes." Textile Research Journal **58**(2): 91-96.
- Fukatsu, K. and M. Isa (1986). "Interaction of wool keratin fibers and copper(II) ions." Textile Research Journal **56**: 774-775.
- Galster, H. (1991). pH measurement: Fundamentals, methods, applications, instrumentation. Weinheim, Germany, VCH Verlagsgesellschaft.
- Garside, P. and M. M. Brooks (2006). Probing the microstructure of protein and polyamide fibres. The Future of the 20th Century: Collecting, Interpreting and Conserving Modern Materials. C. Rogerson and P. Garside. AHRC Research Centre for Textile Conservaiton and Textile Studies, Archetype Publications Ltd.: 67-71.
- Garside, P. and P. Wyeth (2009). The effect of historic processing methods on the stability of silk artefacts. Ars Textrina International Textiles Conference: Natural Fibres - A world heritage. J. Winder and M. A. Hann. ULITA, Leeds: 24-25.
- Garside, P., P. Wyeth and X. Zhang (2010a). "Understanding the ageing behaviour of nineteenth and twentieth century tin-weighted silks." Journal of the Institute of Conservation **33**(2): 179-193.
- Garside, P., P. Wyeth and X. Zhang (2010b) "The inherent acidic characteristics of silk, Part II - Weighted silks." e-Preservation Science **7**, 126-131 DOI:
- Garside, P., P. Wyeth and X. Zhang (2011). "Use of near IR spectroscopy and chemometrics to assess the tensile strength of historic silk." e-Preservation Science **8**: 68-73.
- Gilchrist, A. and J. Nobbs (1999). "Colour by Numbers." JSDC **115**: 4-7.
- Gill, L., H. Wilson and B. Mackenzie (2010). "Group news and graduate voice: CF10's winning student posters [Poster entitled 'Developing chemically unstable model textiles for treatment evaluation' by Helen Wilson]." ICON News **28**: 22-25.
- Gillespie, J. M., A. Broad and P. J. Reis (1969). "Further study on the dietary-regulated biosynthesis of high-sulphur wool proteins." Biochemical Journal **112**: 41-49.
- Gordon, S. (2007). Cotton fibre quality. Cotton: Science and Technology. S. Gordon and Y.-L. Hsieh. Boston and Cambridge, CRC Press and Woodhead Publishing Limited: 68-102.
- Graf, E. and J. W. Eaton (1990). "Antioxidant functions of phytic acid." Free Radical Biology & Medicine **8**: 61-69.
- GreenEarth Cleaning LLC (2010). "GreenEarth® cleaning fact sheet."
- Green, L. R. and V. D. Daniels (1990). Identification of mordants using analytical techniques. Dyes in History and Archaeology **9**. J. Kirby. York, Archetype Publications Ltd: 10-14.
- Greenspan, L. (1977). "Humidity fixed points of binary saturated aqueous solutions." Journal of Research of the National Bureau of Standards - A. Physics and Chemistry **81A**(1): 89-96.
- Grice, T. (2010). Personal communication. H. Wilson. London.
- Gumienna-Kontecka, E., R. Silvagni, R. Lipinski, M. Lecouvey, F. C. Marincola, G. Crisponi, V. M. Nurchi, Y. Leroux and H. Kozlowski (2002). "Bisphosphonate chelating agents: complexation of Fe(III) and Al(III) by 1-phenyl-1-hydroxymethylene bisphosphonate and its analogues." Inorganica Chimica Acta **339**: 111-118.
- Guthrie, R. E. and S. H. Laurie (1968). "The binding of copper(II) to mohair keratin." Australian Journal of Chemistry **21**: 2437-43.

References

- Hacke, A. M., C. M. Carr, A. Brown and D. Howell (2003). "Investigation into the nature of metal threads in a Renaissance tapestry and the cleaning of tarnished silver by UV/Ozone (UVO) treatment." Journal of Materials Science **38**(15): 3307-3314.
- Hacke, M. (2008). "Weighted silk: history, analysis and conservation." Reviews in Conservation **9**: 3-16.
- Hahn, O. (2010). "Analyses of iron gall and carbon inks by means of X-ray Fluorescence Analysis: A non-destructive approach in the field of Archaeometry and Conservation Science." Restaurator **31**(1): 41-64.
- Haigh, J. (1800). The Dyer's Assistant in the Art of Dying Wool and Woollen Goods. London.
- Hallett, K. and D. Howell (2005). Size exclusion chromatography of silk: inferring the tensile strength and assessing the condition of historic tapestries. ICOM-CC 14th Triennial Meeting, The Hague 12-16 September 2005. J. Bridgland. The Hague, James and James. **II**: 911-919.
- Hanus, J., A. Makova, M. Ceppan, J. Minarikova, E. Hanusova and B. Havlinova (2009). "Survey of historical manuscripts written with iron gall inks in the Slovak Republic." Restaurator **30**: 165-180.
- Hardy, J. G., L. M. Romer and T. R. Scheibel (2008). "Polymeric materials based on silk proteins." Polymer **49**: 4309-4327.
- Hartley, F. R. (1968a). "Studies in chrome mordanting. I. The binding of chromium(VI) anions to wool." Australian Journal of Chemistry **21**(9): 2277-2286.
- Hartley, F. R. (1968b). "Studies in chrome mordanting. II. The binding of chromium(III) cations to wool." Australian Journal of Chemistry **21**(11): 2723-2735.
- Hartley, F. R. (1968c). "The uptake of aluminium by wool." Australian Journal of Chemistry **21**(4): 1013-1022.
- Hartley, F. R. (1970a). "Studies in chrome mordanting. V. Kinetics and mechanism of the interaction of chromium (III) salts with wool." Australian Journal of Chemistry **23**(2): 275-285.
- Havermans, J. B. G. A. and M. A. P. C. de Feber (1999). Emission of volatile organic compounds from paper objects affected with iron-gall ink corrosion. ICOM-CC 12th Triennial Meeting, 29th August - 3rd September 1999, Lyon, James & James.
- Havermans, J. (2003). "Non Destructive Detection of Iron Gall Inks by Means of Multispectral Imaging Part 1: Development of the Detection System." Restaurator **24**: 55-60.
- Havermans, J., H. A. Aziz and N. Penders (2005). "NIR as a Tool for the Identification of Paper and Ink in Conservation Research." Restaurator **26**: 172-180.
- Havermans, J., H. A. Aziz and H. Scholten (2003). "Non-destructive detection of iron gall inks by means of multispectral imaging Part 2: Application on original objects affected with iron-gall-ink corrosion." Restaurator **24**: 88-94.
- Havlinova, B., J. Minarikova, J. Hanus, V. Jancovicova and Z. Szaboova (2007). "The conservation of historical documents carrying iron gall ink by antioxidants." Restaurator **28**(2): 112-128.
- Hearle, J. W. S. (2007). Physical structure and properties of cotton. Cotton: Science and Technology. S. Gordon and Y.-L. Hsieh. Boston and Cambridge, CRC Press and Woodhead Publishing Limited: 35-67.
- Hearle, J. W. S. and R. H. Peters (1963). Fibre Structure. Manchester: London, The Textile Institute: Butterworths.
- Hein, T. (2008). "Siapo: Samoan Tapa Cloth." Retrieved 2008/11/10, from <http://anthromuseum.missouri.edu/minigalleries/tapacloth/intro.shtml>
- Henniges, U. (2012). GPC-MALLS evaluation of results. H. Wilson.
- Henniges, U., L. Bjerregaard, B. Ludwig and A. Potthast (2011). "Controversial influence of aqueous treatments on historic textiles." Polymer Degradation and Stability **96**: 588-594.

References

- Henniges, U. and A. Potthast (2008). "Phytate treatment of metallo-gallate inks: Investigation of its effectiveness on model and historic paper samples." Restaurator **29**: 219-234.
- Henniges, U., T. Prohaska, G. Banik and A. Potthast (2006). "A fluorescence labelling approach to assess the deterioration state of aged papers." Cellulose **13**(4): 421-428.
- Henniges, U., R. Reibke, G. Banik, E. Huhsmann, U. Hahner, T. Prohaska and A. Potthast (2008). "Iron gall ink-induced corrosion of cellulose: Aging, degradation and stabilization. Part 2: Application on historic sample material." Cellulose **15**: 861-870.
- Heritage (ICN). J. A. Mosk and N. H. Tennent. London, James & James (Science Publishers) Ltd.: 34-41.
- Hocker, H. (2002). Fibre Morphology. Wool: Science and Technology. W. S. Simpson and G. H. Crawshaw. Cambridge, Woodhead Publishing Limited in association with The Textile Institute: 60-79.
- Hofenk de Graaff, J., H. (2002). Dyeing and Writing: A comparison of the use and degradation of iron-gall complexes on textiles and paper. Contributions to Conservation - Research in Conservation at the Netherlands Institute for Cultural Heritage (ICN). J. A. Mosk and N. H. Tennent. London, James & James (Science Publishers) Ltd.: 34-41.
- Hofmann-de Keijzer, R. and A. Hartl (2005). Ancient textiles - recent knowledge: a multidisciplinary research project on textile fragments from the prehistoric salt mine of Hallstatt. ICOM-CC 14th Triennial Meeting The Hague: 12-16 September, 2005. I. Verger. The Hague, Maney Publishing. **2**: 920-926.
- Hras, A. R., M. Hadolin, Z. Knez and D. Bauman (2000). "Comparison of antioxidative and synergistic effects of rosemary extract with α -tocopherol, ascorbyl palmitate and citric acid in sunflower oil." Food Chemistry **71**(2): 229-233.
- Hsieh, Y.-L. (2007). Chemical structure and properties of cotton. Cotton: Science and Technology. S. Gordon and Y.-L. Hsieh. Boston and Cambridge, CRC Press and Woodhead Publishing Limited: 3-34.
- Hurst, G., H. (1892). Dyeing Blacks on Silk. Silk Dyeing, Printing, and Finishing. London, George Bell & Sons: 35-57.
- Hurst, G. H. (1892a). Silk Dyeing, Printing and Finishing. London, George Bell & Sons.
- Hynes, M. J. and M. O'Coinceanainn (2001). "The kinetics and mechanisms of the reaction of iron(III) with gallic acid, gallic acid methyl ester and catechin." Journal of Inorganic Biochemistry **85**: 131-142.
- ICOM-CC (2008). Terminology to characterize the conservation of tangible cultural heritage.
- Iglesias, J., E. Garcia de Saldana and J. A. Jaen (2001). "On the tannic acid interaction with metallic iron." Hyperfine Interactions **134**: 109-114.
- Imperato, P. J. and M. Shamir (1970). "Bokolanfini: Mud Cloth of the Bamana of Mali." African Arts **3**(4): 32-80.
- INSTRON. (2012). "5900 Series - Advanced mechanical testing systems." Retrieved 19th June, 2012, from <http://www.instron.co.uk/wa/product/5900-Series-Mechanical-Testing-Systems.aspx>.
- ISO 6588-1:2005 (2005). Paper, board and pulps - Determination of pH of aqueous extracts - Part 1: Cold extraction, ISO.
- ISO 6588-2:2005 (2005). Paper, board and pulps - Determination of pH of aqueous extracts - Part 2: Hot extraction, ISO.
- Jaen, J. A., L. Gonzalez, A. Vargas and G. Olave (2003). "Gallic acid, ellagic acid and pyrogallol reaction with metallic iron." Hyperfine Interactions **148/149**: 227-235.
- James, C. (2000). The evolution of iron gall ink and its aesthetical consequences. The iron gall ink meeting, Newcastle upon Tyne, 4th & 5th September 2000, Newcastle upon Tyne, University of Northumbria.

References

- Jarman, C. (1998). Small-scale textiles: Plant Fibre Processing - A handbook. UK, Intermediate Technology Publications.
- Jarvis, M. C. (2003). Cellulose. Encyclopedia of Applied Plant Sciences. D. J. Murphy, B. G. Murray and B. Thomas, Academic Press: 865-871.
- Jeol Ltd. (2009). SEM A to Z. Tokyo, Jeol Ltd.
- Jeol Ltd. and Jeol Datum Ltd. (2009). SEM Q&A. Tokyo, Jeol Ltd./Jeol Datum Ltd.
- Jokilehto, J. (2005). Definition of cultural heritage - References to documents in history, ICCROM Working Group 'Heritage and Society'.
- Jones, L. N., D. E. Rivett and D. J. Tucker (1998). Wool and Related Mammalian Fibers. Handbook of Fiber Chemistry. M. Lewin and E. Pearce, M. New York, Marcel Dekker, Inc.: 355-414.
- Kabacinska, Z., R. Krzyminiewski, B. Dobosz and D. Nawrocka (2012). "ESR investigation of structure and dynamics of paramagnetic centres in lime mortars from Budinjak, Croatia." Radiation Measurements.
- Karolia, A., J. Nagrani and H. Raval (2009). Value addition of Khadi spun silk by hand block printing using natural dyes. Ars Textrina International Textiles Conference, Leeds, ULITA, University of Leeds.
- Katayama, T., A. Ide-Ektessabi, K. Funahashi and R. Nishimura (2008). Application of XRF and AMS techniques to textiles in the Mongol Empire. Materials Issues in Art and Archaeology VIII. P. B. Vandiver, B. McCarthy, R. H. Tykot, J. L. Ruvalcaba-Sil and F. Casadio. Warrendale, PA, Materials Research Society 321-329.
- Kelley, S. S., R. M. Rowell, M. Davis, C. K. Jurich and R. Ibach (2004). "Rapid analysis of the chemical composition of agricultural fibers using near infrared spectroscopy and pyrolysis molecular beam mass spectrometry." Biomass and Bioenergy **27**: 77-88.
- Kennedy, J. A. and H. K. J. Powell (1985). "Polyphenol interactions with aluminium(III) and iron(III): their possible involvement in the podzolization process." Australian Journal of Chemistry **38**(6): 879-888.
- Khanbabaee, K. and T. van Ree (2001). "Tannins: Classification and Definition." Natural Product Reports **18**: 641-649.
- Khokhar, S. and R. K. Owusu Apenten (2003). "Iron binding characteristics of phenolic compounds: some tentative structure-activity relations." Food Chemistry **81**: 133-140.
- Kim, J. and P. Wyeth (2009). "Towards a routine methodology for assessing the condition of historic silk." e-Preservation Science **6**: 60-67.
- Kim, J., X. Zhang and P. Wyeth (2008). "The inherent acidic characteristics of aged silk." e-Preservation Science **5**: 41-46.
- Kipton, H., J. Powell and M. C. Taylor (1982). "Interactions of iron(II) and iron(III) with gallic acid and its homologues: a potentiometric and spectrophotometric study." Australian Journal of Chemistry **35**(4): 739-756.
- Klein, G. A. (2010). Industrial Color Physics. London, Springer.
- Kokot, S. (1993). "Sites for Cu (II) stabilization in wool keratin." Textile Research Journal **63**(3): 159-161.
- Kokot, S. and M. Feughelman (1973). "An electron spin resonance study of the copper (II) interaction with wool-keratin: Part II : The natures of the copper (II) interaction with wool-keratin." Textile Research Journal **43**: 146-153.
- Kokot, S., M. Feughelman and R. M. Golding (1972). "An electron spin resonance study of the copper (II) interaction with wool-keratin: Part I: An interpretation and the properties of a copper (II)/wool ESR spectrum." Textile Research Journal **42**: 704-708.
- Kokot, S., M. Feughelman and R. M. Golding (1974). "An electron spin resonance study of the copper (II) interaction with wool-keratin, Part III: A kinetic model for the Cu (II)/wool interaction." Textile Research Journal **44**: 523-527.

References

- Kolar, J., A. Mozir, A. Balazic, M. Strlic, G. Ceres, V. Conte, V. Mirruzzo, T. Steemers and G. De Bruin (2008). "New antioxidants for treatment of transition metal containing inks and pigments." Restaurator **29**(3): 184-198.
- Kolar, J., M. Strlic, G. Novak and B. Pihlar (1998). "Aging and stabilisation of alkaline paper." Journal of Pulp and Paper Science **24**: 89-94.
- Kolar, J., A. Mozir, M. Strlic, G. Ceres, V. Conte, V. Mirruzzo, T. Steemers and G. de Bruin (2008). New antioxidants for treatment of transition metal containing inks. Durability of Paper and Writing 2: 2nd International Symposium and Workshops, Ljubljana, Slovenia, July 5-7, 2008. M. Strlic and J. Kolar. Ljubljana, Faculty of Chemistry and Chemical Technology: 20-21.
- Kolar, J. and M. Strlic, Eds. (2006). Iron gall inks: On manufacture, characterisation, degradation and stabilisation. Ljubljana, National and University Library.
- Kolar, J., M. Sala, M. Strlic and V. S. Selih (2005). "Stabilisation of Paper Containing Iron-Gall Ink with Current Aqueous Processes." Restaurator **26**: 181-189.
- Kolar, J., J. Malesic and M. Strlic (2005). Antioxidants for stabilization of iron gall ink corrosion. ICOM 14th Triennial Meeting, The Hague, 12-16th September 2005. The Hague, The Netherlands, James & James/Earthscan. **1**.
- Kolar, J., A. Mozir, M. Strlic, G. de Bruin, B. Pihlar and T. Steemers (2007). "Stabilisation of iron gall ink: aqueous treatment with magnesium phytate." e-PreservationScience **4**: 19-24.
- Kolar, J. and G. Novak (1996). "Effect of various deacidification solutions on the stability of cellulose pulps." Restaurator **17**: 25-31.
- Kolar, J., A. Stolf, M. Strlic, M. Pompe, B. Pihlar, M. Budnar, J. Simcic and B. Reissland (2006). "Historical iron gall ink containing documents - Properties affecting their condition." Analytica Chimica Acta **555**: 167-174.
- Kolar, J. and M. Strlic (2004). "Evaluating the effects of treatments on iron gall ink corroded documents. A new analytical methodology." Restaurator **25**(2): 94-103.
- Kolar, J., M. Strlic, A. Balazic, M. Smodis, J. Malesic and M. Sala (2006). Prototype INKCOR treatments: Evaluation of effectiveness. Iron Gall Inks: On Manufacture, Characterisation, Degradation and Stabilisation. J. Kolar and M. Strlic. Ljubljana, National and University Library: 247-253.
- Kolar, J. and M. Strlic (2006). Ageing and stabilisation of paper containing iron gall ink. Iron Gall Inks: On Manufacture, Characterisation, Degradation and Stabilisation. M. Strlic and J. Kolar. Ljubljana, National and University Library: 181-194.
- Kolar, J., M. Strlic and B. Pihlar (2006). Methodology and analytical techniques in studies of iron gall ink and its corrosion. Iron gall inks: On manufacture, characterisation, degradation and stabilisation. J. Kolar and M. Strlic. Ljubljana, National and University Library: 95-118.
- Krekel, C. (1999). "The chemistry of historical iron gall inks." International Journal of Forensic Document Examiners **5**: 54-58.
- Leed, D. (2008). "Dye Recipes from the Innsbruck Manuscript." Retrieved 2008/11/12/, from <http://www.elizabethancostume.net/dyes/innsbruck/#>
- Leeder, J. D. (1986). "The cell membrane complex and its influence on the properties of the wool fibre." Wool Science Review **63**: 3-35.
- Leeder, J. D., L. A. Holt, J. A. Rippon and I. W. Stapleton (1990). Diffusion of dyes and other reagents into the wool fibre. 8th International Wool Textile Research Conference, Christchurch New Zealand, Wool Research Organisation of New Zealand (Inc.).
- Leeder, J. D. and R. C. Marshall (1982). "Readily-extracted proteins from merino wool." Textile Research Journal **52**(4): 245-249.
- Letelier, M. E., A. M. Lepe, M. Faundez, J. Salazar, R. Marin, P. Aracena and H. Speisky (2005). "Possible mechanisms underlying copper-induced damage in biological

References

- membranes leading to cellular toxicity." Chemico-Biological Interactions **151**(2): 71-82.
- Letelier, M. E., S. Sanchez-Jofre, L. Peredo-Silva, J. Cortes-Troncoso and P. Aracena-Parks (2010). "Mechanisms underlying iron and copper ions toxicity in biological systems: Pro-oxidant activity and protein-binding effects." Chemico-Biological Interactions **188**(1): 220-227.
- Lewis, D. M. (1989). "Some aspects of the photochemistry of fibrous proteins." Colourage: 25-31.
- Lewis, D. M. (1992). Wool Dyeing. Bradford, Society of Dyers and Colourists.
- Lichtblau, D. and M. Anders (2006). Designing non-aqueous treatments to counteract ink corrosion. Iron Gall Inks: On Manufacture, Characterisation, Degradation and Stabilisation. M. Strlic and J. Kolar. Ljubljana, National and University Library: 195-214.
- LookChem.com. (2008). "Melanin." Retrieved 28th June, 2012, from <http://www.lookchem.com/Melanin/>.
- Lopes, G. K. B., H. M. Schulman and M. Hermes-Lima (1999). "Polyphenol tannic acid inhibits hydroxyl radical formation from Fenton reaction by complexing ferrous ions." Biochimica et Biophysica Acta **1472**: 142-152.
- Luo, M. R., G. Cui and B. Rigg (2001). "The development of the CIE 2000 colour-difference formula: CIEDE2000." Color research & application **26**(5): 340-350.
- Luxford, N., D. Thickett and P. Wyeth (2011). Non-destructive testing of silk: problems and possibilities. ICOM-CC 16th Triennial Conference, 19-23 September 2011. Lisbon, Portugal, Critério - Produção Gráfica, Lda., Lisbon. **CD**: 1-9.
- Maclaren, J. A. and B. Milligan (1981). Wool Science - The chemical reactivity of the wool fibre. Marrickville, Science Press.
- Malawer, E. G. (1995). Introduction to size exclusion chromatography. Handbook of size exclusion chromatography. C.-s. Wu. New York, Marcel Dekker, Inc: 1-24.
- Malesic, J., D. Kocar and A. Balazic Fabjan (2012). "Stabilization of copper- and iron-containing papers in mildly alkaline environment." Polymer Degradation and Stability **97**(1): 118-123.
- Malesic, J., J. Kolar, M. Strlic and S. Polanc (2005). "The use of halides for stabilisation of iron gall ink containing paper - The pronounced effect of cation." e-Preservation Science **2**(13-18).
- Malesic, J., J. Kolar, M. Strlic and S. Polanc (2006). "The influence of halide and pseudo-halide antioxidants in Fenton-like reaction schemes." Acta Chim. Slov. **53**: 450-456.
- Manhita, A., V. Ferreira, H. Vargas, I. Ribeiro, A. Candeias, D. Teixeira, T. Ferreira and C. B. Dias (2011). "Enlightening the influence of mordant, dyeing technique and photodegradation on the colour hue of textiles dyed with madder - A chromatographic and spectrometric approach." Microchemical Journal **98**(1): 82-90.
- Marmolle, F., E. Leize, I. Mila, A. Van Dorsselaer, A. Scalbert and A. M. Albrecht-Gary (1997). "Polyphenol metallic complexes: Characterization by electrospray mass spectrometric and spectrophotometric methods." Analysis Magazine **25**(8): 53-55.
- Marques, G., J. del Rio and A. Gutierrez (2010). "Lipophilic extractives from several nonwoody lignocellulosic crops (flax, hemp, sisal, abaca) and their fate during alkaline pulping and TCF/ECF bleaching." Bioresource Technology **101**(1): 260-267.
- Martin, T. (1813). The Circle of the Mechanical Arts. London.
- Martinez, S. and I. Stern (1999). "Ferric-tannate formation and anticorrosive properties of mimosa tannin in acid solutions." Chemical and Biochemical Engineering Quarterly **13**(4): 191-199.
- Martinez, A. T., J. Rencoret, G. Marques, A. Gutierrez, D. Ibarra, J. Jimenez-Barbero and J. del Rio (2008). "Monolignol acylation and lignin structure in some nonwoody plants: A 2D NMR study." Phytochemistry **69**(16): 2831-2843.

References

- Mascall, L. (1589). A profitable booke declaring dyuers approoued remedies, to take out spottes and staines, in silkes, veluets, linnen and woollen clothes With diuers colours how to die veluets and sylkes, linnen and woollen, fustian and threade Also to dresse leather, and to colour felles. How to gild, graue, sowder, and vernishe. And to harden and make softe yron and steele. Uery necessarie for all men, specially for those which hath or shall haue any doinges therein: with a perfite table hereunto, to finde all things readye, not the like reuealde in Englishe heeretofore. London, Thomas Purfoote.
- Masschelein-Kleiner, L., J. Lefebvre and M. Geulette (1981). The use of tannins in ancient textiles. ICOM-CC 6th triennial meeting, Ottawa, 21-25 September 1981, Ottawa, ICOM.
- McCafferty, E. (2010). Thermodynamics of Corrosion: Pourbaix Diagrams. Introduction to Corrosion Science. E. McCafferty. New York, Springer New York: 95-117.
- McDonald, M., I. Mila and A. Scalbert (1996). "Precipitation of metal ions by plant polyphenols: Optimal conditions and origin of precipitation." Journal of Agricultural and Food Chemistry **44**(2): 599-606.
- McMurry, J. (1996). Organic Chemistry. London, Brooks/Cole Publishing Company.
- Meybeck, A. and J. Meybeck (1978). Electron spin resonance. Applied Fibre Science. F. Happey. London, Academic Press Inc. **1**: 505-556.
- Miller, J. E. and B. M. Reagan (1989). "Degradation in weighted and unweighted historic silks." Journal of the American Institute for Conservation **28**(2): 97-115.
- Millington, K. R. (2000). "Comparison of the effects of gamma and ultraviolet radiation on wool keratin." Journal of the Society of Dyers and Colourists **116**: 266-272.
- Millington, K. R. and J. S. Church (1997). "The photodegradation of wool keratin II. Proposed mechanisms involving cystine." Journal of Photochemistry and Photobiology B: Biology **39**: 204-212.
- Mills, J. and R. White (1994). The Organic Chemistry of Museum Objects, Butterworth-Heinemann.
- Minolta Co. Ltd. (1998). Precise color communication: color control from perception to instrumentation. Japan, Minolta Co. Ltd.
- More, N., G. Smith, R. Te Kanawa and I. Miller (2000). Iron-sensitised degradation of black-dyed Maori textiles. Dyes in History and Archaeology 19, the Royal Museum, National Museums of Scotland, Edinburgh, 19-20 October 2000, Edinburgh, Archetype Publications.
- Morton, W. E. and J. W. S. Hearle (1997). Physical Properties of Textile Fibres. Manchester, The Textile Institute.
- Muros, V., S. Warmlander, D. Scott and J. Theile (2006). Characterization of metal threads from the Colonial Andes. American Institute for Conservation of Historic & Artistic Works 35th Annual Meeting Richmond, VA, AIC.
- Needles, H., L. (1986). Textile fibers, dyes, finishes, and processes. New Jersey, Noyes Publications.
- Neevel, J. G. (1995). "Phytate: a potential conservation agent for the treatment of ink corrosion caused by iron gall inks." Restaurator **16**: 143-160.
- Neevel, J. G. (2002). (Im)possibilities of the phytate treatment of ink corrosion. Contributions to Conservation, James & James.
- Neevel, J. G. (2006). The development of in-situ methods for identification of iron gall inks. Iron Gall Inks: On Manufacture, Characterisation, Degradation and Stabilisation. M. Strlic and J. Kolar. Ljubljana, National and University Library: 147-172.
- Neevel, J. G. (2009). "Application Issues of the Bathophenanthroline Test for Iron(II) Ions." Restaurator **30**: 3-15.
- Neevel, J. G. and B. Reissland (2005). "Bathophenanthroline indicator paper." PapierRestaurierung **6**: 28-36.

References

- Negut, C.-D., V. Bercu and O.-G. Dului (2012). "Defects induced by gamma irradiation in historical pigments." Journal of Cultural Heritage(0).
- Nelkon, M. and P. Parker (1971). Advanced Level Physics. London, Heinemann Educational Books Ltd.
- Nevell, T. P. and S. H. Zeronian (1985). Cellulose chemistry fundamentals. Cellulose chemistry and its applications. T. P. Nevell and S. H. Zeronian. Chichester, Ellis Horwood Limited: 15-29.
- New Zealand Maori Arts and Crafts Institute (Te Puia). (2010). "Te Puia - National Weaving School (Te Rito)." Retrieved 28/10/11, 2011, from http://www.tepuia.com/wananga_new_zealand_national_weaving_school.htm.
- Nilsson, J., F. Vilaplana, S. Karlsson, J. Bjurman and T. Iversen (2010). "The validation of artificial ageing methods for silk textiles using markers for chemical and physical properties of Seventeenth-Century silk." Studies in Conservation **55**: 55-65.
- Orsega, E. F., F. Agnoli and G. A. Mazzocchin (2006). "An EPR study on ancient and newly synthesised Egyptian blue." Talanta **68**(3): 831-835.
- O'Connor, D. and A. Richards (1999). The Right Mud: Studies in Mud-Tannic Dyeing in West China and West Surrey. Dyes in History and Archaeology 18, the Royal Institute for Cultural Heritage, Brussels, 21-22 October 1999, Brussels, Archetype Publications Ltd.
- O'Sullivan, A. C. (1997). "Cellulose: the structure slowly unravels." Cellulose **4**(3): 173-207.
- Ottenberg, S. (2007). "Decorated Hu Ronko shirts from Northern Sierra Leone - Birth, life, and decline." African Arts(Winter 2007): 14-31.
- Oxford Instruments plc. (2008, 2008). "X-ray Fluorescence (XRF)." Oxford Instruments Retrieved 22/09, 2009, from <http://www.oxford-instruments.com/applications-markets/environment/environmental-monitoring/rohs/Pages/x-ray-fluorescence-xrf.aspx>.
- Packer, T. (1830). The Dyer's Guide. London, Printed for Sherwood, Gilbert, and Piper.
- Parton, K. (2002). Practical Wool Dyeing. Wool: Science and Technology. W. S. Simpson and G. H. Crawshaw. Cambridge, Woodhead Publishing Limited in association with The Textile Institute: 237-257.
- Pendergrast, M. and D. C. Starzecka (1996). The Fibre Arts. Maori Art and Culture. London, British Museum Press: 114-146.
- Petrosian-Husa, C. (1995). Changes in Colouring: Observations on the Islands of the Rei Metau in Micronesia, York, Textiles Research Associates.
- Phan, K. H., H. Thomas and E. Heine (1995). Structure of the cuticle of fine wool fibres. 9th International Wool Textile Research Conference, Biella, Italy, International Wool Secretariat.
- Polikreti, K. and Y. Maniatis (2004). "Distribution changes of Mn²⁺ and Fe³⁺ on weathered marble surfaces measured by EPR spectroscopy." Atmospheric Environment **38**(22): 3617-3624.
- Porck, H. J. (2000). Rate of paper degradation - The predictive value of artificial aging tests. Amsterdam, European Commission on Preservation and Access.
- Potthast, A., U. Henniges and G. Banik (2008). "Iron gall ink-induced corrosion of cellulose: aging, degradation and stabilization. Part 1: model paper studies." Cellulose **15**: 849-859.
- Potthast, A., J. Rohrling, T. Rosenau, A. Borgards, H. Sixta and P. Kosma (2003). "A novel method for the determination of carbonyl groups in celluloses by fluorescence labeling. 3. Monitoring oxidative processes." Biomacromolecules **4**: 743-749.
- Pouli, P., C. Fotakis, B. Hermosin, C. Saiz-Jimenez, C. Domingo, M. Oujja and M. Castillejo (2008). "The laser-induced discoloration of stonework; a comparative

References

- study on its origins and remedies." Spectrochimica Acta Part A: Molecular and Biomolecular Spectroscopy **71**(3): 932-945.
- Poulten Selfe & Lee Ltd. (2004). "Poulten Selfe & Lee Ltd." Retrieved 18th June, 2012.
- Presciutti, F., D. Capitani, A. Sgamellotti, B. G. Brunetti, F. Costantino, S. Viel and A. Segre (2005). "Electron Paramagnetic Resonance, Scanning Electron Microscopy with Energy Dispersion X-ray Spectrometry, X-ray Powder Diffraction, and NMR Characterization of Iron-Rich Fired Clays." The Journal of Physical Chemistry B **109**(47): 22147-22158.
- Preservation Equipment Ltd. (2012). "Iron gall ink test paper." Retrieved 18th June, 2012, from <http://www.preservationequipment.com/Store/Products/Conservation-Materials/Other-Materials/Iron-Gall-Ink-Test-Paper>.
- Pullan, M. and A. Baldwin (2008). The evolution of a treatment strategy for an Akali Sikh turban. ICOM-CC 15th Triennial Meeting, 22-26 September 2008, Delhi, India, Allied Publishers Pvt.
- Qureshi, M. S. and S. A. Kazmi (1994). "Kinetics and mechanism of formation of trisgallatoiron(III) complex from monogallatotetraquo iron(III) and bisgallato diaquo iron(III) complexes." Journal of the Chemical Society of Pakistan **16**(4): 248-253.
- Quye, A., D. Littlejohn, R. A. Pethrick and R. A. Stewart (2011). "Accelerated ageing to study the degradation of cellulose nitrate museum artefacts." Polymer Degradation and Stability **96**(10): 1934-1939.
- Ramalho, O., A.-L. Dupont, C. Egasse and A. Lattuati-Derieux (2009). "Emission rates of volatile organic compounds from paper." e-Preservation Science **6**: 53-59.
- Reissland, B. (1999). "Ink corrosion aqueous and non-aqueous treatment of paper objects - State of the art." Restaurator **20**: 167-180.
- Reissland, B. (2001). Ink corrosion: side-effects caused by aqueous treatments for paper objects. The Iron Gall Ink Meeting, 4-5th September 2000, The University of Northumbria. A. J. E. Brown. The University of Northumbria, Newcastle upon Tyne, Conservation of Fine Art, The University of Northumbria: 109-114.
- Reissland, B., R. van Gulik and A. de la Chapelle (2006). Non-aqueous prototype treatment agents for ink-corroded papers: evaluation of undesirable side effects. Iron Gall Inks: On Manufacture, Characterisation, Degradation and Stabilisation. M. Strlic and J. Kolar. Ljubljana, National and University Library: 215-246.
- Reissland, B. (2002). Iron-gall ink corrosion - Progress in visible degradation. Contributions to Conservation - Research in Conservation at the Netherlands Institute for Cultural Heritage (ICN). J. A. Mosk and N. H. Tennent. London, James & James (Science Publishers) Ltd.: 113-118.
- Reissland, B. and M. W. Cowan (2002). The light sensitivity of iron gall inks. Works of art on paper: books, documents and photographs: techniques and conservation: contributions to the Baltimore Congress, 2-6 September 2002. V. D. Daniels, A. Donnithorne and P. Smith, International Institute for Conservation: 180-184.
- Rezk, B. M., G. R. M. M. Haenen, W. J. F. van der Vijgh and A. Bast (2004). "The extraordinary antioxidant activity of vitamin E phosphate." Biochimica et Biophysica Acta **1683**(1): 16-21.
- Rippon, J. A. (1992). The Structure of Wool. Wool Dyeing. D. M. Lewis, Society of Dyers and Colourists: 1-35.
- Robinson, S. (1969). A history of dyed textiles. London, Studio Vista Limited.
- Robson, R. M. (1985). Silk: Composition, Structure, and Properties. Handbook of Fiber Chemistry. M. Lewin and E. M. Pearce. New York, Marcel Dekker, Inc. **15**: 649-700.
- Robson, R. M. (1998). Silk: Composition, Structure, and Properties. Handbook of Fiber Chemistry. M. Lewin and E. M. Pearce. New York, Marcel Dekker, Inc. **15**: 415-464.

References

- Rohrling, J., A. Potthast, T. Rosenau, T. Lange, A. Borgards, H. Sixta and P. Kosma (2002). "A novel method for the determination of carbonyl groups in celluloses by fluorescence labelling. 2. Validation and applications." Biomacromolecules **3**: 969-975.
- Rosetti, G. (1548). The Plietho of Gioanventura Rosetti; Instructions in the Art of the Dyers which Teaches the Dyeing of Woolen Cloths, Linens, Cottons, and Silk by the Great Art as Well as by the Common. Translation of the First Edition of 1548 by Sidney M. Edelstein and Hector C. Borghetty. Cambridge, Massachusetts, MIT Press.
- Rouchon, V., B. Durocher, E. Pellizzi and J. Stordiau-Pallot (2009). "The water sensitivity of iron gall ink and its risk assessment." Studies in Conservation **54**: 236-253.
- Rouchon, V., E. Pellizzi, M. Duranton, F. Vanmeert and K. Janssens (2011). "Combining XANES, ICP-AES, and SEM/EDS for the study of phytate chelating treatments used on iron gall ink damaged manuscripts." Journal of Analytical Atomic Spectrometry **26**(12): 2434-2441.
- Rowland, S. P. (1977). Cellulose: Pores, Internal Surfaces, and the Water Interface. Textile and Paper Chemistry and Technology. J. C. Arthur. Washington, American Chemical Society: 20-45.
- Sala, M., J. Kolar, M. Strlic and M. Kocevar (2006). "Synthesis of myo-inositol 1,2,3-tris- and 1,2,3,5-tetrakis(dihydrogen phosphate)s as a tool for the inhibition of iron-gall-ink corrosion." Carbohydrate Research **341**.
- Saleeby, M. (1915). Abaca (Manila Hemp) in the Philippines (Musa Textilis). Manila, Bureau of Printing.
- Sandy, M. and L. Bacon (2008). A tensile testing method for monocotyledon leaves with parallel venation. ICOM-CC 15th Triennial Meeting, 22-26 September 2008, New Delhi, India, Allied Publishers Pvt
- Sandy, M., A. Manning and F. Bollet (2010). "Changes in the crystallinity of cellulose in response to changes in relative humidity and acid treatment." Restaurator **31**(1): 1-18.
- Sato, M., S. Okubayashi, S. Sukigara and M. Sato (2011). "Non-destructive evaluation of historic textiles by compression measurement using the "Kawabata Evaluation System" (KES)." e-Preservation Science **8**: 55-61.
- Sato, M. and S. Okubayashi (2010). "Consolidation treatment of Japanese ceremonial doll's hair at Edo Period with polyethylene glycol." Journal of Textile Engineering **56**(3): 65-70.
- Sato, M., S. Okubayashi and M. Sato (2011). "Development of conservation procedures for late Edo period Japanese ceremonial dolls' hair: Evaluation of effective treating reagents by using artificially degraded black-dyed silk fibres." Journal of Cultural Heritage **12**(2): 157-163.
- Saunders, D. (2006). British Museum storage guidelines and standards.
- Saverwyns, S., V. Sizaire and J. Wouters (2002). The acidity of paper. Evaluation of methods to measure the pH of paper samples. ICOM-CC 13th Triennial Meeting, 22-27 September 2002. R. Vontobel. Rio de Janeiro, James & James: 628-634.
- Schoeser, M., J. MacDonald and B. Marcondalli (2007). Appendix: The Science of Silk. Silk. London, Yale University Press: 232-243.
- Schwepe, H. (1986). Identification of dyes in historic textile materials. Historic Textile and Paper Materials I - Conservation and Characterization. H. Needles, L. and S. H. Zeronian. Washington, American Chemical Society. **1**: 153-174.
- Scott, D. and G. Eggert (2009). Iron oxides and hydroxides. Iron and steel in art. London, Archetype: 35-52.
- Scott, G. (1985). "Antioxidants *in vitro* and *in vivo*." Chemistry in Britain **July 1985**: 648-653.

References

- Scott, G. (1993a). Autoxidation and antioxidants: Historical perspective. Atmospheric oxidation and antioxidants. G. Scott. Amsterdam, Elsevier Science Publishers B.V. **1**: 1-44.
- Scott, G. (1993b). Initiators, prooxidants and sensitisers. Atmospheric oxidation and antioxidants. G. Scott. Amsterdam, Elsevier Science Publishers B.V. **1**: 83-119.
- Scott, G. (1993c). Antioxidants: Chain breaking mechanisms. Atmospheric oxidation and antioxidants. G. Scott. Amsterdam, Elsevier Science Publishers B.V. **1**: 121-160.
- Selih, V. S., M. Strlic, J. Kolar and B. Pihlar (2007). "The role of transition metals in oxidative degradation of cellulose." Polymer Degradation and Stability **92**: 1476-1481.
- Selih, V. S., M. Strlic and J. Kolar (2004). Catalytic activity of transition metals during oxidative degradation of cellulose. ICOM-CC Graphic Documents Interim Meeting, Ljubljana, 11-12 March 2004. J. Kolar, M. Strlic and J. Wouters. Ljubljana, Slovenia, National and University Library, Ljubljana: 71-72.
- Sequeira, S., C. Casanova and E. J. Cabrita (2006). "Deacidification of paper using dispersions of Ca(OH)₂ nanoparticles in isopropanol. Study of efficiency." Journal of Cultural Heritage **7**(4): 264-272.
- Shahani, C. J. and G. Harrison (2002). Spontaneous formation of acids in the natural aging of paper. Works of art on paper, books, documents and photographs: Techniques and conservation. V. D. Daniels, A. Donnithorne and P. Smith. London, IIC: 189-192.
- Shahani, C. J. (1995). Accelerated aging of paper: Can it really foretell the permanence of paper. Research and Testing Series. Washington, DC, Library of Congress.
- Shahani, C. J. and F. H. Hengemihle (1986). The influence of copper and iron on the permanence of paper. Historic textiles and paper materials - Conservation and characterization. H. Needles, L. and S. H. Zeronian. Washington, DC, American Chemical Society: 387-410.
- Sharma, G., W. Wu and E. N. Dalal (2005). "The CIEDE2000 color-difference formula: Implementation notes, supplementary test data, and mathematical observations." Color research & application **30**(1): 21-30.
- Sharples, A. (1954). "The hydrolysis of cellulose part II. Acid sensitive linkages in egyptian cotton." Journal of Polymer Science **14**(73): 95-104.
- Shimizu, F. (2000). Adsorption behaviour of metal ions on silk and their effect on the photo-degradation of the silk. Structure of Silk Yarn Part B: Chemical Structure and Processing of Silk Yarn. N. Hojo. Enfield, NH, Science Publishers, Inc.: 159-172.
- Shroff, D. H. and A. W. Stannett (1985). "A review of paper aging in power transformers." Generation, Transmission and Distribution, IEE Proceedings C **132**(6): 312-319.
- Sideris, V., L. A. Holt and I. H. Leaver (1990). Dye diffusion in wool and selective photomodification of various morphological components of the fibre. 8th International Wool Textile Research Conference, Christchurch New Zealand, Wool Research Organisation of New Zealand (Inc.).
- Silicones Environmental Health and Safety Council of North America (2008). "D₅ in dry cleaning."
- Simpson, W. S. (2002). Wool Chemistry. Wool: Science and Technology. W. S. Simpson and G. H. Crawshaw. Cambridge, Woodhead Publishing Limited in association with The Textile Institute: 130-159.
- Sistach, M. C. (1990). Scanning Electron Microscopy and Energy Dispersive X-ray Microanalysis applied to metallogallic inks. ICOM Committee for Conservation, 9th Triennial Meeting, 26-31 August 1990. Dresden, International Council of Museums. **2**: 489-496.

References

- Sistach, M. C. and I. Espedaler (1993). Organic and inorganic components of iron gall inks. Preprints of the ICOM Committee for Conservation 10th Triennial Meeting, Washington D.C., Washington D.C., ICOM Committee for Conservation.
- Sistach, M. C., J. M. Gibert and R. Areal (1999). "Ageing of laboratory iron gall inks studied by reflectance spectrometry." Restaurator **20**: 151-166.
- Skelton, M. and L. Lee-Whitman (1986). A systematic method for differentiating between 18th century painted-printed Chinese and Western silks. Historic Textile and Paper Materials I - Conservation and Characterization. H. Needles, L. and S. H. Zeronian. Washington, DC, American Chemical Society: 131-151.
- Slavin, J. and J. I. M. Hanlan (1992). "An investigation of some environmental factors affecting migration-induced degradation in paper." Restaurator **13**(2): 78-94.
- Slawinska, D., J. Slawinski, K. Polewski and W. Pukacki (1979). "Chemiluminescence in the peroxidation of tannic acid." Photochemistry and Photobiology **30**(1): 71-80.
- Smith, A. W. (2011). Aqueous deacidification of paper. Paper and Water: A guide for conservators. G. Banik and I. Bruckle. London, Butterworth-Heinemann: 341-388.
- Smith, G. J. (1974). "Effect of bound metal ions on photosensitivity of wool." New Zealand Journal of Science **17**: 349-350.
- Smith, G. J. (1975). "Effect of metal ions on the photoyellowing of wool." Textile Research Journal **45**: 483-485.
- Smith, G., R. Te Kanawa, I. Miller and G. Fenton (2001). Stabilization of cellulosic textiles decorated with iron-containing dyes. Dyes in History and Archaeology **20**, 1-2 November 2001. J. Kirby. Amsterdam, Archetype Publications: 89-94.
- Smodis, M. and M. Strlic (2003). Unpublished results.
- South, P. K. and D. D. Miller (1998). "Iron binding by tannic acid: effects of selected ligands." Food Chemistry **63**(2): 167-172.
- Stefanis, E. and C. Panayiotou (2007). "Protection of lignocellulosic and cellulosic paper by deacidification with dispersions of micro- and nano-particles of Ca(OH)₂ and Mg(OH)₂ in alcohols." Restaurator **28**: 185-200.
- Stijnman, A. (2006). Iron Gall Inks in History: Ingredients and Productivity. Iron Gall Inks: On Manufacture, Characterisation, Degradation and Stabilisation. M. Strlic and J. Kolar. Ljubljana, National and University Library: 25-68.
- Strlic, M., L. Csefalvayova, J. Kolar, E. Menart, J. Kosek, C. Barry, C. Higgitt and M. Cassar (2010). "Non-destructive characterisation of iron gall ink drawings: Not such a galling problem." Talanta **81**(1-2): 412-417.
- Strlic, M., J. Kolar, D. Kocar, T. Drnovsek, V. S. Selih, R. Susic and B. Pihlar (2004). "What is the pH of alkaline paper?" e-Preservation Science **1**: 35-47.
- Strlic, M., J. Kolar, V. S. Selih, M. Budnar, J. Simcic, P. Kump, M. Necemer, M. Marinsek and B. Pihlar (2006). Chemical analysis of metals in paper and ink. Iron Gall Inks: On Manufacture, Characterisation, Degradation and Stabilisation. J. Kolar and M. Strlic. Ljubljana, CIP: 119-140.
- Strlic, M., J. Kolar, M. Zigon and B. Pihlar (1998). "Evaluation of size-exclusion chromatography and viscometry for the determination of molecular masses of oxidised cellulose." Journal of Chromatography. A **805**: 93-99.
- Strlic, M., J. Kolar and B. Pihlar (2001). "Some preventive cellulose antioxidants studied by an aromatic hydroxylation assay." Polymer Degradation and Stability **73**: 535-539.
- Strlic, M., T. Radovic, J. Kolar and B. Pihlar (2002). "Anti- and prooxidative properties of gallic acid in Fenton-type systems." Journal of Agricultural and Food Chemistry **50**: 6313-6317.
- Strlic, M., J. Kolar, D. Kocar and J. Rychly (2005). Thermo-oxidative degradation. Ageing and stabilisation of paper. M. Strlic and J. Kolar. Ljubljana, CIP: 111-132.
- Strlic, M. and J. Kolar (2005). Ageing and Stabilisation of Paper. Ljubljana, National and University Library.

References

- Strlic, M., J. Kolar and S. Scholten (2005). Paper and durability. Ageing and Stabilisation of Paper. M. Strlic and J. Kolar. Ljubljana, National and University Library: 3-8.
- Strlic, M., J. Kolar and B. Pihlar (2005). Methodology and analytical techniques in paper stability studies. Ageing and Stabilisation of Paper. M. Strlic and J. Kolar. Ljubljana, National and University Library: 27-47.
- Strlic, M., J. Kolar, V. S. Selih, D. Kocar and B. Pihlar (2003). "A comparative study of several transition metals in Fenton-like reaction systems at circum-neutral pH." Acta Chimica Slovenica **50**: 619-632.
- Strlic, M., E. Menart, I. K. Cigic, J. Kolar, G. De Bruin and M. Cassar (2010). "Emission of reactive oxygen species during degradation of iron gall ink." Polymer Degradation and Stability **95**: 66-71.
- Strlic, M., V. S. Selih and J. Kolar (2006). Model studies of the catalytic role of transition metals. Iron Gall Inks: On Manufacture, Characterisation, Degradation and Stabilisation. M. Strlic and J. Kolar. Ljubljana, National and University Library: 173-180.
- Sumner, H. H. (1989). Thermodynamics of dye sorption. The theory of coloration of textiles. A. Johnson. Bradford, The Society of Dyers and Colourists: 255-372.
- Sun, R., J. M. Fang, A. Goodwin, J. M. Lawther and A. J. Bolton (1998). "Fractionation and characterization of polysaccharides from abaca fibre." Carbohydrate Polymers **37**: 351-159.
- Sun, R., J. M. Fang, A. Goodwin, J. M. Lawther and A. J. Bolton (1998). "Isolation and characterization of polysaccharides from abaca fiber." Journal of Agricultural and Food Chemistry **46**: 2817-2822.
- Sungur, S. and A. Uzar (2008). "Investigation of complexes tannic acid and myricetin with Fe(III)." Spectrochimica Acta Part A **69**: 225-229.
- Sykes, P. (1970). A guidebook to mechanism in organic chemistry. London, Longman Group Limited.
- Takahashi, Y., M. Gehoh and K. Yuzuriha (1999). "Structure refinement and diffuse streak scattering of silk (*Bombyx mori*)." International Journal of Biological Macromolecules **24**: 127-138.
- TAPPI T 435 Hydrogen ion concentration (pH) of paper extracts - Hot extraction method, TAPPI.
- TAPPI T 509 Hydrogen ion concentration (pH) of paper extracts - Cold extraction method, TAPPI.
- TAPPI T 529 om-09 Surface pH measurement of paper, TAPPI.
- Tasneem, Z., S. A. Kazmi and K. Sultana (1991). "Role of water in aqueous solution of iron gallic acid complexes." Pakistan Journal of Scientific and Industrial Research **34**(1): 45-48.
- Te Kanawa, R., S. Thomsen, G. Smith, I. Miller, C. Andary and D. Cardon (1999). Traditional Maori dyes. Dyes in History and Archaeology **18**, the Royal Institute for Cultural Heritage, Brussels, 21-22 October 1999. J. Kirby. Brussels, Archetype Publications: 47-50.
- Te Kanawa, R. and G. J. Smith (2009). Zinc alginate consolidation treatment of a piupiu - Maori waist garment. Natural Fibres in Australasia: Proceedings of the Combined (NZ and AUS) Conference of The Textile Institute, Dunedin 15-17 April 2009, Dunedin, New Zealand, The Textile Institute (NZ).
- Te Kanawa, R., G. J. Smith, G. A. Fenton, I. J. Miller and C. L. Dunford (2002). Evaluation of consolidants for black iron-tannate-dyed Maori textiles. Dyes in History and Archaeology: 21. Avignon and Lauris, France 2002, Avignon and Lauris, France, Archetype Publications Ltd.
- The Association for the Promotion of Traditional Craft Industries. (2009-2011). "Oshima Pongee: Overview." from <http://kougeihin.jp/en/crafts/introduction/weaving/2810>.

References

- The Association for the Promotion of Traditional Craft Industries. (2009-2011). "Oshima Pongee: Production." Retrieved 21st October 2011, 2011, from <http://kougeihin.jp/en/crafts/introduction/weaving/2810?m=pd>.
- Thomas, H. and K. H. Phan (1990). Alteration of wool proteins during dyeing. 8th International Wool Textile Research Conference, Christchurch New Zealand, Wool Research Organisation of New Zealand (Inc.).
- Thornalley, P. J. and A. Stern (1984). "The production of free radicals during the autoxidation of monosaccharides by buffer ions." Carbohydrate Research **134**(2): 191-204.
- Timar-Balazsy, A. and D. Eastop (1998). Chemical principles of textile conservation. Oxford, Butterworth-Heinemann.
- Titus, S., R. Schneller, E. Huhsman, U. Hahner and G. Banik (2009). "Stabilising local areas of loss in iron gall ink copy documents from the Savigny estate." Restaurator **30**: 16-50.
- Toerien, E. S. (2003). "Mud cloth from Mali: its making and use." Journal of Family Ecology and Consumer Sciences **31**: 52-57.
- Trathnigg, B. (1995). "Determination of MWD and chemical composition of polymers by chromatographic techniques." Progress in Polymer Science **20**(4): 615-650.
- Trustees of the British Museum. (2012a). "History of the British Museum." Retrieved 7th July, 2012, from http://www.britishmuseum.org/about_us/the_museums_story/general_history.aspx.
- Trustees of the British Museum. (2012b). "Treasure." Retrieved 7th July, 2012, from http://www.britishmuseum.org/about_us/departments/coins_and_medals/research/treasure.aspx.
- Tse, S. (2007). Guidelines for pH measurement in conservation. Ottawa, CCI.
- Uchida, Y., M. Inaba and T. Kijima (2007). "Evaluation of aqueous washing methods of paper by the measurement of organic acid extraction." Restaurator **28**(3): 169-184.
- UCL. (2012). "Science and Heritage Programme." Retrieved 7th July, 2012, from <http://www.ucl.ac.uk/silva/heritagescience/index-9-03-11>.
- UNESCO (2001). 25. UNESCO Universal Declaration on Cultural Diversity. General Conference, 31st Session, Paris, 15 October to 3 November 2001. Paris, UNESCO. **1**: 61-64.
- UNESCO. (2007). "Heritage." Retrieved 5th May, 2011, from http://portal.unesco.org/culture/en/ev.php-URL_ID=35028&URL_DO=DO_TOPIC&URL_SECTION=201.html.
- van Oosten, T., B. (1994). Degradation: Investigation into the degradation of weighted silk. Contributions of the Central Research Laboratory to the field of conservation and restoration. H. Verschoor and J. Mosk. Amsterdam, Central Research Laboratory for Objects of Art and Science: 65-76.
- Vargas, J. B., T. E. Arias, J. L. P. Rodriguez and A. J. Erbez (2006). "Colour in the Seventeenth-Century miniatures of Spanish choir books." Restaurator **27**: 143-161.
- Virro, K., E. Mellikov, O. Volobujeva, V. Sammelselg, J. Asari, L. Paama, J. Jürgens and I. Leito (2008). "Estimation of uncertainty in electron probe microanalysis: iron determination in manuscripts, a case study." Microchimica Acta **162**(3): 313-323.
- von Lerber, K., S. Pentzien, M. Strlic and W. Kautek (2005). Laser cleaning of silk: a first evaluation. ICOM 14th Triennial Meeting The Hague: 12-16 September, 2005, The Hague, ICOM.
- Vuori, J. and S. Tse (2005b). Preliminary study of a micro extraction method for measuring the pH of textiles. American Institute for Conservation of Historic & Artistic Works 33rd Annual Meeting, June 2005: Textile Speciality Group K. MacKay, B. Szuhay and J. Thompson. Minneapolis, Minnesota, AIC. **15**: 63-73.

References

- Vuori, J. and S. Tse (2005a). A preliminary study of the use of bathophenanthroline iron test strips on textiles. ICOM-CC 14th Triennial Meeting, The Hague 12-16 September 2005. J. Bridgland. The Hague, James and James. **II**: 989-995.
- Wagner, B., E. Bulska, A. Hulanicki, M. Heck and H. M. Ortner (2001). "Topochemical investigation of ancient manuscripts." Fresenius' Journal of Analytical Chemistry **369**(7): 674-679.
- Wagner, B. and E. Bulska (2003). "Towards a new conservation method for ancient manuscripts by inactivation of iron via complexation and extraction." Analytical and Bioanalytical Chemistry **375**(8): 1148-1153.
- Wagner, B., E. Bulska, B. Stahl, M. Heck and H. M. Ortner (2004). "Analysis of Fe valence states in iron-gall inks from XVIth century manuscripts by ⁵⁷Fe Mössbauer spectroscopy." Analytica Chimica Acta **527**(2): 195-202.
- Wakelyn, P. J., N. R. Bertoniere, A. D. French, S. H. Zeronian, T. P. Nevell, D. P. Thibodeaux, E. J. Blanchard, T. A. Calamari, B. A. Triplett, C. K. Bragg, C. M. Welch, J. D. Timpa, W. R. Goynes Jr., W. E. Franklin, R. M. Reinhardt and T. L. Vigo (1998). Cotton Fibers. Handbook of Fiber Chemistry. M. Lewin and E. M. Pearce. New York, Marcel Dekker, Inc. **15**: 577-724.
- Wakui, M., K. Yamazaki and M. Saito (2002). "The amounts of mordants on black and red fabrics dyed with natural dyes [Original title and text in Japanese]." Bunkazai hozon-syuhuku gakkaisi **46**: 48-57.
- Wakui, M., M. Yatagai, N. Kohara, C. Sano, H. Ikuno, Y. Magoshi and M. Saito (2001). "ICP-AES and X-ray Fluorescence Determinations of Mordants on Fabric Dyed with Natural Dyes [Original title and text in Japanese]." Bunkazai hozon-syuhuku gakkaisi **45**: 12-26.
- Wetzel, F. H., J. H. Elliot and A. F. Martin (1953). "Variable shear viscometers for cellulose intrinsic viscosity determinations." TAPPI **36**: 564-571.
- Whiston, C., Ed. (1987). X-ray methods. Analytical chemistry by Open Learning. Chichester, John Wiley & Sons.
- Whitmore, P. M. and J. Bogaard (1994). "Determination of the cellulose scission route in the hydrolytic and oxidative degradation of paper." Restaurator **15**: 26-45.
- Whitmore, P. M. (2011). Paper ageing and the influence of water. Paper and Water: A guide for conservators. G. Banik and I. Bruckle. London, Butterworth-Heinemann: 219-254.
- Wills, B. and M. Hacke (2007). Conservation, colour and plant material in Ancient Egyptian basketry. ICON Archaeology Group/Fitzwilliam Museum (University of Cambridge) Conference 2001; Decorated Surfaces on Ancient Egyptian Objects, Technology, Deterioration and Conservation. Cambridge: 6-9.
- Wilson, H. L. (2007). Analysis of the current research into the chemistry of Iron Gall Ink and its implications for Paper Conservation. Chemistry. Oxford, Oxford University. **MChem**: 124.
- Wilson, H. (2010). Investigation into iron diffusion into wool, silk, cotton and abaca textiles using SEM-EDX [Poster]. IIC 2010 Congress - Conservation and the Eastern Mediterranean, 20th - 23rd September 2010, Istanbul, Turkey, IIC.
- Wilson, H., C. Carr and M. Hacke (2012). "Production and validation of model iron-tannate dyed textiles for use as historic textile substitutes in stabilisation treatment studies." Chemistry Central Journal **6**(44).
- Wilson, K. (1979). A History of Textiles. Boulder, Westview Press Inc.
- Wilson, W. K. and E. J. Parks (1979). "An analysis of the aging of paper: possible reactions and their effects on measurable properties." Restaurator **3**(1-2): 37-61.
- Wilson, W. K. and E. J. Parks (1980). "Comparison of accelerated aging of book papers in 1937 with 36 years natural aging." Restaurator **4**(1): 1-56.
- Wittekind, J. (1994). "The Battelle Mass Deacidification Process: a New Method for Deacidifying Books and Archival Materials." Restaurator **15**: 189-207.

References

- Wolfe, H. (2012). "Personal communication."
- Wortmann, F.-J., G. Wortmann and H. Zahn (1997). "Pathways for dye diffusion in wool fibers." Textile Research Journal **67**(10): 720-724.
- Wortmann, F.-J. and H. Zahn (1994). "The stress/strain curve of α -keratin fibers and the structure of the intermediate filament." Textile Research Journal **64**(12): 737-743.
- Wunderlich, C. H. (1991). "Über Eisengallustinte." Zeitung der Anorganischen Allgemeinen Chemie **598-599**: 371-376.
- Wunderlich, C. H. (1994). "Geschichte und Chemie der Eisengallustinte - Rezepte, Reaktionen und Schädwirkungen." Restauro **100**: 414-421.
- Wyatt, P. J. (1993). "Light scattering and the absolute characterization of macromolecules." Analytica Chimica Acta **272**(1): 1-40.
- Yanagi, Y., Y. Kondo and K. Hirabayashi (2000). "Deterioration of silk fabrics and their crystallinity." Textile Research Journal **70**(10): 871-875.
- Yanagi, Y., K. Yasuda and K. Hirabayashi (1994). "Deterioration of silk fibers mordanted with ferrous sulfate after treatment with tannic acid." J. Silk Sci. Tech. **Jan. 3**: 30-33.
- Ziegler, M. (2008). "A Little Dye Book." Retrieved 2008/11/12, from <http://www.elizabethancostume.net/dyes/zieglerdyebook.html>
- Zervos, S. and A. Moropoulou (2005). "Cotton cellulose ageing in sealed vessels. Kinetic model of autocatalytic depolymerization." Cellulose **12**(5): 485-496.
- Zou, X., N. Gurnagul, T. Uesaka and J. Bouchard (1994). "Accelerated aging of papers of pure cellulose: Mechanism of cellulose degradation and paper embrittlement." Polymer Degradation and Stability **43**: 393-402.
- Zou, X., T. Uesaka and N. Gurnagul (1996a). "Prediction of paper permanence by accelerated ageing I. Kinetic analysis of the aging process." Cellulose **3**: 243-267.
- Zou, X., T. Uesaka and N. Gurnagul (1996b). "Prediction of paper permanence by accelerated aging II. Comparison of the predictions with natural aging results." Cellulose **3**(1): 269-279.

This Provisional PDF corresponds to the article as it appeared upon acceptance. Fully formatted PDF and full text (HTML) versions will be made available soon.

Production and validation of model iron-tannate dyed textiles for use as historic textile substitutes in stabilisation treatment studies

Chemistry Central Journal 2012, 6:44 doi:10.1186/1752-153X-6-44

Helen Wilson (helenlouisewilson@gmail.com)
Chris Carr (chris.carr@manchester.ac.uk)
Marei Hacke (mhacke@thebritishmuseum.ac.uk)

ISSN 1752-153X

Article type	Research article
Submission date	8 November 2011
Acceptance date	22 May 2012
Publication date	22 May 2012

Article URL <http://journal.chemistrycentral.com/content/6/1/44>

This peer-reviewed article was published immediately upon acceptance. It can be downloaded, printed and distributed freely for any purposes (see copyright notice below).

Articles in *Chemistry Central Journal* are listed in PubMed and archived at PubMed Central.

For information about publishing your research in *Chemistry Central Journal* or any Chemistry Central Journal, go to

<http://journal.chemistrycentral.com/info/instructions/>

For information about other Chemistry Central publications go to

<http://www.chemistrycentral.com>

© 2012 Wilson et al.; licensee Chemistry Central Ltd.
This is an open access article distributed under the terms of the Creative Commons Attribution License (<http://creativecommons.org/licenses/by/2.0>), which permits unrestricted use, distribution, and reproduction in any medium, provided the original work is properly cited.

Production and validation of model iron-tannate dyed textiles for use as historic textile substitutes in stabilisation treatment studies

Helen Wilson^{1,2*}

* Corresponding author

Email: helenlouisewilson@gmail.com

Chris Carr¹

Email: chris.carr@manchester.ac.uk

Marei Hacke²

Email: mhacke@thebritishmuseum.ac.uk

¹ Textiles and Paper, The School of Materials, The University of Manchester, Oxford Road, Manchester M13 9PL, UK

² Department of Conservation and Scientific Research, British Museum, Great Russell Street, London WC1B 3DG, UK

Abstract

Background

For millennia, iron-tannate dyes have been used to colour ceremonial and domestic objects shades of black, grey, or brown. Surviving iron-tannate dyed objects are part of our cultural heritage but their existence is threatened by the dye itself which can accelerate oxidation and acid hydrolysis of the substrate. This causes many iron-tannate dyed textiles to discolour and decrease in tensile strength and flexibility at a faster rate than equivalent undyed textiles. The current lack of suitable stabilisation treatments means that many historic iron-tannate dyed objects are rapidly crumbling to dust with the knowledge and value they hold being lost forever.

This paper describes the production, characterisation, and validation of model iron-tannate dyed textiles as substitutes for historic iron-tannate dyed textiles in the development of stabilisation treatments. Spectrophotometry, surface pH, tensile testing, SEM-EDX, and XRF have been used to characterise the model textiles.

Results

On application to textiles, the model dyes imparted mid to dark blue-grey colouration, an immediate tensile strength loss of the textiles and an increase in surface acidity. The dyes introduced significant quantities of iron into the textiles which was distributed in the exterior and interior of the cotton, abaca, and silk fibres but only in the exterior of the wool fibres. As seen with historic iron tannate dyed objects, the dyed cotton, abaca, and silk textiles lost tensile strength faster and more significantly than undyed equivalents during accelerated

thermal ageing and all of the dyed model textiles, most notably the cotton, discoloured more than the undyed equivalents on ageing.

Conclusions

The abaca, cotton, and silk model textiles are judged to be suitable for use as substitutes for cultural heritage materials in the testing of stabilisation treatments.

Background

Iron-tannate complexes have been used as inks (iron gall inks) and dyes for thousands of years and are now present in objects of cultural significance worldwide. While iron gall inks have been used predominantly on paper and parchment, iron-tannate dyes have been used to colour a vast array of woven and non-woven materials shades of black, grey, or brown, including proteinaceous materials such as silk (Figure 1), wool, skin, and leather, and cellulosic materials such as cotton, abaca, *Phormium tenax* (New Zealand flax) (Figure 2), and raffia.

Figure 1 Losses to the iron-tannate dyed hair (silk) on a Japanese ceremonial Hina doll (British Museum, Department of Asia, AS1981.0808.227). Image © The Trustees of the British Museum

Figure 2 A Maori *piu piu* (ceremonial skirt), approximately 15 years old, produced from New Zealand flax (*Phormium tenax*) (owned by Dr Vincent Daniels)

Iron-tannate dyes are formed through the combination of iron ions (usually iron(II)) and tannic acids (usually hydrolysable) in water. Historically, iron ions were often sourced from iron-rich mud or iron(II) sulphate (vitriol) while tannic acid (condensed, hydrolysable, or a mixture) was sourced from plant material such as bark, leaves, and galls. Hydrolysable tannins from galls for example include gallotannins and ellagitannins which can be hydrolysed to glucose and gallic acid or ellagic acid, respectively [1]. On combination with ferrous ions hydrolysable tannins form blue-black coloured iron(II)-tannate dye complexes; the colour being due to a reversible charge transfer across the Fe(II)-O bond in the iron(III)-tannate, or iron(III)-gallate, complex [2]. Condensed tannins (proanthocyanidins) are oligomers or polymers of flavan-3-ol (catechin) monomers [1] which form green-black coloured dye complexes on combination with iron(III) ions [3,4]. The exact shade of black, brown, or grey of iron-tannate dyes varies depending on the method of dyeing used and the types and quality of reagents included [5]. Additionally, the dyes can become browner with age as the dye complex is broken down and coloured degradation products such as brown quinones and iron(III) oxides, and yellow ellagic acid are formed [6,7]. See Additional file 1 for further detail on the colour, acidity, and complex structure of iron-tannate dyes.

Unfortunately, iron gall inks and iron-tannate dyes pose a significant threat to the lifetime of the materials they colour due to their acidity and metal ion content which can accelerate acid hydrolysis and oxidation (see Additional file 1 for more details). This causes tensile strength loss, embrittlement, and discolouration in the substrate. Consequently, many iron-tannate dyed materials are brown rather than black, fragile, exhibit physical losses, or in some cases have crumbled to dust (Figure 3).

Figure 3 Remains of a Maori cloak and *piu piu* that has disintegrated in the iron-tannate dyed areas (Horniman Museum)

While much research has been undertaken into understanding the degradation processes and development of stabilisation treatments for iron gall ink on paper [2,8,9] significantly less research has been undertaken on the iron-tannate dyed textiles that are the focus of this paper [3,4,10–13], and at present there is no suitable non-aqueous treatment with which to stabilise these objects.

In 2008 an AHRC/EPSRC Science and Heritage Programme collaborative PhD project was established at the University of Manchester and the British Museum to investigate non-aqueous stabilisation treatments for iron-tannate dyed organic materials. The use of historic material in these treatment studies was deemed unsuitable for ethical and practical reasons and necessitated the production and use of substitute iron-tannate dyed textiles that:

- Exhibit relatively uniform iron and colour distribution to ensure that the iron-catalysed degradation of the dyed textiles occurs as uniformly as possible, thus minimising analytical variability in accelerated ageing and stabilisation treatment studies;
- Lose tensile strength and possibly discolour more than undyed equivalent textiles on accelerated ageing, as is seen with naturally aged iron-tannate dyed objects worldwide including in the British Museum's collections [4,10].

In this paper the production of the substitute textiles is described. The validity for the use of the textiles as substitutes for historic iron-tannate dyed material in accelerated ageing and stabilisation treatment studies is assessed through their characterisation before and after accelerated ageing.

Production of substitute textiles

Small quantities of iron-tannate dyed silk [12], New Zealand flax [3], and raffia [13] yarns/fibre bundles and textiles have been produced in laboratories by several researchers. For this research significantly larger quantities of uniformly dyed woven textiles were needed and so four textiles (cotton, abaca, silk, and wool) and six specifically developed dye formulations (Table 1) were used on industrial equipment at the University of Manchester's dyehouse to produce an unprecedented 80 m² of substitute textiles. The pH of the clear and colourless dye bath solutions was tested using pH-Fix 0–14 Fisherbrand pH indicator strips and found to be typically pH 4 to 6 for both tannic acid solutions and metal ion solutions. More detailed information on the development and dyeing of the substitute textiles is presented in Additional file 2.

Table 1 Dye formulations used to produce substitute iron-tannate dyed textiles

Dye code	Substrate	Liquor: Fabric ^a	Dyebath A ^b	Dyebath B	Dyebath A+	Dyeing sequence
Proteinaceous	p1 Wool + silk	200 : 3.23	0.02 M FeSO ₄ ·7H ₂ O 55°C, 1 hour	6.5 g L ⁻¹ TA 55°C, 3 hours	0.009 M FeSO ₄ ·7H ₂ O 55°C, 1 hour	A B A B A+
	p2 Wool + silk	200 : 3.23	0.02 M FeSO ₄ ·7H ₂ O + 0.002 M CuSO ₄ ·5H ₂ O 55°C, 1 hour	6.5 g L ⁻¹ TA 55°C, 3 hours	0.009 M FeSO ₄ ·7H ₂ O + 0.009 M CuSO ₄ ·5H ₂ O 55°C, 1 hour	A B A B A+
	p3 Silk	200 : 0.62	0.005 M FeSO ₄ ·7H ₂ O 55°C, 1 hour	3.5 g L ⁻¹ Gx 55°C, 3 hours	0.002 M FeSO ₄ ·7H ₂ O 55°C, 1 hour	A B A B A+
Cellulosic	c1 Cotton + abaca	60 : 2.01	15 g L ⁻¹ TA 20°C, 2 hours	0.04 M FeSO ₄ ·7H ₂ O 20°C, 2 hours	-	A B A B A B
	c2 Cotton + abaca	60 : 2.01	15 g L ⁻¹ TA 20°C, 2 hours	0.04 M FeSO ₄ ·7H ₂ O + 0.005 M CuSO ₄ ·5H ₂ O 20°C, 2 hours	-	A B A B A B
	c3 Cotton	60 : 1.22	16.6 g L ⁻¹ Gx 20°C, 2 hours	0.024 M FeSO ₄ ·7H ₂ O 20°C, 2 hours	-	A B A B A B

a. Ratio in litres of dyebath : total mass of fabric in kilograms

b. Abbreviations are as follows: TA; 50/50 mixture of non-purified and purified tannic acid extracts from Chinese galls and sumac, respectively; Gx: non-purified gall powder

c. In p1, the final quantity of iron (A+) was added directly to the final dyebath B but in p2 and p3, it was applied in a separate dyebath due to substantial and problematic foam formation in p1. Since an unknown quantity of tannic acid remained in the final dyebath B in p1 when the iron (A+) was added, the effective concentration of iron ions available for binding with tannic acid on or within the textile fibres is lower than that in p2 and p3.

Results and discussion

Characterisation of unaged iron-tannate dyed model textiles

Metal ion content and distribution, including uniformity, in iron-tannate dyed model textiles (XRF and SEM-EDX analysis)

XRF was used to assess the overall metal ion content and uniformity throughout the dyed textiles since an uneven distribution could cause uneven degradation during accelerated ageing.

All iron-tannate dye formulations introduced significant quantities of iron (and copper for the p2 and c2 formulations) into the dyed textiles (Table 2). Dye formulation 3 resulted in the highest levels of iron detected probably due to a greater quantity of tannic acid and gallic acid being present in the aqueous gall powder extract compared to in the mixture of tannic acids used in dye formulations 1 and 2.

Table 2 The uniformity of metal ion and colour distribution in unaged substitute textiles determined using XRF and spectrophotometry, respectively

Sample	XRF ^a (elemental ratios)				Colour measurement	
	Fe	Cu	L*	a*	b*	
Wool undyed (WU)	12 (1) ^b	5 (1)	78.39 (0.39)	-1.06 (0.04)	6.67 (0.24)	
Wool dyed with p1 (Wp1)	590 (60)	11 (1)	33.53 (1.03)	1.31 (0.04)	-1.11 (0.12)	
Wool dyed with p2 (Wp2)	786 (68)	333 (27)	31.03 (0.79)	0.93 (0.07)	-1.05 (0.18)	
Silk undyed (SU)	17 (2)	4 (1)	75.36 (0.36)	-0.20 (0.02)	0.97 (0.12)	
Silk dyed with p1 (Sp1)	2124 (526)	9 (5)	20.75 (0.37)	1.46 (0.03)	-3.90 (0.09)	
Silk dyed with p2 (Sp2)	2413 (292)	204 (26)	18.76 (0.30)	1.61 (0.03)	-4.37 (0.07)	
Silk dyed with p3 (Sp3)	2628 (145)	11 (10)	17.79 (0.20)	1.38 (0.03)	-4.09 (0.07)	
Abaca undyed (AU)	24 (5)	4 (3)	74.25 (1.66)	1.91 (0.41)	13.56 (1.09)	
Abaca dyed with c1 (Ac1)	1459 (338)	9 (2)	21.66 (0.75)	0.56 (0.05)	-2.22 (0.12)	
Abaca dyed with c2 (Ac2)	1490 (190)	371 (53)	23.34 (0.83)	0.50 (0.04)	-2.65 (0.17)	
Cotton undyed (CU)	15 (1)	3 (1)	84.31 (0.51)	-0.26 (0.02)	0.67 (0.09)	
Cotton dyed with c1 (Cc1)	683 (145)	5 (3)	35.7 (0.91)	0.70 (0.06)	-4.33 (0.15)	
Cotton dyed with c2 (Cc2)	742 (41)	83 (11)	33.58 (0.50)	0.80 (0.04)	-4.89 (0.12)	
Cotton dyed with c3 (Cc3)	1115 (44)	3 (3)	29.61 (1.01)	0.57 (0.05)	-4.62 (0.13)	
Black silk (1881.0802.158 or PRN: RRM 10294 ^c)	2370	587	ND ^d	ND	ND	
Black dyed North American skin bag (1937.0617.1 ^c)	4163	44	ND	ND	ND	
Brown braided area of modern <i>piu piu</i> owned by Dr Vincent Daniels (Figure 2)	1918	2	ND	ND	ND	
Black fibres of broken Maori cloak and <i>piu piu</i> from the Horniman Museum (Figure 3)	5924	3	ND	ND	ND	

a. Iron and copper content ratios (net elemental peak area: net Compton peak area) multiplied by 1000

b. Standard deviations of mean data are in parentheses

c. British Museum registration number

d. Not done because the samples were too small or the surface too uneven for analysis

The most uniform metal distributions were achieved with dye formulation 3 (a maximum of 6% variation from the mean) and the least with dye formulation 1 (a maximum of 25% variation from the mean). The production method, particularly the efficacy of the post-dyeing rinsing may have caused these variations in iron content. High levels of iron were also detected in a range of samples from iron-tannate dyed museum objects.

SEM-EDX of the dyed (p1 and c1) and undyed substitute textile cross-sections identified a high variability of iron content in the fibre bundles/yarns, with iron concentration increasing with increasing proximity to the fibre bundle/yarn surface. This variation in the iron content with the location of the fibre within the fibre bundles/yarns will occur throughout the textiles and therefore will not affect the results from tensile testing or spectrophotometry which will be averaged by analysis of multiple fibres.

Importantly, for the individual fibres of abaca, cotton, and silk, iron was easily detected on the exterior and the interior of each fibre and was most concentrated on the exterior (Figure 4). Iron in the wool fibres was primarily located at the exterior of the fibres (cuticle) with minimal or no iron detected inside the fibres (cortex), Figure 5. This is due to the

hydrophobic and highly cross-linked cuticle layer present in only the wool fibres, which restricts diffusion of the water-based dye into the cortex of the wool fibres [14]. The lack of a cuticle layer in the silk explains the greater iron content in the silk than in the simultaneously dyed wool (Table 2). Improved dye diffusion into the wool fibres may be achieved through use of a higher temperature such as the 90–100°C usually used for wool dyeing, rather than the 55°C used in these dye formulations. In this study, 55°C was selected in order to minimise thermal damage to the simultaneously dyed silk.

Figure 4 SEM images and EDX spectra of a dyed abaca (A), cotton (B), and silk (C and D) fibres in cross-section. The dyed silk fibres in C are from the interior of the yarn while those in D are on the crown of the weave

Figure 5 SEM image and EDX spectra of a dyed wool fibre near the crown of the weave

It is likely that the majority of the metal in the substitute textiles is bound in iron-tannate complexes or directly to the fibres since significant or complete removal of water-soluble unbound ions will have occurred in the post-dyeing rinsing. The iron-tannate dye complexes can be physically bonded to the textile fibres via Van der Waals' forces [15–17] or chemically bonded via the mordant of the dye. In the proteinaceous dye formulations, the metal ions acted as mordants so that fibre/iron/tannic acid interactions will predominate [18]; in the cellulosic dye formulations tannic acid was the mordant and so fibre/tannic acid/iron interactions will predominate. Iron ions and copper ions can bind to hydroxyl, carbonyl, and carboxyl groups in proteinaceous and cellulosic textiles as well as to amine, amide, and thiol groups present in proteinaceous textiles [15,16,19]. Copper ions bind more strongly than iron ions, particularly to thiols [20–22]. Carboxylate anion groups are the major binding sites in wool [20] and silk [23]. The isoelectric points of wool and silk are approximately at pH 5.6 and 2.8, respectively [24], and are the pH values at which the proteins are electrically neutral, having equal quantities of positive (e.g. $-\text{NH}_3^+$) and negative (e.g. $-\text{COO}^-$) functional groups. Since the pH of the dye baths for the model textiles ranged between pH 4 and 6, it is likely that the silk fibroin will be slightly negatively charged which will attract the metal cations, while the wool will be either slightly positively charged which will repel the metal cations, or will be electrically neutral. In the silk the metal ions can bind by co-ordinate bonds to un-ionised groups such as amines and hydroxyl groups as well as by ionic bonds to negatively charged groups such as carboxylate and sulphonate groups [25–27]. In the wool the metal ions will be repelled by positively charged groups such as protonated amines but can bind to un-ionised groups such as amine groups, and to the ionised carboxyl groups that account for the majority or all of the carboxyl groups present in the wool since the pH of dye baths are close to the isoelectric point of wool. Wool p2 contains more copper ions than silk p2 because of its greater aspartic acid, glutamic acid [28], and thiol content [15].

The carbonyl, carboxyl, and hydroxyl groups in cellulosic materials can bind to tannic acid (by hydrogen bonding) as well as to metal ions [15,16]. Dyed abaca contains more iron and copper than equivalently dyed cotton probably because of the greater presence of non-cellulosic components such as lignin and hemicellulose which also contain hydroxyl and carboxyl groups [29,30].

Iron-tannate dyed textile colour and colour uniformity

The colour of textiles can be described using reflectance spectra such as those in Figure 6, or quantified using co-ordinates of a colour space system such as CIE $L^* a^* b^*$ (Table 2). The

co-ordinate values L^* , a^* , and b^* correspond to the blackness ($L^* = 0$), whiteness ($L^* = 100$), redness (+a), greenness (–a), yellowness (+b), and blueness (–b), respectively [31]. A uniform colour distribution is needed to minimise error in characterising colour changes associated with ageing and stabilisation treatment studies.

Figure 6 Visible reflectance spectra of the unaged cellulosic (A) and proteinaceous (B) substitute textiles

All of the iron-tannate dyes caused similar mid to dark blue/grey colouration of the substitute textiles (Figure 6). The colour is due to a charge transfer in the iron-tannate dye complex [2] which causes a relatively strong absorption of red light (600–700 nm with an absorption maximum at pH 4 of 620 nm [6]). Comparable reflectance spectra have been reported with laboratory produced iron gall ink [6] and traditionally dyed *Phormium tenax* (New Zealand flax) [32]. Increasing levels of iron in the textiles (Table 2) correlate well with their L^* , a^* , and b^* values.

Examination of the dyed fabrics indicated that relatively uniform textile colouration was achieved with variations in L^* , a^* , and b^* being generally less than 10% of the mean.

Surface pH of model textiles

Iron-tannate dyed textiles are typically acidic, primarily due to the hydroxyl and carboxyl functionalities of the tannic acid (see Additional file 1 for more details). This is demonstrated by the surface pH of iron-tannate dyed museum objects (Table 3) and the aqueous pH results from the same or similar iron-tannate dyed objects reported in the literature [10,33]. Correspondingly, the dyed substitute textiles were found to be acidic, exhibiting surface pH values between 2.65 and 3.91 which is significantly lower than the surface pH of the undyed equivalents which ranged between pH 5.36 and 7.46 (Table 3).

Table 3 The surface pH, breaking load, and extension of the unaged substitute textiles and iron-tannate dyed museum objects

Sample	Surface pH	Tensile testing	
		Breaking load (N)	Extension (%)
Wool undyed (WU)	7.46 (0.49) ^a	ND ^b	ND ^b
Wool dyed with p1 (Wp1)	3.91 (0.10)	ND	ND
Wool dyed with p2 (Wp2)	3.84 (0.11)	ND	ND
Silk undyed (SU)	7.24 (0.09)	70.2 (4.9)	28.2 (1.7)
Silk dyed with p1 (Sp1)	3.60 (0.06)	62.9 (4.9)	25.0 (2.6)
Silk dyed with p2 (Sp2)	3.69 (0.09)	56.4 (2.5)	22.9 (1.7)
Silk dyed with p3 (Sp3)	3.57 (0.06)	55.3 (3.8)	22.6 (1.6)
Abaca undyed (AU)	5.36 (0.18)	239.9 (43.1)	3.9 (0.5)
Abaca dyed with c1 (Ac1)	2.86 (0.07)	105.9 (18.3)	2.1 (0.3)
Abaca dyed with c2 (Ac2)	2.67 (0.08)	130.1 (24.8)	2.5 (0.5)
Cotton undyed (CU)	6.61 (0.11)	73.2 (7.7)	10.5 (1.1)
Cotton dyed with c1 (Cc1)	2.72 (0.06)	68.3 (5.3)	6.9 (0.7)
Cotton dyed with c2 (Cc2)	2.65 (0.07)	51.0 (4.8)	9.2 (1.3)
Cotton dyed with c3 (Cc3)	2.48 (0.04)	45.7 (8.6)	10.2 (1.9)
Dyed areas of modern <i>piu piu</i> owned by Dr Vincent Daniels (Figure 2)	3.72 (0.28)	ND	ND
Black fibres of broken Maori cloak and <i>piu piu</i> from the Horniman Museum (Figure 3)	2.89 (0.19)	ND	ND
Black cotton Akali Sikh turban (2005, 7-27.1 ^c)	3.39	ND	ND

a. Standard deviations are noted in parentheses when more than one analysis of a sample was taken

b. Not done due to either slippage of sample in the jaws of the tensile tester (wool samples) or the samples being too small to test (historic samples)

c. British Museum registration number

Changes in substitute textile tensile strength and extensibility due to dye application

Generally, the application of the dyes caused significant loss of tensile strength (breaking load) and extensibility in the textiles, even before any accelerated ageing had occurred (Table 3). Dyeing of abaca caused the greatest tensile strength loss of all the substitute textiles, followed by cotton, and finally silk. Wool was not tested since the high tensile strength of the wool led to unacceptable slippage of the sample during testing. The damage could be due to the acidity (pH 4 to 6) and, for the silk, the elevated temperature (55°C) of the dyebath solutions. Harsh dyeing conditions could be a major factor in the tensile strength loss seen in historic iron-tannate dyed textiles, especially as soluble iron ions and acid can be removed from the textiles during post-dyeing rinsing [34].

Characterisation of model textiles following accelerated ageing (tensile testing and spectrophotometry)

Despite showing the greatest variation in iron ion distribution (Table 2), the c1 and p1 substitute textiles were chosen to be aged as they were dyed with the highest purity and most essential reagents (iron ions and tannic acids) only, thus minimising the influence of impurities.

Little or no change in tensile strength (breaking load) or extensibility was seen in the undyed materials after four weeks of ageing. However, significant loss of tensile strength and extensibility occurred in the dyed abaca and cotton (Ac1 and Cc1) after one week of accelerated ageing and in the dyed silk (Sp1) after two weeks of ageing (Figure 7 and Table 4). The extent of degradation exhibited by the dyed textiles correlates well with their initial surface pH (Table 3), iron content (Table 2), and the presence of iron in the structurally important internal areas of the dyed fibres, suggesting that the degradation has occurred by acid hydrolysis and metal-catalysed oxidation, similar to that observed in historic iron-tannate dyed textiles [10]. The proportion of degradation occurring by the two mechanisms may be different to those experienced during natural ageing due to the elevated environmental conditions during accelerated ageing, but the essential result of catalysed loss of tensile strength and extensibility of iron-tannate dyed textiles has been determined.

Figure 7 Effect of accelerated ageing on the breaking load (A) and extension (B) of the substitute textiles

Table 4 Changes in colour, tensile breaking load (N), and extension (%) of substitute textiles during accelerated ageing (80°C, 58% RH)

Sample	Extent of ageing (weeks)	Difference in colour (aged versus unaged)				Mean tensile properties	
		ΔE_{00}^*	ΔL^*	Δa^*	Δb^*	Breaking load (N)	Extension (%)
WU	0	0.00	0.00	0.00	0.00	ND ^a	ND
	1	1.14	0.05	-0.40	1.38	ND	ND
	2	1.33	0.32	-0.48	1.58	ND	ND
	3	1.75	0.17	-0.61	2.16	ND	ND
SU	4	2.44	-0.22	-0.72	3.17	ND	ND
	0	0.00	0.00	0.00	0.00	70.2 (4.9) ^b	28.2 (1.7) ^b
	1	1.04	-0.06	-0.32	1.00	64.2 (4.4)	25.2 (0.8)
	2	1.57	0.00	-0.44	1.54	65.5 (4.8)	24.9 (2.5)
AU	3	2.16	-0.48	-0.54	2.17	62.3 (4.7)	24.8 (2.7)
	4	2.59	-0.40	-0.57	2.70	61.6 (4.3)	21.7 (2.1)
CU	0	0.00	0.00	0.00	0.00	239.9 (43.1)	3.9 (0.5)
	1	2.39	-2.17	0.67	2.78	255.5 (38.1)	3.7 (0.5)
	2	3.08	-2.82	1.05	3.43	262.8 (47.3)	3.8 (0.5)
	3	3.03	-1.63	1.39	4.22	250.0 (40.3)	3.9 (0.6)
CUI	4	3.95	-2.64	1.76	5.29	248.8 (28.9)	3.5 (0.5)
	0	0.00	0.00	0.00	0.00	117.1 (9.2)	9.1 (0.8)
	1	0.62	-0.15	-0.10	0.61	101.9 (15.7)	8.2 (1.0)
	2	1.20	0.06	-0.06	1.26	107.2 (11.6)	8.2 (0.7)
Wpl	3	1.52	-0.84	-0.07	1.48	107.1 (8.3)	8.6 (0.5)
	4	1.82	-0.28	-0.06	1.92	108.2 (11.0)	8.1 (0.5)
Spl	0	0.00	0.00	0.00	0.00	ND	ND
	1	ND	ND	ND	ND	ND	ND
	2	2.74	-0.50	-0.39	2.73	ND	ND
	3	3.64	0.42	-0.46	3.70	ND	ND
Acl	4	5.70	3.33	-0.62	5.21	ND	ND
	0	0.00	0.00	0.00	0.00	62.9 (4.9)	25.0 (2.6)
	1	1.07	-0.61	-0.17	1.13	55.6 (6.1)	19.7 (1.4)
	2	1.78	-0.31	-0.30	1.98	46.0 (3.7)	14.5 (0.7)
Ccl	3	2.15	0.25	-0.41	2.37	34.2 (9.4)	13.2 (1.5)
	4	3.27	2.02	-0.39	3.24	33.2 (6.1)	10.1 (1.8)
	0	0.00	0.00	0.00	0.00	105.9 (18.3)	2.1 (0.3)
	1	3.04	0.24	0.11	3.17	14.6 (4.9)	1.8 (0.4)
Ccl	2	4.54	-0.37	0.63	4.64	6.5 (1.9)	1.0 (0.3)
	3	5.33	-0.68	1.20	5.34	ND ^c	ND ^c
	4	4.96	-2.00	1.08	4.75	ND ^c	ND ^c
	0	0.00	0.00	0.00	0.00	68.3 (5.3)	6.9 (0.7)
Ccl	1	7.35	-4.23	0.30	6.92	29.5 (3.9)	4.9 (0.6)
	2	10.49	-4.68	1.29	10.55	13.0 (0.4)	3.7 (0.6)
	3	12.15	-5.71	2.29	12.24	7.7 (1.1)	3.5 (0.2)
	4	13.24	-6.72	3.02	13.22	6.2 (0.7)	3.5 (0.2)

a. Not done

b. Standard deviations of mean data are in parentheses

c. Not done because the samples were too brittle to be prepared for analysis

Ac1 lost tensile strength and extensibility faster than Cc1 and was too fragile for tensile testing after 2 weeks of ageing. This faster rate of degradation is congruent with the greater presence of non-cellulosic components such as hemicellulose [29,30], and the higher iron content (Table 2) in Ac1 than Cc1.

The L^* , a^* , b^* colour coordinates of a sample identify a point in 3D CIELAB colour space that describes the colour of the sample. The colour difference between two samples, e.g. between the aged and unaged substitute textiles, is described by ΔE_{00}^* which is the distance in 3D CIELAB colour space between the points that describe the colour of these samples. The CIE2000 colour difference formula that is based on the law of Pythagoras is used to calculate ΔE_{00}^* [31,35]. Depending on various factors such as surface texture, background, and viewing angle, 50% of observers can perceive a colour difference between samples of $\Delta E_{00}^* = 1$, while the majority can perceive a colour difference of 3 or more [36].

After 4 weeks of accelerated ageing there was little overall change in colour of the undyed textiles ($\Delta E_{00}^* < 4$) (Figure 8 and Table 4). The dyed textiles (p1 and c1) changed colour more than the simultaneously aged undyed equivalents. The dyed cotton showed significantly greater colour change ($\Delta E_{00}^* = 13.24$) than the other dyed textiles ($\Delta E_{00}^* < 6$).

Figure 8 The effect of accelerated ageing on the colour difference (ΔE_{00}^*) of substitute textiles

More specifically, a small yellowing ($+\Delta b^*$) of the undyed textiles occurred during accelerated ageing which for the cotton, wool, and silk was less than that seen in the dyed equivalents. The dyed textiles (Figure 9 and Table 4) showed an increase in redness ($+\Delta a^*$) and a greater reflectance of 600–700 nm light), particularly for the dyed cotton and abaca, and yellowness ($+\Delta b^*$) and a greater reflectance of 560–600 nm light) with age. These results are explained by the breakdown of the blue-black iron-tannate dye complex with thermal ageing as previously described [6,7] (see also Additional file 1), which has been observed with model iron gall inks on paper and traditionally dyed New Zealand flax on ageing [6,32]. The reflectance spectra of the four week accelerated aged dyed cotton and abaca correlate well with the reflectance spectra of the cellulosic museum objects analysed (Figure 9).

Figure 9 Visible reflectance spectra of cellulosic substitute textiles after 0 and 4 weeks of accelerated ageing (80°C, 58% RH) and of cellulosic museum objects

Experimental

Dyeings

The dyeings were performed on a Winch and a Jigger machine at the University of Manchester's dyehouse. Further information including material sources can be found in Additional file 2.

Accelerated ageing

Substitute textiles were accelerated aged in two stacks (one for the dyed and one for the undyed samples) at 80°C and 58% RH for 1, 2, 3, and 4 weeks in a Sanyo Gallenkamp Environmental Chamber. These are similar to the conditions used in iron gall ink studies (80°C, 65% RH) [37]. The stacks were arranged in the order of abaca, cotton, silk, and wool from the shelf upwards. The sample stacks were not rotated during ageing but were moved around on the shelf throughout ageing to counter any location-dependent variations in temperature and relative humidity in the chamber. See Additional file 3: Experimental section for more details.

Analytical techniques

Characterisation of the unaged substitute textiles and historic material was achieved using XRF, spectrophotometry, tensile testing, SEM-EDX, and surface pH testing. The aged substitute textiles were characterised using spectrophotometry and tensile testing. Brief methodologies for these techniques are described below. See Additional file 3: Experimental section for further details.

XRF

A Bruker ArtTax μ -XRF spectrometer with a molybdenum X-ray tube and ArtTax4.9 software was used to analyse the unaged substitute textiles and the historic samples semi-quantitatively. Single thicknesses of substitute textiles were analysed in 8 locations on filter paper for 100 s, using a 1.5 mm collimator, 50 kV, and 500 μ A in air. Analysis of material from museum objects occurred using the same experimental conditions as above with small samples such as a few short strands being adhered to a carbon tab on filter paper for analysis.

Elemental peak areas were divided by the Compton peak area and multiplied to 1000 to give the XRF ratio values that are reported in Table 2.

SEM-EDX

Resin mounted cross-sections of dyed (p1 and c1) and undyed substitute textile fabrics were analysed using an Hitachi S-4800 Field Emission SEM and an Hitachi variable pressure S-3700 N SEM (operating at 30 Pa). The SEMs were operated at 20 kV and a 12 mm working distance for all analyses. Analysis was conducted using Oxford Instruments energy dispersive X-ray analysers with INCA software. EDX spectra were collected for varying lifetimes after optimisation of the iron peak versus total time taken for analysis: 200 s for abaca and silk; 200–300 s for cotton and 500–1000 s for wool. Dyed and undyed samples of the same material were analysed using the same conditions for comparison.

Surface pH analysis

Individual sheets of substitute textile were laid on a clean glass sheet and a drop of deionised water added. A Mettler Toledo InLab@Surface pH electrode attached to a Hanna Instruments HI2210 pH meter with temperature probe was then applied to the wetted area and held in place until the pH value stabilised. Ten analyses per substitute textile were made on randomly selected locations of randomly selected textile sheets, pH 4.01 and pH 7.01 buffer solutions were used to calibrate the equipment prior to analysis.

Samples of museum objects were analysed as above one and four times depending on sample size.

Tensile testing

70–100 mm long strips of cotton and silk textiles (10 mm wide) and strips of abaca textiles (11 fibre bundles wide) were tested using an Instron 4411 tensile tester with 500 N static load cell and Series IX software. The warp direction of the cotton, abaca and silk fabrics was tested. The strips had been conditioned to approximately 21°C and 50% RH overnight before

testing. Between eight and ten strips were analysed per sample (as sample size allowed) using a 50 mm gauge length and 10 mm min⁻¹ extension speed as used by Garside, Wyeth and Zhang [38]. Exponential trend lines were fitted to tensile testing data using MS Excel.

Spectrophotometry

Average L*, a*, b* values of SCI/100 and SCE/100 data were collected using a Konica/Minolta CM-2600d spectrophotometer, Spectramagic 3.60 software and the following settings: SCI + SCE, medium aperture, UV included, 10° observer and D65 illuminant. The spectrophotometer was calibrated using a white standard before analysis and the textiles were analysed on black velvet.

10 randomly selected sheets of each unaged substitute textile were analysed in 3 randomly selected locations while each aged substitute textile sample was analysed in 5 randomly selected locations. Single layers of textile were analysed except for the unaged abaca textiles which were folded so that two layers were measured simultaneously due to the looseness of the weave compared to the other textiles. Aged abaca was too brittle to be folded without breaking and so one layer of aged abaca was measured at a time.

CIE2000 was used to calculate the ΔE_{00}^* , ΔL^* , Δa^* , Δb^* from SCE/100 data from the aged textile compared to the unaged equivalent textile.

The small aperture rather than medium aperture was used to analyse up to three areas of the historic samples as sample size allowed. All other conditions were the same as for spectrophotometry of substitute textiles.

Conclusions

Cotton, abaca, wool, and silk iron-tannate dyed substitute fabrics have been produced on a large and unprecedented scale for use in stabilisation treatment studies. The achieved colours were characteristic of iron-tannate complexes. The harsh dyeing conditions led to immediate deterioration of mechanical properties of the textiles. Dyeing introduced significant acid and metal ion content to the textiles which was shown to be present in the structurally important internal areas of the dyed cotton, abaca, and silk fibres. The use of a higher temperature during dyeing would have improved dye diffusion into the internal areas of the wool fibres. Colour, surface pH, and metal ion content were found to be suitably uniform across the textiles for the needs of this accelerated ageing study and future stabilisation treatment studies.

The dyed cotton, abaca, and silk substitute textiles lost tensile strength and extensibility significantly faster than undyed equivalents on accelerated thermal ageing, as has been known for hundreds of years to occur to iron-tannate dyed objects. Discolouration of the dyed textiles was also observed during accelerated ageing due to the breakdown of the iron-tannate dye complex resulting in colours of cellulosic textiles being comparable to the colours of naturally aged cellulosic museum objects. Consequently, the cotton, abaca, and silk model textiles were found to be valid substitutes for historic iron-tannate dyed textiles in stabilisation treatment studies.

- November 1998* (Kirby J ed, pp 211–215. Lyon and Greenwich: Archetype Publications Ltd 2002; 1998:211–215. ISBN: 1-873132-97-2).
5. O'Connor D, Richards A: **The Right Mud: Studies in Mud-Tannic Dyeing in West China and West Surrey.** In *Dyes in History and Archaeology 18, the Royal Institute For Cultural Heritage, Brussels, 21-22 October 1999*. Edited by Jo K. Brussels: Archetype Publications Ltd; 2002:41–46. ISBN 1-873132-33-6.
6. Sistach MC, Gilbert JM, Areal R: Ageing of laboratory iron-gall inks studied by reflectance spectrometry. *Restaurator* 1999, 20:151–166.
7. Neevel JG: The development of in-situ methods for identification of iron gall inks. In *Iron Gall Inks: On Manufacture, Characterisation, Degradation and Stabilisation*. Edited by Strlic M, Kolar J. Ljubljana: National and University Library; 2006:147–172.
8. Kolar J, Strlic M (Eds): *Iron Gall Inks: On Manufacture, Characterisation, Degradation and Stabilisation*. Ljubljana: National and University Library; 2006.
9. Neevel JG: Phytate: a potential conservation agent for the treatment of ink corrosion caused by iron-gall inks. *Restaurator* 1995, 16:143–160.
10. Daniels V: Factors affecting the deterioration of the cellulosic fibres in black-dyed New Zealand Flax (Phormium Tenax). *Stud Conserv* 1999, 44:73–85.
11. Te Kanawa R, Smith GJ, Fenton GA, Miller II, Dunford CL: Evaluation of Consolidants for Black Iron-Tannate-Dyed Maori Textiles. In *Dyes in History and Archaeology: 21 Avignon and Lauris, France 2002*. Edited by Kirby J, Avignon and Lauris: Archetype Publications Ltd; 2008:224–229. ISSN: 0959-0641.
12. Sato M, Okabayashi S: Consolidation treatment of Japanese ceremonial doll's hair at Edo Period with polyethylene glycol. *J Text Eng* 2010, 56:65–70.
13. Sandy M, Bacon L: A tensile testing method for monocotyledon leaves with parallel venation. In *ICOM Committee for Conservation, ICOM-CC, 15th Triennial Conference New Delhi, 22-26 September 2008*. New Delhi: Allied Publishers Pvt Ltd; 2008:198–205. ISBN 9788184243444.
14. Simpson WS: Wool Chemistry. In *Wool: Science and Technology*. Edited by Simpson WS, Crawshaw GH. Cambridge: Woodhead Publishing Limited in association with The Textile Institute; 2002:130–159.
15. Hearle JWS, Peters RH: *Fibre Structure*. Manchester: The Textile Institute; Butterworths; 1963.
16. Christie RM: *Colour Chemistry*. Cambridge: The Royal Society of Chemistry; 2001.
17. Frazier RA, Deaville ER, Green RJ, Stringano E, Willoughby I, Plant J, Mueller-Harvey J: Interactions of tea tannins and condensed tannins with proteins. *J Pharm Biomed Anal* 2010, 51:490–495.
- ## Abbreviations
- SEM-EDX, Scanning Electron Microscopy-Energy Dispersive X-ray Microanalysis; XRF, X-ray Fluorescence; C, Cotton; A, Abaca (*Musa textilis*); W, Wool; S, Silk; p1-3, Dye formulations 1–3 described in Table 1 for proteinaceous textiles; c1-3, Dye formulations 1–3 described in Table 1 for cellulosic textiles; U, Undyed model textile; CIE2000, Commission Internationale de L'Eclairage 2000 colour space formula
- ## Competing interests
- The authors declare that they have no competing interests.
- ## Authors' contributions
- MH and CC proposed the project. HW developed the dye formulations used on the model textiles and with assistance from Phil Cohen from the University of Manchester, produced the dyed model textiles in the dyehouse at the University of Manchester. HW performed all the analyses and data interpretation presented. Supervision was provided when required by CC and MH. All authors read and approved the final manuscript.
- ## Acknowledgements
- We thank AHRC, EPSRC, and the Science and Heritage Programme for their financial and other support given to this project. We also thank Dr Vincent Daniels, Dr Muriel Rigout, and Pippa Cruickshank for their assistance in this project, Phil Cohen for assisting in the production of the model textiles, Adrian Handley for assisting in the tensile testing, Nigel Meeks for assisting with SEM-EDX, Dr Huw Owens for assisting with spectrophotometry data, Dr David Pegg for the use of and assistance with the environmental chamber at the National Gallery, and Louise Bacon from the Horniman Museum for the deteriorated Maori samples.
- ## References
1. Khanbabae K, van Ree T: Tannins: classification and definition. *Nat Prod Rep* 2001, 18:641–649.
 2. Krekel C: The chemistry of historical iron gall inks. *Int J Forensic Doc Exam* 1999, 5:54–58.
 3. More N, Smith G, Te Kanawa R, Miller I: Iron-sensitised degradation of black-dyed Maori textiles. In *Dyes in History and Archaeology 19, the Royal Museum, National Museums of Scotland, Edinburgh, 19-20 October 2003*. Edited by Kirby J. Edinburgh: Archetype Publications; 2003:144–148. ISBN 1-873132-14-X.
 4. Daniels VD: Degradation of Artefacts caused by Iron-Containing Dyes. In *Dyes in History and Archaeology 16/17, Lyons, 11–12 December 1997 and Greenwich, 26–27*

18. Bhattacharya SD, Shah AK: Metal ion effect on dyeing of wool fabric with catechu. *J Soc Dyers Colourists* 2000, 116:10–12.
19. Fukatsu K, Isa M: Interaction of wool keratin fibers and copper(II) ions. *Text Res J* 1986, 56:774–775.
20. MacLaren JA, Milligan B: *Wool Science - The chemical reactivity of the wool fibre*. Marriackville: Science Press; 1981.
21. Letelier ME, Sanchez-Jofre S, Peredo-Silva L, Cortes-Troncoso J, Aracena-Parks P: Mechanisms underlying iron and copper ions toxicity in biological systems: Pro-oxidant activity and protein-binding effects. *Chem Biol Interact* 2010, 188:220–227.
22. Letelier ME, Lepe AM, Faundez M, Salazar J, Marin R, Aracena P, Speisky H: Possible mechanisms underlying copper-induced damage in biological membranes leading to cellular toxicity. *Chem Biol Interact* 2005, 151:71–82.
23. Chen WX, Lu SF, Yao YY, Pan Y, Shen ZQ: Copper(II)-Silk Fibroin Complex Fibers as Air-Purifying Materials for Removing Ammonia. *Text Res J* 2005, 75:326–330.
24. Timar-Balazsy A, Eastop D: *Chemical principles of textile conservation*. Oxford: Butterworth-Heinemann; 1998.
25. Hartley FR: The uptake of aluminium by wool. *Aust J Chem* 1968, 21:1013–1022.
26. Hartley FR: Studies in chrome mordanting. II. The binding of chromium(III) cations to wool. *Aust J Chem* 1968, 21:2723–2735.
27. Bird CL: *The theory and practice of wool dyeing*. 4th edition. Bradford: The Society of Dyers and Colourists; 1972.
28. Guthrie RE, Laurie SH: The binding of copper(II) to mohair keratin. *Aust J Chem* 1968, 21:2437–2443.
29. Hsieh Y-L: Chemical structure and properties of cotton. In *Cotton: Science and Technology*. Edited by Gordon S, Hsieh Y-L. Boston and Cambridge: CRC Press and Woodhead Publishing Limited; 2007:3–34.
30. Sun R, Fang JM, Goodwin A, Lawther JM, Bolton AJ: Fractionation and characterization of polysaccharides from abaca fibre. *Carbohydr Polym* 1998, 37:351–359.
31. Luo MR, Cui G, Rigg B: The development of the CIE 2000 colour-difference formula: CIEDE2000. *Color Res Appl* 2001, 26:340–350.
32. Te Kanawa R, Thomsen S, Smith G, Miller I, Andary C, Cardon D: Traditional Maori Dyes. In *Dyes in History and Archaeology 18, the Royal Institute for Cultural Heritage, Brussels, 21-22 October 1999*. Edited by Kirby J. Brussels: Archetype Publications; 2002:47–50.
33. Pullan M, Baldwin A: The evolution of a treatment strategy for an Akali Sikh turban. In *ICOM Committee for Conservation, ICOM-CC, 15th Triennial Conference, 22-26 September 2008*. Edited by Bridgland J. Delhi: Allied Publishers Pvt; 2008:191–197. ISBN 9788184243444.
34. HofenckdeGraaff JH: Dyeing and Writing: A comparison of the use and degradation of iron-gall complexes on textiles and paper. In *Contributions to Conservation - Research in Conservation at the Netherlands Institute for Cultural Heritage (ICN)*. Edited by Mosk JA, Tennent NH. London: James & James (Science Publishers) Ltd; 2002:34–41. ISBN 1-902916-09-3.
35. Broadbent AD: *Basic Principles of Textile Coloration*. Bradford: Society of Dyers and Colourists; 2001.
36. Kolar J, Strlic M, Pihlar B: Methodology and analytical techniques in studies of iron gall ink and its corrosion. In *Iron Gall Inks: On Manufacture, Characterisation, Degradation and Stabilisation*. Edited by Kolar J, Strlic M. Ljubljana: National and University Library; 2006:95–118.
37. Kolar J, Mozir A, Balazic A, Strlic M, Ceres G, Conte V, Miruzzo V, Steemers T, De Bruin G: New antioxidants for treatment of transition metal containing inks and pigments. *Restaurator* 2008, 2008:184–198.
38. Garside P, Wyeth P, Zhang X: Understanding the ageing behaviour of nineteenth and twentieth century tin-weighted silks. *J Inst Conserv* 2010, 33:179–193.
39. Wunderlich CH: Über Eisengallustinte. *Zeitung der Anorganischen Allgemeinen Chemie* 1991, 598–599:371–376.
40. Wunderlich CH: Geschichte und Chemie der Eisengallustinte - Rezepte, Reaktionen und Schädwirkungen. *Restaurator* 1994, 100:414–421.
41. Taseem Z, Kazni SA, Sultana K: Role of water in aqueous solution of iron gallic acid complexes. *Pak J Sci Ind Res* 1991, 34:45–48.
42. Marmolle F, Leize E, Mila I, Van Dorsselaer A, Scalbert A, Albrecht-Gary AM: Polyphenol metallic complexes: characterization by electrospray mass spectrometric and spectrophotometric methods. *Analyst Magazine* 1997, 25:53–55.
43. Hynes MJ, O'Coincinnainn M: The kinetics and mechanisms of the reaction of iron(III) with gallic acid, gallic acid methyl ester and catechin. *J Inorg Biochem* 2001, 85:131–142.
44. Sungur S, Uzar A: Investigation of complexes tannic acid and myricetin with Fe(III). *Spectrochim Acta A* 2008, 69:225–229.
45. Jaen JA, Gonzalez L, Vargas A, Olave G: Gallic Acid, Ellagic Acid and Pyrogallol Reaction with Metallic Iron. *Hyperfine Interactions* 2003, 148/149:227–235.

46. Delamare F, Repoux M: Studying dyes by Time of Flight Secondary Ion Mass Spectrometry. In *Dyes in History and Archaeology 20*; Amsterdam. Edited by Kirby J.; Archetype Publications; 2001.
47. Darbour M: *Les encres métallurgiques*. Université de Paris VI: Étude de la dégradation de l'acide gallique et analyse du complexe ferrogallique; 1980.
48. Iglesias J, Garcia de Saldana E, Jaen JA: On the Tannic Acid Interaction with Metallic Iron. *Hyperfine Interactions* 2001, **134**:109–114.
49. Kipton H, Powell J, Taylor MC: Interactions of Iron(II) and Iron(III) with Gallic Acid and its Homologues: a Potentiometric and Spectrophotometric Study. *Aust J Chem* 1982, **35**:739–756.
50. Darbour M, Bonmassies S, Fliedner F: Les encres métallurgiques. Étude de la dégradation de l'acide gallique et analyse du complexe ferrogallique. In *ICOM-CC 6th Triennial Meeting*. Los Angeles, USA: ICOM-CC; 1981:1–14.
51. Wagner B, Bulska E, Stahl B, Heck M, Ortner HM: Analysis of Fe valence states in iron-gall inks from XVIIIth century manuscripts by 57Fe Mössbauer spectroscopy. *Anal Chim Acta* 2004, **527**:195–202.
52. Daniels VD: The Chemistry of Iron Gall Ink. In *The Iron Gall Ink Meeting - First triennial conservation conference* (Brown AJE ed. pp. 31–36. Newcastle upon Tyne: Conservation of Fine Art, University of Northumbria; 2000:31–36.
53. Slawinska D, Slawinski J, Polewski K, Pukacki W: Chemiluminescence in the peroxidation of tannic acid. *Photochemistry and Photobiology* 1979, **30**:71–80.
54. Sistiach MC, Espedaler I: Organic and inorganic components of iron gall inks. In *Preprints of the ICOM Committee for Conservation 10th Triennial Meeting*. Washington DC, Washington D.C.: ICOM Committee for Conservation; 1993:485–490.
55. Shahani CJ, Hengemihle FH: The influence of copper and iron on the permanence of paper. In *Historic textiles and paper materials - Conservation and characterization*. Edited by Needles H, L., Zeronian SH. Washington, DC: American Chemical Society; 1986: 387–410.[Comstock MJ (Series Editor): *Advances in Chemistry Series*].
56. Neevel JG: (Im)possibilities of the phytate treatment of ink corrosion. In *Contributions to Conservation*. Edited by Mosk JA, Tennent NH.; James & James; 2002:74–86.
57. McDonald M, Mila I, Scalbert A: Precipitation of metal ions by plant polyphenols: Optimal conditions and origin of precipitation. *J Agric Food Chem* 1996, **44**:599–606.
58. Kolar J, Stofa A, Strlic M, Pompe M, Pihlar B, Budnar M, Simcic J, Reissland B: Historical iron gall ink containing documents - Properties affecting their condition. *Anal Chim Acta* 2006, **555**:167–174.
59. IUPAC: *Compendium of Chemical Terminology*. Oxford: Blackwell Scientific Publications; 1997.
60. Selih VS, Strlic M, Kolar J, Pihlar B: The role of transition metals in oxidative degradation of cellulose. *Polym Degradation Stability* 2007, **92**:1476–1481.
61. Budnar M, Simcic J, Ursic M, Rupnik Z, Pelicon P: Transition metals in historical documents, determined by In-Air PIXE. In *Iron Gall Inks: On Manufacture, Characterisation, Degradation and Stabilisation*. Edited by Strlic M, Kolar J. Ljubljana: National and University Library; 2006:141–146.
62. Rosetti G: *The Plietho of Gioaventura Rosetti: Instructions in the Art of the Dyers which Teaches the Dyeing of Woolen Cloths, Linens, Cottons, and Silk by the Great Art as Well as by the Common*. Translation of the First Edition of 1548 by Sidney M. Edelstein and Hector C. Borghetty. Cambridge, Massachusetts: MIT Press; 1548.
63. Anonymous: *Black Silks, Textile Colorist* 1898, **20**:287–288.
64. Bird FI: *The Dyer's Hand-book*. Manchester: John Heywood; 1876.
65. Haigh J: *The Dyer's Assistant in the Art of Dying Wool and Woollen Goods*. London;; 1800.
66. Packer T: *The Dyer's Guide*. 2nd., corrected and materially improved edn. London: Printed for Sherwood, Gilbert, and Piper; 1830.
67. Porck HJ: *Rate of Paper Degradation - The Predictive Value of Artificial Aging Tests*. Amsterdam: European Commission on Preservation and Access; 2000.

Additional files

Additional_file_1 as DOC

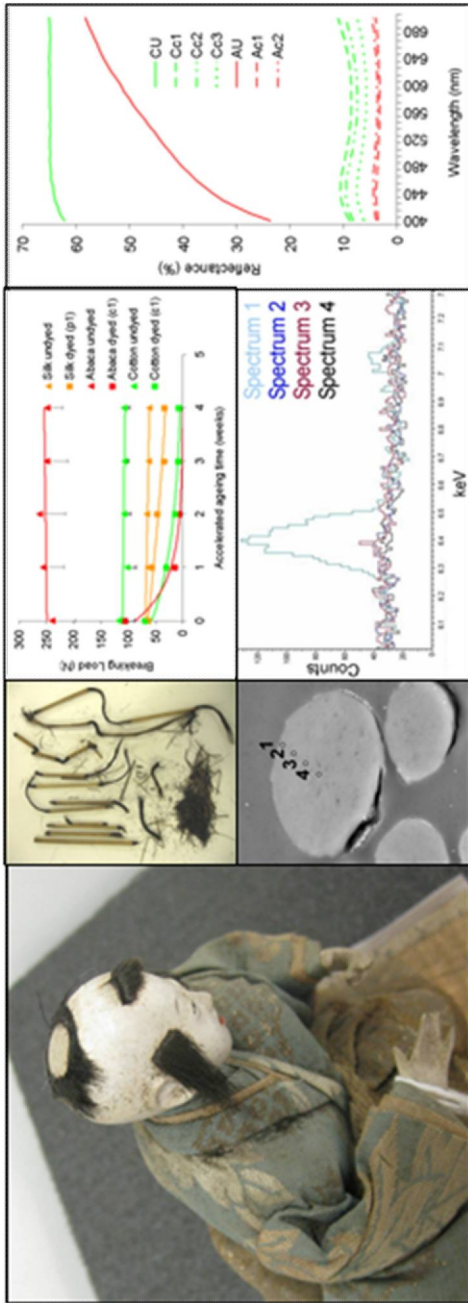
Additional file 1: Iron-tannate dye chemistry. Text and schemes [2-7,9,10,39-61]

Additional_file_2 as DOC

Additional file 2: Further substitute textile development and dyeing method details. Text and images [62–66]

Additional_file_3 as DOC

Additional file 3: Experimental section. Text only [37,38,67]



Graphical abstract



Figure 1



Figure 2



Figure 3

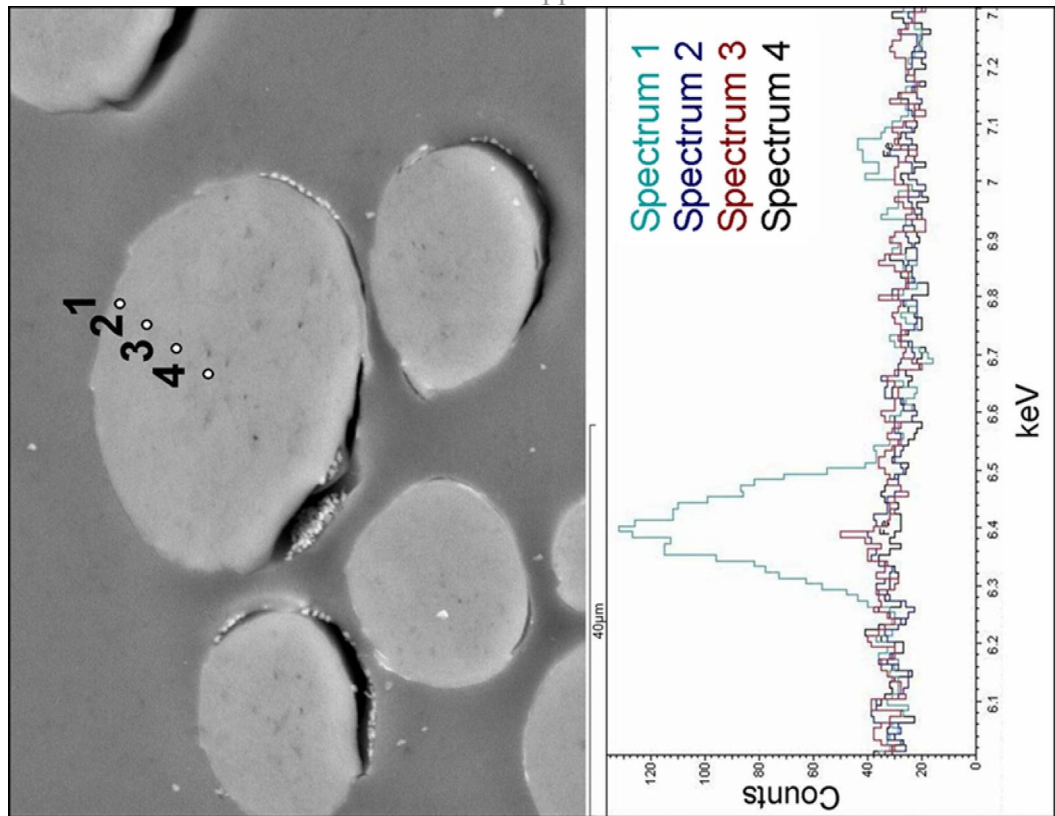


Figure 5

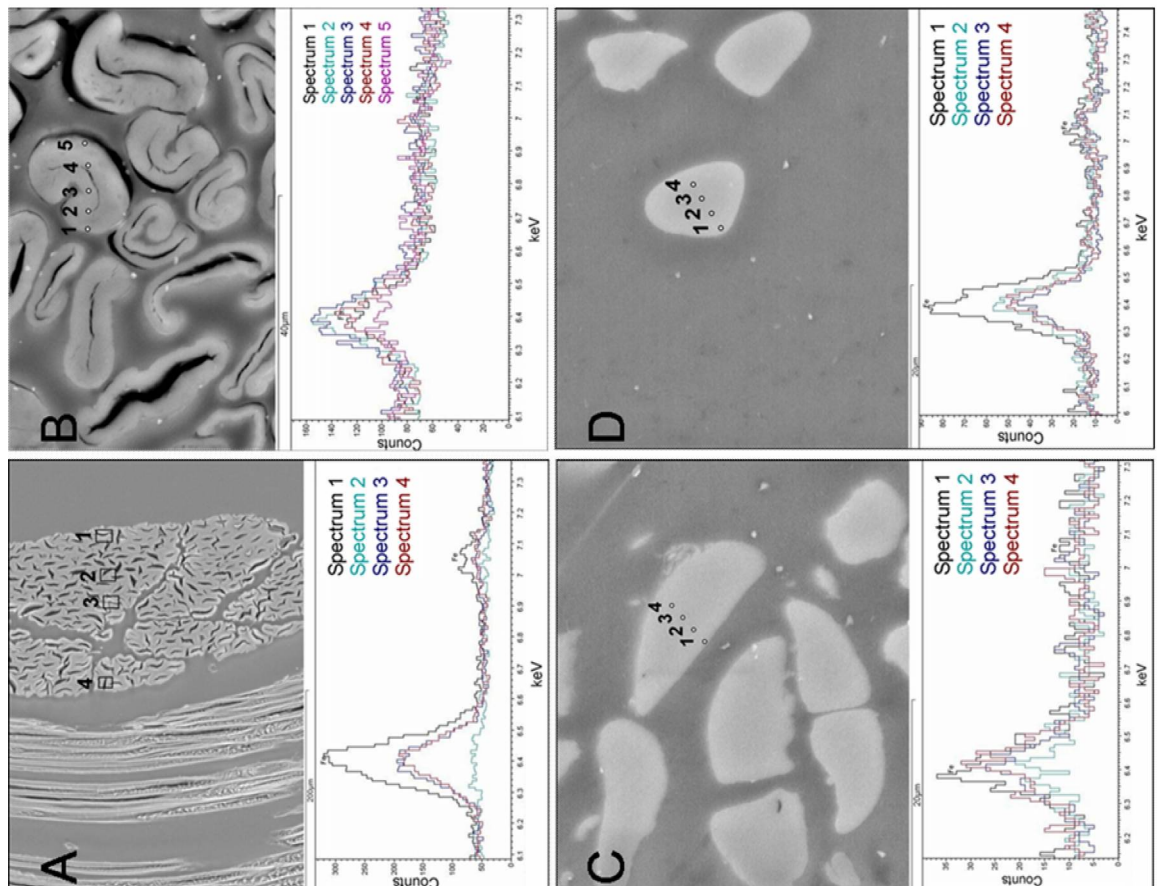


Figure 4

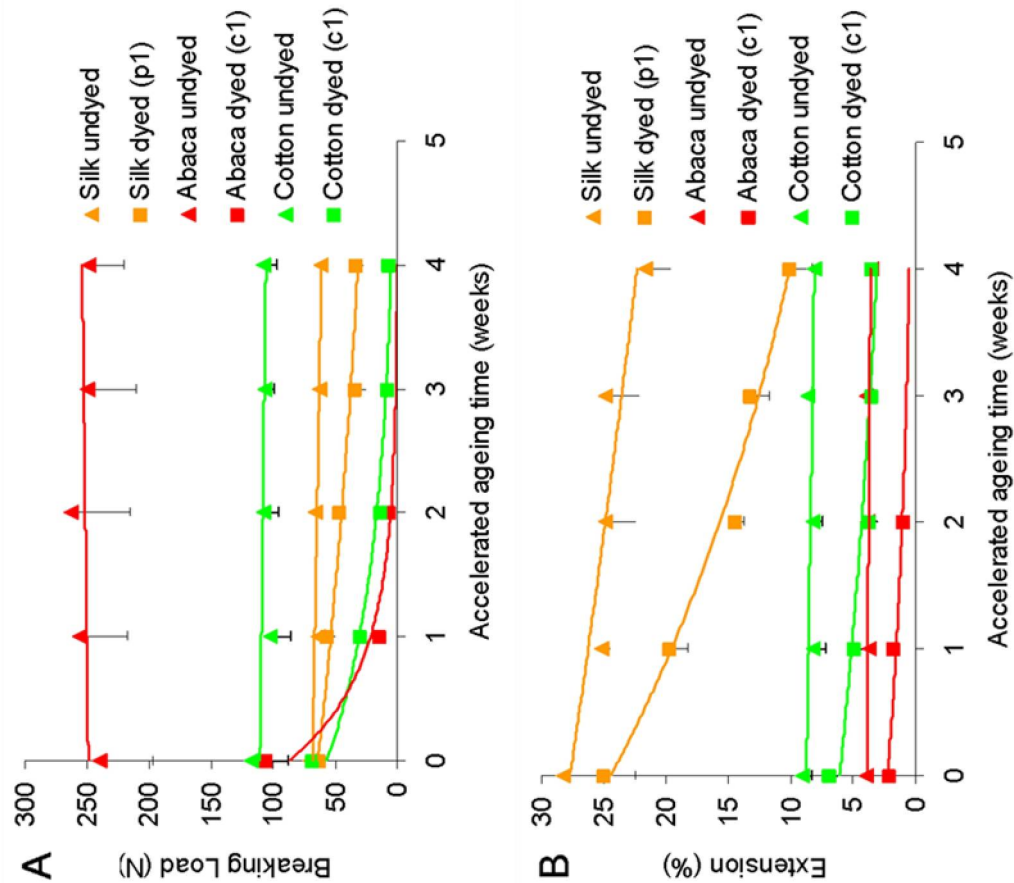


Figure 7

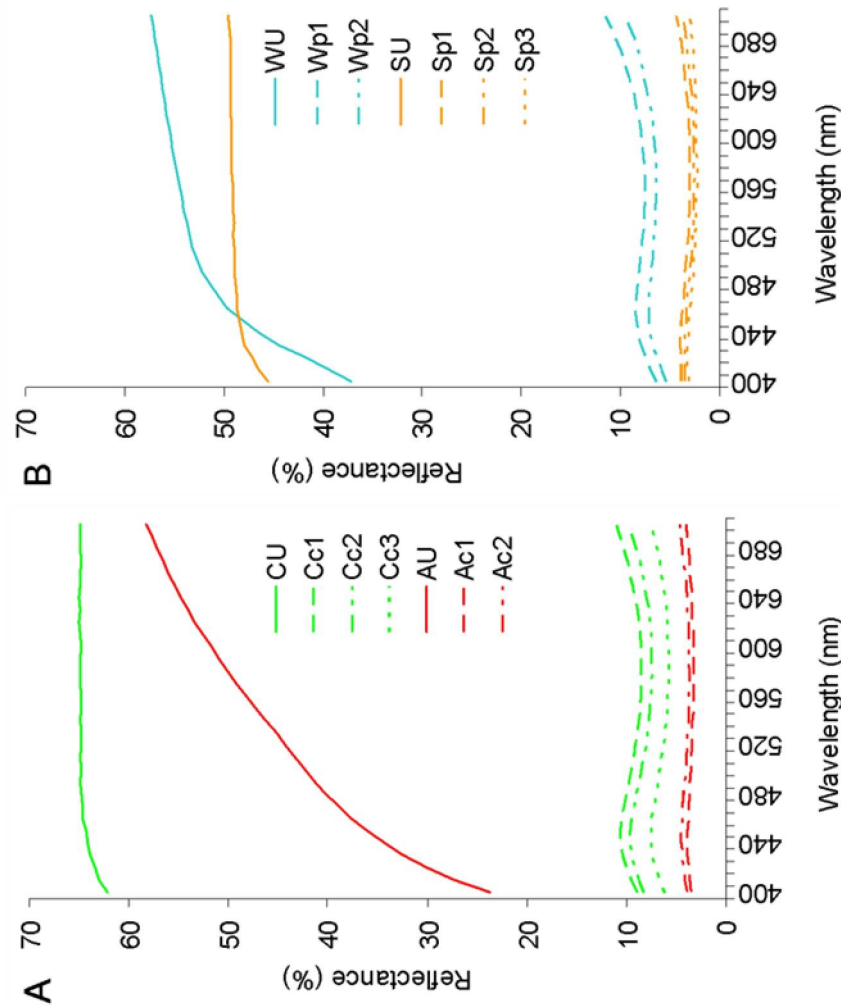


Figure 6

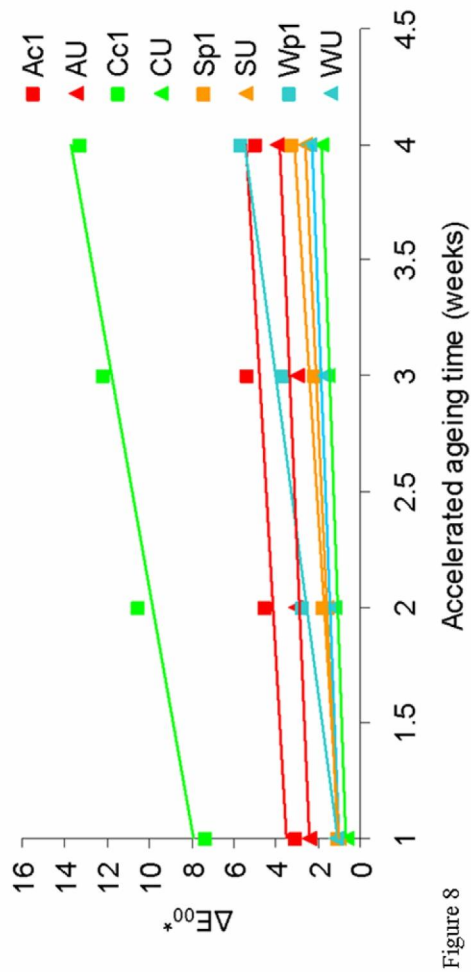


Figure 8

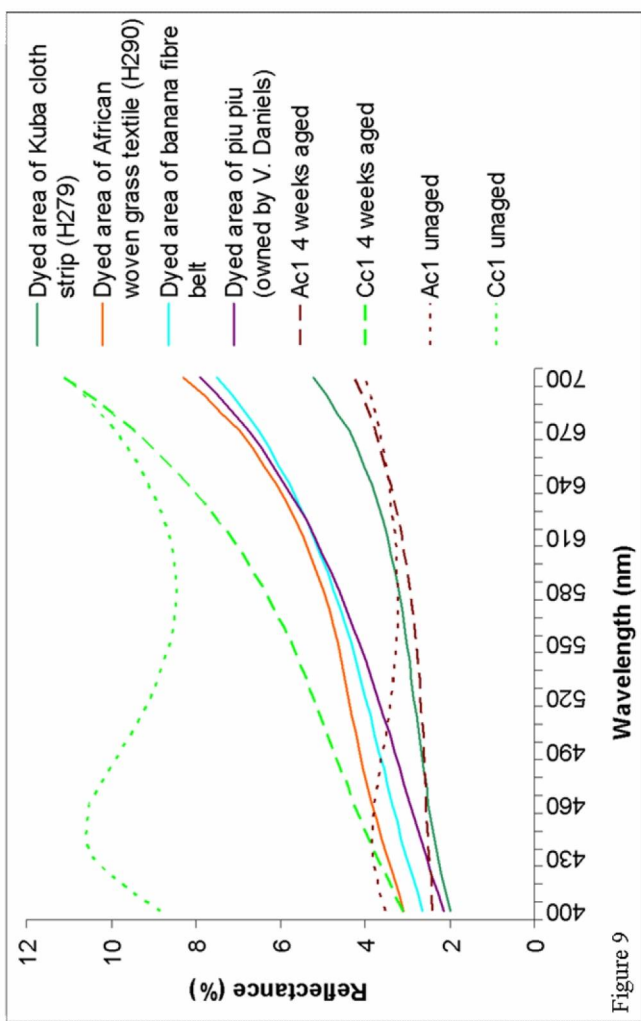


Figure 9

Additional files provided with this submission:

Additional file 1: Additional file 1b.pdf, 38K
<http://www.journal.chemistrycentral.com/media/4435725626816476/suppl1.pdf>
 Additional file 2: Additional file 2b.pdf, 359K
<http://www.journal.chemistrycentral.com/media/6570986446816477/suppl2.pdf>
 Additional file 3: Additional file 3.pdf, 27K
<http://www.journal.chemistrycentral.com/media/1875290976704179/suppl3.pdf>

APPENDIX 2 ICOM-CC 16th Triennial Conference publication, 2011

The peer-reviewed paper presented at the 16th international triennial ICOM-CC conference in Lisbon, Portugal, from the 19th to the 23rd September 2011

HELEN WILSON*

The University of Manchester
Manchester, UK
The British Museum
London, UK
helen.louise.wilson@gmail.com

PIPPA CRUICKSHANK

The British Museum
London, UK
pcruickshank@thebritishmuseum.ac.uk

MAREI HACKE

The British Museum
London, UK
mhacke@thebritishmuseum.ac.uk

REBECCA STACEY

The British Museum
London, UK
rstacey@thebritishmuseum.ac.uk

CHRIS CARR

The University of Manchester
Manchester, UK
christopher.m.carr@manchester.ac.uk

VINCENT DANIELS

The British Museum
London, UK
vdaniels@thebritishmuseum.ac.uk

MURIEL RIGOUT

The University of Manchester
Manchester, UK
Muriel.Rigout@manchester.ac.uk
*Author for correspondence

INVESTIGATION OF NON-AQUEOUS REMEDIAL TREATMENTS FOR IRON-TANNATE DYED TEXTILES

Keywords: iron, tannin, dye, textile, black, non-aqueous, antioxidant, deacidifier

ABSTRACT

Iron-tannate dyes accelerate the degradation of the substrates they colour, severely decreasing the material's lifetime. This paper presents preliminary results focusing on the development of non-aqueous remedial conservation treatment(s) to inhibit degradation. A range of antioxidants and deacidifiers in organic solvent applied to model iron-tannate dyed cotton and silk fabrics and the effects of the treatments on accelerated ageing of the cotton have been evaluated using spectrophotometry and handling tests. The results show that there is little correlation between colour and strength of the samples after ageing. Strength-retention is considered of greater importance than colour-retention. The protective agents showing most potential are Tinuvin 292, Tinuvin 144, alpha-tocopherol, phytic acid, etidronic acid and magnesium ethoxide. Completion of the cotton and silk analyses will identify the most promising treatments for further investigation.

RÉSUMÉ

Les colorants au tannate de fer accélèrent la dégradation des substrats qu'ils colorent, diminuant drastiquement la durée de vie du matériau. Cet article présente les résultats préliminaires à propos du développement de traitement(s) de conservation curative non aqueux afin d'interrompre la dégradation. Une gamme d'antioxydants et de produits de désacidification dans un solvant organique appliqué sur des modèles de tissus en soie et en coton teints au tannate de fer et les effets des traitements sur le coton vieilli de façon accélérée ont été évalués par spectrophotométrie et par des essais de manipulation. Les résultats ont montré qu'il n'existe qu'une faible corrélation entre la couleur et la résistance

INTRODUCTION

Iron-tannate dyes have been used to colour a wide variety of organic materials worldwide for thousands of years and are present in many museum collections. The dyes produce shades of black, grey, and brown. Unfortunately, even under ambient environmental conditions the dyes accelerate the degradation of the substrates they colour and can eventually lead to complete disintegration of dyed objects in unusually short timescales (Figures 1 and 2). Currently, there are no suitable remedial conservation treatments to inhibit this dye-catalysed degradation for fragile textiles or objects with iron-tannate-dyed organic components; this project seeks to address this problem. Firstly, model iron-tannate dyed woven textiles (cotton, abaca, wool, and silk) were developed. Secondly, a range of antioxidants and deacidifiers in non-aqueous solutions were applied to a proportion of the cotton and silk model textiles. These treatments are being evaluated for their effect on textile colour and handle both before and after accelerated ageing, and pH testing, viscometry (cotton only) and SEM will also be performed. The spectrophotometric, visual colour assessment and handling test results for cotton are reported here. Based on all of the results, several treatments will be investigated further on pre-aged cotton, abaca, wool and silk model textiles.

IRON-TANNATE DYE CATALYSED DEGRADATION

Iron-tannate dyes accelerate oxidation and acid hydrolysis of the substrates they colour through the presence of reactive, unbound iron(II) ions. These ions may originate from the dyeing process or from the breakdown of the blue-black iron(III)-tannate complex which occurs when iron(III) is converted to iron(II) during the oxidation of carbohydrates to acids. Unbound iron(II) ions accelerate oxidation via the Fenton reaction. The resulting acid groups increase the rate of acid hydrolysis, which in turn converts iron(III) to reactive iron(II) ions, restarting the cycle of accelerated degradation. Iron-tannate dyes frequently also contain copper and other metal ions, either as deliberate inclusions in the dye recipe or as contamination from impure iron sources. These can also accelerate the cycle via a similar mechanism. This cycle of accelerated degradation is also seen with iron gall inks on paper, since these inks are chemically similar to iron-tannate dyes.

des échantillons après vieillissement. La rétention de résistance est considérée comme plus importante que la rétention de couleur. Les agents protecteurs faisant preuve du plus fort potentiel sont le Tinuvin 292, le Tinuvin 144, l'alpha-tocophérol, l'acide phytique, l'acide éthydronique et l'éthoxide de magnésium. À terme, les analyses du coton et de la soie identifieront les traitements les plus prometteurs pour des recherches ultérieures.

RESUMEN

Los tintes de tanato de hierro aceleran la degradación de los sustratos que tiñen, disminuyendo drásticamente la vida del material. Este artículo presenta los resultados preliminares centrados en el desarrollo de tratamientos de conservación no acuosos para inhibir la degradación. A través de espectrofotometría y pruebas de manipulación se evaluó una serie de antioxidantes y desacidificantes en disolventes orgánicos aplicados a muestras de algodón y tejidos de seda teñidos con tanato de hierro, así como los efectos de los tratamientos al someter el algodón a envejecimiento acelerado. Los resultados muestran que hay poca relación entre el color y la resistencia de las muestras después del envejecimiento. La retención de la resistencia se considera de mayor importancia que la retención del color. Los agentes protectores que mostraron mayor potencial fueron: Tinuvin 292, Tinuvin 144, alfa-tocoferol, ácido fítico, ácido etidróico y etóxido de magnesio. Una vez finalizados los análisis del algodón y la seda se identificarán los tratamientos más prometedores para continuar con la investigación.



Figure 1
 Reverse of an African printed cotton
 Adinkra cloth (Registration number:
 Af1818,1114.23), acquired by the British
 Museum in 1818, showing textile loss and
 discolouration due to the dye

EXISTING REMEDIAL CHEMICAL TREATMENTS

To inhibit the acceleration of substrate degradation caused by iron gall inks and iron-tannate dyes, antioxidants such as metal ion chelators and radical scavengers, as well as alkaline compounds for deacidification, have been investigated. This has led to the development of aqueous treatments based on phytate as a metal ion chelator (Neevel 2002, Kolar et al. 2007). However, aqueous treatments are often unsuitable for use on fragile organic materials, partly due to the swelling of fibres caused by water.

Non-aqueous treatments for iron-gall ink on paper are currently being researched (Kolar et al. 2008) and their applicability to proteinaceous and cellulosic textiles is investigated in this project. Consolidation treatments that can inhibit discolouration have also been developed (Te Kanawa 2008).

NON-AQUEOUS REMEDIAL TREATMENT REQUIREMENTS

Any successful non-aqueous remedial treatment developed in this project should significantly inhibit degradation of iron-tannate dyed textiles. The treatment should have minimal effect on textile handle and colour and if possible, be non-toxic, and easy to apply to large or three-dimensional objects that may be made of composite materials using readily available chemicals, solvents and equipment. Treatment application methods will be investigated upon completion of the chemical tests planned for future work.

The established aqueous magnesium phytate treatment will be used as a control to measure the success of the potential non-aqueous treatments.

EXPERIMENTAL METHOD

Model textiles

Woven textiles of abaca, cotton, wool and silk were chosen as model textiles following research into the types of iron-tannate dyed materials within the British Museum's collections. The textiles have been dyed using up to three different iron-tannate dye formulations. The dyes comprise iron sulphate, copper sulphate, purified tannic acids and gall extracts and are based on historical dye recipes and experimental results (Gill et al. 2010).

Treatment solutions

Ten chemicals and five organic solvents were investigated (Table 1). I1425 and M were not soluble in the organic solvents tested and so not investigated further.

A variety of chemical concentrations and combinations, in each case using the least toxic solvent possible (Table 2), were applied to model textile samples. When available, published precedents or manufacturer guidelines were used to choose treatment concentrations for study (Kolar et al. 2007, Kolar et al. 2008). When unavailable, the choice of chemical concentration was

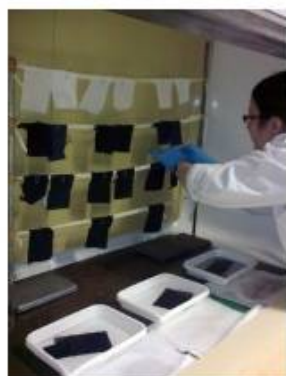


Figure 2
Black silk hair of a Japanese ceremonial Hina doll (Registration number: A51981,0808,229) embrittled by the dye

Figure 3
Textile samples being treated and hung to dry

Figure 4
Treated samples prepared for accelerated aging

Table 1
Chemicals and solvents under investigation

Stabilisation role	Chemical/Solvent ^a	Chemical abbreviation
Peroxide decomposer	1-ethyl-3-methylimidazolium bromide	EBR
Radical scavenging antioxidant	Alpha-tocopherol	AT
	Irganox 1135	I1135
	Irganox 1425	I1425
	Tinuvin 144	T144
	Tinuvin 292	T292
Metal ion chelating antioxidant	Phytic acid	PA
	Etidronic acid	EA
	Melaneze	M
Deacidifier	Magnesium ethoxide	ME
Solvent	Ethanol (100%)	EtOH
	Industrial methylated spirits	IMS
	Tetrachloroethylene	T
	n-Hexane	H
	Cyclosiloxane D5 (GreenEarth)	GE

a. IUPAC names are given in the materials list.

influenced by the concentrations used for chemicals of similar stabilisation role, e.g. radical scavenger. All concentrations were calculated with respect to the mass of fabric being treated so that the mass of chemical per mass of textile remained the same for sample comparability. Consequently, the concentrations for the dyed and undyed samples differ.

Magnesium phytate (MP), the control, was produced by combining magnesium carbonate hydrate (MC) and PA(MP) in water. Dried MP treated textile samples were immersed in two consecutive calcium bicarbonate (CB) solutions. These solutions were formed as described by Kolar et al. (2007) using 26.6832 g CB in 7.2 l deionised water.

Treatment application to model textiles

Samples of undyed cotton and silk model textiles (15 x 10 cm) and those dyed with dye formulation 3, a combination of iron sulphate and aqueous extract of gall powder (Gill et al. 2010), were used in all tests. The samples were immersed in treatment solution (300 ml) for 30 minutes and were hung to dry in the fume cupboard. Cross-contamination of dye was eliminated through separate treatment of dyed and undyed samples except for the AT200 test (Figure 3).

Accelerated ageing

A portion of each treated and untreated sample (5 x 10 cm) was accelerated aged for two weeks with an untreated control at 80°C and 65% RH in a Sanyo Gallenkamp environmental chamber with Format 550 Programmer. The labelled samples were stacked according to treatment types on a piece of Munktell CXD pHoton Aqua Forte High Wet Strength absorbent paper (90 grams per square meter) on the chamber shelf (Figure 4).

Table 2
Chemical concentrations used

Chemical	Solvent	ME ~30% textile weight ^a	Chemical mass in 300 ml of solvent as approximate % textile weight ^b	Concentration, M	
				Dyed ^c	Undyed ^d
Antioxidants					
AT	GE		2.00	0.00052	0.00047
			3.00	0.00078	0.00070
			6.00	0.00155	0.00141
		Y	6.00	0.00157	0.00141
AT ^b	GE		200.00	0.05146	0.05146
EA	IMS		0.40	0.00019	0.00017
		Y	0.40	0.00019	0.00017
			2.00	0.00097	0.00087
			4.00	0.00195	0.00174
		Y	4.00	0.00195	0.00174
EBR	EtOH		6.00	0.00335	0.00300
			30.00	0.01675	0.01500
			60.00	0.03350	0.03001
I1135	GE		2.00	0.00057	0.00051
			3.00	0.00086	0.00077
			6.00	0.00172	0.00154
			43.00	0.01229	0.01229
		Y (in IMS)	43.00	0.01229	0.01229
PA	IMS		3.00	0.00047	0.00044
			15.00	0.00243	0.00219
			30.00	0.00486	0.00438
		Y (in IMS)	30.00	0.00487	0.00436
T144	T		2.00	0.00033	0.00029
			3.00	0.00049	0.00044
			6.00	0.00098	0.00088
		Y	6.00	0.00099	0.00088
			450.00	0.07282	0.07282
T292	GE		2.00	0.00025	0.00023
			3.00	0.00038	0.00034
			6.00	0.00077	0.00069
		Y	6.00	0.00077	0.00069
			260.00	0.03277	0.03277
PA (MP)	Water		5.00	0.00098	0.00044
			15.00	0.00244	0.00218
			30.00	0.00487	0.00436
MC	Water		0.82	0.00108	0.00107
			4.66	0.00617	0.00562
			9.37	0.01241	0.01125
Deacidifier					
ME	EtOH		6.00	0.00558	0.00502
			30.00	0.02793	0.02496
			60.00	0.05603	0.05000

a. Y (yes) means a separate application of ME30 was made to a treated sample.

b. Combination of these values and the chemical abbreviation form the treatment codes referred to from now on e.g.

AT200. IMS is included in the treatment code when used with PA to highlight the use of organic solvent. The magnesium phytate and calcium bicarbonate treatment is noted as MPx/2CBx, where 'x' is the mass of PA(MP) as percentage of textile weight.

c. In some cases, concentrations for undyed and dyed textiles vary because of differing textile masses; the mass of chemical per mass of textile is equal. In other cases the concentration is independent of textile mass.

d. A very small piece of undyed textile was added to the dyed sample treatment bath rather than treating 10 cm x 15 cm undyed samples separately due to insufficient quantity of solvent.

Handling tests

After ageing, the dyed samples were assessed by comparing aged treated samples (T) with the aged untreated sample (U). The handling tests were conducted by the same person in a well-lit area for consistency.

Strength was assessed by gently pulling individual fibres apart, folding and pressing a corner of the sample until it broke or four folds was reached, and folding and rolling a fibre together between fingers to see if it broke.

Surface rub resistance was assessed by rubbing the sample gently between the thumb and forefinger and judging the quantity of dark fibres left on the nitrile glove.

Colour was assessed by visually comparing the aged treated samples next to the aged untreated control sample. Spectrophotometry was used to obtain an objective measure of colour changes.

Spectrophotometry

A Minolta CM-2600d spectrophotometer was used with Spectramagic 3.60 software. Medium aperture, D65 illumination, 10° observer and UV included settings were used. A single thickness of each sample was analysed on a black velvet background in five randomly selected locations. Colour differences (ΔE_{00}) between aged treated and untreated samples were calculated using the CIE2000 (Commission Internationale de L'Eclairage) formula.

RESULTS

Colour

Reasonable correlation exists between the colour differences assessed visually and through spectrophotometric analysis. However, the spectrophotometric data is used in the following discussion as it provides the most accurate assessment of subtle colour changes. This could be because only samples of the same treatment were compared simultaneously, and comparison between samples of different treatments was not undertaken. Consequently, the spectrophotometric data provides a more accurate assessment of colour-retention, especially where subtle changes are involved.

ΔE_{00} indicates the difference in colour between the aged treated and aged untreated dyed cotton samples. This reflects colour changes due to treatment application and subsequent ageing. All treated samples retained colour comparably or better than the untreated sample ($+\Delta E_{00}$) (Table 3). The majority of treated samples were darker ($-\Delta L^*$) and bluer ($-\Delta b^*$) than the untreated sample and approximately half of the treated samples, primarily those containing ME, EBR and MPx/2CBx were greener or less red ($-\Delta a^*$).

T292260, EBR60, EBR30 and ME60 retained colour the best ($\Delta E_{00} > 3$), better than the MPx/2CBx treatments ($2 > \Delta E_{00} < 3$) (Table 3). Generally the

Table 3

Results from handling tests and spectrophotometry of two week aged (80°C, 65% RH) treated and untreated dyed cotton samples

Treatment code	Handling test			Spectrophotometry			
	Strength ^a	Surface rub resistance ^a	Colour ^a	ΔE_{∞}	ΔL^*	Δa^*	Δb^*
U	0	0	0	0.00	0.00	0.00	0.00
ME6	+	0	+	1.51	-1.68	0.19	-0.88
ME30	++	++	++	3.88	-4.26	-0.35	-2.67
ME60	++	+++	+++	3.99	-4.18	-0.27	-3.00
ME60/IMS	++	+++	+++	4.25	-4.50	-0.35	-3.13
EA0.4	+	+	0	1.30	1.51	0.37	0.10
EA0.4/ME30	++	++	+	2.59	-2.73	-0.19	-1.93
EA2	+	+	0	1.66	-2.03	0.23	-0.53
EA4	++	++	+	2.41	-2.83	0.34	-1.12
EA4/ME30	++	++	+	1.88	-2.20	0.45	-0.59
EBR6	-	-	+	3.48	-3.92	-0.14	-2.25
EBR30	+	0	++	5.19	-4.25	-0.53	-4.89
EBR60	+	0	++	5.91	-4.60	-0.42	-5.67
EBR60/IMS	0	0	++	5.29	-3.20	-0.59	-5.59
T1442	+	+	+	2.61	-3.24	0.11	-0.97
T1443	++	+	+	1.41	-1.71	0.31	-0.27
T1446	++	+	+	2.00	-2.53	0.29	-0.25
T1446/ME30	+++	+++	++	2.34	-2.33	-0.27	-1.91
T144450	++	++	+	2.43	-3.03	-0.26	-0.83
T2922	+	0	+	1.58	-1.42	0.31	-1.27
T2923	+	0	+	2.55	-3.08	0.12	-1.15
T2926	+	0	0	1.39	-1.67	0.08	-0.62
T2926/ME30	++	++	++	2.11	-2.25	-0.26	-1.52
T292260	+++	+++	+++	6.09	-6.42	0.61	-4.18
AT2	0/+	+	0	0.68	-0.78	0.18	-0.17
AT3	+	+	0	0.48	-0.33	0.27	0.30
AT6	+	+	0	0.30	-0.19	0.18	0.20
AT6/ME30	++	++	++	2.61	-2.71	-0.35	-1.98
AT200	++	++	+	2.71	-3.42	0.45	0.49
PA10/IMS/ME30	+++	+++	++	2.83	-2.96	-0.01	-2.12
PA10ME60/IMS	++	++	+	1.04	-0.90	0.35	-0.68
PA10MC15/IMS	++	++	+	1.00	-0.84	0.38	-0.60
PA5/IMS	0	+	0	1.56	-1.89	0.25	-0.51
PA15/IMS	+	++	0	0.52	0.25	0.35	-0.06
PA30/IMS	++	++	-	2.86	3.33	0.59	1.09
PA30/IMS/ME30	+++	++	0	1.22	-0.82	0.34	-1.10
MP5/2CB5	+++	+++	+	2.44	-1.95	-0.41	-2.40
MP15/2CB15	+++	+++	++	2.48	-2.04	-0.23	-2.42
MP30/2CB30	+++	+++	++	2.70	-2.28	-0.24	-2.59
I11352	+	++	0	0.97	-1.09	0.30	-0.21
I11353	+	++	0	0.77	-0.89	0.23	-0.07
I11356	+	++	0	1.21	-1.55	0.08	-0.09
I113543	0	+	0	1.42	-1.76	0.26	-0.08
I113543/ME30	+	++	0	1.51	-1.90	0.11	-0.33

a. Classification of treated (T) and untreated (U) samples followed a five point scale:

- T exhibits poorer property retention than U.
- 0 No difference between T and U.
- +
- ++ T exhibits slightly better property retention than U.
- +++ T exhibits better property retention than U.
- ++++ T exhibits markedly better property retention than U.

b. L*, a*, and b* describe the colour of a sample in CIELAB colour space. They indicate lightness (L*) from 0-100 (black to white), redness (+a*), greenness (-a*), yellowness (+b*), and blueness (-b*).

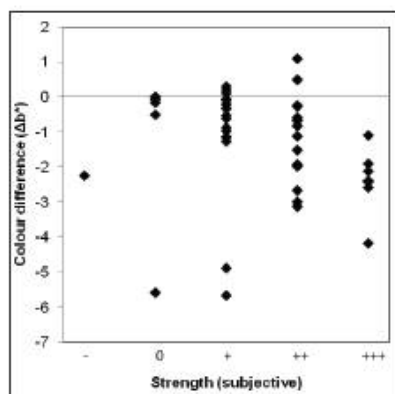


Figure 5
 Graph of correlation between colour difference (Δb^*) and strength-retention (assessed by handling tests) of treated dyed cotton samples after two weeks of ageing at 80°C, 65% RH

combination of ME30 and antioxidant caused greater colour-retention than antioxidant alone and many examples including T2926/ME30 and T1446/ME30 have $\Delta E_{00} > 2$. Colour-retention is often concentration dependent with the lowest concentrations achieving $\Delta E_{00} < 1$. I1135 resulted in least colour-retention with colour change for all concentrations being comparable to the untreated sample ($\Delta E_{00} < 1$).

Exceptions to these trends exist and could arise due to uneven treatment application, natural colour variation of the model textile samples and uneven exposure during ageing. However, every effort was made to minimise these variations.

Strength and surface rub resistance

The strength and surface rub resistance of aged samples treated with antioxidant and ME30 were often significantly higher, i.e. better, than the results of the equivalent samples treated with antioxidant alone (Table 3).

Of the samples treated with antioxidant alone, AT200, T292260, T144450, EA4, PA10MC15/IMS, and PA30/IMS show the most potential with strength and rub resistance scores of '+' or '++'. All the MPx/2CBx samples scored '+++'.

Treatment success is often concentration dependent, as demonstrated by the majority of results of the higher concentration samples compared to the lower concentration samples of the same chemical (Table 3).

Interestingly, there is little correlation between strength- and colour-retention of the samples after ageing (Figure 5).

DISCUSSION

The handling tests were made as objective as possible through consistency in method. The results clearly indicate the comparative effectiveness of the treatments. The concentration-dependence of antioxidant success suggests that the less successful antioxidants in this study might prove more successful at an untested, higher concentration.

Little correlation exists between strength- and colour-retention of the treated samples (Figure 5). EBR for example is very good for colour-retention but poor for strength-retention (Table 3). Clearly colour cannot be used to estimate the strength of the aged treated model textiles. The low correlation could be due to textile strength and colour changes occurring via different mechanisms, for example colour change may be pH dependent. Further analysis will identify this.

Strength-retention is considered more important than colour-retention for a stabilisation treatment for iron-tannate dyed textiles because the primary aim is to prevent eventual textile disintegration. The fibres treated with PA10/IMS/ME30, PA30/IMS/ME30, T292260, and T1446/ME30

retained their strength best and comparably with the MPx/CBx treatments with '+++' (Table 3).

FURTHER WORK

Completion of analysis of the treated cotton and silk samples from these tests in addition to consideration of ease of use, toxicity levels, cost and availability of the treatments and chemicals will result in a final decision as to which non-aqueous treatments will be tested further. The chosen treatments will be applied to 15 x 10 cm sized, pre-aged, dyed and undyed model textiles (cotton, abaca, wool, and silk) followed by further accelerated ageing. Treatment success will be assessed using SEM, spectrophotometry, pH testing, and tensile testing. Also, real-time ageing studies will be started to indicate how long the treatments can protect the iron-tannate dyed samples under ambient environmental conditions.

CONCLUSIONS

A range of non-aqueous treatments involving antioxidants and deacidifier has been applied to specially developed model textiles. The treatments were evaluated for their success in inhibiting the degradation of iron-tannate dyed model textiles using spectrophotometry, visual colour assessment and handling tests. The most successful treatments so far include the antioxidants: Tinuvin 292, Tinuvin 144, alpha-tocopherol, phytic acid, etidronic acid, and deacidifier magnesium ethoxide. These were comparable or slightly less successful than the magnesium phytate, calcium bicarbonate treatment. Combination of antioxidant and deacidifier was generally more successful than use of antioxidant alone. Completion of analysis will conclude which treatments will be investigated alongside the established phytate treatment on cotton, abaca, wool, and silk textiles.

ACKNOWLEDGEMENTS

Thanks to The Science and Heritage Programme, AHRC, EPSRC; Tim Grice for supplying the GreenEarth®; Dass Chahal for supplying the melaneze; Chris Addie for supplying the Tinuvin and Irganox chemicals; David Peggie for monitoring the environmental chamber; and Huw Owens for advising on colour analysis.

REFERENCES

- GILL, L., H. WILSON, and B. MACKENZIE. 2010. Group news and graduate voice: CF10's winning student posters. In *ICON News* (28): 22–25. [Poster entitled 'Developing chemically unstable model textiles for treatment evaluation' by Helen Wilson].
- KOLAR, J., A. MOZIR, M. STRLIČ, G. DE BRUIN, B. PIHLAR, and T. STEEMERS. 2007. Stabilisation of iron gall ink: aqueous treatment with magnesium phytate. *e-Preservation Science* 4: 19–24. <http://www.morana-rtd.com/e-preservation-science/2007/Kolar-30-12-2007.pdf>.
- KOLAR, J., A. MOZIR, M. STRLIČ, G. CERES, V. CONTE, V. MIRRUZZO, T. STEEMERS, and G. DE BRUIN. 2008. New antioxidants for treatment of transition metal containing inks. In *Durability of Paper and Writing 2: 2nd International Symposium*

and *Workshops, Ljubljana, Slovenia, 5–7 July 2008*, ed. M. Strlič and J. Kolar, 20–21. Ljubljana: Faculty of Chemistry and Chemical Technology.

NEEVEL, J. 2002. (Im)possibilities of the phytate treatment of ink corrosion. In *Contributions to conservation – research in conservation at the Netherlands Institute for Cultural Heritage (ICN)*, ed. J. Mosk and N. Tennent, 74–86. London: James and James.

TE KANAWA, R., G.J. SMITH, G.A. FENTON, I.J. MILLER, and C.L. DUNFORD. 2008. Evaluation of consolidants for black iron-tannate-dyed Maori textiles. In *Dyes in History and Archaeology: 21. Avignon and Lauris, France 2002*, ed. J. Kirby, 224–229. London: Archetype Publications Ltd.

MATERIALS LIST

n-Hexane, tetrachloroethylene, DMS, and ethanol

VWR (<https://www.vwrsp.com/index.cgi>)

1-ethyl-3-methylimidazolium bromide, etidronic acid (1-hydroxyethane 1,1-diphosphonic acid), calcium carbonate, magnesium carbonate hydrate, phytic acid solution (~40% in water) (1r,2R,3S,4s,5R,6S)-cyclohexane-1,2,3,4,5,6-hexayl hexakis[dihydrogen (phosphate)]) and alpha-tocopherol

Sigma Aldrich (<http://www.sigmaaldrich.com/united-kingdom.html>)

Tinuvin 292 (Bis(1,2,2,6,6-pentamethyl-4-piperidyl) sebacate and Methyl 1,2,2,6,6-pentamethyl-4-piperidyl sebacate), Tinuvin 144 (Bis (1,2,2,6,6-pentamethyl-4-piperidiny)-[[3,5-bis(1,1-dimethylethyl)-4-hydroxyphenyl]methyl]butylmalonate), Irganox 1135 (Benzenepropanoic acid, 3,5-bis (1,1-dimethyl-ethyl)-4-hydroxy-.C7-C9 branched alkyl esters) and Irganox 1425 (1:1-Combination of Calcium-bis (((3,5-bis(1,1-dimethylethyl)-4-hydroxyphenyl)methyl)-ethylphosphonate) and polyethylene-wax)

CIBA (<http://www.basf.com/group/corporate/en/>)

melaneze (synthetic melanin)

Croda (<http://www.croda.com/home.aspx?s=1&r=70>)

GreenEarth® (cyclsiloxane D5)

Johnson Cleaners UK Ltd. (www.johnsoncleaners.com)

Munktel CXD pHoton Aqua Forte High Wet Strength absorbent paper, 90 gsm

Conservation by Design Limited (<http://www.conservation-by-design.co.uk/>)

Investigation into iron diffusion into wool, silk, cotton and abaca textiles using SEM-EDX

Helen Wilson

The University of Manchester and the British Museum

INTRODUCTION

Iron-tannate dyes have been used worldwide for thousands of years to colour a huge variety of materials in shades of black, grey and brown. Unfortunately, iron-tannate dyes can severely accelerate the degradation of the substrates they colour.

Unbound iron ions originating from the dyeing process or the breakdown of the dye complex accelerate fibre oxidation via the Fenton reaction. Highly reactive radicals are formed which react quickly with nearby polymer chains or other compounds.

During oxidation, polymer cross-links and acid groups are formed, which increase fibre brittleness and accelerate the rate of acid hydrolysis, respectively. Acid hydrolysis breaks the polymer chains, decreasing the fibre strength, and promotes oxidation through the reduction of ferric ions to the catalytic ferrous ions, thereby initiating the acceleration of the degradation cycle.

A collaborative project between the University of Manchester and the British Museum is investigating non-aqueous treatments to inhibit these processes using model iron-tannate dyed textiles [1, 2].

Differences in strength-loss have been observed following accelerated ageing of model textiles. Dyed cotton and abaca suffered significant strength-loss after one week of exposure to 80°C and cycling relative humidity (35-80% every 3 hours). Dyed silk was noticeably weakened by four weeks of exposure, but dyed wool retained much of its strength. These differences could arise from the susceptibility of the textile substrates to iron catalysed degradation, the amount of iron-tannate dye present in the fibres and/or the availability and location of unbound iron ions. The high reactivity of the radicals formed during the Fenton reaction result in accelerated degradation close to the unbound iron ions.

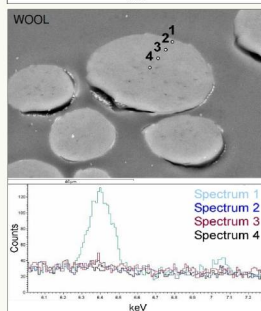
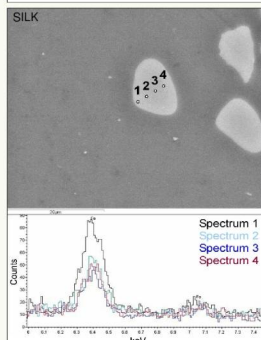
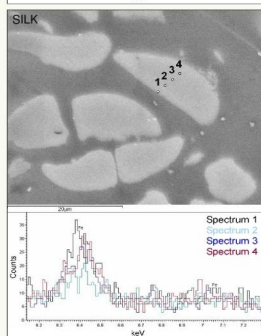
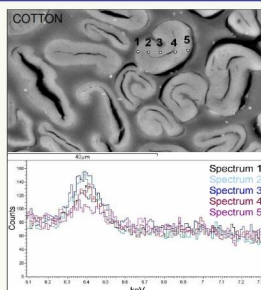
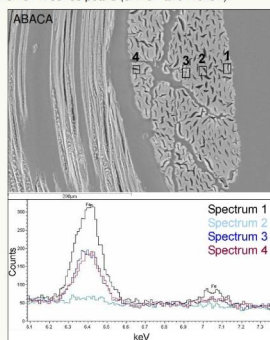
In this poster, a correlation between the location of iron throughout model textile fibres and the extent of fibre degradation upon accelerated ageing is investigated.

EXPERIMENTAL

Cross-sections of the resin (bisphenol A-epichlorohydrin) embedded, undyed and dyed, model textiles were prepared and polished. Analysis of the cross-sections was undertaken using a Hitachi Ultra High Resolution S-4800 FE-SEM and an Hitachi VP-SEM S-3700N (30Pa). The SEMs were operated at 20kV and a 12mm working distance for all analyses. EDX spectra were collected for varying lifetimes after optimisation of the iron peak versus total time taken for analysis: 200s for abaca and silk; 200-300s for cotton and 500-1000s for wool. Dyed and undyed samples of the same material were analysed using the same conditions for comparison.



Variations in iron content in both individual fibres and in fibre bundles or yarns were investigated. Lack of standards for these materials makes quantification unreliable so all data should be viewed as semi-quantitative. Therefore only the presence or absence of peaks in a particular sample and the relative heights of peaks from the same sample area have been compared. General trends rather than precise conclusions can be drawn. The EDX spectra presented here are limited to the iron K series peaks (6.4keV and 7.0keV).



RESULTS AND DISCUSSION

1. In all the model textiles the dyed samples showed iron peaks while the undyed did not.
2. The iron content in the fibre bundles/yarns was highly variable but seems to be linked to the penetration of the dye. For example, the fibres on the more exposed edges of a fibre bundle or yarn, e.g. the crown of the weave, often contained more iron than fibres on the less exposed edge, e.g. where warp and weft yarns are compressed against one another. Variable iron levels in abaca fibre bundles, Figure 2, can be explained by the cracks in the bundles which enable dye complexes to penetrate fibres deeper within the bundle.
3. For individual fibres of abaca, cotton and silk iron was easily detected on the edge and the interior of each fibre. Some of this iron will be unbound and much smaller in size than the dye complex. Consequently it is possible that unbound iron ions diffused further into the fibres than the dye complex. As the types of iron are indistinguishable with SEM-EDX the extent of dye complex diffusion is unknown, but potentially extends throughout the fibres Figures 3-5.
4. An iron concentration gradient decreasing from the edge to the interior was often seen and could depend on location within the fibre bundle or yarn.
5. Iron in wool fibres was primarily located in the outer surface of the fibres (cuticle) with minimal or no iron detected inside the fibres (cortex), Figure 6. This can be attributed to the hydrophobic cuticle layer preventing water-based dye from entering the cortex of the wool fibres.

Some of the iron ions detected by SEM-EDX will be unbound and catalytic. The small size of the ions suggest that, if not located close to bound iron (dye complexes), the unbound ions will be located further into the fibres. Consequently, unbound ions will be present throughout the cotton, abaca and silk fibres but only in the cuticle of wool fibres. This correlates well with the strength-loss seen in the accelerated ageing studies. Accelerated degradation throughout the cotton, abaca and silk fibres caused severe strength-loss while wool suffered accelerated degradation in the cuticle only, thus retaining much of its strength.

CONCLUSION

Iron concentrations in iron-tannate dyed textiles varied throughout fibre bundles and yarns. A concentration gradient was identified from the surface to the interior of many individual fibres. While iron was detected throughout individual fibres of cotton, abaca and silk, the iron in wool was primarily located in the cuticle of the fibres. The observed differences in iron-tannate dye diffusion into the textile fibres offer an explanation for the different extents of fibre degradation seen during accelerated ageing studies.

FIGURE CAPTIONS

- Figure 1 Top view of cross-sections used in analysis. From left to right: abaca, cotton, silk and wool.
- Figure 2 SEM image and EDX spectra of dyed abaca in cross-section. Spectrum 2 was recorded from a point inside a fibre bundle and does not show any iron peak while spectrum 1, recorded at the crown of the weave, shows the highest iron signal.
- Figure 3 SEM image and EDX spectra of dyed cotton. Iron was detected throughout the fibres.
- Figure 4 SEM image and EDX spectra of dyed silk fibre located inside the yarn. A decrease in iron concentration from the outside to the inside of the fibre is seen.
- Figure 5 SEM image and EDX spectra of a dyed silk fibre on the crown of the weave. Iron ions are detected throughout the fibre with the largest concentration at the edge of the fibre closest to the crown of the weave. Note that overall iron concentration was higher in this fibre compared to the fibre from the inside of the yarn, Figure 4.
- Figure 6 SEM image and EDX spectra of a dyed wool fibre near the crown of the weave. A significant iron signal is present at the edge of the fibre only.
- Figure 7 Samples of the dyed model textiles analysed using SEM-EDX.

ACKNOWLEDGEMENTS

Thanks to: Nigel Meeks at the British Museum for training me in the SEM-EDX and cross-section preparation; Chris Carr and Muriel Rigout for their supervision at The University of Manchester; Mari Hache and Rebecca Slacey for their supervision at the British Museum.

REFERENCES

1. Wilson, H., Daniels, V., Hache, M., and Carr, C., Ars Textura Conference, ULTA, Leeds (2009). http://ulta.leeds.ac.uk/doc/Ars_TexturaAbstracts2009.pdf (accessed 7 June 2010).
2. Gill, L., Wilson, H., and Mackenzie, B., 'Group news and graduate voice: CF10's winning student posters', in ICON News (28) (2010) 22-25 [Poster entitled 'Developing chemically unstable model textiles for treatment evaluation' by Helen Wilson].

SAMPLES OF MODEL TEXTILES ANALYSED			
ABACA	COTTON	SILK	WOOL

APPENDIX 4 ICON CF10 conference poster, 2010

Poster presented at the ICON CF10 conference in Cardiff from the 25th to the 26th March 2010. This poster won the Judges' vote for the best poster presented.



MANCHESTER
1824

THE BRITISH MUSEUM

Developing chemically unstable model textiles

Helen Wilson

Textiles and Paper Science, School of Materials, The University of Manchester
Department of Conservation and Scientific Research, The British Museum

Engineering and Physical Sciences
Research Council

Arts & Humanities
Research Council

EPSRC

Helen.Wilson@postgrad.manchester.ac.uk

Introduction

The combination of iron(II) (ferrous) ions and tannic acids has been used worldwide for hundreds of years to dye natural fibres black, grey or brown.



Figure 1 This iron cloth Oxi1904, -282 from Oceania demonstrates the effect of the increasing brittleness and strength-loss of natural fibres dyed with iron-tannate dyes.

Many iron-tannate dyed organic materials are present in museum collections on objects of cultural significance. However, like the chemically similar iron gall ink, these iron-tannate dyes accelerate the degradation of the objects they colour, severely decreasing their useful lifetime, i.e. [1,2].

This research aims to develop a non-aqueous treatment to inhibit this accelerated degradation. Model iron-tannate dyed textiles have been produced to which possible treatments will be applied.

Collections Research

- Iron-tannate dyes were identified in British Museum objects from Europe, Asia, Africa, America and Oceania which were constructed from organic materials such as raphia, cotton, silk, leather and New Zealand flax (*Phormium tenax*).
- X-ray fluorescence (XRF) was used to confirm high levels of iron in these objects, implying the presence of iron-tannate dyes.



Figure 2 XRF spectra of beige and black areas of (inset) African Kuba cloth (amalgamated) demonstrating the unusually high iron peak in the black area.

Literature Research

Historical iron-tannate dye recipes from the 16th to 20th centuries were identified and assessed for methodology, ingredients and use, i.e. [3-5]. The methods described ranged considerably in complexity and clarity, and there was substantial variation in the type and quality of ingredients. However, iron(II) ions and tannic acids were present in all.

Experimentation

Materials and variables were chosen based on collections and literature research to include in small-scale lab experiments. Three dye formulations were produced which were scaled up for use on 20 metre lengths of textile fabric at The University of Manchester's dyehouse. The dyeing profiles were further adapted to improve colour depth and dyeing efficiency [6].



Figure 3 Left: Dyeing cotton and abaca on The Jigger Machine. Right: Dyeing wool and silk on the Wind Machine.

Dye	Dye bath 1	Dye bath 2
1	Fe	Purified tannin extracts (Sunach + Chinese Gall)
2	Fe + Cu	Purified tannin extracts (Sunach + Chinese Gall)
3	Fe	Raw gall extract

Accelerated Ageing Studies

- Model textiles were exposed to both constant and variable relative humidity over a temperature range of 70-90°C for a maximum of 8 weeks.
- Significant strength loss was seen in dyed cotton and abaca within less than 1 week of heat/humidity exposure. In contrast, the dyed wool and undyed textiles retained much of their strength after 6 weeks of heat/humidity exposure.
- All dyed textiles showed discolouration after ageing.

Conclusions

- Approximately 100 metres of model iron-tannate dyed textiles have been produced using methodologies derived from collections and literature research and experimentation.
- Accelerated ageing studies have shown that the model dyed textiles degrade significantly faster than the undyed counterparts, which reflects the behaviour observed in iron-tannate dyed museum objects.
- Future work involves pre-ageing the model textiles before treatment application. Further accelerated ageing and analysis will evaluate the success of the treatments.

Acknowledgements

Many thanks go to the Science and Heritage Programme, AHRC and EPSRC: G Carr, M. Rigout, and P. Cohen at The University of Manchester; conservators, curators and scientists at The British Museum; in particular C. Higgit, M. Hacke, V. Daniels, P. Cruickshank, M. Sandy and M. Yarni at Camberwell College of Arts and D. Peggie at The National Gallery.

References

- Neveel, J. G. (2002) In Mosk, J. A. & Tennent, N. H. (Eds.) *Contributions to Conservation*. James & James.
- Kolar, J. & Strick, M. (Eds.) (2006) *Iron Gall Inks: On Manufacture, Identification, Degradation and Stabilisation*. Ljubljana, National and University Library.
- Rosetti, G. (1548). *The Pilchro of Gioanventura Rosetti*. translation by Edelstein, S. M. & Borghetty, H. C., MIT Press, 1969.
- Haigh, J. (1800). *The Dyer's Assistant in the Art of Dying Wool and Woollen Goods*. London.
- Donne, J. B. (1973). *Man* 8(1): 104-107.
- Wilson, H. L. et al (2009). *Arts Textiles International Textiles Conference 2nd-3rd September 2009*. Leeds, ULTA.

APPENDIX 5 Experimental methods for the 16 iterative experiments (Section 4.6.2) used to produce the dye formulations detailed in Table 4.3

Experiment number and title	Fabrics included in dyebath	Reagent concentration (x10 ⁻³ M)			Temperature (°C)	Dyebath volume (ml)	Liquor: fabric	Immersion time per dyebath (h)	Method of reagent application	Number of full dyeing cycles completed
		Iron(II) sulphate heptahydrate	Tannic acid	Other reagent						
1	One-stage vs two-stage dyeing methods	100	40		16-17	250	63:1	1	A ¹ : Combined in one solution (one-stage method) made the night before immersion (old solution) or immediately before immersion (fresh solution). B: Separate application either tannic acid first (T-I) or iron sulphate first (I-T)	3
2	Temperature	33	19.5		A: 19-20; B: 53-55; C: 90-100	250	63:1	1	A ¹ : T-I; B ¹ : I-T	1
3	Reagent concentration (Part 1)	A: 33.10; B: 16.50; C: 8.27; D: 6.62; E: 3.31	A: 19.5; B: 9.76; C: 4.88; D: 3.90; E: 1.95		20	250	126:1	1	A ¹ : T-I; B ¹ : I-T	2
		A: 16.50; B: 6.62; C: 3.31	A: 9.76; B: 3.90; C: 1.95		55	250	111:1	1	A ¹ : T-I; B ¹ : I-T	2
4	Immersion time (Part 1)	3.31	1.95		20	250	126:1	A: 1; B: 2; C: 3; D: 4; E: ~24	T-I	2
		6.62	3.9		55	250	111:1	A: 1; B: 2; C: 3; D: 4; E: ~24	I-T	2

5	Reagent ratio (Part 1)	Cotton, Abaca, Silk	A: 3.31; B: 6.62; C: 9.93	0.331	20	250	126:1	2	T-I	2
		Wool, Silk, Cotton	A: 6.62; B: 13.24; C: 19.86	0.662	55	250	111:1	2	I-T	2
6	Substitution of tannic acid with powdered galls (Part 1)	Cotton, Abaca, Silk	3.31	-	20	250	126:1	1	G-I	2
								0.28		
7	Substitution of tannic acid with powdered galls (Part 2)	Cotton, Abaca, Silk	6.62	-	20	250	126:1	2	G-I	2
								A: 0.14; B: 0.28, C: 0.42		
8	Immersion time (Part 2)	Wool, Silk, Cotton	13.24	-	55	250	111:1	2	I-G	2
								A: 0.28; B: 0.56, C: 0.84		
9	Reagent concentration (Part 2)	Cotton, Abaca, Silk	6.62	0.33	20	250	126:1	A: 2-2; B: 2-1; C: 2- 0.5; D: 3-1	T-I	2
		Wool, Silk, Cotton	13.4	0.6	55	250	111:1	A: 2-2; B: 1-2; C: 0.5- 2; D: 1-3	I-T	2
9	Reagent concentration (Part 2)	Cotton, Abaca, Silk	A: 13.24; B: 19.86	A: 0.66; B: 0.99	20	250	126:1	2-2	T-I	2
		Wool, Silk, Cotton	A: 26.8; B: 40.2	A: 1.2; B: 1.8	55	250	111:1	1-3	I-T	2

10	Liquor: fabric ratio	Cotton, Abaca, Silk	6.62	0.33	20	A: 250; B: 150; C: 50	A: 126:1; B: 75:1; C: 25:1	2-2	T-I	2
		Wool, Silk, Cotton	13.4	0.6	55	A: 250; B: 150; C: 50	A: 111:1; B: 67:1; C: 22:1	1-3	I-T	2
		Cotton, Abaca, Silk	6.62	-	20	Gallie acid: 3.31×10^{-3} M	126:1	2	GA-I	2
11	Substitution of tannic acid with gallic acid	Wool, Silk, Cotton	13.4	-	55	Gallie acid: 6.62×10^{-3} M	111:1	2	I-GA	2
		Cotton, Abaca, Silk	16.5	A: 1.64; B: 2.47; C: 3.29	20	250	126:1	2-2	T-I	2
	Reagent ratio (Part 2)	Wool, Silk, Cotton	13.24	A: 1.32; B: 2.00; C: 2.63	55	250	111:1	1-3	I-T	2
13	Addition of copper(II) sulphate pentahydrate	Cotton, Abaca, Silk	16.5	9.87	20	Copper sulphate(II) pentahydrate: $A: 0 \times 10^{-3}$ M; $B: 2 \times 10^{-3}$ M	126:1	2-2	T-I	2
		Wool, Silk, Cotton	13.24	7.89	55	Copper(II) sulphate pentahydrate: $A: 0 \times 10^{-3}$ M; $B: 1.44 \times 10^{-3}$ M	111:1	1-3	I-T	2
		Cotton, Abaca, Silk	49.5	9.87	20	250	126:1	2-2	T-I	2
14	Reagent concentration (Part 3)	Wool, Silk, Cotton	39.72	7.89	55	250	111:1	1-3	I-T	2
		Cotton, Abaca, Silk	49.5	9.87	20	250	126:1	2-2	T-I	2
		Wool, Silk, Cotton	39.72	7.89	55	250	111:1	1-3	I-T	2

15	Liquid extract of gall powder	Cotton, Abaca, Silk	16.5	-	A: 100 ml liquid extract of 30 g of gall powder soaked for 3-4 days in 800 ml water; B: 5 g of gall powder	20	250	126:1	2-2	T-I	2
		Wool, Silk, Cotton	13.24	-	A: 250 ml liquid extract of 30 g of gall powder soaked for 3-4 days in 800 ml water; B: 10 g of gall powder	55	250	111:1	1-3	I-T	2
16	Substituting tannic acid with purified sumach tannic acid	Cotton, Abaca, Silk	16.5	-	0.56 g per 250 ml	20	250	126:1	2-2	T-I	2
		Wool, Silk, Cotton	13.24	-	1.12 g per 250 ml	55	250	111:1	A: 1-3; B: 3-1	A: I-T; B: T-I	2

Note:

I. A, B, C etc have been used to list all of the conditions used in an experiment where more than one exists e.g. the different temperatures tested. Where the concentrations of both iron sulphate and tannic acid have been altered to maintain the same ratio of reagents, the concentrations of each that were used together to produce the iron-tannate dye are listed by using the same letter e.g. A, B, C etc. Where two separate variables were tested in one experiment e.g. dyebath order and dyebath temperature, the variations in one are listed as A, B, C etc. while those in the other factor are listed as A', B', C' etc.

APPENDIX 6 XRF Fe ratios of historic samples

The semi-quantitative XRF analysis (XRF ratios) of iron in British Museum and other objects is presented below and complements the information provided in Table 6.2. The XRF ratios have been determined by normalising the metal ion peak to the Compton peak and multiplying the result by 1000.

Registration number	XRF number	Name	Material dyed	Continent of production	Sample colour	XRF ratio	
						Iron	Copper
British Museum objects							
1881,0802.48 P+E	HW2	Gorget/breast-plate/back-plate made of leather, textile, and metal.	P	Europe	black	9145	61
1909,5,19,8	HW3	Printing brush		Asia	black	477	15
1957,As11,9	HW4	Black Apatani rain cape	C	Asia	black	49	2
1979,Af,1,2397	HW5	African mask	C	Africa	black	153	ND
1981,0808.225	HW6	Hina doll hair	P	Asia	black	238	ND
6317	HW7	Egyptian basket	C	Africa	black	1450	6
21789	HW8	Coptic textile	C	Africa	black	30	ND
43369	HW13	Black and cream Egyptian textile	C	Africa	black	106	54
Af1938,1004.13	HW15	African mask	C	Africa	black	307	ND

Appendix 6

No number	HW20	Horse chain mail with black lining		Asia	black	1868	561
M4-S-22 37119	HW21	Black and white textile (mainly black) with many losses	C	Africa	beige	75	3
	HW22				black	127	ND
M4-S-22 37129	HW23	Black and beige strip of woven textile	C	Africa	beige	116	6
	HW24				black	134	6
OA+7279	HW28	Saddle		Asia	black	511	23
Thailand Siam Royal Cypher Medal1926	HW30	Medal		Asia	black	69	36
Af1818,1114.23	HW32	Adinkra (mourning cloth)	C	Africa	black	508	2
	HW33				black	263	5
1881,0802.158	HW34	Islamic steel helmet (lining)	C	Asia	black	2370	587
1,904,282	HW35	Loin cloth of banana or hibiscus fibre	C	Micronesia	dark brown	406	39
	HW36				light brown	95	16
1906-0524-8, Oc1906,0524.8	HW37	Belt worn by a chief "Tol"	C	Oceania	black	925	2
1936,1211.5	HW38	Machine woven adinkra cloth	C	Africa	black	340	5

Appendix 6

<i>Am1937,0617.1</i>	<i>HW39</i>	<i>North American skin bag</i>	<i>P (skin)</i>	<i>North America</i>	<i>black</i>	<i>4163</i>	<i>44</i>
<i>Am1933,1216.1</i>	<i>HW40</i>	<i>Andean textile</i>		<i>South America</i>		<i>71</i>	<i>13</i>
<i>Am1933,1216.3</i>	<i>HW41</i>	<i>Andean textile</i>		<i>South America</i>	<i>light brown</i>	<i>22</i>	<i>17</i>
	<i>HW42</i>				<i>green-black</i>	<i>54</i>	<i>13</i>
	<i>HW43</i>				<i>red</i>	<i>33</i>	<i>13</i>
	<i>HW44</i>				<i>yellow</i>	<i>60</i>	<i>40</i>
<i>Am1933,1216.4</i>	<i>HW45</i>	<i>Andean textile</i>		<i>South America</i>	<i>light brown</i>	<i>46</i>	<i>43</i>
	<i>HW46</i>				<i>dark brown</i>	<i>47</i>	<i>29</i>
	<i>HW47</i>				<i>light brown</i>	<i>136</i>	<i>278</i>
<i>Am1934,0714.2</i>	<i>HW48</i>	<i>Andean textile</i>		<i>South America</i>	<i>black</i>	<i>75</i>	<i>7</i>
<i>Am1934,0714.8</i>	<i>HW49</i>	<i>Andean textile</i>		<i>South America</i>	<i>black</i>	<i>46</i>	<i>14</i>
	<i>HW50</i>				<i>black</i>	<i>44</i>	<i>8</i>
<i>Am1954,04.555</i>	<i>HW51</i>	<i>Andean textile</i>		<i>South America</i>		<i>90</i>	<i>6</i>
<i>Am1954,05.565</i>	<i>HW52</i>	<i>Andean textile</i>		<i>South America</i>	<i>red</i>	<i>38</i>	<i>24</i>
	<i>HW53</i>					<i>89</i>	<i>12</i>
	<i>HW54</i>					<i>32</i>	<i>49</i>
<i>H279</i>	<i>HW56</i>	Woven strip with black tufts caught into the weave to produce a black on beige triangular	<i>C</i>	<i>Africa</i>	<i>beige</i>	<i>418</i>	<i>11</i>
	<i>HW57</i>				<i>black</i>	<i>767</i>	<i>7</i>

Appendix 6

pattern							
H288 5J	HW58	Woven textile with tufts of yellow and black fibres incorporated into the weave to produce a black, yellow and beige diamond and striped pattern	C	Africa	beige	204	7
	HW59				yellow	154	11
	HW60				black	542	7
H290 9C	HW61	Woven textile with black woven striped areas and fringed ends	C		beige	74	6
	HW62				beige	90	10
	HW63				black	2844	14
	HW64				black	4499	9
NA	HW65	Model iron-tannate dye precipitate	Organic	Europe	black	7486	ND
NA	HW66	Model iron-tannate dyed raffia provided by Mark Sandy, Camberwell College of Arts	C	Europe	black	814	0
	HW67				black	1242	3
	HW68				black	731	5
NA	HW69	Model undyed raffia provided by Mark Sandy, Camberwell College of Arts	C	Europe	beige	163	4
	HW70				beige	296	4
NA	HW71	Fragile historic piu piu/Maori cloak pieces from the Horniman Museum	C	Oceania	beige	105	2
	HW72				black	5924	3
NA	HW73	Modern piu piu	C	Oceania	beige	35	6
	HW74				black	1918	2
	HW75				black	1989	4
Am1957,11.10	HW76	Black Apatani composite hat	C	Asia	black	205	6
	HW77				black	36	3
	HW78				black	62	3
	HW79				neutral	6	2

Appendix 6

Coins & Medals handling collection	HW85				black	983	13
	HW86	Kuba cloth	C	Africa	black	1152	14
	HW87				beige	380	61
	HW88				beige	202	148
Oc4253, Oc1866C1.4253, and Oc1866E6.54	HW89	Decorated tiputa (poncho) made from tapa, bark cloth.	C	Oceania	black	168	6
Oc9954A, Oc1876C1.19954, Oc1876C1118.7, and Oc1876E6.63	HW90	Barkcloth two layer garment (possibly mourning dress)	C	Oceania	black	924	9
SLM2105, 1. Af,SLMisc2105	HW92	Colourful striped woven textile from Madagascar	C	Africa	black	96	6
	HW93				brown	56	3
2005,0727.1	HW94	Akali Sikh turban cotton cloth	C	Asia	black	1408	13
No number	HW95	19th Century banana fibre belt from the Caroline Islands	C	Micronesia	brown	3502	7
Samples from the Museum of Islamic Art, Berlin (Anna Beselin)							
I.0007/62	AB1.1	Islamic carpet	P		Red	0	0
	AB1.2				Brown	502	35
KGM1880,919	AB1.3	Islamic carpet	P		Red	146	4
	AB1.4				Brown	696	12
KGM1882,707	AB1.5	Islamic carpet	P		Green	101	21
	AB1.6				Brown	574	30

Appendix 6

I. 5526	AB1.7	Islamic carpet	P	Red	158	38
	AB1.8			Brown	1951	249
KGM1900,55A	AB1.9	Islamic carpet	P	Blue	222	97
	AB1.10			Black	357	62
KGM1885,248a	AB2.1	Islamic carpet	P	Blue	84	59
	AB2.2			Brown	1029	30
I.0072/62	AB2.3	Islamic carpet	P	Blue-green	386	35
	AB2.4			Brown	486	14
KGM1882,703	AB2.5	Islamic carpet	P	Red	141	37
	AB2.6			Brown	465	27
KGM1875,197	AB2.7	Islamic carpet	P	Red	197	34
	AB2.8			Black/ brown	75	26
	AB2.9			Brown	1109	30
I. 0001/64	AB3.1	Islamic carpet	P	Yellow	49	6
	AB3.2			Brown	278	9
I. 0041/70	AB3.3	Islamic carpet	P	Green	76	28
	AB3.4			Black	455	39
KGM1886,500	AB3.5	Islamic carpet	P	Red	80	9
	AB3.6			Brown	241	8
KGM1875,111	AB3.7	Islamic carpet	P	Yellow	63	7
	AB3.8			Brown	222	6
	AB3.9			Black/ dark green	214	9
KGM1883,522	AB4.1	Islamic carpet	P	Green	2	54
	AB4.2			Brown	0	4

Appendix 6

KGM1885,247	AB4.3	Islamic carpet	P		Red	4	22
	AB4.4				Brown	5	19
KGM1889,150	AB4.5	Islamic carpet	P		Red	2	31
	AB4.6				Brown/ black	6	23
	Axminster carpet samples obtained on visit to Tetley Studios, Saltram House, and the Axminster Factory						
TC920D3	HT1.1	Axminster carpet in Tetley Studio	P	Europe	Dark brown	217	3
	HT1.2				Black (restauration wool)	9	2
	HT1.3				Yellow	50	4
	HT1.4				Red	45	6
PC976	HT1.5	Grimstone chenille rug in Tetley Studio	P	Europe	Originally red (now faded to green/ yellow)	34	112
	HT1.6				Peach	10	4
	HT1.7				Coral	15	4
NA	HT1.8	Appletons brown groundings 584 dyed wool used in carpet conservation	P	Europe	Brown	4	5
NA	HT2.1	Axminster carpet in the Saloon of Saltram House	P	Europe	Brown/ black (original wool)	28	2
	HT2.2				Brown	113	9
	HT2.3				Brown (restauration wool)	21	4
	HT2.4				Green	15	5
	HT2.5				Brown	13	14
NA	HT2.6	Axminster carpet in the dining room of Saltram House	P	Europe	Brown	11	12
	HT2.7				Brown (restauration wool)	11	17
NA	HT2.8	Axminster carpet fin the Saloon of Saltram House	P	Europe	Brown	12	8
NA	HT2.9	Wool from Axminster Factory	P	Europe	Black (contempora ry wool)	8	2

Note:

a. Cellulosic and proteinaceous materials are denoted by a 'C' and 'P', respectively.

Appendix 7

APPENDIX 7 Samples of the model textiles (see Table 5.1 for dye formulations)

CU	AU
Cc1	Ac1
Cc2	Ac2
Cc3	

Appendix 7

SU	WU
Sp1	Wp1
Sp2	Wp2
Sp3	